



UNIVERSITAT DE
BARCELONA

**Mitochondrial and autophagic alterations
in human-derived cell models of Parkinson's disease
related to LRRK2^{G2019S} and GBA^{N370S} mutations**

Diana Luz Juárez Flores



Aquesta tesi doctoral està subjecta a la llicència **Reconeixement 4.0. Espanya de Creative Commons.**

Esta tesis doctoral está sujeta a la licencia **Reconocimiento 4.0. España de Creative Commons.**

This doctoral thesis is licensed under the **Creative Commons Attribution 4.0. Spain License.**

**MITOCHONDRIAL AND
AUTOPHAGIC ALTERATIONS IN
HUMAN-DERIVED CELL MODELS OF
PARKINSON'S DISEASE RELATED
TO *LRRK2*^{G2019S} AND *GBA*^{N370S}
MUTATIONS**

Thesis presented by

Diana Luz Juárez Flores

For the degree of Doctor by the University of Barcelona

Thesis directed by

Glòria Garrabou and Constanza Morén



**UNIVERSITAT DE
BARCELONA**

Faculty of Medicine and Health Sciences, University of Barcelona
Barcelona, 2019.

Por Suseli, Nidia y Emi,

Para Montse

Gracias a mis papás porque es por ustedes que he llegado a tener un doctorado, ustedes me enseñaron que con trabajo duro y constante se obtiene lo que se desea. Mi papá me ha animado siempre a no tener miedo de embarcarme en aventuras nuevas y mi mamá me ha enseñado que el trabajar duro trae buenos resultados. Gracias por venirme a visitar a Barcelona, y por acompañarme algunas noches al laboratorio para que no tuviera miedo, incluso a mis treinta y tantos años.

Marcos, gracias por esta vida tan bonita que tenemos. Gracias por enseñarme a andar en bicicleta, por los paseos, por heredar tu carácter a Montse, por ceder a mi necesidad de tener perro, y por acompañarme a buscar hojitas en el parque. Hemos hablado muchas veces de cómo hacer un doctorado ha sido el reto profesional más duro de los dos; compartir contigo profesión, y vocación, hace que el esfuerzo sea muy disfrutable. Gracias por aceptarme tan exigente y rígida, por esforzarte tanto, por hacerte cargo de nuestro hogar cuando lo necesité y gracias por esperar pacientemente a que te alcanzara en el final del doctorado. Casarme contigo ha sido la mejor decisión de mi vida.

Hace seis años, cuando conocí a las autoras de “el artículo de la sepsis”, intuí que mi vida daría un giro, pero nunca imaginé lo que vendría a continuación. De la mano del **Lluís Palacios**, nos dirigimos al laboratorio a preguntar por las autoras y nos recibió Glòria, con la sonrisa de siempre, nos ofreció un café, nos explicó las líneas de investigación del laboratorio y nos presentó con todos los que iban y venían, haciendo la mudanza del lab 302 a la planta 4B del Cellex.

Glòria, tu entusiasmo, tu ilusión, tu generosidad y tu manera de explicar en términos simples tu complicadísimo trabajo, no deja indiferente; si ya tenía yo antes una extraña obsesión con las mitocondrias, conocerte me convenció de que tenía que intentar ser un poquito como tu. Meses después, **Glòria** y **Cons** me entrevistaron para entrar al laboratorio a hacer el doctorado. Y es por esta primera oportunidad que empezó esta increíble aventura y el primer motivo de mi agradecimiento. Gracias por dedicarme una hora de su tiempo aquella mañana para explicarme el proyecto del Parkinson, gracias por tomarme en serio. Esta tesis es de ustedes.

Gracias a ambas por aceptarme como parte del grupo y permitirme una flexibilidad que me permitió estar con Montse los primeros años de su vida. Ustedes son el mejor ejemplo de cómo podemos ayudarnos para lograr la tan deseada conciliación laboral, cuenten con mi ayuda ahora y siempre en todos los proyectos nuevos de su vida, estaré por siempre en deuda con ustedes.

Gràcies **Glòria** per compartir la teva experiència i la teva saviesa, pel teu somriure de sempre i per ser tan bona mestra i amiga. Gràcies pel teu optimisme i gràcies per no permetre conformar-me mai, i per acompanyar-me a superar els meus límits com mai hagués imaginat.

Gràcies **Cons** per la teva visió pràctica de la ciència, per sempre saber com millorar les coses. Gràcies per la paciència que has tingut amb mi i per animar-me a intentar coses noves. Moltes gràcies per treballar colze a colze amb mi, per fer-me sentir que som col·legues quan sempre has estat una gran mestra.

Ingrid, vas tenir la difícil tasca de ensenyar-me a caminar pel laboratori, a fer experiments i fins i tot a organitzar-me. Gràcies per la teva infinita paciència i gràcies per fer-me participar de la teva tesi. Moltes gràcies per ser tan propera a la meua família, per ser l'heroïna de la Montse durant més de dos anys i per preocupar-te sempre per ella. Gràcies per ser la seva cangur! Sempre et portarà al seu cor, i espero que sempre porti una mica de tu a la seva manera de ser.

Mariona, gràcies pel teu exemple de constància, serenitat i organització. Sempre portes serenitat al laboratori i vull que sàpigues que tots aquests anys t'he admirat profundament. Gràcies per parlar-me sempre en català i ser pacient en els meus intents de respondre't així, gràcies per compartir mirades que sovint deien molt més del que podria expressar amb paraules!

Un dels meus records més vívids del laboratori, és d'un dia que vaig llançar la b actina a la pica i vaig entrar en pànic, el **Marc** em va dir "has de saber quines són les coses greus que et poden passar, i aquesta no és una d'elles ". **Marc**, treballar amb tu va ser determinant per no perdre el cap aquesta i moltes altres vegades, ets un gran científic i un gran artista. Gràcies per imaginar-te situacions de la vida i descriure-les d'una manera que sempre em van fer riure i somriure.

A la meua veïna de taula, **Ester Tobi**, m'has ensenyat molt del laboratori i més de la vida. Gràcies per repetir-me incansablement que no corri, que prengui les coses com van arribant i per animar-me a ser com tu: original i espontània.

Portaré per sempre al meu cor aquell mati en cultius quan ho estava passant malament i plorava: tots els mitos van venir a abraçar-me i a oferir-me ajuda. Han estat el meu major suport en els moments més difícils d'aquests anys.

Estic profundament agraïda als caps clínics del grup, el **Dr. Francesc Cardellach** i el **Dr. Josep María Grau** per acceptar-me con part de l'equip, pel temps que s'han pres en mirar presentacions, llegir "drafts" d'articles i pel respecte amb el

que consideren totes les idees prevenients del laboratori, las meves incloses. Sobretot, per l'exemple d'integritat en l'actuar metge, docent i investigador.

Els últims mesos del meu temps al laboratori haguessin estat impossibles de no haver comptat amb els consells de la **Nekane** i la **Roser**. **Nekane**, gràcies a tu vaig fer un ELISA per primera vegada, el meu experiment preferit fins ara, i gràcies a la **Roser** vaig aconseguir fer unes immunocitoquímiques de les que em sento molt i molt orgullosa. Quina sort tinc de que a més, he pogut compartir amb vostès xerrades i somnis. En un temps en què la meva emoció per la ciència estava desapareixent, i que sentia que el meu ímpetu s'havia acabat amb la maternitat, parlar i somiar amb vostès em va tornar les ganes d'intentar coses noves i no conformar-me amb la vida com és. Gràcies per deixar-me gaudir amb el vostre talent i brillantor.

Gemma S. gràcies per ensenyar-me un feminisme que no coneixia i que m'ha convençut de ser una més de les moltes dones lluitant per demostrar que podem aconseguir el que ens proposem sense renúncies a la nostra essència.

Merche, gràcies per entendre tant els meus moments de "crisi maternal" i per estar amb mi en aquests moments. Per compartir la teva saviesa i per les teves boníssimes idees per fer coses diferents amb la gent del laboratori.

Siscu, crec que puc afirmar, sense por d'equivocar-me, que ets el millor mestre que he conegut a la vida. La teva infinita paciència i amor pel coneixement en totes les àrees són la barreja ideal per enamorar als teus alumnes. Moltíssimes gràcies pel temps que dediques a respondre cadascuna de les meves preguntes. Gràcies per les rialles al laboratori en el teu temps de ser mitoboy; la teva estada al lab va ser dels meus moments favorits del doctorat (mentre escric, recordo i torno a riure), i em vas donar un gran exemple d'humilitat i perseverança.

Marc (Panda) gràcies per la teva creativitat, per ser tan detallista sempre i per estar sempre pendent de totes les persones del laboratori. Mai havia conegut ningú com tu! Tens una família maquíssima i ha sigut increïble poder veure créixer als teus nens. Gràcies per compartir els teus ideals i conviccions.

Ester P. Veure't treballar al meu costat en els primers mesos al laboratori em va ensenyar quan laboriós és ser un bon científic. Et vaig veure deixar-te la vida en els teus projectes i en la teva tesi, i et recordo com un exemple a seguir en els meus moments de cansament o quan he volgut buscar el camí fàcil. Gràcies per explicar-me pacientment com interpretar el WB de la proteïna fosforilada aquella... que per descomptat, no va sortir.

En este laboratorio se hacen amigos para toda la vida. He tenido la fortuna de compartir momentos con muchas personas que, aunque ya no estaba físicamente en el laboratorio cuando yo llegué, también fueron moldeando mi estancia con las anécdotas que de ellos se contaban, con mensajes que me hacían reír y con lo bien que la pase conociéndolos fuera del lab: **Palmi, Gemma Ch, Francesc, Saraí, y Alex**. Al equipo de predis: **Rosa, Ana, Irene, Margarida y Sara**, mil gracias por los consejos de ciencia y las pláticas de pasillo que hacen más llevaderos los tiempos duros.

A los estudiantes de master que han pasado por el laboratorio en este tiempo, **Vicente, Sergio, Juanjo, Joan y Laura**. Gracias por dejarme ser parte de su master, por ayudarme a aprender cosas nuevas a su lado y por la adaptabilidad a mis raros horarios cuando les tocaba trabajar conmigo.

M'agradaria agrair de manera especial a la **Raquel Fucho**, la **Montserrat Battle**, la **Maria Calvo** i l'**Elisenda Coll** per la seva inavaluable ajuda en diferents experiments, per trobar el temps d'explicar-me conceptes nous i per ajudar-me a tirar endavant el doctorat, que per moments vaig pensar inabastable. La seva ajuda desinteressada i l'empatia que van mostrar quan em sentia incapaç d'entendre i dur a terme algunes parts de la meva tesi em van animar en el pla professional i personal.

Ya me habían hablado de lo solitario y duro que es hacer un doctorado. A nivel personal, tengo la fortuna de haber encontrado cerca de mi casa a tres personas que, sin proponérselo, se convirtieron en mi puerto seguro cada noche de los casi 5 años que ha durado el proceso. **Cristóbal, Antonia y Josep María**, muchas gracias por sus sonrisas y sus ánimos, por ser aquellas personas las que Montse les quiere enseñar sus logros, gracias por los minutos de calma que me dan cada día al saludarlos, y por los buenos días, todos los días.

Gracias a **Lorena y Mercè** por dejarme ser parte de su cotidianeidad, por compartir conmigo su vida, sus proyectos, sus personalidades, y por quererme como soy. Pasar tiempo con ustedes me devuelve 20 años, me llena de energía y me mantiene la sonrisa al menos 7 días por sesión. Gracias por la confianza para revisar y tratar a las niñas cuando están enfermas, ese gesto me devolvió la confianza en mi misma de una manera que no se pueden imaginar. **Oscar y Marc**, gracias por dar equilibrio a nuestras reuniones y por todas las noches se encargan de las niñas para que nosotras pudiéramos salir y hablar. **Lúa, Claudia, Martina y Emma**, ojala y cuando sean mayores lean estas líneas y sepan que han motivado mucho mi esfuerzo; verlas crecer junto a Montse ha sido, por mucho, la mejor parte de estos años de mi vida. Tengan por seguro que cuando sean mayores y yo viejita tendrán en mi casa otro hogar.

A mi nueva amiga y hermana, **Meli**. Gracias por ayudarme a mantenerme viva los primeros meses del doctorado; porque algunos días comí gracias a ti, literalmente. Gracias por darme el honor de ser una familia para **Santi y Fran**.

Gracias **Agus** por tu amistad de tantos años, por siempre encontrar la manera de estar cerca y por dejarte abrazar, aunque sean poquitas veces. Te quiero hasta el infinito.

Finalmente, gracias a toda la gente que ha influido en mi vida, aunque no directamente en ésta tesis, porque a lo largo de mi camino, nunca me ha faltado cariño y palabras de ánimo.



INDEX



1. ABBREVIATIONS	5
2. INTRODUCTION	13
2.1 PARKINSON'S DISEASE	15
2.1.1 History	15
2.1.2 Epidemiology and risk factors	19
2.1.3 Clinical features	20
2.1.4 Diagnosis	22
2.1.5 Treatment	26
2.2 MOLECULAR MECHANISMS INVOLVED IN PD PATHOGENESIS	29
2.2.1 Mitochondria	30
2.2.1.1 Mitochondrial structure, function and genome	30
2.2.1.2 Mitochondrial dynamics	32
2.2.1.3 Mitochondrial dysfunction in PD	34
2.2.2 Autophagy	36
2.2.2.1 Subtypes of autophagy	36
2.2.2.2 Selective autophagy processes and control	39
2.2.2.3 Autophagy dysfunction in PD	41
2.3. GENETICS IN PD	45
2.3.1 Leucine Rich Repeat Kinase 2 (<i>LRRK2</i>)	48
2.3.2 Glucocerebrosidase (<i>GBA</i>)	51
2.4 NOVEL APPROACHES IN PD RESEARCH	57
2.4.1 Animal models	57
2.4.2 Cellular models	59
2.4.2.1 Fibroblasts	62
2.4.2.2 Neural stem cells	64

3. HYPOTHESIS AND OBJECTIVES	67
4. METHODS	71
4.1 STUDY 1: Characterization of <i>LRRK2</i>^{G2019S} fibroblasts	75
4.1.1 Study design and population	75
4.1.2 Cell model development	75
4.1.2.1 Fibroblast culture	76
4.1.2.2 Metabolic stress test	76
4.1.2.3 Cell growth and protein content	76
4.1.3 Mitochondrial phenotyping	77
4.1.3.1 Mitochondrial genetics, transcript and protein expression	77
4.1.3.2 Mitochondrial function	79
4.1.3.3 Mitochondrial damage markers	82
4.1.3.4 Mitochondrial dynamics	84
4.1.4 Autophagy characterization	86
4.1.4.1 Western blot immunoquantification	86
4.1.4.2 Immunocytochemistry	88
4.1.5 Statistical analysis	89
4.2 STUDY 2: Characterization of <i>GBA</i>^{N370S} neurospheres	91
4.2.1 Study design and population	91
4.2.2 Cell model development	91
4.2.2.1 Neurosphere culture and characterization	92
4.2.2.2 Uncoupling stress test	95
4.2.3 Mitochondrial phenotyping	96
4.2.3.1 Mitochondrial content and biogenesis	96
4.2.3.2 Mitochondrial function	96
4.2.4 Autophagy characterization	97
4.2.4.1 Western blot immunoquantification	97

4.2.4.2 Mitophagy-associated mRNA levels	97
4.2.5 Statistical analysis	99
5. RESULTS	101
5.1 STUDY 1: Characterization of <i>LRRK2</i>^{G2019S} fibroblasts	103
5.1.1 Epidemiological and clinical data	105
5.1.2 Mitochondrial phenotype	106
5.1.3 Autophagy characterization	114
5.2 STUDY 2: Characterization of <i>GBA</i>^{N370S} neurospheres	119
5.2.1 Epidemiological data	121
5.2.2 Characterization of the neurosphere model	121
5.2.3 Mitochondrial phenotype	128
5.2.4 Autophagy characterization	133
6. DISCUSSION	137
7. CONCLUSIONS	153
8. REFERENCES	157
9. SUPPLEMENTARY MATERIAL	183
10. ANNEX	191

1. ABBREVIATIONS

A AD: Alzheimer's disease
ADP: Adenosine diphosphate
AMPK: Adenosine monophosphate-activated protein kinase
ATP: Adenosine triphosphate
AR: Aspect ratio

B BAF: Bafilomycin A1
BCA: Bicinchoninic Acid Assay
BSA: Bovine serum albumin
BvFTD: Behavioural variant frontotemporal dementia

C CBE: Condurotol- β -epoxide
CCCP: Carbonyl cyanide *m*-chlorophenyl hydrazine
Circ: Circularity
CI: Complex I of the MRC
CIV: Complex IV of the MRC
CMA: Chaperone-mediated autophagy
CNS: Central nervous system
CO₂: Carbon dioxide
CoQ: Coenzyme Q
COXII: Cytochrome oxidase subunit II
COXIV: Cytochrome oxidase subunit IV
CS: Citrate synthase

D DJ-1: Protein/nucleic acid deglycase DJ-1
DMEM: Dulbecco's Modified Eagle Medium
DMSO: Dimethyl sulfoxide
DNA: Deoxyribonucleic acid
Drp1: Dynamin related protein 1
DTNB: 5,5'-dithiobis-2-nitrobenzoic acid

E EDS: excessive daytime sleepiness
EDTA: Ethylenediaminetetraacetic acid
EGF: Epidermal growth factor
ER: Endoplasmic reticulum
ERAD: Endoplasmic reticulum associated degradation
ETC: Electron transport chain

F FBS: Fetal bovine serum
FGF: Fibroblast growth factor
FF: Form factor

G GADPH: Glyceraldehyde-3-phosphate dehydrogenase
GBA: Glucocerebrosidase gene
 GBA^{N370S} : GBA^{N370S} -mutation
 $GBA^{N370S} / GBA^{N370S}$: homozygotes for GBA^{N370S} -mutation
 wt / GBA^{N370S} : heterozygotes for GBA^{N370S} -mutation
GBA-PD: GBA-associated PD
GCase: β -glucocerebrosidase
GD: Gaucher's disease
GWAS: Genome-wide association studies

H HAE: 4-hydroxyalkenal
haNCSc: Human adipose neural crest stem cells
HD: Huntington's disease
HEPES: 4-(2-hydroxyethyl)-1-piperazineethanesulfonic acid
HEX: β -hexosaminidase
Hsc70: Heat-shock cognate 70
HCl: Hydrochloric acid

I IMM: Inner mitochondrial membrane
IMS: Intermembrane space
iPD: Idiopathic PD
iPSC: Induced pluripotent stem cells

J JC-1: Tetraethyl benzimidazolocarboyanine iodide

L LAMP-1: Lysosomal-associated membrane protein-1
LC3B: (Microtubule-associated protein 1) light-chain 3 beta
LRRK2: Leucine rich repeat kinase 2
LRRK2: Leucine rich repeat kinase 2 gene
LRRK2^{G2019S}: *LRRK2*^{G2019S}-mutation
LRRK2-PD: *LRRK2*-associated PD
LSD: Lysosomal storage disorders

M MAMS: Mitochondrial-associated membranes
MAP2: Microtubule-associated protein 2
MCI: Mild cognitive impairment
MDA: Malondialdehyde
MDS: Movement Disorders Society
MES: 2 (N morpholino) ethane sulphonic acid
MFN 2: Mitofusin-2
MM: Mitochondrial matrix
MMP: Mitochondrial membrane potential
MOPS: 3-(N-morpholino)propanesulfonic acid
MPP+: 1-methyl-4-phenylpyridinium
MPTP: 1-methyl-4-phenyl-1, 2, 3, 6-tetrahydropyridine
MRC: Mitochondrial respiratory chain
MRI: Magnetic resonance imaging

mtDNA: Mitochondrial DNA
mtRNA: Mitochondrial RNA
mTOR: Mammalian target of rapamycin

N NAD⁺: Oxidized form of nicotinamide adenine dinucleotide
NADH: Reduced form of nicotinamide adenine dinucleotide
NBIA: Neurodegeneration with brain iron accumulation
NcSC: Neural crest stem cells
NM-*LRRK2*^{G2019S}: Non-manifesting carriers of *LRRK2*^{G2019S}-mutation.

O O₂: Oxygen
OMM: Outer mitochondrial membrane
OPA-1: Optic atrophy protein 1
OXPHOS: Oxidative phosphorylation system

P *PARK*: Parkin gene
PBS: Phosphate-buffered saline
PCA: Principal component analysis
PCR: Polymerase chain reaction
PD: Parkinson's disease
PD-*LRRK2*^{G2019S}: *LRRK2*^{G2019S}-carriers diagnosed with PD
PET: Positron emission tomography
PGC1 α : Peroxisome proliferator-activated receptor γ coactivator 1 α
P: Phosphate
PI: Propidium iodide
PINK-1: PTEN-induced kinase1
PMox: Pyruvate-malate oxidation
PPAR γ : Peroxisome proliferator-activated receptor- γ
PTEN: Phosphatidylinositol 3,4,5-trisphosphate 3-phosphatase and dual-specificity protein phosphatase

PVDF: Polyvinylidene difluoride membrane

R RBD: REM sleep behaviour disorder
REM: Rapid-eye movement
RIPA: Radioimmunoprecipitation assay
RNA: Ribonucleic acid
 rRNA: Ribosomal RNA
 tRNA: transfer RNA
RNase P: Ribonuclease P
ROS: Reactive oxygen species

S SEM: Standard error of mean
SDHA: Succinate dehydrogenase complex, subunit A
SNpc: *Substantia nigra* pars compacta
SPECT: Single-photon emission computed tomography
SQSTM1/p62: Sequestosome 1/p62

T TFAM: Mitochondrial transcription factor A
TFEB: Transcription factor EB
TNB: 2-nitro-5-thiobenzoic acid
TMRM: Tetramethylrhodamine methyl ester
TOM20: Translocase of outer mitochondrial membrane 20
TORC1: mTOR coactivator1

U Ub: Ubiquitin
UKPDSBB: United Kingdom Parkinson's Disease Society Brain Bank
UPR^{mt}: Mitochondrial uncoupled protein response
UPS: Uncoupling protein system
UT: Untreated

V VDAC: Voltage-dependent anion channel

W Wt: wildtype
wt/*GBA*^{N370S}: heterozygotes for *GBA*^{N370S}-mutation



2. INTRODUCTION



2.1 PARKINSON'S DISEASE

Parkinson's disease (PD) is classically described as a clinical syndrome encompassing muscular rigidity, rest tremor, bradykinesia, postural instability and gait impairment associated with the presence of Lewy bodies (α -synuclein aggregates in the *substantia nigra, pars compacta* of the mesencephalon (SNpc)) (1). Recently PD has been associated with numerous non-motor symptoms, redefining long lasting concepts that in the last years have led to significant increase in knowledge of the pathology of the disease. The current definition of PD is: ***a slowly progressive neurodegenerative disorder, affecting multiple neuroanatomical areas, that results from a combination of genetic and environmental factors and manifests with a broad range of symptoms*** (2).

2.1.1 History

The earliest historical records with succinct descriptions of parkinsonism are from ancient Indian and Chinese medicine from around 1000 BC (3). Dr. James Parkinson published PD in 1817 the first medical description of what is today known as PD under the title "An Essay on the Shaking Palsy", which consists in the description of 6 male subjects with resting tremor and rigidity (4) (**Figure 1**).

Years later, on 1872, Dr. Jean-Martin Charcot made a more detailed characterization of the disease, which incorporated bradykinesia and postural instability; he also suggested it to be named "Parkinson's disease" (5). Many years of clinical characterization followed, where atypical forms of PD were described and that for some years were diagnosed as Parkinson-plus syndromes. These similar diseases, and their further classification as independent clinical entities, have helped to define novel pathological mechanisms and gain insight into the diversity of events that may lead to similar clinical phenotypes (6).

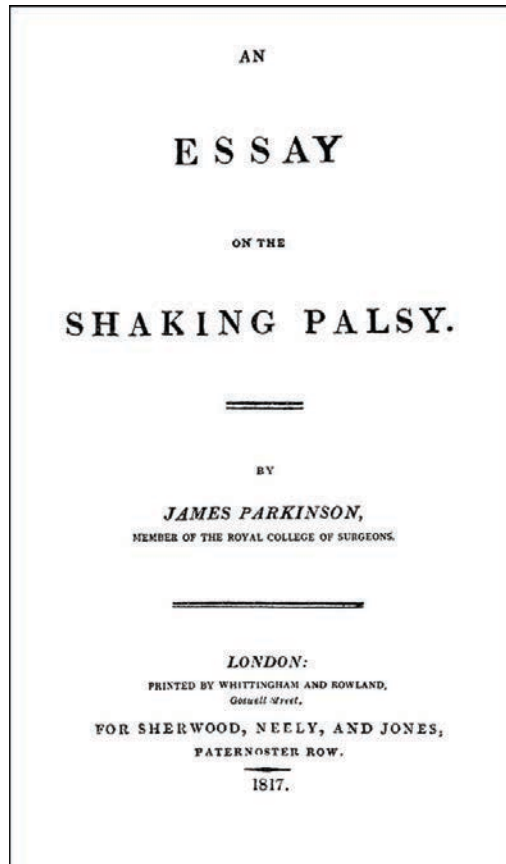


Figure 1. Essay on the Shaking Palsy.

The first medical description of what is today known as Parkinson's disease (PD). Some other manifestations, currently known as "non-motor symptoms" of PD were also described in some patients, but were not thought to be related to the disease, and were not included in the definition of the syndrome.

Source: <https://archive.org/details/essayonshakingpa00parkuoft/page/n4>

Greenfield and Bosanquet described the characteristic pathologic lesions in 1953. In their work, the presence of intracellular aggregates, called Lewy bodies, was well demonstrated in distinct forms of parkinsonism (7). Morbidity and clinical progression of PD was profoundly studied by Hoehn and Yahr, introducing the first internationally recognized staging system (8).

The observation of a group of young patients with symptoms of PD led to the discovery that the causative agent was 1-methyl-4-phenyl-1,2,3,6-tetrahydropyridine (MPTP), a narcotic that selectively damages the *substantia nigra*. This led to the possibility to develop animal models of PD that remain to be the most used model in preclinical studies of new treatments for PD (9). Most importantly for this thesis, mitochondrial toxicity was acknowledged as one of the possible mechanisms for the development of the disease, since MPTP and its active metabolite 1-methyl-4-phenylpyridinium (MPP+) exert their toxicity by targeting the complex I (CI) of the mitochondrial respiratory chain (MRC) (10). Drug and toxin-induced parkinsonisms and other parkinsonian disorders, such as some lysosomal storage disorders (LSD) and neurodegeneration with brain iron accumulation (NBIA), have helped to increase the understanding of the biological basis of PD (11,12).

On behalf of the treatment for PD, Dr Parkinson was the first to suggest that treatment should be started preferentially in the early stages of the disease in order to stop its progression (4). Several approaches have been addressed to modify the natural history of PD, being the most notable advance the administration of dopamine or agonists of dopamine receptors as the mainstream of the treatment (3). Deep brain stimulation, surgery, placebo, relaxation therapies and some other chemical compounds have also shown some benefit in PD, but there is currently no definite cure available for the neurodegeneration process (13).

A brief summary of the most relevant events in history of PD is schematically presented in **Figure 2**.

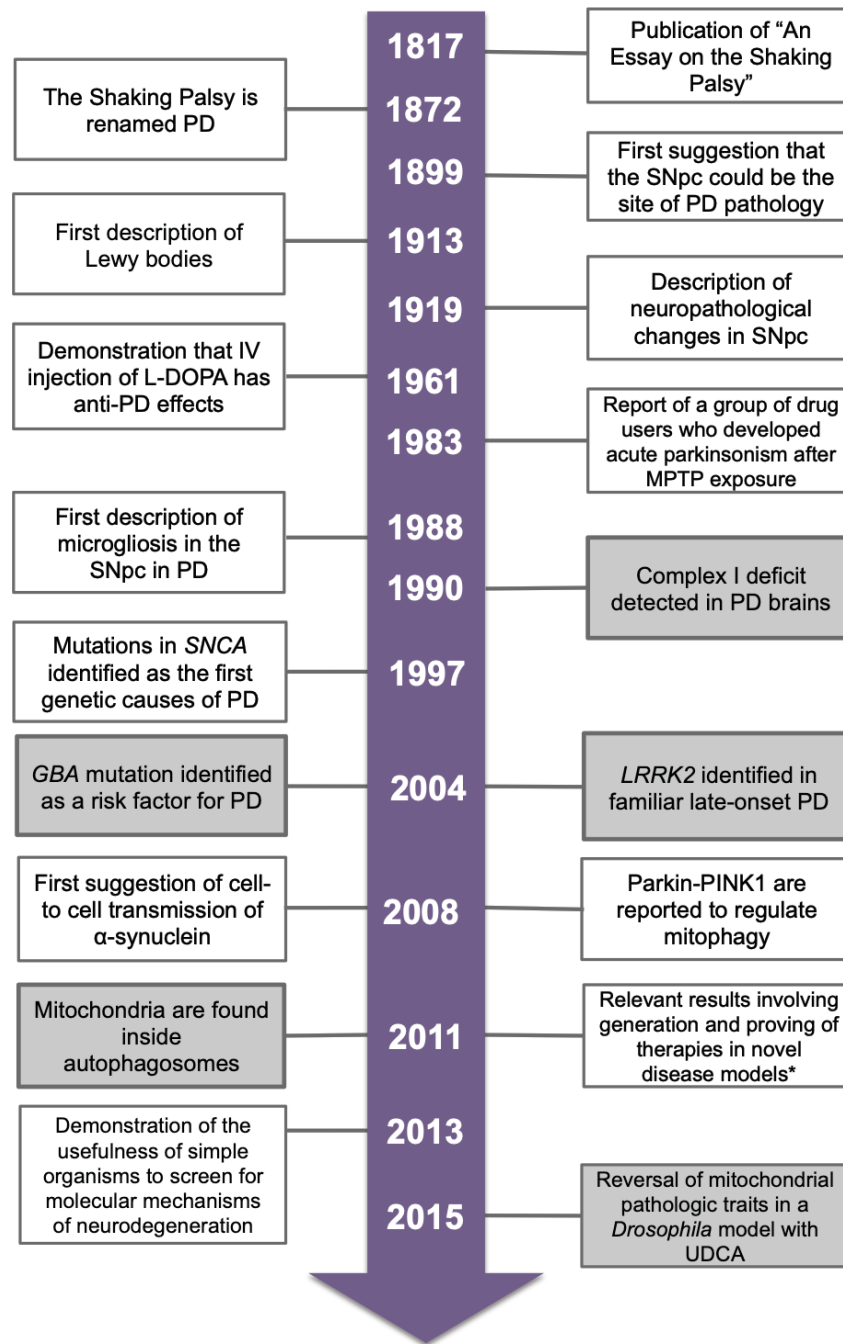


Figure 2. History of Parkinson's Disease (PD)

Historical timeline summarizing the most relevant advances that have led to the current knowledge of PD as a complex neurodegenerative process. The most relevant discoveries in terms of this thesis are highlighted. *GBA*: Glucocerebrosidase; *LRRK2*: Leucine-rich repeat kinase 2; PD: Parkinson's disease SNpc: *Sustantia nigra pars compacta*; SNCA: α -synuclein. Adapted from: Przedborski S. *Nat Rev Neurosci.* 2017;18(4):251-259 (6).

2.1.2 Epidemiology and risk factors

Parkinson's disease is the second most common neurodegenerative disease worldwide, affecting 1-2% of the population over 65 years. The greatest risk factor for the development of PD is ageing; its appearance is rare before the 6th decade of life, but the incidence increases 5-10 fold from 60 to 90 years old (14).

The estimated heritability for PD is of 34% when calculated in twin studies and 23% when calculated using genome-wide association studies (GWAS) (15). In addition, large GWAS confirm that PD-associated genes are also affected in idiopathic PD (iPD) (16,17).

Men are twice proner than women to PD. Some populations, like Ashkenazi Jews and Native American communities, have a higher prevalence of PD (18). Genes associated with PD have been identified in these population groups, such as leucine-rich repeat/kinase 2 (*LRRK2*) and glucocerebrosidase (*GBA*) (19). Pathologic variants of α -synuclein and tau have also been identified as risk factors for developing PD (20). Other geographical and societal groups may have a higher prevalence of PD, but it seems that socioeconomic rather than biological causes may underlie such associations. Environmental risks have been long known to increase the risk for developing PD, such as head injuries, pesticide exposure and traumatic brain injury (21).

Although a cure is not available at the present time, improvements in health care and symptomatic treatment have made possible that a person with PD can live up to 20 years after the diagnosis is made, after which mortality considerably increases. The number of people living with PD is estimated to double from 2005 to 2030, with the consequent increment in the personal, social and economic costs as the population ages (22).

2.1.3 Clinical features

The cardinal symptoms of PD are tremor at rest, bradykinesia, muscular rigidity, and postural instability. Additionally, flexed posture and motor blocks have been included among the classic features of PD (2). Onset of motor symptoms is usually unilateral and the asymmetry persists throughout the disease. Motor symptoms of PD appear when neurodegeneration of more than 50% of dopaminergic neurons has occurred, preceded by several years of prodromal stage and followed by a rapid progression of the disease (23) (**Table 1**).

Non-motor symptoms are a common feature of PD that for a long time were neglected; nowadays, their presence defines the prodromal phase of PD (24). Alternatively, non-motor symptoms may arise later in the disease, and may even dominate the clinical picture at the end stage of the disease becoming the main determinants of quality of life (25) (**Table 1**).

Table 1. Motor and non-motor symptoms of PD.

Motor symptoms	Non-motor symptoms
Tremor, bradykinesia, rigidity, postural instability	Cognitive impairment, bradyphrenia, tip-of-the tongue phenomenon
Hypomimia, dysarthria, dysphagia, sialorrhoea	Depression, apathy, anhedonia, fatigue, other behavioural and psychiatric problems
Decreased arm swing, shuffling gait, festination difficulty arising from chair, turning in bed	Sensory symptoms: anosmia, ageusia, pain (shoulder, back), paresthesias.
Micrographia, Daily living difficulties (cutting food, feeding, hygiene)	Dysautonomia (orthostatic hypotension, constipation, urinary and sexual dysfunction, abnormal sweating, seborrhoea), weight loss
Glabellar reflex, blepharospasm, dystonia, striatal deformity, scoliosos, campyocornia.	Sleep disorders (REM behaviour disorder, vivid dreams, daytime drowsiness, sleep fragmentataion, restless legs syndrome).

REM: Rapid-eye movement.

Reproduced from: Jankovic J. *J Neurol Neurosurg Psychiatry*. 2008;79(4):368-376 (24).

The premotor or prodromal phase of PD is characterized by impaired olfaction, constipation, depression, excessive daytime sleepiness, and rapid eye movement (REM) sleep behaviour disorder (RBD) (26). These symptoms may develop even 20 years before motor symptoms appear. The establishment of the diagnosis of PD in its prodromal phase offers a unique opportunity to study early biomarkers and to start neuroprotective treatment which may modify the natural history of the disease (27).

The progression of PD is characterized by the worsening of motor features. In addition to this, the complications derived from long-lasting symptomatic treatment (motor and non-motor fluctuations, dyskinesia, drug-induced psychosis), dementia and autonomic dysfunction significantly contribute to disability and mortality (2) (**Figure 3**).

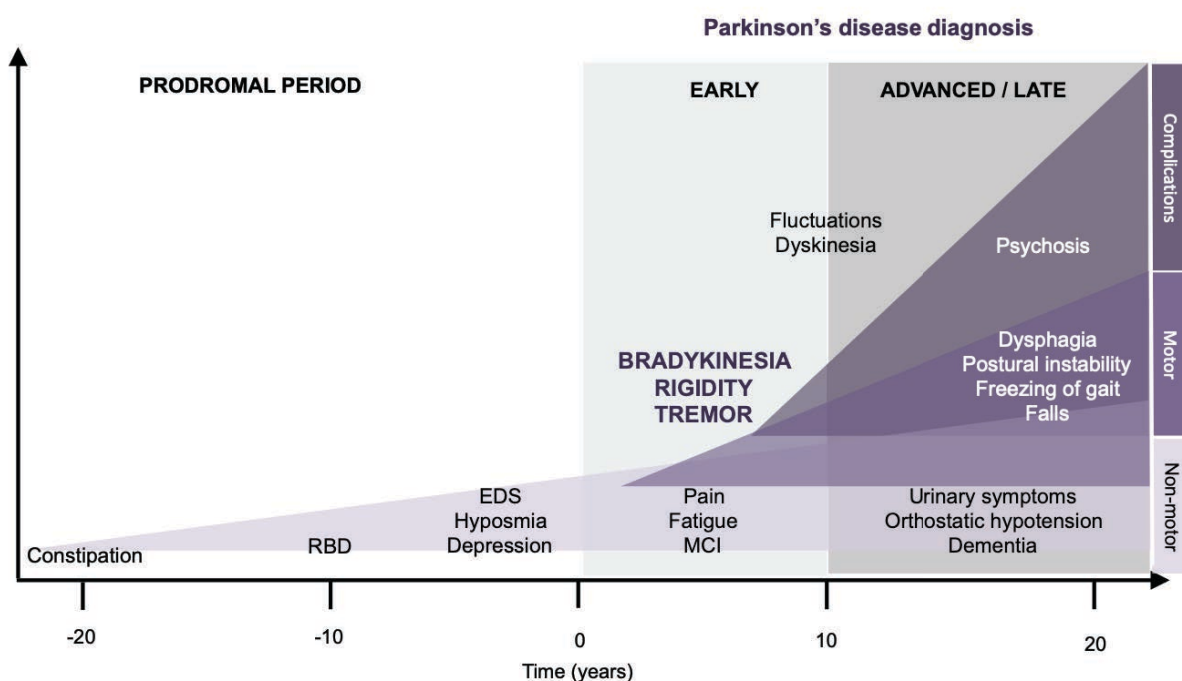


Figure 3. Natural history of PD.

The classical clinical presentation of PD may be preceded by up to 20 years of prodromal symptoms, followed by a non-linear progression that is largely variable among patients.

EDS: excessive daytime sleepiness. MCI: mild cognitive impairment. RBD=REM sleep behaviour disorder.

Source: Kalia L V, Lang AE. *Lancet*. 2015;386(9996):896-912 (2).

2.1.4 Diagnosis

The United Kingdom Parkinson's Disease Society Brain Bank (UKPDSBB) Criteria was the first formal tool for clinical diagnosis of PD. It is the most widely used diagnostic criteria used in clinical trials and in routine clinical practice. According to these, bradykinesia (including hypokinesia and akinesia) is the core feature for PD and is mandatory in order to establish the diagnose of PD (**Table 2**) (28).

Table 2. The United Kingdom Parkinson's Disease Society Brain Bank clinical diagnostic criteria.

Step 1. Diagnosis of parkinsonism	Step 2. Exclusion criteria for PD	Step 3. Supportive criteria for PD (≥ 3 required for definite diagnosis)
Bradykinesia ¹ and ≥1 of the following: Muscular rigidity 4-6 Hz rest tremor Postural instability ²	Repeated strokes with stepwise progression Repeated head injury Definite encephalitis Oculogyric crises Use of neuroleptic or dopamine-depleting agents at onset of symptoms > 1 affected relative Sustained remission Strictly unilateral features after 3 years Supranuclear gaze palsy Cerebellar signs Early severe disautonomy Early severe dementia with disturbances of memory, language or praxis Babinsky sign Cerebral tumor or communicating hydrocephalus on neuroimaging Negative response to large doses of levodopa (malabsortion excluded) Exposure to known neurotoxin (p ej MPTP)	Unilateral onset Rest tremor Progressive disorder Persistent assymetry affecting side of onset most Excellent response (70-100%) to levodopa Severe levodopa-induced chorea Levodopa response for ≥ 5 years Clinical course od ≥ 10 years

PD: Parkinson's disease; MPTP: 1-methyl-4-phenyl-1,2,3,6-tetrahydropyridine. ¹Delayed onset of voluntary movement with increasing reduction of amplitude and speed of repetitive movements. ²Unrelated to primary visual, cerebellar, vestibular or propioceptive dysfunction. Reproduced from: Gibb WR, Lees AJ. *J Neurol Neurosurg Psychiatry*. 1988;51(6):745-752 (28)

In recent years, these and other criteria have been criticized due to the lack of inclusion of non motor features, leaving few space for diagnosis of prodromal PD (29). Also, in step 2, genetic risk factors (>1 relative affected) exclude the diagnosis of PD, which is no longer acceptable since genetic variants of PD are now well recognized (30).

Accordingly, the Movement Disorders Society (MDS) released in 2015 the MDS-PD criteria (31). Specifically designed for its use in research, the motor syndrome remains the core feature of the disease, but non-motor manifestations have been incorporated into the diagnostic criteria and a new diagnostic category was added: prodromal PD, which from is now considered a true initial stage of PD (**Figure 4**) (26).

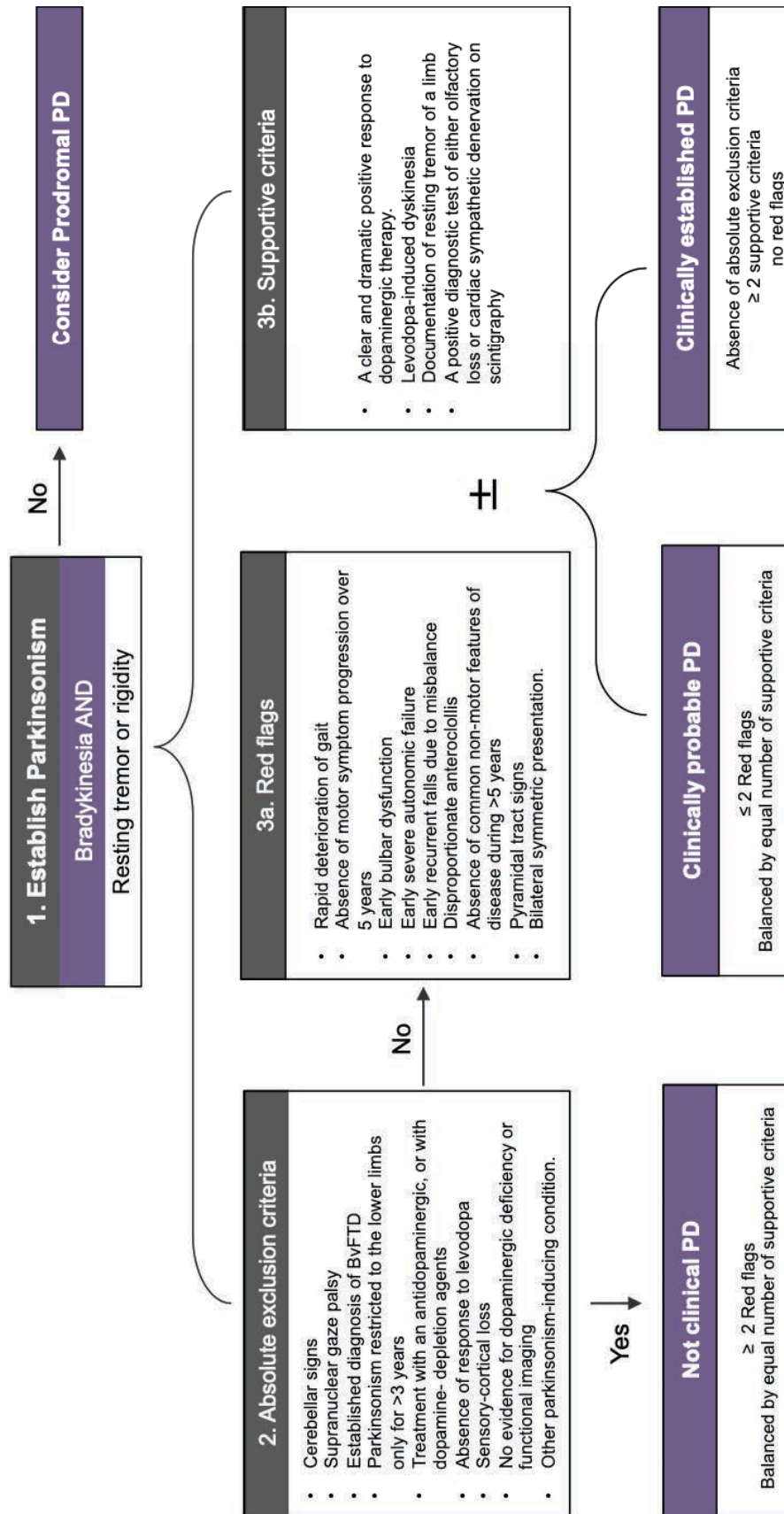


Figure 4 (Previous page). Summary of the MDS Diagnostic Criteria.

Released in 2015 and designed primarily for research purposes, the most relevant item is the consideration of diagnosing prodromal PD, based on the presence of non-motor symptoms.

BvFTD: Behavioural variant frontotemporal dementia; PD: Parkinson's disease.

Modified from: Postuma RB, Berg D, Stern M, et al. *Mov Disord.* 2015;30(12):1591-1601 (32)

The predictive value of the MDS remains to be tested, but it is calculated to have a 99.2% positive predictive value, and a negative predictive value of 99%. Taken together, the above described diagnostic criteria can have an error rate as high as 24%; differential diagnosis must take into account multiple system atrophy, progressive supranuclear palsy and corticobasal neurodegeneration (33).

Among other diagnostic tests currently used in PD are: positron emission tomography (PET), single-photon emission computed tomography (SPECT) and structural magnetic resonance imaging (MRI). The use of these imaging techniques in combination with the clinical presence of non-motor symptoms of PD, such as hyposmia, RBD and constipation can improve the sensitivity and specificity of the prediction for conversion from pre-symptomatic to symptomatic PD. However, the diagnostic gold standard for PD remains to be *postmortem* pathological examination (25).

All of the above highlights the need for less invasive diagnostic tests and biomarkers to enhance diagnostic accuracy and early detection that would open the window to start disease-modifying therapies in its prodromal stages (22).

Genetic testing as a diagnostic tool in clinical routine is limited due to the incomplete penetrance and large variable expression of some of these genes. Also, there is no current treatment that could justify the genetic assessment of the rare genetic variants of PD. However, in the near future this approach will be probably modified, since it is known that genetic variations may conduct to special phenotypes (like increased prevalence of dementia in *GBA* carriers) that may benefit from early interventions.

2.1.5 Treatment

The mainstay of PD treatment consists of drugs that increase dopamine concentration, or dopamine receptors antagonists. Today it is known that PD also results from alterations in neurotransmitters other than dopamine, and regions of the nervous system outside the basal ganglia, so research efforts are directed toward systemic therapies that may alter the natural history of the disease and modify the molecular pathways that lead to dopaminergic cell death. Ideally, disease-modifying therapies could be administered at the prodromal phase of PD, which provides a potential temporal window where the development and progression of PD could be stopped (26,34) (**Figure 5**).

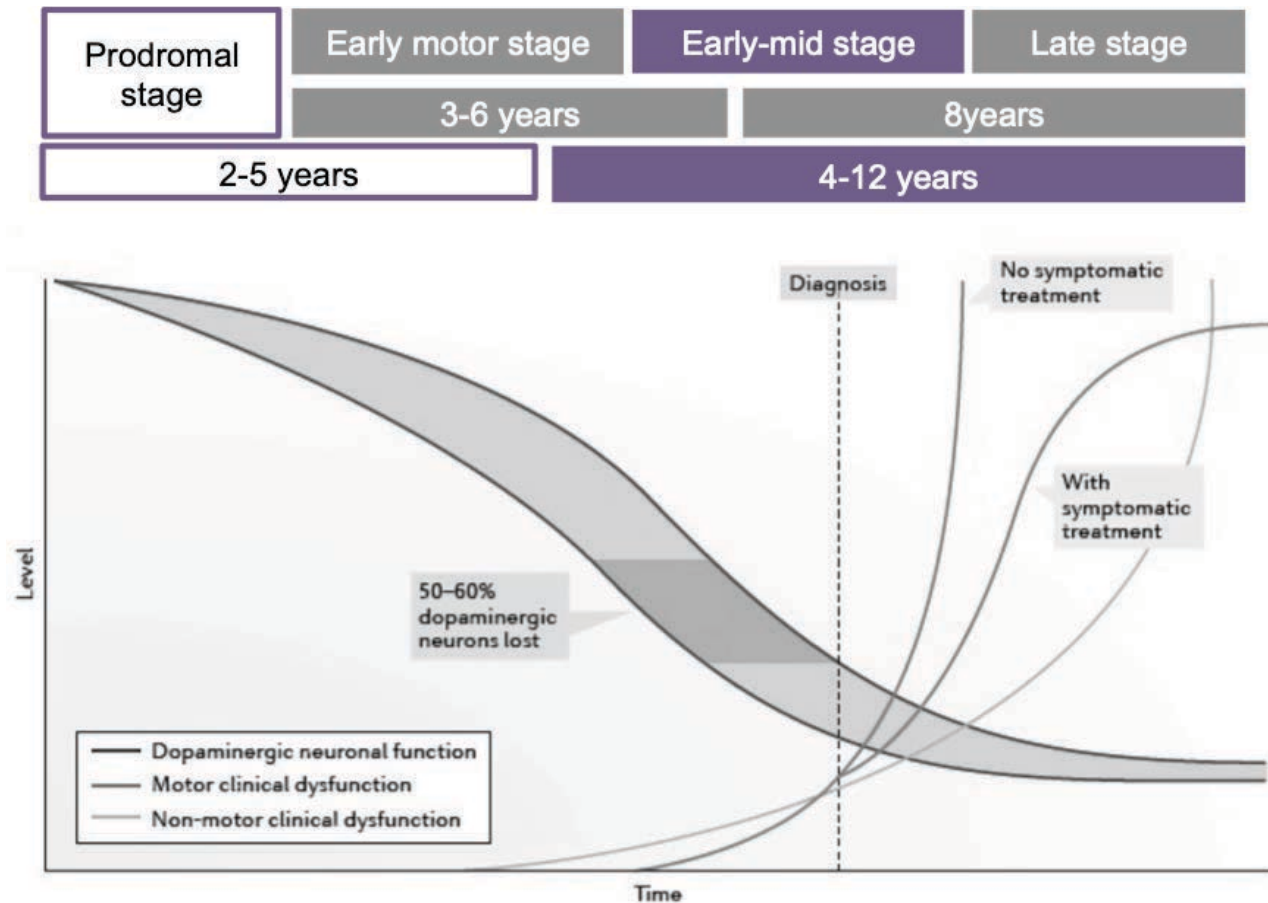


Figure 5 (Previous page). Progression of motor and non-motor symptoms of PD and effect of symptomatic treatment in the natural course of the disease.

The progression of PD would be rapid and almost linear without symptomatic treatment. Motor symptoms appear when approximately 50% of dopaminergic neurons have been lost (dark grey area), while non-motor symptoms begin early at the pre-motor stage but lead to a greater disability. As the great part of the non-motor features are not related to dopaminergic cell loss, they are unaffected by dopamine replacement therapy and may be targeted by novel therapies, directed to prevent or stop neurodegeneration.

Source: Schapira AHV, Chaudhuri KR, Jenner P. *Nat Rev Neurosci.* 2017;18(7):435-450 (25).

Therapies directed to ameliorate non-motor symptoms, such as depression, sleep disorders, autonomic dysfunction and non-medical treatment such as transcranial magnetic stimulation, deep brain stimulation therapy and life style modifications to increase the quality of life of the patient should also be taken into account throughout the evolution of the disease (35–37) .

Further understanding of the molecular alterations that lead to neurodegeneration in PD is mandatory in order to develop early biomarkers and disease modifying therapies that will effectively decrease the burden caused by PD to patients and society in general. Perhaps the most promising strategy to prevent the development of the disease and to achieve neuroprotection is to target those molecular pathways that have been described from studies in genetic forms of PD (38).

2.2 MOLECULAR MECHANISMS INVOLVED IN PD PATHOGENESIS

The main pathological feature that characterizes PD is the neuronal loss in specific areas of SNpc and intracellular protein aggregates in the remaining neurons, of which α -synuclein is by far the most abundant (Lewy body pathology). In early-stage disease, loss of dopaminergic neurons is restricted to the ventrolateral *substantia nigra*, reaching structures of the limbic system and brainstem at the end-stage of the disease (39). Some studies support that, as proposed by the Braak model (40), Lewy body pathology correlates in many cases with the progression of the disease (41).

Great controversy has risen since some PD cases not only do not comply with the pathological staging (42), but also do not show Lewy bodies, and a unique pathologic mechanistic description that fits all cases of PD has still not been found (43–45). Other molecular pathways that have been shown to trigger the neuropathology characteristic of PD are: mitochondrial dysfunction and increased oxidative stress, deficient axonal transport, neuroinflammation, altered autophagy and missfolded protein aggregation other than α -synuclein (22).

Investigation efforts are currently focused on understanding the compensatory mechanisms, intracellular interactions and coordinated responses to the numerous pathogenic features of the disease, so that preventive and disease modifying therapies may be developed.

For the purposes of this thesis the mechanisms that lead to neurodegeneration and comprise alterations in mitochondrial and autophagic function will be described in detail.

2.2.1 Mitochondria

Ever since it was shown that the exposure to mitochondrial toxics such as rotenone and MPTP could trigger parkinsonism (46), mitochondrial implication in neurodegeneration, and specifically in PD, has been documented by a great number of studies (47–49).

2.2.1.1 Mitochondrial structure, function and genome

Mitochondria are intracellular organelles originated from the symbiotic relationship established between primitive aerobic bacteria and primordial eukaryotic cells and by which the latter became capable of using oxygen as a metabolite to produce energy in the form of adenosine triphosphate (ATP) (50).

Mitochondria are involved in different functions crucial for cells such as thermogenesis, biosynthesis of heme and iron–sulfur clusters (Fe-S), calcium homeostasis and, in case of pathologic conditions, they are the main source of reactive oxygen species (ROS) generation and apoptosis triggering (51).

Located in the cytoplasm, they consist of two membranes, the outer mitochondrial membrane (OMM) and the inner mitochondrial membrane (IMM). In the latter, the oxidative phosphorylation system (OXPHOS), composed by the electron transport chain (ETC) and the ATP/H⁺ synthase, is embedded. The mitochondrial matrix is the most inner part, where mitochondrial DNA (mtDNA) freely floats and biochemical reactions such as fatty acid oxidation, Krebs cycle, urea cycle, gluconeogenesis and ketogenesis occur (**Figure 6**) (52).

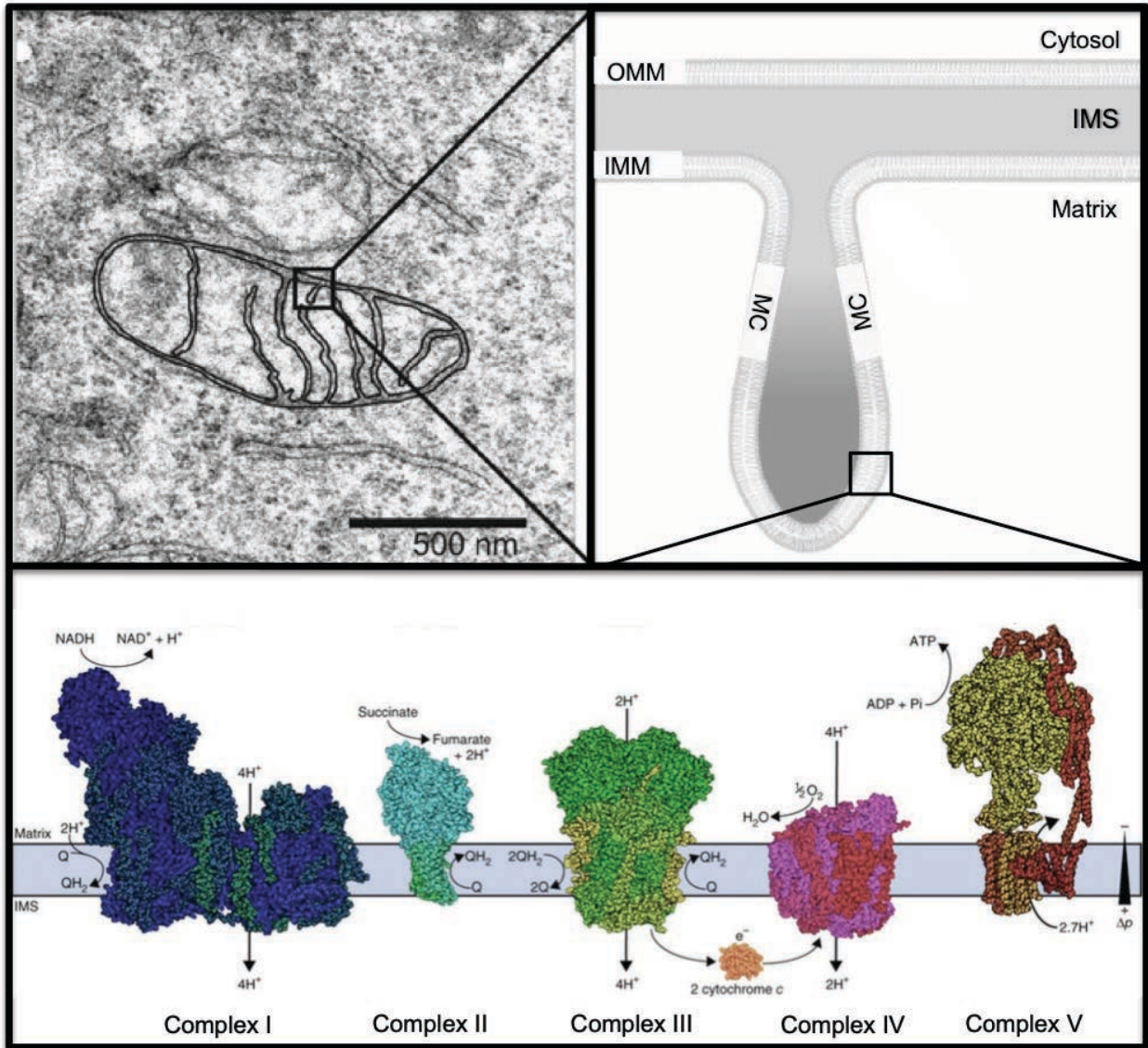


Figure 6. Schematic representation of mitochondrial ultrastructure.

Mitochondria have two membranes. The OMM isolates the mitochondria from the cytosol and contains different porins and enzymes that regulate the interchange of nucleotides, ions and metabolites and enzymes involved in diverse metabolic activities, as fatty acid oxidation. The IMM is highly impermeable to all molecules and contains the cristae where the ETC is embedded. The chemiosmotic theory of Mitchell (53) postulates that high-energy electrons are extracted from the breakage of nutrients (NADH^+H^+ or FADH_2) and imported into the mitochondria, where complex I (NADH dehydrogenase) or complex II (succinate dehydrogenase) receive electrons that are then transferred to CoQ and delivered to complex III (cytochrome c reductase). Cytochrome c then shuttles the electrons to complex IV

(cytochrome c oxidase), which constitutes the last step in the ETC where molecular oxygen is reduced to water. The proton gradient generates a proton moving force that generates ATP synthesis by complex V (ATP/H⁺ synthase). Even though for academic purposes the schematic vision of the ETC is adequate, the five complexes are not independently moving within the membrane. On the contrary, they can physically associate in different combinations called respiratory supercomplexes (54). These associations are dynamic and can be modified to optimize energy production, implying that this system is more versatile than it was thought and that can be fine-tuned by this structural plasticity to efficiently obtain energy from different sources and depending on different, specialized cell types.

OMM: Outer mitochondrial membrane; IMM: Inner mitochondrial membrane; IMS: intermembrane space; NADH: Nicotinamide adenine dinucleotide; NAD⁺: reduced form of nicotinamide adenine dinucleotide; CoQ: Coenzyme Q; ATP: adenosine triphosphate; ADP: adenosine diphosphate; P: phosphate.

Modified from: Koob S, Reichert AS. *Biol Chem*. 2014;395(3):285-296 (55) and: Letts JA, Sazanov LA. *Nat Struct Mol Biol*. 2017;24(10):800-808 (56).

The mtDNA consists of 37 genes (16.6 kb), of which only 13 codify subunits of the OXPHOS system, and the rest (2 ribosomal RNA (rRNA) and 22 transfer RNA (tRNA)) are coded for their translation (57). The nuclear genome encodes for the approximately 100 other proteins that compose the OXPHOS system, and contains also the rest of genes encoding for the rest of metabolic and structural proteins (approximately 4500). Consequently, mitochondrial function is controlled by both genomes and the intergenomic communication is essential for its adequate function (58).

2.2.1.2 Mitochondrial dynamics

Mitochondria actively divide and fuse with one another in an important series of processes enclosed under the name of mitochondrial dynamics. This process is highly complex and requires close regulation in which, by constant fusion and fission processes and the resulting cristae remodelling, mitochondrial homeostasis is maintained (59). Mitochondrial fusion allows communication between organelles, surpassing transient mitochondrial defects by facilitating access to molecules that

may be of use to correct the initial defect. On the other hand, mitochondrial fission facilitates mitochondrial distribution and transport to distant locations on demand (Figure 7).

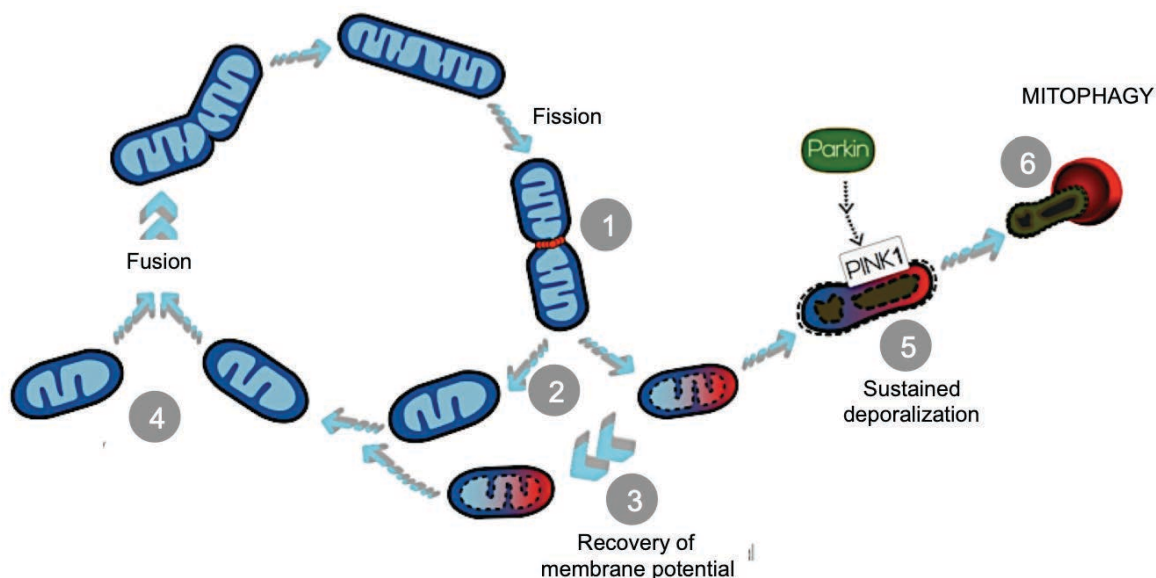


Figure 7. Mitochondrial dynamics.

Continuous cycles of fission and fusion occur constantly in order to maintain a healthy mitochondrial pool. Fission of mitochondria is carried out by recruiting the Drp1 (red dots) GTPase from the cytosol to the OMM (1). After fission, daughters with different mitochondrial membrane potential are obtained (2), some of which are able to restore the mitochondrial membrane potential (MMP) by fusion with other mitochondria (3). After solitary periods, mitochondria may also fuse with other mitochondria if the MMP passes a quality threshold (4). Sustained depolarization triggers cleavage of Optic atrophy protein 1 (Opa1), reduction in mitofusin capacity and accumulation of PINK1/Parkin in the OMM (5), targeting a clearance process called mitophagy (6), which will be addressed below.

Drp1: Dynamin related protein;

Source: Twig G, Shirihai OS. *Antioxid Redox Signal*. 2011;14(10):1939-1951 (60).

The maintenance of an adequate mitochondrial function and quality control, and the capacity to actively respond to changes in the cellular environment greatly depends on this highly complex feature, and a correct balance between fusion and fission is important for the maintenance and distribution of mtDNA (61). Therefore,

proper function of mitochondrial dynamics and effective mitochondrial trafficking to exchange mitochondrial components and promote mitochondrial removal must be readily available and fully functional to ensure a healthy pool of mitochondria (62,63). Alterations in mitochondrial dynamics have been associated with numerous neurodegenerative diseases such as Alzheimer's disease (AD), Huntington's disease (HD), fragile X syndrome and PD (64,65).

2.2.1.3 Mitochondrial dysfunction in PD

Mitochondria could be directly responsible or interplay with most of the molecular hallmarks associated to PD. For instance, a relationship between mitochondrial dysfunction and protein aggregation has been described by the dysfunction of mitochondrial-associated membranes (MAMs) in PD that endangers the relationship between mitochondria and endoplasmic reticulum (ER) structures, where cytosolic proteins are synthesised (66).

Similarly, mitochondrial involvement in neuroinflammation has also been demonstrated. The primarily identified cause is an increase in ROS that leads to the activation of the inflammatory cascade primarily by the cells in the neuroglia (67).

Various genes that have been identified in the pathogenesis of PD have been associated to mitochondrial function, being Parkin (*PARK*), PTEN-induced kinase 1 (*PINK1*), Protein/Nucleic Acid Deglycase DJ-1 (*DJ-1*) and Leukine rich-repeat kinase 2 (*LRRK2*) the most widely studied (19). Patients that carry such mutations may develop PD at earlier ages, with a more rapid progression and the presence of some symptoms not observed in classical PD.

CI of the MRC is the most recognized target of mitochondrial dysfunction in PD (47,49). Increased oxidative stress, altered mitochondrial dynamics and alterations in mitochondrial membrane potential (MMP) have also been described in different experimental models of PD (62,63,68,69).

High levels of mtDNA deletions have been associated with ETC deficiency in SNpc from PD patients (70). The circular conformation and localization of the mtDNA makes it prone to insults and to accumulate mutations that cause alterations in mitochondrial proteins, resulting in an impaired mitochondrial function which may lead to premature cell death (71).

When mitochondrial alterations are detected, mitochondrial chaperone and quality control protease genes are induced to facilitate *de novo* protein folding and degrade damaged proteins and/or organelles. The mitochondrial unfolded protein response (UPR^{mt}) is activated by multiple forms of mitochondrial dysfunction and regulated by mitochondrial-to-nuclear communication (72). The UPR^{mt} promotes the import of mitochondrial-targeted proteins into the matrix, and multiple components that limit ROS toxicity are induced (73,74).

The peroxisome proliferator-activated receptor γ (PPAR γ) coactivator 1 α (PGC1 α) is a mitochondrial transcriptional master regulator that coordinates mitochondrial biogenesis and respiration (75). This transcription factor is highly expressed in tissues with high-energy demands, as the brain (76), and it has proven to have neuroprotective effects by inducing the expression of downstream target genes involved in mitochondrial biogenesis, transcription factors such as the mitochondrial transcription factor A (TFAM) and antioxidant defences (77).

The final result of the equilibrium between mitochondrial biogenesis and turnover is mitochondrial content which, together with adequate mitochondrial function, accounts for *mitohormesis* (78). The recent focus to identify and describe pathways and molecules implicated in the beneficial effects of mitohormesis may allow to open novel areas of therapies to prevent neurodegeneration, among PD and other age-related diseases (79,80).

2.2.2 Autophagy

Until now this thesis has presented mitochondrial mechanisms to preserve cellular bioenergetic status and homeostasis. However, if mitochondria are submitted to severe injury, autophagy is the principal mechanism for clearance of the damaged organelles. Autophagy is responsible for the digestion and recycling of most long-lived intracytoplasmatic proteins and organelles and plays a crucial role in cell fate determinations, such as preservation of genomic integrity, immune responses and metabolic circuitries (81).

Lysosomes are the major sites for degradation of cellular proteins and organelles and pivot cells between anabolic and catabolic processes (82). Even when the primary and most known function of lysosomes is the digestion or recycling of autophagic cargoes, lysosomes also influence the initial stages of autophagy. This occurs through a signaling complex that reversibly docks the mTOR coactivator 1 (TORC1) and the transcription factor EB (TFEB). When TFEB is translocated to the nucleus, it upregulates the expression of most genes involved in lysosome biogenesis and additional genes required for autophagosome formation (83,84). Alterations in the hydrolytic functions of lysosomes impair autophagic flux in the same way that lysosomal function requires normal autophagic flux (85).

2.2.2.1 Subtypes of autophagy

Three subtypes of autophagy have been identified, macroautophagy, microautophagy, and chaperone-mediated autophagy (CMA) (86). Each of these subtypes involves different mechanisms of substrate delivery, being lysosomal digestion the common cardinal feature that defines autophagy (**Figure 8**).

1) Macroautophagy encompasses a highly specific system for determined cargoes. It is an essential component in mammalian developmental and differentiation processes, including the elimination of paternal mitochondria from the fertilized egg, removal of mitochondria during red-blood cell maturation and beige to white adipocyte differentiation (84). The process by which damaged mitochondria are

cleared is known as “mitophagy”. Mitophagy maintains normal cellular metabolism, reduces mitochondrial generation of ROS and prevents the mitochondrial release of proapoptotic factors (87).

2) Microautophagy is a lysosomal degradative process that involves direct engulfment of cytoplasmic cargo by autophagic tubes. The main functions of microautophagy are maintenance of organellar size, membrane homeostasis, and cell survival under nitrogen restriction (88). Although specific mitochondrial micromitophagy (micromitophagy) has been described in yeast, in mammals microautophagy seems to be less specific and functions in a coordinated way with macroautophagy and CMA (81,89).

3) CMA is a specific lysosomal-dependent protein degradation pathway that targets cellular proteins and in which the protein cargo is directly delivered into the lysosomal lumen through the interaction with chaperones specific for this process (90).

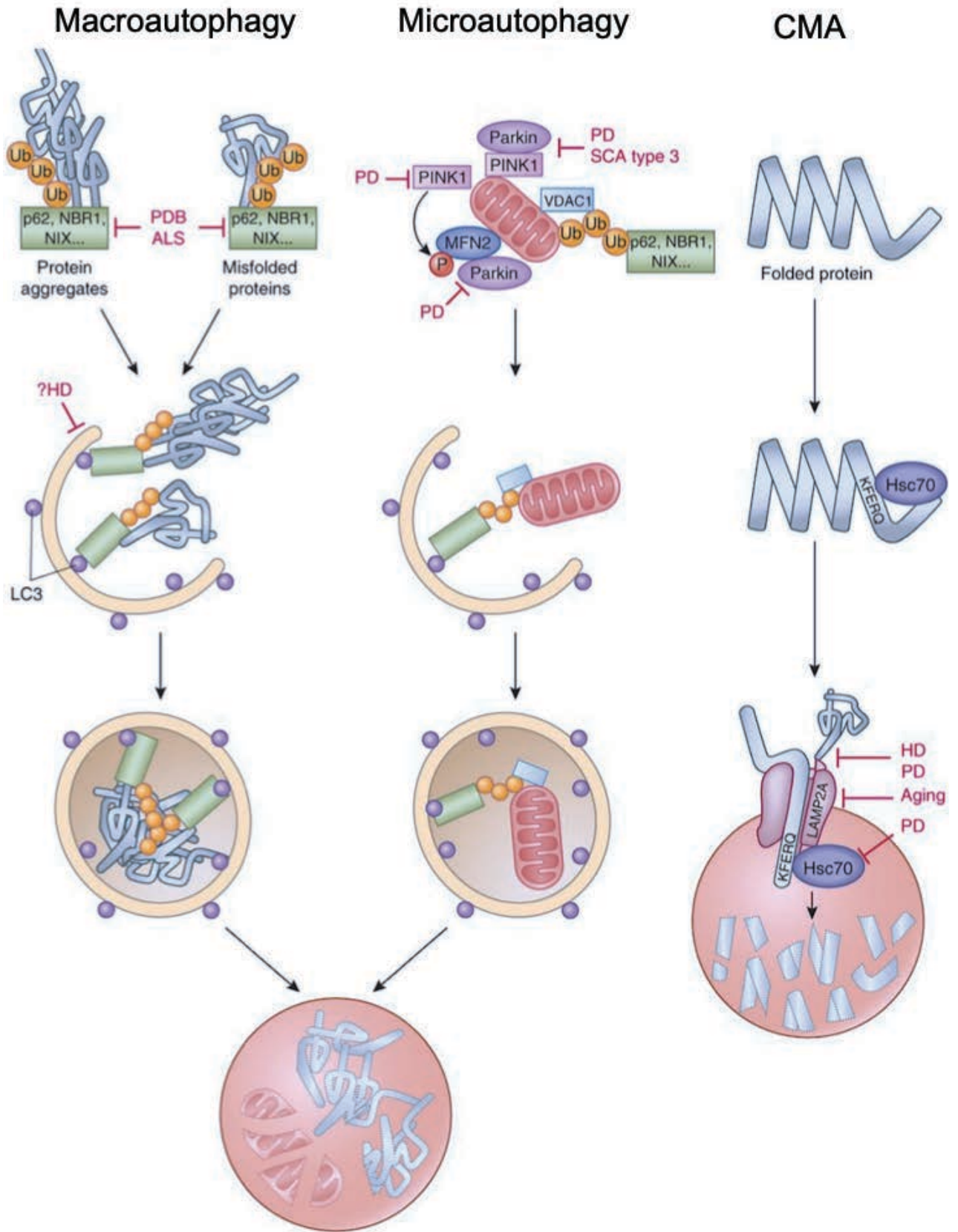


Figure 8. Subtypes of autophagy.

Briefly, macroautophagy and microautophagy involve the direct sequestration of whole areas of the cytosol by a membrane that seals to form a double-membrane autophagosome (macroautophagy) or by invaginations at the lysosomal membrane (microautophagy). In CMA, cargo is selectively recognized by a complex of cytosolic chaperones that mediate its delivery to a receptor at the lysosomal membrane. In all cases, the cargo is degraded by the lysosomal hydrolases.

CMA: Chaperone-mediated autophagy; Hsc70: heat-shock cognate 70; LAMP: lysosomal-associated membrane protein-1; LC3: Microtubule associated Light chain 3 beta; MFN2: mitofusin 2; PD: Parkinson's disease; p62; sequestrosome (SQSTM1)/P62; Ub: ubiquitin; VDAC1: Voltage-dependent anion channel 1.

Source: Nixon RA. *Nat Med.* 2013;19(8):983-997 (86).

2.2.2.2 Selective autophagy processes and control

The process of macro and micro autophagy involves multiple steps. The earliest event is the formation of the isolation membrane of the autophagosome. Cargo sequestration follows and consists on the recognition of certain post-translational modifications that account for the high selectivity of the process. Several levels of control are needed to dictate and target the cargo in autophagy in front of constitutively or potentially harmful components for the cell or obsolete products of cell differentiation (**Figure 9**) (91).

Autophagy may be initiated via mammalian target of rapamycin (mTOR) inhibition or adenosine monophosphate-activated protein kinase (AMPK) activation which are triggered as well by different signals of cellular stress such as low ATP levels, hypoxia, some protein aggregates and ER stress (92).

Autophagy initiation, cargo recognition, cargo engulfment, and vesicle closure is dependent on the Microtubule-associated Light Chain 3 (LC3)/ Gamma-aminobutyric acid receptor-associated protein (GABARAP) family (**Figure 9**) (84). Damaged mitochondria are targeted for mitophagy by Parkin and PINK1. PINK1 is

located on the OMM and it enables Parkin to bind and ubiquitinate exposed membrane proteins, recruiting sequestrosome p62 (SQSTM/p62) and LC3B finally initiating mitophagy (93).

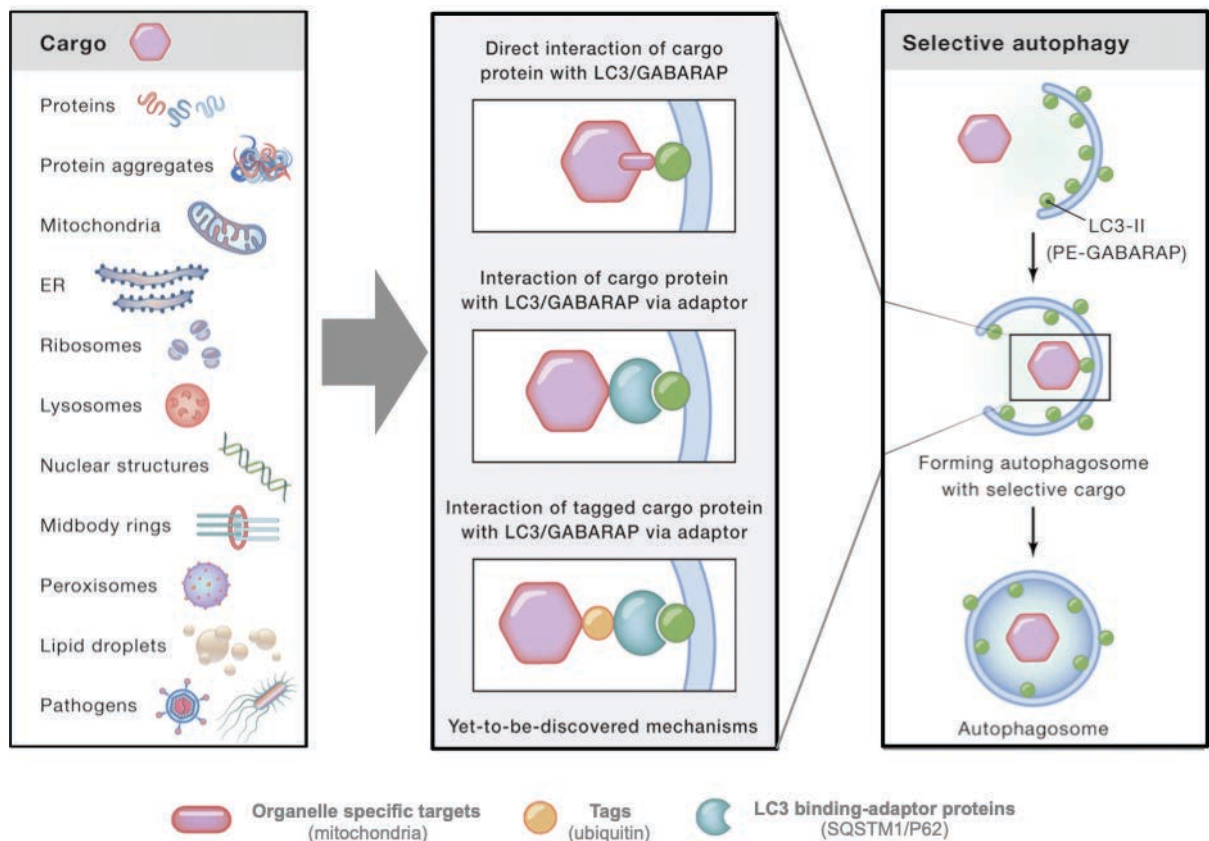


Figure 9. Selective autophagy.

Different cargoes, organelle-specific binding proteins and LC3/GABARAP-binding adaptor proteins that are degraded by autophagy are shown. The steps involved in the autophagy process are also shown in the right panel: formation of the isolation membrane, cargo sequestration and autophagosome elongation and closure, which will finally lead to autophagosome clearance. Source: Levine B, Kroemer G. *Cell*. 2019;176:11-42 (84).

Membrane elongation and autophagosome closure depends on an adequate cytoskeleton function and the last step, autophagosome clearance, occurs after autophagosomes fuse to lysosomes for further digestion (94).

2.2.2.3 Autophagy dysfunction in PD

Alterations in autophagy have been described in several neurodegenerative diseases, such as AD and HD (86) depending on the stage at which autophagy is primarily affected, cellular homeostasis is disrupted and diverse clinical phenotypes are observed (95). Moreover, autophagy has been demonstrated to be altered at multiple stages of PD (96).

An increasing amount of evidence has found genetic, epidemiological and molecular links between PD and LSD. Mutations in genes that regulate lysosomal biogenesis or function lead to accumulation of non-degraded substrates and cause LSD. LSD are a heterogeneous group of disorders of which the vast majority are early onset and have a fatal course with variable implication of central nervous system (CNS), among many other clinical features, resulting from the accumulation of degradation products of cell metabolism (11). This has led to the discovery of parallel mechanisms between rare paediatric LSDs and common adult diseases, such as the relationship between the most common LSD, Gaucher's disease (GD), and PD (97).

Interestingly, mutations in genes that code for Parkin and PINK1 account for the majority of autosomal-recessive cases of PD which impede mitophagy, favouring the accumulation of damaged mitochondria and promoting apoptosis (19). DJ-1 is another PD related protein with mitochondrial localization which plays a role in mitochondrial function and autophagy, and a couple of studies suggest that an alteration in mitochondrial function has a detrimental impact on the function of the lysosomal compartment in PD (98,99).

The failure to induce autophagosome formation or an inefficient cargo recognition may result in cytosolic persistence of unsequestered cargo such as damaged mitochondria, which may be a source of oxidative damage and further mitochondrial malfunctioning (94). Altered autophagy is also responsible for the accumulation of missfolded proteins, such as α -synuclein (94). Poor clearance of autophagosomes may interfere with intracellular trafficking, become a source of cytotoxic products and release lysosomal enzymes which may ultimately activate cell death (100). Finally, the impact of autophagy cannot be fully understood without taking into account the reutilization of autophagosome components in biosynthetic pathways, which may become dysfunctional under many pathological conditions (101).

In summary, mitochondrial function, mitochondrial dynamics, autophagy and lysosomal degradation play an important role in PD-associated neurodegeneration (102). The exact mechanisms by which neural death occurs remain to be elucidated but it has become clear that there are several influencing factors coexisting rather than a unique molecular pathway responsible for the neurodegenerative process (**Figure 10**).

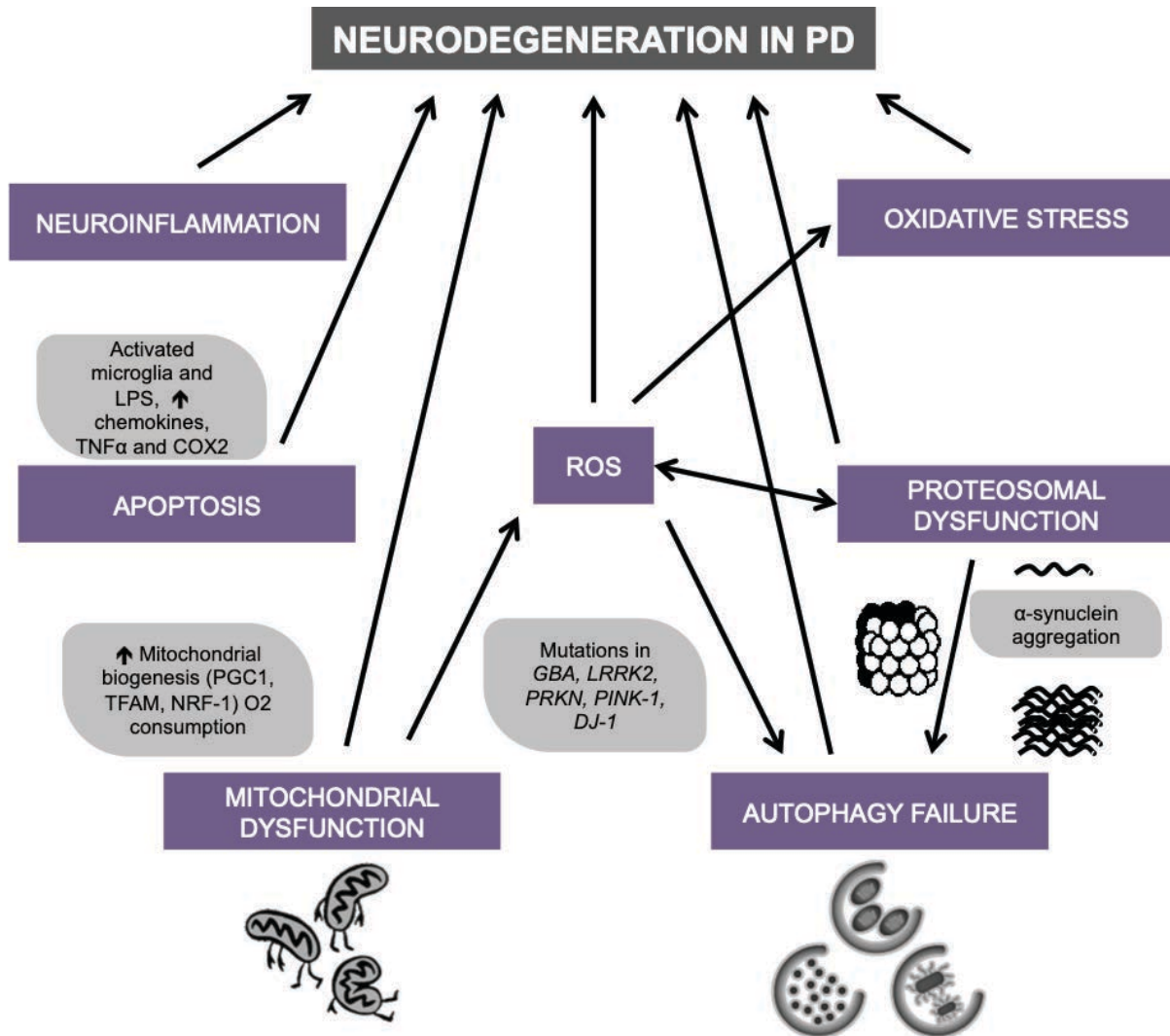


Figure 10. Summary of molecular mechanisms involved in PD neurodegeneration.

Mitochondrial dysfunction, oxidative stress, altered proteostasis, neuroinflammation, autophagy and apoptosis are all implicated in the pathogenesis of PD. The gray-rounded rectangles account for diverse factors that may lead to alterations in the principal pathways leading to neurodegeneration.

DJ-1: Protein/nucleic acid deglycase DJ-1; GBA: Glucocerebrosidase; LRRK2: Leucine rich-repeat kinase 2; PINK: PTEN-induced kinase 1; ROS: Reactive oxygen species.

Modified from: Corona JC, Duchen MR. *Neurochem Res.* 2015;40(2):308-316.(77).

2.3 GENETICS IN PD

To date, the etiology of PD remains unknown in up to 90% of the cases, making iPD the most common form of the disease. Although hereditary forms of PD only represent 5-10% of all cases, the discovery of genes associated to PD, or those that represent an increased risk factor for its development, have provided crucial insights to the understanding of the pathology of the disease (**Figure 11**).

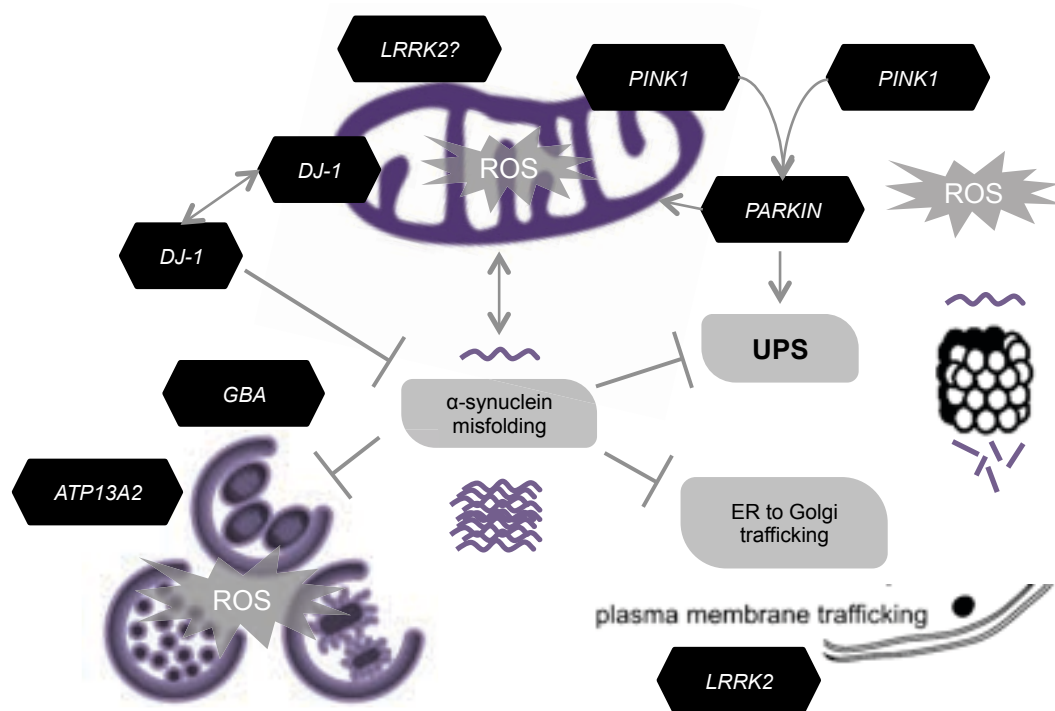


Figure 11. PD-associated gene products and their prospective sites of cellular function.

PD is hypothesized to be a consequence of the dysfunction of intersecting and compensatory organelle and protein degradation components, Accordingly, mutations in genes that code for proteins associated to mitochondrial function and autophagy pathways, have been further implicated in PD by increasing the production of ROS, which accelerate protein damage and neurodegeneration and decrease the clearance of toxic component for cell metabolism. DJ-1: Protein/nucleic acid deglycase DJ-1; ER: Endoplasmic reticulum; GBA: Glucocerebrosidase; LRRK2: Leucine rich-repeat kinase 2; PINK: PTEN-induced kinase 1; ROS: Reactive oxygen species; UPS: Uncoupling protein system

Modified from: Caldwell GA, Caldwell KA. *Dis Model Mech.* 2008;1(1):32-36(103).

The list of mutations causing monogenic types of PD continues to grow (16) and the number of genes associated with complex phenotypes that include parkinsonism is also increasing (**Table 3**). Genes that are currently known to contribute to an increased risk for the sporadic form of the disease such as, *GBA1* and *ATP13A2*, are also responsible of LSD or a risk factor for its development (104). Finally, genes responsible for less frequent child-onset neurodegenerative disorders presenting with parkinsonism, such as LSD, have been found to be present in late-onset forms of PD (12,105).

This thesis focused on the study of two genetic factors associated to PD: *LRRK2*, which is the most common gene for familiar PD, and *GBA*, which is known to be the single most common risk factor for developing PD (106,107). In both cases, the clinical characteristics of the disease are undistinguishable from iPD, so they are relevant in terms of dissecting the molecular etiopathology of the most common form of the disease, that accounts for iPD (108). In addition to this, healthy carriers of mutations in these genes have been identified, which is of great relevance to the study of mechanistic of genetic alterations in neurodegeneration pathways (106,109) because they may represent the prodromal stage of the disease.

Table 3. Summary of genes associated with PD.

Gene	Locus	Protein	Location	Inheritance	Onset	Function
<i>SNCA</i>	<i>PARK1/4</i>	α -synuclein	4q21.3-q22	Dominant Risk factor	Early	Synaptic vesicles trafficking
<i>PARKIN</i>	<i>PARK2</i>	Parkin	6q25.2-q27	Recessive	Early	Mitophagy
Unknown	<i>PARK3</i>		2p13	Dominant	Late	?
<i>UCHL1</i>	<i>PARK5</i>	Ubiquitin carboxy-terminal hydrolase L1	4p13	Dominant	Late	Proteasome
<i>PINK1</i>	<i>PARK6</i>	PTEN-induced putative kinase 1	1p36.12	Recessive	Early	Mitophagy
<i>DJ-1</i>	<i>PARK7</i>	DJ-1	1p36.23	Recessive	Early	Mitophagy
<i>LRRK2</i>	<i>PARK8</i>	Leucine-rich repeat kinase 2	12q12	Dominant Risk factor	Late	Autophagy, citoeskeleton moviility, mitochondrial
<i>ATP13A2</i>	<i>PARK9</i>	ATPase cation transporting 13A2	1p36	Recessive	Early	Lysosomes
Unknown	<i>PARK10</i>		1p32	Risk factor	?	?
<i>GIGYF2</i>	<i>PARK11</i>	GRB10-interacting GYF protein 2	2q36-7	Recessive	Early	Insulin-like growth factors (IGFs) signaling
Unknown	<i>PARK12</i>		Xq21-q22	Risk factor	?	?
<i>HTRA2</i>	<i>PARK13</i>	High temperature requirement protein A2	2p13.1	Dominant	?	Mitophagy,
<i>PLA2G6</i>	<i>PARK14</i>	Phospholipase A2 group VI	22q13.1	Recessive	Early	Lipids metabolism
<i>FBXO7</i>	<i>PARK15</i>	F-box protein 7	22q12.3	Recessive	Early	Mitophagy
Unknown	<i>PARK16</i>		1q32	Risk factor	?	?
<i>VPS35</i>	<i>PARK17</i>	Vacuolar protein sorting 35	16q12	Dominant	Late	Endosomes
<i>EIF4G1</i>	<i>PARK18</i>	Eukaryotic Translation Initiation Factor 4 Gamma 1	3q27.1	Dominant	Late	Protein translation
<i>DNAJC6</i>	<i>PARK19</i>	DnaJ heat shock protein family member C6	1p31.3	Recessive	Early	Endosomes
<i>SYNJ1</i>	<i>PARK20</i>	Synaptojanin 1	21q22.11	Recessive	Early	Endosomes
<i>DNAJC13</i>	<i>PARK21</i>	DnaJ Heat Shock Protein Family Member C13	3q22.1	Dominant	Late	Endosomes
<i>CHCHD2</i>	<i>PARK22</i>	Coiled-Coil-Helix Domain Containing 2	7p11.2	Dominant	Early or late	Mitochondria-mediated apoptosis and metabolism
<i>VPS13C</i>	<i>PARK23</i>	Vacuolar protein sorting 13 honolog C	15q22.2	Recessive	Early	Mitophagy
<i>GBA</i>	–	Gluccerebrosidase	1q22	GD Risk factor	Late	Lysosomes
<i>MAPT</i>	–	Microtubule Associated Protein Tau	17q21.31	Sporadic Risk factor		Microtubules

Modified from: Del Rey NL-G, Quiroga-Varela A, Garbayo E, et al. Advances in Parkinson's Disease: 200 Years Later. *Front Neuroanat.* 2018;12:113 (13)

2.3.1 Leucine Rich Repeat Kinase 2 (*LRRK2*)

LRRK2 mutations are the most common cause of late-onset hereditary PD. Frequencies vary between ethnic groups, being North African Arabs and Ashkenazi Jews the most affected populations (110). Increasing evidence suggests that *LRRK2* is associated with a range of diseases, such as Crohn's disease (CD), leprosy, and that it may increase the risk to develop particular types of cancer, however the molecular pathways leading to these diseases still remain elusive (111).

LRRK2 mutations typically cause a PD-typical phenotype, with no sex association and where most of the patients were from white ethnicity. Autopsies of such patients show prominent loss of melanised dopaminergic neurons in the SNpc. A large systematic review of *LRRK2*-associated PD cases reports that age of onset was 57 years, a median disease duration of 10 years. The cardinal symptoms of PD were reported with the following frequency: bradykinesia in 99%, rigidity in 99%, tremor in 88% and postural instability in 65%, while atypical signs of PD have been reported only anecdotally (15). A number of non-pathologic variants are also known and some others variants that may act as PD risk factors have been reported using GWAS (112).

The *LRRK2* gene (PARK8) is located in chromosome 12, contains 51 exons and spans a genomic distance of 144kb. It encodes for a 2527 amino-acid multi-domain protein also known as dardarin, from the Basque word "dardara" that means trembling. This protein is a member of the leucine-rich repeat kinase family. *LRRK2* has primarily an enzymatic activity: both kinase and GTPase, and has been implied in many cellular functions such as vesicle trafficking and movement, autophagy and mitochondrial function (113–115).

The *LRRK2* gene (**Figure 12**) coding sequence includes 7500 nucleotides. Even when deterministic mutations have been found, penetrance is age dependent and estimated between 30% and 74% (116). Its most frequent mutation, *G2019S* (*LRRK2*^{*G2019S*}), is responsible for 1% of apparently sporadic PD and 4% of familial PD (117).

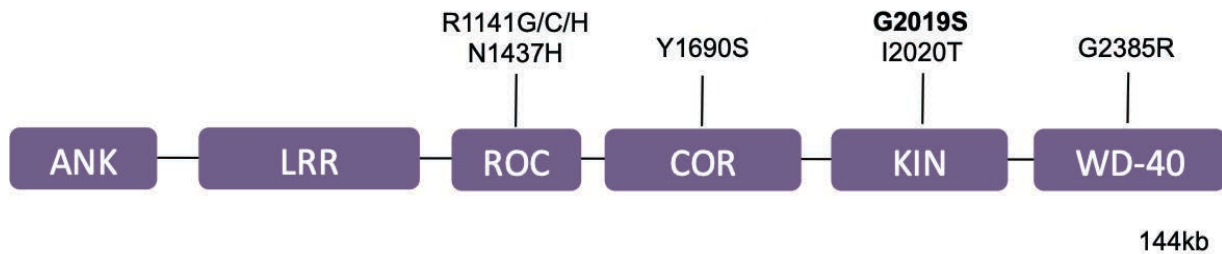


Figure 12. Schematic representation of *LRRK2* gene.

The altered sites of PD pathogenic mutations are shown. Nomenclature is based in the guidelines from the International Union of Biochemistry and Molecular Biology.

Modified from: Esteves a. R, Swerdlow RH, Cardoso SM. *Exp Neurol.* 2014;261:206-216 (118)

LRRK2 protein is expressed in most organs including brain, heart, liver and circulating immune cells. Within cells, *LRRK2* associates with various intracellular membranes and vesicular structures including the endosomes, the lysosomes, the multivesicular bodies, the OMM, lipid rafts, microtubule associates vesicles, golgi complex and the ER (119). *LRRK2* function is also associated with microtubule dynamics and trafficking; changes in autophagy are consistently observed when mutant *LRRK2* is knocked down or overexpressed, but the specific mechanisms for these alterations are still unclear (**Figure 13**) (102,120).

Studies consisting in modifications in the expression of *LRRK2* in different neural-cell based models report an altered synaptic vesicle trafficking and endocytosis (121,122). A protective role against oxidative stress has been reported for wild-type *LRRK2*, which seems to be lost in mutant forms of *LRRK2* (123). *LRRK2* dysfunction has also been demonstrated to play a role in different pathologic

scenarios, such as α -synuclein phosphorylation, microtubule dynamics, alterations in the uncoupling protein system (UPS) and in neurite growth and branching regulation leading to neurodegeneration (124). Silencing of *LRRK2* reduced the inflammatory response in different human cell-derived and animal models (125).

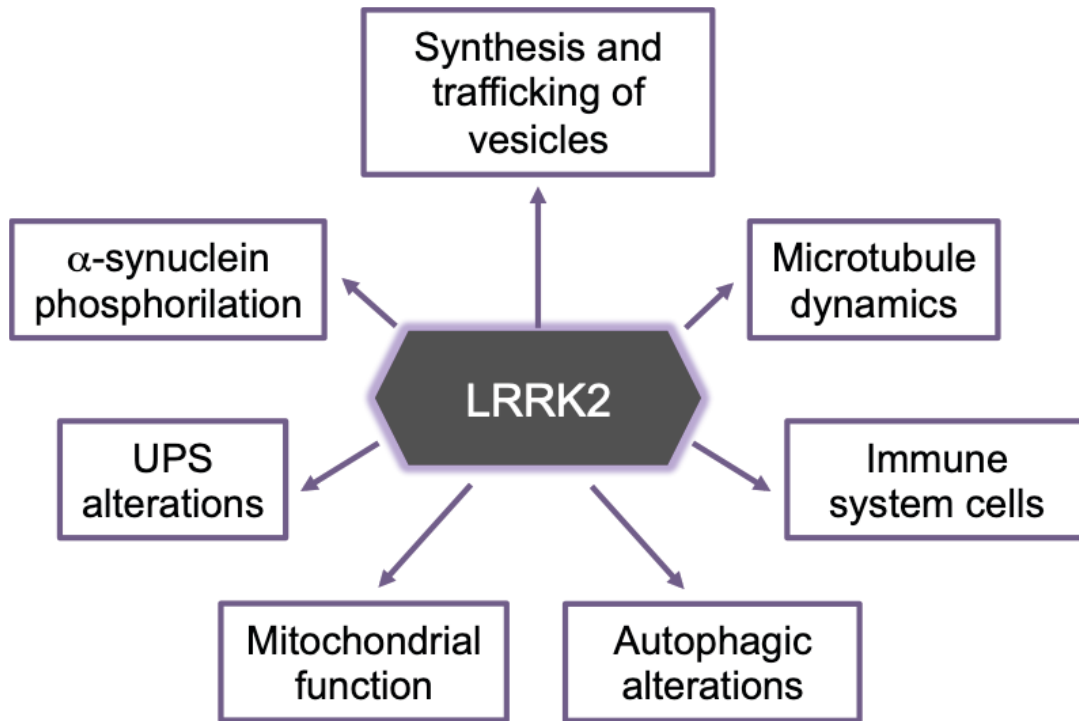


Figure 13. LRRK2 interactions in cellular mechanisms.

The boxes represent the cellular processes that have been associated with LRRK2 function in physiology and/or disease. A hierarchical order cannot be established among these processes and it is not exactly known which of these processes are directly controlled by LRRK2, which of them are LRRK2 partially-regulated or which are just consequences of other LRRK2 primary functions. Whether all of these functions co-occur in a single cell type, or if LRRK2 orchestrates different, specific functions in different cell types also remains unknown.

UPS: Uncoupling protein system.

Modifies from: Esteves a. R, Swerdlow RH, Cardoso SM. *Exp Neurol.* 2014;261:206-216 (118)

The *G2019S* (*LRRK2*^{*G2019S*}) mutation increases kinase activity by increasing the catalytic rate and facilitating the substrate access to the enzyme, but not by enhancing substrate affinity. These changes in *LRRK2* kinase activity appear to be toxic, and seem to induce degeneration of dopaminergic neurons (126).

Mutations associated with genetic forms of PD have been associated with deregulated mitochondrial function and autophagy. *LRRK2*^{*G2019S*} mutation is associated with impaired mitochondrial function and dynamics (127), as well as with imbalanced autophagy and aggregation of α -synuclein (128), and has also been linked to defects in endosomal-lysosomal trafficking, lysosomal pH and calcium regulation and CMA impairment (120,129)

Investigations on the implication of *LRRK2* mutations in PD etiology suggest that, although the genetic compound is clearly defined, it may not be determinant to produce neurodegeneration, and that many other factors should be taken into consideration to elucidate the mechanism of the disease which may, in turn, explain the reduced penetrance of this mutation (130).

2.3.2 Glucocerebrosidase (GBA)

GBA is the most common genetic risk factor for PD. Homozygous *GBA* defects cause GD and heterozygous defects predispose to PD (131). Mutations in *GBA* increase the risk of PD in carriers who are not developmentally affected by GD.

The clinical phenotype of *GBA*- PD has many common features with iPD. Importantly, the prodromal features associated with iPD are also found in the *GBA*-PD population (107). PD patients with *GBA* mutations cannot be differentiated from iPD without having a clinical background or any other factor that may raise the suspicion of a genetic condition (familiar, clinical or pathological).

Non-motor symptoms are the earliest presenting symptoms in *GBA*-PD, as well as in iPD, but they have been reported to be more severe in *GBA*-mutation

carriers (132). The age of onset of PD patients with *GBA* mutations is approximately 5 years earlier than iPD, and cognitive impairment is more frequent in this subset of patients (133).

As *GBA*-PD is more widely known, the clinical features of *GBA* carriers have been described in some series, highlighting the slight clinical particularities shown by these patients. For instance, bradykinesia is a more common clinical symptom, and motor progression seems to be more rapid when compared to the iPD group (134) but remains to be fully defined. Treatment response to dopaminergic agents and to deep brain stimulation is the same as in iPD (135,136).

The *GBA* gene is found on chromosome 1q21 and consists of 11 exons and 10 introns. It encodes the lysosomal enzyme glucocerebrosidase (GCase), it spans a genomic distance of 10kb. Mutations in *GBA* decrease Gcase activity, leading to defects in autophagic-lysosomal function and α -synuclein aggregate accumulation (137).

The presence of a mutation in *GBA* is always associated with a reduced Gcase activity and Gcase activity progressively declines with physiologic aging (138), increasing the risk for PD. Depending on the mutation, homozygous patients may have <1% of and heterozygous carriers may have 50-60% of residual activity.

The pathology of *GBA*-associated PD (*GBA*-PD) is similar to iPD. While some studies have suggested that Lewy body deposition is more extensive in *GBA* mutant positive brains, others have not confirmed this finding (131). Gcase has been found in Lewy bodies and 5% of brains exhibiting PD pathological characteristics were found to be *GBA* positive in a retrospective analysis (139,140).

Over 300 mutations of the gene have been discovered to date, the most common being *N370S* (*GBA*^{*N370S*}) and *L444P*, which are point mutations in exon 9 and 10, respectively. The location of the mutations is not a reliable predictor of

disease severity and the same mutation may lead to a great clinical variability, suggesting the existence of modifying factors yet unknown (**Figure 14**).

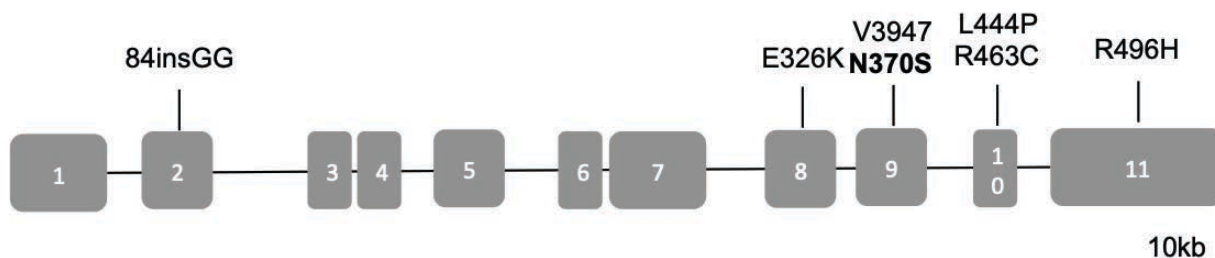


Figure 14. Schematic representation of *GBA* gene.

The most common altered sites of PD pathogenic mutations are shown in red. Nomenclature is based in the guidelines from the International Union of Biochemistry and Molecular Biology Source: Ziegler SG, Eblan MJ, Gutti U, et al. *Mol Genet Metab.* 2007;91(2):195-200 (135)

Gcase is a 497 amino acid protein of approximately 62 kDa with three domains and GCcase activity. It is localized in the lysosomes, where it remains associated with the lysosomal membrane. The active site of the protein is located at domain 3.

Among the several candidate pathways through which Gcase deficiency may promote the pathogenesis of PD are defective clearance and recycling of α -synuclein, lysosomal dysfunction, ER associated degradation (ERAD), calcium deregulation and mitochondrial abnormalities (**Figure 15**) (141,142).

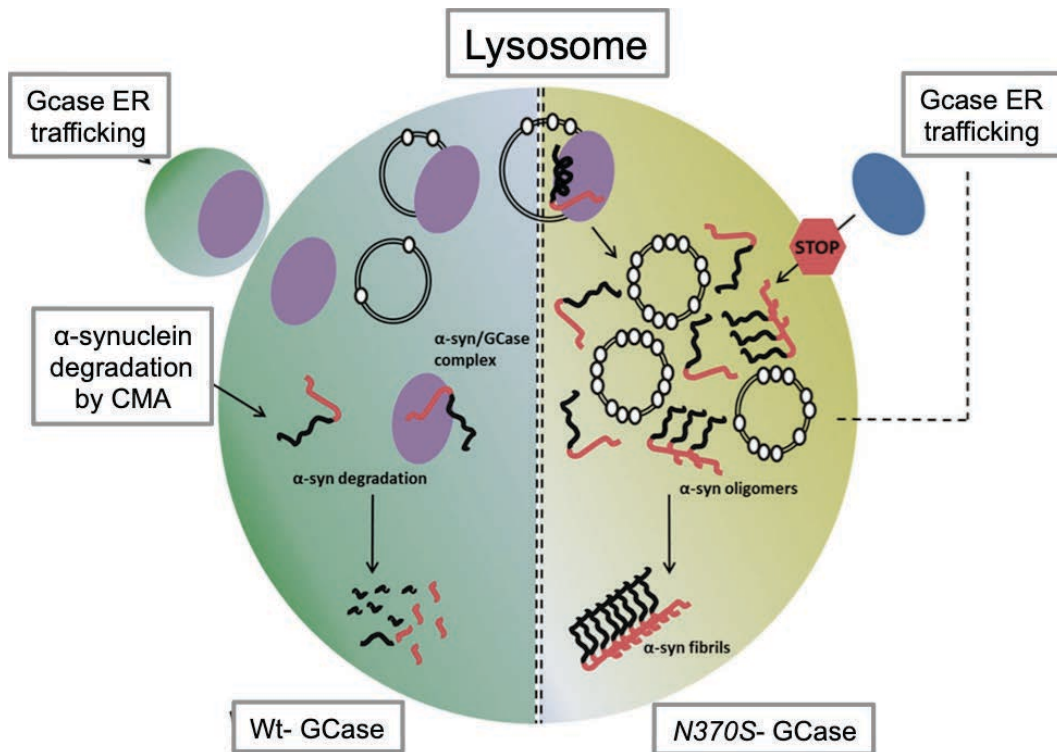


Figure 15. Proposed molecular alterations produced by mutant GCase.

In normal functioning lysosomes (left, green), wild-type GCase (purple) enters the lysosome via vesicle transport. Upon lysosomal entry, GCase hydrolyses the substrate GlcCer (open white circles), on intralysosomal vesicles, and the components of autophagosomes. In compromised lysosomes (right, yellow) with mutant *GBA* (blue), several scenarios may occur. GCase mutations (blue), resulting in its decrease in activity or levels, cause the build-up of GlcCer (note more open circles) on intralysosomal vesicles, α -syn fibrils are formed and defective mitochondria are accumulated. Lysosomal leakage may then occur, increasing ROS levels perpetuating cell damage by various pathways.

CMA: Chaperone-mediated autophagy; ER: Endoplasmic reticulum; GCase: Glucocerebrosidase; α -syn: α -synuclein

Modified from: McGlinchey RP, Lee JC. *Biochem Soc Trans.* 2013;41(6):1509-1512 (143).

Characterizing in detail the signature features of *GBA*-PD helps us to gain insight, not only to the molecular mechanisms of PD, but also into prodromal and “transitional” PD contributing to the understanding of iPD pathology and identification of biomarkers of preclinical features and ultimately widen these findings to other PD groups (144).

The Gcase chaperone ambroxol has been tested in PD models, positively increasing Gcase activity in GD patients, *GBA*-mutation carriers with and without PD, iPD patients and controls. Ambroxol also improved endoplasmic ERAD, ROS damage and decreased α -synuclein levels, probably by TFEB activation. The importance of these results lays on the potential use of Gcase chaperones as a neuroprotective agent against PD and LSD related neurodegeneration (133).

In summary, *LRRK2*-PD and *GBA*-PD both exhibit clinical and anatomical characteristics almost identical to those of iPD, which makes the study of these genetic forms very attractive in terms of understanding the molecular basis of the PD. A detailed description of the role of *LRRK2* and *GBA* and their association to mitochondrial and autophagic alterations in PD pathogenesis may be of benefit to discover novel biomarkers and neuroprotective strategies treatments aimed to modify the clinical course of PD (145,146).

2.4 NOVEL APPROACHES IN PD RESEARCH

Despite a great deal of investigation efforts, the physiopathological basis of neurodegeneration leading to PD remains unknown. The description of the multiple functions of PD related genes, such as *LRRK2* and *GBA* in several models has greatly helped to acknowledge the complicated interplay of multiple molecular pathways leading to PD particular kind of neurodegeneration. For example, molecular alterations that are common to PD and LSD, such as the presence of insoluble, oligomeric or fibrillar α -synuclein aggregations have been observed in neurons of the *sustantia nigra*, hippocampus and cerebral cortex of patients with GD (97).

Since the target tissue of the disease, the CNS, is not readily available for investigation, several experimental models have been developed in the pursuit of unravelling PD pathophysiology (147,148)]. Animal models, yeast and eukaryotic cell models are fundamental tools to identify and validate the molecular and cellular mechanisms underlying genetically linked diseases.

It has come to attention that PD is not a disease confined to the CNS, but that it also encompasses molecular defects in non-neural tissues, such as skeletal muscle, colon, submaxilar gland and fibroblasts (48,151–154). In these regards, the fact that the altered molecular pathways of systemic diseases such as CD, leprosy, LSD and mitochondrial disease, which are common to neurodegenerative diseases are also observed in peripheral tissues opens an interesting window for novel research strategies (155).

2.4.1 Animal models of PD

Non-human primates (NHP) have been used to generate the most robust and clinically useful models of PD. The current gold standard animal model of PD is the NHP MPTP induced model, which shows stable, bilateral clinical features that closely

resemble iPD (156) and may even exhibit some features of RBD (157). However, this model does not model the major pathophysiological hallmark of iPD, such as Lewy body pathology, and its utility for the study of prodromal PD has still not been validated (158).

Although evidence of neuroinflammation following administration of neurotoxins exists in animal models, dopaminergic neurons cell death happens in cultured neurons in the absence of neuroinflammatory cell type-drivers, and neuroinflammation occurs but in manners distinct to PD (156). Many model organisms have been shown to exhibit dopaminergic neurodegeneration and neuropathology such as nematode worms, *Drosophila melanogaster* (*D. melanogaster*), mouse and rat models (159).

In order to study the expression of genes in animal models, models using genetically edited viral vectors have been developed. These models are not easily suitable for *LRRK2* delivery due to the big size of *LRRK2* and the limited packaging capacity of the system. However, some groups have demonstrated a loss of dopaminergic neurons after successfully injecting *LRRK2*^{G2019S} and wild type (wt) *LRRK2* (160,161). Models of genetic signaling using RNA interference of other PD related genes (*PINK*, *DJ-1* and *PRKN*) have not satisfactorily displayed a PD phenotype. In summary, viral vector production, upscaling and purification require a great amount of time and technology investment in order to obtain reproducible results, which for some kinds of PD have not proven to be useful (162).

Yeast exhibit a high degree of conservation of basin protein function and cellular function with mammalian cells that are implicated in neurodegeneration, such as vesicular trafficking, protein folding and aggregation, protein catabolism and mitochondrial function (163). This model is very useful to identify molecular pathways and biological processes associated with or regulated by a given protein (164). The toxicity of *LRRK2* overexpression was first observed in a *Saccharomyces cerevisiae*

(*S. cerevisiae*). Puzzlingly, when genetic PD-pathogenic variants of this gene were overexpressed, the toxicity was not observed (159).

D. melanogaster and *Caenorhabditis elegans* (*C.elegans*) have provided a great deal of information on the mechanism of action of LRRK2 and the enzyme activities that it exerts. Moreover, the beneficial effect of ursodeoxycholic acid (UDCA) on mitochondrial function and its impressive pharmacological effect was recently demonstrated in a *D. melanogaster* model of PD (127). However, neither *Drosophila* nor *C elegans* contain true orthologs, but most likely paralogs, of human LRRK2, and the translational process to develop an effective treatment for humans is still challenging (165).

A mouse model for a severe neurological form of GD showed impaired autophagy and a profound alteration in mitochondrial function consisting of reduced MMP, severely impaired respiration and mitochondrial fragmentation (166) and other animal models of LSD have proven useful to study neurodegenerative pathways (167). GBA deficiency in the brains of mice and flies leads to an accumulation of GlcCer, impaired autophagic-lysosomal flux, α -synuclein aggregate accumulation and neurodegeneration, such as observed in brains of PD patients (97).

Even though animal models have largely helped to understand the pathology of the disease, and to develop potential treatment strategies, the main concern is the interspecies variability that becomes more evident when translating the results to human research, and the fact that they do not carry the genetic and epigenetic background of patients (168).

2.4.2 Cellular models of PD

The purpose of any cellular model is to simplify the experimental variables and to enable more precise manipulation of specific genes and environmental factors. In

multifactorial disorders, such as PD, it is desirable to dissect the complex pathological processes into simpler molecular events (169).

By using cellular models, it is possible to generate homogeneous populations of cells and to obtain a sufficient quantity of material for most experimental procedures. To repeat experiments in the same conditions but at different time points is also possible when working with cell models, since the culturing conditions are relatively simple to replicate.

Immortalized cell lines such as the neuroblastoma SH-SY5Y lineage have a human origin, neuronal properties that are easy to be maintained, have a rapid proliferation rate and enable large-scale studies (170). However, genetic modifications are necessary in order to immortalize the lines, and they do not exhibit a dopaminergic neuronal phenotype unless they are induced with retinoic acid (169,171). The latter has led to the development of differentiated dopaminergic cell models derived from human and mouse neural cell lines treated with different methods (172). A big caveat of cancer cell lines is that they rely almost exclusively on glycolysis instead of mitochondrial respiration (Warburg effect), which may cover up mitochondrial defects that need to be evaluated (173).

Patient-derived cellular models allow the study of the genetic mutations directly on the human physiology and therefore provide an important, yet complementary, model in which to understand the mechanistic of the disease representing an important advantage over other cell models (169). On the counterpart, information provided by cell models cannot recapitulate *in vivo* systemic physiology, nor the physiological diversity resulting from the intercellular specializations and interactions in a specialized organ environment, particularly that of the CNS (150,174).

The development of iPSC derived neurons has permitted to investigate the consequences of genetic mutations in several patient-derived cell subtypes where the genome and transcriptional control are mostly intact (175). The greatest

advantage of iPSC-derived neurons is that they can mimic the microenvironment of PD cells *in vitro*, opening new avenues to explore gene-environment interactions (176); the clear involvement of nigrostriatal dopaminergic neurons in disease and the well-developed capacity to generate iPSC-derived dopaminergic neurons (177). The main limitation of iPSC is the poor efficiency of differentiating stem cells into specific neuronal subtypes, which consequently makes drug screening and target validation difficult to implement.

Cell co-cultures in three-dimensional surroundings, such as microfluidic brain-on-a-chip devices are very promising and may mimic the *in vivo* microenvironment allowing to best study the neurodegeneration process (178,179). However, until date to perform therapy targeted-studies in large cohorts is still technically challenging.

Many systems have been used as tools to understand the molecular and cellular mechanisms of familial *LRRK2* and *GBA* mutations, among these, primary neuronal culture models have been extensively used to understand the pathogenic effects of *LRRK2* mutations and *in silico* models have been developed to study *GBA* mutations (124,167).

When developing neural cell models of PD, it should be taken into account that neural tissue is highly dependent on oxidative metabolism. Moreover, because of its postmitotic nature, autophagy alterations have a big impact on their long term viability and functionality. iPSC and immortalized cell lines rely on glycolytic metabolism, which may potentially mask mitochondrial failure and associated autophagic clearance of dysfunctional organelles. In these regards, research on primary mitochondrial diseases uses galactose-based models that unravel mitochondrial alterations that in glycolytic conditions may be surpassed (180,181).

In iPSC and neural stem cells (NSCs) derived from *LRRK2*^{G2019S}, passage-dependent deficiencies have been observed to correlate with epigenetic changes such as those observed during cellular aging (182,183). Even when getting a very

accurate model that may mimic neuronal function NSCs or iPSC derived neurons still cannot recapitulate the complexity of brain circuitry (159).

Dopaminergic neurons derived from iPSC obtained from donors carrying heterozygous *GBA* mutations show increased α -synuclein and mono-amine oxidase B (MAO-B), defect in lysosomal protein degradation, and weak competence in dopamine synthesis and release (184,185). Finally, mitochondrial and autophagic defects have also been reported in fibroblasts and iPSC-derived neurons of patients with *GBA* mutations (186,187). However, studies in cell models have been performed in glycolytic conditions, where mitochondrial metabolism is bypassed and autophagy is down regulated, consequently, a pathologic phenotype may be disregarded.

2.4.2.1. Fibroblasts

The great individual variability presented in PD, and the urgent need to find novel biomarkers targeted to the prodromal phase of the disease makes it imperative to develop patient-derived, easily accessible where PD cases can be studied in an individual basis, such as skin-derived fibroblasts (188). An ideal biomarker would be an easily assayed biological parameter, from a replicable model that informs on PD-relevant pathological changes and reliably tracks clinical symptoms.

Fibroblasts offer several advantages, since they are accessible cells, which can be derived from PD affected patients, controls and subjects carrying genetic mutations associated to PD. It should be noted that fibroblasts make dynamic cell-to-cell contacts when cultured, which is similar to neuronal cells (189). Consequently, they provide a patient-specific culture system retaining the specific environmental and aging history, and polygenic risk factors of the patient. Furthermore, fibroblasts can be propagated in culture, cryopreserved and stored for long periods of time, and transformed in cell types that exhibit molecular characteristics of the target tissue of the disease, the nervous system. Additionally, they offer a cell platform to depict disease etiopathogenesis and develop high throughput drug screening with low costs

of maintenance and they have been validated before for the study of mitochondrial diseases, neurodegenerative diseases and drug toxicity, among others (190,191).

The greatest proportion of PD is of unknown cause, and the great complexity of the disease, encompassing unknown genetic and epigenetic factors and environmental lesions has made it difficult to find an accessible model that recapitulates the pathogeny of PD. Studies in skin derived fibroblasts from patients with iPD have thrown relevant and consistent information regarding molecular pathways altered in this type of neurodegeneration. A recent study showed that fibroblasts from iPD patients have higher growth rates, altered morphology, increased mitochondrial susceptibility to ultraviolet (UV)- exerted stress and autophagic alterations (188).

Multiple studies have shown disease-relevant changes in fibroblasts derived from different hereditary types of PD, such as increased oxidative stress, MRC deficiencies, ineffective mitochondrial dynamics and autophagy and transcriptomic and postranslational alterations (102,192–197).

Mitochondrial phenotypes have been characterized in fibroblasts at baseline and under conditions of pharmacological stress. The most used pharmacological approaches used to date include mitochondrial toxins such as MPTP, valinomycin, oligomycin, CCCP and rotenone, but as these approaches may mimic mitochondrial toxicity, they are far from dissecting the mitochondrial pathways affected under physiological conditions (198). Smith et al demonstrated an increased sensitivity to valinomycin in a subset, but not all, of fibroblasts derived from PD patients, pinpointing again the great interindividual variability and, outstandingly, that the molecular characteristics of patient-derived cell models do not always correlate with the clinical presentation of the disease (199).

Other pathogenic characteristics of PD have been also found in fibroblast studies, such as α -synuclein accumulation and altered GCase expression, supporting the adequacy of this model to study the altered molecular mechanisms of the disease in a patient-derived model (133,194).

Mortiboys *et al* reported for the first time mitochondrial alterations in fibroblasts of human *LRRK2*^{G2019S}-mutation carriers, consisting in reduced MMP, reduced intracellular ATP levels, mitochondrial elongation and increased mitochondrial interconnectivity (197). These findings were further confirmed by Papkovskaia *et al*, who described decreases MMP and ATP levels in fibroblasts and neuroblastoma cells (200). Finally, Cooper *et al* showed that fibroblast-derived iPSC carrying *LRRK2* mutations (although not only *G2019S*) had a defective mitochondrial respiration, increased proton leak and impaired mitochondrial dynamics (183).

Mitochondrial dysfunction has been demonstrated on dermal fibroblasts from GD patients (187). An elegant study by Collins *et al* showed that *GBA*-mutant fibroblast lines have GCase activity impairment and autophagic flux alterations are present in fibroblasts from *GBA*-PD and GD patients, but not in fibroblasts from iPD patients or controls (201). Moreover, novel pharmacologic therapies have been proven effective in fibroblasts from *GBA*-PD (141).

2.4.2.2. Neural stem cells (neurospheres)

Neural stem cells (NSC) are self-renewing multipotent populations of cells present in the developing and adult mammalian CNS. They generate the neurons and glia of the developing brain and also account for the limited regenerative potential of the adult brain (202). The physiological relevance of the neural stem cell models is still a matter of debate.

Neurospheres are free-floating 3D-aggregates of neural progenitors, each potentially derived from a single NSC and generated through tissue microdissection and exposure to mitogens (176). For their expansion, cells are plated in low-

attachment tissue culture plastic dishes in conditions where differentiating or differentiated cells are expected to die, whilst NSCs respond to the mitogens, divide and form floating aggregates (primary neurospheres) which can be further dissociated and re-plated to generate secondary neurospheres (203).

This model represents a patient-derived method that exhibits hallmarks of NSC and that can be obtained and propagated from multipotent stem cells found in olfactory mucosa and adipose tissue, among others. Olfactory mucosa-derived neurospheres have been proven to be a robust and informative model where molecular pathways associated with neurological disorders and found in other tissues replicate, offering the advantage neurodevelopmental pathways that are not observed in other cell models (204).

The main caveat of neurospheres is the limited efficiency in terms of neurogenic competence and differentiation, but it can certainly be useful for generating large number of neurons *in vitro* and testing some pathological pathways (205).

As previously mentioned, mitochondrial alterations and autophagy deregulation are common to PD and LSD, such as GBA. However, the exact molecular mechanisms leading to neurodegeneration, and the pathogenic alterations that lead to dopaminergic neural destruction are far unknown. One of the main reasons for this is the lack of cellular models that may help to dissect the molecular pathways altered and to establish a genotype-phenotype correlation, which can be translated to clinical biomarkers and disease modifying therapies.

This thesis aims to contribute in the understanding neurodegeneration in two genetic forms of PD and to validate two cell models in response to the exposition to different insults that may evidence underlying molecular alterations that lead to the appearance of clinically manifest PD.



3. HYPOTHESIS AND OBJECTIVES



The hypothesis of this thesis is that cell models derived from subjects carrying PD -related mutations exhibit mitochondrial and autophagic alterations that partially reproduce the pathology of PD offering cell platforms to advance in the study of disease etiology, thus providing support for further development of potential biomarkers and therapeutic strategies.

Thus, the main objectives of this thesis are:

To validate two different patient-derived cellular models to study the pathology of the most common genetic forms of PD.

Skin-derived fibroblasts from *LRRK2*^{G2019S}-mutation carriers

STUDY 1

To assess genotype-phenotype correlation and molecular changes of skin-derived fibroblasts from *LRRK2*^{G2019S} mutation carriers in correspondence to the presence of PD symptoms.

To characterize the mitochondrial state and autophagic phenotype of skin-derived fibroblasts obtained from asymptomatic carriers of *LRRK2*^{G2019S} mutation and *LRRK2*-PD patients in standard conditions.

To evidence the mitochondrial and autophagic response after forcing oxidative metabolism by subjecting fibroblasts to mitochondrial challenging conditions.

Adipocyte-derived neurospheres from *GBA*^{N370S}-mutation carriers

STUDY 2

To assess genotype-phenotype correlation and molecular changes of adipocyte-derived neurospheres from *GBA*^{N370S} mutation carriers in correspondence to zygosity and neurosphere's developmental stage.

To characterize the mitochondrial state and autophagyc phenotype of adipocyte-derived neurospheres obtained from heterozygous and homozygous *GBA*^{N370S}-mutation carriers in standard conditions.

To evidence the mitochondrial and autophagic response after a mitochondrial insult by subjecting neurospheres to mitochondrial uncoupling.



4. METHODS



This thesis comprises two studies that assess the mitochondrial and autophagic function in two different cell models from subjects carrying the most common PD-associated mutations.

Study 1 consisted of an exhaustive mitochondrial characterization and autophagy print assessment of skin-derived fibroblasts from asymptomatic carriers of *LRRK2*^{G2019S}-mutation and *LRRK2*^{G2019S}-PD patients. This study was carried out in Hospital Clinic of Barcelona in collaboration with the Neurology Department and with the Laboratory of Neurodegenerative diseases

Study 2 comprised a broader assessment of mitochondrial content and its relation to autophagy initiation in neural stem cells derived from subjects carrying heterozygous and homozygous *GBA*^{N370S}-mutation. This study was carried out in the University College of London in collaboration with the Department of Clinical and Movement Neurosciences.

Since the studies were conducted in distinct cellular models of PD and in two different cohorts of patients, the methods are described separately and further divided in:

1. Study design and population
2. Cell model development
3. Mitochondrial experimental parameters
4. Autophagy experimental parameters
5. Statistical analysis

4.1 STUDY 1: Characterization of *LRRK2*^{G2019S} fibroblasts

4.1.1 Study design and population

A single-site, cross-sectional, observational study was conducted. Twenty-one age and gender paired subjects were included: six carriers of *LRRK2*^{G2019S}-mutation without clinical manifestations of PD (Non-manifesting carriers: NM-*LRRK2*^{G2019S}), seven PD patients carrying *LRRK2*^{G2019S}-mutation (PD-*LRRK2*^{G2019S}) and eight healthy, unrelated controls (C). Clinical examination and categorization of PD-*LRRK2*^{G2019S} patients was performed according to the UK Brain Bank Criteria for PD (206). The control group included *LRRK2*^{G2019S} negative relatives of patients who voluntarily underwent skin biopsy.

Subjects with comorbidities, mitochondrial disorders, and those consuming mitochondrial toxic drugs were not included in any of those groups (207). The study was approved by the ethics committee of the Hospital Clínic of Barcelona (Spain) and by the Commission on Guarantees for Donation and Use of Human Tissues and Cells of the Instituto de Salud Carlos III (ISCIII). Every participant signed a written consent form, according to the Declaration of Helsinki.

4.1.2 Cell model development

Fibroblasts were obtained by a 6 mm of diameter punch skin biopsy from the alar surface of the non-dominant arm of the subjects and washed twice with Dulbecco's Modified Eagle Media (DMEM) (Gibco™). Small pieces were dissected from the sample and were explanted in a 25cm² Nunc™ EasYFlask™ (Thermo Fisher Scientific Inc), media was changed once a week until cells reached 70% confluence. After that, cells were dissociated from the flask with trypsin and either seeded for further propagation or cryopreserved with 10% Dimethyl sulfoxide (DMSO) (Sigma®). Mutation screening was performed as previously described (208).

4.1.2.1 Fibroblast culture

Cells were grown in 25mM glucose DMEM (Gibco™) supplemented with 10% heat-inactivated fetal bovine serum (FBS) and 1% penicillin-streptomycin at 37°C, in a humidified 5% CO₂ air incubator until 80% optimal confluence was reached. Cells were collected at the same pass number <10 with 2.5% Trypsin (Gibco™) and harvested by centrifugation 8 minutes at 500 g.

4.1.2.2 Metabolic stress test

In order to assess whether mitochondrial and autophagic function was directly implicated in the pathogenesis of *LRRK2^{G2019S}*, cells were exposed for 24-hours to either 25mM glucose (standard) or 10mM galactose (mitochondrial-challenging) media (181).

Table 4. Specific composition of glucose media was:

Glucose	Galactose
DMEM	DMEM
Phenol red	No phenol red
Glucose 25mM	D-galactose 10mM
L-glutamine 4mM	L-glutamine 2mM
FBS 10%	FBS 4%
Sodium pyruvate 1mM	Sodium pyruvate 1mM
P/S 1%	P/S 1%

DMEM: Dulbecco's Modified Eagle's Medium; FBS: Fetal bovine serum

In vivo experiments, oxygen consumption and MMP, were performed in parallel including one subject from each cohort, at the same passage, both in glucose and galactose media. Fixation of cells for immunofluorescence and quantification of mitochondrial dynamics was also performed at this time point. Cell pellets from each line were kept at -80°C for further experimental procedures.

4.1.2.3 Cell growth and protein content

Cell growth rate was manually determined through cell counting with the Neubauer chamber using trypan blue staining at the times of seeding and harvesting the cells. To calculate cell growth rate the following formula was applied, and results were expressed as Δ cell growth/hours:

$$\frac{\left[\frac{\text{Number of cells at time of harvesting} - \text{Number of cells at time of seeding}}{\text{Number of cells at time of seeding}} \right]}{\text{Time (hours)}}$$

Total protein content was quantified through colorimetric detection from cell suspensions and cell protein lysates prior to biochemical and protein expression analyses by using the Pierce Bicinchoninic Acid Assay (BCA) Kit (#23225; Thermo Scientific™) according to manufacturer's protocol and by quadruplicate. A standard curve was prepared with bovine serum albumin (BSA) with concentrations ranging from 0.06 to 2 mg/mL, from which total protein concentration in the samples was quantified. Samples were diluted 1/4 and 1/8 and were loaded together with BSA standards in duplicates in a 96-well plate. 200 μ L of the kit A+B solution were added to each well and the plate was incubated at 37°C for 30 min before determining the absorbance at 580 nm using the Multiskan Ascent plate reader (Thermo Fischer™).

4.1.3 Mitochondrial phenotyping

4.1.3.1 Mitochondrial genetics, transcript and protein expression

In order to assess if mtDNA mutations or altered mitochondrial protein content could be responsible for mitochondrial alterations, the mtDNA, transcripts and protein expression in the context of *LRRK2*^{G2019S} mutation were measured as follows:

Mitochondrial DNA (mtDNA)

Total DNA was extracted by standard phenol chloroform procedure as previously reported (209) and total DNA concentration was measured using a Q5000 UV-Vis spectrophotometer. Samples were diluted to 5 ng/ μ L with 10 mM Tris pH 8.5.

To assess mtDNA content, fragments of the highly conserved mitochondrial 12S rRNA gene and the constitutive nuclear Ribonuclease P gene (RNase P) were simultaneously amplified by multiplex qRT-PCR in a 7900HT Sequence Detection system (Applied Biosystems™)(210). Polymerase chain reaction (PCR) was performed in triplicates in a final reaction volume of 20 µl containing 25 ng of total DNA. The reaction mix contained: 10 µl TaqMan Universal PCR Master Mix (Applied Biosystems™), 1 µl 20x RNaseP (Applied Biosystems™), 2.5 µl of RNase-free water, 2 mM of MgCl₂, 125 µM of forward mtF805 (50-CCACGGGAAACAGCAGTGAT-30), 125 µM of reverse mtR927 (50-CTATTGACTTGGGTTAATCGTGTGA-30) mitochondrial primers and 125 µM of TaqMan mitochondrial probe (6FAM-50TGCCAGCCACCGCG-30-MGB) (Sigma®). Settings of thermal cycling conditions were: 2 min at 50°C, 10 min at 95°C, followed by 40 cycles of 15 sec of denaturalization at 95°C and by 60 sec of annealing/extension at 60°C, according to manufacturer's instructions (Thermo Fisher Scientific Inc). mtDNA content, estimated through 12S rRNA expression, was corrected by simultaneous measurements of the single copy nuclear RNase P gene. Results were expressed as the ratio between a mtDNA encoded gene respect to the nuclear encoded one (mt12SrRNA/nRNaseP)(209).

Mitochondrial RNA (mtRNA)

Total RNA was extracted by affinity micro columns using SpeedTools Total RNA Extraction Kit® (Biotools™), following manufacturer's instructions and quantified using Quawell UV-Vis Spectrophotometer Q5000 in triplicates. After quantification, reverse transcription was performed by using random hexamer primers before the RTqPCR experiment. Mitochondrial RNA content was afterwards analysed through the amplification of ND2/18SrRNA cDNA. The results were expressed as the ratio between mitochondrial to nuclear RNA (mt12SrRNA/nRNaseP)(209).

Mitochondrial protein content

Western Blotting and immunoquantification was performed in duplicates with 15 µg of total protein through 7/13% SDS-PAGE and transferred using the iBlot Dry

Blotting System (Invitrogen) to nitrocellulose membranes 7 minutes at 20 V (iBlot Gel Transfer Stacks, Life Technologies). Blots were probed with VDAC, mt-COXII, n-COXIV and β -actin, the latter was used for sample normalization (**Table 9**).

Protein subunits quantification was performed by chemiluminescence with ImageQuantLD® and results were expressed as VDAC/ β -actin (mitochondrial content per cell), COXII/ β -actin (nuclear encoded mitochondrial proteins), COXIV/ β -actin (mitochondrial encoded mitochondrial proteins) and COXII/COXIV ratios (211).

4.1.3.2 Mitochondrial function

Complex I (CI) and complex IV (CIV) of the MRC have been previously associated to PD. Consequently, these two complexes were measured by spectrophotometry at 37°C following standardized procedures (212). Enzymatic activities were calculated as nanomoles of consumed substrate per minute and milligram of protein (nmoles/min*mg protein) and then normalized to citrate synthase (CS) activity to relativize the enzymatic activity by mitochondrial content.

Complex I enzymatic activity

Since CI transfers electrons from NADH to ubiquinone, its activity can be determined monitoring the decrease in absorbance of NADH at 340 nm. The ubiquinone or CoQ, a hydrophobic natural acceptor, is then converted into decylubiquinone, which is a hydrophilic compound.

Measurement of CI activity required previous treatment of cells with triton and digitonin detergents to obtain specific mitochondrial NADH-dehydrogenase activity (193). The specific activity of CI is calculated by subtracting the unspecific rotenone-insensitive activity from the total activity without rotenone because the activity of NADH cytochrome b₅ oxidoreductase, which also oxidises NADH, is not sensitive to rotenone, but rotenone is a specific inhibitor of CI.

Table 5. Reaction mix composition for measurement of CI enzymatic activity.

Complex I	
NADH	100mM
Decilubiquinone	100mM
Potassic phosphate	50mM
BSA	3.75mg/ml

BSA: Bovine serum albumin. NADH: Reduced form of nicotinamide adenine dinucleotide

Complex IV enzymatic activity

This complex transfers electrons from reduced cytochrome c to oxygen, and its activity can be determined monitoring the decrease in absorbance corresponding to the oxidation of reduced cytochrome c at 550 nm.

Table 6. Reaction mix composition for measurement of CIV enzymatic activity.

Complex IV	
Potassic phosphate	50mM
Reduced Cyt C	100mM

Cyt c: Cytochrome c.

Citrate synthase activity

Mitochondrial content was determined through the enzymatic activity of citrate synthase (CS). CS catalyses the formation of citrate from oxaloacetate and acetyl-CoA. The reduced form of CoA, CoA-SH, that is produced in last reaction transforms the 5,5'-dithiobis-2-nitrobenzoic acid (DTNB) into 2-nitro-5-thiobenzoic acid (TNB), at 412 nm. Thus, the citrate synthase activity can be evaluated by monitoring the increase of TNB absorbance at 412 nm.

Table 7. Reaction mix composition for measurement of citrate synthase enzyme activity.

Citrate synthase	
DTNB	100mM
Tris HCl pH 8.1	100mM
Acetyl-CoA	300mM
Oxaloacetate	500mM
Triton 100x	0.10%

DTNB: 5,5'-Dithiobis (2-nitrobenzoic acid); HCl: hydrochloric acid

Internal quality controls of known reference values were run in parallel simultaneously including controls and patients. In all cases, 20µl of sample were added to the reaction mix. Absorbance changes were monitored in a HITACHI U2900 spectrophotometer through the UV-Solution software v2.2 and were expressed as nanomols of consumed substrate or generated product per minute and milligram of protein (nmols/min*mg protein).

Table 8. Summary of reagents, wavelength and inhibitors used to measure the MRC enzymatic activities and citrate synthase.

	Monitored reagent	λ (nm)	Electron donor	Electron acceptor	Abs. Variation	Enzyme activity inhibitor
Complex I	NADH	340	NADH	Decylubiquinone	Negative	Rotenone
Complex IV	Reduced cyt c	550	Reduced cyt c	Oxygen	Negative	-
Citrate synthase	TNB	412	CoA	TNB	Positive	-

λ: Wavelength. NADH: Reduced form of nicotinamide adenine dinucleotide. TNB: 2-nitro-5-thiobenzoic acid. Cyt c: cytochrome c.

Mitochondrial Complex I-stimulated oxygen consumption

Mitochondrial respiration is the result of oxygen consumption by the MRC. CI stimulated oxygen consumption was assessed through pyruvate-malate oxidation (PMox) by high-resolution respirometry using Oroboros™ Oxygraph-2K® (Innsbruck,

Austria) in permeabilized fibroblasts, following manufacturer protocols (213). Briefly, 1 million of living fibroblasts were obtained and resuspended in ice-cold respiration MiR05 medium (0.5 mM EGTA, 3 mM MgCl₂, 60 mM K-lactobionate, 20 mM taurine, 10 mM KH₂PO₄, 20 mM HEPES, 110 mM sucrose and 0.1% BSA (w/v), pH 7.1). Data recording and analysis were performed using DatLab software v5.1.1.9 (Oroboros Instruments), respectively, following manufacturer's protocol. The oxygen consumption under the stimulation of mitochondrial CI with NAD-linked substrates was evaluated in digitonin-permeabilized cells.

Results were normalized by protein concentration and were expressed as pmol O₂/s·million cells (nmoles/min*mg protein).

Total cellular ATP.

In order to quantify the bioenergetic efficiency of mitochondrial respiration, total cellular ATP was measured in duplicates by using the Luminescent ATP detection assay kit® (#ab113849; Abcam™), according to manufacturer's instructions. Results were normalized by protein levels and expressed as picomoles of ATP per microliter and milligram of cell protein (pmol ATP / μ l*mg prot).

4.1.3.3 Mitochondrial damage markers

In order to assess if the presence of *LRRK2*^{G2019S} mutation is associated with a mitochondrial lesion, or if mitochondria are more prone to mitochondrial damage in front of challenging conditions, MMP, lipid peroxidation and apoptotic rate were measured.

Mitochondrial Membrane Potential

MMP is a marker of early mitochondrial lesion that may resolve after mitochondrial fusion or progress to mitochondrial clearance by autophagy or destruction, with increase of ROS.

MMP was evaluated in triplicates by flow cytometry in a BD FACSCalibur™ cell analyser (BD Biosciences) using 5,5',6,6'-tetrachloro-1,1',3,3' tetraethyl benzimidazolocarboyanine iodide dye (JC-1). JC-1 is a cationic carboyanine dye that exhibits potential-dependent accumulation in mitochondria, indicated by a fluorescence emission shift from green (~525 nm) to red (~590 nm). Mitochondrial depolarization is indicated by a decrease in the red/ green fluorescence intensity ratio. The potential-sensitive colour shift is due to concentration dependent formation of red fluorescent J-aggregates (214).

In order to measure MMP in fibroblasts, 0.5 million cells were resuspended in DMEM and stained with 2.5 µg/mL of JC-1 for 10 min at room temperature and protected from light. Cells were then washed with PBS 1x and the pellet was resuspended in PBS 1x for immediate flow cytometric analysis. Both, green and red fluorescent emissions of each cell population were simultaneously measured, as reported elsewhere (215) Results were obtained as percentage of cells with specific fluorescence indicating polarized or depolarized mitochondria.

The results were expressed as the percentage of fibroblasts with depolarized mitochondria, with respect to total cells (% cells with depolarized mt/total cells) as previously described (216).

Oxidative damage

Lipid peroxidation was measured as an indicator of oxidative damage of ROS into cellular lipid compounds using the Colorimetric assay for Lipid Peroxidation Kit #21012; Bioxytech® LPO-586™, OxisResearch™, by the spectrophotometric measurement of malondialdehyde (MDA) and 4-hydroxyalkenal (HAE), both products derived from fatty acid peroxide decomposition, at 586 nm (216). Oxidative damage analysis was carried out in duplicates.

Results were normalized by protein content, and expressed as MDA and HAE concentration (in micromoles per litre) per milligram of cell protein (μM MDA + 4-HAE/mg prot).

Apoptotic rate

Advanced apoptosis and necrosis phenomena were assessed to explore the failure to recover from mitochondrial lesion using the annexin V and propidium iodide (PI) ratio by means of flow cytometric analysis in a BD FACSCalibur™ cell analyzer (BD Biosciences) as previously reported (217). Briefly, a total of 1 ml of complete culture media containing roughly 2×10^5 cells was prepared for dye and subjected to incubation with 0.05% annexin V plus PI (556463; BD Biosciences) for 10 min. to assess advanced apoptotic and necrotic events.

Results were reported as the percentage of double stained cells, with respect to total cells (% stained cells/total cells).

4.1.3.4 Mitochondrial dynamics

The maintenance of mitochondrial homeostasis is greatly dependent on mitochondrial dynamics. LRRK2 has been suggested to play a role in mitochondrial fission and cytoskeleton integrity.

For immunocytochemistry, fibroblasts were seeded in a 16-well glass slide (Nunc™ #178599 Lab-Tek® Chamber Slide™) in both, glucose and galactose media, for 24 h. Mitochondrial network was stained by incubation with rabbit Tom20 Antibody (FL-145) (Santa Cruz Biotechnology) and secondary antibody donkey anti-rabbit Alexa Fluor® 488 IgG (Life Technologies). Wheat Germ Agglutinin Alexa Fluor® 594 conjugate (Life Technologies) and TO-PRO 3® iodide #T3605 (Life Technologies) were used for cytoplasm immunostaining and nuclei detection, respectively. Images were obtained with a Leica™ TCS SP5 laser scanning confocal system using 63X oil immersion objective. Analysis was performed using 2.5X zoom for each cell in at

least 3 cells per patient and quantification of parameters was done by using a semi-automatized macro for Image J (218) software.

The following parameters were assessed for mitochondrial dynamics evaluation (**Figure 16**):

1) Mitochondrial network or mitochondrial content: Mitochondrial network refers to the total number of mitochondria within the total cell area (219); higher mitochondrial network values are accountable for healthy mitochondria.

2) Circularity (Circ): This parameter indicates mitochondrial isolation. The formula for its calculation is:

$$\frac{4\pi \times \text{area}}{\text{Perimeter}^2}$$

Circ=1 refers to poor mitochondrial dynamics, since circular mitochondria have less interaction sites with other mitochondria.

3) Aspect Ratio (AR): AR refers to mitochondrial elongation and its value increases as mitochondria elongate and become more elliptical, which is considered a beneficial sign of mitochondrial dynamics. It is calculated as:

$$\frac{\text{Major axis}}{\text{minor axis}}$$

AR=1 indicates a perfect circle which translates into poor mitochondrial dynamics.

4) Form factor (FF): Mitochondrial branching defines FF. It is calculated as the inverse value of circularity:

$$\text{Circ}^{-1};$$

FF=1 corresponds to a circular, unbranched mitochondrion and high FF values indicate a branched, connected and active mitochondrion which is favourable for mitochondrial function.

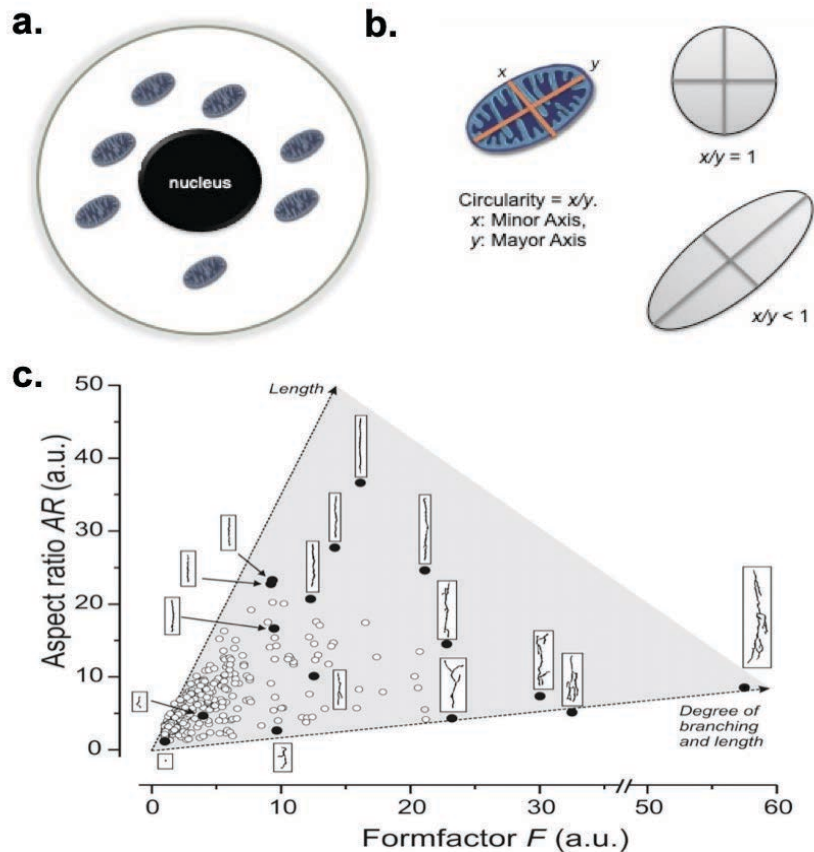


Figure 16. Morphological descriptors of mitochondrial shape.

a. Mitochondrial network; **b.** Circularity. Circular mitochondria are considered to present more pathological features since they have less interaction sites with other mitochondria **c.** Aspect ratio and form factor: Mitochondrial elongation and branching. Both are considered to be indicators of healthy mitochondrial dynamics. Modified from: H Koopman, *Am J Physiol Cell Physiol* 2005, 288, 1440–1450 (220).

4.1.4 Autophagy characterization

In order to assess autophagic alterations in the context of *LRRK2*^{G2019S} mutations, we aimed to characterize autophagic print in glycolytic conditions and after exposure to galactose media.

4.1.4.1 Western blot immunoquantification

Characterization of steady-state autophagic print was carried out by Western Blotting and immunoquantification of autophagic related proteins after 24 hour exposition to both media (glucose and galactose). To further assess autophagosome

formation, cells were seeded again in 6-well plaques with glucose and galactose media for 24 hours, after which 100 nM bafilomycin A1 (BAF) was added at two different time points (4 and 8 hours). Bafilomycin A1 is a proton pump inhibitor that neutralizes lysosomal pH preventing fusion of autophagosomes with lysosomes and thus allowing monitoring of autophagosome synthesis by measuring the accumulation of both, SQSTM1/p62 and LC3B2 (221).

Cells were harvested in ice-cold PBS and centrifuged 8 min at 500 g. Next, cell pellets were lysed with radioimmunoprecipitation assay (RIPA) buffer and Halt Protease Inhibitor Single-Use Cocktail EDTA-Free (#78425, ThermoScientific™) and maintained in agitation 30 min on ice followed by centrifugation at 14,000 g at 4°C for 10 min. Soluble fractions were retained for Western Blot analysis. Electrophoresis was performed with 15 µg of total protein through 7/15% SDS-PAGE and transferred into nitrocellulose membranes (iBlot® Gel Transfer Stacks, #IB301001, Invitrogen™) using a iBlot Dry Blotting System (Invitrogen™) for 7 minutes at 20 V following 3 hour-blocking with 10% skimmed milk. Membranes were hybridized with Anti-SQSTM1/p62 and anti-LC3B antibodies overnight at 4 °C. Protein expression was normalized by β-actin protein content in all cases, as a cell loading control (**Table 9**). Chemiluminescence was quantified with ImageQuantLD® and results were expressed and interpreted as:

Autophagy initiation

SQSTM1/p62 is an ubiquitin-binding scaffold protein that acts as a cargo receptor recruited to autophagosomes through LC32 interaction. It serves as an autophagy substrate widely used as a marker of autophagy initiation [13]. Results were expressed as (SQSTM1/p62)/β-actin after 0, 4 and 8 hours of BAF.

Autophagosome number

LC3B is an ubiquitin-like protein that is a necessary for the formation of the autophagosome. LC3B1 is unspecific and expressed in the autophagosome membrane but can also be located in cytoplasm or other organelles. Its lipidation and

migration to the autophagosome membrane (LC3B2) is the lipidated form of the autophagy receptor and is considered to be a marker of autophagosome number (222). Results were expressed as (LC3B2/ β -actin) after 0, 4 and 8 hours of BAF.

Table 9. Antibodies used for Western Blot and summary of optimal conditions.

Protein	Primary antibody	Band size (KDa)	Dilution used	SDS-PAGE	Secondary antibody
VDAC1	Anti-VDAC1/Porin antibody Abcam ab14734	37	1:1000	7/13%	Anti-mouse
mt-COXII	MTCO2 antibody Invitrogen™ #A-6404	25.6	1:1000	7/13%	Anti-mouse
n-COXIV	Complex IV Monoclonal antibody Invitrogen™ #A-6404	15	1:1000	7/13%	Anti-mouse
β -actin	β -actin antibody Sigma-Aldrich® #A2228	42	1:30.000	7/13%	Anti-mouse
SQSTM1/p62	Anti-SQSTM1/p62 antibody Abcam ab56416	62	1:60.000	7/15%	Anti-mouse
LC3B	LC3B antibody Cell Signaling® #2775	14 and 16	1:250	7/15%	Anti-rabbit

VDAC1: Voltage-dependent anion-selective channel 1; mt-COXII: Cytochrome c oxidase subunit II; n-COXIV: Cytochrome c oxidase subunit IV; SQSTM1/p62: Sequestrosome1 p62; LC3B: (Microtubule-associated protein 1) light-chain 3 beta

4.1.4.2 Immunocytochemistry

To further characterize autophagosome formation in glucose and galactose media in the basal state and after 8 h exposure to 100 nM BAF, immunostaining and confocal microscopy was used. Briefly, cultured skin fibroblasts were washed with PBS before fixation with 4% paraformaldehyde for 15 min. Fixed cells were washed, permeabilized with 0.1% Digitonin in blocking solution (1% BSA). Cells were incubated for 1 hour using Anti-LC3 (1:1000, PM036, MBL) followed by Goat anti-Rabbit IgG secondary antibody; Alexa Fluor 488 (A11008, Thermofisher™). Counterstaining with DAPI Fluoromount-G® (0100-20, Southern Biotech was

performed for nucleus visualization. Images were obtained with a Zeiss LSM 880 laser scanning confocal system using 63X oil immersion objective.

4.1.5 Statistical analysis

Results were expressed as mean \pm standard error of mean (SEM) and as a percentage (%) of increase/decrease with respect to controls, which were arbitrarily assigned as a 0% baseline. Two statistical approaches were performed for each media (glucose or galactose): (i) Non-parametric Mann–Whitney analysis for independent samples to detect inter-group differences for individual parameters and (ii) Principal Component Analysis (PCA) to define the component with the largest possible variance and to show whether the studied population would be clustered by group, age or sex. Statistical analysis was performed with SPSS 20.00 (for Mann-Whitney test) and R Studio Desktop 1.0.153, missMDA, estim_ncpPCA and imputPCA R functions (for PCA). Statistical significance was set at $p < 0.05$ in all cases.

4.2 STUDY 2: Characterization of GBA^{N370S} neurospheres

4.2.1 Study design and population

A single-site, cross-sectional, observational study was conducted. Six age and gender paired subjects were included: heterozygotes for GBA^{N370S} -mutation (wt/GBA^{N370S} , n=2), homozygotes for GBA^{N370S} -mutation (GBA^{N370S}/GBA^{N370S} , n=2), and healthy, unrelated controls (wt/wt , n=2).

Subjects with mitochondrial disorders, and those consuming mitochondrial toxic drugs were not included in any of those groups (207).

All patients and controls included presented their informed consent according to the Declaration of Helsinki. The Royal Free Research Ethics Committee (REC number 10/H0720/21) approved this study. Methods have been performed in accordance with the appropriate guidelines and regulations of University College of London.

4.2.2 Cell model development

Skin-punch biopsies containing subcutaneous adipose tissues (6 mm in diameter) were obtained from the arm of participants; the subcutaneous adipose tissues were dissected from skin and used for cell isolation.

Human subcutaneous adipose tissues were washed once with growth medium and dissected into small pieces (less than 0.2 cm diameter). The small pieces of adipose tissues were explanted in fibronectin-coated 6-well plates. A sterilized coverslip was used to cover the tissue in order to prevent tissue floating in the medium. Media was changed every 4 days until migrated cells reached 60%–70%

confluence; at this time, migrated cells are human adipose neural crest stem cells (haNCSc).

4.2.2.1 Neurosphere culture and characterization

The haNCSc were dissociated from the well with Accutase (Millipore) and seeded in normal culture dishes with DMEM media supplemented with 10% foetal bovine serum, 1mM pyruvate, 0.5 ml uridine (50mg/ml) and 0.5% penicillin-streptomycin-fungizone. When haNCSc reached 70%–80% confluence, the growth medium was removed; cells were washed with PBS without Ca²⁺ and were incubated with accutase (1 mL/dish; 100 × 20 mm) at 37°C for 3–5 min.

Growth medium was added to the dissociated cells and the medium containing cells was divided over three individual dishes. Cells were cultured and maintained in growth medium at 37°C with 5% CO₂.

Neurosphere formation and maintenance

When haNCSC reached to 70%–80% confluence, cells were dissociated with accutase at 37°C for 3–5 min. Growth medium was added to the dish to inhibit accutase activity. Cells were collected and pelleted by centrifugation at 200 × g for 10 min. The cell pellet was resuspended with neurosphere formation medium (DMEM-F12 (1:1) containing the following supplements and growth factors, 1x B27, 20µL leukaemia inhibitor (10ng/mL), basic fibroblast growth factor (40ng/mL FGF2), epidermal growth factor (10ng/mL EGF) and 1% penicillin-streptomycin-fungizone, transferred to an uncoated 12-well plate, and incubated at 37°C with 5% CO₂. Neurospheres formed within 24 hours in neurosphere formation medium. The neurospheres were cultured and maintained in the same conditions with medium changes every 5 days (142).

Neurosphere characterization

To identify the time point when neurospheres become biochemically stable, in which the influence of *GBA*^{N370S} zygosity on neurosphere formation was compared, and to confirm the presence and dedifferentiation to neural stem cells, protein levels of neuronal markers β -III tubulin and Microtubule-associated protein 2 (MAP2) were measured twice by Western Blotting from the 6 lines over time, as described in the following section (**Table10**).

Levels of mRNA

Stem-cell marker, Nestin, was measured through mRNA expression was assessed in duplicates as follows: RNA was extracted from cells using RNeasy kit (Qiagen). RNA was converted to cDNA and relative mRNA levels were measured using SYBERgreen (Applied Biosystems).

Relative expression of Nestin mRNA (forward 5' ACCAAGAGACATTCAGACTCC 3' and reverse 3' CCTCATCCTCATTTTCCACTCC 5') was measured with Power SYBRgreen kit (Applied Biosystems) using a STEP One PCR device (Applied Biosystems). Glyceraldehyde-3-Phosphate Dehydrogenase (GAPDH) mRNA levels GAPDH mRNA levels (forward 5' GAA GGT GAA GGT CGG AGT 3' and reverse 3' GAA GAT GGT GAT GGG ATT TC 5') were used to normalize data. Relative expression was calculated using the Δ CT method.

Lysosomal enzyme assays

Lysosomal enzyme analyses were also performed twice as part of the characterization and validation of neurospheres as a proper model for the effects of *GBA* mutation. GCCase, β -hexosaminidase (HEX) and β -galactosidase (β -gal) enzyme activities were determined in duplicates at 37 °C. CE-sensitive GCCase activity (end-point measurement) was determined as described at pH 5.4 using 4-methylumbelliferyl- β -d-glucopyranoside as substrate in a plate reader and its activity is reported in the presence of the activator sodium taurocholate (Sigma®). The increase in fluorescence of released 4-methylumbelliferone at 460 nm following

excitation at 360 nm was followed after 1 h (Synergy, LabTech). Total HEX and β -gal were assayed with 4-methylumbelliferyl-2-acetoamido-2-deoxy-6-sulpho-b-D-glucopyransoside and 4-methylumbelliferyl-B-D-galactopyransoside as substrates, respectively. Enzyme activities were normalised to the amount of protein of the samples and results were expressed as nmol/minute*mg protein.

Western blot Immunoquantification

Neurospheres were lysed and placed on ice for 15 min with RIPA buffer supplemented with 1x Halt protease inhibitor cocktail (Pierce). Cell lysates were centrifuged at 21,000g at 4°C for 5min and soluble material was retained for Western Blot analysis.

Total protein content was determined by quadruplicate using the Pierce BCA Protein Assay Kit (#23225; Thermo Scientific™), as described in section 4.1.2.

Equal amounts of protein (20 μ g) from the soluble material were resolved under reducing conditions in either: i) NuPAGE 4-12% polyacrylamide precast gels (Invitrogen) using the 2 (N morpholino) ethane sulphonic acid (MES) buffer or: ii) NuPAGE 12% (Invitrogen) using 3-(N-morpholino) propanesulfonic acid (MOPS) buffer and transferred onto Immobilon polyvinylidene difluoride membrane (PVDF) (Millipore). Blocking was made with 10% skimmed milk powder in PBS.

Antibodies detecting MAP2, β -III tubulin and α -synuclein were incubated overnight at 4°C. β actin was used as a loading control. Horseradish peroxidase conjugated secondary antibodies against mouse and rabbit IgG were used as specified in (**Table 10**). ECL reagent (GE Healthcare) was used to develop the blots and signals detected through the Chemidoc MP System (BioRad) and band densities measured using ImageLab analysis software (BioRad).

4.2.2.2-Uncoupling stress test

All mitochondrial experimental parameters were measured upon Carbonyl cyanide *m*-chlorophenyl hydrazine (CCCP) treatment to evaluate the basal mitochondrial state and the effect of uncoupling mitochondria from the neurospheres of the three groups included in the study.

Induction of mitophagy through mitochondrial uncoupling was performed/conducted by treating the neurospheres with 10 μ M CCCP for 24 hours. CCCP is a nitrile, hydrazone and protonophore that causes an uncoupling of the proton gradient that during the normal activity of electron carriers in the MRC. It acts essentially as an ionophore and reduces the ability of ATP synthase to function optimally.

To confirm CCCP-derived mitochondrial depolarization 3 approaches were conducted:

1) MMP was assessed by flow cytometry over time of CCCP treatment using tetramethylrhodamine methyl ester (TMRM). TMRM is a cell-permeant, cationic, red fluorescent dye. Because of its positive charge, TMRM accumulates in negatively charged mitochondria. When mitochondria are depolarized, stored anions are released and TMRM concentration also decreases. TMRM is a cell-permeant dye that accumulates in active mitochondria with intact membrane potentials. If the cells are healthy and have functioning mitochondria, the signal will be bright. Upon loss of the MMP, TMRM accumulation will cease and the signal will dim or disappear.

2) The switch of the long isoform of optic atrophy protein 1 (L-OPA1) to the short form of the protein (S-OPA1) was assessed by Western Blot as described above (**Table 10**).

3) Decrease in the widely used mitochondrial marker Tom20 upon CCCP treatment over time, assessed by Western Blot as described above (**Table 10**).

4.2.3 Mitochondrial phenotyping

To assess for if mitochondrial alterations could exist in the context of *GBA*^{N370S} mutation, the following mitochondrial experimental parameters were performed in neurospheres, in basal conditions and after CCCP uncoupling, to evaluate the mitochondrial response to an external insult.

4.2.3.1 Mitochondrial content and biogenesis

Mitochondrial content markers

Mitochondrial markers from: i) outer mitochondrial membrane (VDAC-1), ii) inner mitochondrial membrane (Succinate dehydrogenase complex, subunit A: SDHA) and iii) mitochondrial matrix (Mitochondrial transcription factor A: TFAM) were measured in duplicates by Western Blot as described in the previous section and used as biomarkers of mitochondrial content (**Table 10**) (223,224).

Mitochondrial biogenesis

Following CCCP treatment, RNA was extracted from cells using RNeasy kit (Qiagen). RNA was converted to cDNA (Primer Design) and relative mRNA levels were measured using SYBERgreen (Applied Biosystems). Relative expression of the mitochondrial TFEB (forward CCA GAA GCG AGA GCT CAC AGA T and reverse TGT GAT TGT CTT TCT TCT GCC G) and Peroxisome proliferator-activated receptor gamma coactivator 1-alpha (PGC-1 α) (forward CAG AGA ACA GAA ACA GCA GCA and reverse TGG GGT CAG AGG AAG AGA TAA A) were measured as described in section 4.2.2.3, as a reliable markers of mitochondrial biogenesis (77). Data was normalized by GAPDH mRNA levels (forward GAA GGT GAA GGT CGG AGT and reverse GAA GAT GGT GAT GGG ATT TC) and relative expression was calculated using the Δ CT method.

4.2.3.2 Mitochondrial function

ATP levels before and after mitochondrial uncoupling were measured with the ATP Bioluminescence Assay Kit CLS II (#11699695001, Roche), in triplicates following manufacturer's instructions. Briefly, different dilutions of samples and serial

diluted ATP standards were included as an internal curve in a black opaque microplate. Then, a volume of 50µl luciferase reagent was added and luminescence was immediately measured in a synergy device (Synergy, LabTech). ATP levels were normalised to the amount of total protein. Results were expressed as femtomolATP/µl*mgprot (FmolATP/µl*mgprot).

4.2.4 Autophagy characterization

4.2.4.1 Western blot immunoquantification

Steady state levels of autophagy were in duplicates measured by immunoquantification of SQSTM1/p62 and LC3B2, normalized by β-actin as described before (**Table 10**). BAF treatment was performed for 4 hours at 0.5 µM.

4.2.4.2 Mitophagy-associated mRNA levels

To evaluate mitophagy, *PINK1* mRNA levels (forward 5' GGA CGC TGT TCC TCG TTA 3' and reverse 3' ATC TGC GAT CAC CAG CCA 5') were measured in duplicates by PCR and normalized by GAPDH mRNA levels as described in section 4.2.2.3.

Table 10 Antibodies used for Western Blot and summary of optimal conditions.

Protein	Primary antibody	Band size (KDa)	Dilution used	SDS-PAGE	Secondary antibody
MAP2	MAP2 antibody Invitrogen # 13-1500	37	1:1000	7/12%	Anti-mouse
β III tubulin	Anti-beta III Tubulin antibody Abcam, ab7751	52	1:1000	7/12%	Anti-mouse
α -syn	Anti-alpha-synuclein antibody abcam ab27766	14	1:1000	7/12%	Anti-mouse
OPA 1	Anti-OPA1 BD Transduction laboratories BD/612606	110	1:500	7/12%	Anti-mouse
TOM20	Tom20 policlonal antibody Santa Cruz sc-11415	15	1:1000	7/12%	Anti-rabbit
VDAC	Anti-VDAC1/Porin antibody Abcam ab14734	31	1:1000	7/12%	Anti-mouse
SDHA	Anti-SDHA antibody Abcam ab14715	70	1:1000	7/12%	Anti-mouse
TFAM	TFAM monoclonal antibody Thermofisher MA5-16148	25	1:1000	7/12%	Anti-mouse
SQSTM/p62	Anti-SQSTM1 / p62 antibody Abcam ab56416	62	1:1666	7/12%	Anti-mouse
LC3B	LC3B antibody Cell Signaling® #2775	14	1:1000	7/12%	Anti-rabbit
β -actin	β -actin antibody Sigma-Aldrich® #A2228	42	1:10.000	7/12%	Anti-mouse

MAP2: Microtubule-associated protein 2; α -syn: alfa-synuclein; OPA1: optic atrophy protein 1; Tom20 (Translocase of outer mitochondrial membrane 20); VDAC-1: Voltage-dependent anion-selective channel 1; SDHA: Succinate dehydrogenase complex, subunit A; TFAM: Mitochondrial transcription factor A SQSTM1/p62: Sequestrosome1 p62; LC3B: (Microtubule-associated protein 1) light-chain 3 beta.

4.2.5 Statistical analysis

Results were expressed as means \pm SEM. Even though we acknowledge the small sample size of this study, for a better interpretation of the results, one-way ANOVA followed by Bonferroni's post-hoc correction was performed using SPSS Version 20 to assess whether differences between groups were present. Significance cut off was set at $p < 0.05$.



5. RESULTS



5.1 STUDY 1: Characterization of *LRRK2*^{G2019S} fibroblasts

Title:

Exhaustion of mitochondrial and autophagic reserve may contribute to the development of *LRRK2*^{G2019S}-Parkinson's disease

Authors:

Diana Luz Juárez-Flores, Ingrid González-Casacuberta, Mario Ezquerra, María Bañó, Francesc Carmona-Pontaque, Marc Catalán-García, Mariona Guitart-Mampel, Juan José Rivero, Ester Tobías, José César Milisenda, Eduard Tolosa, Maria Jose Marti, Ruben Fernández-Santiago, Francesc Cardellach, Constanza Morén and Glòria Garrabou

Reference:

J Transl Med (2018) 16:160

<https://doi.org/10.1186/s12967-018-1526-3>

IF 2017: 4.19 (Q1)

See Annex section, page 197

The objective of the first study of this thesis was to assess the genotype-phenotype correlation and to characterize the mitochondrial and autophagic phenotype in standard conditions and after a mitochondrial insult (exposure to galactose media) in fibroblasts of *LRRK2*^{G2019S}-associated PD. We also aimed to identify a molecular hallmark that could either predict or characterize the development of PD-symptoms in subjects carrying *LRRK2*^{G2019S}-mutation.

The results of study 1 are presented in three parts:

- 1) The first part consists of epidemiological and clinical data of the subjects included in the study.
- 2) The second part encompasses an exhaustive description of mitochondrial genetics, function and dynamics of NM-*LRRK2*^{G2019S} subjects and PD-*LRRK2*^{G2019S} patients compared to controls in a standard vs. mitochondrial challenging conditions (glucose vs. galactose).
- 3) The third part includes the assessment of autophagic flux in standard and mitochondrial challenging conditions

Raw data obtained from the experimental work is available in Supplementary material.

5.1.1 Epidemiological and clinical data

Epidemiological and clinical data of the studied cohorts at the time of skin biopsy are shown in **Table 11**. No significant differences in age and gender between groups were found, suggesting that further observed changes among cohorts or conditions should not be attributed to epidemiologic characteristics.

Table 11. Epidemiological characteristics of cohorts

GROUP	N	GENDER		AGE		
		Male	Female	Range	Mean	SEM (\pm)
NM- <i>LRRK2</i> ^{G2019S}	6	3 (50%)	3 (50%)	34-61	46.67	4.04
PD- <i>LRRK2</i> ^{G2019S}	7	3 (42.85%)	4 (57.14%)	44-71	60.57	3.15
Control	8	3 (37.50%)	5 (62.50%)	41-69	56	3.63
TOTAL	21	9 (42.85%)	12 (57.14%)	34-71	54.86	2.34

N: number of subject included in the study; NM-*LRRK2*^{G2019S}: Non-manifesting carriers of *G2019S*LRRK2 mutation; PD-*LRRK2*^{G2019S}: Manifesting carriers of *G2019S*LRRK2 mutation; SEM: Standard error of the mean

Clinical characteristics of PD-*LRRK2*^{G2019S} patients are shown in **Table 12**. None of the NM-*LRRK2*^{G2019S} subjects had developed clinical symptoms of the disease at the time of results analysis confirming their asymptomatic status throughout and after the study.

Table 12 Clinical characteristics of PD-*LRRK2*^{G2019S} patients (n=7)

CLINICAL FEATURES AT TIME OF BIOPSY		PRESENT	NOT PRESENT	UNKNOWN
MUTATION	<i>G2019S</i>	7	0	0
FAMILY HISTORY	Parkinsonism	5	0	2
	Dementia	0	5	2
DIAGNOSTIC CRITERIA	Unilateral tremor at beginning	6	0	1
	Tremor at rest	5	1	1
	Progressive disease	6	0	1
	Assymetric persistence	5	1	1
CLINICAL FEATURES AT TIME OF BIOPSY	Tremor at rest	5	1	1
	Dementia	1	5	1
	Deep brain stimulation	2	3	2
	Clinical course > 10 years	4	1	2
RESPONSE TO TREATMENT	First response to Ldopa	5	0	2
	Response to Ldopa>5 years	3	0	4

5.1.2 Mitochondrial phenotype

***Mitochondrial phenotype of NM-LRRK2*^{G2019S}**

Mitochondrial parameters were preserved in NM-*LRRK2*^{G2019S} subjects in glucose media with respect to controls, except for early MMP depolarization (54.14%, $p=0.04$, **Figure 17.a.8** and **19.f**) and increased mitochondrial network (38.32%, $p=0.04$, **Figure 17.a.11** and **Figure 20.b**) suggesting a conserved mitochondrial function in this condition.

After galactose exposure, CI enzymatic function, O₂ consumption stimulated for CI, CIV enzymatic function and ATP levels of NM-*LRRK2*^{G2019S} trended to overcome the level of controls (76.92%, 76.87%, 88.48% and 61.98%; $p=0.18$, $p=0.35$, $p=0.14$ and $p=0.76$, respectively), suggesting an adaptation to mitochondrial challenging conditions (**Figure 17.a.4 – 17.a.7**, **Figure 19.b – 19.e**). Mitochondrial dynamics ameliorated in fibroblasts of NM-*LRRK2*^{G2019S} with respect to controls when

exposed to galactose medium, evidenced by 17.54% decreased circularity ($p=0.002$) and 42.53% increased form factor ($p=0.051$) (**Figure 17.a.12** and **17.a.14**), accounting for longer, more branched mitochondria (**Figure 20.c** and **20.e**), which can be interpreted as an outstanding adaptation to mitochondrial-challenging conditions.

All of the above suggests that mitochondrial function of NM-LRRK2^{G2019S} was almost preserved in standard conditions (glucose) and ameliorated when subjected to mitochondrial challenging conditions (galactose), in order to maintain ATP production over controls.

Mitochondrial phenotype of PD-LRRK2^{G2019S}

In fibroblasts from PD-LRRK2^{G2019S} patients in glucose media, CI enzyme function, O₂ consumption stimulated for CI and ATP levels seemed to decrease with respect to controls (**Figure 17.b.4, 17.b.5, 17.b.7, Figure 19. b, 19.c** and **19.e**). Noticeably, although not significantly, depolarized mitochondria augmented to 101.34% ($p=0.14$), accompanied by a 90% increase of oxidative stress ($p=0.46$) with respect to controls (**Figure 17.b.8, 17.b.9, Figure 19.f** and **19.g**) suggesting a pre-existing mitochondrial lesion in this group of patients.

Exposure of PD-LRRK2^{G2019S} fibroblasts to galactose media increased CI enzyme function compared to controls (84.62%, $p=0.04$), but such increase was neither translated into heightened oxygen consumption, nor enhanced CIV enzyme function or ATP synthesis (**Figure 17.b.4 - 17.b.7** and **Figure 19.b -19.e**), as formerly observed in asymptomatic carriers. Instead, oxidative damage increased 144.64% ($p=0.13$) (**Figure 17.b.9** and **Figure 19.g**) and, in detriment to mitochondrial dynamics, aspect ratio decreased 37.7% ($p=0.053$) after exposure to mitochondrial challenging conditions (**Figure 17.b.13** and **Figure 20d**).

In summary, PD-LRRK2^{G2019S} showed mitochondrial alterations in standard (glucose) media and aggravated their performance when subjected to mitochondrial-challenging (galactose), resulting in an inefficient increase of CI activity that yielded towards increased oxidative stress and altered mitochondrial dynamics. Overall, these results reproduce the mitochondrial pathologic hallmarks described in PD described in previous studies, such as CI dysfunction and increased oxidative stress.

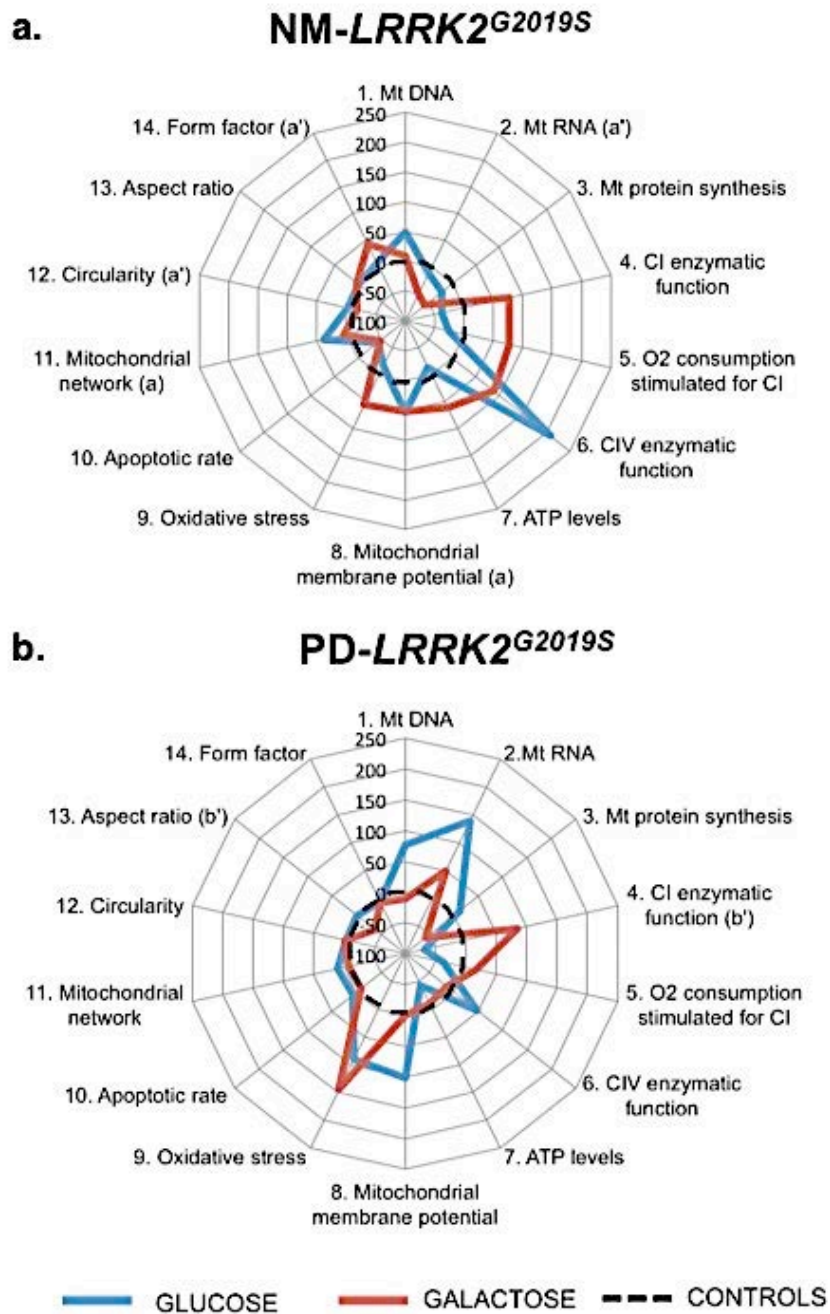


Figure 17 (Previous page). Mitochondrial phenotype of *LRRK2*^{G2019S}-mutation carriers.

Mitochondrial parameters measured in *LRRK2*^{G2019S}-mutation carriers, represented as a percentage of decrease/increase when compared to healthy controls, arbitrarily assigned as 0% (black, dotted line) in glucose (blue line) and galactose media (red line). The letters (a), (a'), (b) and (b'), indicate those cases in which a statistical difference within the two analysed groups and controls was found: (a) $p < 0.05$ when comparing NM-*LRRK2*^{G2019S} to controls in glucose media, (a') $p < 0.05$ when comparing NM-*LRRK2*^{G2019S} to controls in galactose media, (b) $p < 0.05$ when comparing PD-*LRRK2*^{G2019S} to controls in glucose media and (b') $p < 0.05$ when comparing PD-*LRRK2*^{G2019S} to controls in galactose media.

In summary, fibroblasts of NM-*LRRK2*^{G2019S} showed a pattern similar to controls in glucose, except for early disruption of MMP. When subjected to mitochondrial challenging conditions, global mitochondrial function and dynamics trended to ameliorate, towards ATP production **(a)**. Fibroblasts of PD-*LRRK2*^{G2019S} in glucose trended towards a deranged mitochondrial function when compared to controls. When subjected to galactose media, PD-*LRRK2*^{G2019S} fibroblasts presented an inefficient increase of mitochondrial function and worsened mitochondrial dynamics, leading to increased oxidative stress **(b)**.

The above-presented information and its interpretation derive from a thorough analysis of the results presented in **Figure 18**, **Figure 19** and **Figure 20**.

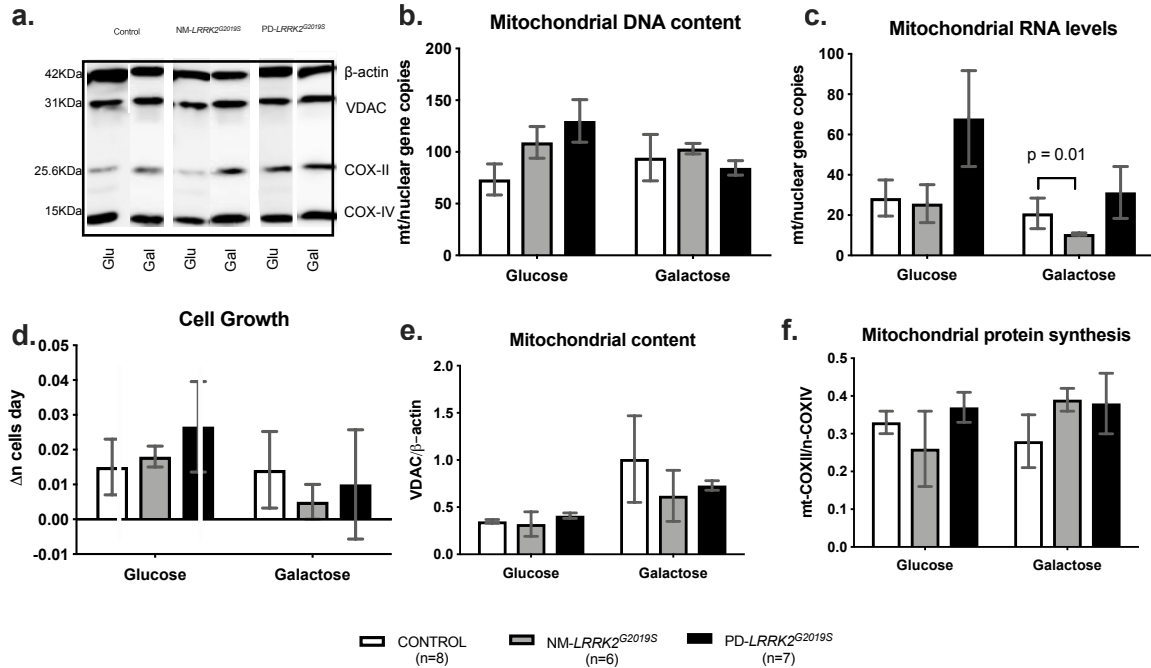


Figure 18. Cell growth, mitochondrial genome, content and protein synthesis.

Results are represented by means \pm SEM, comparing controls (white bars), NM-*LRRK2*^{G2019S}, (grey bars) and PD-*LRRK2*^{G2019S} (black bars) in glucose and galactose media. **a.** Representative image of Western Blot of mitochondrial proteins in either glucose (Glu) or galactose (Gal) media of the three cohorts studied. Mitochondrial DNA was conserved in both groups and media (**b**), while mtRNA levels were significantly decreased in NM-*LRRK2*^{G2019S} when compared to controls in galactose media (**c**). However, there was not an effect in protein translation, and cell growth (**d**), mitochondrial content (**e**) and protein synthesis (**f**) did not show differences between groups, in either condition. This findings suggest minimal changes on measured cell and mitochondrial parameters.

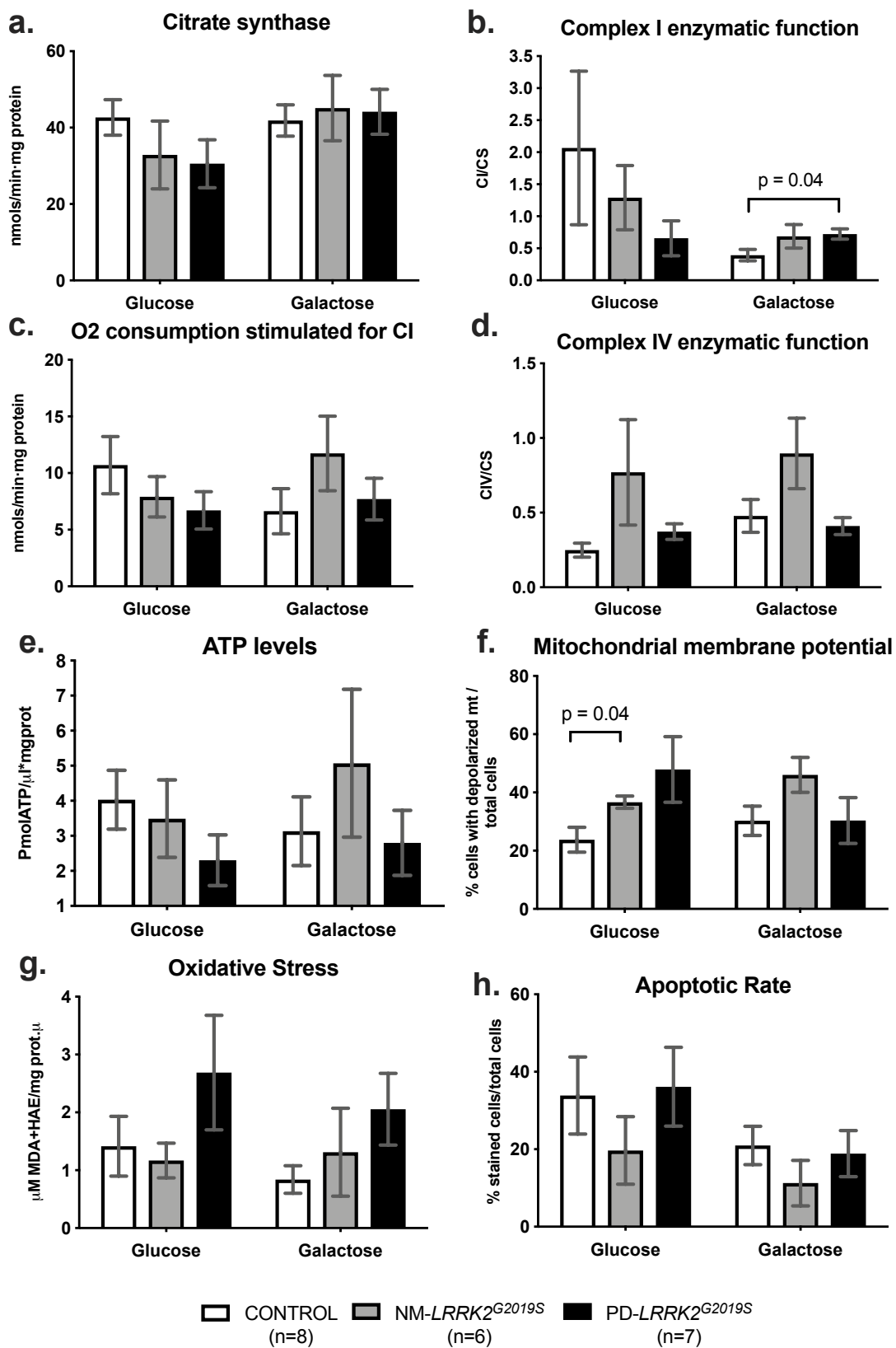


Figure 19 (Previous page). Mitochondrial function.

Results are represented by means \pm SEM, comparing controls (white bars), NM-*LRRK2*^{G2019S} (grey bars) and PD-*LRRK2*^{G2019S} (black bars) in glucose and galactose media. A specific functional parameter that describes mitochondrial dysfunction could not be evidenced. Citrate synthase levels remained preserved between groups in both media **(a)**. A trend to decrease CI enzymatic activity in NM-*LRRK2*^{G2019S} and PD-*LRRK2*^{G2019S} was observed in glucose media, and PD-*LRRK2*^{G2019S} patients harbouring the mutation increased their activity with respect to controls in galactose media ($p=0.04$). **(b)** Oxygen consumption trended to reproduce the pattern of CI enzymatic activity. After exposure to galactose media, a non-significant increment in O₂ consumption was observed in fibroblasts of NM-*LRRK2*^{G2019S} subjects with respect to controls ($p=0.35$). **(c)** Complex IV enzymatic function remained similar in all groups, showing a trend to increase in NM-*LRRK2*^{G2019S} subjects with respect to controls in glucose and galactose media ($p=0.14$ in both cases). **(d)** ATP levels tended to decrease in both mutant groups in glucose media ($p=0.18$ when comparing PD-*LRRK2*^{G2019S} with controls) **(e)**. Finally, the number of depolarized mitochondria was increased in NM-*LRRK2*^{G2019S} when compared to controls in glucose media ($p=0.04$), with the same trend observed for PD-*LRRK2*^{G2019S} although without reaching statistical significance ($p=0.14$). **(f)** Oxidative damage trended to increase in PD-*LRRK2*^{G2019S} patients in both conditions when comparing them to controls. **(g)** Apoptotic rate tended to decrease in the NM-*LRRK2*^{G2019S} group in both media **(h)**. Altogether, these results suggest that the overall mitochondrial function is conserved in the NM-*LRRK2*^{G2019S} in standard conditions (glucose) and enhanced after the mitochondrial challenge (galactose), but not in PD-*LRRK2*^{G2019S}, where mitochondrial alterations are observed in standard conditions and worsened by the exposure to mitochondrial challenging media.

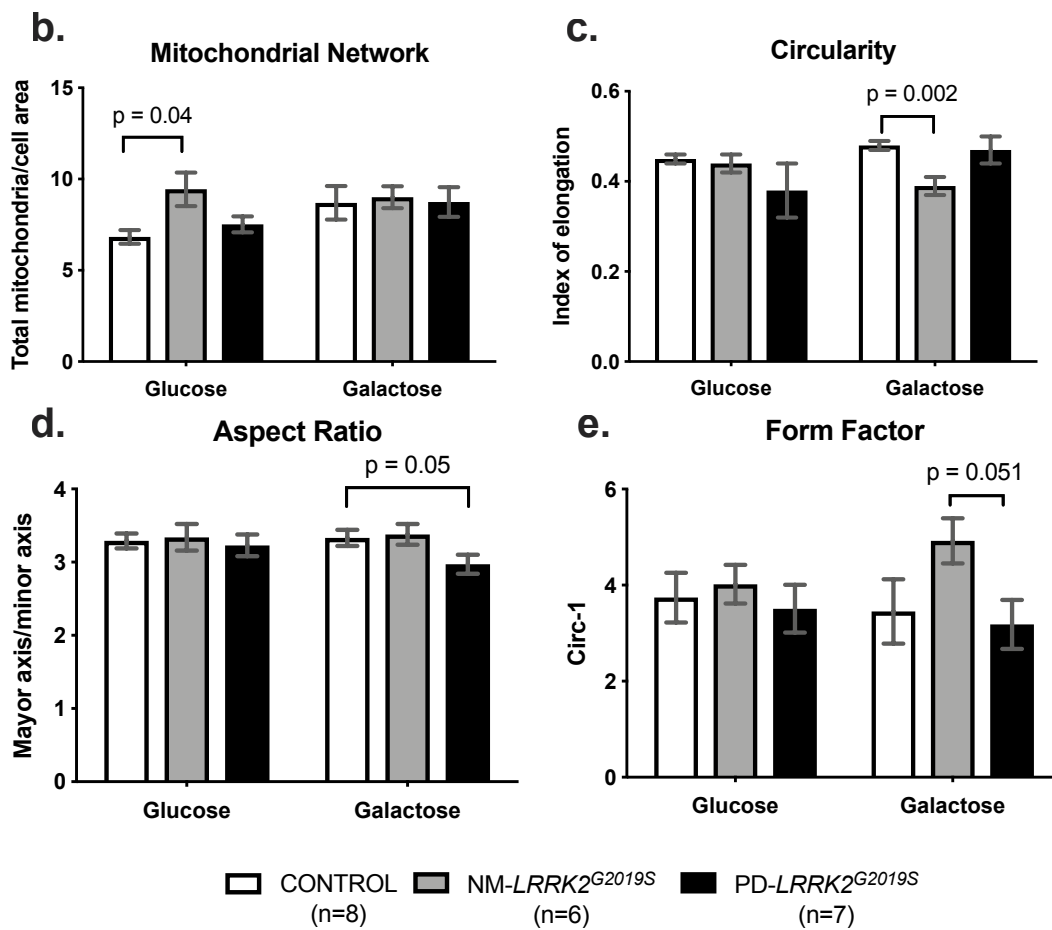
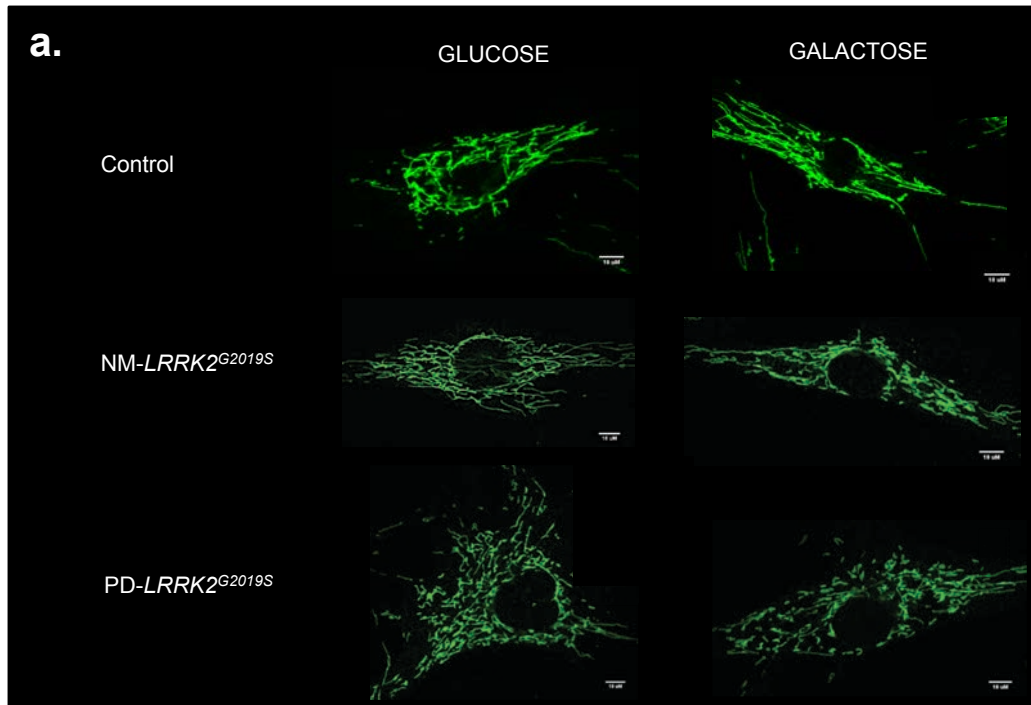


Figure 20 (Previous page) Mitochondrial dynamics.

Results are represented by mean \pm SEM, comparing controls (white bars), NM-*LRRK2*^{G2019S} (grey bars) and PD-*LRRK2*^{G2019S} (black bars) in glucose and galactose media. **a** Representative images of mitochondrial network obtained by confocal microscopy. Mitochondrial dynamics in fibroblasts of NM-*LRRK2*^{G2019S} showed an increased mitochondrial network in standard conditions when compared to controls (**b**). When NM-*LRRK2*^{G2019S} fibroblasts were subjected to mitochondrial challenging conditions (galactose), mitochondrial dynamics improved by decreasing circularity (**c**) and trends to increase form factor (**e**), accounting for longer, more branched mitochondria. Fibroblasts of PD-*LRRK2*^{G2019S} showed a pattern similar to controls in standard (glucose) conditions and a handicapped response when exposed to mitochondrial challenging conditions (galactose) as shown by decreased aspect ratio (**d**), accounting for shorter mitochondria. Globally these findings stand for a greater adaptation of mitochondrial dynamics when fibroblasts of NM-*LRRK2*^{G2019S} were subjected to a mitochondrial challenge (galactose), not observed in PD-*LRRK2*^{G2019S}.

5.1.3 Autophagy characterization

Autophagy in NM-*LRRK2*^{G2019S}

A significant increase in autophagy substrate expression (SQSTM1/p62) in fibroblasts of NM-*LRRK2*^{G2019S} was observed when compared to controls in glucose media (118.4%, $p = 0.014$), and in galactose, after 4 hours of BAF exposure (114.44% increase, $p = 0.009$) (**Figure 21.b**). These increased signaling for autophagy initiation was accompanied by trends to increase autophagosome formation at 4 and 8 hours of BAF treatment (LC3B2/ β actin: +145.22% and +287.21%, respectively, $p = 0.051$) when compared to controls in glucose media, but not in galactose media, where autophagosome formation seemed to be decreased (**Figure 21c**).

Autophagy initiation signaling increased in NM-*LRRK2*^{G2019S} subjects in glucose and galactose media, but autophagosome formation was only upregulated in glucose media suggesting an efficient autophagic response of this group to the adaptive mitochondrial enhanced function.

Autophagy in PD-LRRK2^{G2019S}

Autophagy substrate expression was increased in PD-LRRK2^{G2019S} after 8 hours of BAF treatment in glucose media (226.14%, p = 0.04) and at 4 hours in galactose media when compared to controls (78.5%, p = 0.02) (**Figure 21b**). However, these increased signaling for autophagy initiation was not accompanied by autophagosome formation in any media, and a significant decrease in LC3B2 levels was demonstrated when compared to NM-LRRK2^{G2019S} subjects at 4 and 8 h of BAF treatment in glucose media (-79 %, p = 0.042 and -71.26%; p=0.22, respectively) (**Figure 21c**).

These results suggest that autophagosome formation was decreased in PD-LRRK2^{G2019S} despite increased autophagy initiation in both media, which may be accountable for LRRK2^{G2019S} mutation.

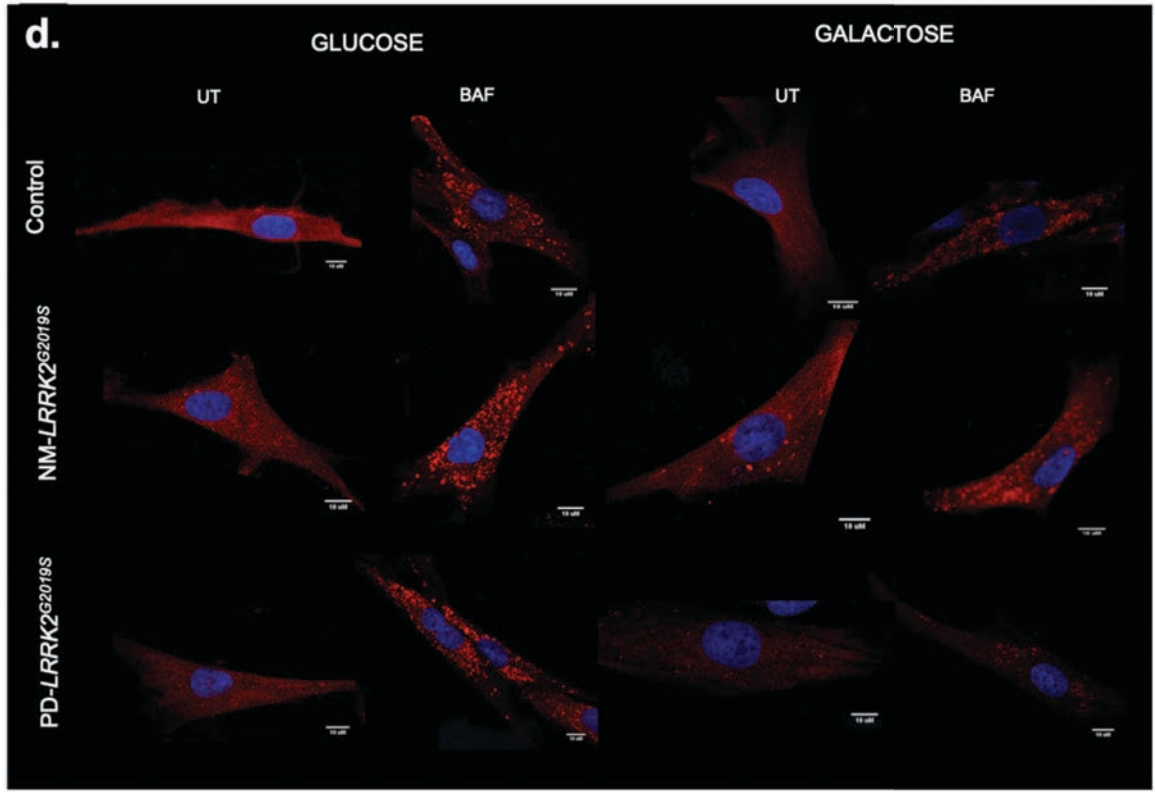
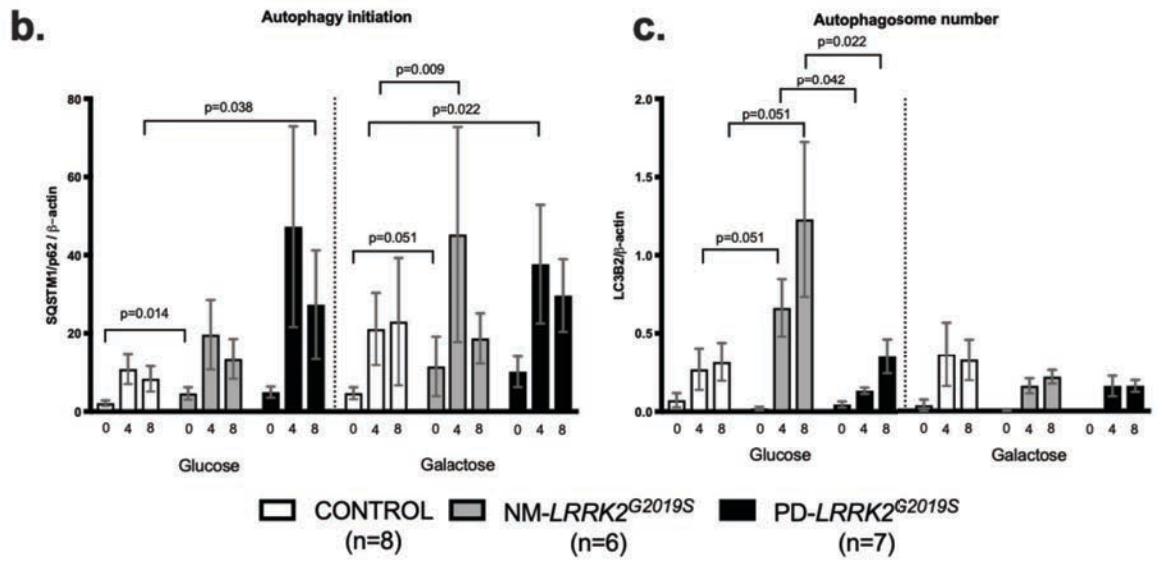
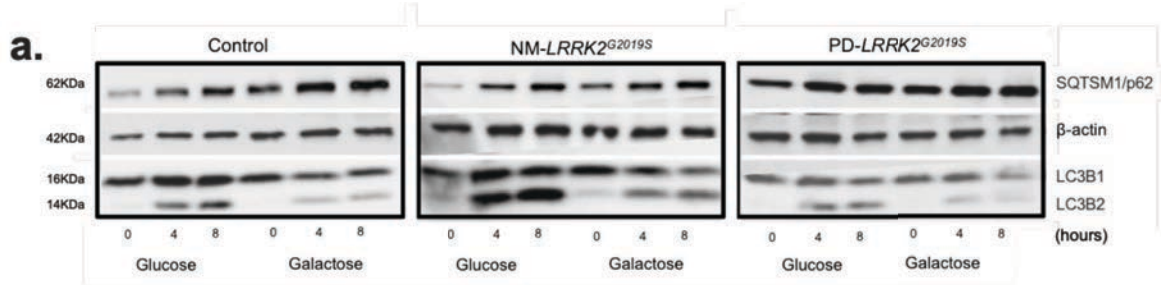


Figure 21 (Previous page). Autophagy.

Results are represented by mean \pm SEM, comparing controls (white bars), NM-*LRRK2*^{G2019S} (grey bars) and PD-*LRRK2*^{G2019S} (n=7; black bars) in either glucose or galactose media and at basal state, and after 4 and 8 hours treatment with BAF (0, 4, 8).

a. Representative images of autophagy markers measured by Western blot comparing: controls, NM-*LRRK2*^{G2019S} and PD-*LRRK2*^{G2019S}. (SQSTM1/p62)/ β -actin: Autophagy substrate. LC3B2/ β -actin: autophagy receptor, lipidated form. **b.** Autophagy initiation was upregulated in NM-*LRRK2*^{G2019S} subjects in glucose and galactose media when compared to controls (+ 118.4% SQSTM1/p62, p = 0.014 and + 114.44% SQSTM1/p62, p = 0.009, respectively) and trends to increase autophagy substrate were observed in PD-*LRRK2*^{G2019S} in both media. **b.** Autophagosome number tended to increase at 4 and 8 h of BAF treatment in NM-*LRRK2*^{G2019S} and was significantly decreased in PD-*LRRK2*^{G2019S} when compared to NM-*LRRK2*^{G2019S} subjects in glucose media at 4 and 8 hours of BAF treatment (- 79 to 86%, p = 0.042 and - 71.26%, p = 0.22 respectively). **d.** Representative images of autophagosome formation at time-point 0 (untreated: UT) and accumulation after 8 h of treatment with 100 nM BAF obtained by confocal microscopy.

In summary, an exhaustion of mitochondrial bioenergetic and functional reserve and the concomitant deregulation of autophagy described in fibroblasts from *LRRK2*^{G2019S} mutation carriers, may contribute to the development of PD in this genetically prone-population.

5.2 STUDY 2: Characterization of *GBA*^{N370S} neurospheres

Title:

***GBA* mutation influences mitophagy in 3D neurosphere models**

Authors:

Constanza Morén, Diana Luz Juárez-Flores, Kai-Yin Chau, Matthew Gegg, Glòria Garrabou, Ingrid González-Casacuberta, Mariona Guitart-Mampel, Eduard Tolosa, Maria Jose Marti, Francesc Cardellach, and Anthony Henry Schapira

Submitted to: Aging

IF 2017: 5.17 (Q1)

The objective of the second study of this thesis was to assess the genotype-phenotype correlation and to characterize the mitochondrial and autophagic phenotype in a model of adipocyte-derived neurospheres of *GBA*^{N370S}-mutation carriers in basal state and after mitochondrial uncoupling. We also aimed to validate the neurosphere model to study mitochondrial and autophagic alterations in neurospheres.

The results of study 2 are presented in four parts:

- 1) The epidemiological data of the cohorts included in the study.
- 2) The second part describes the characterization of the neurosphere model and the validation of the uncoupler treatment to induce mitophagy.
- 3) Third, the assessment of mitochondrial content after mitophagy induction.
- 4) The fourth part encompasses an overall view of autophagic flux.

Raw data obtained from the experimental work is available in Supplementary material.

5.2.1 Epidemiological data

No significant differences were found in age or gender between groups confirming that populations were homogenous and that the main difference between them was the genotype.

Table 13. Epidemiological data of the studied cohorts at the time of biopsy.

GROUP	N	GENDER		AGE		
		Male	Female	Range	Mean	SEM (\pm)
wt/wt	2	1	1	56-73	64.5	8.5
wt/ <i>GBA</i> ^{N370S}	2	1	1	45-75	60	15
<i>GBA</i> ^{N370S} / <i>GBA</i> ^{N370S}	2	1	1	58-76	67	9
Total	6	3	3	45-76	63.83	10.83

N: Number of cases included in the study; wt/wt: controls; wt/*GBA*^{N370S}: heterozygous subjects for *GBA*^{N370S} mutation and *GBA*^{N370S}/*GBA*^{N370S}: homozygous patients with *GBA* mutation. SEM: Standard error of the mean.

5.2.2. Characterization of the neurosphere model

The morphological change of NcSC upon induction to neurospheres is shown in **Figure 22** demonstrating the acquisition of expected cell architecture and morphometry characteristic of this cell model.

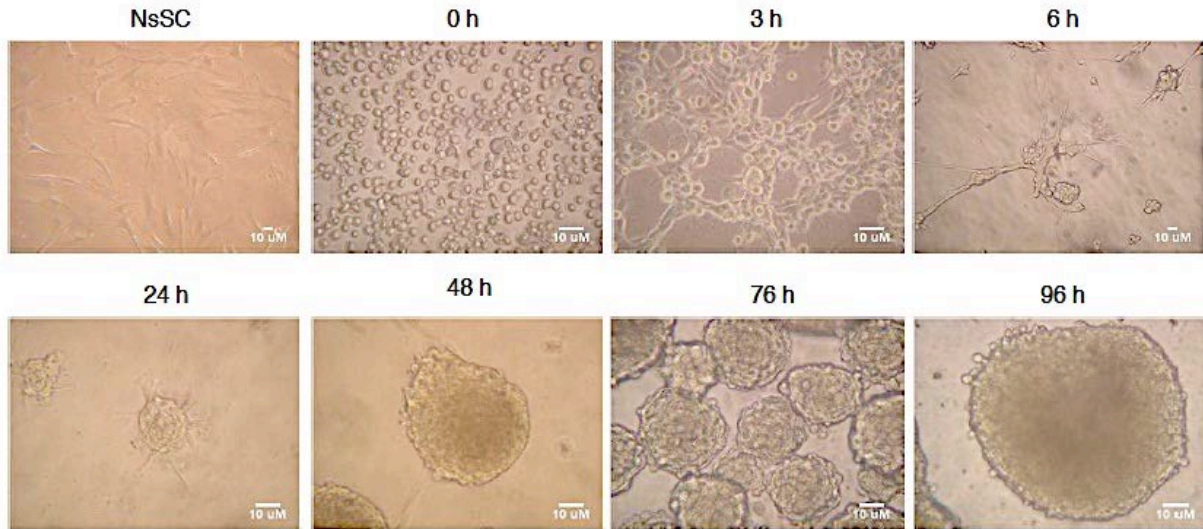


Figure 22. Neurosphere formation and morphology from neural crest stem cells to 4 days of development.

NcSC: neural crest stem cells. Cell aggregates began to form within 24 hours and the spherical structures grew in size as time progressed (48,72 and 96 h).

Neural and stemness markers

To identify the length of time the neurospheres become biochemically stable, to compare the influence of *GBA*^{N370S} zygosity on neurosphere formation and to confirm the presence of neural stem cells in the model, protein levels of neuronal markers (β -III tubulin MAP2), and the mRNA level of the neuroectodermal stem cell marker (nestin), were measured over time. β -III tubulin and MAP2 were stable (**Figure 23.a-b**) and nestin levels (**Figure 23.c**) were not significantly different between the lines at 4 days suggesting that at this time they were biochemically stable; consequently, this time point was selected to perform the rest of experimental work.

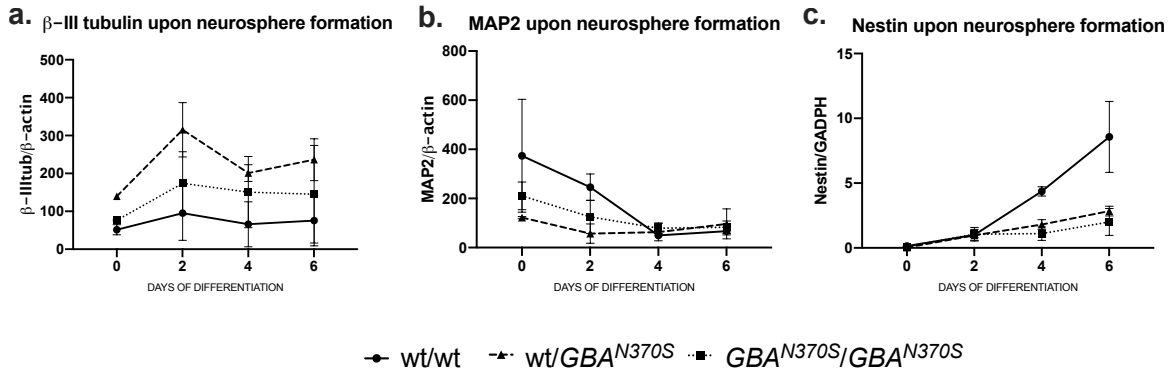


Figure 23. Characterization of neurosphere development by analysis of β -III tubulin, MAP2 and Nestin markers.

Values are plotted over time as single dots \pm SEM of controls (wt/wt, \square continuous line), wt/ GBA^{N370S} (\blacktriangle , discontinuous line) GBA^{N370S}/GBA^{N370S} (\blacksquare , dotted line), AU: arbitrary units.

Both neural markers showed stabilized expression on day 4 of development. β -III tubulin (a) and MAP2 levels (b) confirmed neural properties of neurospheres. Increasing levels of mRNA nestin confirmed neural stem cell properties of neurospheres during development. (c). No significant differences were found at 4 day of development, thus at this point further molecular and cell phenotyping was performed in all cohorts.

Genotype-phenotype correlation

GCCase, HEX and β -gal enzymatic activities were also measured at 0, 2, 4 and 6 days of differentiation. At 4 days, GCCase activity was 33% decreased ($p=NS$) in heterozygotes for GBA^{N370S} -mutation (wt/ GBA^{N370S}) and: and 98% decreased ($p=0.049$) in homozygotes for GBA^{N370S} -mutation (GBA^{N370S}/GBA^{N370S}) when compared to controls (wt/wt) measured at pH 5.4 in the presence of sodium taurocholate. As a confirmation, measurement of GCCase at pH 4.5 in the absence of the GCCase activator sodium taurocholate yielded similar results, while HEX and β -gal were unaffected (Figure 24) confirming that GCCase activity was affected secondary to GBA^{N370S} mutation.

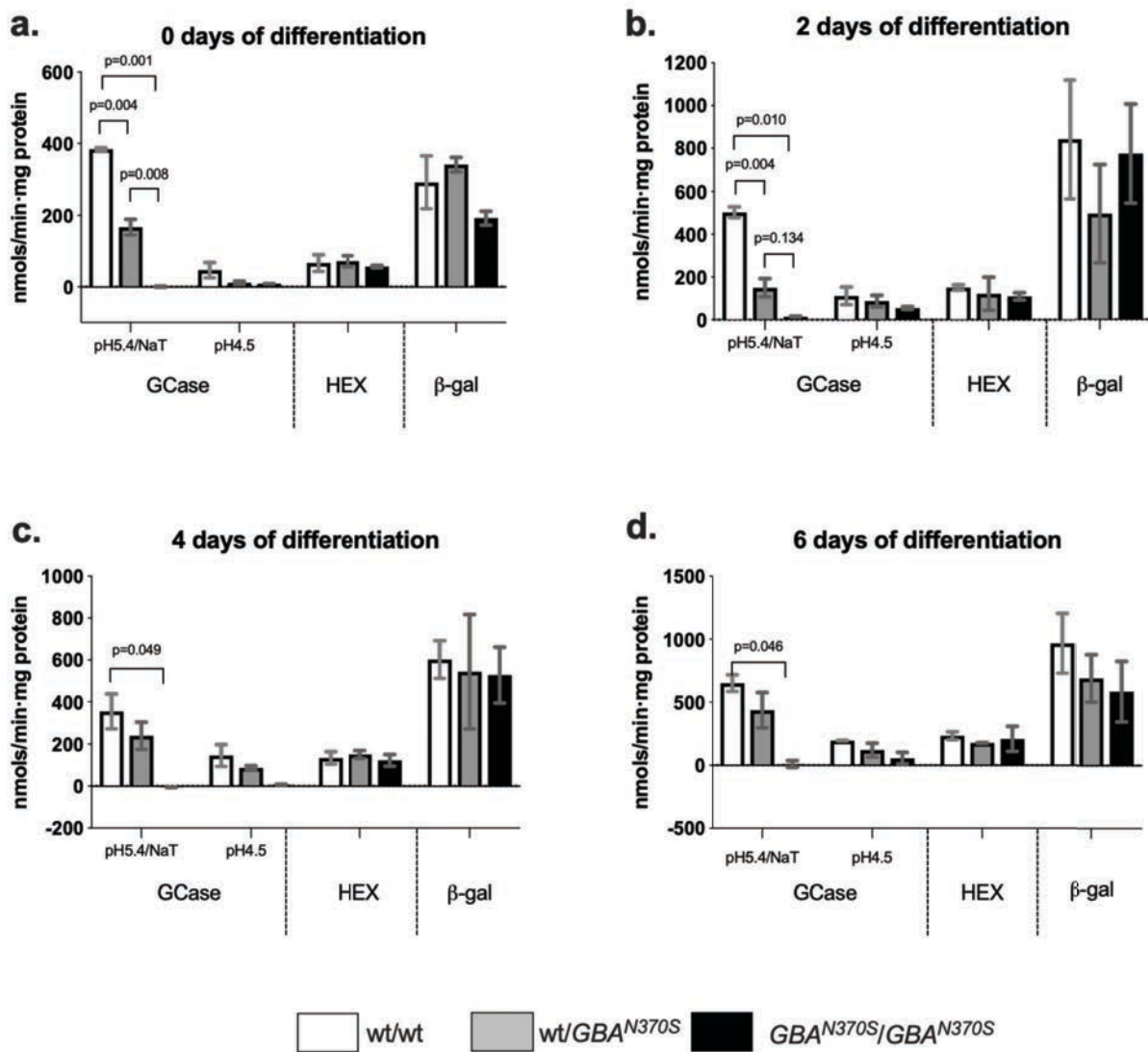


Figure 24 GCCase, HEX and β -gal enzymatic activities from 0 to 6 days of differentiation. Results are represented by mean \pm SEM comparing wt/wt, (white bars), wt/*GBA*^{N370S} (grey bars) and *GBA*^{N370S}/*GBA*^{N370S} (black bars).

GCCase activity decreased as expected for the respective genotypes when measured at pH 5.4 in the presence of sodium taurocholate. Measurement of GCCase at pH 4.5 in the absence of the GCCase activator sodium taurocholate yielded similar results, while HEX and β -gal were unaffected standing for the expected mutation phenotype in this model.

During development of neurospheres, the mutant lines showed trends to increase α -synuclein protein levels. Despite this, at 4 days of differentiation, the three lines showed the same levels of protein expression (**Figure 25**).

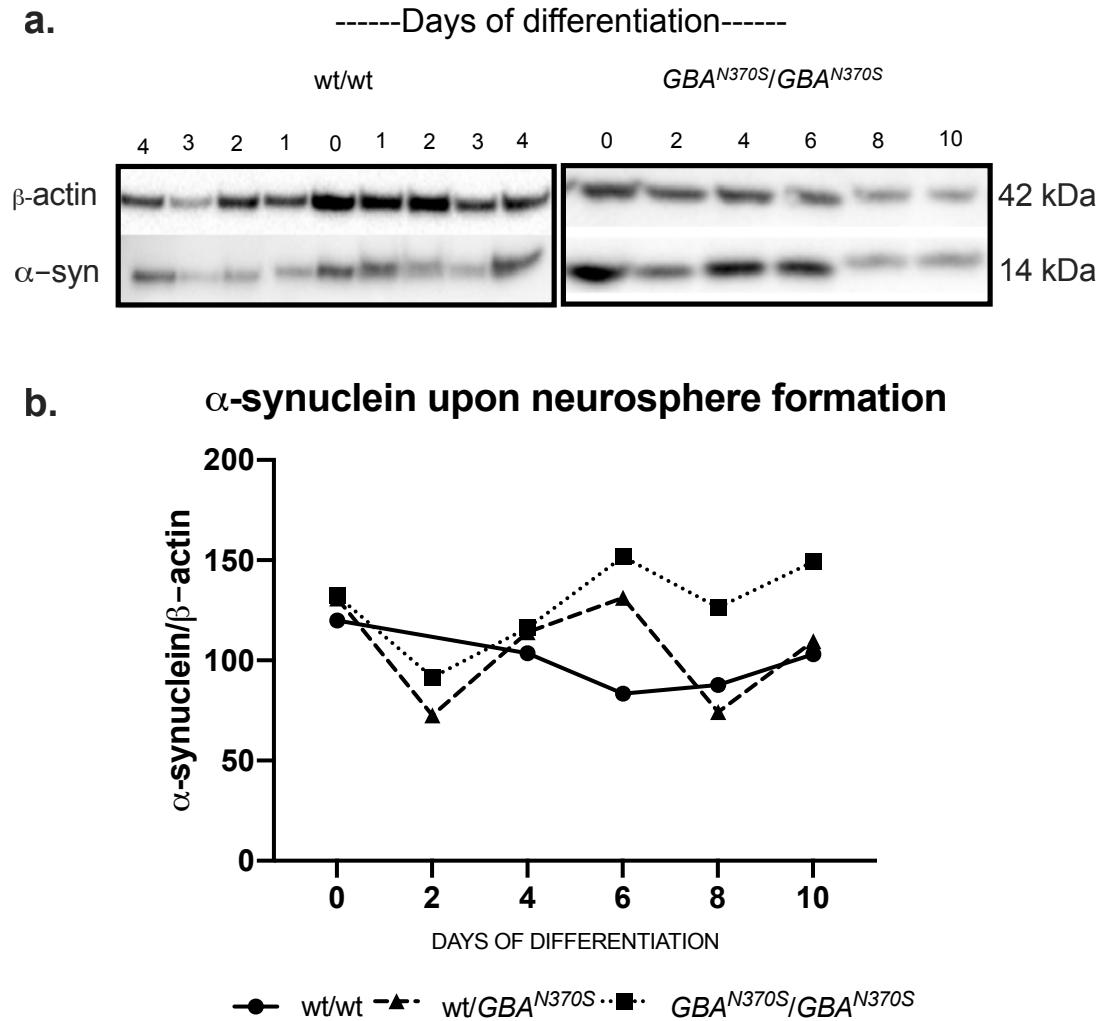


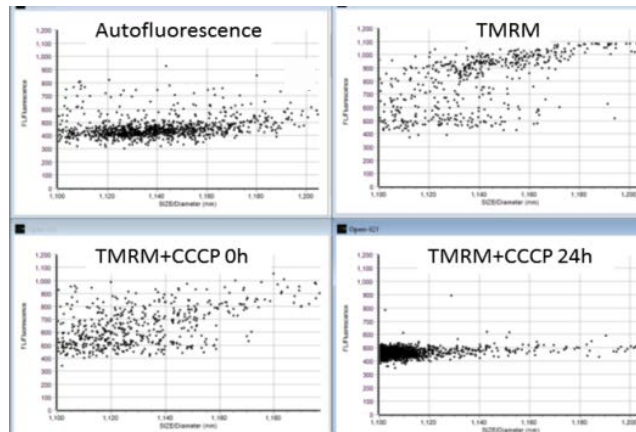
Figure 25. α -synuclein protein levels during neurospheres development.

a. Representative blots of α -synuclein protein expression levels during neurospheres development. **b.** Quantification of the protein expression levels, individual values are plotted over time as single dots \pm SEM of controls (wt/wt: continuous line), wt/*GBA*^{N370S} (discontinuous line) *GBA*^{N370S}/*GBA*^{N370S} (dotted line), No differences in α -synuclein levels were observed at 4 days of differentiation but trends towards higher α -synuclein expression were observed in mutant lines along time recapitulating the altered α -synuclein degradation for which *GBA* mutations have been previously accountable for.

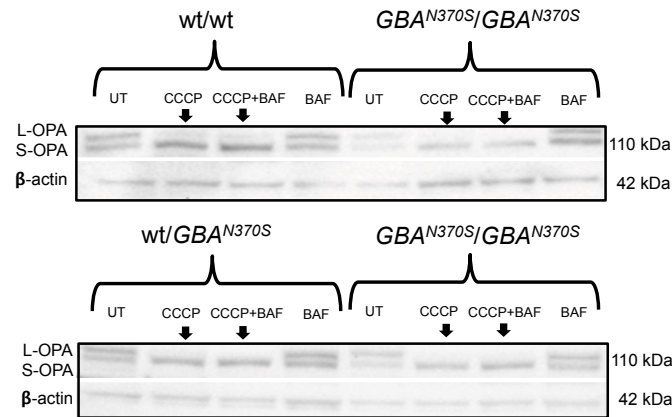
Validation of uncoupler treatment to dissipate MMP and to induce mitophagy in the neurosphere model

Similar to other cell models, treatment of neurospheres with 10 μ M CCCP for up to 24 hours decreased TMRM staining for MMP (**Figure 26.a**). Mitochondrial depolarization following mitochondrial uncoupling was confirmed by loss of the long isoform of optic atrophy protein 1 (l-OPA1/s-OPA1); (**Figure 26.b**) and was similar in all three genotypes discarding the presence of differences exerted by the experimental procedure and validating the methodological procedure. Mitophagy induction was confirmed through the decrease of mitochondrial content as measured by Tom20 protein level reduction during the 24h CCCP treatment (**Figure 26.c**).

a. TMRM fluorescence upon CCCP treatment



b. Mitochondrial uncoupling following CCCP treatment



c. Mitophagy upon CCCP treatment over time

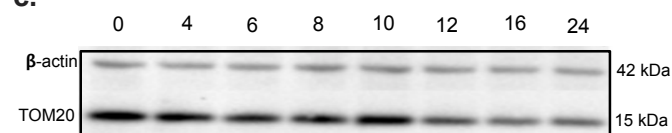


Figure 26. Confirmation of mitochondrial uncoupling with CCCP in the neurosphere model.

a. Detection of mitochondrial membrane potential upon 10 μ M CCCP treatment **b.**

Representative blots of OPA1 isoforms **c.** Representative blot showing how TOM20 levels

progressively decrease from 0 to 24h in a control line.

TMRM: tetramethylrhodamine methyl ester BAF, bafilomycin; L-OPA1, long isoform of optic atrophy 1 protein OPA1; S-OPA1, short isoform of OPA1; UT, untreated.

TMRM fluorescence decreased upon mitochondrial uncoupling. Expected changes from L-OPA1 to S-OPA1 isoforms were observed upon CCCP treatment in all the genotypes, and mitochondrial content decreased in the control line upon CCCP treatment, suggesting an adequate mitophagy induction.

5.2.3 Mitochondrial phenotype

We compared the steady-state levels of mitochondrial content between the three different genotypes. As shown in **Figure 27**, higher levels of mitochondrial markers were observed in the homozygous lines under basal conditions with respect to the controls, which may suggest mitochondrial accumulation in the presence of double *GBA* mutation.

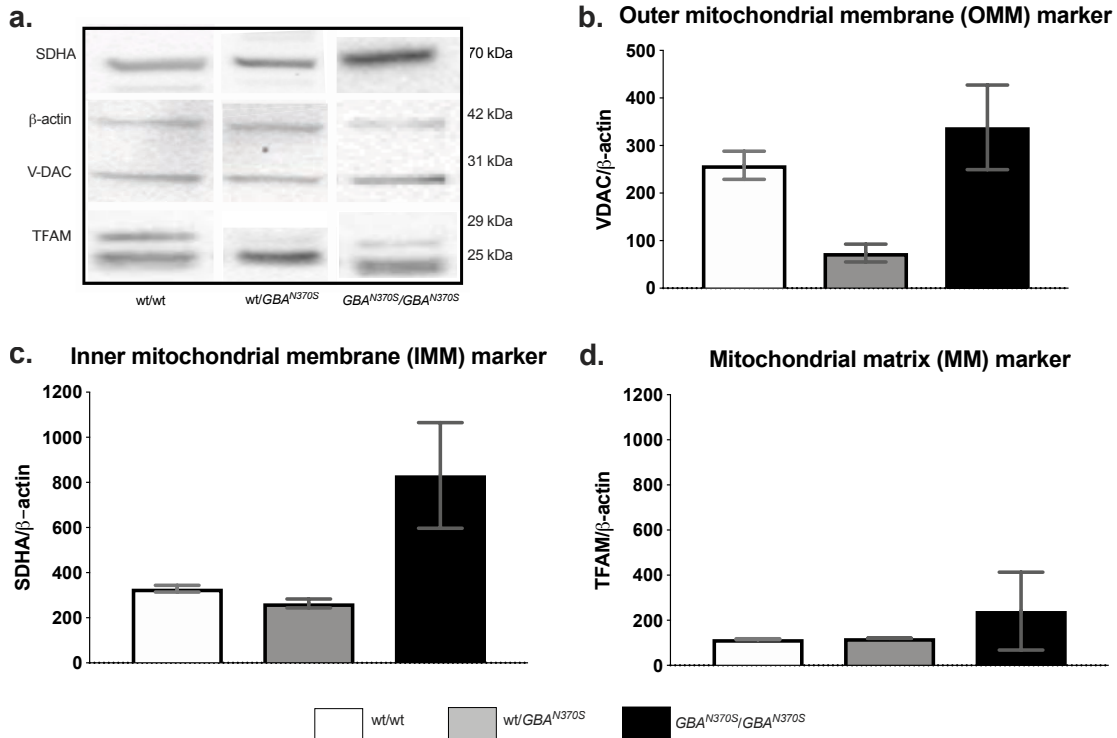


Figure 27. Mitochondrial content under basal conditions.

Results are represented by mean \pm SEM comparing wt/wt, (white bars), wt/*GBA*^{N370S} (grey bars) and *GBA*^{N370S}/*GBA*^{N370S} (black bars).

a. Representative blot of different mitochondrial markers in neurospheres of the three groups included. **b.** VDAC1: outer mitochondrial membrane, **c.** SDHA: inner mitochondrial membrane and **d.** TFAM: matrix.

All markers tended to increase in *GBA*^{N370S}/*GBA*^{N370S} neurospheres in basal conditions, when compared to control lines, suggesting an increased content of mitochondria in the homozygous neurospheres.

As expected, protein levels of VDAC1, SDHA and TFAM decreased following CCCP treatment for 24 hours in control lines (**Figure 28.b-d**) confirming the induction of mitophagy. However, mitochondrial markers of wt/*GBA*^{N370S} neurospheres did not respond to CCCP uncoupling (**Figure 28.b-d**). In fact, an increase of TFAM was observed in mutant lines with respect to controls after mitochondrial uncoupling (300% in wt/*GBA*^{N370S}, p=0.017 and 152% in *GBA*^{N370S}/*GBA*^{N370S} p= 0.002) and TFAM significantly increased in the heterozygous lines when compared to its basal state (187%, p=0.033) (**Figure 28.d**) suggesting that mitochondrial biogenesis increased in response to mitochondrial uncoupling.

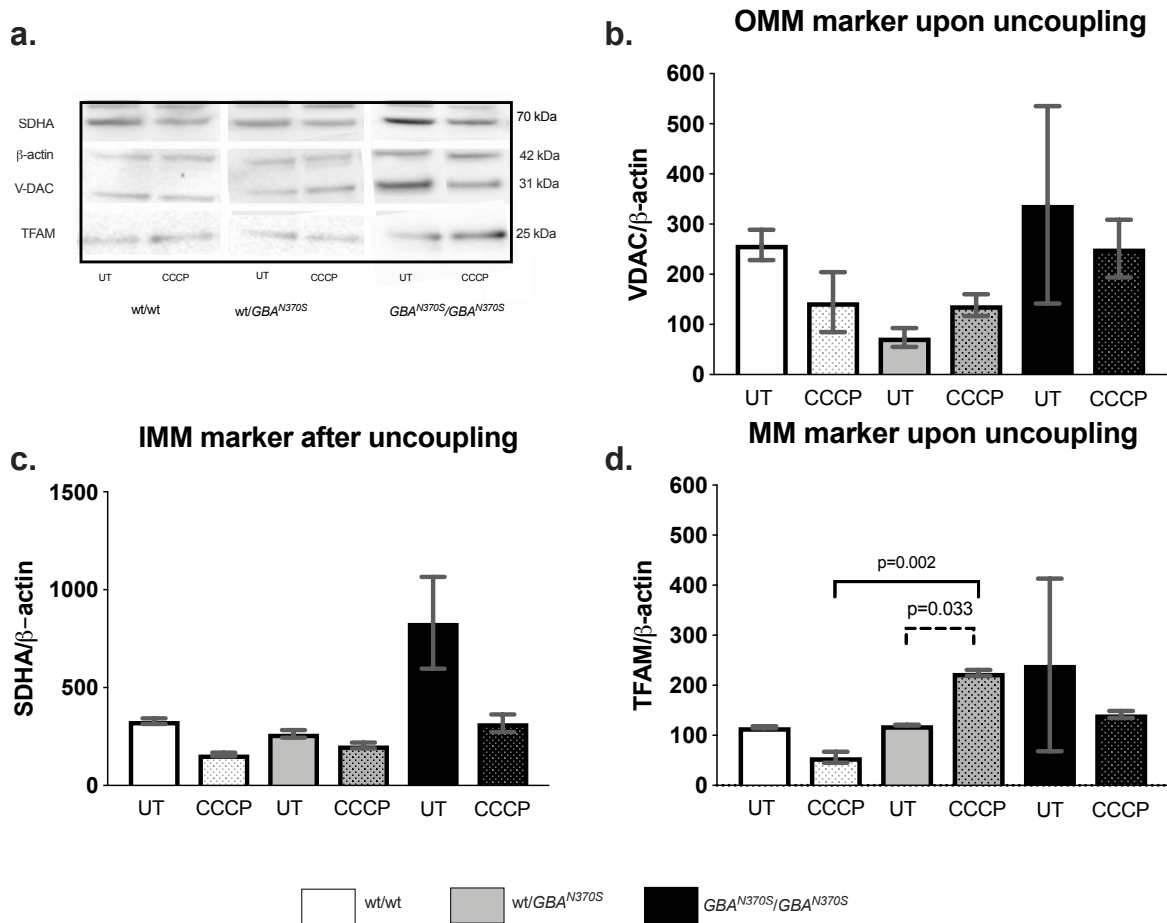


Figure 28. Mitochondrial content upon mitochondrial uncoupling

Results are represented by mean \pm SEM comparing wt/wt, (white bars), wt/*GBA*^{N370S} (grey bars) and *GBA*^{N370S}/*GBA*^{N370S} (black bars). OMM: outer mitochondrial membrane, IMM: inner mitochondrial membrane, MM: mitochondrial matrix. UT: untreated, CCCP; 10uM CCCP. **a.** Representative blot of different mitochondrial markers in neurospheres before and after mitochondrial uncoupling using CCCP treatment **b.** VDAC1: outer mitochondrial membrane, **c.** SDHA: inner mitochondrial membrane and **d.** TFAM: mitochondrial matrix. A reduction of protein level in a panel of mitochondrial markers was present upon uncoupler treatment in the control lines (wt/wt), but not for mutant lines, most evident in TFAM for wt/*GBA*^{N370S}. These results suggest that even after uncoupling, mitochondrial content can be conserved in wt/*GBA*^{N370S} perhaps in an attempt to maintain ATP levels.

Since mitochondrial content is not only maintained by mitochondrial turnover but also mitochondrial biogenesis, mRNA levels of PGC1 α transcript and one of its upstream regulators, TFEB, were measured in untreated and CCCP-uncoupled neurospheres (**Figure 29**). Mitochondrial depolarization led to a substantial and significant increase in PGC1 α transcript in *wt/GBA^{N370S}* compared to *wt/wt* and *GBA^{N370S}/GBA^{N370S}*. The steady-state levels of TFEB mRNA expression were found inversely increased to the GCase level (**Figure 24**) suggesting that *GBA* deficiency alone is enough to stimulate TFEB activation (**Figure 29.b**). Treatment of *wt/GBA^{N370S}* or *GBA^{N370S}/GBA^{N370S}* neurospheres with CCCP resulted in the same TFEB mRNA levels, compared to control. These results suggest that mitochondrial biogenesis is significantly increased in *wt/GBA^{N370S}*, probably as a compensatory mechanism, and that lysosomal biogenesis tend to decrease in both mutant groups after mitophagy induction.

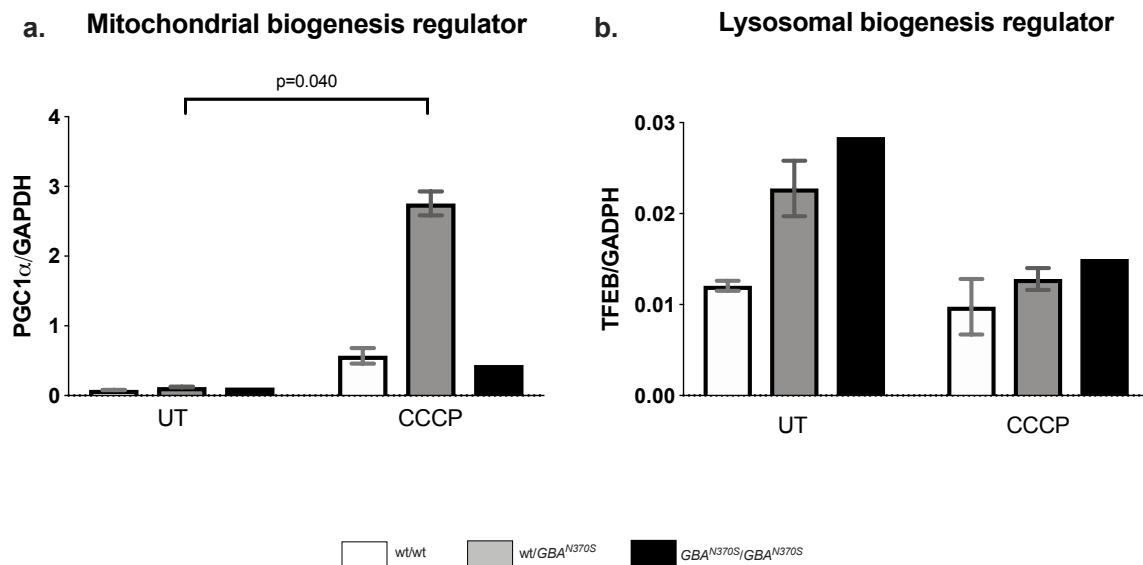


Figure 29. mRNA levels of TFEB and PGC1 α in basal state and upon uncoupling treatment. Results are represented by mean \pm SEM; *wt/wt*, (white bars); *wt/GBA^{N370S}* (grey bars) and *GBA^{N370S}/GBA^{N370S}* (black bars). UT: untreated, CCCP; 10uM CCCP. **a.** PGC1 α significantly increased upon CCCP induction in *wt/N370SGBA*, probably in an attempt to compensate for the underlying mitochondrial defects by increasing mitochondrial biogenesis. **b.** TFEB mRNA levels tended to decrease in *wt/GBA^{N370S}*, and *GBA^{N370S}/GBA^{N370S}* *GBA* after mitochondrial uncoupling in an attempt to compensate lysosomal defects by increasing lysosomal biogenesis.

Despite the increase in mitochondrial content under basal conditions, steady state levels of ATP in GBA^{N370S}/GBA^{N370S} were lower than control cells suggesting mitochondrial dysfunction (**Figure 30**). As expected after uncoupler treatment, ATP levels decreased in the control lines. However, the decrease of ATP levels upon induced mitophagy was less important in the wt/GBA^{N370S} and not observed at all in GBA^{N370S}/GBA^{N370S} (**Figure 31**), confirming defective mitochondrial clearance previously observed by augmented mitochondrial content markers in the presence of the GBA mutation.

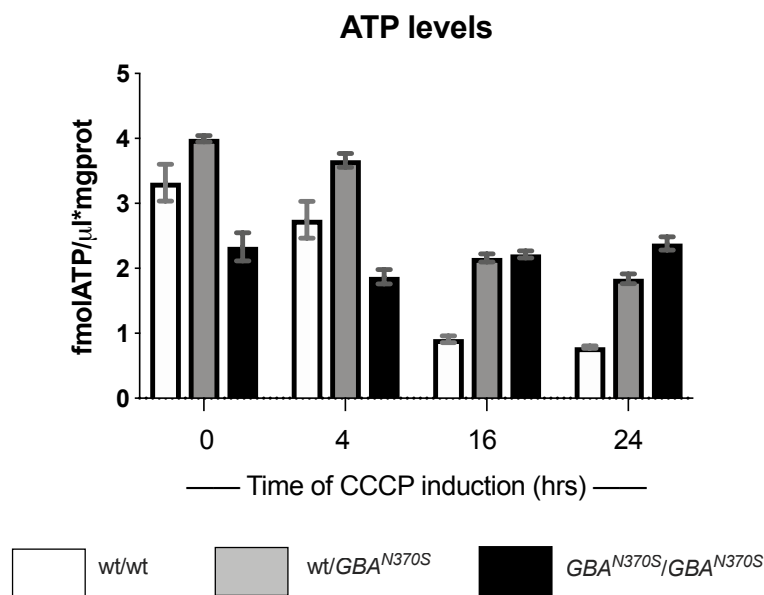


Figure 30. ATP levels upon CCCP induction.

Results are represented by mean \pm SEM comparing wt/wt, (white bars), wt/ GBA^{N370S} (grey bars) and GBA^{N370S}/GBA^{N370S} (black bars). Despite an increase in mitochondrial mass in untreated conditions, ATP levels remained unchanged in wt/ GBA^{N370S} and GBA^{N370S}/GBA^{N370S} neurospheres suggesting the lack of mitochondrial response to mitophagy induction.

5.2.4 Autophagy characterization

To investigate if mitophagy was impaired in neurospheres with GCase deficiency, macroautophagy flux was measured by LC3B2 and SQSTM1/p62 levels. Under basal conditions, SQSTM1/p62 and LC3B were similar between groups (**Figure 31. b and c**).

To measure macroautophagy flux we treated cells with BAF, which prevents the fusion of autophagosomes to lysosomes. As expected BAF increased SQSTM/p62 and LC3B2 in all groups (**Figure 31.b and c**). However, there was no significant difference between the groups treated with BAF, suggesting that macroautophagy flux is not noticeably affected.

Interestingly, only the *GBA*^{N370S}/*GBA*^{N370S} group showed a significant increase in autophagosome number after treatment with bafilomycin, which could be interpreted as a pre-existent impairment of autophagosome formation.

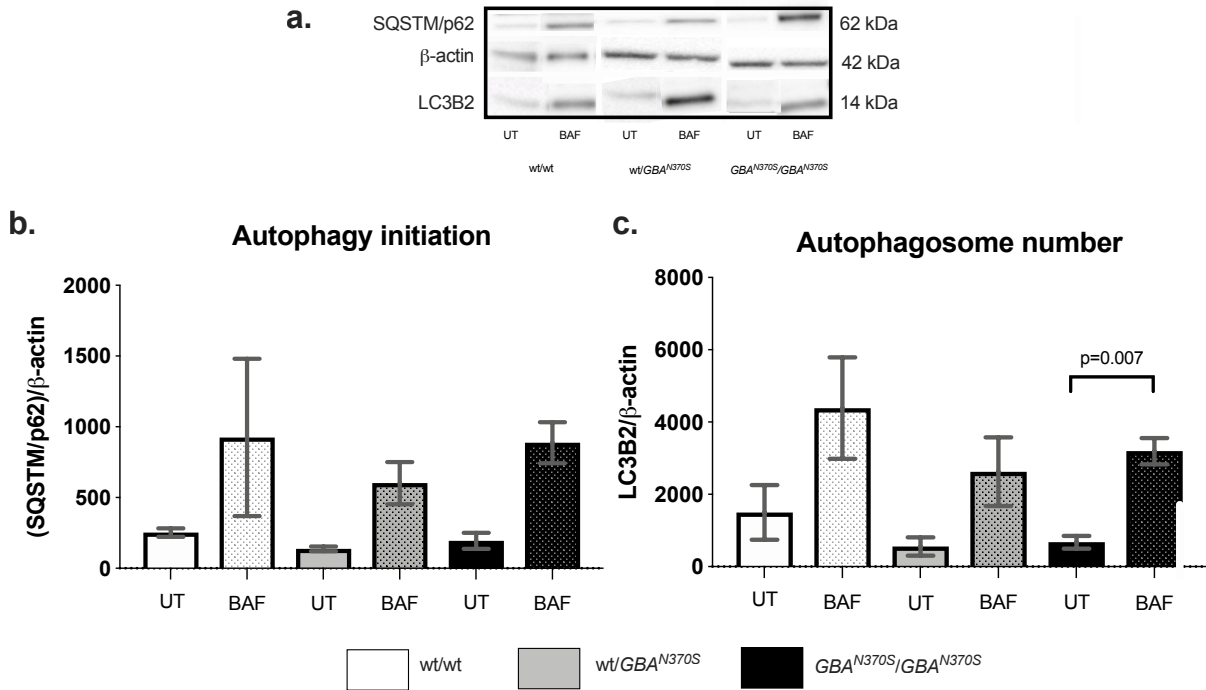


Figure 31. Autophagy flux measurement.

Results are represented by mean \pm SEM comparing wt/wt, (white bars), wt/ GBA^{N370S} (grey bars) and GBA^{N370S}/GBA^{N370S} (black bars). UT: untreated, BAF; 0.5 μ M bafilomycin. **a.** Representative blot of macroautophagy flux before and after treatment with bafilomycin. As expected, SQSTM1/p62 and LC3B2 levels increased after treatment with BAF. The most significant change was observed in autophagosome number after BAF treatment in GBA^{N370S}/GBA^{N370S} neurospheres. These findings suggest that in standard conditions, autophagosome formation may be deficient.

PINK1 mRNA levels followed the same pattern as in TFEB, increasing its levels in the wt/ GBA^{N370S} group, where mitochondrial biogenesis also increased.

These results suggest that if mitophagy was impaired, it would probably not be due to lower *PINK1* levels but to other not explored *PINK*-*Parkin* independent mitophagy pathways, and adding evidence that mitochondrial compensatory mechanisms may be present in basal conditions in wt/ GBA^{N370S} cell lines but not in GBA^{N370S}/GBA^{N370S} (**Figure 32**).

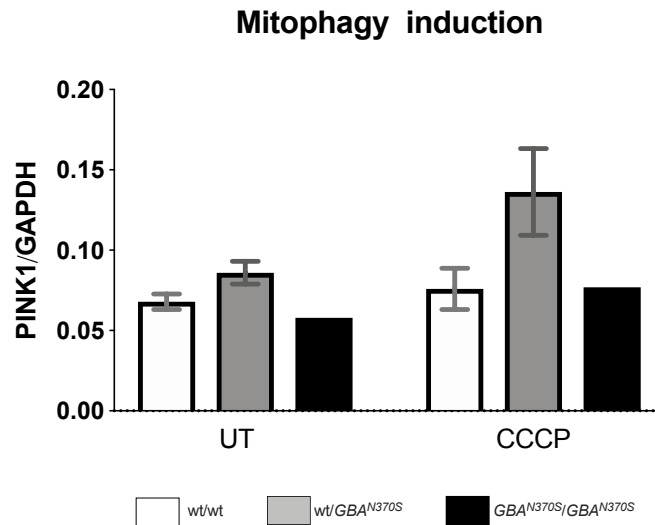


Figure 32. mRNA levels of PINK1

Results are represented by mean \pm SEM comparing wt/wt, (white bars), wt/*GBA*^{N370S} (grey bars) and *GBA*^{N370S}/*GBA*^{N370S} (black bars). UT: untreated, CCCP: 10uM CCCP.

After CCCP uncoupling, mitophagy induction seemed to increase in the wt/*GBA*^{N370S} group, further supporting the increased basal mitochondrial content in this group.

The fact that ATP levels of *GBA*^{N370S}/*GBA*^{N370S} remained unchanged throughout CCCP induction along time, even when autophagosome number significantly increased (473%, $p=0.007$), suggests that preexistent mitochondrial alterations may account for the pathogenesis in *GBA* mutant neurospheres.

In summary, adipocyte derived neurospheres from *GBA* mutation carriers exhibit a basal defect in autophagy that corresponds to the expected enzyme activity that corresponds to the phenotype. Also, an enhanced mitochondrial function and compensatory mitochondrial biogenesis was observed in adipocyte-derived neurospheres from wt/*GBA*^{N370S}, while increased mitochondrial basal content and failure to induce mitophagy was observed in adipocyte-derived neurospheres from *GBA*^{N370S}/*GBA*^{N370S} patients, accounting for pre-existent autophagic and mitochondrial failure.



6. DISCUSSION



Parkinson's disease represents the second most common neurodegenerative disorder. A great rise in the incidence of this disease is expected in the coming years mainly because of the increase in life expectancy of the population (2). Thus, the description of the pathological mechanisms that lead to PD as well as the development of biomarkers, preventive measures and effective treatments is utterly important (22).

Neurodegenerative diseases share common molecular pathways with each other, and also with other less common metabolic disorders such as LSD, including mitochondrial and autophagic alterations that lead to a wide range of clinical phenotypes. For instance, iron accumulation and increased oxidative stress are common to neurodegenerative disorders with parkinsonism with child and adult onset (12). Most interestingly, common alterations among molecular pathways described on rare diseases and PD provide important insights and advances towards the development of biomarkers and therapeutic targets for the most common neurodegenerative diseases (97,225).

The brain is often affected when mutations of mitochondrial genes and genes involved in the autophagy system are present because high levels of ATP production are needed to ensure an adequate neural activity. Neurons rely almost exclusively on oxidative metabolism and do not actively regenerate, so an efficient mitochondrial and vesicle transport and an adequate digestion and recycling of waste products is upmost important (226,227).

The particularity of PD among the rest of neurodegenerative disorders is the loss of dopaminergic neurons in the *SNpc*, which is responsible for the motor features that define the condition of our interest. Dopaminergic neurons have been suggested to be particularly prone to metabolic and oxidative stress because: (i) Dopamine and its metabolites increase oxidative stress, (ii) They possess particularly long, unmyelinated axons, and require big amounts of energy to be sustained, and

(iii) the pacemaker activity requires a high calcium interchange and is also very demanding in energetic terms (228).

There is a great need to develop and validate experimental models that may reproduce the altered molecular pathways of the disease and that can be easily translated to the clinical context of the disease. By validating models that recreate the genotype-phenotype correspondence and metabolism of the altered systems, great advances will be made that can potentially translate into early biomarkers, diagnostic tools and disease-modifying therapies of all kinds.

For many years, PD research almost solely focused on neurodegeneration (103). Animal models, such as the MPTP or rotenone induced PD of primates and mice, have been largely used to investigate the mechanisms involved in the death of dopaminergic neurons, but they do not reproduce all the molecular mechanisms of neurodegeneration. On the other hand, genetically modified animals exhibit mitochondrial alterations, increased oxidative stress and altered autophagy but offer different pathological phenotypes from humans (103,168).

Since the *SNpc* of patients is accessible only *post mortem*, human-derived cell models of study have been developed over the years in an attempt to study all the above-mentioned stages of the disease, aiming to reproduce the mechanisms leading to neurodegeneration (229,230). Possibly the most widely known model are iPSC that may be differentiated to dopaminergic neurons, however the genetic modifications needed to produce the iPSC, the high costs derived from their generation and maintenance, the low efficiency of the model and their dependence on glycolytic metabolism have been mentioned among the disadvantages of this models (185,231).

Fibroblasts are a relatively well established model to study PD, pathological features of iPD and other genetic forms of the disease have been previously described at many levels (153,196,197,199,232). Phenotyping of fibroblasts from iPD

patients has also been successful, so they continue to represent an adequate, accessible and relatively easy-to-maintain model, with patient-derived cells (188) that has been previously validated for the study of mitochondrial and neurodegenerative disease (191,233). The added feature of the model proposed in this thesis is the evaluation of mitochondrial and autophagic phenotyping in conditions of mitochondrial stress. Perhaps the greatest caveat of fibroblasts as a model of PD is the distinct embryonic origin from neurons, and that dopamine-related oxidative stress cannot be studied. However, as the mechanistics of neural damage exerted by dopamine and the dopaminergic nature of neurons have already been described, the study of patient-derived cells, which conserve the genetic and epigenetic background of patients, is of great utility to dissect the molecular pathways that lead to alterations at the neural level and that are part of the systemic disease in a similar environment to that of neurons (181).

Neurospheres represent a closer phylogenetic, yet readily accessible, model that may unveil some mechanisms specific to neural cells. Additionally, they also conserve the genetic and epigenetic background of the patient, and do not require genetic modifications to express neural properties (204). Although some disadvantages have been described to this model, such as the elevated costs of maintenance and the limited efficiency of the models, they represent an excellent option as a second step in evaluation of molecular pathways that have been previously detected on other models that permit large-scale phenotyping (234). The model *per se* is not new, but the addition of the mitochondrial uncoupler CCCP permitted to evaluate mitophagy induction, and the exposure to galactose media could yield to interesting observations.

Mitochondrial and autophagic implication in the pathophysiology of PD has been well-documented (47–49,62,86), and it is now recognized that mitochondrial health is widely dependent on adequate mitochondrial dynamics, turnover and renewal through autophagy (235). Recent reports in patients, animal and cell models

have described differential mitochondrial functional phenotypes in idiopathic and some monogenic forms of PD (196,236,237).

Lysosomal dysfunction cannot explain the preferential neuronal vulnerability in PD by itself, and the presence of *GBA* mutations (even in homozygous forms) is not determinant for presenting neural degeneration in the context of GD, suggesting that compensatory mechanisms in the cellular metabolism, such as enhanced mitochondrial metabolism, autophagy activation or the presence of protective factors that are yet unknown play an important role in the pathogeny of PD and other neurodegenerative disorders (238). Several studies have shown that lysosomal dysfunction and impaired mitophagy correlate and may be related to alterations in other pathways such as mitochondrial biogenesis, missfolded protein aggregation and ROS production (83,225,239,240). However, more studies are needed to understand whether impairment of the autophagy-lysosomal pathway is associated with mitochondrial defects because they prompt the accumulation of defective mitochondria through failed mitophagy or whether other pathways are involved (241).

UPR_{mt} and mitophagy can be simultaneously activated, and their role in cellular metabolism is transcription adaptation and promoting recovery of mitochondrial activity in front of a severely damaged mitochondrial context. UPR_{mt} aberrant or prolonged activation results in cells being in a state of constant mitochondrial recovery, accumulating at the same time deleterious mitochondria and mtDNA, accounting for a persistence in cellular deterioration (73). By all of the above, UPR_{mt} transcripts can function as biomarkers of mitochondrial dysfunction and perhaps provide therapeutic approaches that prevent or modify neurodegeneration (72), and they can be studied in patient-derived cellular models.

The exhaustive description of the molecular pathways involved in genetic forms of PD that are linked to mitochondrial function, autophagy regulation and lysosomal degradation provides a valuable foundation for the development of therapies directed, among others, to enhance lysosomal function, enhancing

mitophagy, promoting degradation of α -synuclein and blocking the accumulation of potentially harmful dopamine oxidation products (238). The hereditary forms of PD associated to mutations in mitochondrial genes, exhibit alterations in autophagy (242), as familial forms of PD associated with mutations of proteins involved in the autophagic-lysosomal pathway coexist with mitochondrial defects (243).

In two large studies of GWAS comprising large cohorts of PD cases and controls, a significant number of damaging variants in genes from LSD, apart from GBA, were found, supporting the possibility of an oligogenic risk model for PD, in which multiple hits act in combination to degrade cellular metabolism, enhancing disease susceptibility (104). The discovery of genes associated with PD has permitted to study different molecular pathways related to neurodegeneration. In this context, the study of *LRRK2* as the most common cause of hereditary PD, and the study of *GBA* as the most frequent risk factor to develop PD, are of great importance to unravel which cellular alterations are responsible for neuronal death (109,244).

Mitochondrial dysfunction in *LRRK2*^{G2019S}-mutation associated PD has been characterized in several disease models by mtDNA disarrangements (245), CIV deficiency and decreased ATP levels (127), MMP alterations (192,200,246) and mitochondrial dynamics dysfunction (246,247). Accumulating evidence points towards a fundamental role of autophagy in neurodegenerative diseases and, specifically in PD, *LRRK2* inhibition has been studied as a therapeutic target for PD and impaired autophagy (86,115,192,248,249). *LRRK2* mutations and also aggregation of α -synuclein can be involved in deregulation of autophagic and endo-lysosomal pathways and are associated with a suboptimal mitochondrial function (200,250).

Mitochondrial and autophagic abnormalities have been associated with *GBA* mutations (166,232,251,252) and recent data has also shown that mitochondrial dysfunction and mitophagy alterations are present in *post mortem* tissues of PD patients, cell and animal models with the second most common *GBA*-mutation,

GBA^{L444P} (253), but the exact mechanisms underlying the coexistence of mitochondrial and autophagic alterations are still not known.

Two important factors that support the relevance of the study of these PD-associated genes are (i) the fact that none of the two mutations are determinant but may only cause PD in some cases, making healthy mutation-carriers an interesting population of study, and (ii) the opportunity to identify subjects with prodromal PD and to follow from the beginning the, still unknown, pathological process, in order to establish biomarkers and maybe disease modifying therapies (26).

In this thesis, two different cell models derived from familiar forms of PD were evaluated: *LRRK2*^{G2019S} and *GBA*^{N370S}.

Characterization of *LRRK2*^{G2019S} fibroblasts

Study 1 consisted in the exhaustive analysis of mitochondrial phenotype and autophagic print of fibroblasts from *LRRK2*^{G2019S} mutation carriers. The added feature of the cell model herein presented is the exposure to galactose media aiming to enhance mitochondrial metabolism and the evaluation of mitochondrial performance in these challenging conditions (181).

Briefly, in standard conditions (glucose), the NM-*LRRK2*^{G2019S} fibroblasts showed a preserved mitochondrial phenotype, except for a significant disruption of MMP that may represent an early event in PD (197,200,246,248). In response to mitochondrial-challenging conditions (galactose), a pattern of mitochondrial enzymatic and respiratory function enhancement was observed, resulting in an increase of ATP production and morphological features characteristic of improved mitochondrial dynamics. In PD-*LRRK2*^{G2019S} fibroblasts, biases toward deranged mitochondrial phenotype were found in glucose media, such as decreased CI enzyme function, oxygen consumption and ATP production, and increased oxidative stress. Exposure to galactose revealed an inefficient increase in mitochondrial function, trends to increase oxidative stress and deranged mitochondrial dynamics.

Our study partially reproduces the mitochondrial phenotype described by Mortiboys et al. (127), where CI enzyme activity, oxygen consumption and ATP levels progressively decreased in NM-*LRRK2*^{G2019S} and PD-*LRRK2*^{G2019S}. Papkovskaia et al. (200) also found decreased ATP levels and depolarization in fibroblasts of PD-*LRRK2*^{G2019S}. However, both studies were only conducted in glycolytic conditions so mitochondrial alterations might have been concealed.

Oxidative stress is a hallmark of mitochondrial involvement on PD and neurodegeneration (49,62). Grünewald et al. (254), found increased levels of the antioxidant superoxide dismutase, but no significant alteration of oxidative stress in fibroblasts of NM-*LRRK2*^{G2019S}, suggesting the existence of compensatory mechanisms against early-stage production of ROS. Liou et al, (123) reported a protective effect against oxidative stress-mediated apoptosis mediated by wild type *LRRK2* which is lost in PD-associated mutations. In our study, trends towards reduced apoptosis in NM-*LRRK2*^{G2010S} in despite of trends to increase oxidative stress was found, which suggests the existence of other protecting mechanisms that are yet to be described, or maybe that a certain level of oxidative stress is important to maintain cellular health (79).

This study corroborated the impairment in mitochondrial dynamics in PD-*LRRK2*^{G2019S} patients exposed to glucose media described by others (127,246,247,255). Additionally, a healthier pattern in mitochondrial dynamics in NM-*LRRK2*^{G2019S} subjects was demonstrated. Whether alterations in mitochondrial dynamics are the cause or consequence of mitochondrial dysfunction, and the mechanism by which *LRRK2* mediates such alterations, is still a matter of debate (115).

Trends towards upregulation in autophagy in NM-*LRRK2*^{G2019S} were observed, which may be explained by any of the previously described effects of *LRRK2*^{G2019S} mutation in autophagy, such as defects in vesicle trafficking and lysosomal degradation (128,249,256) or by an increased attempt to eliminate damaged

subcellular compounds. A further increase in autophagy initiation signaling in PD-*LRRK2*^{G2019S} patients was found, probably in response to mitochondrial dysfunction and the resulting decrease in ATP levels evidenced by galactose exposure (177,257). The inability to continue with autophagosome formation and closure, and the resulting accumulation of damaged mitochondria among other waste product of cell metabolism, may explain the pathologic state in this group. Further studies should confirm the present findings, where mitophagy and autophagic flux may be characterized in more detail (258).

The most differential mitochondrial bioenergetic and dynamics response between NM-*LRRK2*^{G2019S} subjects and PD-*LRRK2*^{G2019S} patients was shown in response to mitochondrial-challenging conditions. This is the first study reporting that the exposition of fibroblasts from NM-*LRRK2*^{G2019S} to mitochondrial challenging conditions tends to enhance mitochondrial performance, even above the values of controls (250). Herein, we suggest that alternative models of PD should also be tested in oxidative conditions (259).

In accordance with other previous studies where NM-*LRRK2*^{G2019S} subjects perform as good as controls in motor (260), neuropsychological (261) and neuroimaging tests (262), our results suggest that *LRRK2*^{G2019S}-mutation may not trigger the development of clinical manifest PD by itself (117,257,263), but that another “hit” is needed to start the neurodegeneration process. In the non-manifesting group, enhanced mitochondrial function (evidenced upon stressful galactose condition) and improved autophagic performance may explain their asymptomatic state, providing two interesting therapeutic targets to test. Scientific efforts focused on promoting mitochondrial optimal performance and autophagy regulation should be translated into prophylactic measures that modify the natural history of PD (80).

Characterization of *GBA*^{N370S} neurospheres

Study 2 consisted in the assessment of the genotype-phenotype correlation of adipocyte-derived neurospheres from *GBA*^{N370S} mutation carriers, and the evaluation of the potential effect of *GBA*^{N370S} mutation in mitochondrial function and mitophagy induction. By exposing neurospheres to a uncoupling test, we aimed to induce and evaluate mitophagy and mitochondrial biogenesis.

The first part of this study encompassed the validation of the model since, to our knowledge, this is the first study characterizing mitochondrial performance and autophagy in neurospheres derived from carriers of *GBA*^{N370S}. This model would theoretically reproduce, with increased target-tissue specificity with respect to other cellular models, the mitochondrial and autophagic molecular alterations that may be responsible for neurodegeneration. Indeed, the characterization of the model was carried out successfully, as seen by the decreased GCCase activity in mutant neurospheres over time. The activity of GCCase has been found to impact the accumulation of α -synuclein, not only by a lack of digestion in the lysosomes, but also because of a vicious circle that includes a GCCase-directed toxicity by α -synuclein aggregates (143). Although at four days of differentiation synuclein levels were the same for all lines, it can be seen that over 10 days of differentiation, a trend to increase in α -synuclein levels is observed in the homozygous group, while the heterozygous and controls showed equal levels.

Our data suggests that homozygous *GBA*^{N370S} display increased mitochondrial content under basal conditions, while uncoupling resulted in defective clearance of mitochondrial content. Intriguingly heterozygous *GBA*^{N370S} lines tended to increase mitochondrial content following mitochondrial uncoupling, according to the literature (264) together with a large increase in PGC1- α . Most interestingly, ATP basal levels were increased in the heterozygous *GBA*^{N370S} group when compared to controls, and they progressively decreased with mitochondrial uncoupling in heterozygotes and controls, but not in homozygotes, confirming the accumulation of defective mitochondria.

Our macroautophagy flux data did not indicate a significant problem in the fusion of autophagosomes and lysosomes in mutant neurospheres, suggesting that, if mitophagy is impaired in these cells, it could be due to a problem with the initiation of mitophagy or excessive mitochondrial biogenesis, as observed by PGC1- α increase (265), although this has not been confirmed in the present study. Dysfunctional mitochondrial accumulation occurred in homozygous *GBA*^{N370S} neurospheres under basal conditions, and mitophagy did not seem to decrease mitochondrial content after mitochondrial uncoupling in heterozygous *GBA*^{N370S} neurospheres. Alternatively, if mitochondrial accumulation was not due to defective organelle clearance, it may be due to increased mitochondrial biogenesis.

GCase deficiency in neuronal models is typically associated with an impairment of macroautophagy flux (186,266,267). The increased mRNA levels of TFEB and associated increase in mitochondrial biogenesis, is the most likely explanation why we do not see changes in macroautophagy flux. Perhaps neurons are unable to maintain this compensatory mechanism, as they develop, particularly if mitochondrial dysfunction is occurring in these cells, and changes in autophagy flux are observed in more mature neurons.

Mitochondrial fission, as measured by the disappearance of the long isoform of OPA1, was similar between lines suggesting an alteration at other mechanistic level rather than the autophagic machinery required for the degradation of damaged mitochondria. PINK1 mRNA levels were also similar, and we were unable to detect either endogenous PINK1 or parkin protein levels suggesting either PINK1/parkin mitophagy occurs at an undetectable rate, or does not occur at all in neurospheres. Mitochondria in cortical neurons from *GBA-knock out* mice have been shown to recruit GFP-tagged parkin upon depolarization to a similar level as controls (166). Other mitophagy initiators (268,269) might be required for mitophagy in neurospheres. For instance, other proteins related to mitophagy such as BNIP3, FUND1, SMURF1 and ATG32 could also be affected. However, in this study only PINK/PARK dependent mitophagy was explored.

Although further studies are needed to assess whether mitochondrial optimal performance may influence the initiation of pathogenic pathways in this genetic context, as could be demonstrated in NM-*LRRK2*^{G2019S} subjects in study 1, findings that may provide important insights and prophylactic strategies will certainly shed light in the years to come.

Ever since the acknowledgment that PD pathology is not confined to the *SNpc*, and that the prodromal stage of the disease may precede it by as long as 20 years, it has been suggested that PD is the final stage of a systemic disorder where neurodegeneration is the common and final end-point (270). Moreover, different pathological pathways have been described, and subtle clinical and histologic differences have been identified, widening the lines of investigation focused on the study of the disease (19).

The efficiency with which a cell can regenerate mitochondria declines with aging and disease; the ability to balance increased mitochondrial degradation with increased biogenesis may determine the outcome of mitophagy in neurons and other cells that are highly dependent on mitochondrial metabolism (51,69,271). Also, the balance between mitochondrial biogenesis and autophagy, or mitophagy, determines the cellular adaptation to physiological and pathological stressors. An imbalanced response to these stressors contributes to cellular degeneration and susceptibility to cell death (101).

Autophagy induction and autophagic overexpressed genes in response to mutant or damaged proteins and aggregates could be compensatory and neuroprotective at early stages of the disease. This response is only pathologic if lysosomal clearance becomes compromised (86). However, a pathological level of autophagy induction has been inferred in a few neuropathological states so it must be stated that, even though modulation of autophagy may be a logical interventional strategy, the high complexity of this interventions still need to be largely studied

(240). For instance, although macroautophagy and CMA are not redundant processes, cells respond to blockage of CMA by activating macroautophagy and viceversa (239,272,273), which may be an explanation to the upregulation of macroautophagy observed in our study. A better understanding of the compensatory mechanisms and autophagic alternatives that are activated when autophagy fails will surely help to design therapeutic strategies.

Based on all our results, this thesis proposes that the enhanced mitochondrial and autophagic function of NM-*LRRK2*^{G2019S} subjects and the increased ATP levels and mitochondrial content in *GBA*^{N370S} heterozygous represents a biological rescue mechanism, which may prevent the neurodegenerative process with compensatory increased bioenergetic cell demand in early mitochondrial damage. It may be deduced that mitochondrial and autophagic optimal function could have a protective role in mutation carriers who have not yet developed symptoms of PD. In other words, mitochondria from NM-*LRRK2*^{G2019S} and wt/*GBA* may have an increased adaptative response to stress and increased biogenesis until a maximal threshold beyond which neurodegeneration may occur.

Even though there is still no explanation on why cell death only occurs in certain neuronal subtypes in PD, it can be deduced that neural integrity greatly relies on efficient mitochondrial metabolism and autophagy. If autophagic deficiencies are evident in mitotic cells, or in young neurons (or a model resembling young neurons, such as neurospheres) it may be inferred that these alterations account for an increased vulnerability in mature neurons since autophagic vacuoles generated in axons must travel longer distances to reach lysosomes, and because of their postmitotic nature, neurons face more difficulties in preventing accumulation of dysfunctional organelles.

There is a positive correlation between age and PD onset in *LRRK2*^{G2019S} mutation carriers (117), suggesting that some NM-*LRRK2*^{G2019S} may eventually develop PD. However, it must be emphasized that no age-related differences in

mitochondrial and autophagic parameters were observed and that, up to date, none of NM-LRRK2 patients has developed PD. Finally, many other molecular triggers may be taking place in PD, where the loss of dopaminergic neurons may be the common manifestation of a complex disease where mitochondrial alterations and autophagic deregulation are two of manifold molecular events leading to neurodegeneration. GCase activity is also decreased with ageing; which most probably influences the development of PD in this subset of population.

Some limitations of the present studies must be acknowledged. A unique mitochondrial parameter has not been demonstrated to be affected and, thus, the availability of a single, accessible and reliable biomarker is still lacking. The approaches to study autophagy in the works presented by this thesis are, unfortunately, limited to the description of macroautophagic flux. However, three main core features of mitochondrial biology are now on focus as candidates after studying different hereditary forms of PD and other related parkinsonian disorders, including: 1. ETC, 2. Mitochondrial dynamics and 3. UPRmt.

Although the study of less frequent forms of PD due to inherited mutations reduces the potential study of bigger cohorts, the small sample size of this study may explain a common pitfall of the reported outcomes, which is the limited number of statistically significant differences. Additionally, the inter-individual variability in environmental conditions potentially influencing molecular parameters may also hinder the homogeneity of the distinct groups. More specifically for study 2, the reduced number of samples from each group cannot support any taxative conclusion on behalf of mitochondrial and autophagic performance. On this respect, we would like to emphasize the reduced variability within the control and heterozygous groups, and the great variability that the homozygous patients presented. In the future, when more patients and controls are available, and once the model is recognized for its utility, an increment in the cases included would be desirable to study an extended mitochondrial profile of heterozygous with respect to whether they present PD or not. Fortunately, being these two mutations the most common genetic factor and the

greatest common risk for hereditary PD, it is a matter of time that more subjects are identified and more studies encompassing human-derived models can be performed. In this promising scenario, perhaps the greatest challenge is to have access to detailed clinical data and negative results derived from research efforts in different countries in order to be able to elaborate reliable conclusions.

Future studies may be carried on in human-derived cellular models to dissect the molecular mechanisms of PD, establish novel biomarkers and potential therapeutic candidates. The asymptomatic mutation carriers represent the most valuable population for research in early onset stages, since early neurodegenerative events can be identified and disease-modifying therapies can thus be developed in which the use of cell stressors may be of utility to highlight differences between cases and controls.

Despite all the gaps remaining in the description of the etiologic mechanisms leading to neurodegeneration in PD, the works contained in the present thesis validate two patient-derived cell models of disease. These models derived from the less frequent types of PD and other rare diseases, such as mitochondrial diseases and LD are of a great value to the investigation of molecular pathways altered in common forms of neurodegenerative diseases, resulting in promising protective and early disease-modifying therapies that, most importantly can be promptly translated to the clinical setting.



7. CONCLUSIONS



1. A global analysis of skin-derived fibroblasts from NM-*LRRK2*^{G2019S} and PD-*LRRK2*^{G2019S} demonstrated that both mutant groups showed a genotype-phenotype correspondence and a distinct mitochondrial and autophagic performance.
2. In standard (glucose) conditions, skin-derived fibroblasts from NM-*LRRK2*^{G2019S} exhibited a conserved mitochondrial and autophagic phenotype whilst PD-*LRRK2*^{G2019S} showed a pre-existing mitochondrial lesion and decreased autophagosome formation.
3. In mitochondrial-challenging conditions (galactose), skin-derived fibroblasts from NM-*LRRK2*^{G2019S} showed an outstanding mitochondrial and autophagic response to mitochondrial challenging conditions (galactose); on the contrary, PD-*LRRK2*^{G2019S} show an inefficient increase in mitochondrial function and defective autophagy yielded towards increased oxidative damage.
4. Adipocyte-derived neurospheres exhibit molecular changes associated to the decreased activity of GCase throughout developmental stages, and mitochondrial dysfunction is an early event preceding macroautophagy flux in adipocyte-derived neurospheres from pathogenic *GBA*^{N370S}-mutation carriers.
5. In standard conditions, adipocyte-derived neurospheres from *GBA*^{N370S} heterozygotes showed a compensatory mitochondrial state, while *GBA*^{N370S} homozygotes showed a dysfunctional mitochondrial profile and decreased autophagy.
6. Induction of mitochondrial uncoupling of adipocyte-derived neurospheres from *GBA*^{N370S} heterozygotes showed an increased mitochondrial biogenesis, which was not present in *GBA*^{N370S} homozygotes.
7. The study of asymptomatic subjects carrying *LRRK2*^{G2019S} and *GBA*^{N370S} mutations represent a valuable group of study where early molecular alterations and compensatory mechanisms may be dissected to target for potential disease-modifying therapies.
8. Skin-derived fibroblasts and adipocyte-derived neurospheres exhibit PD pathological characteristics, such as mitochondrial and autophagic alterations, which validate these cell models of disease and confirm the presence of molecular alterations beyond the neural tissues.



8. REFERENCES



1. Pahwa R, Lyons KE. Early diagnosis of Parkinson's disease: recommendations from diagnostic clinical guidelines. *Am J Manag Care* [Internet]. 2010 Mar [cited 2016 Feb 15];16 Suppl 1:S94-9. Available from: <http://www.ncbi.nlm.nih.gov/pubmed/20297872>
2. Kalia L V, Lang AE. Parkinson's disease. *Lancet* [Internet]. 2015 Aug 29 [cited 2018 Oct 3];386(9996):896–912. Available from: <http://www.ncbi.nlm.nih.gov/pubmed/25904081>
3. Goetz CG. The History of Parkinson's Disease: Early Clinical Descriptions and Neurological Therapies. *Cold Spring Harb Perspect Med* [Internet]. 2011 [cited 2019 Jan 14];1(1):a008862. Available from: www.perspectivesinmedicine.org
4. Parkinson J. An Essay on the Shaking Palsy. *J Neuropsychiatry Clin Neurosci* [Internet]. 2002 May [cited 2019 Jan 14];14(2):223–36. Available from: <http://psychiatryonline.org/doi/abs/10.1176/jnp.14.2.223>
5. Goetz CG. Charcot on Parkinson's disease. *Mov Disord* [Internet]. 1986 [cited 2019 May 28];1(1):27–32. Available from: <http://www.ncbi.nlm.nih.gov/pubmed/3332804>
6. Przedborski S. The two-century journey of Parkinson disease research. *Nat Rev Neurosci* [Internet]. 2017 Apr 1 [cited 2019 Jan 15];18(4):251–9. Available from: <http://www.nature.com/articles/nrn.2017.25>
7. Greenfield. Ground water pollution in Germany by nitrate: a nationwide GIS supported model analysis. *Eng Geol Environ Proc Symp Athens, 1997 Vol 2* [Internet]. 1993 Nov [cited 2019 Jan 14];16(4):2265–70. Available from: <http://www.ncbi.nlm.nih.gov/pubmed/13109537>
8. Hoehn MM, Yahr MD. Parkinsonism: onset, progression and mortality. *Neurology* [Internet]. 1967 May [cited 2019 Jan 14];17(5):427–42. Available from: <http://www.ncbi.nlm.nih.gov/pubmed/6067254>
9. Blesa J, Phani S, Jackson-Lewis V, Przedborski S. Classic and New Animal Models of Parkinson's Disease. *J Biomed Biotechnol*. 2012;
10. Langston JW. The MPTP Story. *J Parkinsons Dis* [Internet]. 2017 [cited 2019 Jan 14];7(s1):S11–9. Available from: <http://www.ncbi.nlm.nih.gov/pubmed/28282815>
11. Platt FM, d'Azzo A, Davidson BL, Neufeld EF, Tiffit CJ. Lysosomal storage diseases. *Nat Rev Dis Prim* [Internet]. 2018 Dec 1 [cited 2019 May 23];4(1):27. Available from: <http://www.nature.com/articles/s41572-018-0025-4>
12. Tello C, Darling A, Lupo V, Pérez-Dueñas B, Espinós C. On the complexity of clinical and molecular bases of neurodegeneration with brain iron accumulation. *Clin Genet* [Internet]. 2018 Apr 1 [cited 2019 May 23];93(4):731–40. Available from: <http://doi.wiley.com/10.1111/cge.13057>
13. Del Rey NL-G, Quiroga-Varela A, Garbayo E, Carballo-Carbajal I, Fernández-Santiago R, Monje MHG, et al. Advances in Parkinson's Disease: 200 Years Later. *Front Neuroanat* [Internet]. 2018 [cited 2019 Jan 20];12:113. Available from: <http://www.ncbi.nlm.nih.gov/pubmed/30618654>
14. Gazewood JD, Richards DR, Clebak K. Parkinson disease: an update. *Am Fam Physician* [Internet]. 2013 Mar 15;87(4):267–73. Available from: <http://www.ncbi.nlm.nih.gov/pubmed/24291875>
15. Trinh J, Zeldenrust FMJ, Huang J, Kasten M, Schaake S, Petkovic S, et al. Genotype-phenotype relations for the Parkinson's disease genes SNCA, LRRK2, VPS35:

- MDSGene systematic review. *Mov Disord* [Internet]. 2018 Dec [cited 2019 Jan 20];33(12):1857–70. Available from: <http://www.ncbi.nlm.nih.gov/pubmed/30357936>
16. Trinh J, Lohmann K, Baumann H, Balck A, Borsche M, Brüggemann N, et al. Utility and Implications of Exome Sequencing in Early-Onset Parkinson's Disease. 2018 [cited 2019 Jan 20]; Available from: <https://onlinelibrary-wiley-com.sire.ub.edu/doi/pdf/10.1002/mds.27559>
 17. Gorostidi A, Martí-Massó JF, Bergareche A, Rodríguez-Oroz MC, López de Munain A, Ruiz-Martínez J. Genetic Mutation Analysis of Parkinson's Disease Patients Using Multigene Next-Generation Sequencing Panels. *Mol Diagn Ther* [Internet]. 2016 Jun 13 [cited 2016 Aug 25]; Available from: <http://www.ncbi.nlm.nih.gov/pubmed/27294386>
 18. de Lau LML, Breteler MMB. Epidemiology of Parkinson's disease. *Lancet Neurol* [Internet]. 2006 Jun 1 [cited 2019 Feb 13];5(6):525–35. Available from: <http://www.ncbi.nlm.nih.gov/pubmed/16713924>
 19. Corti O, Lesage S, Brice A. What genetics tells us about the causes and mechanisms of Parkinson's disease. *Physiol Rev* [Internet]. 2011 Oct [cited 2015 Dec 17];91(4):1161–218. Available from: <http://www.ncbi.nlm.nih.gov/pubmed/22013209>
 20. De Rosa P, Marini ES, Gelmetti V, Valente EM. Candidate genes for Parkinson disease: Lessons from pathogenesis. *Clin Chim Acta*. 2015;449:68–76.
 21. Tysnes O-B, Storstein A. Epidemiology of Parkinson's disease. *J Neural Transm* [Internet]. 2017 Aug 1 [cited 2019 Jan 20];124(8):901–5. Available from: <http://www.ncbi.nlm.nih.gov/pubmed/28150045>
 22. Poewe W, Seppi K, Tanner CM, Halliday GM, Brundin P, Volkmann J, et al. Parkinson disease. *Nat Rev Dis Prim* [Internet]. 2017 Mar 23 [cited 2018 Oct 3];3:17013. Available from: <http://www.nature.com/articles/nrdp201713>
 23. Kordower JH, Olanow CW, Dodiya HB, Chu Y, Beach TG, Adler CH, et al. Disease duration and the integrity of the nigrostriatal system in Parkinson's disease. *Brain* [Internet]. 2013 Aug [cited 2016 Aug 2];136(Pt 8):2419–31. Available from: <http://www.ncbi.nlm.nih.gov/pubmed/23884810>
 24. Jankovic J. Parkinson's disease: clinical features and diagnosis. *J Neurol Neurosurg Psychiatry* [Internet]. 2008 Apr 1 [cited 2019 Jan 15];79(4):368–76. Available from: <http://www.ncbi.nlm.nih.gov/pubmed/18344392>
 25. Schapira AHV, Chaudhuri KR, Jenner P. Non-motor features of Parkinson disease. *Nat Rev Neurosci* [Internet]. 2017 Jun 8 [cited 2019 Jan 20];18(7):435–50. Available from: <http://www.ncbi.nlm.nih.gov/pubmed/28592904>
 26. Mahlke P, Seppi K, Poewe W. The Concept of Prodromal Parkinson's Disease. *J Parkinsons Dis* [Internet]. 2015 [cited 2019 Jan 15];5(4):681–97. Available from: <http://www.ncbi.nlm.nih.gov/pubmed/26485429>
 27. Postuma RB, Berg D. Advances in markers of prodromal Parkinson disease. *Nat Rev Neurol* [Internet]. 2016 Nov 1 [cited 2019 Jan 15];12(11):622–34. Available from: <http://www.nature.com/articles/nrneurol.2016.152>
 28. Gibb WR, Lees AJ. The relevance of the Lewy body to the pathogenesis of idiopathic Parkinson's disease. *J Neurol Neurosurg Psychiatry* [Internet]. 1988 Jun 1 [cited 2019 Jan 15];51(6):745–52. Available from: <http://www.ncbi.nlm.nih.gov/pubmed/2841426>
 29. Gelb DJ, Oliver E, Gilman S. Diagnostic Criteria for Parkinson Disease. *Arch Neurol*

- [Internet]. 1999 Jan 1 [cited 2019 Jan 15];56(1):33. Available from: <http://archneur.jamanetwork.com/article.aspx?doi=10.1001/archneur.56.1.33>
30. Marsili L, Rizzo G, Colosimo C. Diagnostic criteria for Parkinson's disease: From James Parkinson to the concept of prodromal disease [Internet]. Vol. 9, *Frontiers in Neurology*. 2018 [cited 2019 Jan 15]. Available from: www.frontiersin.org
 31. Postuma RB, Berg D, Stern M, Poewe W, Olanow CW, Oertel W, et al. MDS clinical diagnostic criteria for Parkinson's disease. *Mov Disord* [Internet]. 2015 Oct 1 [cited 2019 Jan 14];30(12):1591–601. Available from: <http://doi.wiley.com/10.1002/mds.26424>
 32. Berg D, Postuma RB, Adler CH, Bloem BR, Chan P, Dubois B, et al. MDS research criteria for prodromal Parkinson's disease. *Mov Disord* [Internet]. 2015 Oct [cited 2019 Jan 14];30(12):1600–11. Available from: <http://doi.wiley.com/10.1002/mds.26431>
 33. Mahlkecht P, Gasperi A, Willeit P, Kiechl S, Stockner H, Willeit J, et al. Prodromal Parkinson's disease as defined per MDS research criteria in the general elderly community. *Mov Disord* [Internet]. 2016 Sep 1 [cited 2019 Jan 20];31(9):1405–8. Available from: <http://doi.wiley.com/10.1002/mds.26674>
 34. Djaldetti R, Lev N, Melamed E. Lesions outside the CNS in Parkinson's disease. *Mov Disord*. 2009;24(6):793–800.
 35. Dayal V, Limousin P, Foltynie T. Subthalamic Nucleus Deep Brain Stimulation in Parkinson's Disease: The Effect of Varying Stimulation Parameters. *J Parkinsons Dis* [Internet]. 2017 May 16 [cited 2019 Mar 26];7(2):235–45. Available from: <http://www.ncbi.nlm.nih.gov/pubmed/28505983>
 36. Bloem BR, de Vries NM, Ebersbach G. Nonpharmacological treatments for patients with Parkinson's disease. *Mov Disord* [Internet]. 2015 Sep 15 [cited 2019 Mar 26];30(11):1504–20. Available from: <http://www.ncbi.nlm.nih.gov/pubmed/26274930>
 37. Witt K, Kalbe E, Erasmi R, Ebersbach G. Nichtmedikamentöse Therapieverfahren beim Morbus Parkinson. *Nervenarzt* [Internet]. 2017 Apr 1 [cited 2019 Mar 26];88(4):383–90. Available from: <http://www.ncbi.nlm.nih.gov/pubmed/28251243>
 38. Olanow CW, Schapira AH V. Therapeutic prospects for Parkinson disease. *Ann Neurol* [Internet]. 2013 Sep 1 [cited 2019 Jan 14];74(3):337–47. Available from: <http://doi.wiley.com/10.1002/ana.24011>
 39. Dickson DW. Neuropathology of Parkinson disease. *Parkinsonism Relat Disord* [Internet]. 2018 Jan [cited 2019 Feb 17];46:S30–3. Available from: <http://www.ncbi.nlm.nih.gov/pubmed/28780180>
 40. Braak H, Del Tredici K, Rüb U, de Vos RAI, Jansen Steur ENH, Braak E. Staging of brain pathology related to sporadic Parkinson's disease. *Neurobiol Aging* [Internet]. [cited 2019 Feb 17];24(2):197–211. Available from: <http://www.ncbi.nlm.nih.gov/pubmed/12498954>
 41. Dickson DW, Uchikado H, Fujishiro H, Tsuboi Y. Evidence in favor of Braak staging of Parkinson's disease. *Mov Disord* [Internet]. 2010 [cited 2019 Feb 17];25(S1):S78–82. Available from: <http://www.ncbi.nlm.nih.gov/pubmed/20187227>
 42. Cao H, Shi J, Cao B, Kang B, Zhang M, Qu Q. Evaluation of the Braak staging of brain pathology with 1 H-MRS in patients with Parkinson's disease. *Neurosci Lett* [Internet]. 2017 Nov 1 [cited 2019 Feb 17];660:57–62. Available from:

- <http://www.ncbi.nlm.nih.gov/pubmed/28844732>
43. Johansen KK, Torp SH, Farrer MJ, Gustavsson EK, Aasly JO. A Case of Parkinson's Disease with No Lewy Body Pathology due to a Homozygous Exon Deletion in Parkin. *Case Rep Neurol Med* [Internet]. 2018 [cited 2019 Feb 17];2018:6838965. Available from: <http://www.ncbi.nlm.nih.gov/pubmed/30050705>
 44. Gaig C, Martí MJ, Ezquerra M, Rey MJ, Cardozo A, Tolosa E. G2019S LRRK2 mutation causing Parkinson's disease without Lewy bodies. *J Neurol Neurosurg Psychiatry* [Internet]. 2007 Jun [cited 2019 Feb 17];78(6):626–8. Available from: <http://www.ncbi.nlm.nih.gov/pubmed/17210620>
 45. Rietdijk CD, Perez-Pardo P, Garssen J, van Wezel RJA, Kraneveld AD. Exploring Braak's Hypothesis of Parkinson's Disease. *Front Neurol* [Internet]. 2017 Feb 13 [cited 2019 Feb 17];8:37. Available from: <http://www.ncbi.nlm.nih.gov/pubmed/28243222>
 46. Singer TP, Ramsay RR, Sonsalla PK, Nicklas WJ, Heikkila RE. Biochemical mechanisms underlying MPTP-induced and idiopathic parkinsonism. *New vistas. Adv Neurol* [Internet]. 1993 Jan [cited 2016 Feb 22];60:300–5. Available from: <http://www.ncbi.nlm.nih.gov/pubmed/8380523>
 47. Schapira AH V. Mitochondria in the aetiology and pathogenesis of Parkinson's disease. *Lancet Neurol* [Internet]. 2008 Jan;7(1):97–109. Available from: <http://www.ncbi.nlm.nih.gov/pubmed/18093566>
 48. Cardellach F, Martí MJ, Fernández-Solá J, Marín C, Hoek JB, Tolosa E, et al. Mitochondrial respiratory chain activity in skeletal muscle from patients with Parkinson's disease. *Neurology* [Internet]. 1993 Nov [cited 2015 May 12];43(11):2258–62. Available from: <http://www.ncbi.nlm.nih.gov/pubmed/8232939>
 49. Keeney PM, Xie J, Capaldi R a, Bennett JP. Parkinson's disease brain mitochondrial complex I has oxidatively damaged subunits and is functionally impaired and misassembled. *J Neurosci* [Internet]. 2006 May 10 [cited 2014 May 6];26(19):5256–64. Available from: <http://www.ncbi.nlm.nih.gov/pubmed/16687518>
 50. Margulis L. Symbiotic theory of the origin of eukaryotic organelles; criteria for proof. *Symp Soc Exp Biol* [Internet]. 1975 Jan [cited 2015 Sep 6];(29):21–38. Available from: <http://www.ncbi.nlm.nih.gov/pubmed/822529>
 51. Nunnari J, Suomalainen A, Ahlqvist KJ, Hämäläinen RH, Yatsuga S, Uutela M, et al. Mitochondria: in sickness and in health. *Cell* [Internet]. 2012 Mar 16 [cited 2016 Dec 13];148(6):1145–59. Available from: <http://www.ncbi.nlm.nih.gov/pubmed/22424226>
 52. Gorman GS, Chinnery PF, DiMauro S, Hirano M, Koga Y, McFarland R, et al. Mitochondrial diseases. *Nat Rev Dis Prim* [Internet]. 2016 Oct 20 [cited 2019 Feb 10];2:16080. Available from: <http://www.nature.com/articles/nrdp201680>
 53. Mitchell P. Coupling of phosphorylation to electron and hydrogen transfer by a chemi-osmotic type of mechanism. *Nature* [Internet]. 1961 Jul 8 [cited 2019 May 14];191:144–8. Available from: <http://www.ncbi.nlm.nih.gov/pubmed/13771349>
 54. Cogliati S, Calvo E, Loureiro M, Guaras AM, Nieto-Arellano R, Garcia-Poyatos C, et al. Mechanism of super-assembly of respiratory complexes III and IV. *Nature* [Internet]. 2016 Nov 24 [cited 2019 Apr 2];539(7630):579–82. Available from: <http://www.nature.com/articles/nature20157>
 55. Koob S, Reichert AS. Novel intracellular functions of apolipoproteins: the ApoO protein

- family as constituents of the Mitofilin/MINOS complex determines cristae morphology in mitochondria. *Biol Chem* [Internet]. 2014 Jan 1 [cited 2019 Feb 17];395(3):285–96. Available from: <http://www.ncbi.nlm.nih.gov/pubmed/24391192>
56. Letts JA, Sazanov LA. Clarifying the supercomplex: the higher-order organization of the mitochondrial electron transport chain. *Nat Struct Mol Biol* [Internet]. 2017 Oct 5 [cited 2019 Feb 17];24(10):800–8. Available from: <http://www.nature.com/doi/10.1038/nsmb.3460>
 57. Anderson S, Bankier AT, Barrell BG, de Bruijn MH, Coulson AR, Drouin J, et al. Sequence and organization of the human mitochondrial genome. *Nature* [Internet]. 1981 Apr 9 [cited 2016 Nov 5];290(5806):457–65. Available from: <http://www.ncbi.nlm.nih.gov/pubmed/7219534>
 58. Herst PM, Rowe MR, Carson GM, Berridge M V. Functional Mitochondria in Health and Disease. *Front Endocrinol (Lausanne)* [Internet]. 2017 Nov 3 [cited 2017 Nov 24];8:296. Available from: <http://www.ncbi.nlm.nih.gov/pubmed/29163365>
 59. Dagda RK, Chu CT. Mitochondrial quality control: insights on how Parkinson's disease related genes PINK1, parkin, and Omi/HtrA2 interact to maintain mitochondrial homeostasis. *J Bioenerg Biomembr* [Internet]. 2009 Dec 10 [cited 2018 Feb 5];41(6):473–9. Available from: <http://link.springer.com/10.1007/s10863-009-9255-1>
 60. Twig G, Shirihai OS. The Interplay Between Mitochondrial Dynamics and Mitophagy. *Antioxid Redox Signal* [Internet]. 2011 May 15 [cited 2019 Apr 3];14(10):1939–51. Available from: <http://www.liebertpub.com/doi/10.1089/ars.2010.3779>
 61. Burté F, Carelli V, Chinnery PF, Yu-Wai-Man P. Disturbed mitochondrial dynamics and neurodegenerative disorders. *Nat Rev Neurol* [Internet]. 2014;11(1):11–24. Available from: <http://www.nature.com/doi/10.1038/nrneurol.2014.228>
 62. Haelterman N a, Yoon WH, Sandoval H, Jaiswal M, Shulman JM, Bellen HJ. A Mitocentric View of Parkinson's Disease. *Annu Rev Neurosci* [Internet]. 2014;37:137–59. Available from: <http://www.ncbi.nlm.nih.gov/pubmed/24821430>
 63. Van Laar VS, Berman SB. Mitochondrial dynamics in Parkinson's disease. *Exp Neurol* [Internet]. 2009;218(2):247–56. Available from: <http://dx.doi.org/10.1016/j.expneurol.2009.03.019>
 64. Bertholet AM, Delerue T, Millet AM, Moulis MF, David C, Daloyau M, et al. Mitochondrial fusion/fission dynamics in neurodegeneration and neuronal plasticity. *Neurobiol Dis* [Internet]. 2016 Jun [cited 2019 May 17];90:3–19. Available from: <http://www.ncbi.nlm.nih.gov/pubmed/26494254>
 65. Alvarez-Mora MI, Rodriguez-Revenga L, Madrigal I, Guitart-Mampel M, Garrabou G, Milà M. Impaired Mitochondrial Function and Dynamics in the Pathogenesis of FXTAS. *Mol Neurobiol* [Internet]. 2017 Nov 22 [cited 2019 May 17];54(9):6896–902. Available from: <http://link.springer.com/10.1007/s12035-016-0194-7>
 66. Rodríguez-Arribas M, Yakhine-Diop SMS, Pedro JMB-S, Gómez-Suaga P, Gómez-Sánchez R, Martínez-Chacón G, et al. Mitochondria-Associated Membranes (MAMs): Overview and Its Role in Parkinson's Disease. *Mol Neurobiol* [Internet]. 2017 Oct 6 [cited 2019 May 17];54(8):6287–303. Available from: <http://www.ncbi.nlm.nih.gov/pubmed/27714635>
 67. Trudler D, Nash Y, Frenkel D. New insights on Parkinson's disease genes: the link

- between mitochondria impairment and neuroinflammation. *J Neural Transm* [Internet]. 2015 Oct 17 [cited 2019 Feb 13];122(10):1409–19. Available from: <http://www.ncbi.nlm.nih.gov/pubmed/25894287>
68. Camilleri A, Vassallo N. The centrality of mitochondria in the pathogenesis and treatment of Parkinson's disease. *CNS Neurosci Ther* [Internet]. 2014 Jul [cited 2016 Mar 15];20(7):591–602. Available from: <http://www.ncbi.nlm.nih.gov/pubmed/24703487>
 69. Swerdlow RH. The neurodegenerative mitochondrialopathies. *J Alzheimers Dis* [Internet]. 2009 Jan [cited 2015 Sep 6];17(4):737–51. Available from: <http://www.pubmedcentral.nih.gov/articlerender.fcgi?artid=2896000&tool=pmcentrez&rendertype=abstract>
 70. Kravtsov Y, Kudryavtseva E, McKee AC, Geula C, Kowall NW, Khrapko K. Mitochondrial DNA deletions are abundant and cause functional impairment in aged human substantia nigra neurons. *Nat Genet* [Internet]. 2006 May 9 [cited 2019 Feb 18];38(5):518–20. Available from: <http://www.ncbi.nlm.nih.gov/pubmed/16604072>
 71. Cha M-Y, Kim DK, Mook-Jung I. The role of mitochondrial DNA mutation on neurodegenerative diseases. *Exp Mol Med* [Internet]. 2015;47(3):e150. Available from: <http://www.nature.com/doi/10.1038/emm.2014.122>
 72. Shpilka T, Haynes CM. The mitochondrial UPR: mechanisms, physiological functions and implications in ageing. *Nat Rev Mol Cell Biol* [Internet]. 2017 Nov 22 [cited 2019 Feb 18];19(2):109–20. Available from: <http://www.ncbi.nlm.nih.gov/pubmed/29165426>
 73. Lin Y-F, Schulz AM, Pellegrino MW, Lu Y, Shaham S, Haynes CM. Maintenance and propagation of a deleterious mitochondrial genome by the mitochondrial unfolded protein response. *Nature* [Internet]. 2016 May 2 [cited 2019 Feb 22];533(7603):416–9. Available from: <http://www.ncbi.nlm.nih.gov/pubmed/27135930>
 74. Stefani IC, Wright D, Polizzi KM, Kontoravdi C. The role of ER stress-induced apoptosis in neurodegeneration. *Curr Alzheimer Res* [Internet]. 2012 Mar [cited 2016 Apr 19];9(3):373–87. Available from: <http://www.ncbi.nlm.nih.gov/pubmed/22299619>
 75. Puigserver P. Tissue-specific regulation of metabolic pathways through the transcriptional coactivator PGC1- α . *Int J Obes* [Internet]. 2005 Mar 14 [cited 2019 Feb 18];29(S1):S5–9. Available from: <http://www.ncbi.nlm.nih.gov/pubmed/15711583>
 76. Esterbauer H, Oberkofler H, Krempler F, Patsch W. Human Peroxisome Proliferator Activated Receptor Gamma Coactivator 1 (PPARGC1) Gene: cDNA Sequence, Genomic Organization, Chromosomal Localization, and Tissue Expression. *Genomics* [Internet]. 1999 Nov 15 [cited 2019 Feb 18];62(1):98–102. Available from: <http://www.ncbi.nlm.nih.gov/pubmed/10585775>
 77. Corona JC, Duchon MR. PPAR γ and PGC-1 α as therapeutic targets in Parkinson's. *Neurochem Res* [Internet]. 2015 Feb [cited 2019 Jan 20];40(2):308–16. Available from: <http://www.ncbi.nlm.nih.gov/pubmed/25007880>
 78. Carvalho C, Correia SC, Cardoso S, Plácido AI, Candeias E, Duarte AI, et al. The role of mitochondrial disturbances in Alzheimer, Parkinson and Huntington diseases. *Expert Rev Neurother* [Internet]. 2015 Jan [cited 2016 Apr 19];15(8):867–84. Available from: <http://www.ncbi.nlm.nih.gov/pubmed/26092668>
 79. Ristow M. Unraveling the Truth About Antioxidants: Mitohormesis explains ROS-

- induced health benefits. *Nat Med* [Internet]. 2014 Jul 7 [cited 2019 May 17];20(7):709–11. Available from: <http://www.nature.com/articles/nm.3624>
80. Bárcena C, Mayoral P, Quirós PM. Mitohormesis, an Antiaging Paradigm. In: *International review of cell and molecular biology* [Internet]. 2018 [cited 2019 May 17]. p. 35–77. Available from: <http://www.ncbi.nlm.nih.gov/pubmed/30072093>
 81. Cuervo AM. Autophagy: many paths to the same end. *Mol Cell Biochem* [Internet]. 2004 Aug [cited 2019 Apr 3];263(1–2):55–72. Available from: <http://www.ncbi.nlm.nih.gov/pubmed/15524167>
 82. Xu H, Ren D. Lysosomal Physiology. *Annu Rev Physiol* [Internet]. 2015 Feb 10 [cited 2019 May 23];77(1):57–80. Available from: <http://www.ncbi.nlm.nih.gov/pubmed/25668017>
 83. Puertollano R, Ferguson SM, Brugarolas J, Ballabio A. The complex relationship between TFEB transcription factor phosphorylation and subcellular localization. *EMBO J* [Internet]. 2018 Jun 1 [cited 2019 Feb 27];37(11):e98804. Available from: <http://www.ncbi.nlm.nih.gov/pubmed/29764979>
 84. Levine B, Kroemer G. Biological Functions of Autophagy Genes: A Disease Perspective. *Cell* [Internet]. 2019 [cited 2019 Jan 19];176:11–42. Available from: <https://doi.org/10.1016/j.cell.2018.09.048>
 85. Seranova E, Connolly KJ, Zatyka M, Rosenstock TR, Barrett T, Tuxworth RI, et al. Dysregulation of autophagy as a common mechanism in lysosomal storage diseases. *Essays Biochem* [Internet]. 2017 Dec 12 [cited 2019 May 23];61(6):733–49. Available from: <http://essays.biochemistry.org/lookup/doi/10.1042/EBC20170055>
 86. Nixon RA. The role of autophagy in neurodegenerative disease. *Nat Med* [Internet]. 2013 Aug 6 [cited 2017 Feb 17];19(8):983–97. Available from: <http://www.nature.com/doi/10.1038/nm.3232>
 87. López-Otín C, Galluzzi L, Freije JMP, Madeo F, Kroemer G. Metabolic Control of Longevity. *Cell* [Internet]. 2016 Aug 11 [cited 2019 Feb 27];166(4):802–21. Available from: <https://www.sciencedirect.com/science/article/pii/S0092867416309813>
 88. Li W, Li J, Bao J. Microautophagy: lesser-known self-eating. *Cell Mol Life Sci* [Internet]. 2012 Apr 12 [cited 2019 Apr 3];69(7):1125–36. Available from: <http://link.springer.com/10.1007/s00018-011-0865-5>
 89. Kissová I, Salin B, Schaeffer J, Bhatia S, Manon S, Camougrand N. Selective and non-selective autophagic degradation of mitochondria in yeast. *Autophagy* [Internet]. [cited 2019 Apr 3];3(4):329–36. Available from: <http://www.ncbi.nlm.nih.gov/pubmed/17377488>
 90. Alfaro IE, Alborno A, Molina A, Moreno J, Cordero K, Criollo A, et al. Chaperone Mediated Autophagy in the Crosstalk of Neurodegenerative Diseases and Metabolic Disorders. *Front Endocrinol (Lausanne)* [Internet]. 2019 Jan 31 [cited 2019 Feb 28];9:778. Available from: <https://www.frontiersin.org/article/10.3389/fendo.2018.00778/full>
 91. Grumati P, Dikic I. Ubiquitin signaling and autophagy. *J Biol Chem* [Internet]. 2018 Apr 13 [cited 2019 Feb 27];293(15):5404–13. Available from: <http://www.ncbi.nlm.nih.gov/pubmed/29187595>
 92. Kroemer G, Mariño G, Levine B. Autophagy and the Integrated Stress Response. *Mol*

- Cell [Internet]. 2010 Oct 22 [cited 2019 Feb 25];40(2):280–93. Available from: <http://www.ncbi.nlm.nih.gov/pubmed/20965422>
93. Geisler S, Holmström KM, Skujat D, Fiesel FC, Rothfuss OC, Kahle PJ, et al. PINK1/Parkin-mediated mitophagy is dependent on VDAC1 and p62/SQSTM1. *Nat Cell Biol* [Internet]. 2010 Feb 24 [cited 2019 Feb 25];12(2):119–31. Available from: <http://www.ncbi.nlm.nih.gov/pubmed/20098416>
 94. Wong E, Cuervo AM. Autophagy gone awry in neurodegenerative diseases. *Nat Neurosci* [Internet]. 2010 Jul [cited 2015 Oct 28];13(7):805–11. Available from: <http://dx.doi.org/10.1038/nn.2575>
 95. Jing K, Lim K. Why is autophagy important in human diseases? *Exp Mol Med*. 2012;44(2):69–72.
 96. Karabiyik C, Lee MJ, Rubinsztein DC. Autophagy impairment in Parkinson’s disease. *Essays Biochem* [Internet]. 2017 Dec 12 [cited 2019 Feb 18];61(6):711–20. Available from: <http://www.ncbi.nlm.nih.gov/pubmed/29233880>
 97. Aflaki E, Westbroek W, Sidransky E. The Complicated Relationship between Gaucher Disease and Parkinsonism: Insights from a Rare Disease. *Neuron* [Internet]. 2017 Feb 22 [cited 2019 Feb 27];93(4):737–46. Available from: <http://www.ncbi.nlm.nih.gov/pubmed/28231462>
 98. McCoy MK, Cookson MR. DJ-1 regulation of mitochondrial function and autophagy through oxidative stress. *Autophagy* [Internet]. 2011 [cited 2019 Feb 28];7(5):531. Available from: <https://www.ncbi.nlm.nih.gov/pmc/articles/PMC3127213/>
 99. Hao L-Y, Giasson BI, Bonini NM. DJ-1 is critical for mitochondrial function and rescues PINK1 loss of function. *Proc Natl Acad Sci U S A* [Internet]. 2010 [cited 2019 Feb 28];107(21):9747. Available from: <https://www.ncbi.nlm.nih.gov/pmc/articles/PMC2906840/>
 100. Kaasik A, Rikk T, Piirsoo A, Zharkovsky T, Zharkovsky A. Up-regulation of lysosomal cathepsin L and autophagy during neuronal death induced by reduced serum and potassium. *Eur J Neurosci* [Internet]. 2005 Sep [cited 2019 Feb 27];22(5):1023–31. Available from: <http://www.ncbi.nlm.nih.gov/pubmed/16176344>
 101. Zhu J, Wang KZ, Chu CT. After the banquet. *Autophagy* [Internet]. 2013 Nov 3 [cited 2019 Jan 20];9(11):1663–76. Available from: <http://www.tandfonline.com/doi/abs/10.4161/auto.24135>
 102. Chen H, Chan DC. Mitochondrial dynamics-fusion, fission, movement, and mitophagy-in neurodegenerative diseases. *Hum Mol Genet*. 2009;18(R2):169–76.
 103. Caldwell GA, Caldwell KA. Traversing a wormhole to combat Parkinson’s disease. *Dis Model Mech* [Internet]. 2008 Jul 1 [cited 2019 Mar 4];1(1):32–6. Available from: <http://www.ncbi.nlm.nih.gov/pubmed/19048050>
 104. Robak LA, Jansen IE, van Rooij J, Uitterlinden AG, Kraaij R, Jankovic J, et al. Excessive burden of lysosomal storage disorder gene variants in Parkinson’s disease. *Brain* [Internet]. 2017 Dec 1 [cited 2019 May 22];140(12):3191–203. Available from: <http://www.ncbi.nlm.nih.gov/pubmed/29140481>
 105. Shamir R, Klein C, Amar D, Vollstedt E-J, Bonin M, Usenovic M, et al. Analysis of blood-based gene expression in idiopathic Parkinson disease. *Neurology* [Internet]. 2017 Oct 17 [cited 2018 Oct 3];89(16):1676–83. Available from:

- <http://www.ncbi.nlm.nih.gov/pubmed/28916538>
106. Sierra M, González-Aramburu I, Sánchez-Juan P, Sánchez-Quintana C, Polo JM, Berciano J, et al. High frequency and reduced penetrance of LRRK2 G2019S mutation among Parkinson's disease patients in Cantabria (Spain). *Mov Disord* [Internet]. 2011 Nov [cited 2016 Aug 22];26(13):2343–6. Available from: <http://www.ncbi.nlm.nih.gov/pubmed/21954089>
 107. Sidransky E, Nalls MA, Aasly JO, Aharon-Peretz J, Annesi G, Barbosa ER, et al. Multicenter Analysis of Glucocerebrosidase Mutations in Parkinson's Disease. *N Engl J Med* [Internet]. 2009 Oct 22 [cited 2019 Jan 13];361(17):1651–61. Available from: <http://www.ncbi.nlm.nih.gov/pubmed/19846850>
 108. Reed X, Bandrés-Ciga S, Blauwendraat C, Cookson MR. The role of monogenic genes in idiopathic Parkinson's disease. *Neurobiol Dis* [Internet]. 2018 [cited 2019 Jan 20];124:230–9. Available from: www.elsevier.com/locate/ynbdi
 109. Sidransky E, Lopez G. The link between the GBA gene and parkinsonism. *Lancet Neurol* [Internet]. 2012 Nov [cited 2019 Jan 21];11(11):986–98. Available from: <http://www.ncbi.nlm.nih.gov/pubmed/23079555>
 110. Correia Guedes L, Ferreira JJ, Rosa MM, Coelho M, Bonifati V, Sampaio C. Worldwide frequency of G2019S LRRK2 mutation in Parkinson's disease: a systematic review. *Parkinsonism Relat Disord* [Internet]. 2010 May [cited 2016 Feb 15];16(4):237–42. Available from: <http://www.ncbi.nlm.nih.gov/pubmed/19945904>
 111. Bae JR, Lee BD. Function and dysfunction of leucine-rich repeat kinase 2 (LRRK2): Parkinson's disease and beyond. *BMB Rep* [Internet]. 2015 [cited 2019 May 24];48(5):243. Available from: <https://www.ncbi.nlm.nih.gov/pmc/articles/PMC4578562/>
 112. Islam MS, Moore DJ. Mechanisms of LRRK2-dependent neurodegeneration: role of enzymatic activity and protein aggregation. *Biochem Soc Trans* [Internet]. 2017 Feb 8 [cited 2019 Feb 13];45(1):163–72. Available from: <http://www.ncbi.nlm.nih.gov/pubmed/28202670>
 113. Cookson MR. LRRK2 Pathways Leading to Neurodegeneration. *Curr Neurol Neurosci Rep* [Internet]. 2015 Jul [cited 2016 Feb 15];15(7):42. Available from: <http://www.ncbi.nlm.nih.gov/pubmed/26008812>
 114. Migheli R, Del Giudice MG, Spissu Y, Sanna G, Xiong Y, Dawson TM, et al. LRRK2 affects vesicle trafficking, neurotransmitter extracellular level and membrane receptor localization. *PLoS One* [Internet]. 2013 Jan [cited 2015 Jul 14];8(10):e77198. Available from: <http://www.pubmedcentral.nih.gov/articlerender.fcgi?artid=3805556&tool=pmcentrez&endertype=abstract>
 115. Wallings R, Manzoni C, Bandopadhyay R. Cellular processes associated with LRRK2 function and dysfunction. *FEBS J* [Internet]. 2015 Aug [cited 2016 Feb 8];282(15):2806–26. Available from: <http://www.pubmedcentral.nih.gov/articlerender.fcgi?artid=4522467&tool=pmcentrez&endertype=abstract>
 116. Ozelius LJ, Senthil G, Saunders-Pullman R, Ohmann E, Deligtisch A, Tagliati M, et al. LRRK2 G2019S as a Cause of Parkinson's Disease in Ashkenazi Jews. *N Engl J Med*

- [Internet]. 2006 Jan 26 [cited 2018 Jan 4];354(4):424–5. Available from: <http://www.nejm.org/doi/abs/10.1056/NEJMc055509>
117. Healy DG, Falchi M, O’Sullivan SS, Bonifati V, Durr A, Bressman S, et al. Phenotype, genotype, and worldwide genetic penetrance of LRRK2-associated Parkinson’s disease: a case-control study. *Lancet Neurol* [Internet]. 2008 Jul 7 [cited 2015 Apr 13];7(7):583–90. Available from: <http://www.pubmedcentral.nih.gov/articlerender.fcgi?artid=2832754&tool=pmcentrez&endertype=abstract>
 118. Esteves a. R, Swerdlow RH, Cardoso SM. LRRK2, a puzzling protein: Insights into Parkinson’s disease pathogenesis. *Exp Neurol* [Internet]. 2014;261:206–16. Available from: <http://dx.doi.org/10.1016/j.expneurol.2014.05.025>
 119. Cookson MR. Cellular effects of LRRK2 mutations. *Biochem Soc Trans* [Internet]. 2012 Oct [cited 2016 Jan 31];40(5):1070–3. Available from: <http://www.pubmedcentral.nih.gov/articlerender.fcgi?artid=4662252&tool=pmcentrez&endertype=abstract>
 120. Gómez-Suaga P, Fdez E, Fernández B, Martínez-Salvador M, Blanca Ramírez M, Madero-Pérez J, et al. Novel insights into the neurobiology underlying LRRK2-linked Parkinson’s disease. *Neuropharmacology*. 2014;85:45–56.
 121. Shin N, Jeong H, Kwon J, Heo HY, Kwon JJ, Yun HJ, et al. LRRK2 regulates synaptic vesicle endocytosis. *Exp Cell Res* [Internet]. 2008 Jun 10 [cited 2019 Mar 2];314(10):2055–65. Available from: <http://www.ncbi.nlm.nih.gov/pubmed/18445495>
 122. Piccoli G, Condliffe SB, Bauer M, Giesert F, Boldt K, De Astis S, et al. LRRK2 Controls Synaptic Vesicle Storage and Mobilization within the Recycling Pool. *J Neurosci* [Internet]. 2011 Feb 9 [cited 2019 Mar 2];31(6):2225–37. Available from: <http://www.ncbi.nlm.nih.gov/pubmed/21307259>
 123. Liou AKF, Leak RK, Li L, Zigmond MJ. Wild-type LRRK2 but not its mutant attenuates stress-induced cell death via ERK pathway. *Neurobiol Dis* [Internet]. 2008 Oct [cited 2015 Dec 1];32(1):116–24. Available from: <http://www.pubmedcentral.nih.gov/articlerender.fcgi?artid=2580823&tool=pmcentrez&endertype=abstract>
 124. Dächsel JC, Behrouz B, Yue M, Beevers JE, Melrose HL, Farrer MJ. A comparative study of Lrrk2 function in primary neuronal cultures. *Parkinsonism Relat Disord* [Internet]. 2010 Dec [cited 2016 Feb 15];16(10):650–5. Available from: <http://www.pubmedcentral.nih.gov/articlerender.fcgi?artid=3159957&tool=pmcentrez&endertype=abstract>
 125. Lopez de Maturana R, Aguila JC, Sousa A, Vazquez N, del Rio P, Aiausti A, et al. Leucine-rich repeat kinase 2 modulates cyclooxygenase 2 and the inflammatory response in idiopathic and genetic Parkinson’s disease. *Neurobiol Aging* [Internet]. 2014 May [cited 2017 Jul 24];35(5):1116–24. Available from: <http://www.ncbi.nlm.nih.gov/pubmed/24360742>
 126. West AB, Moore DJ, Choi C, Andrabi SA, Li X, Dikeman D, et al. Parkinson’s disease-associated mutations in LRRK2 link enhanced GTP-binding and kinase activities to neuronal toxicity. *Hum Mol Genet* [Internet]. 2007 Jan 15 [cited 2019 Mar 2];16(2):223–32. Available from: <http://www.ncbi.nlm.nih.gov/pubmed/17200152>

127. Mortiboys H, Furnston R, Bronstad G, Aasly J, Elliott C, Bandmann O. UDCA exerts beneficial effect on mitochondrial dysfunction in LRRK2(G2019S) carriers and in vivo. *Neurology* [Internet]. 2015 Sep 8 [cited 2016 Jan 28];85(10):846–52. Available from: <http://www.ncbi.nlm.nih.gov/pubmed/26253449>
128. Manzoni C. The LRRK2-macroautophagy axis and its relevance to Parkinson's disease. *Biochem Soc Trans* [Internet]. 2017 [cited 2018 Feb 1];45(1):155–62. Available from: <http://www.ncbi.nlm.nih.gov/pubmed/28202669>
129. Orenstein SJ, Kuo S-H, Tasset I, Arias E, Koga H, Fernandez-Carasa I, et al. Interplay of LRRK2 with chaperone-mediated autophagy. *Nat Neurosci* [Internet]. 2013 Mar 3 [cited 2017 Feb 20];16(4):394–406. Available from: <http://www.nature.com/doi/10.1038/nn.3350>
130. Paisán-Ruiz C, Lewis PA, Singleton AB. LRRK2: cause, risk, and mechanism. *J Parkinsons Dis* [Internet]. 2013 Jan [cited 2016 Feb 15];3(2):85–103. Available from: <http://www.pubmedcentral.nih.gov/articlerender.fcgi?artid=3952583&tool=pmcentrez&endertype=abstract>
131. Schapira AHV. Glucocerebrosidase and Parkinson disease: Recent advances. *Mol Cell Neurosci* [Internet]. 2015 May [cited 2019 Jan 13];66(Pt A):37–42. Available from: <http://www.ncbi.nlm.nih.gov/pubmed/25802027>
132. Cilia R, Tunesi S, Marotta G, Cereda E, Siri C, Tesi S, et al. Survival and Dementia in GBA-Associated Parkinson's Disease: The Mutation Matters. [cited 2019 Jan 13]; Available from: www.aimn.it
133. McNeill A, Magalhaes J, Shen C, Chau K-Y, Hughes D, Mehta A, et al. Ambrinol improves lysosomal biochemistry in glucocerebrosidase mutation-linked Parkinson disease cells. *Brain* [Internet]. 2014 May 1 [cited 2019 Mar 4];137(5):1481–95. Available from: <http://www.ncbi.nlm.nih.gov/pubmed/24574503>
134. Beavan M, McNeill A, Proukakis C, Hughes DA, Mehta A, Schapira AH V. Evolution of Prodromal Clinical Markers of Parkinson Disease in a GBA Mutation–Positive Cohort. *JAMA Neurol* [Internet]. 2015 Feb 1 [cited 2019 Jan 13];72(2):201. Available from: <http://www.ncbi.nlm.nih.gov/pubmed/25506732>
135. Ziegler SG, Eblan MJ, Gutti U, Hruska KS, Stubblefield BK, Goker-Alpan O, et al. Glucocerebrosidase mutations in Chinese subjects from Taiwan with sporadic Parkinson disease. *Mol Genet Metab* [Internet]. 2007 Jun 1 [cited 2019 Mar 4];91(2):195–200. Available from: <https://www.sciencedirect.com/science/article/pii/S1096719207001023>
136. Angeli A, Mencacci NE, Duran R, Aviles-Olmos I, Kefalopoulou Z, Candelario J, et al. Genotype and phenotype in Parkinson's disease: Lessons in heterogeneity from deep brain stimulation. *Mov Disord* [Internet]. 2013 Sep 1 [cited 2019 Mar 4];28(10):1370–5. Available from: <http://doi.wiley.com/10.1002/mds.25535>
137. Hallett PJ, Huebner M, Brekk OR, Moloney EB, Rocha EM, Priestman DA, et al. Glycosphingolipid levels and glucocerebrosidase activity are altered in normal aging of the mouse brain. *Neurobiol Aging* [Internet]. 2018 Jul [cited 2019 Jan 26];67:189–200. Available from: <http://www.ncbi.nlm.nih.gov/pubmed/29735433>
138. Rocha EM, Smith GA, Park E, Cao H, Brown E, Hallett P, et al. Progressive decline of glucocerebrosidase in aging and Parkinson's disease. *Ann Clin Transl Neurol*

- [Internet]. 2015 Apr 1 [cited 2019 Mar 4];2(4):433–8. Available from: <http://doi.wiley.com/10.1002/acn3.177>
139. Neumann J, Bras J, Deas E, O’Sullivan SS, Parkkinen L, Lachmann RH, et al. Glucocerebrosidase mutations in clinical and pathologically proven Parkinson’s disease. *Brain* [Internet]. 2009 Jul 1 [cited 2019 Mar 4];132(7):1783–94. Available from: <https://academic.oup.com/brain/article-lookup/doi/10.1093/brain/awp044>
 140. Wong K, Sidransky E, Verma A, Mixon T, Sandberg GD, Wakefield LK, et al. Neuropathology provides clues to the pathophysiology of Gaucher disease. *Mol Genet Metab* [Internet]. 2004 Jul 1 [cited 2019 Mar 4];82(3):192–207. Available from: <https://www.sciencedirect.com/science/article/pii/S1096719204001179>
 141. Sanchez-Martinez A, Beavan M, Gegg ME, Chau K-Y, Whitworth AJ, Schapira AH V. Parkinson disease-linked GBA mutation effects reversed by molecular chaperones in human cell and fly models. *Sci Rep* [Internet]. 2016 Nov 19 [cited 2019 Jan 26];6(1):31380. Available from: <http://www.nature.com/articles/srep31380>
 142. Yang S-Y, Beavan M, Chau K-Y, Taanman J-W, Schapira AH V. Stem Cell Reports Article A Human Neural Crest Stem Cell-Derived Dopaminergic Neuronal Model Recapitulates Biochemical Abnormalities in GBA1 Mutation Carriers. *Stem Cell Reports* [Internet]. 2017 [cited 2019 Jan 26];8:728–42. Available from: <http://dx.doi.org/10.1016/j.stemcr.2017.01.011>
 143. McGlinchey RP, Lee JC. Emerging insights into the mechanistic link between α -synuclein and glucocerebrosidase in Parkinson’s disease. *Biochem Soc Trans* [Internet]. 2013 Dec 1 [cited 2019 Mar 5];41(6):1509–12. Available from: <http://www.ncbi.nlm.nih.gov/pubmed/24256245>
 144. O’regan G, Desouza R-M, Balestrino R, Schapira AH. Glucocerebrosidase Mutations in Parkinson Disease. *J Parkinsons Dis* [Internet]. 2017 [cited 2019 Jan 13];7:411–22. Available from: <https://content.iospress.com/download/journal-of-parkinsons-disease/jpd171092?id=journal-of-parkinsons-disease%2Fjpd171092>
 145. Kalia L V, Lang AE, Hazrati L-N, Fujioka S, Wszolek ZK, Dickson DW, et al. Clinical correlations with Lewy body pathology in LRRK2-related Parkinson disease. *JAMA Neurol* [Internet]. 2015 Jan [cited 2016 Feb 15];72(1):100–5. Available from: <http://www.pubmedcentral.nih.gov/articlerender.fcgi?artid=4399368&tool=pmcentrez&rendertype=abstract>
 146. O’Regan G, deSouza R-M, Balestrino R, Schapira AH. Glucocerebrosidase Mutations in Parkinson Disease. *J Parkinsons Dis* [Internet]. 2017 Aug 8 [cited 2019 Jan 13];7(3):411–22. Available from: <http://www.ncbi.nlm.nih.gov/pubmed/28598856>
 147. Alberio T, Lopiano L, Fasano M. Cellular models to investigate biochemical pathways in Parkinson’s disease. *FEBS J* [Internet]. 2012 Apr [cited 2019 Mar 3];279(7):1146–55. Available from: <http://www.ncbi.nlm.nih.gov/pubmed/22314200>
 148. Chiu AY, Rao MS. Cell-based therapy for neural disorders--anticipating challenges. *Neurotherapeutics* [Internet]. 2011 Oct [cited 2016 Apr 19];8(4):744–52. Available from: <http://www.pubmedcentral.nih.gov/articlerender.fcgi?artid=3250286&tool=pmcentrez&rendertype=abstract>
 149. Jiang P, Dickson DW. Parkinson’s disease: experimental models and reality. *Acta*

- Neuropathol [Internet]. 2017 Nov 18 [cited 2018 Jan 4];135(1):13–32. Available from: <http://www.ncbi.nlm.nih.gov/pubmed/29151169>
150. Alberio T, Lopiano L, Fasano M. Cellular models to investigate biochemical pathways in Parkinson's disease. *FEBS J* [Internet]. 2012 Apr [cited 2015 Jun 19];279(7):1146–55. Available from: <http://www.ncbi.nlm.nih.gov/pubmed/22314200>
 151. Adler CH, Dugger BN, Hentz JG, Hinni ML, Lott DG, Driver-Dunckley E, et al. Peripheral Synucleinopathy in Early Parkinson's Disease: Submandibular Gland Needle Biopsy Findings. *Mov Disord* [Internet]. 2016 Feb [cited 2019 Apr 5];31(2):250–6. Available from: <http://www.ncbi.nlm.nih.gov/pubmed/26799362>
 152. Schneider SA, Boettner M, Alexoudi A, Zorenkov D, Deuschl G, Wedel T. Can we use peripheral tissue biopsies to diagnose Parkinson's disease? A review of the literature. *Eur J Neurol* [Internet]. 2016 Feb [cited 2019 Apr 5];23(2):247–61. Available from: <http://www.ncbi.nlm.nih.gov/pubmed/26100920>
 153. González-Casacuberta I, Morén C, Juárez-Flores D-L, Esteve-Codina A, Sierra C, Catalán-García M, et al. Transcriptional alterations in skin fibroblasts from Parkinson's disease patients with parkin mutations. *Neurobiol Aging*. 2018;65.
 154. Morén C, González-Casacuberta Í, Navarro-Otano J, Juárez-Flores D, Vilas D, Garrabou G, et al. Colonic Oxidative and Mitochondrial Function in Parkinson's Disease and Idiopathic REM Sleep Behavior Disorder. *Parkinsons Dis*. 2017;2017.
 155. Phelix CF, Bourdon AK, Villareal G, LeBaron RG. Modeling non-clinical and clinical drug tests in Gaucher disease. In: 2016 38th Annual International Conference of the IEEE Engineering in Medicine and Biology Society (EMBC) [Internet]. IEEE; 2016 [cited 2019 May 19]. p. 1434–8. Available from: <http://www.ncbi.nlm.nih.gov/pubmed/28268595>
 156. Johnston TM, Fox SH. Symptomatic Models of Parkinson's Disease and L-DOPA-Induced Dyskinesia in Non-human Primates. In: Current topics in behavioral neurosciences [Internet]. 2014 [cited 2019 Mar 2]. p. 221–35. Available from: <http://www.ncbi.nlm.nih.gov/pubmed/25158623>
 157. Verhave PS, Jongsma MJ, Van den Berg RM, Vis JC, Vanwersch RAP, Smit AB, et al. REM sleep behavior disorder in the marmoset MPTP model of early Parkinson disease. *Sleep* [Internet]. 2011 Aug 1 [cited 2019 Mar 2];34(8):1119–25. Available from: <http://www.ncbi.nlm.nih.gov/pubmed/21804674>
 158. Barraud Q, Lambrecq V, Forni C, McGuire S, Hill M, Bioulac B, et al. Sleep disorders in Parkinson's disease: The contribution of the MPTP non-human primate model. *Exp Neurol* [Internet]. 2009 Oct [cited 2019 Mar 2];219(2):574–82. Available from: <http://www.ncbi.nlm.nih.gov/pubmed/19635479>
 159. Daniel G, Moore DJ. Modeling LRRK2 Pathobiology in Parkinson's Disease: From Yeast to Rodents. In: Current topics in behavioral neurosciences [Internet]. Springer, Berlin, Heidelberg; 2014 [cited 2019 Mar 2]. p. 331–68. Available from: <http://www.ncbi.nlm.nih.gov/pubmed/24850078>
 160. Li X, Patel JC, Wang J, Avshalumov M V., Nicholson C, Buxbaum JD, et al. Enhanced Striatal Dopamine Transmission and Motor Performance with LRRK2 Overexpression in Mice Is Eliminated by Familial Parkinson's Disease Mutation G2019S. *J Neurosci* [Internet]. 2010 Feb 3 [cited 2019 Mar 2];30(5):1788–97. Available from:

- <http://www.ncbi.nlm.nih.gov/pubmed/20130188>
161. Dusonchet J, Kochubey O, Stafa K, Young SM, Zufferey R, Moore DJ, et al. A Rat Model of Progressive Nigral Neurodegeneration Induced by the Parkinson's Disease-Associated G2019S Mutation in LRRK2. *J Neurosci* [Internet]. 2011 Jan 19 [cited 2019 Mar 2];31(3):907–12. Available from: <http://www.ncbi.nlm.nih.gov/pubmed/21248115>
 162. Van der Perren A, Van den Haute C, Baekelandt V. Viral Vector-Based Models of Parkinson's Disease. In: *Current topics in behavioral neurosciences* [Internet]. 2014 [cited 2019 Mar 2]. p. 271–301. Available from: <http://www.ncbi.nlm.nih.gov/pubmed/24839101>
 163. Pereira C, Miguel Martins L, Saraiva L. LRRK2, but not pathogenic mutants, protects against H₂O₂ stress depending on mitochondrial function and endocytosis in a yeast model. *Biochim Biophys Acta - Gen Subj*. 2014;1840(6):2025–31.
 164. Xiong Y, Coombes CE, Kilaru A, Li X, Gitler AD, Bowers WJ, et al. GTPase Activity Plays a Key Role in the Pathobiology of LRRK2. MacDonald ME, editor. *PLoS Genet* [Internet]. 2010 Apr 8 [cited 2019 Mar 2];6(4):e1000902. Available from: <https://dx.plos.org/10.1371/journal.pgen.1000902>
 165. Marín I. Ancient Origin of the Parkinson Disease Gene LRRK2. *J Mol Evol* [Internet]. 2008 Jul 4 [cited 2019 Mar 2];67(1):41–50. Available from: <http://www.ncbi.nlm.nih.gov/pubmed/18523712>
 166. Osellame LD, Rahim AA, Hargreaves IP, Gegg ME, Richard-Londt A, Brandner S, et al. Mitochondria and Quality Control Defects in a Mouse Model of Gaucher Disease—Links to Parkinson's Disease. *Cell Metab* [Internet]. 2013 Jun 4 [cited 2019 Feb 28];17(6):941–53. Available from: <http://www.ncbi.nlm.nih.gov/pubmed/23707074>
 167. Barranger J, Vallor MJ. Models of Lysosomal Storage Disorders Useful for the Study of Gene Therapy. In: *Gene Therapy* [Internet]. Basel: Birkhäuser Basel; 2012 [cited 2019 May 19]. p. 123–36. Available from: http://link.springer.com/10.1007/978-3-0348-7011-5_9
 168. Bezard E, Yue Z, Kirik D, Spillantini MG. Animal models of Parkinson's disease: Limits and relevance to neuroprotection studies. *Movement Disorders*. 2013.
 169. Lázaro DF, Pavlou MAS, Outeiro TF. Cellular models as tools for the study of the role of alpha-synuclein in Parkinson's disease. *Exp Neurol* [Internet]. 2017 Dec [cited 2019 Jan 14];298(Pt B):162–71. Available from: <http://www.ncbi.nlm.nih.gov/pubmed/28526239>
 170. Xicoy H, Wieringa B, Martens GJM. The SH-SY5Y cell line in Parkinson's disease research: a systematic review. *Mol Neurodegener* [Internet]. 2017 [cited 2019 Apr 5];12(1):10. Available from: <http://www.ncbi.nlm.nih.gov/pubmed/28118852>
 171. Falkenburger BH, Schulz JB. Limitations of cellular models in Parkinson's disease research. *J Neural Transm Suppl* [Internet]. 2006 [cited 2019 Apr 5];(70):261–8. Available from: <http://www.ncbi.nlm.nih.gov/pubmed/17017539>
 172. Tremblay RG, Sikorska M, Sandhu JK, Lanthier P, Ribocco-Lutkiewicz M, Bani-Yaghoub M. Differentiation of mouse Neuro 2A cells into dopamine neurons. *J Neurosci Methods* [Internet]. 2010 Jan 30 [cited 2019 Mar 3];186(1):60–7. Available from: <http://www.ncbi.nlm.nih.gov/pubmed/19903493>
 173. Senyilmaz D, Teleman AA. Chicken or the egg: Warburg effect and mitochondrial

- dysfunction. F1000Prime Rep [Internet]. 2015 Jan [cited 2015 Jun 23];7:41. Available from:
<http://www.pubmedcentral.nih.gov/articlerender.fcgi?artid=4447048&tool=pmcentrez&endertype=abstract>
174. Astashkina A, Mann B, Grainger DW. A critical evaluation of in vitro cell culture models for high-throughput drug screening and toxicity. *Pharmacol Ther* [Internet]. 2012 Apr [cited 2019 Mar 3];134(1):82–106. Available from: <http://www.ncbi.nlm.nih.gov/pubmed/22252140>
 175. Nguyen HN, Byers B, Cord B, Shcheglovitov A, Byrne J, Gujar P, et al. LRRK2 Mutant iPSC-Derived DA Neurons Demonstrate Increased Susceptibility to Oxidative Stress. *Cell Stem Cell* [Internet]. 2011 Mar 4 [cited 2019 Mar 2];8(3):267–80. Available from: <http://www.ncbi.nlm.nih.gov/pubmed/21362567>
 176. Zhang Q, Chen W, Tan S, Lin T. Stem Cells for Modeling and Therapy of Parkinson's Disease. *Hum Gene Ther* [Internet]. 2017 Jan [cited 2019 Mar 3];28(1):85–98. Available from: <http://www.ncbi.nlm.nih.gov/pubmed/27762639>
 177. Sánchez-Danés A, Richaud-Patin Y, Carballo-Carbajal I, Jiménez-Delgado S, Caig C, Mora S, et al. Disease-specific phenotypes in dopamine neurons from human iPSC-based models of genetic and sporadic Parkinson's disease. *EMBO Mol Med* [Internet]. 2012 May [cited 2018 Jan 4];4(5):380–95. Available from: <http://www.ncbi.nlm.nih.gov/pubmed/22407749>
 178. Park J, Lee BK, Jeong GS, Hyun JK, Lee CJ, Lee S-H. Three-dimensional brain-on-a-chip with an interstitial level of flow and its application as an in vitro model of Alzheimer's disease. *Lab Chip* [Internet]. 2015 Jan 7 [cited 2019 Mar 3];15(1):141–50. Available from: <http://www.ncbi.nlm.nih.gov/pubmed/25317977>
 179. Moreno EL, Hachi S, Hemmer K, Trietsch SJ, Baumuratov AS, Hankemeier T, et al. Differentiation of neuroepithelial stem cells into functional dopaminergic neurons in 3D microfluidic cell culture. *Lab Chip* [Internet]. 2015 [cited 2019 Mar 3];15(11):2419–28. Available from: <http://xlink.rsc.org/?DOI=C5LC00180C>
 180. Pereira C V, Oliveira PJ, Will Y, Nadanaciva S. Mitochondrial bioenergetics and drug-induced toxicity in a panel of mouse embryonic fibroblasts with mitochondrial DNA single nucleotide polymorphisms. *Toxicol Appl Pharmacol* [Internet]. 2012 Oct 15 [cited 2016 Jan 13];264(2):167–81. Available from: <http://www.sciencedirect.com/science/article/pii/S0041008X12003316>
 181. Aguer C, Gambarotta D, Mailloux RJ, Moffat C, Dent R, McPherson R, et al. Galactose enhances oxidative metabolism and reveals mitochondrial dysfunction in human primary muscle cells. Luque RM, editor. *PLoS One* [Internet]. 2011 Jan 15 [cited 2016 Feb 25];6(12):e28536. Available from: <http://dx.plos.org/10.1371/journal.pone.0028536>
 182. Liu G-H, Qu J, Suzuki K, Nivet E, Li M, Montserrat N, et al. Progressive degeneration of human neural stem cells caused by pathogenic LRRK2. *Nature* [Internet]. 2012 Nov 17 [cited 2019 Mar 2];491(7425):603–7. Available from: <http://www.ncbi.nlm.nih.gov/pubmed/23075850>
 183. Cooper O, Seo H, Andrabi S, Guardia-Laguarta C, Graziotto J, Sundberg M, et al. Pharmacological Rescue of Mitochondrial Deficits in iPSC-Derived Neural Cells from

- Patients with Familial Parkinson's Disease. *Sci Transl Med* [Internet]. 2012 Jul 4 [cited 2019 Mar 2];4(141):141ra90-141ra90. Available from: <http://www.ncbi.nlm.nih.gov/pubmed/22764206>
184. Mazzulli JR, Xu Y-H, Sun Y, Knight AL, McLean PJ, Caldwell GA, et al. Gaucher Disease Glucocerebrosidase and α -Synuclein Form a Bidirectional Pathogenic Loop in Synucleinopathies. *Cell* [Internet]. 2011 Jul 8 [cited 2019 Mar 3];146(1):37–52. Available from: <http://www.ncbi.nlm.nih.gov/pubmed/21700325>
185. Woodard CM, Campos BA, Kuo S-H, Nirenberg MJ, Nestor MW, Zimmer M, et al. iPSC-Derived Dopamine Neurons Reveal Differences between Monozygotic Twins Discordant for Parkinson's Disease. *Cell Rep* [Internet]. 2014 Nov 20 [cited 2019 Mar 3];9(4):1173–82. Available from: <http://www.ncbi.nlm.nih.gov/pubmed/25456120>
186. Schöndorf DC, Aureli M, McAllister FE, Hindley CJ, Mayer F, Schmid B, et al. iPSC-derived neurons from GBA1-associated Parkinson's disease patients show autophagic defects and impaired calcium homeostasis. *Nat Commun* [Internet]. 2014 Dec 6 [cited 2019 Feb 28];5(1):4028. Available from: <http://www.ncbi.nlm.nih.gov/pubmed/24905578>
187. de la Mata M, Cotán D, Oropesa-Ávila M, Garrido-Maraver J, Cordero MD, Villanueva Paz M, et al. Pharmacological Chaperones and Coenzyme Q10 Treatment Improves Mutant β -Glucocerebrosidase Activity and Mitochondrial Function in Neuronopathic Forms of Gaucher Disease. *Sci Rep* [Internet]. 2015 Sep 5 [cited 2019 Feb 28];5(1):10903. Available from: <http://www.ncbi.nlm.nih.gov/pubmed/26045184>
188. Teves JMY, Bhargava V, Kirwan KR, Corenblum MJ, Justiniano R, Wondrak GT, et al. Parkinson's Disease Skin Fibroblasts Display Signature Alterations in Growth, Redox Homeostasis, Mitochondrial Function, and Autophagy. *Front Neurosci* [Internet]. 2017 [cited 2018 Oct 3];11:737. Available from: <http://www.ncbi.nlm.nih.gov/pubmed/29379409>
189. Konrad C, Kawamata H, Bredvik KG, Arreguin AJ, Cajamarca SA, Hupf JC, et al. Fibroblast bioenergetics to classify amyotrophic lateral sclerosis patients. *Mol Neurodegener* [Internet]. 2017 Dec 24 [cited 2019 Mar 3];12(1):76. Available from: <http://www.ncbi.nlm.nih.gov/pubmed/29065921>
190. Tenreiro S, Reimão-Pinto MM, Antas P, Rino J, Wawrzycka D, Macedo D, et al. Phosphorylation Modulates Clearance of Alpha-Synuclein Inclusions in a Yeast Model of Parkinson's Disease. Shorter J, editor. *PLoS Genet* [Internet]. 2014 May 8 [cited 2019 Jun 19];10(5):e1004302. Available from: <https://dx.plos.org/10.1371/journal.pgen.1004302>
191. Marroquin LD, Hynes J, Dykens JA, Jamieson JD, Will Y. Circumventing the Crabtree Effect: Replacing Media Glucose with Galactose Increases Susceptibility of HepG2 Cells to Mitochondrial Toxicants. *Toxicol Sci* [Internet]. 2007 Jan 18 [cited 2018 Apr 1];97(2):539–47. Available from: <https://academic.oup.com/toxsci/article-lookup/doi/10.1093/toxsci/kfm052>
192. Yakhine-Diop SMS, Bravo-San Pedro JM, Gómez-Sánchez R, Pizarro-Estrella E, Rodríguez-Arribas M, Climent V, et al. G2019S LRRK2 mutant fibroblasts from Parkinson's disease patients show increased sensitivity to neurotoxin 1-methyl-4-phenylpyridinium dependent of autophagy. *Toxicology* [Internet]. 2014 Oct 3 [cited

- 2017 Jul 24];324:1–9. Available from: <http://linkinghub.elsevier.com/retrieve/pii/S0300483X14001346>
193. Chretien D, Bénit P, Chol M, Lebon S, Rötig A, Munnich A, et al. Assay of mitochondrial respiratory chain complex I in human lymphocytes and cultured skin fibroblasts. *Biochem Biophys Res Commun* [Internet]. 2003 Jan [cited 2013 Jan 3];301(1):222–4. Available from: <http://www.sciencedirect.com/science/article/pii/S0006291X02030164>
194. Hoepken H-HH, Gispert S, Azizov M, Klinkenberg M, Ricciardi F, Kurz A, et al. Parkinson patient fibroblasts show increased alpha-synuclein expression. 2008 Aug [cited 2016 Jul 19];212(2):307–13. Available from: <http://www.ncbi.nlm.nih.gov/pubmed/18511044>
195. González-Casacuberta I, Morén C, Juárez-Flores D-LD-L, Esteve-Codina A, Sierra C, Catalán-García M, et al. Transcriptional alterations in skin fibroblasts from Parkinson's disease patients with parkin mutations. *Neurobiol Aging* [Internet]. 2018 May 7 [cited 2018 Mar 12];65:206–16. Available from: <http://www.ncbi.nlm.nih.gov/pubmed/29501959>
196. Mortiboys H, Thomas KJ, Koopman WJH, Klaffke S, Abou-Sleiman P, Olpin S, et al. Mitochondrial function and morphology are impaired in parkin-mutant fibroblasts. *Ann Neurol* [Internet]. 2008 Nov [cited 2015 Sep 3];64(5):555–65. Available from: <http://www.pubmedcentral.nih.gov/articlerender.fcgi?artid=2613566&tool=pmcentrez&endertype=abstract>
197. Mortiboys H, Johansen KK, Aasly JO, Bandmann O. Mitochondrial impairment in patients with Parkinson disease with the G2019S mutation in LRRK2. *Neurology* [Internet]. 2010 Nov 30 [cited 2015 Sep 10];75(22):2017–20. Available from: <http://www.ncbi.nlm.nih.gov/pubmed/21115957>
198. Trentadue R, Raffaella T, Fiore F, Massaro F, Fabrizia M, Papa F, et al. Induction of mitochondrial dysfunction and oxidative stress in human fibroblast cultures exposed to serum from septic patients. *Life Sci* [Internet]. 2012 Sep 17 [cited 2013 Jun 12];91(7–8):237–43. Available from: <http://www.ncbi.nlm.nih.gov/pubmed/22820545>
199. Smith GA, Jansson J, Rocha EM, Osborn T, Hallett PJ, Isacson O. Fibroblast Biomarkers of Sporadic Parkinson's Disease and LRRK2 Kinase Inhibition. *Mol Neurobiol* [Internet]. 2015 Sep 23 [cited 2016 Feb 12];53(8):5161–77. Available from: <http://www.ncbi.nlm.nih.gov/pubmed/26399642>
200. Papkovskaia TD, Chau K-YY, Inesta-Vaquera F, Papkovsky DB, Healy DG, Nishio K, et al. G2019S leucine-rich repeat kinase 2 causes uncoupling protein-mediated mitochondrial depolarization. *Hum Mol Genet* [Internet]. 2012 Oct 1 [cited 2015 Sep 10];21(19):4201–13. Available from: <http://www.pubmedcentral.nih.gov/articlerender.fcgi?artid=3441120&tool=pmcentrez&endertype=abstract>
201. Collins LM, Drouin-Ouellet J, Kuan W-L, Cox T, Barker RA. Dermal fibroblasts from patients with Parkinson's disease have normal GCCase activity and autophagy compared to patients with PD and GBA mutations. *F1000Research* [Internet]. 2018 Feb 9 [cited 2019 May 19];6:1751. Available from: <http://www.ncbi.nlm.nih.gov/pubmed/29527290>

202. Temple S. The development of neural stem cells. *Nature* [Internet]. 2001 Nov 1 [cited 2019 Mar 3];414(6859):112–7. Available from: <http://www.ncbi.nlm.nih.gov/pubmed/11689956>
203. Singec I, Knoth R, Meyer RP, Maciaczyk J, Volk B, Nikkhah G, et al. Defining the actual sensitivity and specificity of the neurosphere assay in stem cell biology. *Nat Methods* [Internet]. 2006 Oct [cited 2019 Mar 3];3(10):801–6. Available from: <http://www.ncbi.nlm.nih.gov/pubmed/16990812>
204. Matigian N, Abrahamsen G, Sutharsan R, Cook AL, Vitale AM, Nouwens A, et al. Disease-specific, neurosphere-derived cells as models for brain disorders. *Dis Model Mech* [Internet]. 2010 Oct 12 [cited 2019 Jan 26];3(11–12):785–98. Available from: <http://www.ncbi.nlm.nih.gov/pubmed/20699480>
205. Conti L, Cattaneo E. Neural stem cell systems: physiological players or in vitro entities? *Nat Rev Neurosci* [Internet]. 2010 Mar 28 [cited 2019 Jan 26];11(3):176–87. Available from: <http://www.nature.com/articles/nrn2761>
206. Hughes AJ, Ben-Shlomo Y, Daniel SE, Lees AJ. What features improve the accuracy of clinical diagnosis in Parkinson's disease: a clinicopathologic study. *Neurology* [Internet]. 1992 Jun [cited 2017 Jul 15];42(6):1142–6. Available from: <http://www.ncbi.nlm.nih.gov/pubmed/1603339>
207. Morén C, Juárez-Flores D, Cardellach F, Garrabou G. The Role of Therapeutic Drugs on Acquired Mitochondrial Toxicity. *Curr Drug Metab* [Internet]. 2016 Mar 22 [cited 2016 Jul 19];17(999):1–1. Available from: <http://www.eurekaselect.com/openurl/content.php?genre=article&doi=10.2174/1389200217666160322143631>
208. Gaig C, Ezquerro M, Marti MJ, Muñoz E, Valldeoriola F, Tolosa E. LRRK2 Mutations in Spanish Patients With Parkinson Disease. *Arch Neurol* [Internet]. 2006 Mar 1 [cited 2017 Jul 15];63(3):377. Available from: <http://archneur.jamanetwork.com/article.aspx?doi=10.1001/archneur.63.3.377>
209. Morén C, Noguera-Julián A, Garrabou G. Mitochondrial disturbances in HIV pregnancies. *Aids* [Internet]. 2015 [cited 2016 Feb 17]; Available from: http://journals.lww.com/aidsonline/Abstract/2015/01020/Mitochondrial_disturbances_in_HIV_pregnancies.2.aspx
210. Montero R, Grazina M, López-Gallardo E, Montoya J, Briones P, Navarro-Sastre A, et al. Coenzyme Q10 deficiency in mitochondrial DNA depletion syndromes. *Mitochondrion* [Internet]. 2013 Jul [cited 2019 Feb 5];13(4):337–41. Available from: <http://www.ncbi.nlm.nih.gov/pubmed/23583954>
211. Garrabou G, Morén C, Gallego-Escuredo JM, Milinkovic A, Villarroya F, Negrodo E, et al. Genetic and Functional Mitochondrial Assessment of HIV-Infected Patients Developing HAART-Related Hyperlactatemia. *JAIDS J Acquir Immune Defic Syndr* [Internet]. 2009 Dec [cited 2017 Jul 24];52(4):443–51. Available from: <http://content.wkhealth.com/linkback/openurl?sid=WKPTLP:landingpage&an=00126334-200912010-00002>
212. Medja F, Allouche S, Frachon P, Jardel C, Malgat M, de Camaret BM, et al. Development and implementation of standardized respiratory chain spectrophotometric assays for clinical diagnosis. *Mitochondrion* [Internet]. 2009 Sep 1

- [cited 2019 Apr 23];9(5):331–9. Available from: <https://www.sciencedirect.com/science/article/pii/S1567724909000877?via%3Dihub>
213. Pesta D, Gnaiger E. High-resolution respirometry: OXPHOS protocols for human cells and permeabilized fibers from small biopsies of human muscle. [Internet]. Vol. 810, *Methods in molecular biology* (Clifton, N.J.). 2012 [cited 2016 Jan 27]. p. 25–58. Available from: <http://www.ncbi.nlm.nih.gov/pubmed/22057559>
 214. Smiley ST, Reers M, Mottola-Hartshorn C, Lin M, Chen A, Smith TW, et al. Intracellular heterogeneity in mitochondrial membrane potentials revealed by a J-aggregate-forming lipophilic cation JC-1. *Proc Natl Acad Sci U S A* [Internet]. 1991 May 1 [cited 2019 Feb 5];88(9):3671–5. Available from: <http://www.ncbi.nlm.nih.gov/pubmed/2023917>
 215. Noguera-Julian A, Morén C, Rovira N, Garrabou G, Catalán M, Sánchez E, et al. Decreased Mitochondrial Function Among Healthy Infants Exposed to Antiretrovirals During Gestation, Delivery and the Neonatal Period. *Pediatr Infect Dis J* [Internet]. 2015 Dec [cited 2016 Nov 22];34(12):1349–54. Available from: <http://content.wkhealth.com/linkback/openurl?sid=WKPTLP:landingpage&an=00006454-201512000-00015>
 216. Morén C, Garrabou G, Noguera-Julian A, Rovira N, Catalán M, Hernández S, et al. Study of oxidative, enzymatic mitochondrial respiratory chain function and apoptosis in perinatally HIV-infected pediatric patients. *Drug Chem Toxicol* [Internet]. 2013 Oct 27 [cited 2016 Dec 28];36(4):496–500. Available from: <http://www.tandfonline.com/doi/full/10.3109/01480545.2013.776578>
 217. Morén C, González-Casacuberta I, Álvarez-Fernández C, Bañó M, Catalán-García M, Guitart-Mampel M, et al. HIV-1 promonocytic and lymphoid cell lines: an in vitro model of in vivo mitochondrial and apoptotic lesion. *J Cell Mol Med* [Internet]. 2017 [cited 2019 Feb 5];21(2):402–9. Available from: <http://www.ncbi.nlm.nih.gov/pubmed/27758070>
 218. Schindelin J, Arganda-Carreras I, Frise E, Kaynig V, Longair M, Pietzsch T, et al. Fiji: an open-source platform for biological-image analysis. *Nat Methods* [Internet]. 2012 Jun 28 [cited 2016 Sep 13];9(7):676–82. Available from: <http://www.nature.com/doi/10.1038/nmeth.2019>
 219. Dagda RK, Chu CT. NIH Public Access. *J Bioenerg*. 2010;41(6):473–9.
 220. H Koopman WJ, Verkaart S, Visch H-J, van der Westhuizen FH, Murphy MP, P J van den Heuvel LW, et al. Inhibition of complex I of the electron transport chain causes O₂-mediated mitochondrial outgrowth. *Am J Physiol Cell Physiol* [Internet]. 2005 [cited 2019 Feb 5];288:1440–50. Available from: www.ajpcell.org
 221. Rubinsztein DC, Cuervo AM, Ravikumar B, Sarkar S, Korolchuk V, Kaushik S, et al. In search of an “autophagometer.” *Autophagy* [Internet]. 2009 Jul [cited 2018 Apr 15];5(5):585–9. Available from: <http://www.ncbi.nlm.nih.gov/pubmed/19411822>
 222. Klionsky DJ, Abdelmohsen K, Abe A, Abedin MJ, Abeliovich H, Arozena AA, et al. Guidelines for the use and interpretation of assays for monitoring autophagy (3rd edition). *Autophagy* [Internet]. 2016 [cited 2018 Apr 15];12(1):1. Available from: <https://www.ncbi.nlm.nih.gov/pmc/articles/PMC4835977/>
 223. Gouspillou G, Sgarioto N, Norris B, Barbat-Artigas S, Aubertin-Leheudre M, Morais

- JA, et al. The Relationship between Muscle Fiber Type-Specific PGC-1 α Content and Mitochondrial Content Varies between Rodent Models and Humans. Schuelke M, editor. PLoS One [Internet]. 2014 Aug 14 [cited 2019 May 19];9(8):e103044. Available from: <http://dx.plos.org/10.1371/journal.pone.0103044>
224. Morén C, Bañó M, González-Casacuberta I, Catalán-García M, Guitart-Mampel M, Tobías E, et al. Mitochondrial and apoptotic *in vitro* modelling of differential HIV-1 progression and antiretroviral toxicity. J Antimicrob Chemother [Internet]. 2015 Aug [cited 2019 May 19];70(8):2330–6. Available from: <http://www.ncbi.nlm.nih.gov/pubmed/25921514>
 225. Plotegher N, Duchen MR. Mitochondrial Dysfunction and Neurodegeneration in Lysosomal Storage Disorders. Trends Mol Med [Internet]. 2017 Feb [cited 2019 Feb 28];23(2):116–34. Available from: <http://www.ncbi.nlm.nih.gov/pubmed/28111024>
 226. Sun A. Lysosomal storage disease overview. Ann Transl Med [Internet]. 2018 Dec [cited 2019 May 24];6(24):476–476. Available from: <http://www.ncbi.nlm.nih.gov/pubmed/30740407>
 227. Debrosse S, Parikh S. Neurologic disorders due to mitochondrial DNA mutations. Semin Pediatr Neurol [Internet]. 2012 Dec [cited 2013 Jun 13];19(4):194–202. Available from: <http://www.ncbi.nlm.nih.gov/pubmed/23245552>
 228. Dexter DT, Jenner P. Parkinson disease: from pathology to molecular disease mechanisms. Free Radic Biol Med [Internet]. 2013 Sep [cited 2015 May 14];62:132–44. Available from: <http://www.sciencedirect.com/science/article/pii/S0891584913000282>
 229. Auburger G, Klinkenberg M, Drost J, Marcus K, Morales-Gordo B, Kunz WS, et al. Primary skin fibroblasts as a model of Parkinson’s disease. Mol Neurobiol [Internet]. 2012 Aug [cited 2016 Apr 19];46(1):20–7. Available from: <http://www.pubmedcentral.nih.gov/articlerender.fcgi?artid=3443476&tool=pmcentrez&endertype=abstract>
 230. Smith R, Bagga V, Fricker-Gates RA. Embryonic Neural Progenitor Cells: The Effects of Species, Region, and Culture Conditions on Long-Term Proliferation and Neuronal Differentiation. J Hematother Stem Cell Res [Internet]. 2003 Dec [cited 2019 Mar 3];12(6):713–25. Available from: <http://www.ncbi.nlm.nih.gov/pubmed/14977480>
 231. Jacobs BM. Stemming the hype: what can we learn from iPSC models of Parkinson’s disease and how can we learn it? J Park Dis. 2014;4(1):15–27.
 232. Gegg ME, Schapira AHV. Mitochondrial dysfunction associated with glucocerebrosidase deficiency. Neurobiol Dis [Internet]. 2016 Jun 1 [cited 2019 Jan 13];90:43–50. Available from: <http://www.ncbi.nlm.nih.gov/pubmed/26388395>
 233. Carelli V, Rugolo M, Sgarbi G, Ghelli A, Zanna C, Baracca A, et al. Bioenergetics shapes cellular death pathways in Leber’s hereditary optic neuropathy: A model of mitochondrial neurodegeneration. Biochim Biophys Acta - Bioenerg. 2004;1658(1–2):172–9.
 234. Jensen JB, Parmar M. Strengths and Limitations of the Neurosphere Culture System. Mol Neurobiol [Internet]. 2006 Dec [cited 2019 Mar 10];34(3):153–62. Available from: <http://www.ncbi.nlm.nih.gov/pubmed/17308349>
 235. Detmer S a, Chan DC. Functions and dysfunctions of mitochondrial dynamics. Nat

- Rev Mol Cell Biol [Internet]. 2007 Nov [cited 2014 Apr 29];8(11):870–9. Available from: <http://www.ncbi.nlm.nih.gov/pubmed/17928812>
236. Lopez-Fabuel I, Martin-Martin L, Resch-Beusher M, Azkona G, Sanchez-Pernaute R, Bolaños JP. Mitochondrial respiratory chain disorganization in Parkinson's disease-relevant PINK1 and DJ1 mutants. *Neurochem Int* [Internet]. 2017 Apr 11 [cited 2017 Jul 25]; Available from: <http://www.ncbi.nlm.nih.gov/pubmed/28408307>
237. Ryan BJ, Hoek S, Fon EA, Wade-Martins R. Mitochondrial dysfunction and mitophagy in Parkinson's: from familial to sporadic disease. *Trends Biochem Sci* [Internet]. 2015 Apr [cited 2016 May 14];40(4):200–10. Available from: <http://www.sciencedirect.com/science/article/pii/S0968000415000225>
238. Ysselstein D, Shulman JM, Krainc D, Davee R, Duncan D, Shulman J. Emerging Links Between Pediatric Lysosomal Storage Diseases and Adult Parkinsonism. 2019 [cited 2019 May 14]; Available from: <https://onlinelibrary-wiley-com.sire.ub.edu/doi/pdf/10.1002/mds.27631>
239. Webb JL, Ravikumar B, Atkins J, Skepper JN, Rubinsztein DC. α -Synuclein Is Degraded by Both Autophagy and the Proteasome. *J Biol Chem* [Internet]. 2003 Jul 4 [cited 2019 Feb 27];278(27):25009–13. Available from: <http://www.ncbi.nlm.nih.gov/pubmed/12719433>
240. Rubinsztein DC, Codogno P, Levine B. Autophagy modulation as a potential therapeutic target for diverse diseases. *Nat Rev Drug Discov* [Internet]. 2012 Sep 1 [cited 2019 Feb 25];11(9):709–30. Available from: <http://www.ncbi.nlm.nih.gov/pubmed/22935804>
241. Diogo C V., Yambire KF, Fernández Mosquera L, Branco F. T, Raimundo N. Mitochondrial adventures at the organelle society. *Biochem Biophys Res Commun* [Internet]. 2018 May 27 [cited 2019 Feb 28];500(1):87–93. Available from: <http://www.ncbi.nlm.nih.gov/pubmed/28456629>
242. González-Casacuberta I, Juárez-Flores D-L, Ezquerra M, Fucho R, Catalán-García M, Guitart-Mampel M, et al. Mitochondrial and autophagic alterations in skin fibroblasts from Parkinson disease patients with Parkin mutations. *Aging (Albany NY)* [Internet]. 2019 Jun 9 [cited 2019 Jun 20];11(11):3750–67. Available from: <http://www.ncbi.nlm.nih.gov/pubmed/31180333>
243. Plotegher N, Duchen MR. Crosstalk between Lysosomes and Mitochondria in Parkinson's Disease. *Front Cell Dev Biol* [Internet]. 2017 Dec 12 [cited 2019 Jan 13];5:110. Available from: <http://journal.frontiersin.org/article/10.3389/fcell.2017.00110/full>
244. Ishihara L, Warren L, Gibson R, Amouri R, Lesage S, Dürr A, et al. Clinical Features of Parkinson Disease Patients With Homozygous Leucine-Rich Repeat Kinase 2 G2019S Mutations. *Arch Neurol* [Internet]. 2006 Sep 1 [cited 2016 Aug 22];63(9):1250. Available from: <http://archneur.jamanetwork.com/article.aspx?doi=10.1001/archneur.63.9.1250>
245. Sanders LH, Laganière J, Cooper O, Mak SK, Vu BJ, Huang YA, et al. LRRK2 mutations cause mitochondrial DNA damage in iPSC-derived neural cells from Parkinson's disease patients: reversal by gene correction. *Neurobiol Dis* [Internet]. 2014 Feb [cited 2015 Jul 16];62:381–6. Available from:

- <http://www.sciencedirect.com/science/article/pii/S096999611300288X>
246. Grünewald A, Arns B, Meier B, Brockmann K, Tadic V, Klein C. Does uncoupling protein 2 expression qualify as marker of disease status in LRRK2-associated Parkinson's disease? *Antioxid Redox Signal* [Internet]. 2014 May 1 [cited 2017 Jul 24];20(13):1955–60. Available from: <http://online.liebertpub.com/doi/abs/10.1089/ars.2013.5737>
 247. Su Y-C, Qi X. Inhibition of excessive mitochondrial fission reduced aberrant autophagy and neuronal damage caused by LRRK2 G2019S mutation. *Hum Mol Genet* [Internet]. 2013 Nov 15 [cited 2017 Jul 24];22(22):4545–61. Available from: <https://academic.oup.com/hmg/article-lookup/doi/10.1093/hmg/ddt301>
 248. Esteves AR, G-Fernandes M, Santos D, Januário C, Cardoso SM. The Upshot of LRRK2 Inhibition to Parkinson's Disease Paradigm. *Mol Neurobiol* [Internet]. 2015 Dec 15 [cited 2017 Jul 24];52(3):1804–20. Available from: <http://link.springer.com/10.1007/s12035-014-8980-6>
 249. Bravo-San Pedro JM, Niso-Santano M, Gómez-Sánchez R, Pizarro-Estrella E, Aiastui-Pujana A, Gorostidi A, et al. The LRRK2 G2019S mutant exacerbates basal autophagy through activation of the MEK/ERK pathway. *Cell Mol Life Sci* [Internet]. 2013 Jan 8 [cited 2017 Feb 17];70(1):121–36. Available from: <http://link.springer.com/10.1007/s00018-012-1061-y>
 250. Juárez-Flores DL, González-Casacuberta I, Ezquerra M, Bañó M, Carmona-Pontaque F, Catalán-García M, et al. Exhaustion of mitochondrial and autophagic reserve may contribute to the development of LRRK2G2019S-Parkinson's disease. *J Transl Med* [Internet]. 2018 Dec 8 [cited 2018 Jun 19];16(1):160. Available from: <https://translational-medicine.biomedcentral.com/articles/10.1186/s12967-018-1526-3>
 251. Xu Y, Xu K, Sun Y, Liou B, Quinn B, Li R, et al. Multiple pathogenic proteins implicated in neuronopathic Gaucher disease mice. *Hum Mol Genet* [Internet]. 2014 Aug 1 [cited 2019 Mar 10];23(15):3943–57. Available from: <http://www.ncbi.nlm.nih.gov/pubmed/24599400>
 252. Keatinge M, Bui H, Menke A, Chen Y-C, Sokol AM, Bai Q, et al. Glucocerebrosidase 1 deficient *Danio rerio* mirror key pathological aspects of human Gaucher disease and provide evidence of early microglial activation preceding alpha-synuclein-independent neuronal cell death. *Hum Mol Genet* [Internet]. 2015 Dec 1 [cited 2019 Mar 10];24(23):6640–52. Available from: <http://www.ncbi.nlm.nih.gov/pubmed/26376862>
 253. Li H, Ham A, Ma TC, Kuo S-H, Kanter E, Kim D, et al. Mitochondrial dysfunction and mitophagy defect triggered by heterozygous *GBA* mutations. *Autophagy* [Internet]. 2019 Jan 2 [cited 2019 Mar 10];15(1):113–30. Available from: <http://www.ncbi.nlm.nih.gov/pubmed/30160596>
 254. Grünewald A, Arns B, Meier B, Brockmann K, Tadic V, Klein C. Does *Uncoupling Protein 2* Expression Qualify as Marker of Disease Status in *LRRK2* -Associated Parkinson's Disease? *Antioxid Redox Signal* [Internet]. 2014 May 1 [cited 2017 Jul 14];20(13):1955–60. Available from: <http://www.ncbi.nlm.nih.gov/pubmed/24251413>
 255. Su B, Wang X, Zheng L, Perry G, Smith M a, Zhu X. Abnormal mitochondrial dynamics and neurodegenerative diseases. *Biochim Biophys Acta* [Internet]. 2010 Jan [cited 2014 May 1];1802(1):135–42. Available from:

- <http://www.pubmedcentral.nih.gov/articlerender.fcgi?artid=2790543&tool=pmcentrez&endertype=abstract>
256. Bang Y, Kim K-S, Seol W, Choi HJ. LRRK2 interferes with aggresome formation for autophagic clearance. *Mol Cell Neurosci* [Internet]. 2016 Sep 1 [cited 2018 Feb 1];75:71–80. Available from: <https://www-sciencedirect-com.sire.ub.edu/science/article/pii/S1044743116300562?via%3Dihub>
 257. Manzoni C, Mamais A, Dihanich S, McGoldrick P, Devine MJ, Zerle J, et al. Pathogenic Parkinson's disease mutations across the functional domains of LRRK2 alter the autophagic/lysosomal response to starvation. *Biochem Biophys Res Commun* [Internet]. 2013 Nov 29 [cited 2017 Sep 28];441(4):862–6. Available from: <http://linkinghub.elsevier.com/retrieve/pii/S0006291X13018615>
 258. Loos B, du Toit A, Hofmeyr J-HS. Defining and measuring autophagosome flux—concept and reality. *Autophagy* [Internet]. 2014 [cited 2018 Mar 15];10(11):2087–96. Available from: <http://www.ncbi.nlm.nih.gov/pubmed/25484088>
 259. Hall CN, Klein-Flügge MC, Howarth C, Attwell D. Oxidative phosphorylation, not glycolysis, powers presynaptic and postsynaptic mechanisms underlying brain information processing. *J Neurosci* [Internet]. 2012 Jun 27 [cited 2016 Feb 25];32(26):8940–51. Available from: <http://www.pubmedcentral.nih.gov/articlerender.fcgi?artid=3390246&tool=pmcentrez&endertype=abstract>
 260. Marras C, Schuele B, Munhoz RP, Rogaeva E, Langston JW, Kasten M, et al. Phenotype in parkinsonian and nonparkinsonian LRRK2 G2019S mutation carriers.
 261. Lohmann E, Leclere L, De Anna F, Lesage S, Dubois B, Agid Y, et al. A clinical, neuropsychological and olfactory evaluation of a large family with LRRK2 mutations. *Parkinsonism Relat Disord*. 2009;15(4):273–6.
 262. Brockmann K, Gröger A, Di Santo A, Liepelt I, Schulte C, Klose U, et al. Clinical and brain imaging characteristics in leucine-rich repeat kinase 2-associated PD and asymptomatic mutation carriers. *Mov Disord* [Internet]. 2011 Nov [cited 2016 Aug 22];26(13):2335–42. Available from: <http://www.ncbi.nlm.nih.gov/pubmed/21989859>
 263. Infante J, Prieto C, Sierra M, Sánchez-Juan P, González-Aramburu I, Sánchez-Quintana C, et al. Comparative blood transcriptome analysis in idiopathic and LRRK2 G2019S-associated Parkinson's disease. *Neurobiol Aging* [Internet]. 2016 Feb [cited 2017 Jul 24];38:214.e1-214.e5. Available from: <http://linkinghub.elsevier.com/retrieve/pii/S0197458015005382>
 264. Sardiello M, Palmieri M, di Ronza A, Medina DL, Valenza M, Gennarino VA, et al. A Gene Network Regulating Lysosomal Biogenesis and Function. *Science* (80-) [Internet]. 2009 Jul 24 [cited 2019 Mar 10];325(5939):473–7. Available from: <http://www.ncbi.nlm.nih.gov/pubmed/19556463>
 265. Ciron C, Lengacher S, Dusonchet J, Aebischer P, Schneider BL. Sustained expression of PGC-1 α in the rat nigrostriatal system selectively impairs dopaminergic function. *Hum Mol Genet* [Internet]. 2012 Apr 15 [cited 2019 Jan 20];21(8):1861–76. Available from: <http://www.ncbi.nlm.nih.gov/pubmed/22246294>
 266. Magalhaes J, Gegg ME, Migdalska-Richards A, Doherty MK, Whitfield PD, Schapira AHV. Autophagic lysosome reformation dysfunction in glucocerebrosidase deficient

- cells: relevance to Parkinson disease. *Hum Mol Genet* [Internet]. 2016 Aug 15 [cited 2019 Mar 10];25(16):3432–45. Available from: <https://academic.oup.com/hmg/article-lookup/doi/10.1093/hmg/ddw185>
267. Fernandes HJR, Hartfield EM, Christian HC, Emmanouilidou E, Zheng Y, Booth H, et al. ER Stress and Autophagic Perturbations Lead to Elevated Extracellular α -Synuclein in GBA-N370S Parkinson's iPSC-Derived Dopamine Neurons. *Stem Cell Reports* [Internet]. 2016 Mar 8 [cited 2019 Mar 10];6(3):342–56. Available from: <http://www.ncbi.nlm.nih.gov/pubmed/26905200>
268. Yuan Y, Zheng Y, Zhang X, Chen Y, Wu X, Wu J, et al. BNIP3L/NIX-mediated mitophagy protects against ischemic brain injury independent of PARK2. *Autophagy* [Internet]. 2017 Oct 3 [cited 2019 Mar 10];13(10):1754–66. Available from: <http://www.ncbi.nlm.nih.gov/pubmed/28820284>
269. Chu CT, Ji J, Dagda RK, Jiang JF, Tyurina YY, Kapralov AA, et al. Cardiolipin externalization to the outer mitochondrial membrane acts as an elimination signal for mitophagy in neuronal cells. *Nat Cell Biol* [Internet]. 2013 Oct 15 [cited 2019 Mar 10];15(10):1197–205. Available from: <http://www.ncbi.nlm.nih.gov/pubmed/24036476>
270. Titova N, Padmakumar C, Lewis SJG, Chaudhuri KR. Parkinson's: a syndrome rather than a disease? *J Neural Transm* [Internet]. 2017 [cited 2019 Feb 18];124(8):907–14. Available from: <http://www.ncbi.nlm.nih.gov/pubmed/28028643>
271. Collier TJ, Kanaan NM, Kordower JH. Aging and Parkinson's disease: Different sides of the same coin? *Mov Disord* [Internet]. 2017 Jul 1 [cited 2018 Oct 3];32(7):983–90. Available from: <http://doi.wiley.com/10.1002/mds.27037>
272. Massey AC, Kaushik S, Sovak G, Kiffin R, Cuervo AM. Consequences of the selective blockage of chaperone-mediated autophagy. *Proc Natl Acad Sci* [Internet]. 2006 Apr 11 [cited 2019 Feb 27];103(15):5805–10. Available from: <http://www.ncbi.nlm.nih.gov/pubmed/16585521>
273. Kaushik S, Massey AC, Mizushima N, Cuervo AM. Constitutive Activation of Chaperone-mediated Autophagy in Cells with Impaired Macroautophagy. Subramani S, editor. *Mol Biol Cell* [Internet]. 2008 May [cited 2019 Feb 27];19(5):2179–92. Available from: <http://www.ncbi.nlm.nih.gov/pubmed/18337468>



9. SUPPLEMENTARY MATERIAL

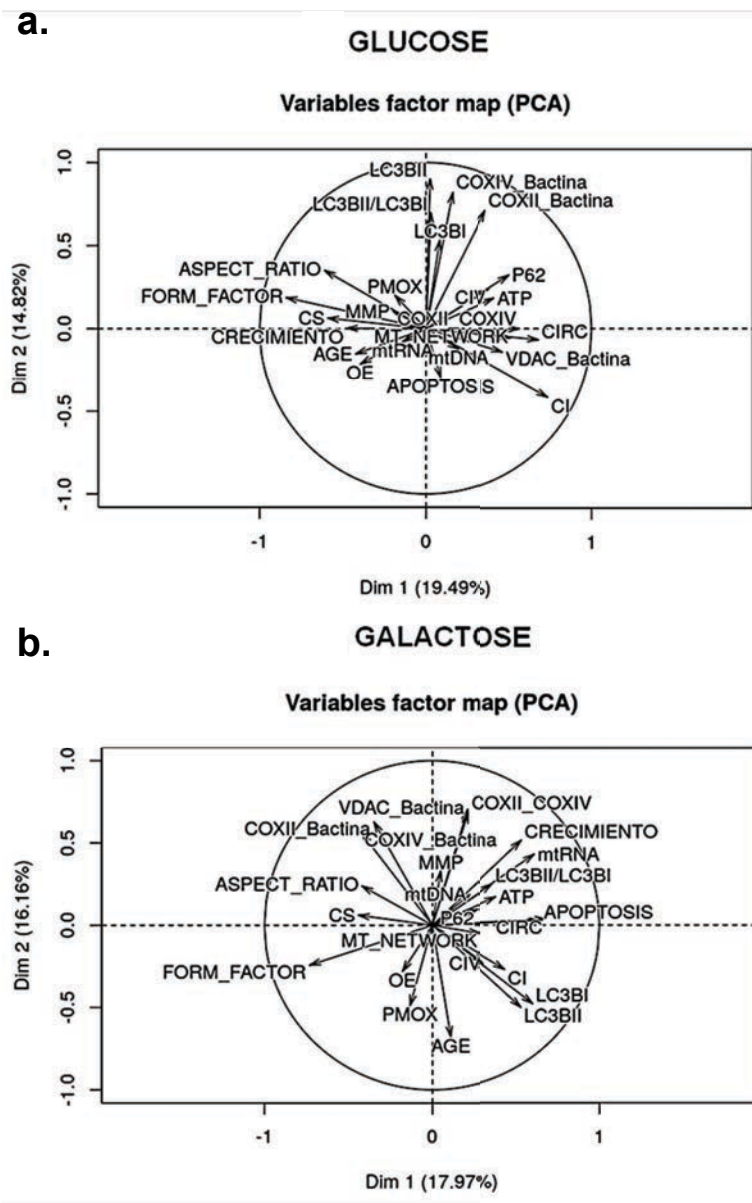


9.1 RESULTS

(SUPPLEMENTARY MATERIAL)

STUDY 1.

Groups were not differentially clustered nor variables correlated among each other by performing principal component analysis (PCA) (**Supplementary figure 1**).



Supplementary figure 1 (Previous page) Principal component analysis (PCA) for patients and controls in both media.

Variables factor map showing that individual variability in glucose media **(A)** was best expressed by mitochondrial dynamics parameters -circularity and mitochondrial network- for component 1 (horizontal axis), and autophagy parameters for component 2 (vertical axis). When subjected to mitochondrial challenging conditions **(B)**, circularity expressed the greatest variability for component 1 (horizontal axis), and MMP better expressed component 2 variability (vertical axis). The longer vectors and those which are more aligned to the corresponding axis (depicted as dotted lines) are the ones with the greatest variability among individuals, which interestingly have been documented to be associated with PD, despite none of the parameters represent a greater variability between groups.

MtDNA: mitochondrial-DNA; mtRNA: mitochondrial-RNA; VDAC/ β actin: Mitochondrial content; COXII/ β actin: Mitochondrial encoded protein content COXIV/ β actin; Nuclear encoded protein content; CI: Complex I enzymatic function; PMox: oxygen consumption stimulated by pyruvate-malate; CIV: Complex IV enzymatic function; MMP: Mitochondrial membrane potential; OE: Oxidative stress; Circ: Circularity; P62: Autophagy substrate LC3BI: Autophagy receptor, basal form; LC3BII: Lipidated form of the autophagy receptor, LC3BII/LC3BI: autophagic turnover, LC3BII/P62: autophagic flux.

Supplementary Table 1. Raw data of mitochondrial phenotype and autophagic print parameters of study 1.

		Parameter (Units)	Media	CONTROL (n=8)		NM-LRRK2 ^{G2019S} (n=6)				PD-LRRK2 ^{G2019S} (n=7)				P _c
				MEAN	SEM (±)	MEAN	SEM (±)	%	P _s	MEAN	SEM (±)	%	P _s	
MITOCHONDRIAL PHENOTYPE	Genetics and protein content	mtDNA (mt12SrRNA/nRNaseP)	Glu	73.43	14.98	109.24	15.33	48.77	0.14	129.99	20.57	77.03	0.07	0.37
			Gal	94.48	22.39	103.21	5.07	9.24	0.95	84.57	7.03	-10.49	0.72	0.08
		mtRNA (mt12SrRNA/nRNaseP)	Glu	28.47	8.95	25.71	9.41	-9.70	0.83	67.94	23.80	138.64	0.19	0.15
			Gal	20.84	7.59	10.60	0.57	-49.14	0.01	31.25	12.88	49.95	0.90	0.26
		Mitochondrial protein synthesis (mt-COX2/n-COX4)	Glu	0.33	0.03	0.26	0.10	-21.45	0.63	0.37	0.04	11.82	0.53	0.80
			Gal	0.28	0.07	0.39	0.03	-57.8	0.29	0.38	0.08	-58.83	0.55	1.00
	Mitochondrial function	Citrate synthase (nmoles/min*mg protein)	Glu	42.67	4.65	32.86	8.87	-22.99	0.28	30.56	6.28	-28.38	0.11	0.94
			Gal	41.88	4.11	45.11	8.54	7.72	0.85	44.16	5.86	5.45	1.00	0.94
		CI enzymatic function (Rate/CS)	Glu	2.07	1.19	1.29	0.50	-37.58	0.94	0.66	0.27	-68.19	0.61	0.61
			Gal	0.39	0.08	0.69	0.18	76.92	0.18	0.72	0.07	84.62	0.04	0.91
		O₂ consumption stimulated by CI substrate (nmoles/min*mg protein)	Glu	10.70	2.53	7.91	1.78	-26.07	0.49	6.71	1.65	-37.29	0.34	0.37
			Gal	6.64	1.99	11.74	3.29	76.87	0.35	7.7	1.84	16.01	0.69	0.63
CIV enzymatic function (rate/CS)		Glu	0.25	0.04	0.77	0.35	208.00	0.14	0.37	0.05	48.00	0.14	0.59	
		Gal	0.48	0.11	0.90	0.23	88.48	0.14	0.41	0.06	-14.07	0.57	0.18	
ATP levels (pmol ATP/μl*mg prot)		Glu	4.03	0.84	3.49	1.10	-13.40	0.66	2.30	0.72	-42.85	0.18	0.31	
		Gal	3.13	0.98	5.07	2.11	61.98	0.76	2.8	0.92	-10.49	0.76	0.59	
Mitochondrial Membrane Potential (% cells with depolarized mt/total cells)		Glu	23.78	4.26	36.65	2.10	54.14	0.04	47.88	11.27	101.34	0.14	0.94	
		Gal	30.27	5.01	46.03	5.98	52.08	0.11	30.36	7.87	0.29	0.76	0.13	
Oxidative stress (μM MDA + 4-HAE/mg prot)	Glu	1.42	0.51	1.17	0.30	-17.36	0.84	2.69	0.99	90.01	0.46	0.53		
	Gal	0.84	0.23	1.31	0.76	55.95	0.79	2.06	0.62	144.64	0.13	0.31		
Apoptotic rate (% dyed cells/total cells)	Glu	33.87	9.96	19.70	8.72	-41.84	0.35	36.14	10.19	6.70	0.78	0.23		
	Gal	20.97	4.97	11.26	5.87	-46.3	0.28	18.87	5.94	-10.01	0.96	0.37		
Mitochondrial dynamics	Mitochondrial network (Total mitochondria/cell area)	Glu	6.83	0.37	9.44	0.92	38.32	0.04	7.52	0.44	10.10	0.18	0.13	
		Gal	8.7	0.92	9.01	0.6	3.6	0.73	8.74	0.81	-8.22	0.62	0.63	
	Circularity (4π.area/perimeter ²)	Glu	0.45	0.01	0.44	0.02	-2.22	0.76	0.38	0.06	-2.60	0.34	0.45	
		Gal	0.48	0.01	0.39	0.02	-17.54	0.00	0.47	0.03	-1.35	0.95	0.18	
	Aspect ratio (major/minor axis)	Glu	3.29	0.10	3.34	0.18	-1.40	0.85	3.23	0.15	-1.99	0.66	0.94	
		Gal	3.33	0.11	3.38	0.14	1.44	0.73	2.97	0.13	-37.7	0.05	0.07	
	Form factor (Circ ⁻¹)	Glu	3.74	0.52	4.02	0.40	7.33	0.85	3.51	0.50	-6.12	0.95	0.59	
		Gal	3.45	0.67	4.92	0.47	42.53	0.05	3.18	0.51	-7.98	0.71	0.07	

Parameter (Units)		Media	CONTROL (n=8)		NM- <i>LRRK2</i> ^{G2019S} (n=6)				PD- <i>LRRK2</i> ^{G2019S} (n=7)				P _c		
			MEAN	SEM (±)	MEAN	SEM (±)	%	P _a	MEAN	SEM (±)	%	P _b			
AUTOPHAGY	Autophagic print (steady-state levels)	Autophagy substrate ((SQSTM1/p62)/β-actin)	Glu	0.39	0.11	0.64	0.08	64.45	0.37	0.36	0.10	-5.91	0.54	0.234	
			Gal	0.29	0.09	0.47	0.06	61.1	0.23	0.34	0.12	17.48	0.71	0.23	
		Autophagy receptor (LC3B1/β-actin)	Glu	0.18	0.07	0.45	0.18	144.54	0.37	0.44	0.11	135.15	0.13	0.84	
			Gal	0.14	0.05	0.36	0.14	153.28	0.23	0.4	0.11	179.94	0.07	0.84	
		Autophagy receptor lipidated (LC3B2/β-actin)	Glu	0.01	0.00	0.06	0.05	699.29	0.63	0.03	0.02	310.03	0.38	0.79	
			Gal	0.00	0.00	0.01	0	787.09	0.23	0.01	0	629.56	0.17	0.95	
	Autophagic turnover (LC3B2/LC3B1)	Glu	0.05	0.01	0.12	0.05	123.79	0.53	0.11	0.06	107.09	0.81	0.39		
		Gal	0.01	0.01	0.03	0.01	345.79	0.14	0.08	0.05	1088.51	0.10	0.70		
	Autophagic flux (LC3B2/SQSTM1/p62)	Glu	0.05	0.02	0.08	0.05	66.45	0.95	0.21	0.15	359.70	0.54	0.62		
		Gal	0.01	0.01	0.03	0.01	342.2	0.29	0.05	0.02	535.2	0.21	0.83		
	Autophagy (time-course)	Autophagy initiation ((SQSTM1/p62)/β-actin)	0 HRS	Glu	2.12	0.72	4.63	1.58	118.48	0.01	4.96	1.42	133.96	0.10	0.45
				Gal	4.68	1.52	11.52	7.59	145.80	0.05	10.19	3.96	117.51	0.45	0.30
Autophagy initiation ((SQSTM1/p62)/β-actin)		4 HRS	Glu	10.85	3.82	19.65	8.88	81.14	0.18	47.27	25.69	335.68	0.13	0.63	
			Gal	21.10	9.23	45.26	27.50	114.44	0.01	37.67	15.18	78.50	0.02	0.53	
Autophagy initiation ((SQSTM1/p62)/β-actin)		8 HRS	Glu	8.38	3.27	13.45	5.07	60.53	0.20	27.33	13.88	226.15	0.04	0.73	
			Gal	23.00	16.29	18.70	6.39	-18.68	0.10	29.66	9.30	28.96	0.13	0.63	
Autophagy receptor lipidated (LC3B2/β-actin)		0 HRS	Glu	0.07	0.05	0.02	0.01	-73.25	0.84	0.05	0.02	-37.79	0.90	0.45	
			Gal	0.04	0.04	0.00	0.00	-90.96	1.00	0.00	0.00	-100.00	1.00	0.63	
Autophagy receptor lipidated (LC3B2/β-actin)		4 HRS	Glu	0.27	0.13	0.66	0.18	145.23	0.05	0.13	0.02	-50.63	0.90	0.04	
			Gal	0.37	0.20	0.16	0.05	-55.77	1.00	0.16	0.07	-56.06	0.62	0.63	
Autophagy receptor lipidated (LC3B2/β-actin)		8 HRS	Glu	0.32	0.12	1.23	0.50	287.22	0.05	0.35	0.11	11.28	0.54	0.02	
			Gal	0.33	0.13	0.22	0.04	-33.28	0.95	0.16	0.04	-51.05	0.81	0.45	

NM-*LRRK2*^{G2019S}: Non-manifesting carriers of *LRRK2*^{G2019S}-mutation; PD-*LRRK2*^{G2019S}: patients with *LRRK2*^{G2019S}-mutation and clinically manifest PD; Glu: glucose; Gal: galactose; mtDNA: Mitochondrial DNA; mtRNA: Mitochondrial RNA; CI: Complex I; O₂ consumption stimulated for CI: Oxygen consumption stimulated for Complex I substrates (pyruvate, malate and glutamate); CIV: Complex IV.

Statistical analysis was made through non-parametric Mann-Whitney U test. P_a. P value when comparing NM-*LRRK2*^{G2019S} vs. controls; P_b. P value when comparing PD-*LRRK2*^{G2019S} vs. controls; P_c. P value when comparing NM-*LRRK2*^{G2019S} vs. PD-*LRRK2*^{G2019S}

Supplementary Table 2. Raw data of neurosphere characterization, mitochondrial content and autophagy parameters of study 2.

		Parameter (units)	wt/wt (n=2)		wt/GBA ^{N370S} (n=2)				GBA ^{N370S} /GBA ^{N370S} (n=2)				ANOVA	
			MEAN	SEM (±)	MEAN	SEM (±)	%	P _a	MEAN	SEM (±)	%	P _b		
CELL MODEL CHARACTERIZATION	NEURONAL MARKERS	β-III tubulin (AU)	O DOD	51.55	13.43	139.84	7.11	171.27	0.02	76.58	2.32	48.55	0.42	0.01
			2 DOD	95.32	71.73	315.15	71.54	230.62	0.40	174.05	83.21	82.60	1.00	0.26
			4 DOD	65.88	59.25	200.98	21.98	205.07	0.72	150.79	93.86	128.89	1.00	0.44
			6 DOD	75.73	66.91	236.28	55.15	212.00	0.83	145.21	128.56	91.74	1.00	0.52
		MAP2 (AU)	O DOD	373.98	229.95	122.12	4.40	-67.35	0.85	210.60	56.24	-43.69	1.00	0.50
			2 DOD	245.73	58.84	63.04	35.14	-74.35	0.28	79.17	21.29	-67.78	0.65	0.19
			4 DOD	49.42	9.56	0.63	0.35	-98.73	1.00	0.79	0.21	-98.40	1.00	0.72
			6 DOD	67.18	15.41	96.66	60.73	43.89	1.00	83.10	25.19	23.70	1.00	0.87
		Nestin (AU)	O DOD	0.14	0.07	0.03	0.03	-76.36	0.62	0.11	0.03	-22.00	1.00	0.38
			2 DOD	1.00	0.42	0.97	0.19	-2.99	1.00	1.06	0.52	5.21	1.00	0.38
			4 DOD	4.37	0.35	1.81	0.38	-58.60	0.07	1.10	0.52	-74.70	0.04	0.99
			6 DOD	8.57	2.74	2.84	0.37	-66.84	0.29	2.00	1.04	-76.61	0.22	0.13
CELL MODEL CHARACTERIZATION	LYSOSOMAL ENZYME ACTIVITIES	Gcase pH 5.4/NaT (nmols/min·mgprot)	O DOD	384.00	4.00	167.00	22.00	-56.51	0.00	0.50	1.50	-99.87	0.00	0.00
			2 DOD	502.50	25.50	149.50	42.50	-70.25	0.01	14.50	1.50	-97.11	0.00	0.00
			4 DOD	355.00	83.00	239.00	65.00	-32.68	0.81	-6.50	0.50	-101.83	0.07	0.05
			6 DOD	651.50	65.50	438.00	140.00	-32.77	0.58	10.50	26.50	-98.39	0.05	0.03
		Gcase pH 4.5 (nmols/min·mgprot)	O DOD	46.50	21.50	11.00	5.00	-76.34	0.43	8.50	0.50	-81.72	0.38	0.21
			2 DOD	111.50	41.50	87.00	27.00	-21.97	1.00	54.50	6.50	-51.12	0.77	0.47
			4 DOD	145.00	52.00	86.50	9.50	-40.34	0.81	6.50	1.50	-95.52	0.15	0.47
			6 DOD	195.50	1.50	120.50	54.50	-38.36	0.87	56.00	46.00	-71.36	0.29	0.20
		HEX (nmols/min·mgprot)	O DOD	66.50	23.50	71.50	15.50	7.52	1.00	56.50	3.50	-15.04	1.00	0.82
			2 DOD	150.50	12.50	121.50	77.50	-19.27	1.00	109.00	17.00	-27.57	1.00	0.82
			4 DOD	133.50	29.50	150.00	19.00	12.36	1.00	122.00	28.00	-8.61	1.00	0.76
			6 DOD	234.00	31.00	177.00	2.75	-24.36	1.00	209.50	99.50	-10.47	1.00	0.81
		β-gal (nmols/min·mgprot)	O DOD	292.00	73.00	340.50	20.50	16.61	1.00	192.50	19.50	-34.08	0.65	0.21
			2 DOD	842.00	277.00	494.00	230.00	-41.33	1.00	775.00	232.00	-7.96	1.00	0.62
			4 DOD	602.00	90.00	544.00	272.50	-9.63	1.00	528.00	133.00	-12.29	1.00	0.96
			6 DOD	967.50	237.50	692.00	188.00	-28.48	0.69	587.50	240.50	-39.28	0.53	0.54

Parameter (units)			wt/wt (n=2)		wt/ <i>GBA</i> ^{N370S} (n=2)				<i>GBA</i> ^{N370S} / <i>GBA</i> ^{N370S} (n=2)				ANOVA	
			MEAN	SEM (±)	MEAN	SEM (±)	%	P _a	MEAN	SEM (±)	%	P _b		
MITOCHONDRIA	MITOCHONDRIAL CONTENT	Outer mitochondrial membrane (VDAC-1/βactin)	UT	258.64	29.63	73.96	18.69	-71.41	0.30	338.34	88.81	30.82	1.00	0.09
			CCCP	144.48	53.99	138.43	21.85	-4.19	1.00	251.18	58.51	73.85	0.64	0.31
		Inner mitochondrial marker (SDHA/βactin)	UT	328.90	14.77	263.85	19.86	-19.78	0.94	831.23	234.23	152.73	0.15	0.11
			CCCP	158.72	9.02	204.41	14.98	28.79	0.98	318.22	44.52	100.49	0.08	0.06
		Mitochondrial matrix marker (TFAM/βactin)	UT	116.13	1.94	120.46	0.73	3.73	1.00	240.93	172.55	107.47	1.00	0.65
			CCCP	56.12	10.94	224.77	6.17	300.52	0.00	141.74	6.76	152.57	0.02	0.00
	MITOCHONDRIAL BIOGENESIS	Mitochondrial biogenesis regulator (PGC1α/GDAPH)	UT	0.08	0.00	0.12	0.00	49.71	N/A	0.11	n=1	40.87	N/A	0.01
			CCCP	0.57	0.11	2.76	0.17	382.94	N/A	0.44	n=1	-23.21	N/A	0.02
		Lisosomal biogenesis regulator (TFEB/GDAPH)	UT	0.01	0.00	0.02	0.00	88.77	N/A	0.03	n=1	135.47	N/A	0.08
			CCCP	0.01	0.00	0.01	0.00	31.73	N/A	0.02	n=1	53.94	N/A	0.03
	MITOCHONDRIAL FUNCTION	ATP levels (PmolATP/ul*mgprot)	0 HRS	0.01	0.01	0.01	0.00	-29.34	0.36	0.01	0.01	-21.32	0.36	0.05
			4 HRS	0.01	0.01	0.01	0.00	-24.91	0.02	0.01	0.00	-28.16	0.01	0.01
16 HRS			0.00	0.00	0.00	0.00	66.68	0.00	0.01	0.00	190.40	0.00	0.00	
24 HRS			0.00	0.00	0.00	0.00	59.50	0.03	0.01	0.01	253.52	0.01	0.01	
AUTOPHAGY	MITOPHAGY	Mitophagy induction (PINK1/GADPH)	UT	0.07	0.00	0.09	0.01	26.47	N/A	0.06	n=1	-14.84	N/A	0.19
			CCCP	0.08	0.01	0.14	0.03	79.45	N/A	0.08	n=1	1.38	N/A	0.29
	MACROAUTOPHAGY	Autophagy initiation ((SQSTM1/p62)/βactin)	UT	252.42	30.69	137.08	16.69	-45.69	0.23	193.86	56.29	-23.20	1.00	0.18
			BAF	924.84	555.57	602.24	149.36	-34.88	1.00	887.29	145.28	-4.06	1.00	0.78
		Autophagosome number (LC3B2/βactin)	UT	1499.54	754.45	559.01	253.21	-62.72	0.54	674.63	176.19	-55.01	0.61	0.32
			BAF	4385.22	1404.53	2624.67	949.57	-40.15	0.69	3193.41	364.23	-27.18	1.00	0.45

wt/wt: controls; wt/*GBA*^{N370S} heterozygous carriers of *GBA*^{N370S}-mutation; *GBA*^{N370S}/*GBA*^{N370S} homozygous carriers of *GBA*^{N370S}-mutation; AU: arbitrary units; DOD: days of differentiation; UT: untreated; CCCP: 10uM Carbonyl cyanide *m*-chlorophenyl hydrazone; BAF: 0.5 uM bafylomicin. Statistical analysis was made through one-way ANOVA followed by Bonferroni's correction. P_a. P value when comparing wt/*GBA*^{N370S} vs. controls; P_b. P value when comparing *GBA*^{N370S}/*GBA*^{N370S} vs. controls.



10. ANNEX



ORIGINAL ARTICLE RELATED TO THIS THESIS

Exhaustion of mitochondrial and autophagic reserve may contribute to the development of LRRK2_{G2019S}-Parkinson's disease.

Juárez-Flores DL, González-Casacuberta I, Ezquerro M, Bañó M, Carmona-Pontaque F, Catalán-García M, Guitart-Mampel M, Rivero JJ, Tobias E, Milisenda JC, Tolosa E, Martí MJ, Fernández-Santiago R, Cardellach F, Morén C, Garrabou G.

J Transl Med. 2018 Jun 8;16(1):160. doi: 10.1186/s12967-018-1526-3.

OTHER ORIGINAL ARTICLES

Mitochondrial and autophagic alterations in skin fibroblasts from Parkinson disease patients with Parkin mutations.

González-Casacuberta I, **Juárez-Flores DL**, Ezquerro M, Fucho R, Catalán-García M, Guitart-Mampel M, Tobías E, García-Ruiz C, Fernández-Checa JC, Tolosa E, Martí MJ, Grau JM, Fernández-Santiago R, Cardellach F, Morén C, Garrabou G.

Aging (Albany NY). 2019 Jun 9. doi: 10.18632/aging.102014.

Mitochondrial implications in human pregnancies with intrauterine growth restriction and associated cardiac remodelling.

Guitart-Mampel M, **Juarez-Flores DL**, Youssef L, Moren C, Garcia-Otero L, Roca-Agujetas V, Catalan-Garcia M, Gonzalez-Casacuberta I, Tobias E, Milisenda JC, Grau JM, Crispi F, Gratacos E, Cardellach F, Garrabou G.

J Cell Mol Med. 2019 Apr 2. doi: 10.1111/jcmm.14282.

Transcriptional alterations in skin fibroblasts from Parkinson's disease patients with parkin mutations.

González-Casacuberta I, Morén C, **Juárez-Flores DL**, Esteve-Codina A, Sierra C, Catalán-García M, Guitart-Mampel M, Tobías E, Milisenda JC, Pont-Sunyer C, Martí MJ, Cardellach F, Tolosa E, Artuch R, Ezquerro M, Fernández-Santiago R, Garrabou G.

Neurobiol Aging. 2018 May. doi: 10.1016/j.neurobiolaging.2018.01.021

Erratum in: *Neurobiol Aging.* 2018 Sep;69:300.

Cardiac and placental mitochondrial characterization in a rabbit model of intrauterine growth restriction.

Guitart-Mampel M, Gonzalez-Tendero A, Niñerola S, Morén C, Catalán-Garcia M, González-Casacuberta I, **Juárez-Flores DL**, Ugarteburu O, Matalonga L, Cascajo MV, Tort F, Cortés A, Tobias E, Milisenda JC, Grau JM, Crispi F, Gratacós E, Garrabou G, Cardellach F.

Biochim Biophys Acta Gen Subj. 2018 May;1862(5):1157-1167. doi: 10.1016/j.bbagen.2018.02.006.

Imbalance in mitochondrial dynamics and apoptosis in pregnancies among HIV-infected women on HAART with obstetric complications.

Guitart-Mampel M, Hernandez AS, Moren C, Catalan-Garcia M, Tobias E, Gonzalez-Casacuberta I, **Juarez-Flores DL**, Gatell JM, Cardellach F, Milisenda JC, Grau JM, Gratacos E, Figueras F, Garrabou G.

J Antimicrob Chemother. 2017 Sep 1;72(9):2578-2586. doi: 10.1093/jac/dkx187.

Colonic Oxidative and Mitochondrial Function in Parkinson's Disease and Idiopathic REM Sleep Behavior Disorder.

Morén C, González-Casacuberta Í, Navarro-Otano J, **Juárez-Flores D**, Vilas D, Garrabou G, Milisenda JC, Pont-Sunyer C, Catalán-García M, Guitart-Mampel M, Tobias E, Cardellach F, Valldeoriola F, Iranzo A, Tolosa E.

Parkinsons Dis. 2017;2017:9816095. doi: 10.1155/2017/9816095.

HIV-1 promonocytic and lymphoid cell lines: an in vitro model of in vivo mitochondrial and apoptotic lesion.

Morén C, González-Casacuberta I, Álvarez-Fernández C, Bañó M, Catalán-Garcia M, Guitart-Mampel M, **Juárez-Flores DL**, Tobias E, Milisenda J, Cardellach F, Gatell JM, Sánchez-Palomino S, Garrabou G.

J Cell Mol Med. 2017 Feb;21(2):402-409. doi: 10.1111/jcmm.12985.

Mitochondrial DNA disturbances and deregulated expression of oxidative phosphorylation and mitochondrial fusion proteins in sporadic inclusion body myositis.

Catalán-García M, Garrabou G, Morén C, Guitart-Mampel M, Hernando A, Díaz-Ramos À, González-Casacuberta I, **Juárez DL**, Bañó M, Enrich-Bengoia J, Emperador S, Milisenda JC, Moreno P, Tobias E, Zorzano A, Montoya J, Cardellach F, Grau JM.

Clin Sci (Lond). 2016 Oct 1;130(19):1741-51. doi: 10.1042/CS20160080.

BOOK CHAPTER

Drug-Induced Mitochondrial Toxicity During Pregnancy; Mitochondrial Dysfunction Caused by Drugs and Environmental Toxicants

Juárez-Flores DL, Hernández AS, García-Otero L, Guitart-Mampel M, Catalán-García M, González-Casacuberta I, Milisenda JC, Grau JM, Cardellach F, Morén C, Garrabou G.

Hoboken, NJ, USA: John Wiley & Sons, Inc.; 2018 p. 509–20. Available from: <http://doi.wiley.com/10.1002/9781119329725.ch33>

REVIEW

The Role of Therapeutic Drugs on Acquired Mitochondrial Toxicity.

Morén C, **Juárez-Flores DL**, Cardellach F, Garrabou G.

Curr Drug Metab. 2016;17(7):648-62. Review.

LETTER

Mitohormesis and autophagic balance in Parkinson disease.

Juarez-Flores DL, Gonzalez-Casacuberta I, Garrabou G.


Aging (Albany NY). 2019 Jan 16;11(2):301-302. doi: 10.18632/aging.101779.

RESEARCH

Open Access



Exhaustion of mitochondrial and autophagic reserve may contribute to the development of *LRRK2*^{G2019S}-Parkinson's disease

Diana Luz Juárez-Flores^{1,2} , Ingrid González-Casacuberta^{1,2}, Mario Ezquerro^{3,4}, María Bañó^{1,2}, Francesc Carmona-Pontaque⁵, Marc Catalán-García^{1,2}, Mariona Guitart-Mampel^{1,2}, Juan José Rivero^{1,2}, Ester Tobias^{1,2}, Jose Cesar Milisenda^{1,2}, Eduard Tolosa^{3,4}, Maria Jose Marti^{3,4}, Ruben Fernández-Santiago^{3,4}, Francesc Cardellach^{1,2}, Constanza Morén^{1,2*} and Glòria Garrabou^{1,2*}

Abstract

Background: Mutations in *leucine rich repeat kinase 2* (*LRRK2*) are the most common cause of familial Parkinson's disease (PD). Mitochondrial and autophagic dysfunction has been described as etiologic factors in different experimental models of PD. We aimed to study the role of mitochondria and autophagy in *LRRK2*^{G2019S}-mutation, and its relationship with the presence of PD-symptoms.

Methods: Fibroblasts from six non-manifesting *LRRK2*^{G2019S}-carriers (NM-*LRRK2*^{G2019S}) and seven patients with *LRRK2*^{G2019S}-associated PD (PD-*LRRK2*^{G2019S}) were compared to eight healthy controls (C). An exhaustive assessment of mitochondrial performance and autophagy was performed after 24-h exposure to standard (glucose) or mitochondrial-challenging environment (galactose), where mitochondrial and autophagy impairment may be heightened.

Results: A similar mitochondrial phenotype of NM-*LRRK2*^{G2019S} and controls, except for an early mitochondrial depolarization (54.14% increased, $p = 0.04$), was shown in glucose. In response to galactose, mitochondrial dynamics of NM-*LRRK2*^{G2019S} improved (– 17.54% circularity, $p = 0.002$ and + 42.53% form factor, $p = 0.051$), probably to maintain ATP levels over controls. A compromised bioenergetic function was suggested in PD-*LRRK2*^{G2019S} when compared to controls in glucose media. An inefficient response to galactose and worsened mitochondrial dynamics (– 37.7% mitochondrial elongation, $p = 0.053$) was shown, leading to increased oxidative stress. Autophagy initiation (SQSTM1/P62) was upregulated in NM-*LRRK2*^{G2019S} when compared to controls (glucose + 118.4%, $p = 0.014$; galactose + 114.44%, $p = 0.009$), and autophagosome formation increased in glucose media. Despite of elevated SQSTM1/P62 levels of PD-NM-*LRRK2*^{G2019S} when compared to controls (glucose + 226.14%, $p = 0.04$; galactose + 78.5%, $p = 0.02$), autophagosome formation was deficient in PD-*LRRK2*^{G2019S} when compared to NM-*LRRK2*^{G2019S} (– 71.26%, $p = 0.022$).

Conclusions: Enhanced mitochondrial performance of NM-*LRRK2*^{G2019S} in mitochondrial-challenging conditions and upregulation of autophagy suggests that an exhaustion of mitochondrial bioenergetic and autophagic reserve, may contribute to the development of PD in *LRRK2*^{G2019S} mutation carriers.

Keywords: Parkinson's disease, *LRRK2*, *G2019S*, Non-manifesting carriers, Mitochondrial dysfunction, Mitochondrial dynamics, Autophagy, Fibroblasts, Glucose, Galactose

*Correspondence: cmoren1@clinic.ub.es; garrabou@clinic.ub.es

¹ Laboratory of Muscle Research and Mitochondrial Function-CELLEX, Institut d'Investigacions Biomèdiques August Pi i Sunyer (IDIBAPS), Department of Internal Medicine-Hospital Clínic of Barcelona, Faculty of Medicine and Health Sciences, University of Barcelona (UB), Barcelona, Spain
Full list of author information is available at the end of the article



Background

Parkinson's disease (PD) is the second most prevalent neurodegenerative disease. While most of PD cases are idiopathic, monogenic forms of the disease are demonstrated in about 5–10% of patients [1]. Mutations in *leucine-rich repeat kinase 2* (*LRRK2*) are the most common cause of inherited PD and account for 1–2% of sporadic PD cases [2]. *LRRK2* is a large multi-domain protein with kinase and GTPase activity involved in several cellular functions [3]. A glycine to serine substitution in the kinase domain of this protein (*G2019S*), accounts for the majority of genetically-transmitted, late-onset PD and for a variable proportion of sporadic PD, with higher prevalence in Ashkenazi Jews and North-African populations [4, 5]. Previous experimental models of PD have reported that *LRRK2* mutations play a role in α -synuclein phosphorylation and depot, microtubule dynamics regulation, alterations in the ubiquitin–proteasome system and in neurite growth and branching of neurons [6].

Current evidence suggests that the increased kinase activity caused by the *LRRK2*^{G2019S}-mutation (*LRRK2*^{G2019S}), associated with the regulation of mitochondrial dynamics, vesicle trafficking and chaperone mediated autophagy [7–9], plays a pivotal role in the pathogenesis of *LRRK2*^{G2019S}-associated PD, but the molecular mechanisms leading to neurodegeneration remain largely unknown [10].

Neuronal function is strongly dependent on oxidative metabolism and efficient organelle clearance, and mitochondrial homeostasis greatly depends on adequate mitochondrial dynamics, turnover and renewal through autophagy, which makes the study of mitochondrial function and autophagy highly relevant in the elucidation of pathological pathways leading to neurodegeneration [7, 8]. Recent studies have characterized mitochondrial dysfunction and autophagy impairment in *LRRK2*^{G2019S}-associated PD [9–11]. Furthermore, therapeutic strategies in *LRRK2*^{G2019S}-associated PD consisting of drug testing in experimental models directed to reverse mitochondrial alterations, and *LRRK2* inhibition as a therapeutic target for impaired autophagy in PD, have been tested with positive outcomes [12–14]. However, whether mitochondrial and autophagic alterations are cause or effect of the pathophysiology of *LRRK2*^{G2019S} PD is still unclear.

In this regard, the study of *LRRK2*^{G2019S}-carriers without PD symptoms (NM-*LRRK2*^{G2019S}) in contrast to *LRRK2*^{G2019S}-carriers diagnosed with PD (PD-*LRRK2*^{G2019S}), provides the opportunity to investigate early molecular alterations in this condition [6]. Motor symptoms of PD appear when loss of more than 60–70% of dopaminergic neurons has occurred, preceded by

several years of neurodegeneration at different levels, and followed by a rapid progression of the disease [15]. In the last decade, research has focused on clinical and molecular alterations in the prodromal phase of PD [16] and in asymptomatic carriers of PD-linked mutations [14, 17], all of which has raised a great interest in the search of the disease aetiology, novel biomarkers and potential targets to prevent and modify the natural history of the disease.

Since the central nervous system is not readily available for investigation, several experimental models have been developed in the pursuit of unravelling PD pathophysiology [15, 16]. Past studies have provided evidence of molecular alterations of PD in peripheral tissues [18–20], such as skin-derived fibroblasts, where defined mutations and cumulative cellular damage of donors are present [21]. Concerns have risen about the use of toxic insults and non-physiologic metabolic conditions in previous cell or animal models of the disease, which may not reproduce the mitochondrial and autophagic derangements that lead to neurodegeneration. Glucose promotes anaerobic glycolysis in detriment of oxidative mitochondrial metabolism, thus masking potential bioenergetic alterations and consequent autophagic fails which may be more evident in mitochondrial-challenging conditions. In this sense, the use of galactose has been proved useful in the study of primary mitochondrial diseases, since it enhances mitochondrial metabolism, evidencing pre-existent mitochondrial alterations [22] and autophagic derangements.

In the present study, we hypothesized that mitochondrial and autophagic alterations represent a primary and systemic process in PD, which may play a role in the development of symptoms of *LRRK2*^{G2019S}-associated PD, and that such derangements may be exacerbated in mitochondrial-challenging conditions. Consequently, we evaluated the mitochondrial and autophagic phenotype in fibroblasts from NM-*LRRK2*^{G2019S} subjects and PD-*LRRK2*^{G2019S} patients, either in glycolytic or oxidative conditions enabled by the use of galactose.

Methods

Study design and population

A single-site, cross-sectional, observational study was conducted. Twenty-one age and gender paired subjects were included: six NM-*LRRK2*^{G2019S}, seven PD-*LRRK2*^{G2019S}, and eight healthy, unrelated controls (C). All PD-*LRRK2*^{G2019S} patients met the UK Brain Bank Criteria for PD [23]. Control group included *LRRK2*^{G2019S} negative relatives of patients who voluntarily underwent skin biopsy. Subjects with comorbidities, mitochondrial disorders, and those consuming mitochondrial toxic drugs were not included in any of those groups [24].

Fibroblasts culture

Fibroblasts were obtained by a skin punch biopsy and mutation screening was performed as previously described [5].

Cells were grown in 25 mM glucose DMEM medium (Gibco, Life Technologies) supplemented with 10% heat-inactivated fetal bovine serum and 1% penicillin–streptomycin at 37 °C, in a humidified 5% CO₂ air incubator, until 80% optimal confluence was reached. In order to assess whether mitochondrial and autophagic function was directly implicated in the pathogeny of *LRRK2*^{G2019S}, cells were exposed for 24-h to either 25 mM glucose (standard) or 10 mM galactose (mitochondrial-challenging) media [22], where cells are forced to rely on oxidative phosphorylation for ATP production. Fibroblasts were harvested with 2.5% trypsin, (Gibco, Life technologies™) at 500 g for 8 min. In vivo experiments, including oxygen consumption and mitochondrial membrane potential (MMP), were performed in parallel including one subject from each cohort, at the same passage, both in glucose and galactose media. Fixation of cells for immunofluorescent quantification of mitochondrial dynamics was also performed at this time point. Cell pellets from each line were kept at –80 °C for further experimental procedures. All functional assays were performed in cells between passage 5 and 10.

Experimental parameters

In order to address an exhaustive mitochondrial phenotyping and autophagic print, this study contemplated the following experiments:

Mitochondrial phenotype

a. Mitochondrial DNA, RNA and protein content:

Total DNA was extracted by standard phenol chloroform procedure and total RNA was extracted by affinity microcolumns and retro transcribed to cDNA in triplicates, as reported elsewhere [25]. Mitochondrial DNA and RNA content were measured as the ratio between a mtDNA encoded gene/transcript and a nuclear encoded one (mt12SrRNA/nRNAseP). Mitochondrial protein content was assessed by Western Blot in duplicates, through 7/13% SDS-PAGE and immunoquantification of nuclear-encoded VDAC, mitochondrial-encoded COXII, and nuclear-encoded COXIV analysis, normalized by β-actin. Chemiluminescence was quantified with ImageQuantLD® [26].

b. Mitochondrial function:

i. Mitochondrial respiratory chain (MRC) enzyme activities previously associated to PD [14] were measured by spectrophotometry, following Spanish standardized national procedures (unpublished data). Complex I (CI) and Complex IV

(CIV) enzyme activities were then normalized by citrate synthase (CS), widely considered as a reliable marker of mitochondrial content.

ii. Mitochondrial respiration is the result of oxygen consumption by the MRC. CI stimulated oxygen consumption was assessed through pyruvate-malate oxidation (PMox) by high-resolution respirometry using Oroboros™ Oxygraph-2K® (Innsbruck, Austria) in permeabilized fibroblasts, following manufacturer protocols [27].

iii. Total cellular ATP was measured in duplicates by using the Luminescent ATP detection assay kit® #ab113849; Abcam™ (Cambridge, United Kingdom), according to manufacturer's instructions, in order to quantify the bioenergetic efficiency of MRC.

iv. Mitochondrial damage markers were measured to search for mitochondrial lesion in association with the presence of *LRRK2*^{G2019S}. Mitochondrial membrane potential was measured by flow cytometry twice to establish whether punctual mitochondrial alterations in MMP prelude mitochondrial dysfunction, as previously described [28]. Second, lipid peroxidation was measured in duplicates by the spectrophotometric measurement of malondialdehyde (MDA) and 4-hydroxyalkenal (HAE), as indicators of oxidative damage of reactive oxygen species (ROS) into cellular lipid compounds, as reported elsewhere [29]. Finally, to evaluate the apoptotic rate, cells were double-stained for annexin V and propidium iodide and quantified by flow cytometry, as previously reported [30].

c. *Mitochondrial dynamics* has been shown to be crucial in the maintenance of mitochondrial homeostasis, and LRRK2 has been suggested to play a role in mitochondrial fission [31]. Immunocytochemistry using confocal microscopy was performed as previously described [32]. One cell from three different fields for each cell line were randomly selected and analyzed with Image J [33] software to quantify the following parameters of mitochondrial dynamics:

i. Mitochondrial network or mitochondrial content: Total number of mitochondria/total cell area [34]; higher mitochondrial network values are considered a sign of healthy mitochondria.

ii. Circularity (Circ) or mitochondrial isolation: $4\pi \cdot \text{area} / \text{perimeter}^2$; circular mitochondria have less interaction sites with other mitochondria, thus, Circ=1 refers to poor mitochondrial dynamics of isolated mitochondria.

- iii. Aspect ratio (AR) or mitochondrial elongation: major/minor axis, AR=1 indicates a perfect circle; AR increases as mitochondria elongate and become more elliptical, which is considered a beneficial sign of mitochondrial dynamics.
- iv. Form factor (FF) or mitochondrial branching: Circ-1; FF=1 corresponds to a circular, unbranched mitochondrion and high FF values indicate branched and connected mitochondria, which is favourable for mitochondrial function.

Autophagic print

Characterization of autophagic print was carried out twice by quantitative measurement of autophagic-related proteins in both media (basal). To further assess autophagosome formation, 100 nM Bafilomycin A1 was added at two different time points (4 and 8 h) [35]. Briefly, fibroblasts were lysed with RIPA buffer and protease inhibitors followed by centrifugation at 14,000g at 4 °C for 5 min. Soluble fraction was retained for Western Blot analysis. Equal protein load lysates were resolved through 7/15% SDS-PAGE and transferred into nitrocellulose membranes, following blocking with 10% skimmed milk. Membranes were hybridized with Anti-SQSTM1/p62 and anti-LC3B antibodies overnight at 4 °C. Protein expression was normalized by β-actin protein content in all cases, as a cell loading control. Chemiluminescence was quantified with ImageQuantLD® and results were expressed and interpreted as:

- i. Autophagy substrate; (SQSTM/p62)/β-actin is a cargo protein widely used as a marker of autophagy initiation [13].
- ii. Autophagy receptor (LC3BI/β-actin) and lipidated form of the autophagy receptor (LC3BII/β-actin): LC3B is a marker of autophagosomes; LC3BI is unspecific and expressed in the autophagosome membrane but can also be located in cytoplasm or other organelles, its lipidation and migration to the autophagosome membrane (LC3BII) is considered to be a marker of autophagosome formation [36].

Immunocytochemistry was performed to further characterize autophagosome formation in the basal state, in glucose and galactose media, and after 6 h exposure to 100 nM Bafilomycin A1 using confocal microscopy. Briefly, cultured skin fibroblasts were washed with PBS before fixation with 4% paraformaldehyde for 15 min. Fixed cells were washed, permeabilized with 0.1% Digitonin in blocking solution (1% bovine serum albumin). Cells were incubated for 1 h using Anti-LC3 pAB. Counterstaining with DAPI was performed for nucleus visualization.

Experimental parameters were normalized by protein levels, measured by the BCA assay in quadruplicates, when needed. See Additional file 1: Material and methods for detailed protocols and reagents.

Statistical analysis

Results were expressed as mean ± SEM and as a percentage of increase/decrease with respect to controls, which were arbitrarily assigned as a 0% baseline. Two statistical approaches were performed for each media (glucose or galactose): (i) Non-parametric Mann–Whitney analysis for independent samples to detect inter-group differences for individual parameters and (ii) principal component analysis (PCA) to define the component with the largest possible variance and to show whether the studied population would be clustered by group, age or sex. Statistical analysis was performed with SPSS 20.00 (for Mann–Whitney test) and the R programming language version 3.4.3 and its missMDA, package (for PCA) [37]. Statistical significance was set at *p* < 0.05 in all cases.

Results

Epidemiological data of the studied cohorts at the time of skin biopsy are shown in Table 1 and clinical characteristics of PD-*LRRK2*^{G2019S} patients are shown in Additional file 2: Table S1. As expected, no significant differences in age and gender between groups were evidenced by either Mann–Whitney or PCA tests. None of the NM-*LRRK2*^{G2019S} subjects had developed clinical symptoms of the disease at the time of results analysis. Groups were not differentially clustered nor variables correlated

Table 1 Epidemiological characteristics of the cohorts

Group	N	Gender		Age (years)		
		Male	Female	Range	Mean	SEM
NM- <i>LRRK2</i> ^{G2019S}	6	3 (50%)	3 (50%)	34–61	46.67	4.04
PD- <i>LRRK2</i> ^{G2019S}	7	3 (42.85%)	4 (57.15%)	44–71	60.57	3.15
Control	8	3 (37.50%)	5 (62.50%)	41–69	56.00	3.63

Epidemiological data of the studied cohorts at the time of skin biopsy. No significant differences were found in age or gender between groups

NM-*LRRK2*^{G2019S}: Non-manifesting *LRRK2*^{G2019S}-mutation carriers; PD-*LRRK2*^{G2019S}: patients with *LRRK2*^{G2019S}-mutation and clinically manifest PD; N: Number of cases enrolled; SEM: Standard error of the mean

among each other by performing PCA (Additional file 3: Figure S1).

Mitochondrial phenotype

Figure 1 summarizes mitochondrial phenotype and raw data of experimental parameters is provided in Additional file 4: Table S2. Extended versions of graphics corresponding to genetics and mitochondrial protein synthesis can be found in Additional file 5: Figure S2.

- a. Mitochondrial function of NM-*LRRK2*^{G2019S} ameliorated when subjected to mitochondrial challenging conditions, in order to maintain ATP production over controls.

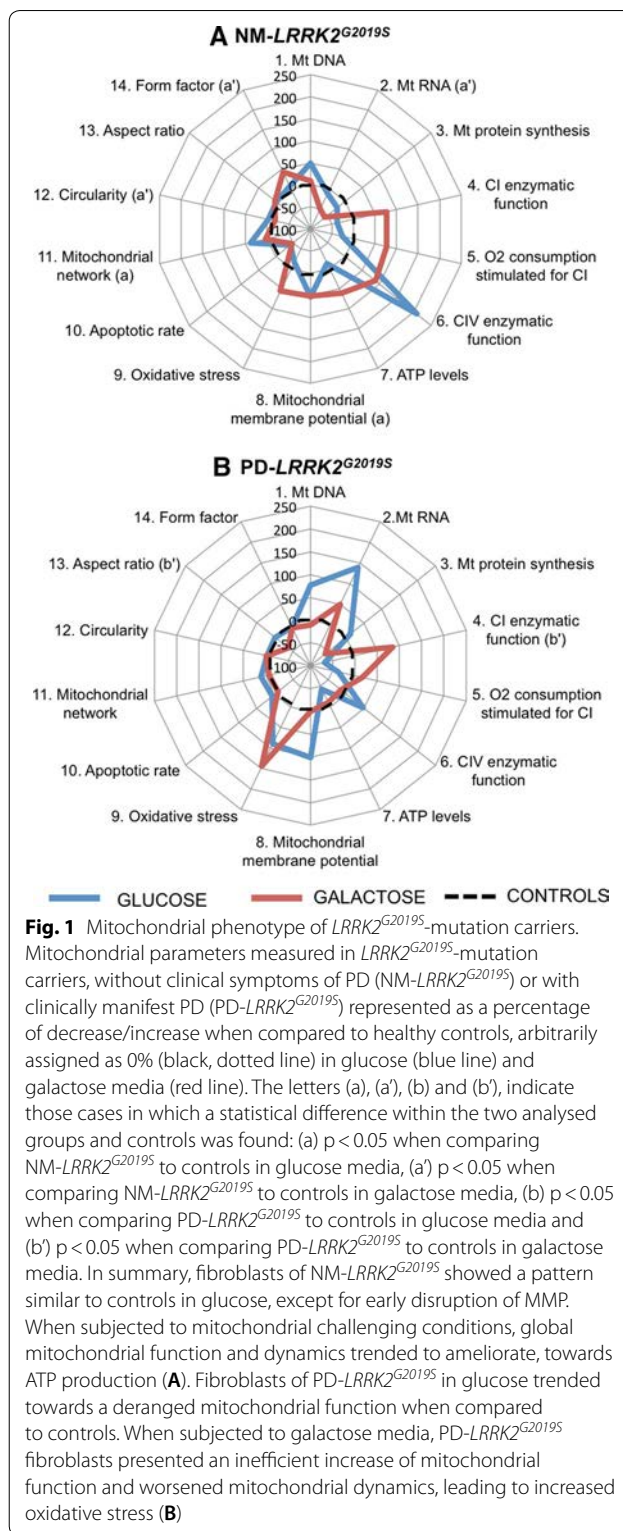
Mitochondrial parameters were preserved in NM-*LRRK2*^{G2019S} subjects in glucose media with respect to controls except for early MMP depolarization (54.14%, $p=0.04$, Figs. 1a.8 and 2f) and increased mitochondrial network (38.32%, $p=0.04$, Figs. 1a.11 and 3b).

After galactose exposure, CI enzymatic function, O₂ consumption stimulated for CI, CIV enzymatic function and ATP levels of NM-*LRRK2*^{G2019S} trended to overcome the level of controls (76.92, 76.87, 88.48 and 61.98%; $p=0.18$, $p=0.35$, $p=0.14$ and $p=0.76$, respectively), suggesting an adaptation to mitochondrial challenging conditions (Figs. 1a.4–7 and 2b–e). Mitochondrial dynamics ameliorated in fibroblasts of NM-*LRRK2*^{G2019S} with respect to controls when exposed to galactose medium, evidenced by 17.54% decreased circularity ($p=0.002$) and 42.53% increased form factor ($p=0.051$) (Fig. 1a.12, 14), accounting for longer, more branched mitochondria (Fig. 3c and e).

- b. PD-*LRRK2*^{G2019S} showed mitochondrial alterations in glucose media, which were worsened when subjected to mitochondrial-challenging conditions, resulting in increased oxidative stress.

In fibroblasts from PD-*LRRK2*^{G2019S} patients in glucose media, CI enzyme function, O₂ consumption stimulated for CI and ATP levels seemed to decrease with respect to controls (Figs. 1b.4, 5, 7 and 2b, c and e). Noticeably, although not significantly, depolarized mitochondria augmented to 101.34% ($p=0.14$), accompanied by a 90% increase of oxidative stress ($p=0.46$) with respect to controls (Figs. 1b.8, 9 and 2f, g).

Exposure of PD-*LRRK2*^{G2019S} fibroblasts to galactose media increased CI enzyme function compared to controls (84.62%, $p=0.04$), but such increase was neither translated into heightened oxygen consumption, nor enhanced CIV enzyme function or ATP synthesis (Figs. 1b.4, 7 and 2b–e), as formerly



observed in asymptomatic carriers. Instead, oxidative damage increased 144.64% ($p=0.13$) (Figs. 1b.9 and 2g) and, in detriment to mitochondrial dynam-

(See figure on next page.)

Fig. 2 Mitochondrial function. Results are represented by mean \pm SEM, comparing controls (n = 8; white bars), NM-*LRRK2*^{G2019S}-mutation, (n = 6; grey bars) and PD-*LRRK2*^{G2019S} (n = 7; black bars) in glucose and galactose media. **a** Citrate synthase levels remained constant between groups in both media. **b** A trend to decrease CI enzymatic activity in NM-*LRRK2*^{G2019S} and PD-*LRRK2*^{G2019S} was observed in glucose media, and PD-*LRRK2*^{G2019S} patients harbouring the mutation increased their activity with respect to controls in galactose media ($p = 0.04$). **c** Oxygen consumption trended to reproduce the pattern of CI enzymatic activity. After exposure to galactose media, a non-significant increment in O₂ consumption was observed in fibroblasts of NM-*LRRK2*^{G2019S} subjects with respect to controls ($p = 0.35$). **d** Complex IV enzymatic function remained similar in all groups, showing a trend to increase in NM-*LRRK2*^{G2019S} subjects with respect to controls in glucose and galactose media ($p = 0.14$ in both cases). **e** ATP levels tended to decrease in both groups in glucose media ($p = 0.18$ when comparing PD-*LRRK2*^{G2019S} with controls). **f** Number of depolarized mitochondria was increased in NM-*LRRK2*^{G2019S} when compared to controls in glucose media ($p = 0.04$), with the same trend observed for PD-*LRRK2*^{G2019S} although without reaching statistical significance ($p = 0.14$). **g** Oxidative damage trended to increase in PD-*LRRK2*^{G2019S} patients in both conditions when comparing them to controls. **h** Apoptotic rate tended to decrease in the NM-*LRRK2*^{G2019S} group in both media

ics, aspect ratio decreased 37.7% ($p = 0.053$) after exposure to mitochondrial challenging conditions (Figs. 1b, 13 and 3d).

media (−79 to 86%, $p = 0.042$ and −71.26%, $p = 0.22$ respectively) (Fig. 4d).

Autophagy

Figure 4 summarizes the autophagic characterization, and raw data of experimental parameters is provided in Additional file 4: Table S2.

- a. Autophagy initiation signalling increased in NM-*LRRK2*^{G2019S} subjects in glucose and galactose media, but autophagosome formation was only upregulated in glucose media.

A significant increase in autophagy substrate expression (SQSTM1/p62) in fibroblasts of NM-*LRRK2*^{G2019S} was observed when compared to controls in glucose media (118.4%, $p = 0.014$), and in galactose, after 4 h of bafilomycin exposure (114.44% increase, $p = 0.009$) (Fig. 4c). These increased signalling for autophagy initiation was accompanied by trends to increase autophagosome formation at 4 and 8 h of bafilomycin treatment (LC3BII/ β actin: +145.22% and +287.21%, respectively, $p = 0.051$) when compared to controls in glucose media, but not in galactose media, where autophagosome formation seemed to be decreased (Fig. 4d).

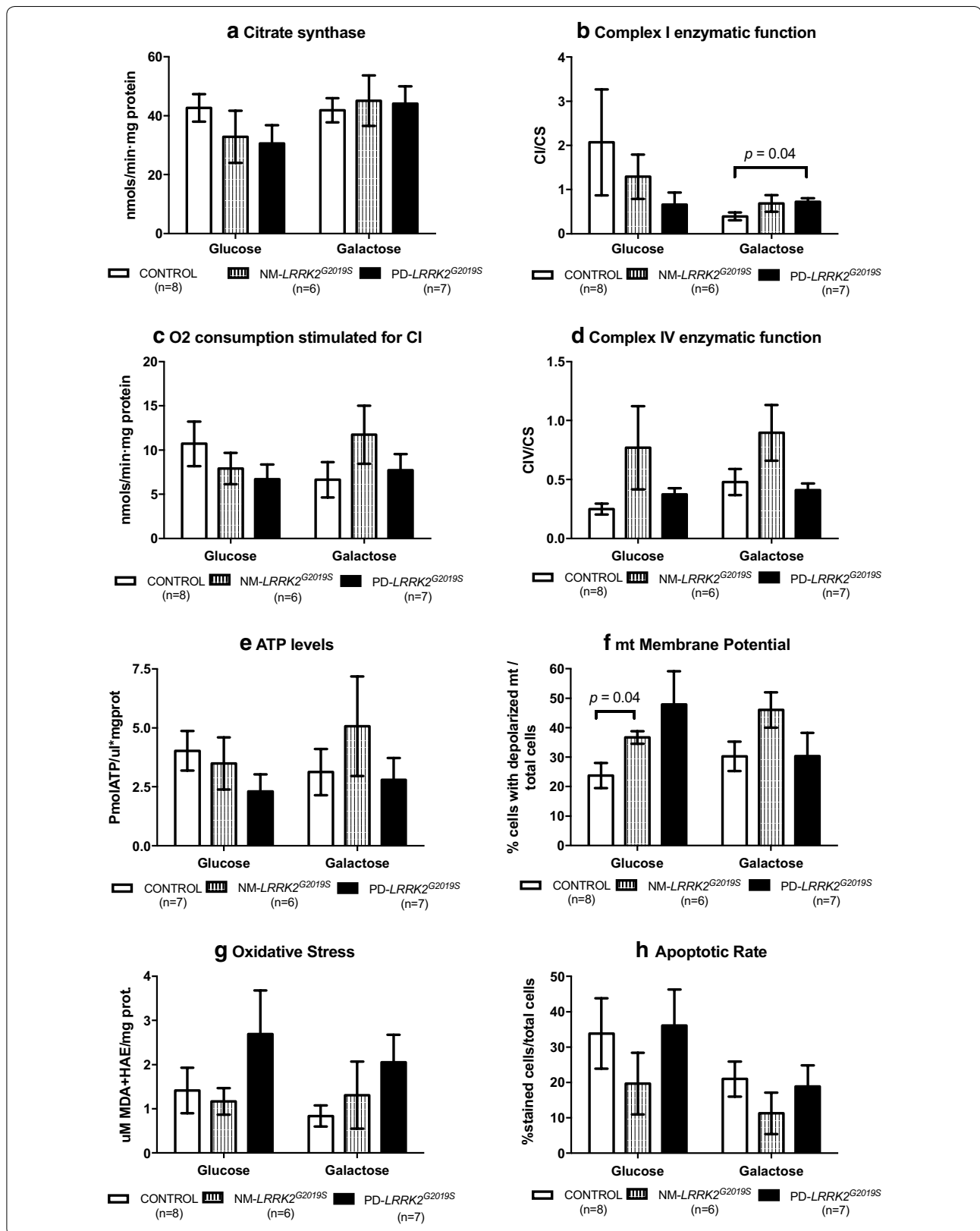
- b. Autophagosome formation was decreased in PD-*LRRK2*^{G2019S} despite increased autophagy initiation in both media.

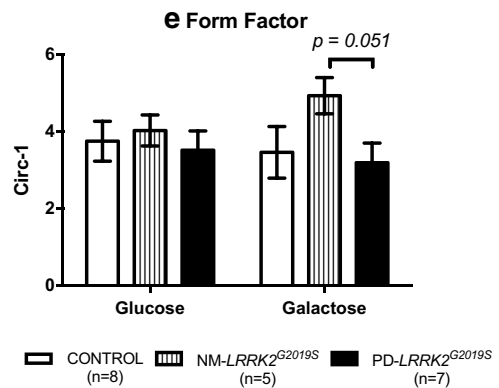
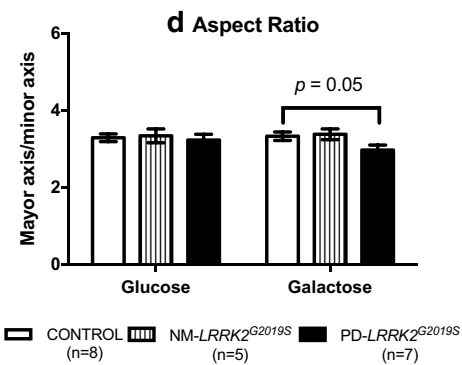
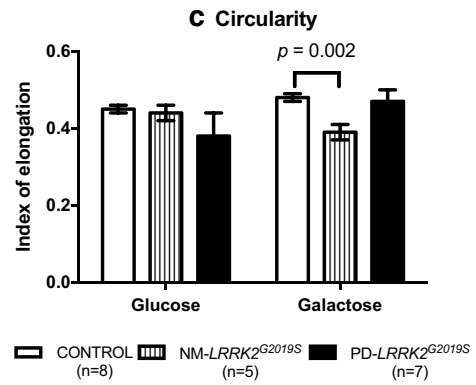
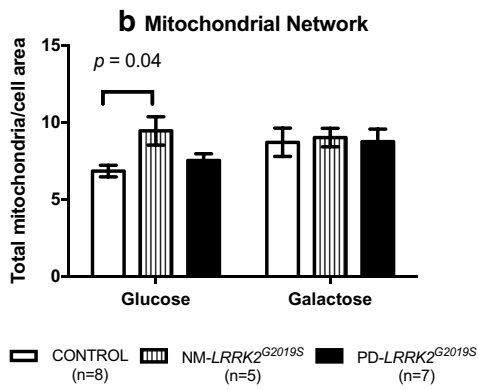
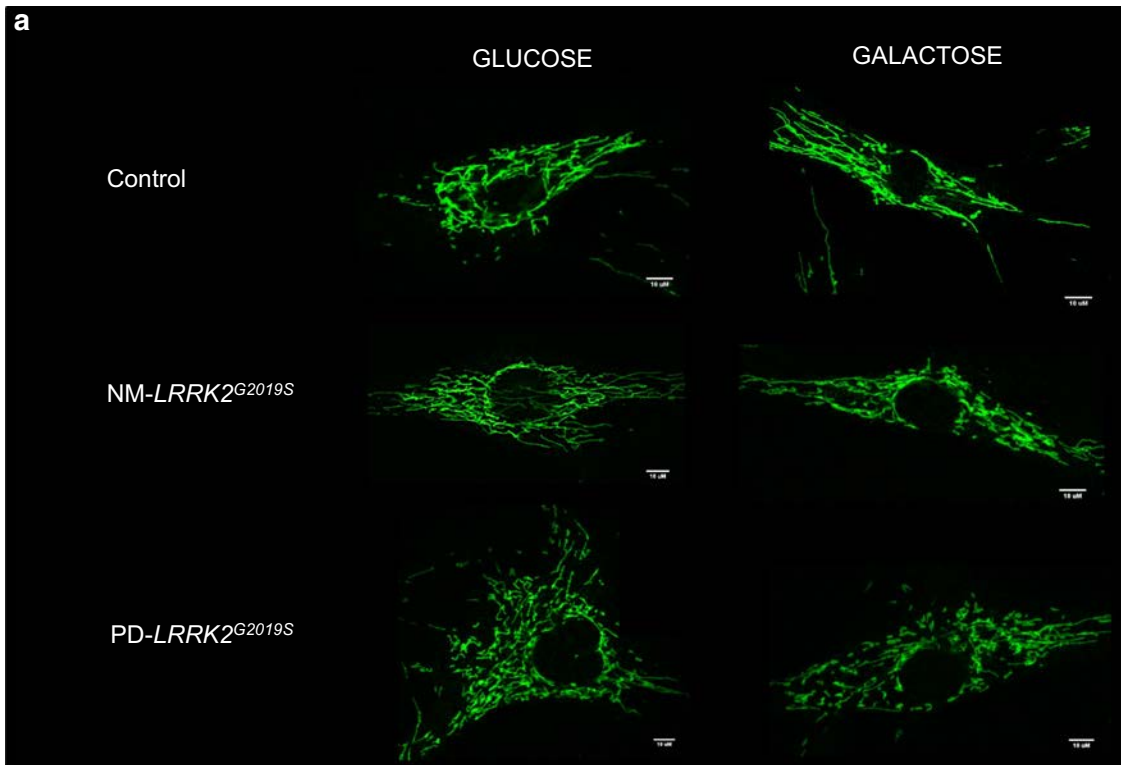
Autophagy substrate expression was increased in PD-*LRRK2*^{G2019S} after 8 h of bafilomycin treatment in glucose media (226.14%, $p = 0.04$) and at 4 h in galactose media when compared to controls (78.5%, $p = 0.02$) (Fig. 4c). However, these increased signalling for autophagy initiation was not accompanied by autophagosome formation in any media, and a significant decrease in LC3BII levels was demonstrated when compared to NM-*LRRK2*^{G2019S} subjects at 4 and 8 h of bafilomycin treatment in glucose

Discussion

The main contribution of this study was the exhaustive analysis of mitochondrial phenotype and autophagic print of fibroblasts from *LRRK2*^{G2019S} mutation carriers with and without clinical evidence of parkinsonism in glucose and galactose media. Briefly, this study suggests that the exhaustion of mitochondrial bioenergetic and autophagic reserve play a role in the onset of *LRRK2*^{G2019S}-associated PD.

Mainly, in standard conditions (glucose), the NM-*LRRK2*^{G2019S} fibroblasts showed a preserved mitochondrial phenotype, except for a significant disruption of MMP that may represent an early event in PD [14, 38–40]. In response to mitochondrial-challenging conditions (galactose), a pattern of mitochondrial enzymatic and respiratory function enhancement was observed, resulting in an increase of ATP production and morphological features characteristic of improved mitochondrial dynamics. In PD-*LRRK2*^{G2019S} fibroblasts, bias toward deranged mitochondrial phenotype were found in glucose media, such as decreased CI enzyme function, oxygen consumption and ATP production, and increased oxidative stress. Exposure to galactose revealed an inefficient increase in mitochondrial function, trends to increase oxidative stress and deranged mitochondrial dynamics. The most differential response between NM-*LRRK2*^{G2019S} subjects and PD-*LRRK2*^{G2019S} patients in mitochondrial functional and dynamic parameters was shown in response to mitochondrial-challenging conditions. In accordance to literature, mitochondrial defects were evidenced in galactose media [22], which leads us to hypothesize that, given their oxidative metabolism and postmitotic nature, neurons may be permanently damaged by mitochondrial and autophagic alterations that in peripheral tissues may be negligible [41, 42]. Ergo, a deficient mitochondrial functional reserve may underlie the





(See figure on previous page.)

Fig. 3 Mitochondrial dynamics. **a** Representative images of mitochondrial network obtained by confocal microscopy. NM-*LRRK2*^{G2019S}. Non-manifesting carriers of *LRRK2*^{G2019S}-mutation; PD-*LRRK2*^{G2019S}; patients with *LRRK2*^{G2019S}-mutation and clinically manifest PD. **b–e**. Results are represented by mean ± SEM, comparing controls (n = 8; white bars), NM-*LRRK2*^{G2019S} (n = 5, gray bars) and PD-*LRRK2*^{G2019S} (n = 7; black bars) in glucose and galactose media. Briefly, in fibroblasts of NM-*LRRK2*^{G2019S} a significant increase in mitochondrial network in standard conditions (glucose) was observed when compared to controls (**b**). When NM-*LRRK2*^{G2019S} fibroblasts were subjected to mitochondrial challenging conditions (galactose), an improvement of mitochondrial dynamics was seen, by decreased circularity (**c**) and trends to increase form factor (**e**), accounting for longer, more branched mitochondria. Fibroblasts of PD-*LRRK2*^{G2019S} showed a pattern similar to controls in standard (glucose) conditions and a handicapped response when exposed to mitochondrial challenging conditions (galactose) as shown by decreased aspect ratio (**d**), accounting for shorter mitochondria

onset of *LRRK2*^{G2019S}-associated PD. The link between mitochondrial health and autophagy initiation may be deduced from these findings, but needs to be assessed in more detail.

Recent reports have described differential mitochondrial functional phenotypes in idiopathic and some monogenic forms of PD [43–45]. Our study partially reproduces the mitochondrial phenotype described by Mortiboys et al. [17], where CI enzyme activity, oxygen consumption and ATP levels progressively decreased in NM-*LRRK2*^{G2019S} and PD-*LRRK2*^{G2019S}. Papkovskaia et al. [39] also found decreased ATP levels and depolarization in fibroblasts of PD-*LRRK2*^{G2019S}.

Oxidative stress is a hallmark of mitochondrial involvement on PD and neurodegeneration [11, 46]. Our results are in accordance with Grünewald et al. [40], who found increased levels of the antioxidant superoxide dismutase, but no significant alteration of oxidative stress in fibroblasts of NM-*LRRK2*^{G2019S}, suggesting the existence of compensatory mechanisms against early-stage production of ROS. Liou et al. [47], reported a protective effect against oxidative stress-mediated apoptosis mediated by wild type *LRRK2* which is lost in PD-associated mutations. In our study, trends towards reduced apoptosis in NM-*LRRK2*^{G2019S} in spite of increased oxidative stress was found, which suggests the existence of other protecting mechanisms that are yet to be described.

This study corroborated the impairment in mitochondrial dynamics in PD-*LRRK2*^{G2019S} patients described by

others [17, 31, 40, 48]. Additionally, a healthier pattern in mitochondrial dynamics in NM-*LRRK2*^{G2019S} subjects was demonstrated. Whether alterations in mitochondrial dynamics are the cause or consequence of mitochondrial dysfunction, and the mechanism by which *LRRK2* mediates such alterations, is still a matter of debate [3].

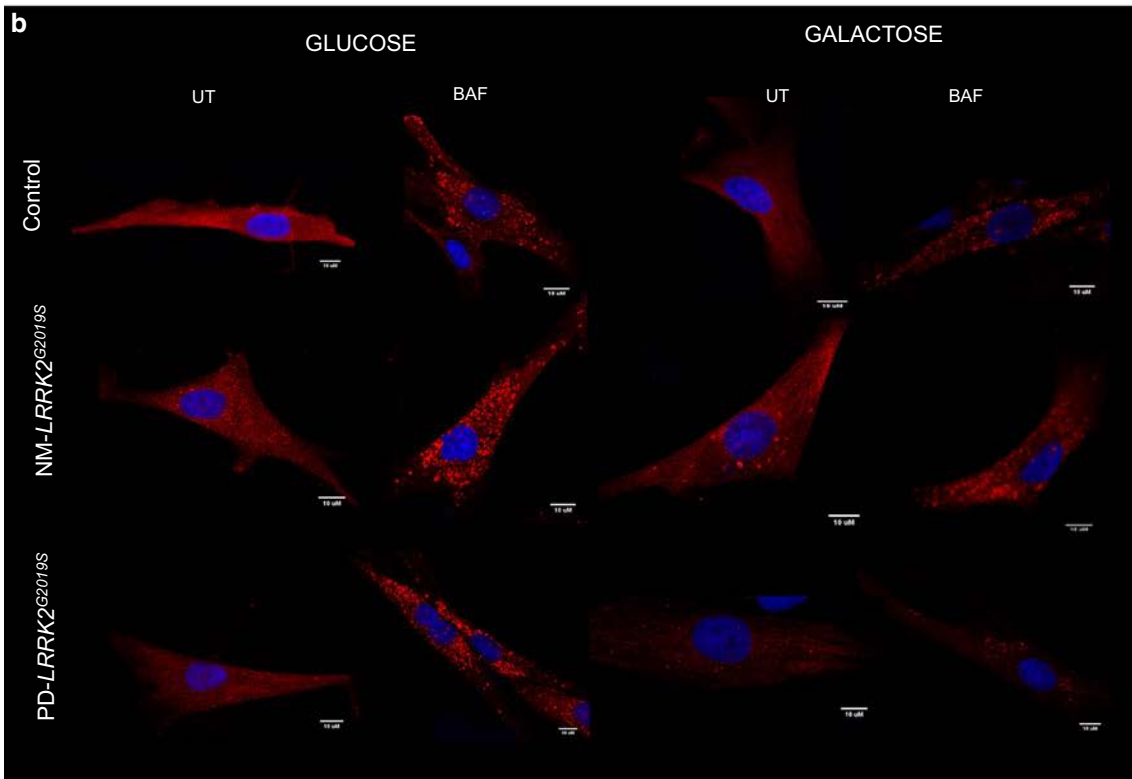
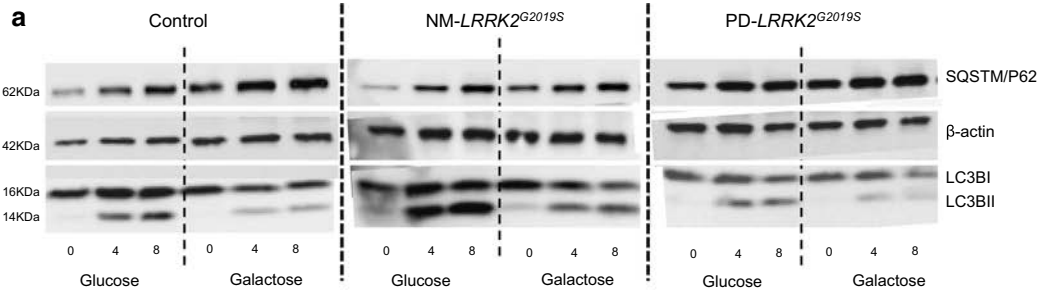
Trends towards upregulation in autophagy in NM-*LRRK2*^{G2019S} were observed, which may be explained by any of the previously described effects of *LRRK2*^{G2019S} mutation in autophagy [49–51] or by an increased attempt to eliminate damaged sub cellular compounds. A further increase in autophagy initiation signalling in PD-*LRRK2*^{G2019S} patients was found, probably in response to mitochondrial dysfunction and the resulting decrease in ATP levels evidenced by galactose exposure [13, 52].

However, the inability to continue with autophagosome formation and closure, and the resulting accumulation of damaged mitochondria among other waste product of cell metabolism, may explain the pathologic state in this group. Further studies should confirm the present findings, where mitophagy and autophagic flux may be characterized in more detail [53].

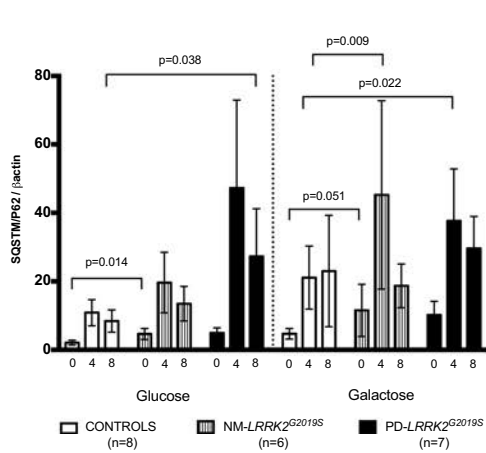
This is the first study reporting that the exposition of fibroblasts from NM-*LRRK2*^{G2019S} to mitochondrial challenging conditions tends to enhance mitochondrial performance, even above the values of controls. We hypothesize that such improvement represents a biological rescue mechanism characteristic of NM-*LRRK2*^{G2019S}, which may protect from the development of symptoms

(See figure on next page.)

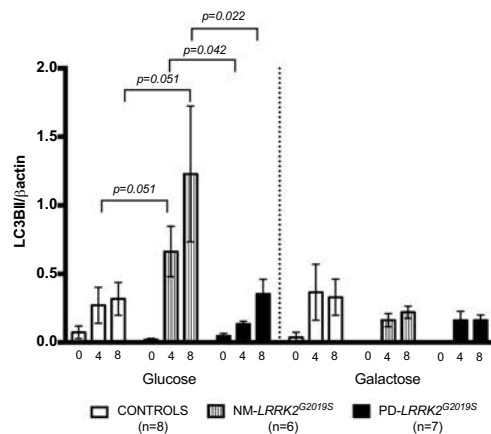
Fig. 4 Autophagy. **a** Representative images (original images have been cropped and are available at request) of autophagy markers measured by Western blot comparing: NM-*LRRK2*^{G2019S}. Non-manifesting carriers of *LRRK2*^{G2019S}-mutation; PD-*LRRK2*^{G2019S}; patients with *LRRK2*^{G2019S}-mutation and clinically manifest PD. (SQSTM1/p62)/β-actin: Autophagy substrate, LC3B-I/β-actin: autophagy receptor, basal form. LC3B-II/β-actin: autophagy receptor, lipidated form. **b** Representative images of autophagosome formation (UT) and accumulation after 8 h of treatment with 100 nM bafilomycin (BAF) obtained by confocal microscopy. **c, d** Results are represented by mean ± SEM, comparing controls (n = 8; white bars), NM-*LRRK2*^{G2019S}-mutation (n = 6, gray bars) and PD-*LRRK2*^{G2019S} (n = 7; black bars) in either glucose or galactose media and at basal state, and after 4 and 8 h treatment with bafilomycin (0, 4, 8). Autophagy initiation was upregulated in NM-*LRRK2*^{G2019S} subjects in glucose and galactose media when compared to controls (+ 118.4% SQSTM1/P62, p = 0.014 and + 114.44% SQSTM1/P62, p = 0.009, respectively) and trends to increase autophagy substrate were observed in PD-*LRRK2*^{G2019S} in both media (**c**). Autophagosome formation trended to increase at 4 and 8 h of bafilomycin treatment in NM-*LRRK2*^{G2019S} and was significantly decreased in PD-*LRRK2*^{G2019S} when compared to NM-*LRRK2*^{G2019S} subjects in glucose media at 4 and 8 h of bafilomycin treatment (− 79 to 86%, p = 0.042 and − 71.26%, p = 0.22 respectively) (**d**)



c Autophagy substrate



d Lipidated autophagy receptor



by compensating an increased bioenergetic cell demand or early mitochondrial damage. It may be deduced that mitochondrial and autophagic optimal function could have a protective role in mutation carriers who have not yet developed symptoms of PD. Mitochondria from NM-*LRRK2*^{G2019S} may retain the capacity to raise their activity until a maximal threshold beyond which PD clinical manifestations can appear.

On account of the above, our results suggest that *LRRK2*^{G2019S}-mutation by itself may not determine the development of clinical manifest PD [2, 52, 54], in accordance with other previous studies where NM-*LRRK2*^{G2019S} subjects perform as good as controls in motor [18], neuropsychological [55] and neuroimaging tests [56]. Scientific efforts focused on promoting mitochondrial optimal performance and autophagy regulation should be translated into prophylactic measures which modify the natural history of PD.

In regard to the experimental model used in this study, the exposure to oxidative metabolism through galactose media unveiled a differential mitochondrial phenotype that may reproduce that of neurons. Herein, we suggest that alternative models of PD should also be tested in oxidative conditions [41].

Some limitations in the present study must be acknowledged. Although the study of rare forms of PD due to inherited mutations reduces the potential study of bigger cohorts, the small sample size of this study may explain a common pitfall of the reported outcomes, which is the limited number of significant differences. Additionally, the inter-individual variability in environmental conditions potentially influencing molecular parameters may also hinder the homogeneity of the distinct groups. There is a positive correlation between age and PD onset in *LRRK2*^{G2019S} mutation carriers [2], suggesting that some NM-*LRRK2*^{G2019S} may eventually develop PD. However, it must be emphasized that no age related differences in mitochondrial and autophagic parameters were observed. Finally, many other molecular triggers may be taking place in PD, where the loss of dopaminergic neurons may be the common manifestation of a complex disease where mitochondrial alterations and autophagic deregulation are only one of manifold molecular events leading to neurodegeneration.

Conclusions

Enhanced mitochondrial performance of NM-*LRRK2*^{G2019S} in mitochondrial-challenging conditions and upregulation of autophagy suggests that an exhaustion of mitochondrial bioenergetic and autophagic reserve, may contribute to the development of PD in *LRRK2*^{G2019S} mutation carriers.

Additional files

Additional file 1: Materials and methods. This part of additional material is provided in a separate word document named "Additional material, materials and methods".

Additional file 2: Table S1. Clinical characteristics of PD-*LRRK2*^{G2019S} patients (n=7). The following legend accompanies the table: NM-*LRRK2*^{G2019S}: Non-manifesting carriers of *LRRK2*^{G2019S}-mutation; PD-*LRRK2*^{G2019S}: patients with *LRRK2*^{G2019S}-mutation and clinically manifest PD.

Additional file 3: Figure S1. Principal component analysis (PCA) for patients and controls in the different media. Variables factor map showing that individual variability in glucose media (**A**) was best expressed by mitochondrial dynamics parameters -circularity and mitochondrial network- for component 1 (horizontal axis), and autophagy parameters for component 2 (vertical axis). When subjected to mitochondrial challenging conditions (**B**), circularity expressed the greatest variability for component 1 (horizontal axis), and MMP better expressed component 2 variability (vertical axis). The longer vectors and those which are more aligned to the corresponding axis (depicted as dotted lines) are the ones with the greatest variability among individuals, which interestingly have been documented to be associated with PD, despite none of the parameters represent a greater variability between groups. MtDNA: mitochondrial-DNA; mtRNA: mitochondrial-RNA; VDAC: Mitochondrial content; COXII/βactin: Mitochondrial encoded protein content COXIV/βactin; Nuclear encoded protein content; CI: Complex I enzymatic function; PMox: oxygen consumption stimulated by pyruvate-malate; CIV: Complex IV enzymatic function; MMP: Mitochondrial membrane potential; OE: Oxidative stress; Circ: Circularity; P62: Autophagy substrate LC3BI: Autophagy receptor, basal form; LC3BII: Lipidated form of the autophagy receptor, LC3BII/LC3BI: autophagic turnover, LC3BII/P62: autophagic flux.

Additional file 4: Table S2. Raw data of mitochondrial phenotype and autophagic print parameters. The following legend accompanies the table: Glu: glucose; Gal: galactose; NM-*LRRK2*^{G2019S}: Non-manifesting carriers of *LRRK2*^{G2019S}-mutation; PD- *LRRK2*^{G2019S}: patients with *LRRK2*^{G2019S}-mutation and clinically manifest PD; mtDNA: Mitochondrial DNA; mtRNA: Mitochondrial RNA; CI: Complex I; O2 consumption stimulated for CI: Oxygen consumption stimulated for Complex I substrates (pyruvate, malate and glutamate); CIV: Complex IV. Pa. P value when comparing NM-*LRRK2*^{G2019S} vs. controls; Pb. P value when comparing PD- *LRRK2*^{G2019S} vs. controls; Pc. P value when comparing NM-*LRRK2*^{G2019S} vs. PD-*LRRK2*^{G2019S}.

Additional file 5: Figure S2. Genetics and mitochondrial protein synthesis. Results are represented by means ± SEM, comparing controls (white bars), non-manifesting carriers of *LRRK2*^{G2019S}-mutation, (NM-*LRRK2*^{G2019S}, grey bars) and patients with *LRRK2*^{G2019S}-mutation and clinically manifest PD (PD-*LRRK2*^{G2019S}, black bars) in glucose and galactose media. **A.** Mitochondrial DNA was conserved in both groups and media. **B.** Mitochondrial RNA levels were significantly decreased in NM-*LRRK2*^{G2019S} when compared to controls in galactose media **C-E.** Cell growth, mitochondrial content and protein synthesis did not show differences between groups, in either condition. **F.** Representative image of Western Blot of mitochondrial proteins in either glucose (Glu) or galactose (Gal) media of the three cohorts studied, the original Blott has been cropped for its better visualization, complete images can be provided at request.

Abbreviations

PD: Parkinson's disease; LRRK2: leucine rich repeat kinase 2; *LRRK2*^{G2019S}: *LRRK2*^{G2019S}-mutation; NM-*LRRK2*^{G2019S}: *LRRK2*^{G2019S}-carriers without PD symptoms; PD-*LRRK2*^{G2019S}: *LRRK2*^{G2019S}-carriers diagnosed with PD; ATP: adenosine triphosphate; MMP: mitochondrial membrane potential; mtDNA: mitochondrial DNA; mtRNA: mitochondrial RNA; VDAC: voltage-dependent anion channel; COXII: cytochrome oxidase subunit II; COXIV: cytochrome oxidase subunit IV; MRC: mitochondrial respiratory chain; CI: Complex I of the MRC; CIV: Complex IV of the MRC; CS: citrate synthase; PMox: oxygen consumption was assessed through pyruvate-malate oxidation; MDA: malondialdehyde; HAE: 4-hydroxyalkenal; ROS: reactive oxygen species; Circ: circularity; AR: aspect

ratio; FF: form factor; (SQSTM/p62)/ β -actin: autophagy substrate; LC3BII/ β -actin: autophagy receptor, lipidated form; SEM: standard error of the mean; PCA: principal component analysis.

Authors' contributions

GG obtained funds to support the study. GG and CM conceived the study and organized the project in collaboration with RF and ME. MJ and ET were responsible for the diagnosis and inclusion of all patients and collected clinical data. RF and ME obtained fibroblasts, participated in the first phase of cell culture and performed genetic testing and identification of mutations. All of the experimental, data collection and statistical analysis was closely supervised by GG and CM. DJ, with help from IG, MG and MB performed fibroblast culture, performed experimental procedures for mitochondrial function and dynamics phenotyping and analysis of this data. DJ, together with MC and JR performed the experimental analysis of the amounts of mtDNA and mtRNA and analysis of mitochondrial protein content by Western blotting. DJ and IG performed autophagy print blotting, with the assistance of JM. ET provided technical assistance for reactive preparation. DJ and IG created a database to collect all clinical and experimental parameters and performed the statistical analysis of the data, under the supervision of GG, CM and FC. FC-P performed PCA and interpreted these results. The first draft for this manuscript was written by DJ, and RF, FC, GG and CM profoundly reviewed and critiqued the manuscript, adding concepts of high relevance. All authors participated in the revision of the manuscript, in accordance with the ICMJE criteria. GG: Glòria Garrabou, CM: Constanza Morén, MJ: María Jose Marti, ET: Eduard Tolosa, RF: Rubén Fernández-Santiago, ME: Mario Ezquerra, DJ: Diana Luz Juárez-Flores, IG: Ingrid González-Casacuberta, MG: Mariona Guitart-Mampel, MB: Maria Bañó, MC: Marc Catalán-García, JR: Juan José Rivero, JM: Jose Milisenda, ET: Ester Tobias, FC: Francisc Cardellach, FC-P: Francisc Carmona Pontaque. All authors read and approved the final manuscript.

Author details

¹ Laboratory of Muscle Research and Mitochondrial Function-CELLEX, Institut d'Investigacions Biomèdiques August Pi i Sunyer (IDIBAPS), Department of Internal Medicine-Hospital Clínic de Barcelona, Faculty of Medicine and Health Sciences, University of Barcelona (UB), Barcelona, Spain. ² Centro de Investigación Biomédica en Red de Enfermedades Raras (CIBERER), Madrid, Spain. ³ Laboratory of Parkinson disease and other Neurodegenerative Movement Disorders: Clinical and Experimental Research, Department of Neurology, Hospital Clínic de Barcelona, Institut d'Investigacions Biomèdiques August Pi i Sunyer (IDIBAPS), University of Barcelona (UB), Barcelona, Spain. ⁴ CIBER de Enfermedades Neurodegenerativas (CIBERNED), Madrid, Spain. ⁵ Department of Genetics, Microbiology and Statistics, University of Barcelona, Barcelona, Spain.

Acknowledgements

The authors would like to thank Melissa Gabriela Altaparro for her counseling in English language writing. We also thank Anna Bosch, Elisenda Coll and Maria Calvo from the Advanced Optical Microscopy department of the University of Barcelona for their support with confocal microscopy.

Competing interests

The authors declare that they have no competing interests.

Availability of data and materials

The datasets used and/or analyzed during the current study are available from the corresponding author on reasonable request.

Consent for publication

Not applicable.

Ethics approval and consent to participate

The study was approved by the ethics committee of the Hospital Clínic de Barcelona (Spain) and by the Commission on Guarantees for Donation and Use of Human Tissues and Cells of the Instituto de Salud Carlos III (ISCIII). Every participant signed a written consent form, according to the Declaration of Helsinki.

Funding

This work was supported by Fondo de Investigación Sanitaria (FIS) ISCIII [PI11/00462], Fundació Privada Cellex [CP042187], CIBER de Enfermedades

Raras (an initiative of Instituto de Salud Carlos III [ISCIII] and FEDER), Suports a Grups de Recerca de la Generalitat de Catalunya 2014/2016 [SGR 893/2017] and CERCA Programme from the Generalitat de Catalunya and Consejo Nacional de Ciencia y Tecnología from México (CONACYT).

Publisher's Note

Springer Nature remains neutral with regard to jurisdictional claims in published maps and institutional affiliations.

Received: 8 February 2018 Accepted: 26 May 2018

Published online: 08 June 2018

References

- Corti O, Lesage S, Brice A. What genetics tells us about the causes and mechanisms of Parkinson's disease. *Physiol Rev*. 2011;91:1161–218.
- Healy DG, Falchi M, O'Sullivan SS, Bonifati V, Durr A, Bressman S, et al. Phenotype, genotype, and worldwide genetic penetrance of LRRK2-associated Parkinson's disease: a case-control study. *Lancet Neurol*. 2008;7:583–90.
- Wallings R, Manzoni C, Bandopadhyay R. Cellular processes associated with LRRK2 function and dysfunction. *FEBS J*. 2015;282:2806–26.
- Ozelius LJ, Senthil G, Saunders-Pullman R, Ohmann E, Deligtisch A, Tagliati M, et al. LRRK2 G2019S as a cause of Parkinson's disease in Ashkenazi Jews. *N Engl J*. 2006;354:424–5.
- Gaig C, Ezquerra M, Marti MJ, Muñoz E, Valldeoriola F, Tolosa E. LRRK2 mutations in Spanish patients with Parkinson disease. *Arch Neurol*. 2006;63:377.
- Dächsel JC, Behrouz B, Yue M, Beevers JE, Melrose HL, Farrer MJ. A comparative study of Lrrk2 function in primary neuronal cultures. *Parkinsonism Relat Disord*. 2010;16:650–5.
- Orenstein SJ, Kuo S-H, Tasset I, Arias E, Koga H, Fernandez-Carasa I, et al. Interplay of LRRK2 with chaperone-mediated autophagy. *Nat Neurosci*. 2013;16:394–406.
- Cookson MR. LRRK2 pathways leading to neurodegeneration. *Curr Neurol Neurosci Rep*. 2015;15:42.
- Migheli R, Del Giudice MG, Spissu Y, Sanna G, Xiong Y, Dawson TM, et al. LRRK2 affects vesicle trafficking, neurotransmitter extracellular level and membrane receptor localization. *PLoS ONE*. 2013;8:e77198.
- Esteves AR, Swerdlow RH, Cardoso SM. LRRK2, a puzzling protein: insights into Parkinson's disease pathogenesis. *Exp Neurol*. 2014;261:206–16.
- Haelterman NA, Yoon WH, Sandoval H, Jaiswal M, Shulman JM, Bellen HJ. A mitocentric view of Parkinson's disease. *Annu Rev Neurosci*. 2014;37:137–59.
- Nixon RA. The role of autophagy in neurodegenerative disease. *Nat Med*. 2013;19:983–97.
- Sánchez-Danés A, Richaud-Patin Y, Carballo-Carbajal I, Jiménez-Delgado S, Caig C, Mora S, et al. Disease-specific phenotypes in dopamine neurons from human iPS-based models of genetic and sporadic Parkinson's disease. *EMBO Mol Med*. 2012;4:380–95.
- Mortiboys H, Johansen KK, Aasly JO, Bandmann O. Mitochondrial impairment in patients with Parkinson disease with the G2019S mutation in LRRK2. *Neurology*. 2010;75:2017–20.
- Kordower JH, Olanow CW, Dodiya HB, Chu Y, Beach TG, Adler CH, et al. Disease duration and the integrity of the nigrostriatal system in Parkinson's disease. *Brain*. 2013;136:2419–31.
- Pont-Sunyer C, Tolosa E, Caspell-García C, Coffey C, Alcalay RN, Chan P, et al. The prodromal phase of leucine-rich repeat kinase 2-associated Parkinson disease: clinical and imaging studies. *Mov Disord*. 2017;32:726–38.
- Mortiboys H, Furnston R, Bronstad G, Aasly J, Elliott C, Bandmann O. UDCA exerts beneficial effect on mitochondrial dysfunction in LRRK2(G2019S) carriers and in vivo. *Neurology*. 2015;85:846–52.
- Marras C, Schuele B, Munhoz RP, Rogaeva E, Langston JW, Kasten M, et al. Phenotype in parkinsonian and nonparkinsonian LRRK2 G2019S mutation carriers. *Neurology*. 2011;77:325–33.
- Jiang P, Dickson DW. Parkinson's disease: experimental models and reality. *Acta Neuropathol*. 2017;135:13–32.

20. Alberio T, Lopiano L, Fasano M. Cellular models to investigate biochemical pathways in Parkinson's disease. *FEBS J*. 2012;279:1146–55.
21. Smith GA, Jansson J, Rocha EM, Osborn T, Hallett PJ, Isaacson O. Fibroblast biomarkers of sporadic Parkinson's disease and LRRK2 kinase inhibition. *Mol Neurobiol*. 2016;53(8):5161–77.
22. Aguer C, Gambarotta D, Mailloux RJ, Moffat C, Dent R, McPherson R, et al. Galactose enhances oxidative metabolism and reveals mitochondrial dysfunction in human primary muscle cells. *PLoS ONE*. 2011;6:e28536.
23. Hughes AJ, Ben-Shlomo Y, Daniel SE, Lees AJ. What features improve the accuracy of clinical diagnosis in Parkinson's disease: a clinicopathologic study. *Neurology*. 1992;42:1142–6.
24. Morén C, Juárez-Flores D, Cardellach F, Garrabou G. The role of therapeutic drugs on acquired mitochondrial toxicity. *Curr Drug Metab*. 2016;17:1–1.
25. Morén C, Noguera-Julían A, Garrabou G. Mitochondrial disturbances in HIV pregnancies. *Aids*. 2015;29:5–12.
26. Garrabou G, Morén C, Gallego-Escuredo JM, Milinkovic A, Villarroya F, Negro E, et al. Genetic and functional mitochondrial assessment of HIV-infected patients developing HAART-related hyperlactatemia. *JAIDS J Acquir Immune Defic Syndr*. 2009;52:443–51.
27. Pesta D, Gnaiger E. High-resolution respirometry: OXPHOS protocols for human cells and permeabilized fibers from small biopsies of human muscle. *Methods Mol Biol*. 2012;810:25–58.
28. Morén C, Garrabou G, Noguera-Julían A, Rovira N, Catalán M, Hernández S, et al. Study of oxidative, enzymatic mitochondrial respiratory chain function and apoptosis in perinatally HIV-infected pediatric patients. *Drug Chem Toxicol*. 2013;36:496–500.
29. Catalán-García M, Garrabou G, Morén C, Guitart-Mampel M, Hernando A, Díaz-Ramos A, et al. Mitochondrial DNA disturbances and deregulated expression of oxidative phosphorylation and mitochondrial fusion proteins in sporadic inclusion body myositis. *Clin Sci*. 2016;130:1741–51.
30. Lugli E, Troiano L, Ferraresi R, Roat E, Prada N, Nasi M, et al. Characterization of cells with different mitochondrial membrane potential during apoptosis. *Cytom Part A*. 2005;68A:28–35.
31. Su Y-C, Qi X. Inhibition of excessive mitochondrial fission reduced aberrant autophagy and neuronal damage caused by LRRK2 G2019S mutation. *Hum Mol Genet*. 2013;22:4545–61.
32. Alvarez-Mora MI, Rodriguez-Revenga L, Madrigal I, Guitart-Mampel M, Garrabou G, Milà M. Impaired mitochondrial function and dynamics in the pathogenesis of FXTAS. *Mol Neurobiol*. 2017;54:6896–902.
33. Schindelin J, Arganda-Carreras I, Frise E, Kaynig V, Longair M, Pietzsch T, et al. Fiji: an open-source platform for biological-image analysis. *Nat Methods*. 2012;9:676–82.
34. Dagda RK, Chu CT. Mitochondrial quality control: insights on how Parkinson's disease related genes PINK1, parkin, and Omi/HtrA2 interact to maintain mitochondrial homeostasis. *J Bioenerg Biomembr*. 2010;41:473–9.
35. Rubinsztein DC, Cuervo AM, Ravikumar B, Sarkar S, Korolchuk V, Kaushik S, et al. In search of an "autophagometer". *Autophagy*. 2009;5:585–9.
36. Klionsky DJ, Abdelmohsen K, Abe A, Abedin MJ, Abeliovich H, Arozana AA, et al. Guidelines for the use and interpretation of assays for monitoring autophagy (3rd edition). *Autophagy*. 2016;12:1.
37. R Core Team. R: a language and environment for computing. Vienna: R Foundation for Statistical Computing; 2017.
38. Esteves AR, G-Fernandes M, Santos D, Januário C, Cardoso SM. The upshot of LRRK2 inhibition to Parkinson's disease paradigm. *Mol Neurobiol*. 2015;52:1804–20.
39. Papkovskaja TD, Chau K-Y, Inesta-Vaquera F, Papkovsky DB, Healy DG, Nishio K, et al. G2019S leucine-rich repeat kinase 2 causes uncoupling protein-mediated mitochondrial depolarization. *Hum Mol Genet*. 2012;21:4201–13.
40. Grünwald A, Arns B, Meier B, Brockmann K, Tadic V, Klein C. Does uncoupling protein 2 expression qualify as marker of disease status in LRRK2-associated Parkinson's disease? *Antioxid Redox Signal*. 2014;20:1955–60.
41. Hall CN, Klein-Flügge MC, Howarth C, Attwell D. Oxidative phosphorylation, not glycolysis, powers presynaptic and postsynaptic mechanisms underlying brain information processing. *J Neurosci*. 2012;32:8940–51.
42. Cha M-Y, Kim DK, Mook-Jung I. The role of mitochondrial DNA mutation on neurodegenerative diseases. *Exp Mol Med*. 2015;47:e150.
43. Lopez-Fabuel I, Martin-Martin L, Resch-Beusher M, Azkona G, Sanchez-Pernaute R, Bolaños JP. Mitochondrial respiratory chain disorganization in Parkinson's disease-relevant PINK1 and DJ1 mutants. *Neurochem Int*. 2017;109:101–5.
44. Ryan BJ, Hoek S, Fon EA, Wade-Martins R. Mitochondrial dysfunction and mitophagy in Parkinson's: from familial to sporadic disease. *Trends Biochem Sci*. 2015;40:200–10.
45. Mortiboys H, Thomas KJ, Koopman WJH, Klaffke S, Abou-Sleiman P, Olpin S, et al. Mitochondrial function and morphology are impaired in parkin-mutant fibroblasts. *Ann Neurol*. 2008;64:555–65.
46. Keeney PM, Xie J, Capaldi RA, Bennett JP. Parkinson's disease brain mitochondrial complex I has oxidatively damaged subunits and is functionally impaired and misassembled. *J Neurosci*. 2006;26:5256–64.
47. Liou AKF, Leak RK, Li L, Zigmund MJ. Wild-type LRRK2 but not its mutant attenuates stress-induced cell death via ERK pathway. *Neurobiol Dis*. 2008;32:116–24.
48. Su B, Wang X, Zheng L, Perry G, Smith MA, Zhu X. Abnormal mitochondrial dynamics and neurodegenerative diseases. *Biochim Biophys Acta*. 2010;1802:135–42.
49. Manzoni C. The LRRK2-macroautophagy axis and its relevance to Parkinson's disease. *Biochem Soc Trans*. 2017;45:155–62.
50. Bravo-San Pedro JM, Niso-Santano M, Gómez-Sánchez R, Pizarro-Estrella E, Aiausti-Pujana A, Gorostidi A, et al. The LRRK2 G2019S mutant exacerbates basal autophagy through activation of the MEK/ERK pathway. *Cell Mol Life Sci*. 2013;70:121–36.
51. Bang Y, Kim K-S, Seol W, Choi HJ. LRRK2 interferes with aggresome formation for autophagic clearance. *Mol Cell Neurosci*. 2016;75:71–80.
52. Manzoni C, Mamais A, Dihanich S, McGoldrick P, Devine MJ, Zerle J, et al. Pathogenic Parkinson's disease mutations across the functional domains of LRRK2 alter the autophagic/lysosomal response to starvation. *Biochem Biophys Res Commun*. 2013;441:862–6.
53. Loos B, du Toit A, Hofmeyr J-HS. Defining and measuring autophagosome flux—concept and reality. *Autophagy*. 2014;10:2087–96.
54. Infante J, Prieto C, Sierra M, Sánchez-Juan P, González-Aramburu I, Sánchez-Quintana C, et al. Comparative blood transcriptome analysis in idiopathic and LRRK2 G2019S-associated Parkinson's disease. *Neurobiol Aging*. 2016;38:214.e1–5.
55. Lohmann E, Leclere L, De Anna F, Lesage S, Dubois B, Agid Y, et al. A clinical, neuropsychological and olfactory evaluation of a large family with LRRK2 mutations. *Parkinsonism Relat Disord*. 2009;15:273–6.
56. Brockmann K, Gröger A, Di Santo A, Liepel I, Schulte C, Klose U, et al. Clinical and brain imaging characteristics in leucine-rich repeat kinase 2-associated PD and asymptomatic mutation carriers. *Mov Disord*. 2011;26:2335–42.

Ready to submit your research? Choose BMC and benefit from:

- fast, convenient online submission
- thorough peer review by experienced researchers in your field
- rapid publication on acceptance
- support for research data, including large and complex data types
- gold Open Access which fosters wider collaboration and increased citations
- maximum visibility for your research: over 100M website views per year

At BMC, research is always in progress.

Learn more biomedcentral.com/submissions



Mitochondrial and autophagic alterations in skin fibroblasts from Parkinson disease patients with Parkin mutations

Ingrid González-Casacuberta^{1,2}, Diana-Luz Juárez-Flores^{1,2}, Mario Ezquerra^{3,4}, Raquel Fucho^{5,6}, Marc Catalán-García^{1,2}, Mariona Guitart-Mampel^{1,2}, Ester Tobías^{1,2}, Carmen García-Ruiz^{5,6,7}, José Carlos Fernández-Checa^{5,6,7}, Eduard Tolosa^{3,4}, María-José Martí^{3,4}, Josep Maria Grau^{1,2}, Rubén Fernández-Santiago^{3,4}, Francesc Cardellach^{1,2}, Constanza Morén^{1,2}, Glòria Garrabou^{1,2}

¹Laboratory of Muscle Research and Mitochondrial Function, Institut d'Investigacions Biomèdiques August Pi i Sunyer (IDIBAPS), University of Barcelona (UB), Department of Internal Medicine-Hospital Clínic of Barcelona (HCB), 08036 Barcelona, Spain

²Centro de Investigación Biomédica en Red (CIBER) de Enfermedades Raras (CIBERER), 28029 Madrid, Spain

³Laboratory of Neurodegenerative Disorders, IDIBAPS, UB, Department of Neurology-HCB, 08036 Barcelona, Spain

⁴CIBER de Enfermedades Neurodegenerativas (CIBERNED), 28031 Madrid, Spain

⁵Cell Death and Proliferation, IDIBAPS, Consejo Superior Investigaciones Científicas (CSIC), Barcelona, Spain

⁶Liver Unit-HCB, IDIBAPS and CIBER de Enfermedades Hepáticas y Digestivas (CIBEREHD), Barcelona, Spain

⁷USC Research Center for ALPD, Keck School of Medicine, Los Angeles, CA 90033, USA

Correspondence to: Constanza Morén, Glòria Garrabou; **email:** CMOREN1@clinic.cat, GARRABOU@clinic.cat

Keywords: Parkinson's disease, Parkin mutation, mitochondrial function, autophagy, fibroblasts

Received: April 1, 2019

Accepted: June 1, 2019

Published: June 9, 2019

Copyright: González-Casacuberta et al. This is an open-access article distributed under the terms of the Creative Commons Attribution License (CC BY 3.0), which permits unrestricted use, distribution, and reproduction in any medium, provided the original author and source are credited.

ABSTRACT

PRKN encodes an E3-ubiquitin-ligase involved in multiple cell processes including mitochondrial homeostasis and autophagy. Previous studies reported alterations of mitochondrial function in fibroblasts from patients with PRKN mutation-associated Parkinson's disease (PRKN-PD) but have been only conducted in glycolytic conditions, potentially masking mitochondrial alterations. Additionally, autophagy flux studies in this cell model are missing.

We analyzed mitochondrial function and autophagy in PRKN-PD skin-fibroblasts (n=7) and controls (n=13) in standard (glucose) and mitochondrial-challenging (galactose) conditions.

In glucose, PRKN-PD fibroblasts showed preserved mitochondrial bioenergetics with trends to abnormally enhanced mitochondrial respiration that, accompanied by decreased CI, may account for the increased oxidative stress. In galactose, PRKN-PD fibroblasts exhibited decreased basal/maximal respiration vs. controls and reduced mitochondrial CIV and oxidative stress compared to glucose, suggesting an inefficient mitochondrial oxidative capacity to meet an extra metabolic requirement. PRKN-PD fibroblasts presented decreased autophagic flux with reduction of autophagy substrate and autophagosome synthesis in both conditions.

The alterations exhibited under neuron-like oxidative environment (galactose), may be relevant to the disease pathogenesis potentially explaining the increased susceptibility of dopaminergic neurons to undergo degeneration. Abnormal PRKN-PD phenotype supports the usefulness of fibroblasts to model disease and the view of PD as a systemic disease where molecular alterations are present in peripheral tissues.

INTRODUCTION

Parkinson's disease (PD) has become increasingly prevalent as the population ages, being the second most prevalent neurodegenerative disorder worldwide [1]. Homozygous and compound heterozygous mutations in the Parkin gene (*PRKN*) are the most common cause of recessively inherited early-onset PD, accounting for up to 50% of familial PD and about 15% of sporadic PD (sPD) with disease onset before 45 years [2]. Parkin-associated PD (PRKN-PD) is clinically similar to sPD besides some specific clinical features and the significant earlier age of onset, which can occur from childhood to the fourth or fifth decade of life [3]. The neuropathological hallmark of PRKN-PD is as in sPD, the prominent death of dopaminergic neurons (DAN) in the *substantia nigra pars compacta* (SNpc). In contrast, the presence of Lewy bodies in PRKN-PD is infrequent [3-5]. The etiopathogenesis of PD has been associated to several molecular events including mitochondrial dysfunction and autophagy impairment [6, 7], which may compromise neuronal survival.

The Parkin protein (PRKN) is a multifunctional E3 ubiquitin ligase that exerts crucial neuroprotective functions in DAN [8, 9]. A key role of PRKN in mitochondrial macroautophagy (mitophagy) has been reported in different models of the disease [10-14]. Specifically, upon mitochondrial depolarization there is a reduced turnover of the PTEN induced putative kinase 1 protein (PINK1) and thus, it accumulates in the outer mitochondrial membrane leading to the recruitment and phosphorylation of PRKN. Subsequently, PRKN mediates the polyubiquitination of many outer mitochondrial membrane proteins. Briefly, the polyubiquitination is the signal for the recruitment of adaptor proteins such as p62, which allows the binding of the microtubule-associated protein 1 light chain 3 (LC3BII) in the forming autophagosome to initiate mitochondrion sequestration and the following clearance upon fusion with the lysosome [7, 15]. Recent evidence suggests that PRKN is also involved in the aggresome-macroautophagy pathway in which it promotes the sequestration of misfolded proteins into aggresomes and its consequent clearance by autophagy through p62 and LC3BII recruitment [16, 17]. In summary, growing evidences point out PRKN as a crucial player in the different pathways that constitute macroautophagy (hereafter called autophagy).

In this scenario, a number of studies have postulated that PRKN-PD may derive from the impaired clearance of bioenergetically compromised mitochondria [8, 18] and the consequent accumulation of dysfunctional mitochondria that trigger an overproduction of intra-

cellular reactive oxygen species (ROS) that eventually may harm cell components. Concurrently, other PRKN protein substrates may accumulate [8, 19] within the cells, eventually compromising their viability [6, 20]. Yet, the precise mechanisms by which *PRKN* loss-of-function mutations lead to neurodegeneration remain elusive.

A major challenge to study PD is the inaccessible nature of the specific neural cell types targeted by the disease which are only available only *post-mortem*. In this context, the development of validated models to study PD is crucial to enable the understanding of the molecular pathways underlying the disease pathogenesis. On the other hand, there is increasing evidence that PD pathology is not confined only in the central nervous system (CNS) but is also present in the peripheral autonomous nervous system and the organs that the latter innervates, including the skin [21]. Skin-derived fibroblasts are accessible peripheral cells that constitute a patient-specific cellular system that retain the genetic background of the patients and potentially preserve the environmental and cumulative age-related events in addition to show relevant expression of most PARK genes [22, 23]. Moreover, they can potentially recapitulate some pathophysiological features of the disease²². In fact, many of the molecular hallmarks occurring in PD-DAN have been reported in fibroblasts from patients with sporadic and monogenic forms of the disease [24-27]. Notwithstanding, previous studies on mitochondrial function in PRKN-PD fibroblasts have been only conducted in glycolytic conditions in which fibroblasts generate most of cell ATP via anaerobic glycolysis, thus potentially masking mitochondrial alterations present in these cells [28]. In case of PRKN-PD fibroblasts phenotyping, these studies have reported controversial outcomes without assessing, in parallel, the cellular impact of *PRKN* mutations on autophagic flux [29-34]. Therefore, growing PRKN-PD fibroblasts in a glucose-free medium such as galactose, which has been previously used for the diagnosis of primary mitochondrial diseases [35, 36], may provide a closer approach to the more oxidative metabolism and the potential associated mitochondrial function alterations present in the DAN of PRKN-PD patients.

In the present study, we aimed to characterize mitochondrial function and autophagy in skin-derived fibroblasts from PRKN-PD patients in parallel in glycolytic (glucose) and mitochondrial-challenging conditions (galactose). The identification of alterations in PRKN-PD fibroblasts under mitochondrial-challenging conditions may provide insight into disease pathogenesis, as the specific neural cell types targeted by the disease are predominantly oxidative.

RESULTS

Mitochondrial respiration

In order to assess the bioenergetic status of fibroblasts, we first performed high-resolution mitochondrial respiration analyses. The overall respiratory control ratios shown in Figure 1 B-F, are obtained from the respiration parameters illustrated in the mitochondrial respiratory flux profile (Figure 1A). In glucose, no significant differences in the respiratory control ratios were found between PRKN-PD and control fibroblasts. Even so, trends to increased basal, ATP-linked and maximal (uncoupled) respirations and a concomitant downward trend in the spare respiratory capacity were observed in PRKN-PD fibroblasts compared to controls.

In galactose, PRKN-PD fibroblasts exhibited a significant decrease in basal/maximal respiratory ratio compared to the control fibroblasts. Although the rest of parameters were preserved, a downward trend in the basal respiration and ATP-linked oxygen consumption was shown. Upon changing from glycolytic to mitochondrial-challenging conditions, control but not PRKN-PD fibroblasts, significantly increased ATP-linked oxygen consumption and the basal/maximal respiratory ratio. In addition, both groups significantly decreased the spare respiratory capacity upon changing cells from glucose to galactose medium (Figure 1 A-E).

To understand the role of mitochondrial complex I (CI) in the overall oxygen consumption, which is reported to be affected in PD, we measured oxygen consumption

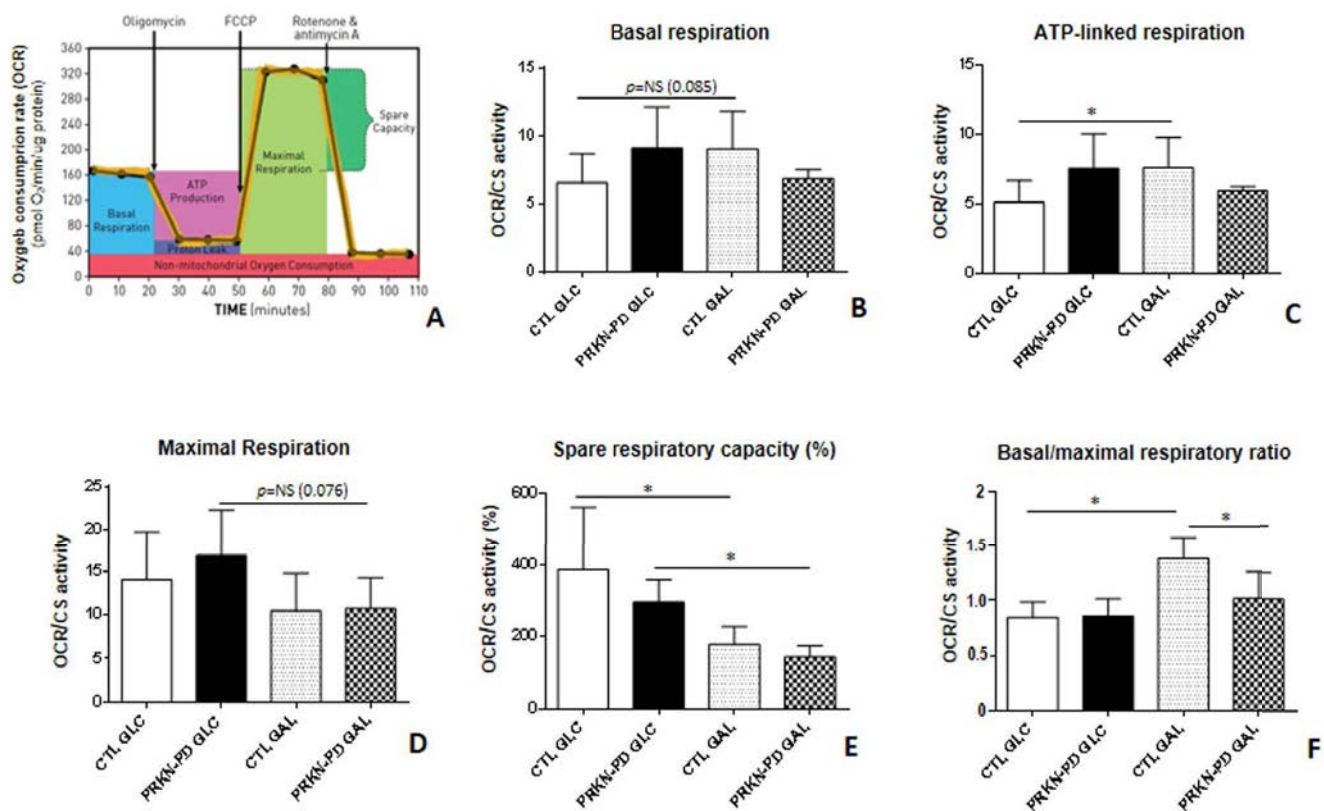


Figure 1. Mitochondrial respiratory control ratios in control and PRKN-PD fibroblasts. Illustrative mitochondrial respiration flux profile indicating respiratory control parameters (image obtained from Agilent Seahorse XF) (A), basal respiration (B), ATP-linked respiration (C), maximal respiration (D), spare respiratory capacity (E) and basal/maximal respiratory ratio (F). In glucose, no significant differences were found between PRKN-PD and control fibroblasts in the respiratory control ratios although trends to increased basal and maximal as well as ATP-linked respirations and decreased spare respiratory capacity were observed. In galactose, PRKN-PD fibroblasts exhibited a significant decrease in basal/maximal respiratory ratio compared to the control fibroblasts as well as a downward trend in the basal respiration and ATP-linked respiration. Controls but not PRKN-PD significantly increased oxygen consumption linked to ATP production and the basal/maximal respiratory ratio in galactose compared to glucose. Both, control and PRKN-PD fibroblasts significantly decreased the spare respiratory capacity upon medium change. Each cell line was seeded in triplicate per condition (n=3 for GLC and n=3 for GAL). The results were expressed as means and standard error of the mean (SEM). * = p<0.05. CTL= Control fibroblasts. GAL= 10 mM galactose medium. GLC= 25 mM glucose medium. NS= not significant. OCR= Oxygen consumption rate. PRKN-PD= Parkin-associated PD fibroblasts. Respiratory control ratios were normalized by total protein content and by citrate synthase activity as a marker of mitochondrial content.

through the specific oxidation of CI-substrates, pyruvate and malate (PMox). Although we did not obtain statistically significant differences, PRKN-PD showed a strong non-significant downward trend in CI-stimulated oxygen consumption compared to control fibroblasts in glucose. Exposure to galactose trended to reduce CI-stimulated oxygen consumption in control, but not in PRKN-PD fibroblasts, when compared to glucose (Figure 2).

Mitochondrial respiratory chain enzymatic activities

We next wanted to determine if the differences observed in mitochondrial respiration analysis between PRKN-PD and control fibroblasts were reflected in the enzymatic activities of the Mitochondrial respiratory chain (MRC) complexes. Although no significant differences were obtained between groups, the same pattern exhibited in CI-stimulated oxygen consumption was

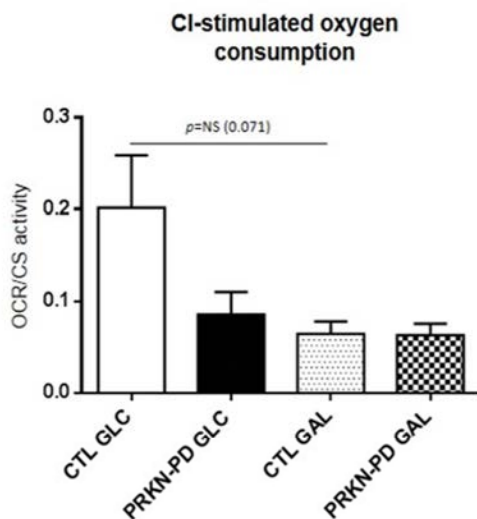


Figure 2. Complex I-stimulated oxygen consumption through pyruvate and malate oxidation measurement in control and PRKN-PD fibroblasts. No statistically significant differences were obtained between groups. In glucose, down-ward trends in CI-stimulated oxygen was shown in PRKN-PD compared to control fibroblasts. Exposure to galactose trended to reduce CI-stimulated oxygen consumption in control fibroblasts when compared to glucose, but not in PRKN-PD cells. The results are expressed as means and standard error of the mean (SEM). CTL= Control fibroblasts. GAL= 10 mM galactose medium. GLC= 25 mM glucose medium. NS= not significant. PRKN-PD= Parkin-associated PD fibroblasts. Oxygen consumption values were normalized by citrate synthase activity as a marker of mitochondrial content.

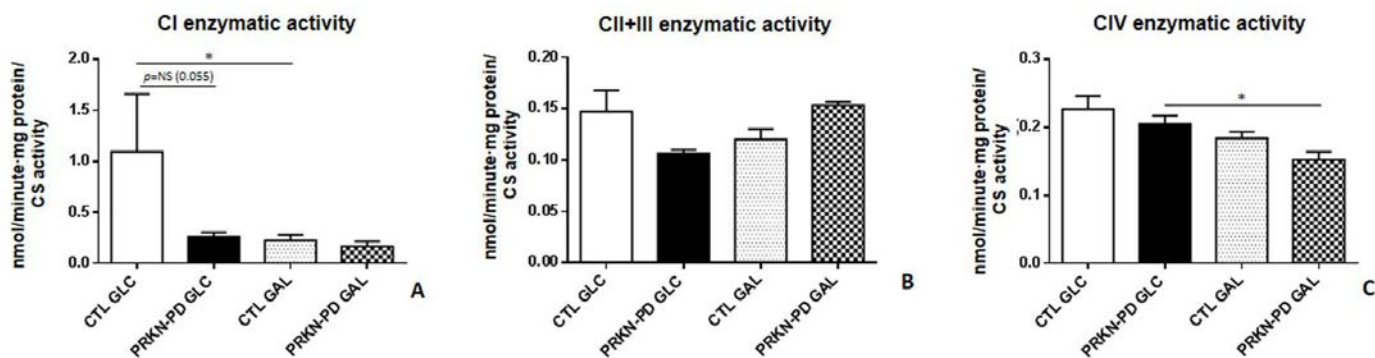


Figure 3. Mitochondrial respiratory chain (MRC) enzymatic activities in control and PRKN-PD fibroblasts. Enzymatic activities of the complexes I (A), II+III (B) and CIV (C) of the MRC. No significant differences were obtained between groups. Exposure to galactose significantly reduced CI-enzymatic activity of control fibroblasts and significantly decreased CIV enzymatic activity of PRKN-PD fibroblasts when compared to glucose. The results were expressed as means and standard error of the mean (SEM). *= $p < 0.05$. CTL= Control fibroblasts. GAL= 10 mM galactose medium. GLC= 25 mM glucose medium. NS= not significant. PRKN-PD= Parkin-associated PD fibroblasts. Enzymatic activity values were normalized by citrate synthase activity as a marker of mitochondrial content.

reflected in CI enzymatic activity, where PRKN-PD showed a strong downward trend compared to control fibroblasts in glucose. Exposure to galactose significantly reduced CI-enzymatic activity of controls, but not PRKN-PD fibroblasts, when compared to glucose, in accordance to CI-stimulated oxygen consumption results. In addition, exposure to galactose significantly decreased CIV enzymatic activity in PRKN-PD fibroblasts when compared to glucose (Figure 3 A-C).

Oxidative stress

Lipid peroxidation was measured as an indicator of ROS-derived oxidative damage. As illustrated in Figure 4, PRKN-PD exhibited an upward trend in lipid peroxidation compared to control fibroblasts in glucose, while exposure to galactose significantly reduced oxidative stress levels in PRKN-PD compared to glucose.

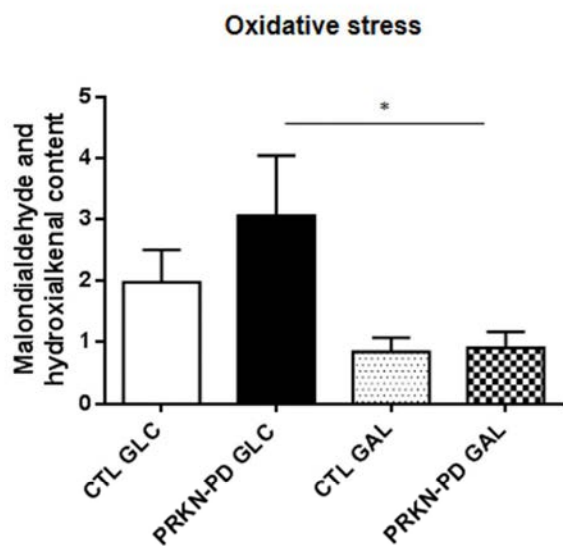


Figure 4. Oxidative stress measured through lipid peroxidation in control and PRKN-PD fibroblasts. In glucose, PRKN-PD exhibited an upward trend in lipid peroxidation compared to control fibroblasts while exposure to galactose significantly reduced oxidative stress levels in PRKN-PD compared to glucose. The results are expressed as means and standard error of the mean (SEM). *= $p < 0.05$. CTL= Control fibroblasts. GAL= 10 mM galactose medium. GLC= 25 mM glucose medium. PRKN-PD= Parkin-associated PD fibroblasts.

Mitochondrial membrane potential

Given that a correct mitochondrial polarization is crucial for mitochondrial integrity, we measured mitochondrial membrane potential in control and PRKN-PD fibroblasts. No significant differences in mitochondrial membrane potential were obtained

between groups. However, upon galactose exposure, control fibroblasts tended to enhance mitochondrial membrane potential as compared to glucose, while PRKN-PD fibroblasts remained preserved (Figure 5).

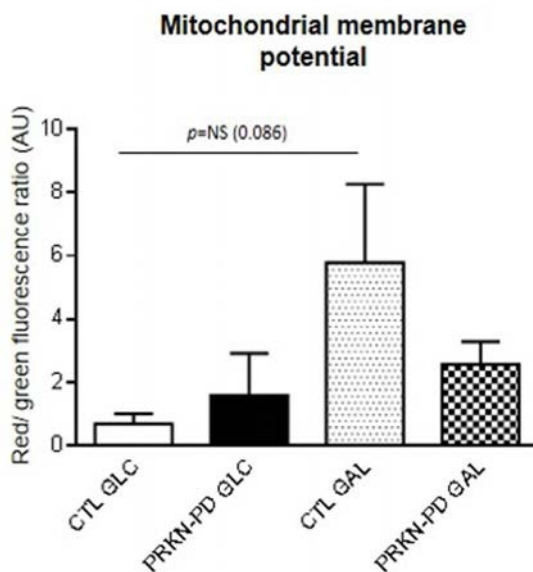


Figure 5. Mitochondrial membrane potential in control and PRKN-PD fibroblasts. Mitochondrial membrane potential is represented as the ratio of red vs. green fluorescence signals of JC-1 representing the cells with correctly polarized vs the cells with depolarized mitochondria. No significant differences in mitochondrial membrane potential were obtained between groups. Upon galactose exposure, control fibroblasts tended to enhance mitochondrial membrane potential as compared to glucose, while PRKN-PD fibroblasts remained unchanged. The results are expressed as means and standard error of the mean (SEM). AU= Arbitrary units. CTL= Control fibroblasts. GAL= 10 mM galactose medium. GLC= 25 mM glucose medium. JC-1: 5,5',6,6'-tetrachloro-1,1',3,3'-tetraethylbenzimidazol-carbocyanine iodide. NS= not significant. PRKN-PD= Parkin-associated PD fibroblasts.

Mitochondrial network complexity

Mitochondrial function is a process intimately associated with changes in mitochondrial dynamics [37]. For this reason, we assessed mitochondrial length Aspect ratio (AR) and branching Form factor (FF) in control and PRKN-PD fibroblasts and found it was comparable between groups in both media (Supplementary Figure 1A and B).

Mitochondrial content

We next evaluated mitochondrial content through the assessment of Mitochondrial DNA (mtDNA) copy number, citrate synthase activity (CS) and mitochondrial

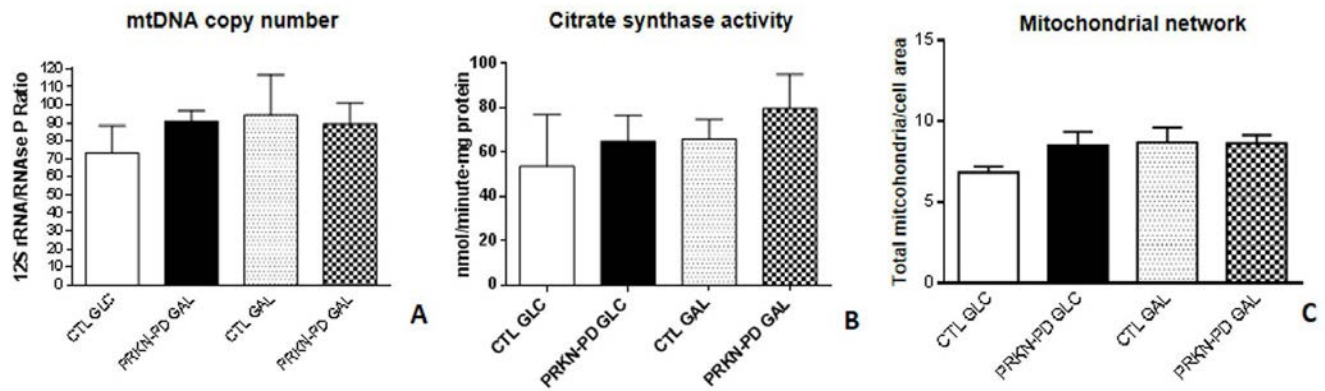


Figure 6. Mitochondrial content in control and PRKN-PD fibroblasts. Mitochondrial content was measured through mtDNA copy number (A), citrate synthase enzymatic activity (B) and mitochondrial network (C). Comparable mitochondrial content was observed between groups in both media. The results are expressed as means and standard error of the mean (SEM). CTL= Control fibroblasts. GAL= 10 mM galactose medium. GLC= 25 mM glucose medium. mtDNA= mitochondrial DNA. PRKN-PD= Parkin-associated PD fibroblasts.

network and found that all parameters were preserved between groups in both media (Figure 6 A-C).

Autophagy

To ascertain the potential impact of *PRKN* mutations on autophagy we quantified p62 and LC3BII protein levels. PRKN-PD fibroblasts presented significant lower basal levels of p62 and LC3BII in both media compared to controls as shown in Figure 7A and B (0h).

The processes of autophagosome synthesis and degradation are spatially and temporally separated. In order to determine whether the decrease in basal p62 and LC3BII protein levels was due to a reduction in autophagosome synthesis or to a later stage in the pathway such as autophagosome degradation, we treated cells with bafilomycin A1. Bafilomycin A1 clamps fusion of autophagosomes with lysosomes and thus blocks autophagosome degradation, allowing measurement of autophagosome synthesis, whereas both synthesis and degradation occur in the untreated samples. The degradation rate can be deduced by subtracting LC3BII levels in the untreated samples from those treated with bafilomycin A1 [38].

In both groups, p62 and LC3BII levels were significantly increased at 4 and 8 hours under bafilomycin A1 treatment compared to basal state, indicating some extent of autophagic flux in both media. However, in glucose, p62 and LC3BII levels at 4 and 8 hours of treatment were significantly lower in PRKN-PD compared to control fibroblasts and the same trends were observed in galactose (Figure 7 A and B; 4h and 8h). Upon exposure to galactose, controls but not PRKN-

PD fibroblasts, showed significantly decreased basal levels of both molecules compared to glucose with concurrent significantly decreased p62 and conserved LC3BII protein levels upon bafilomycin A1 treatment, suggesting an enhancement of autophagic flux in these cells.

Cell growth

We finally investigated cell growth rates in control and PRKN-PD fibroblasts in glucose and galactose media to assess how *PRKN* mutations impact on the overall cellular health. Although not significantly, PRKN-PD fibroblasts showed downward trend in cell growth rate in both media as shown in Figure 8.

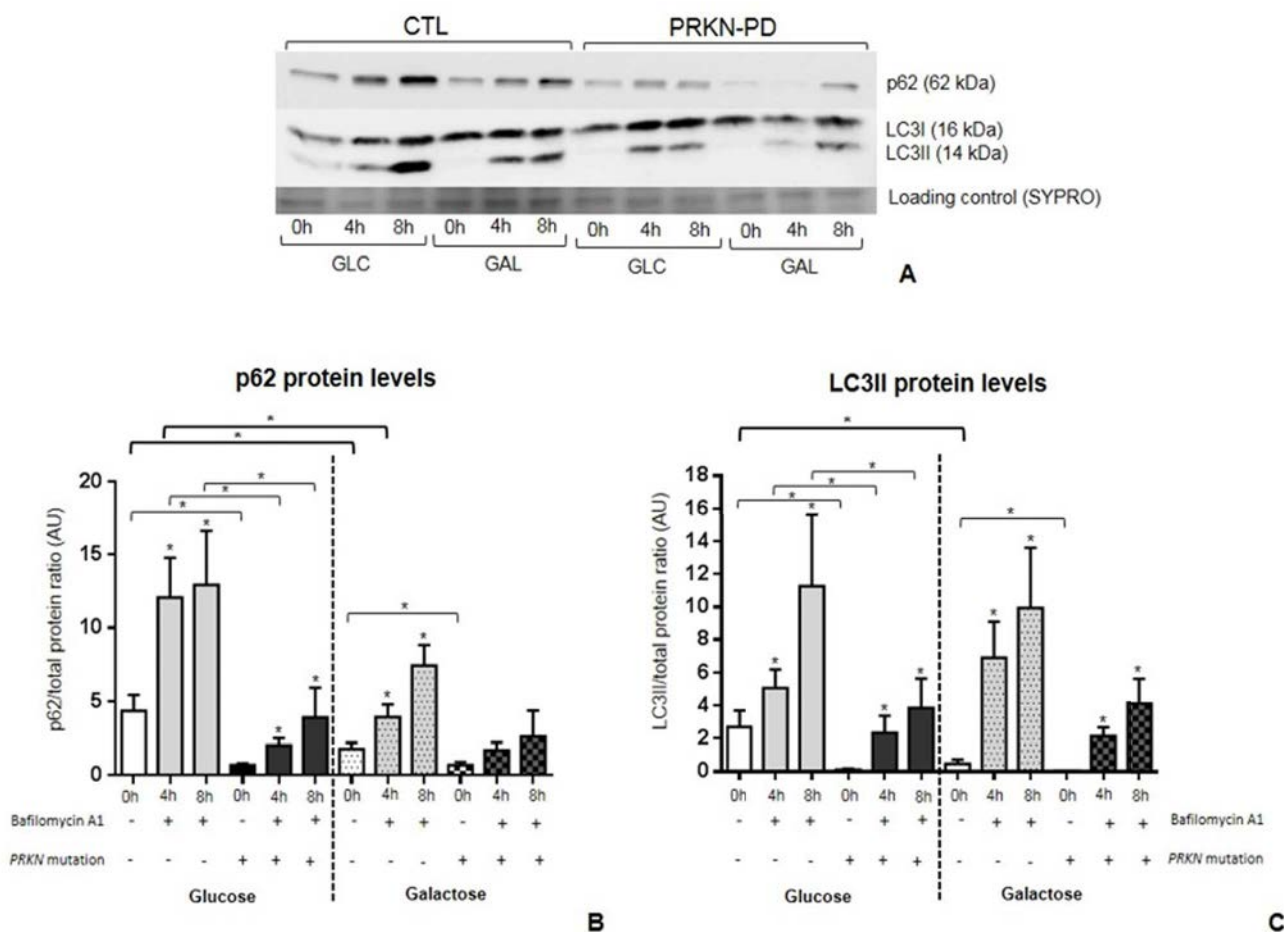
DISCUSSION

To our knowledge, this is the first study exploring the mitochondrial phenotype and the autophagic print in mitochondrial-challenging conditions (galactose) in skin-derived fibroblasts from PRKN-PD patients. Our results suggest that mitochondrial dysfunction and impaired autophagic flux are present in non-neural peripheral tissues of PRKN-PD patients. In addition, the alterations that PRKN-PD fibroblasts exhibited under mitochondrial-challenging conditions may be relevant to disease pathogenesis taking into consideration that the target tissue of the disease is predominantly oxidative.

To date, previous studies reporting altered mitochondrial homeostatic function in PRKN-PD fibroblasts have reported controversial results. Remarkably, all these studies were performed in glycolytic con-

ditions that may partially unveil mitochondrial deficits [29-34]. In this sense, we first explored the mitochondrial function phenotype in glucose conditions and did not find any statistically significant difference between PRKN-PD and control fibroblasts. Interestingly, we found abnormal trend to increased overall mitochondrial respiration in PRKN-PD. More specifically, we observed a bias towards increased mitochondrial basal, ATP-linked and maximal respirations, as likewise reported by previous authors [31, 32]. In contrast to these findings, a previous study that was performed with a different respirometry approach, described an overall decrease in all the aforementioned mitochondrial respiratory parameters of PRKN-PD fibroblasts [29].

To understand if the increased respiration in PRKN-PD cells was physiologically healthy, we assessed mitochondrial CI function as alterations at this level have been described in the CNS and in peripheral tissues of PD patients [33, 39, 40]. Although not statistically significant, we observed a strong downward decline in CI-stimulated oxygen consumption, which accordingly translated into a decreased CI enzymatic activity in PRKN-PD fibroblasts in glucose. In accordance with our results, Pacelli et al. and Mortiboys et al. [29, 33] described CI enzymatic decline in PRKN-PD fibroblasts, while Grünwald et al. observed preserved CI function in isolated mitochondria from a larger cohort [34]. The association between the mode-



rate increased mitochondrial respiration and the decreased MRC CI function in glucose is still a matter of debate but may correspond to an attempt of the PRKN-PD cell to overcome an inefficient oxidative phosphorylation (OXPHOS) function, mainly evidenced by CI deficiency.

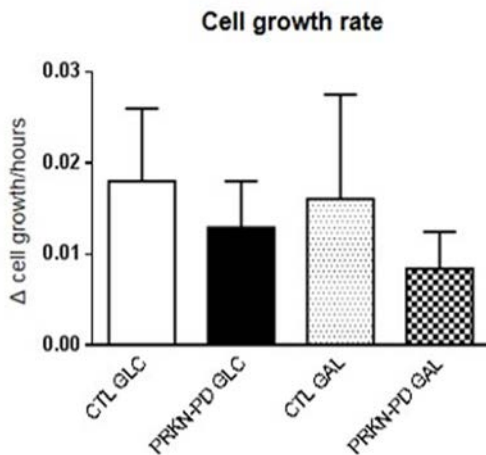


Figure 8. Cell growth rate in control and PRKN-PD fibroblasts. Although not significant, PRKN-PD fibroblasts showed downward trend in cell growth rate in both media. The results are expressed as means and standard error of the mean (SEM). AU= Arbitrary units. CTL= Control fibroblasts. GAL= 10 mM galactose medium. GLC= 25 mM glucose medium. PRKN-PD= Parkin-associated PD fibroblasts.

To evaluate efficiency of the OXPHOS function, we measured oxidative damage which is a hallmark of mitochondrial dysfunction and has often been related with neurodegeneration and specifically with PD [6, 41, 42]. In accordance, we observed a non-significant strong upward trend in lipid peroxidation in the PRKN-PD group in glucose. This moderate increase in oxidative damage could be related to MRC malfunction in PRKN-PD fibroblasts suggested by both the abnormal increased mitochondrial respiration and CI dysfunction, considering CI a major source of ROS [43]. In line with our results, other authors demonstrated increased protein and lipid oxidation in smaller cohorts [29, 34].

PRKN has been implicated in mitochondrial biogenesis [44]. In this context, we assessed mitochondrial content and observed it was preserved in PRKN-PD cells irrespective of the media, in accordance with Mortiboys et al. [33]. We cannot rule out that preserved PRKN-PD mitochondrial content may be triggered by an impairment of the mitochondrial turnover (mitophagy) in these cells that could counteract the lack of mitochondrial

biogenesis. In contrast to our findings, Grunewald et al. reported increased mitochondrial content through an enhancement of the CS activity in isolated mitochondria of PRKN-PD fibroblasts as a compensatory effect for the mild mitochondrial dysfunction observed in these cells [34], whereas Pacelli et al. showed a decrease in this parameter [29]. Similarly, there is considerable controversy in regards of mitochondrial network morphology in PRKN-PD fibroblasts [29-34], although Parkin has been reported to be involved in mitochondrial dynamics [45]. In line with previous studies, we failed to demonstrate significant alterations in mitochondrial network morphology of PRKN-PD in neither of the media [30, 31, 34] despite the specific effectors of mitochondrial dynamics were not analyzed in the present work. Notwithstanding, a previous study reported decreased mitochondrial branching in PRKN-PD fibroblasts [32].

One of the main contributions of the present work is to evaluate the phenotype of PRKN-PD fibroblasts in mitochondrial-challenging conditions. Whereas the glycolytic metabolism of glucose forms pyruvate yielding 2 net ATP, the production of pyruvate via glycolytic metabolism of galactose yields no net ATP production, forcing the cells to rely on mitochondrial oxidative metabolism to obtain the vast majority of the cell ATP²⁸ and approaching them somehow the neuronal metabolism. Moreover, replacing glucose with galactose medium has long been used to diagnose primary mitochondrial diseases in cells derived from patients with OXPHOS deficiencies [35, 36]. This is the first study reporting that the exposition of PRKN-PD fibroblasts to oxidative conditions uncovers a differential mitochondrial function phenotype respect to standard glycolytic conditions. We specifically found a significant decrease in the mitochondrial basal/maximal respiratory ratio in galactose, which indicates that upon an increasing ATP demand that can only be confronted through enhancing mitochondrial metabolism, PRKN-PD cells cannot respond as controls do. Accordingly, we found downward trends in basal and ATP-linked respirations as well as in mitochondrial membrane potential in PRKN-PD compared to controls. In this line, Mortiboys et al. previously described decreased mitochondrial membrane potential in fibroblasts from five PRKN-PD patients in galactose [33]. Consistent with these results, we found a decline in mitochondrial CIV function and oxidative stress in PRKN-PD fibroblasts that was evident upon growing cells in galactose. Previous studies reported mitochondrial CIV deficiency in two PRKN-PD fibroblasts lines [29], while others have reported unaltered enzymatic activity of this complex in glucose medium [33, 34].

The second main finding of this study is the description of autophagic alterations in PRKN-PD fibroblasts. Specifically, we observed significant lower levels of both the autophagy substrate (p62) and autophagosome content markers (LC3BII) in PRKN-PD fibroblasts at basal and after inhibiting autophagosome fusion with lysosomes in both media. These findings suggest that the overall autophagic flux is decreased in *PRKN* mutant fibroblasts. PRKN-PD fibroblasts did not exhibit changes in autophagic flux upon exposure to galactose as compared to glucose. Contrarily, our results suggest that galactose enhances autophagic flux in controls. Although p62 levels decreased in controls upon treatment when compared to glucose, p62 can be degraded through autophagosome-independent mechanisms such as the ubiquitin-proteasome system [46, 47], and thus, may partially evade bafilomycin A1 treatment. The disruption in the autophagosome-lysosome pathway observed in PRKN-PD fibroblasts may promote accumulation of PRKN substrates including defective mitochondria and misfolded and aggregated proteins that, in physiologic conditions, should instead be degraded by the autophagic machinery. Thus, further research should be undertaken to investigate the role of autophagic disruption in PRKN-PD ethiopathogenesis.

In summary, exposure to galactose uncovered a differential mitochondrial phenotype in PRKN-PD fibroblasts compared to glycolytic medium while autophagic flux was reduced in these cells, irrespective of the culture medium. In addition, galactose suggested to enhance both mitochondrial function and autophagy in controls, by improving above all mitochondrial respiration performance and increasing autophagosome degradation. This improvement was not observed in PRKN-PD fibroblasts and may explain overall cell health decay evidenced in PRKN-fibroblasts by trends towards reduced cell growth. As neurons constitute a post-mitotic tissue that strongly relies on mitochondrial oxidative metabolism and autophagy to meet their high energy needs, alterations in these cell processes make them particularly vulnerable. Thus, the mitochondrial phenotype and the autophagic flux alterations exhibited by PRKN-PD fibroblasts under oxidative conditions may be of relevance to disease pathogenesis.

Notwithstanding, our study contains some limitations. First, despite being the study with a larger sample size respect to previous, sample size of our cohort is still limited. Second, the inherent individual variability present in the samples may also contribute to hinder inter-group statistical differences. Also, methodological issues amongst studies may support discrepancies. For

instance, the use of different high-resolution respirometry approaches in which oxygen consumption is measured from seeding fibroblasts or from cells in suspension. Similarly, assessing MRC enzymatic activities in intact cells or in mitochondrial enriched fractions may contribute to outcome disparities. Third, although mitochondrial function has been previously reported as a critical regulator of autophagy in eukaryotic cells [48, 49], the link between mitochondrial function and autophagy alterations in PRKN-PD fibroblasts is not herein explored. In this regard, future mechanistic studies in this field may be helpful in clarifying this issue. Finally, we acknowledge that many other mechanisms may be underlying the ethiopathology of PD, where the loss of DAN may be the common eventual manifestation of this heterogeneous disease.

In conclusion, our work supports the view of PD as a systemic disease where mitochondrial and autophagic alterations play a role also in non-neural peripheral tissues such as skin fibroblasts, and encourages further studies in this model. The alterations that PRKN-PD fibroblasts exhibit under mitochondrial-challenging conditions may be relevant to disease pathogenesis and may be related to the increased susceptibility of patient DAN, which are predominantly oxidative, to undergo degeneration. Future studies with larger sample sizes and different PRKN-PD cohorts are warranted to confirm the results herein reported.

MATERIALS AND METHODS

Subjects and *PRKN* mutational screening

We recruited seven PD patients carrying mutations in the *PRKN* gene (PRKN-PD, n=7), and thirteen unrelated healthy subjects (CTL, n=13) among patients and relatives visiting the Movement Disorders outpatient clinic from the Hospital Clínic of Barcelona (Barcelona, Spain). PRKN-PD patients were diagnosed according to the UK Brain Bank criteria [50] and the mutational screening of the *PRKN* gene was performed as previously described [51]. Clinical and epidemiological data of PRKN-PD patients is summarized in Table 1. Gender and age-paired control group included six males and seven female subjects with an age range of 35-86 years and with a mean age of 58 years. Subjects with comorbidities, mitochondrial disorders, and those consuming mitochondrial toxic drugs were excluded from the study [52]. The study was approved by the ethics committee of the Hospital Clínic of Barcelona, following the guidelines of Helsinki declaration, and subjects were included in the study after signing the informed consent form.

Table 1. Clinical and epidemiological data of patients and control subjects providers of skin biopsy.

Subject	Mutation	Gender	Age of disease onset	Age at skin punch biopsy	Treatment
PRKN-PD 1	Heterozygous <i>PRKN</i> val15met	Male	47	57	L-Dopa
PRKN-PD 2	Homozygous <i>PRKN</i> exon 2-3-4 deletion	Male	35	69	L-Dopa
PRKN-PD 3	Homozygous <i>PRKN</i> exon 5-6 deletion	Female	27	63	L-Dopa
PRKN-PD 4	Compound heterozygous <i>PACRG</i> exon 1 deletion/ <i>PRKN</i> exon 6 deletion	Female	8	35	L-Dopa
PRKN-PD 5	Compound heterozygous <i>PRKN</i> exon 2 duplication/ exon 6 deletion	Male	20	49	L-Dopa
PRKN-PD 6	Homozygous <i>PRKN</i> exon 3 deletion	Male	25	48	L-Dopa
PRKN-PD 7	Compound heterozygous <i>PRKN</i> exon 6 deletion/ exon 8 deletion	Female	38	44	L-Dopa

No differences in mean age and gender were found between PRKN-PD and CTL subjects. Control group included six males and seven female subjects with an age range of 35-86 years and with a mean age of 58 years. CTL= healthy control subjects (not affected by PD or any *PRKN* mutation). *PACRG*=Parkin coregulated gene. PRKN-PD= Parkin-associated Parkinson's disease. Val15Met= Methionine to Valine substitution at position 15.

Cell culture

Fibroblasts were obtained by a 6 mm of diameter punch skin biopsy from the alar surface of the non-dominant arm of the subjects. Fibroblasts were cultured first in DMEM with high glucose (25 mM) supplemented with 10% (v/v) heat-inactivated fetal bovine serum and 1% (v/v) L-glutamine and penicillin/ streptomycin at 37°C and 5% CO₂ until 80-90% optimal confluence was reached. Each cell line was then exposed in parallel to 25 mM glucose (standard) or 10 mM galactose (mitochondrial-challenging) media for 24 hours [28, 53-55]. Fibroblasts were harvested for further analyses as reported elsewhere [56]. All functional assays were performed in cells between passage 5 and 10.

Mitochondrial respiration analysis

Mitochondrial oxygen consumption rates

Oxygen consumption rates (OCRs) were measured in intact adherent fibroblasts through Agilent Seahorse XFe24 Analyzer (Seahorse Bioscience). Briefly, 35,000-40,000 fibroblasts per well were seeded in cus-

tomized 24-well Seahorse cell culture plates and left to adhere overnight in 250 uL of growth medium. Each cell line was seeded in triplicate per condition (n=3 for glucose and n=3 for galactose). After 24 hours, growth medium was removed and wells were washed and replaced with Seahorse XF Base Medium (Seahorse Bioscience) containing either 25 mM glucose or 10 mM galactose plus 1 mM sodium pyruvate and 1 mM glutamine. Afterwards, plates were incubated for 30 min at 37 °C without CO₂ according to manufacturer's protocol. In order to determine the different respiratory control ratios, oxygen consumption was measured under basal conditions and after the addition of oligomycin, which blocks ATP synthase allowing the assessment of the natural proton leak across the inner mitochondrial membrane (IMM). This was followed by the addition of the uncoupler carbonyl cyanide-4-(trifluoromethoxy) phenylhydrazone (FCCP) to measure the maximal respiratory capacity. FCCP is an ionophore that directly transports protons across the IMM bypassing the ATP synthase proton channel thus leading to a rapid consumption of oxygen without the ATP generation. Finally, complex I and III inhibitors, rotenone and antimycin-A, were added to assess

unspecific non-mitochondrial respiration (all reagents from Sigma-Aldrich). In addition, spare respiratory capacity and basal/maximal respiratory ratio were calculated as the maximal after basal OCR subtraction expressed in percentage, and the ratio between basal and maximal OCRs, respectively. All respiration values were normalized to total cell protein content determined in each well through the bicinchoninic acid assay (BCA) assay according to manufacturer's protocol (Thermo Scientific) and CS activity (see mitochondrial respiratory chain enzymatic activities method section).

Mitochondrial complex I-stimulated oxygen consumption

To assess oxygen consumption under the stimulation of mitochondrial CI, 1 million of fibroblasts were obtained and resuspended in ice-cold respiration MiRO5 medium. High-resolution respirometry was performed in digitonin-permeabilized cells using Oroboros™ Oxygraph-2k system® (Innsbruck, Austria) and oxidation of CI substrates, pyruvate and malate (PMox), was monitored following manufacturer's protocol [56, 57]. Results were normalized to cell number and CS activity (see mitochondrial respiratory chain enzymatic activities method section).

Mitochondrial respiratory chain enzymatic activities

In order to study mitochondrial respiratory chain (MRC) function, enzymatic activities of mitochondrial complexes I (CI), II+III (CII+III) and IV (CIV) were spectrophotometrically measured at 37°C in fibroblasts, as reported elsewhere [58, 59]. CS activity was also spectrophotometrically determined at 37°C in fibroblasts, as it is considered a reliable marker of mitochondrial content [60]. Mitochondrial content was further confirmed by alternative methods (see mitochondrial content method section).

All enzymatic assays were performed following national standardized methods and were run in parallel with internal quality controls [58]. Changes in absorbance were registered in a HITACHI U2900 spectrophotometer through the UV-Solution software v2.2 and were expressed as nanomoles of consumed substrate or generated product per minute and milligram of protein (nmol/minute·mg protein). All enzymatic activities were normalized by CS activity.

Lipid peroxidation

Lipid peroxidation levels are indicative of the ROS-derived oxidative damage in cell lipid compounds. Lipid peroxidation was quantified using the BIOXYTECH® LPO-586™ colorimetric assay (Oxy

International Inc., CA, USA). Specifically, the levels of malondialdehyde (MDA) and 4-hydroxyalkenal (HAE) which are peroxides derived from fatty acid oxidation, were quantified in duplicate through spectrophotometry. The results were next normalized by protein content and expressed as $\mu\text{M MDA} + \text{HAE}/\text{mg protein}$, as previously reported [61].

Mitochondrial membrane potential

Mitochondrial membrane potential of fibroblasts was assessed in a BD FACSCalibur™ cell analyzer (BD Biosciences) by JC-1 potentiometric dye and both, green (~525 nm) and red (~590 nm) fluorescent emissions of each cell population were simultaneously monitored by flow cytometry, as reported elsewhere [62, 63]. Results were obtained as percentage of cells with specific fluorescence indicating polarized or depolarized mitochondria. We calculated the red/green ratio indicating the ratio between correctly polarized and depolarized mitochondria, whose decrease indicates mitochondrial depolarization.

Mitochondrial network complexity analysis

Mitochondrial content and mitochondrial network complexity were assessed by immunochemistry and confocal microscopy as reported elsewhere [56, 64]. A minimum of 3 fibroblasts from each subject were visualized and analysed using the Image J software and a macro of instructions was used to perform semi-automatic quantitation [65]. Mitochondrial network of each cell was subjected to particle analysis and the following parameters were assessed: aspect ratio (AR) (major axis/minor axis), form factor (FF), which was calculated as the inverse of the circularity ($4\pi \cdot \text{area}/\text{perimeter}^2$) and, mitochondrial network or content (total number of mitochondria/total cell area). AR and FF values correspond to mitochondrial length and branching, respectively, and are considered parameters of mitochondrial health. AR and FF values of 1 are indicative of circular unbranched mitochondria which are a sign of pathologic mitochondrial isolation. As mitochondria elongate and become more branched, AR and FF values increase indicating mitochondrial health.

Mitochondrial content

The following three approaches were used to quantify mitochondrial content in fibroblasts:

Mitochondrial DNA (mtDNA) copy number

Total DNA from fibroblasts was isolated through the standard phenol–chloroform extraction procedure as previously reported [66]. To assess mitochondrial DNA (mtDNA) content, fragments of the highly conserved

mitochondrial 12S rRNA gene and the constitutive nuclear ribonuclease P gene (RNase P) were amplified in triplicates by multiplex qRT-PCR using Applied Biosystems technology [67]. mtDNA content was expressed as the ratio between the 12S rRNA and RNase P genes.

Citrate synthase enzymatic activity

CS activity was spectrophotometrically determined in fibroblasts (see mitochondrial respiratory chain enzymatic activities method section).

Determination of mitochondrial network

Immunocytochemistry and confocal microscopy were performed to quantify mitochondrial network or content and expressed as the total number of mitochondria per total cell area (see mitochondrial network complexity analysis method section) [68]. In general, higher mitochondrial network values are considered sign of healthy mitochondria.

Autophagic flux analysis

Where indicated, cells were treated with 0.1 μ M bafilomycin A1 (Sigma) for 4 and 8 hours at 37°C in the presence of 5% CO₂. Bafilomycin A1 is a proton pump inhibitor that neutralizes lysosomal pH preventing fusion of autophagosomes with lysosomes and thus allowing monitoring of autophagosome synthesis [38]. Briefly, fibroblasts were lysed with RIPA buffer (Sigma) plus protease inhibitor cocktail (Thermo scientific) followed by shaking and centrifugation at 16,100 g at 4°C for 10 minutes. Soluble fractions were kept at -80 °C until western blot analysis. Electrophoresis and blotting were performed, as reported elsewhere [56, 62]. Blots were probed with anti-SQSTM1/p62 (Abcam) and anti-LC3B (Cell Signaling) antibodies. LC3BII is considered a marker of autophagosome number and p62 is an ubiquitin-binding scaffold protein that labels molecules and organelles that need to be degraded acting as a cargo receptor that is recruited to autophagosomes through LC3BII inter-action [69]. Total protein content was obtained through SYPRO Ruby Protein Blot Stain, according to manufacturer's protocol (Molecular Probes). The intensity of signals was quantified by densitometric analysis (Image Quant TL Software, GE Healthcare). Results were expressed as p62 and LC3BII protein levels normalized by the total cell protein content [70].

Cell growth

Cell growth rate was manually determined through cell counting with the Neubauer chamber using trypan blue staining at the times of seeding and harvesting the cells

[71]. Cell growth rate was calculated by applying the following formula:

$$\frac{\text{No. cells at time of harvesting} - \text{No. cells at the time of seeding}}{\text{No. cells at the time of seeding}} \times \text{Time (hours)}$$

Statistical analysis

Statistical analysis was performed using the Statistical Package for the Social Sciences (SPSS, version 19) software (IBM SPSS Statistics; SPSS Inc). Differences amongst groups were sought by non-parametric tests after filtering for outlier values in the datasets. Specifically, Kruskal-Wallis and Mann-Whitney U statistical tests for independent samples were used when required. Significance was accepted for asymptotic 2-tailed p-values below 0.05 (for a confidence interval of $\alpha= 95\%$). Results were expressed as means \pm the standard error of the mean (SEM).

ACKNOWLEDGEMENTS

The authors thank the patients who participated in the study and their family members. We also want to thank the research team of Silvia Ginés from the Neurosciences Research Institute at the UB, for the kindly donation of two control fibroblast cell lines. We also want to thank the program: Suports a Grups de Recerca de la Generalitat de Catalunya 2017-2019 (grant number SGR 2017/893). We also thank Anna Bosch, Elisenda Coll and Maria Calvo from the Advanced Optical Microscopy department of the University of Barcelona for their support with confocal microscopy.

CONFLICTS OF INTEREST

The authors report no actual or potential conflict of interest including any financial, consultant, institutional or other relationships with other people or organizations within three years of beginning the work submitted that could inappropriately influence this work.

FUNDING

This work was supported by funds from Fondo de Investigaciones Sanitarias of the Instituto de Salud Carlos III (ISCIII) (grant number PI11/00462), the Centro de Investigación Biomédica en Red de

Enfermedades Raras (CIBERER), initiatives of Instituto Carlos III (ISCIII) and FEDER, and Fundació Privada Cellex (CP042187).

REFERENCES

1. Connolly BS, Lang AE. Pharmacological treatment of Parkinson disease: a review. *JAMA*. 2014; 311:1670–83. <https://doi.org/10.1001/jama.2014.3654> PMID:24756517
2. Bonifati V. Genetics of Parkinson's disease--state of the art, 2013. *Parkinsonism Relat Disord*. 2014 (Suppl 1); 20:S23–28. [https://doi.org/10.1016/S1353-8020\(13\)70009-9](https://doi.org/10.1016/S1353-8020(13)70009-9) PMID:24262182
3. Cheon SM, Chan L, Chan DK, Kim JW. Genetics of Parkinson's disease - a clinical perspective. *J Mov Disord*. 2012; 5:33–41. <https://doi.org/10.14802/jmd.12009> PMID:24868412
4. Klein C, Westenberger A. Genetics of Parkinson's disease. *Cold Spring Harb Perspect Med*. 2012; 2:a008888. <https://doi.org/10.1101/cshperspect.a008888> PMID:22315721
5. Bonifati V, Rohé CF, Breedveld GJ, Fabrizio E, De Mari M, Tassorelli C, Tavella A, Marconi R, Nicholl DJ, Chien HF, Fincati E, Abbruzzese G, Marini P, et al, and Italian Parkinson Genetics Network. Early-onset parkinsonism associated with PINK1 mutations: frequency, genotypes, and phenotypes. *Neurology*. 2005; 65:87–95. <https://doi.org/10.1212/01.wnl.0000167546.39375.82> PMID:16009891
6. Poewe W, Seppi K, Tanner CM, Halliday GM, Brundin P, Volkman J, Schrag AE, Lang AE. Parkinson disease. *Nat Rev Dis Primers*. 2017; 3:17013. <https://doi.org/10.1038/nrdp.2017.13> PMID:28332488
7. Nixon RA. The role of autophagy in neurodegenerative disease. *Nat Med*. 2013; 19:983–97. <https://doi.org/10.1038/nm.3232> PMID:23921753
8. Zhang CW, Hang L, Yao TP, Lim KL. Parkin Regulation and Neurodegenerative Disorders. *Front Aging Neurosci*. 2016; 7:248. <https://doi.org/10.3389/fnagi.2015.00248> PMID:26793099
9. Fiesel FC, Caulfield TR, Moussaud-Lamodièrè EL, Ogaki K, Dourado DF, Flores SC, Ross OA, Springer W. Structural and Functional Impact of Parkinson Disease-Associated Mutations in the E3 Ubiquitin Ligase Parkin. *Hum Mutat*. 2015; 36:774–86. <https://doi.org/10.1002/humu.22808> PMID:25939424
10. Seirafi M, Kozlov G, Gehring K. Parkin structure and function. *FEBS J*. 2015; 282:2076–88. <https://doi.org/10.1111/febs.13249> PMID:25712550
11. Park J, Lee SB, Lee S, Kim Y, Song S, Kim S, Bae E, Kim J, Shong M, Kim JM, Chung J. Mitochondrial dysfunction in Drosophila PINK1 mutants is complemented by parkin. *Nature*. 2006; 441:1157–61. <https://doi.org/10.1038/nature04788> PMID:16672980
12. Fiškin E, Dikic I. Parkin promotes cell survival via linear ubiquitination. *EMBO J*. 2013; 32:1072–74. <https://doi.org/10.1038/emboj.2013.70> PMID:23531882
13. Sarraf SA, Raman M, Guarani-Pereira V, Sowa ME, Huttlin EL, Gygi SP, Harper JW. Landscape of the PARKIN-dependent ubiquitylome in response to mitochondrial depolarization. *Nature*. 2013; 496:372–76. <https://doi.org/10.1038/nature12043> PMID:23503661
14. Clark IE, Dodson MW, Jiang C, Cao JH, Huh JR, Seol JH, Yoo SJ, Hay BA, Guo M. Drosophila pink1 is required for mitochondrial function and interacts genetically with parkin. *Nature*. 2006; 441:1162–66. <https://doi.org/10.1038/nature04779> PMID:16672981
15. Ivankovic D, Chau KY, Schapira AH, Gegg ME. Mitochondrial and lysosomal biogenesis are activated following PINK1/parkin-mediated mitophagy. *J Neurochem*. 2016; 136:388–402. <https://doi.org/10.1111/jnc.13412> PMID:26509433
16. Yung C, Sha D, Li L, Chin LS. Parkin Protects Against Misfolded SOD1 Toxicity by Promoting Its Aggresome Formation and Autophagic Clearance. *Mol Neurobiol*. 2016; 53:6270–87. <https://doi.org/10.1007/s12035-015-9537-z> PMID:26563499
17. Olzmann JA, Chin LS. Parkin-mediated K63-linked polyubiquitination: a signal for targeting misfolded proteins to the aggresome-autophagy pathway. *Autophagy*. 2008; 4:85–87. <https://doi.org/10.4161/auto.5172> PMID:17957134
18. Narendra D, Tanaka A, Suen DF, Youle RJ. Parkin is recruited selectively to impaired mitochondria and promotes their autophagy. *J Cell Biol*. 2008; 183:795–803. <https://doi.org/10.1083/jcb.200809125> PMID:19029340
19. Kahle PJ, Haass C. How does parkin ligate ubiquitin to Parkinson's disease? *EMBO Rep*. 2004; 5:681–85. <https://doi.org/10.1038/sj.embor.7400188> PMID:15229644
20. Schapira AH. Mitochondria in the aetiology and pathogenesis of Parkinson's disease. *Lancet Neurol*.

- 2008; 7:97–109. [https://doi.org/10.1016/S1474-4422\(07\)70327-7](https://doi.org/10.1016/S1474-4422(07)70327-7) PMID:18093566
21. Djaldetti R, Lev N, Melamed E. Lesions outside the CNS in Parkinson's disease. *Mov Disord.* 2009; 24:793–800. <https://doi.org/10.1002/mds.22172> PMID:19224610
 22. Auburger G, Klinkenberg M, Drost J, Marcus K, Morales-Gordo B, Kunz WS, Brandt U, Broccoli V, Reichmann H, Gispert S, Jendrach M. Primary skin fibroblasts as a model of Parkinson's disease. *Mol Neurobiol.* 2012; 46:20–27. <https://doi.org/10.1007/s12035-012-8245-1> PMID:22350618
 23. Ivanov NA, Tao R, Chenoweth JG, Brandtjen A, Mighdoll MI, Genova JD, McKay RD, Jia Y, Weinberger DR, Kleinman JE, Hyde TM, Jaffe AE. Strong Components of Epigenetic Memory in Cultured Human Fibroblasts Related to Site of Origin and Donor Age. *PLoS Genet.* 2016; 12:e1005819. <https://doi.org/10.1371/journal.pgen.1005819> PMID:26913521
 24. Hoepken HH, Gispert S, Azizov M, Klinkenberg M, Ricciardi F, Kurz A, Morales-Gordo B, Bonin M, Riess O, Gasser T, Kögel D, Steinmetz H, Auburger G. Parkinson patient fibroblasts show increased alpha-synuclein expression. *Exp Neurol.* 2008; 212:307–13. <https://doi.org/10.1016/j.expneurol.2008.04.004> PMID:18511044
 25. Ambrosi G, Ghezzi C, Sepe S, Milanese C, Payan-Gomez C, Bombardieri CR, Armentero MT, Zangaglia R, Pacchetti C, Mastroberardino PG, Blandini F. Bioenergetic and proteolytic defects in fibroblasts from patients with sporadic Parkinson's disease. *Biochim Biophys Acta.* 2014; 1842:1385–94. <https://doi.org/10.1016/j.bbadis.2014.05.008> PMID:24854107
 26. González-Casacuberta I, Morén C, Juárez-Flores DL, Esteve-Codina A, Sierra C, Catalán-García M, Guitart-Mampel M, Tobías E, Milisenda JC, Pont-Sunyer C, Martí MJ, Cardellach F, Tolosa E, et al. Transcriptional alterations in skin fibroblasts from Parkinson's disease patients with parkin mutations. *Neurobiol Aging.* 2018; 65:206–16. <https://doi.org/10.1016/j.neurobiolaging.2018.01.021> PMID:29501959
 27. Lippolis R, Siciliano RA, Pacelli C, Ferretta A, Mazzeo MF, Scacco S, Papa F, Gaballo A, Dell'Aquila C, De Mari M, Papa S, Cocco T. Altered protein expression pattern in skin fibroblasts from parkin-mutant early-onset Parkinson's disease patients. *Biochim Biophys Acta.* 2015; 1852:1960–70. <https://doi.org/10.1016/j.bbadis.2015.06.015> PMID:26096686
 28. Aguer C, Gambarotta D, Mailloux RJ, Moffat C, Dent R, McPherson R, Harper ME. Galactose enhances oxidative metabolism and reveals mitochondrial dysfunction in human primary muscle cells. *PLoS One.* 2011; 6:e28536. <https://doi.org/10.1371/journal.pone.0028536> PMID:22194845
 29. Pacelli C, De Rasmio D, Signorile A, Grattagliano I, di Tullio G, D'Orazio A, Nico B, Comi GP, Ronchi D, Ferranini E, Pirolo D, Seibel P, Schubert S, et al. Mitochondrial defect and PGC-1 α dysfunction in parkin-associated familial Parkinson's disease. *Biochim Biophys Acta.* 2011; 1812:1041–53. <https://doi.org/10.1016/j.bbadis.2010.12.022> PMID:21215313
 30. van der Merwe C, Loos B, Swart C, Kinnear C, Henning F, van der Merwe L, Pillay K, Muller N, Zaharie D, Engelbrecht L, Carr J, Bardien S. Mitochondrial impairment observed in fibroblasts from South African Parkinson's disease patients with parkin mutations. *Biochem Biophys Res Commun.* 2014; 447:334–40. <https://doi.org/10.1016/j.bbrc.2014.03.151> PMID:24721425
 31. Zanellati MC, Monti V, Barzaghi C, Reale C, Nardocci N, Albanese A, Valente EM, Ghezzi D, Garavaglia B. Mitochondrial dysfunction in Parkinson disease: evidence in mutant PARK2 fibroblasts. *Front Genet.* 2015; 6:78. <https://doi.org/10.3389/fgene.2015.00078> PMID:25815004
 32. Haylett W, Swart C, van der Westhuizen F, van Dyk H, van der Merwe L, van der Merwe C, Loos B, Carr J, Kinnear C, Bardien S. Altered Mitochondrial Respiration and Other Features of Mitochondrial Function in Parkin-Mutant Fibroblasts from Parkinson's Disease Patients. *Parkinsons Dis.* 2016; 2016:1819209. <https://doi.org/10.1155/2016/1819209> PMID:27034887
 33. Mortiboys H, Thomas KJ, Koopman WJ, Klaffke S, Abou-Sleiman P, Olpin S, Wood NW, Willems PH, Smeitink JA, Cookson MR, Bandmann O. Mitochondrial function and morphology are impaired in parkin-mutant fibroblasts. *Ann Neurol.* 2008; 64:555–65. <https://doi.org/10.1002/ana.21492> PMID:19067348
 34. Grünewald A, Voges L, Rakovic A, Kasten M, Vandebona H, Hemmelmann C, Lohmann K, Orolicki S, Ramirez A, Schapira AH, Pramstaller PP, Sue CM, Klein C. Mutant Parkin impairs mitochondrial function and morphology in human fibroblasts. *PLoS One.* 2010; 5:e12962. <https://doi.org/10.1371/journal.pone.0012962>

[PMID:20885945](#)

35. Robinson BH, Petrova-Benedict R, Buncic JR, Wallace DC. Nonviability of cells with oxidative defects in galactose medium: a screening test for affected patient fibroblasts. *Biochem Med Metab Biol.* 1992; 48:122–26. [https://doi.org/10.1016/0885-4505\(92\)90056-5](https://doi.org/10.1016/0885-4505(92)90056-5) PMID:1329873
36. Arroyo JD, Jourdain AA, Calvo SE, Ballarano CA, Doench JG, Root DE, Mootha VK. A Genome-wide CRISPR Death Screen Identifies Genes Essential for Oxidative Phosphorylation. *Cell Metab.* 2016; 24:875–85. <https://doi.org/10.1016/j.cmet.2016.08.017> PMID:27667664
37. Schneeberger M, Dietrich MO, Sebastián D, Imbernón M, Castaño C, Garcia A, Esteban Y, Gonzalez-Franquesa A, Rodríguez IC, Bortolozzi A, Garcia-Roves PM, Gomis R, Nogueiras R, et al. Mitofusin 2 in POMC neurons connects ER stress with leptin resistance and energy imbalance. *Cell.* 2013; 155:172–87. <https://doi.org/10.1016/j.cell.2013.09.003> PMID:24074867
38. Rubinsztein DC, Cuervo AM, Ravikumar B, Sarkar S, Korolchuk V, Kaushik S, Klionsky DJ. In search of an “autophagometer”. *Autophagy.* 2009; 5:585–89. <https://doi.org/10.4161/auto.5.5.8823> PMID:19411822
39. Cardellach F, Martí MJ, Fernández-Solá J, Marín C, Hoek JB, Tolosa E, Urbano-Márquez A. Mitochondrial respiratory chain activity in skeletal muscle from patients with Parkinson’s disease. *Neurology.* 1993; 43:2258–62. <https://doi.org/10.1212/WNL.43.11.2258> PMID:8232939
40. Keeney PM, Xie J, Capaldi RA, Bennett JP Jr. Parkinson’s disease brain mitochondrial complex I has oxidatively damaged subunits and is functionally impaired and misassembled. *J Neurosci.* 2006; 26:5256–64. <https://doi.org/10.1523/JNEUROSCI.0984-06.2006> PMID:16687518
41. Guzman JN, Sanchez-Padilla J, Wokosin D, Kondapalli J, Ilijic E, Schumacker PT, Surmeier DJ. Oxidant stress evoked by pacemaking in dopaminergic neurons is attenuated by DJ-1. *Nature.* 2010; 468:696–700. <https://doi.org/10.1038/nature09536> PMID:21068725
42. Surmeier DJ, Guzman JN, Sanchez-Padilla J, Schumacker PT. The role of calcium and mitochondrial oxidant stress in the loss of substantia nigra pars compacta dopaminergic neurons in Parkinson’s disease. *Neuroscience.* 2011; 198:221–31. <https://doi.org/10.1016/j.neuroscience.2011.08.045> PMID:21884755
43. Scialò F, Fernández-Ayala DJ, Sanz A. Role of Mitochondrial Reverse Electron Transport in ROS Signaling: Potential Roles in Health and Disease. *Front Physiol.* 2017; 8:428. <https://doi.org/10.3389/fphys.2017.00428> PMID:28701960
44. Shin JH, Ko HS, Kang H, Lee Y, Lee YI, Pletinkova O, Troconso JC, Dawson VL, Dawson TM. PARIS (ZNF746) repression of PGC-1 α contributes to neurodegeneration in Parkinson’s disease. *Cell.* 2011; 144:689–702. <https://doi.org/10.1016/j.cell.2011.02.010> PMID:21376232
45. Lim KL, Ng XH, Grace LG, Yao TP. Mitochondrial dynamics and Parkinson’s disease: focus on parkin. *Antioxid Redox Signal.* 2012; 16:935–49. <https://doi.org/10.1089/ars.2011.4105> PMID:21668405
46. Hewitt G, Carroll B, Sarallah R, Correia-Melo C, Ogrodnik M, Nelson G, Otten EG, Manni D, Antrobus R, Morgan BA, von Zglinicki T, Jurk D, Seluanov A, et al. SQSTM1/p62 mediates crosstalk between autophagy and the UPS in DNA repair. *Autophagy.* 2016; 12:1917–30. <https://doi.org/10.1080/15548627.2016.1210368> PMID:27391408
47. Mizushima N, Yoshimori T, Levine B. Methods in mammalian autophagy research. *Cell.* 2010; 140:313–26. <https://doi.org/10.1016/j.cell.2010.01.028> PMID:20144757
48. Graef M, Nunnari J. Mitochondria regulate autophagy by conserved signalling pathways. *EMBO J.* 2011; 30:2101–14. <https://doi.org/10.1038/emboj.2011.104> PMID:21468027
49. Okamoto K. Mitochondria breathe for autophagy. *EMBO J.* 2011; 30:2095–96. <https://doi.org/10.1038/emboj.2011.149> PMID:21629271
50. Hughes AJ, Ben-Shlomo Y, Daniel SE, Lees AJ. What features improve the accuracy of clinical diagnosis in Parkinson’s disease: a clinicopathologic study. *Neurology.* 1992; 42:1142–46. <https://doi.org/10.1212/WNL.42.6.1142>. <http://www.ncbi.nlm.nih.gov/pubmed/1603339> PMID:1603339
51. Schouten JP, McElgunn CJ, Waaijer R, Zwiijnenburg D, Diepvens F, Pals G. Relative quantification of 40 nucleic acid sequences by multiplex ligation-dependent probe amplification. *Nucleic Acids Res.* 2002; 30:e57.

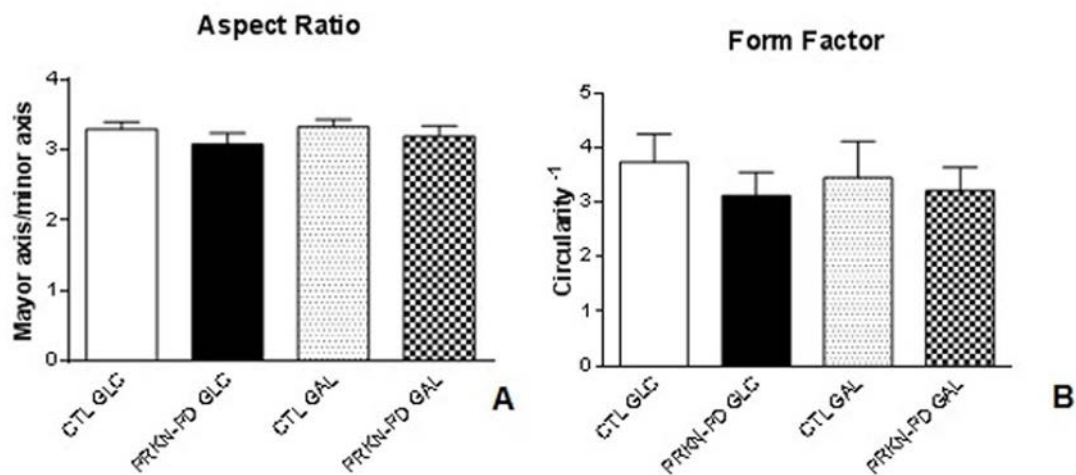
- <https://doi.org/10.1093/nar/gnf056> PMID:12060695
52. Morén C, Juárez-Flores DL, Cardellach F, Garrabou G. The Role of Therapeutic Drugs on Acquired Mitochondrial Toxicity. *Curr Drug Metab*. 2016; 17:648–62. <https://doi.org/10.2174/1389200217666160322143631> PMID:27000075
53. Sanuki Y, Araki T, Nakazono O, Tsurui K. A rapid mitochondrial toxicity assay utilizing rapidly changing cell energy metabolism. *J Toxicol Sci*. 2017; 42:349–58. <https://doi.org/10.2131/jts.42.349> PMID:28496041
54. Tsiper MV, Sturgis J, Avramova LV, Parakh S, Fatig R, Juan-García A, Li N, Rajwa B, Narayanan P, Qualls CW Jr, Robinson JP, Davisson VJ. Differential mitochondrial toxicity screening and multi-parametric data analysis. *PLoS One*. 2012; 7:e45226. <https://doi.org/10.1371/journal.pone.0045226> PMID:23077490
55. Marroquin LD, Hynes J, Dykens JA, Jamieson JD, Will Y. Circumventing the Crabtree effect: replacing media glucose with galactose increases susceptibility of HepG2 cells to mitochondrial toxicants. *Toxicol Sci*. 2007; 97:539–47. <https://doi.org/10.1093/toxsci/kfm052> PMID:17361016
56. Juárez-Flores DL, González-Casacuberta I, Ezquerro M, Bañó M, Carmona-Pontaque F, Catalán-García M, Guitart-Mampel M, Rivero JJ, Tobias E, Milisenda JC, Tolosa E, Marti MJ, Fernández-Santiago R, et al. Exhaustion of mitochondrial and autophagic reserve may contribute to the development of LRRK2^{G2019S} - Parkinson's disease. *J Transl Med*. 2018; 16:160. <https://doi.org/10.1186/s12967-018-1526-3> PMID:29884186
57. Pesta D, Gnaiger E. High-resolution respirometry: OXPHOS protocols for human cells and permeabilized fibers from small biopsies of human muscle. *Methods Mol Biol*. 2012; 810:25–58. https://doi.org/10.1007/978-1-61779-382-0_3 PMID:22057559
58. Medja F, Allouche S, Frachon P, Jardel C, Malgat M, Mousson de Camaret B, Slama A, Lunardi J, Mazat JP, Lombès A. Development and implementation of standardized respiratory chain spectrophotometric assays for clinical diagnosis. *Mitochondrion*. 2009; 9:331–39. <https://doi.org/10.1016/j.mito.2009.05.001> PMID:19439198
59. Catalán-García M, Garrabou G, Morén C, Guitart-Mampel M, Hernando A, Díaz-Ramos À, González-Casacuberta I, Juárez DL, Bañó M, Enrich-Bengoia J, Emperador S, Milisenda JC, Moreno P, et al. Mitochondrial DNA disturbances and deregulated expression of oxidative phosphorylation and mitochondrial fusion proteins in sporadic inclusion body myositis. *Clin Sci (Lond)*. 2016; 130:1741–51. <https://doi.org/10.1042/CS20160080> PMID:27413019
60. Barrientos A. In vivo and in organello assessment of OXPHOS activities. *Methods*. 2002; 26:307–16. [https://doi.org/10.1016/S1046-2023\(02\)00036-1](https://doi.org/10.1016/S1046-2023(02)00036-1) PMID:12054921
61. Garrabou G, Hernández AS, Catalán García M, Morén C, Tobías E, Córdoba S, López M, Figueras F, Grau JM, Cardellach F. Molecular basis of reduced birth weight in smoking pregnant women: mitochondrial dysfunction and apoptosis. *Addict Biol*. 2016; 21:159–70. <https://doi.org/10.1111/adb.12183> PMID:25186090
62. Morén C, González-Casacuberta I, Álvarez-Fernández C, Bañó M, Catalán-García M, Guitart-Mampel M, Juárez-Flores DL, Tobías E, Milisenda J, Cardellach F, Gatell JM, Sánchez-Palomino S, Garrabou G. HIV-1 promonocytic and lymphoid cell lines: an in vitro model of in vivo mitochondrial and apoptotic lesion. *J Cell Mol Med*. 2017; 21:402–09. <https://doi.org/10.1111/jcmm.12985> PMID:27758070
63. Morén C, Bañó M, González-Casacuberta I, Catalán-García M, Guitart-Mampel M, Tobías E, Cardellach F, Pedrol E, Peraire J, Vidal F, Domingo P, Miró Ò, Gatell JM, et al. Mitochondrial and apoptotic in vitro modelling of differential HIV-1 progression and antiretroviral toxicity. *J Antimicrob Chemother*. 2015; 70:2330–36. <https://doi.org/10.1093/jac/dkv101> PMID:25921514
64. Alvarez-Mora MI, Rodriguez-Revenga L, Madrigal I, Guitart-Mampel M, Garrabou G, Milà M. Impaired Mitochondrial Function and Dynamics in the Pathogenesis of FXTAS. *Mol Neurobiol*. 2017; 54:6896–902. <https://doi.org/10.1007/s12035-016-0194-7> PMID:27771901
65. Schindelin J, Arganda-Carreras I, Frise E, Kaynig V, Longair M, Pietzsch T, Preibisch S, Rueden C, Saalfeld S, Schmid B, Tinevez JY, White DJ, Hartenstein V, et al. Fiji: an open-source platform for biological-image analysis. *Nat Methods*. 2012; 9:676–82. <https://doi.org/10.1038/nmeth.2019> PMID:22743772
66. Morén C, Garrabou G, Noguera-Julian A, Rovira N, Catalán M, Hernández S, Tobías E, Cardellach F, Fortuny C, Miró Ò. Study of oxidative, enzymatic mitochondrial respiratory chain function and apoptosis in perinatally HIV-infected pediatric patients. *Drug Chem Toxicol*. 2013; 36:496–500. <https://doi.org/10.3109/01480545.2013.776578> PMID:23534415
67. Montero R, Grazina M, López-Gallardo E, Montoya J,

Briones P, Navarro-Sastre A, Land JM, Hargreaves IP, Artuch R, del Mar O'Callaghan M, Jou C, Jimenez C, Buján N, et al, and Coenzyme Q₁₀ Deficiency Study Group. Coenzyme Q₁₀ deficiency in mitochondrial DNA depletion syndromes. *Mitochondrion*. 2013; 13:337–41.

<https://doi.org/10.1016/j.mito.2013.04.001>
[PMID:23583954](https://pubmed.ncbi.nlm.nih.gov/23583954/)

68. Dagda RK, Chu CT. Mitochondrial quality control: insights on how Parkinson's disease related genes PINK1, parkin, and Omi/HtrA2 interact to maintain mitochondrial homeostasis. *J Bioenerg Biomembr*. 2009; 41:473–79. <https://doi.org/10.1007/s10863-009-9255-1> PMID:20012177
69. Barth S, Glick D, Macleod KF. Autophagy: assays and artifacts. *J Pathol*. 2010; 221:117–24. <https://doi.org/10.1002/path.2694> PMID:20225337
70. Aldridge GM, Podrebarac DM, Greenough WT, Weiler IJ. The use of total protein stains as loading controls: an alternative to high-abundance single-protein controls in semi-quantitative immunoblotting. *J Neurosci Methods*. 2008; 172:250–54. <https://doi.org/10.1016/j.jneumeth.2008.05.003> PMID:18571732
71. Trzaska KA, Kuzhikandathil EV, Rameshwar P. Specification of a dopaminergic phenotype from adult human mesenchymal stem cells. *Stem Cells*. 2007; 25:2797–808. <https://doi.org/10.1634/stemcells.2007-0212> PMID:17656644


SUPPLEMENTARY MATERIAL



Supplementary Figure 1. Mitochondrial network complexity in control and PRKN-PD fibroblasts. Mitochondrial length (aspect ratio) (A) and mitochondrial branching (form factor) (B) were comparable between groups in both media. The results are expressed as means and standard error of the mean (SEM). GAL= 10 mM galactose medium. GLC= 25 mM glucose medium. PRKN-PD= Parkin-associated PD fibroblasts.

ORIGINAL ARTICLE

Mitochondrial implications in human pregnancies with intrauterine growth restriction and associated cardiac remodelling

Mariona Guitart-Mampel^{1,2} | Diana L. Juarez-Flores^{1,2} | Lina Youssef^{3,4} |
 Constanza Moren^{1,2} | Laura Garcia-Otero^{3,4} | Vicente Roca-Agujetas^{1,2} |
 Marc Catalan-Garcia^{1,2} | Ingrid Gonzalez-Casacuberta^{1,2} | Ester Tobias^{1,2} |
 José C. Milisenda^{1,2} | Josep M. Grau^{1,2} | Fàtima Crispi^{3,4} | Eduard Gratacos^{3,4} |
 Francesc Cardellach^{1,2} | Glòria Garrabou^{1,2} 

¹Muscle Research and Mitochondrial Function Laboratory, Faculty of Medicine and Health Sciences, Internal Medicine Service-Hospital Clínic of Barcelona, Cellex-IDIBAPS, University of Barcelona, Barcelona, Spain

²CIBERER-U722, Madrid, Spain

³BCNatal—Barcelona Center for Maternal-Fetal and Neonatal Medicine (Hospital Clínic and Hospital Sant Joan de Déu), IDIBAPS, University of Barcelona, Barcelona, Spain

⁴CIBERER-U719, Madrid, Spain

Correspondence

Glòria Garrabou and Francesc Cardellach,
 Muscle Research and Mitochondrial
 Function Laboratory, Faculty of Medicine
 and Health Science, Internal Medicine
 Service-Hospital Clinic of Barcelona,
 Cellex-IDIBAPS, University of Barcelona,
 Barcelona, Spain.
 Emails: garrabou@clinic.cat;
 fcardell@clinic.cat

Funding information

CIBERER (an initiative of ISCIII); Fundació la Marató de TV3, Grant/Award Number: 87/C/2015; Erasmus + Programme of the European Union, Grant/Award Number: Framework Agreement number: 2013-0040; Fondo de Investigación Sanitaria, Grant/Award Number: FIS PI11/01199, PI14/00226, PI15/00817, PI15/00903, PI15/00130 and INT16/00168; CIBERER; InterCIBER, Grant/Award Number: PIE1400061; Instituto de Salud Carlos III; Suports a Grups de Recerca and CERCA Programme, Grant/Award Number: SGR893/2017 and SGR928/2017; CONACyt; "laCaixa" Foundation; Cerebra

Abstract

Intrauterine growth restriction (IUGR) is an obstetric complication characterised by placental insufficiency and secondary cardiovascular remodelling that can lead to cardiomyopathy in adulthood. Despite its aetiology and potential therapeutics are poorly understood, bioenergetic deficits have been demonstrated in adverse foetal and cardiac development. We aimed to evaluate the role of mitochondria in human pregnancies with IUGR. In a single-site, cross-sectional and observational study, we included placenta and maternal peripheral and neonatal cord blood mononuclear cells (PBMC and CBMC) from 14 IUGR and 22 control pregnancies. The following mitochondrial measurements were assessed: enzymatic activities of mitochondrial respiratory chain (MRC) complexes I, II, IV, I + III and II + III, oxygen consumption (cell and complex I-stimulated respiration), mitochondrial content (citrate synthase [CS] activity and mitochondrial DNA copy number), total ATP levels and lipid peroxidation. Sirtuin3 expression was evaluated as a potential regulator of bioenergetic imbalance. Intrauterine growth restriction placental tissue showed a significant decrease of MRC CI enzymatic activity ($P < 0.05$) and CI-stimulated oxygen consumption ($P < 0.05$) accompanied by a significant increase of Sirtuin3/ β -actin protein levels ($P < 0.05$). Maternal PBMC and neonatal CBMC from IUGR patients presented a not significant

Francesc Cardellach and Glòria Garrabou made an equal contribution.

This is an open access article under the terms of the Creative Commons Attribution License, which permits use, distribution and reproduction in any medium, provided the original work is properly cited.

© 2019 The Authors. Journal of Cellular and Molecular Medicine published by John Wiley & Sons Ltd and Foundation for Cellular and Molecular Medicine.

Foundation for the Brain Injured Child (Carmarthen, Wales, UK); Fundació La Marató de TV3, Grant/Award Number: 87/C/2015; Fundació Privada Cellex, Grant/Award Number: CP042187

decrease in oxygen consumption (cell and CI-stimulated respiration) and MRC enzymatic activities (CII and CIV). Moreover, CS activity was significantly reduced in IUGR new-borns ($P < 0.05$). Total ATP levels and lipid peroxidation were preserved in all the studied tissues. Altered mitochondrial function of IUGR is especially present at placental and neonatal level, conveying potential targets to modulate obstetric outcome through dietary interventions aimed to regulate Sirtuin3 function.

KEYWORDS

bioenergetics, foetal growth, mitochondria, Sirt 3

1 | INTRODUCTION

Intrauterine growth restriction (IUGR) is a common pregnancy complication that arises when the foetus does not achieve its growth potential and affects 5%-10% of all pregnancies.^{1,2} Recent evidence demonstrated that IUGR is associated with foetal cardiovascular remodelling (CVR)^{5,6} which may eventually result in a cardiovascular risk in adulthood.^{7,8}

However, the aetiopathology that underlies IUGR is still a matter of doubt. In many cases, IUGR is associated with placental insufficiency.^{11,12} The placenta is the organ enabling nutrient and oxygen supply to the foetus.^{14,15} Consequently, it plays a pivotal role for the adequate foetal development, since it requires high energy production for metabolic processes and cell growth.^{16,17}

Mitochondria are key organelles responsible for providing cellular energy in terms of ATP synthesised in the mitochondrial respiratory chain (MRC). Thus, mitochondria are essential for successful foetal development^{19,20} and proper cardiac function.^{21,22} Consequently, abnormalities in mitochondrial function and uteroplacental vessels formation have been associated with both adverse perinatal outcomes (preterm birth, IUGR, preeclampsia or stillbirth)²⁰ and cardiac disease.²³

Mitochondria are governed by nuclear effectors such as sirtuins, aimed to modulate mitochondrial disturbances depending on cellular energetic needs and dietetic habits.^{24,25} For instance, there is evidence that Sirtuin3 would modulate mitochondrial respiration and attenuate reactive oxygen species (ROS) production by activating and deactivating mitochondrial target proteins through deacetylation of key lysine residues.^{26,27} The emergent role of Sirtuin3 in regulating diverse pathways in mitochondrial metabolism and stress response is evidenced in a situation of nutrient restriction²⁹ and also in cardiovascular disease.^{24,25} Interestingly, both nutrient and CVR have been associated with IUGR.

However, there are few and quite contradictory mitochondrial studies in human IUGR pregnancies. Some have reported a mitochondrial implication in placenta by transcriptomic analysis,³⁰ metabolic disarrangements in serum of IUGR infants³¹ or less mitochondrial DNA (mtDNA) in cytotrophoblast cells.¹⁸ Mandó et al have also described lower MRC mRNA expression in cytotrophoblast cells but

no alterations at protein level.¹⁸ While others found altered MRC enzymatic activities in human placental homogenate.³²

Overall, these studies pointed out mitochondrial alterations as a potential target in IUGR but also highlighted the need for deep mitochondrial characterisation where Sirtuin3 implication may also be explored. Our group previously evidenced mitochondrial transcriptomic, ultrastructural and function alterations in the target tissue of CVR (heart) and placental insufficiency (placenta) in a rabbit model of IUGR.^{33,34} To validate these findings in human pregnancies, the present work hypothesised that similar mitochondrial disarrangements would be present in human placenta.³⁴ This information could generate fresh insights in disease aetiology that, in turn, could be useful to develop targeted interventions aimed to reverse this obstetric outcome. Secondly, the present study was designed to overcome target tissue limitation of CVR in humans by evaluating potential mitochondrial deficits in peripheral tissues as maternal peripheral blood mononuclear cells (PBMC) and neonatal cord blood mononuclear cells (CBMC). The benefit of finding mitochondrial abnormalities in peripheral tissues would be the development of new potential biomarkers and therapeutic targets.

2 | EXPERIMENTAL

2.1 | Study design

A single-site, cross-sectional and observational study at the Maternal-Fetal Medicine Department of the Hospital Clinic of Barcelona (Spain) was conducted for 2 years.

2.2 | Study population

This study included 14 IUGR pregnancies, defined as estimated birth weight <3rd percentile or, alternatively, <10th percentile in case of abnormal uterine artery Doppler or abnormal cerebroplacental ratio.^{35,36} Birth weight percentile was calculated considering birth weight, weeks of gestation and neonatal gender. Despite final IUGR diagnostic is confirmed at delivery, all potential IUGR pregnancies were monitored by Doppler every week during gestation. In parallel, 22 uncomplicated pregnancies were considered as the control group.¹¹

The inclusion criteria were: >18 years, singleton pregnancies, >22 weeks of gestation and no tobacco consumption in both IUGR and control pregnancies. Pregnant women taking potentially toxic drugs for mitochondria and with familial history of mitochondrial disease were excluded.

The study was approved by the Ethical Committee of our hospital (2013/8246) and followed the Declaration of Helsinki guidelines. All participants provided a written informed consent.

2.3 | Sample collection and processing

At delivery, placental samples were weighted and, after discarding blood residuals, a full thickness section (from both maternal and foetal side) was obtained and processed as follows: 500 mg were homogenised (Caframo technologies, Ontario, Canada) with 10% BSA-SolutionA to isolate fresh mitochondria and immediately perform ex vivo oxygen consumption assays.³⁷ The remaining tissue was immediately cryopreserved at -80°C and further homogenised at 5% (w/v) in Mannitol for the rest of mitochondrial analysis.

Additionally at delivery, 10-20 mL of maternal peripheral blood and neonatal cord blood were collected in ethylenediaminetetraacetic acid-tubes to isolate plasma, PBMC and CBMC by a Ficoll gradient.³⁸ One aliquot of each sample was maintained in fresh conditions to assess ex vivo oxygen consumption. The remaining aliquots were stored at -80°C for mitochondrial analysis.

The usefulness of mononuclear cells for the study of mitochondrial dysfunction has been previously validated. It offers an accessible and non-invasive approach and the possibility to find new potential biomarkers for diagnosis and prognosis.^{39,40}

Protein content was measured through the bicinchoninic acid colorimetric assay following manufacturer's instructions (Thermo Scientific, Waltham, MA) to normalise experimental measurements.

2.4 | BNP levels in cord blood

As a reliable marker of neonatal cardiac remodelling,⁴² brain natriuretic peptide (BNP) levels were measured in neonatal plasma by the CORE laboratory of our Hospital using an Advia Centaur XP.⁴³

2.5 | Mitochondrial oxygen consumption

Based on previous transcriptomic results pointing out MRC complex I (CI) deregulation,³³ oxygen consumption was measured through the stimulation of CI. Briefly, isolated placental mitochondria, PBMC and CBMC were used in fresh conditions to determine oxygen consumption by polarography (Hansatech Instruments, Pentney, UK) in a 'respiration medium' (0.3 mol/L Mannitol, 10 mmol/L KCl, 5 mmol/L $\text{MgCl}_2 \cdot 6\text{H}_2\text{O}$ and 10 mmol/L potassium phosphate).⁴⁴ Cellular oxygen consumption for endogenous substrates (abbreviated as Cellox) was measured in intact PBMC and CBMC. Digitonin was then used to permeabilise blood cells. Manual titration of substrates for CI stimulation (1 mol/L glutamate and 0.5 mol/L malate or 0.25 mol/L pyruvate and 0.5 mol/L malate; referred as GM oxidation, GMox and PM oxidation, PMox) was performed using

Hamilton syringes (Hamilton Company, Reno, NV). Respiratory quality controls were added into the assay by assessing drug response to phosphate acceptors (50 mmol/L Adenine diphosphate), uncouplers (0.25 $\mu\text{mol/L}$ CCCP) and respiratory inhibitors (0.2 mmol/L antimycin a). Data were recorded using O_2 view Software.

The results were expressed as picomoles of consumed oxygen per second and milligram of protein ($\text{pmol O}_2/\text{s mg prot.}$).

2.6 | Mitochondria respiratory chain enzymatic activities and mitochondrial content

2.6.1 | Enzymatic activities of MRC and citrate synthase

The enzymatic activities of MRC complexes I, II, IV, I + III and II + III (CI, CII, CIV, CI + III and CII + III) were measured spectrophotometrically in placenta according to national standardised methods.⁴⁵ Following the same protocols, the measurement of enzymatic activities of MRC in maternal PBMC and neonatal CBMC was restricted to CII and CIV based on previous results of mitochondrial function obtained from the animal model.³⁴

Citrate synthase (CS) activity was also measured spectrophotometrically,^{41,45} as an enzyme belonging to the tricarboxylic acid (TCA) cycle, widely used as a reliable marker of mitochondrial content.⁴⁶

Absorbance changes along time were monitored in a HITACHI-U2900 spectrophotometer using the UV-Solution software 2.2 and were expressed as nanomoles of consumed substrate or generated product per minute and milligram of protein ($\text{nmol/min-mg protein}$).

2.6.2 | Mitochondrial DNA levels

Alternative measurement to determine mitochondrial content was performed by analysing mtDNA copy number. Thus, total DNA was phenol-chloroform-extracted from neonatal CBMC. Multiplex qPCR 7500 Real Time PCR System from Applied Biosystems (Foster City, CA) was used.⁴⁷

Briefly, quantification of the mitochondrial 12S ribosomal RNA (mt12SrRNA) gene and the constitutive nuclear RNaseP gene was performed and results were expressed as the mt12SrRNA/nRNaseP ratio.

2.7 | Total cellular ATP levels

Cellular ATP levels were quantified in each tissue using the Luminescent ATP Detection Assay Kit (Abcam, Cambridge, UK). The results were expressed as picomolar of ATP per milligram of protein ($\text{pmol ATP/mg protein}$).

2.8 | Lipid peroxidation (oxidative damage)

Lipid peroxidation was measured as an indicator of oxidative damage in to lipid membranes using the BIOXYTECH-LPO-586™ assay by the spectrophotometric measurement of malondialdehyde (MDA) and 4-hydroxyalkenal (HAE) levels (Oxis International Inc, Los Angeles,

TABLE 1 Sociodemographic characteristics and perinatal outcomes of the study groups

Parameter	Control N = 22	IUGR N = 14	P value
Maternal age (y)	33.82 ± 1.12	34.43 ± 1.34	NS
Weeks of gestation at delivery	39.47 ± 0.20	35.42 ± 1.03	<0.001
Mode of delivery	20 caesarean section (91%) Two vaginal (9%)	14 caesarean section (100%) 0 vaginal (0%)	NS OR [95% CI] = 0.28 [0.01-6.34]
Birth weight (g)	3440.27 ± 87.59	1742.29 ± 171.31	<0.001
Birth weight percentile	58.32 ± 5.94	0.64 ± 0.23	<0.001
Placental weight (g)	566.67 ± 118.93	329.64 ± 24.26	<0.05
New-born sex	45% women 55% men	54% women 46% men	NS OR [95% CI] = 0.70 [0.17-2.85]
pH umbilical artery cord blood	7.26 ± 0.01	7.24 ± 0.03	NS
Apgar 5'	21 normal (95%) One abnormal (5%)	Nine normal (64%) Five abnormal (36%)	<0.05 OR [95% CI] = 11.67 [1.19-114.65]
Preeclampsia	0 (0%)	4 (28.6%)	<0.05 OR [95% CI] = 0.05 [0.00-1.06]
Cord blood BNP levels (pg/mL)	26.84 ± 3.03	85.68 ± 26.28	<0.05

Values are presented as mean ± SEM or percentage of positive cases within the study cohort. Case-control differences were sought by non-parametric statistical analysis.

BNP, brain natriuretic peptide; CI, confidence interval; g, grams; IUGR, intrauterine growth restriction; N, sample size; NS, not significant; OR, odds ratio; y, years.

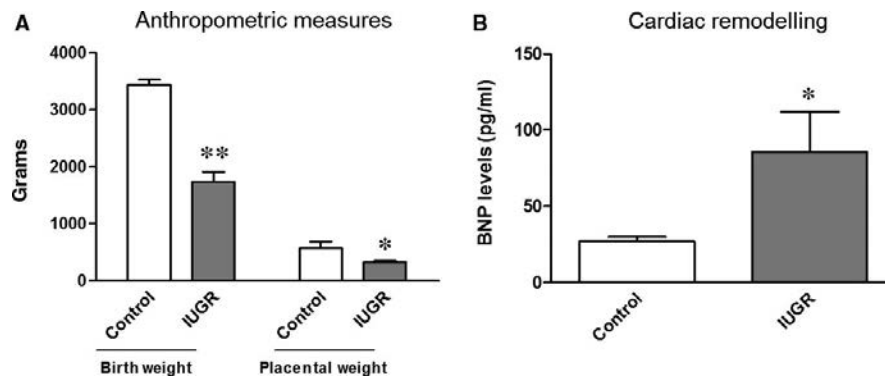


FIGURE 1 A, Anthropometric measures of the study groups. Birth weight is significantly reduced in new-borns from IUGR pregnancies (grey bar) compared to controls (empty bar), as well as placental weight. B, Cardiac remodelling in new-borns from IUGR pregnancies. BNP levels were significantly increased in neonatal plasma from IUGR pregnancies (grey bars) with respect to controls (empty bars). Results are expressed as mean ± SEM. Mann-Whitney tests were used to seek for statistical analysis between groups. BNP, brain natriuretic peptide; IUGR, intrauterine growth restriction; * $P < 0.001$; * $P < 0.05$

CA, USA). The results were expressed as micromolar of MDA and HAE per milligram of protein ($\mu\text{mol/L}$ MDA + HAE/mg protein).

2.9 | Expression of Sirtuin3 in placenta

The protein content of Sirtuin3, a sensor of mitochondrial and metabolic balance, was determined by Western blot. Forty μg of total protein placental homogenate were separated using 7/13% SDS-PAGE and transferred into nitrocellulose membranes (iBlot Gel Transfer Stacks; Life Technologies, Waltham, MA, USA). The membranes were hybridised with anti-Sirtuin3 (44 KD; 1:250; Merck

Millipore, Burlington, MA, USA) overnight and at 4°C. Sirtuin3 protein expression was normalised by β -actin protein (47 KD; 1:30 000; Sigma-Aldrich, St. Louis, MO). The ImageQuantLD program was used to quantify chemiluminescence and the results were expressed as the Sirtuin3/ β -actin ratio.

2.10 | Statistical analysis

Statistics were performed using the 'IBM SPSS Statistics 20' software. Clinical and experimental results were filtered once for outliers and expressed as percentage, means ± SEM or percentage of increase/

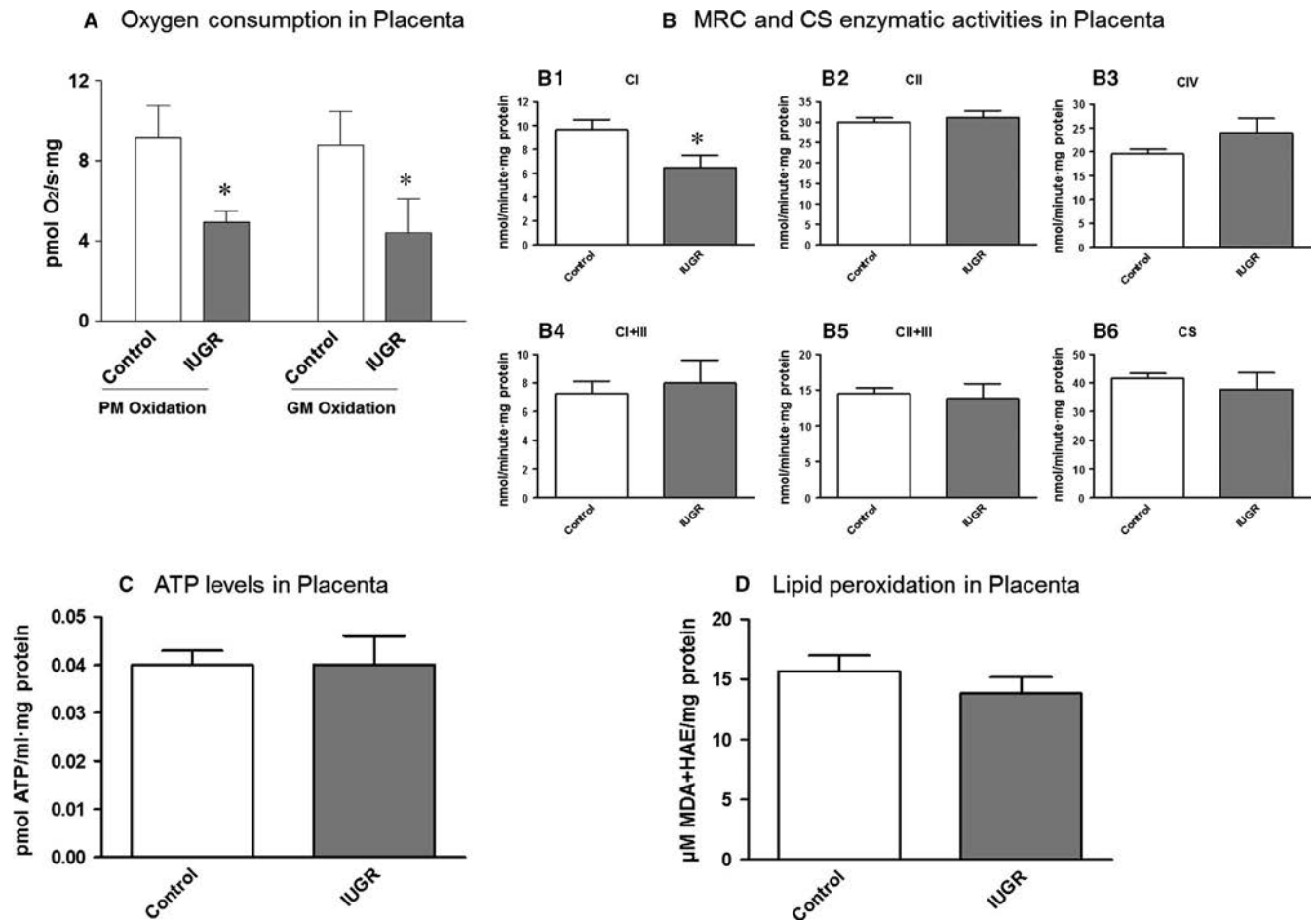


FIGURE 2 A, Oxygen consumption in placental mitochondria of the study groups. A significant decrease in MRC Complex I-stimulated oxygen consumption (both PM and GM Oxidation) was observed in the IUGR cohort (grey bars) compared to controls (empty bars). B, Enzymatic activities of the complexes of the MRC and CS in placental tissue of the study groups. A significant decreased was observed of complex I activity in placenta from IUGR pregnancies (B1: grey bars) while other complexes (B2, B3, B4, B5) and also CS (B6) activity remained conserved. C, Total ATP levels in placental tissue of the study groups. No significant differences were observed between IUGR pregnancies (grey bars) and controls (empty bars). D, Lipid peroxidation as an indicator of oxidative damage in placental tissue of the study groups. No significant differences were evidenced in placental tissue between IUGR pregnancies (grey bars) and controls (empty bars). Results are expressed as mean \pm SEM and Mann-Whitney tests were used to seek for statistical analysis between groups. ATP, adenosine triphosphate; CI, complex I; CII, complex II; CIV, complex IV; CI + III, complex I + III; CII + III, complex II + III; CS, citrate synthase; GM oxidation, glutamate/malate oxidation; HAE, 4-hydroxyalkenal; IUGR, intrauterine growth restriction; MDA, malondialdehyde; PM oxidation, pyruvate/malate oxidation; MRC, mitochondrial respiratory chain; * $P < 0.05$

decrease of IUGR cases compared to controls. Comparisons at placental, maternal or neonatal level were always done between cases and controls (IUGR versus control pregnancies). Nonparametric tests were used to determine: case-control differences (Mann-Whitney independent sample analysis or odds ratio by Fisher's exact test) and parameter correlation (Spearman's rank coefficient). Significance was set at $P < 0.05$.

3 | RESULTS

3.1 | Clinical parameters

Table 1 shows sociodemographic characteristics and perinatal outcomes of study groups. No differences were found between groups

regarding maternal age, mode of delivery, new-born sex or pH umbilical artery cord blood.

As expected, IUGR pregnancies presented abnormal 5-minute Apgar score ($P < 0.05$; Table 1) and an earlier gestational age at delivery compared to controls ($P < 0.001$; Table 1) because our clinical protocol for IUGR indicate induction of delivery about 37 weeks of gestation. Additionally, birth weight, birth weight percentile and placental weight were significantly decreased in IUGR cases with respect to controls ($P < 0.001$; $P < 0.001$ and $P < 0.05$, respectively; Figure 1A; Table 1). Moreover, IUGR group showed higher prevalence of preeclampsia ($P < 0.05$; Table 1).

Brain natriuretic peptide levels were significantly increased by $219.23 \pm 97.91\%$ in IUGR neonatal plasma compared to controls ($P < 0.05$; Figure 1B; Table 1).

3.2 | Mitochondrial study in placenta

3.2.1 | Mitochondrial oxygen consumption

Significant decreases of $46.12 \pm 5.79\%$ and $49.71 \pm 19.54\%$ in CI-stimulated oxygen consumption (PMox and GMox, respectively) were observed in placental mitochondria from IUGR pregnancies compared to controls ($P < 0.05$; Figure 2A; Table S1).

3.2.2 | Mitochondria respiratory chain enzymatic activities and mitochondrial content

Mitochondria respiratory chain CI enzymatic activity was also significantly decreased in placenta from IUGR pregnancies compared to controls ($-32.95 \pm 10.36\%$; $P < 0.05$; Figure 2B; Table S1), despite other MRC complexes (CII, CIV, CI + III and CII + III) were preserved (Figure 2B; Table S1).

Citrate synthase activity was conserved in placenta between groups (Figure 2B; Table S1).

3.2.3 | Total cellular ATP levels

No remarkable differences were observed in ATP content between groups (Figure 2C; Table S1).

3.2.4 | Lipid peroxidation (oxidative damage)

No relevant changes were observed in lipid peroxidation between groups (Figure 2D; Table S1).

3.2.5 | Sirtuin3 protein expression

A significant $117.78 \pm 51.11\%$ (according to Table S1) increase of Sirtuin3/ β -actin protein expression was observed in IUGR placenta with respect to controls ($P < 0.05$; Figure 3A,B; Table S1).

3.3 | Mitochondrial study in maternal and neonatal mononuclear cells

3.3.1 | Mitochondrial oxygen consumption

Peripheral blood mononuclear cells from IUGR pregnant women presented conserved cellular oxygen consumption ($p = \text{NS}$; Figure 4A; Table S2) and trends to decrease of CI-stimulated oxygen consumption compared to controls (PMox: $-31.55 \pm 11.36\%$ and GMox: $-25.00 \pm 10.45\%$; $p = \text{NS}$; Figure 4A; Table S2).

Despite not reaching statistical significance, CBMC from IUGR new-borns presented a tendency to decrease of cellular and CI-stimulated oxygen consumption compared to controls (Cellox: $45.63 \pm 14.19\%$; PMox: -49.90 ± 11.39 ; GMox: -55.73 ± 11.45 ; all $p = \text{NS}$; Figure 4A; Table S3). Noticeably, IUGR new-borns presented greater mitochondrial deficits compared to mothers.

3.3.2 | Mitochondria respiratory chain enzymatic activities and mitochondrial content

No differences in MRC CII and CIV enzymatic activities were observed in maternal PBMC or in neonatal CBMC (Figure 4B; Tables S2 and S3) between IUGR cases and controls.

Moreover, despite conserved CS activity in PBMC from IUGR pregnant women (Figure 4B; Table S2), there was a significant $39.19 \pm 12.61\%$ decrease in CBMC from IUGR new-borns compared to controls ($P < 0.05$; Figure 4B; Table S3).

In order to elucidate if the decrease of CS in CBMC from IUGR new-borns was due to abnormalities in TCA cycle or in mitochondrial content, we measured alternative markers of mitochondrial mass such as levels of mtDNA that resulted unaltered between IUGR and control groups (Table S3).

3.3.3 | Total cellular ATP levels

No differences in ATP content were observed in IUGR group compared to controls (Figure 4C; Tables S2 and S3).

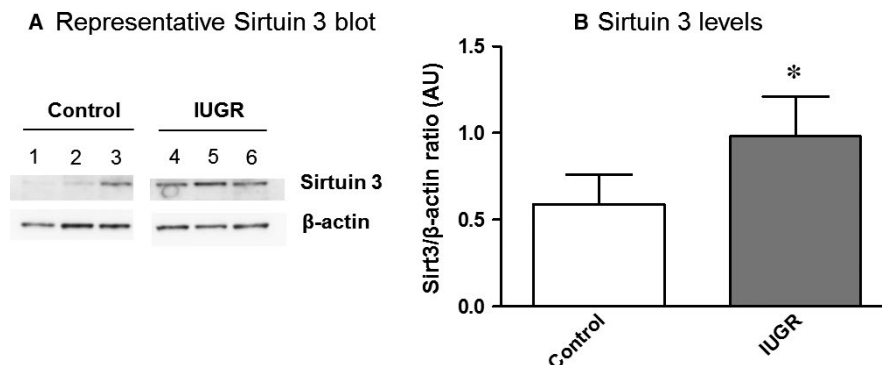


FIGURE 3 Sirtuin3 protein levels in placenta of the study groups. A, A representative Western Blot of Sirtuin3 protein expression in human placenta is shown in both controls (1-3) and IUGR pregnancies (4-6). β -actin was used as the loading control. B, Graph showing the significant increase of Sirtuin3 levels (Sirt3/ β -actin ratio) in IUGR pregnancies (grey bars) compared with controls (empty bars). Results are expressed as mean \pm SEM. Mann-Whitney tests were used to seek for statistical analysis between groups. AU, Arbitrary units; IUGR, Intrauterine growth restriction; Sirt3, Sirtuin3; * $P < 0.05$

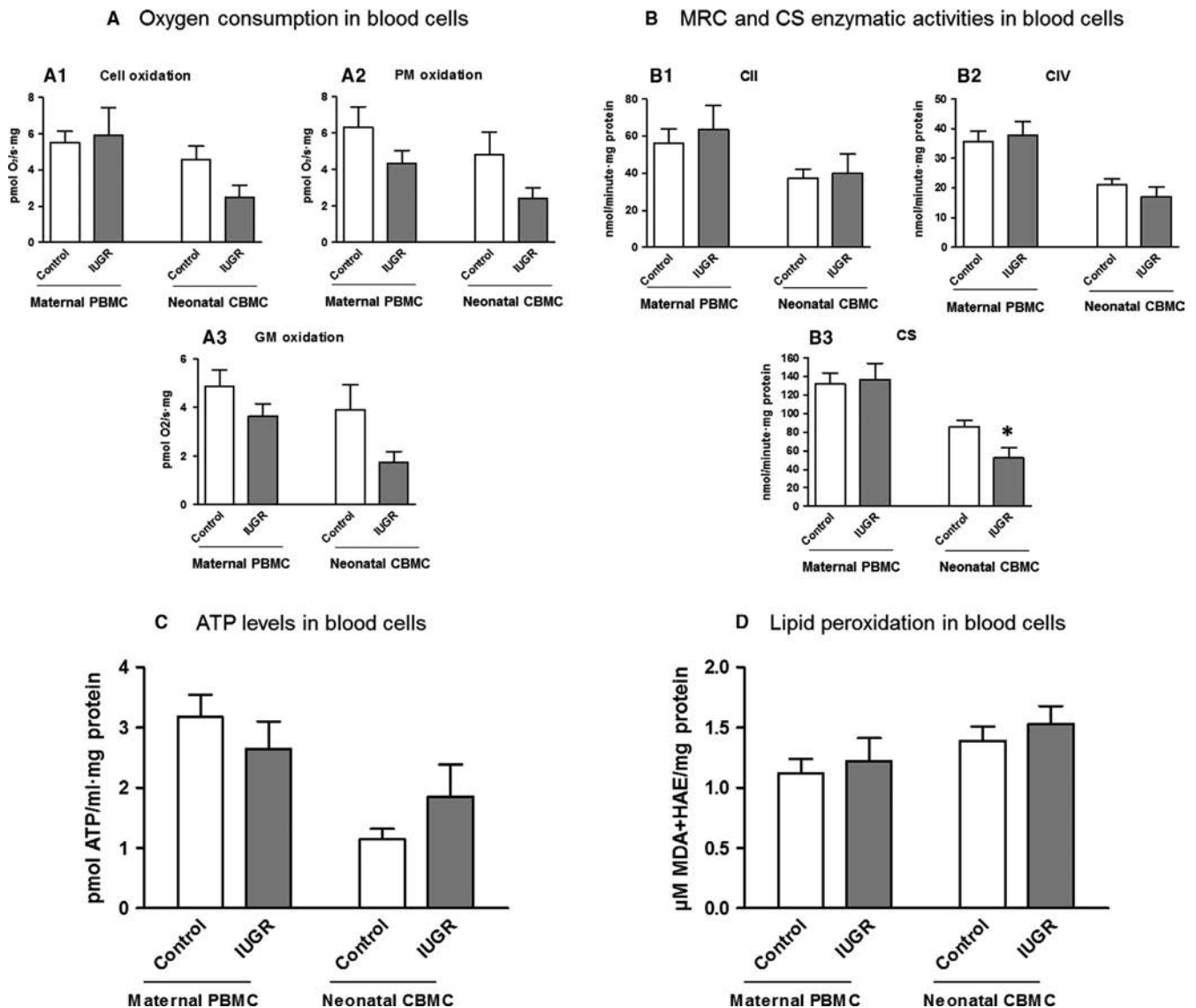


FIGURE 4 A, Oxygen consumption in maternal and neonatal blood cells of the study groups. Maternal PBMC from IUGR pregnant women (grey bars) presented conserved cellular oxygen consumption (A1) and trends to decrease of oxygen consumption stimulated for CI (A2-3) compared to controls (empty bars). Despite not reaching statistical significance, neonatal CBMC from IUGR new-borns (grey bars) presented a tendency to decrease of both cellular and CI-stimulated oxygen consumption (A1-3) compared to controls (empty bars). Additionally, IUGR new-borns presented higher oxygen consumption deficiencies compared to mothers. B, Enzymatic activities of the complexes of the MRC and CS in maternal and neonatal blood cells of the study groups. IUGR cohort is presented as grey bars and controls as empty bars. No remarkable differences were evidenced in maternal PBMC. However, a significant decrease of CS activity was found in neonatal CBMC (B3). C, Total ATP levels in maternal and neonatal blood cells of the study groups. No significant differences were observed either in maternal PBMC or in neonatal CBMC between IUGR pregnancies (grey bars) and controls (empty bars). D, Lipid peroxidation as an indicator of oxidative damage in maternal and neonatal blood cells of the study groups. No significant differences were evidenced either in maternal PBMC and neonatal CBMC between IUGR pregnancies (grey bars) and controls (empty bars). Results are expressed as a percentage of increase or decrease with respect to controls \pm SEM (A,B) and as mean \pm SEM (C,D). Mann-Whitney tests were used to seek for statistical analysis between groups. ATP, adenosine triphosphate; CBMC, cord blood mononuclear cells; cell oxidation, cellular endogen oxidation (without substrates); CI, complex I activity; CII, complex II activity; CIV, complex IV activity; CI + III, complex I + III activity; CII + III, complex II + III activity; CS, citrate synthase activity; GM oxidation, glutamate and malate oxidation; HAE, 4-hydroxyalkenal; IUGR, intrauterine growth restriction; MDA, malondialdehyde; MRC, mitochondrial respiratory chain; PBMC, peripheral blood mononuclear cells; PM oxidation, pyruvate and malate oxidation; * $P < 0.05$

3.3.4 | Lipid peroxidation (oxidative damage)

No changes were observed in lipid peroxidation between IUGR and control groups (Figure 4D; Tables S2 and S3).

3.4 | Associations between clinical data and experimental results

Birth weight, as well as placental weight, were negatively correlated with BNP levels, confirming the association of IUGR with

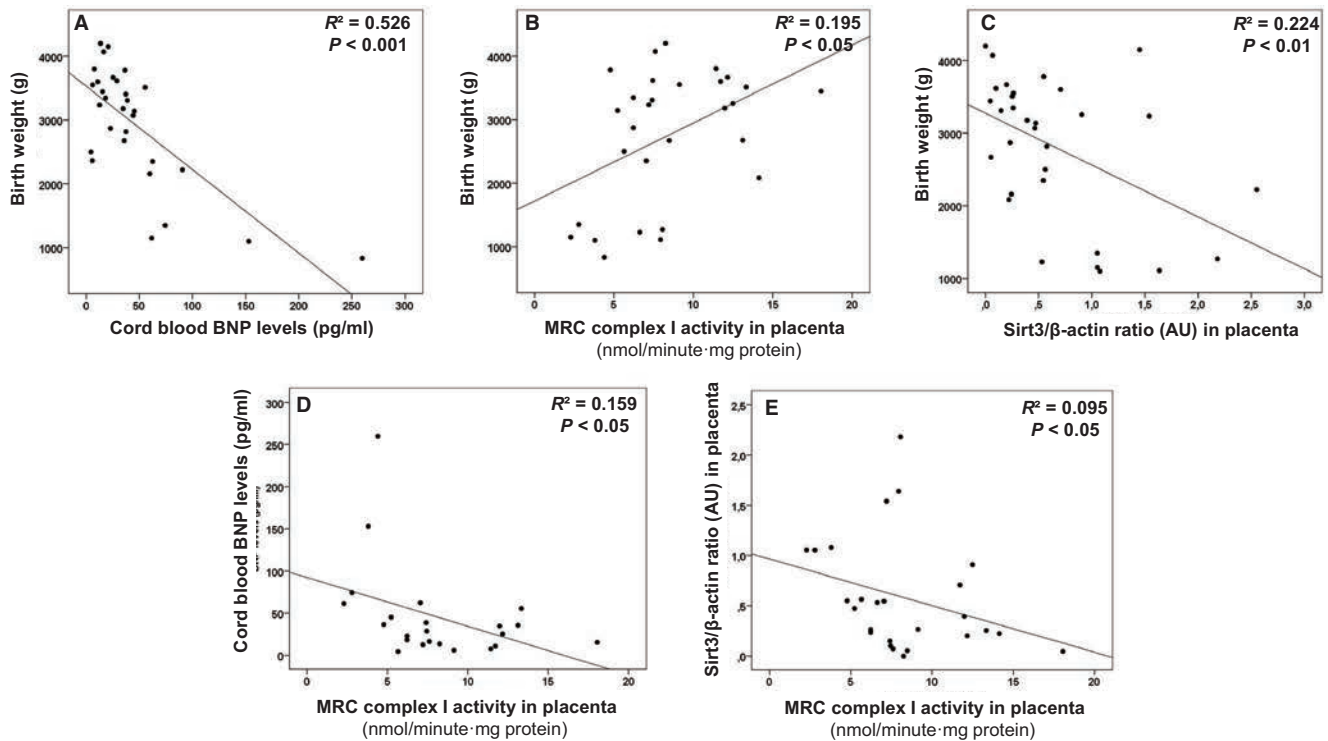


FIGURE 5 Association between clinical data and experimental results from pregnancies complicated by IUGR and controls. Decreased birth weight characteristic of IUGR is associated to increased BNP levels (as sign of cardiovascular remodelling) (A), decreased MRC CI in placenta (B) and enhanced Sirtuin3 protein expression (C). Additionally, impairment in MRC CI in placenta was directly associated to increased neonatal BNP levels (D) and placental Sirtuin3 protein expression (E), demonstrating the strong association among all these parameters. Spearman Rho tests were used to seek for statistical analysis. AU, Arbitrary units; BNP, Brain natriuretic peptide; CBMC, Cord blood mononuclear cells; CI, MRC complex I; g, grams; IUGR, intrauterine growth restriction; MRC, Mitochondrial respiratory chain; Sirt3, Sirtuin3

CVR ($P < 0.001$ and $P < 0.01$, respectively; Figure 5A; Table S4). Secondly, birth weight was also positively correlated with CI-stimulated oxygen consumption (PMox and GMox $P < 0.05$; Table S4) and CI enzymatic activity ($P < 0.05$; Figure 5B; Table S4) in placenta, suggesting that a proper new-born weight promotes optimal MRC CI function in placenta, or more likely, that efficient placental CI function is required to reach a proper birth weight. Additionally, birth weight was negatively correlated with placental Sirtuin3 levels ($P < 0.05$; Figure 5C; Table S4), suggesting the adaptation mechanism of Sirtuin3 up regulation in response to IUGR.

Brain natriuretic peptide levels were also negatively correlated with CI enzymatic activity in placenta ($P < 0.01$; Figure 5D; Table S4) which additionally was negatively correlated with placental Sirtuin3 levels ($P < 0.05$; Figure 5E; Table S4). Those associations suggest that CVR is characterised by CI impairment and adaptive increase of Sirtuin3 levels in the placenta (Figure 6).

Moreover, maternal and neonatal CI-stimulated oxygen consumption were positively correlated (GMox; $P < 0.05$; Table S4), demonstrating the strong dependence of neonatal metabolism on maternal status. Additionally, neonatal oxygen consumption positively correlated with neonatal CS activity (Cell oxidation: $P < 0.05$; PM oxidation: $P < 0.05$; and GM oxidation: $P \leq 0.001$; Table S4), suggesting the dependence of a proper mitochondrial function in

TCA activity. Finally, this neonatal oxygen consumption also positively correlated with placental CI-stimulated oxygen consumption ($P < 0.05$; Table S4), pointing out the dependence of neonatal health on accurate placental function.

4 | DISCUSSION

The molecular basis of IUGR and CVR is still a matter of doubt, but major concerns are raised due to the high prevalence of this obstetric problem and the putative consequences in adulthood. Previous experimental studies pointed out that mitochondrial deficits play a relevant role in IUGR and associated CVR.^{33,34} However, few and contrasting studies were found in the literature investigating mitochondrial alterations in human pregnancies, pointing out the need for a wider study of mitochondrial involvement in patients with this obstetric complication.

Human mitochondrial function alterations in IUGR have been previously demonstrated in placenta, specifically in isolated mitochondria or derived cultured cells.^{18,30,32} Besides, only scarce data studying mitochondrial function in neonatal CBMC have been published so far.⁴⁸ Herein, we present a wide characterisation of mitochondrial function in human placenta together with simultaneous studies in maternal PBMC and neonatal CBMC.

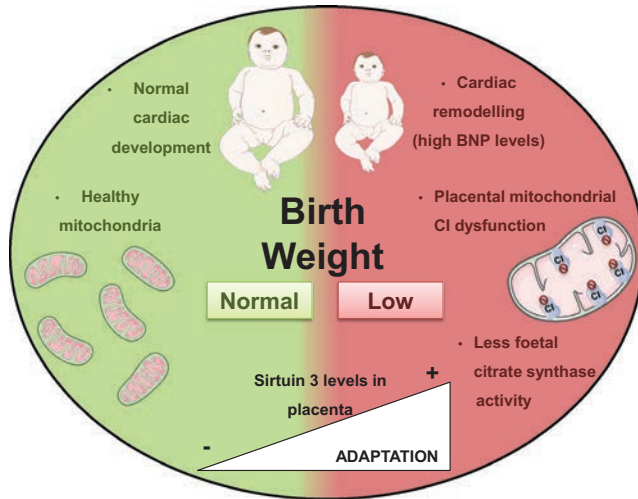


FIGURE 6 Mitochondrial and cardiac features of human pregnancies in two contexts, complicated by intrauterine growth restriction (right side in red) and with no apparent obstetric problems (left side in green). In IUGR new-borns, low birth weight was associated to a higher levels of BNP in new-borns (indicating a potential cardiac remodelling), lower mitochondrial complex I function in placenta and decreased neonatal citrate synthase activity (representative of metabolic mitochondrial activity). In this context, there was an increase of placental protein Sirtuin3 levels, probably as a potential adaptation mechanism aimed to modulate the adverse mitochondrial phenotype reported in this obstetric complication. On the other hand, all these mitochondrial parameters were found within normal ranges in healthy children with no apparent IUGR. BNP, brain natriuretic peptide; CI, mitochondrial respiratory chain complex I; IUGR, intrauterine growth restriction

Our results provided evidence of mitochondrial imbalance in placenta from IUGR pregnancies focused on CI-stimulated oxygen consumption and enzymatic activity (Figure 6). This significant CI deficiency was previously described by our group at transcriptional level in heart tissue of an IUGR animal model³³ and also by Beyramzadeh et al in placenta from high risk pregnancies.³² Conversely to our findings, Mandó et al observed higher oxygen consumption stimulated either through CI + CII or CIV in placenta from IUGR cases.¹⁸ Such discrepancies may be due to differential stimulation of specific MRC complexes and the presence of different cell linages (cytotrophoblasts and syncytiotrophoblasts) that have multiple functions, different mitochondria and also respond differently to stimulus.⁴⁹ In accordance with placental MRC CI impairment in the studied patients, placental Sirtuin3 protein expression significantly increased, probably, as an adaptation mechanism to modulate the adverse mitochondrial phenotype.

This mitochondrial imbalance was also evident in CBMC of IUGR new-borns through the significant decrease of CS activity, not described so far. Citrate synthase is a reliable marker of mitochondrial content,⁴⁶ but it is also an enzyme participating in the TCA cycle. As parallel measurement of alternative markers of mitochondrial content (mtDNA levels) yielded to results suggestive of preserved

mitochondrial mass, we concluded that alterations in CS activity would be mainly related to new-born metabolic imbalance of TCA cycle. Previous studies in obstetric complications associated with placental insufficiency such as IUGR or preeclampsia, showed contrasting results for mitochondrial content.^{18,50,51} Noticeably, in this study, mitochondrial content was maintained also in placenta and in maternal PBMC.

Maternal PBMC were neither affected for mitochondrial function alterations, reinforcing both the placenta and the new-born as the main targets of this obstetric complication.

Remarkably, in the present study, BNP levels were significantly higher in IUGR new-borns, confirming the neonatal CVR previously reported by our group and others.^{42,54,55} Additionally, birth weight was inversely associated with BNP levels confirming the strong association between IUGR and CVR; moreover, birth weight was also directly correlated to placental CI activity and inversely correlated with placental Sirtuin3 expression, thus reinforcing mitochondrial implication in this obstetric complication.

In regard to Sirtuin3, its expression has been associated to increased bioenergetic demands,^{24,25} often in the context of cardiovascular disease, acting as a protective mechanism in front of different stimulus, such as mitochondrial function and oxidative damage.^{29,56} This molecule is becoming of high interest as a potential target to overcome metabolic disarrangements. Additionally, it can be modulated by diet,⁵⁷ emerging as a promising intervention for obstetric complications in which pharmacological interventions are highly discouraged. In the present study, we hypothesised that CI deficiency in placenta may promote the expression of nuclear effectors such as Sirtuin3 to compensate for depressed mitochondrial function, as we previously observed in an IUGR rabbit model.³³ To our knowledge, this is the first study suggesting up-regulation of Sirtuin3 in human IUGR pregnancies, suggesting its usefulness as a therapeutic target.

On the other hand, maternofoetal correlations were observed in mitochondrial parameters, confirming the dependence of neonatal bioenergetics in maternal health status.

Our results showed preserved total ATP levels either in placental tissue, maternal PBMC or neonatal CBMC, suggesting a potential switch from aerobic to faster anaerobic metabolism to preserve ATP supply.⁵⁸ Similarly, we found no differences in lipid peroxidation, as an indicator of oxidative stress, between groups, in any tissue. Previous studies in IUGR reported controversial results in oxidative damage^{49,59,60} but in other pregnancy complications caused by placental insufficiency, such as preeclampsia, it is described an induction of oxidative stress in the placenta and maternal blood,⁵⁹ as well as in certain risk pregnancies depending on the type of delivery (specially vaginal delivery because of intermittent perfusion of intervillous space of the placenta during uterine contractions).⁶¹ In our cohort of IUGR pregnancies, we reduced preeclampsia comorbidity and vaginal delivery to avoid potential confounders. Whether preserved oxidative damage in our sample is linked to deficient oxygen supply due to placental insufficiency and consequent mitochondrial decreased activity,⁶² the presence of antioxidant defences or other compensatory

mechanisms such as Sirtuin3, is still a matter of doubt. Some limitations and technical considerations should be acknowledged in our study. First, IUGR is known to be a multifactorial obstetric condition where many pathways and aetiologies could finally lead to a unique phenotype. Further studies are warranted to better clarify the functional consequences of the decrease of placental MRC CI function and neonatal TCA activity in order to elucidate whether such a deficiency is a consequence or the cause of this obstetric complication. Additionally, larger sample size cohort studies should be used to strengthen statistical findings, in which additional measurements may ideally be studied to investigate mechanistic pathways, as well as the potential contribution of the different cell types of affected tissues in the context of IUGR (as lymphocytes and monocytes in PBMC or syncytiotrophoblast and cytotrophoblast in placenta). For instance, we cannot dismiss that cell composition and type may change in pathological conditions, thus conditioning IUGR or potential blood contamination in placental tissue. Similarly, we cannot exclude that the difference in gestational age at delivery between cases and controls could have influenced the results. This limitation is difficult to overcome as most clinical protocols indicate finalisation of gestation in IUGR with signs of placental insufficiency at 37-38 weeks. Finally, several potential confounders influencing mitochondrial and metabolism regulation (such as vaginal delivery, preeclampsia prevalence, maternal diet and lifestyle) were not considered in this study and may play a role in observed results. Despite these considerations, the consistency of our results, as well as the different associations found between clinical parameters and experimental findings in human pregnancies, or the similarities between human findings and experimental model results,³³ strengthen the validity of the present findings.

In conclusion, IUGR is associated with depressed mitochondrial function, especially at placental and neonatal level. Placental insufficiency seems to directly affect birth weight, CVR and mitochondria, highlighting the necessity to focus therapeutic efforts on those targets, such as dietary interventions aimed to regulate Sirtuin3.

ACKNOWLEDGEMENTS

We would like to sincerely thank all the pregnant women for participating in the study and the involvement of the clinical staff from the Maternity Unit of the Hospital Clinic of Barcelona. The samples used in this Project were provided by the Hospital Clínic-IDIBAPS Biobank with an appropriate ethical approval. We also thank all the financial support by Fondo de Investigación Sanitaria [FIS PI11/01199, PI14/00226, PI15/00817, PI15/00903, PI15/00130 and INT16/00168], CIBERER (an initiative of ISCIII) and InterCIBER [PIE1400061] granted by Instituto de Salud Carlos III, integrated in Plan Estatal de Investigación Científica y Técnica y de Innovación 2013-2016 and co-founded by European Regional Development Fund (FEDER), 'A way to build Europe'; Suports a Grups de Recerca [SGR893/2017 and SGR928/2017] and CERCA Programme from the Generalitat de Catalunya; CONACyT; Erasmus + Programme of

the European Union (Framework Agreement number: 2013-0040); "laCaixa" Foundation; Cerebra Foundation for the Brain Injured Child (Carmarthen, Wales, UK); Fundació La Marató de TV3 [87/C/2015] and Fundació Privada Cellex [CP042187].

CONFLICT OF INTEREST

Authors report no conflict of interest.

AUTHOR CONTRIBUTION

GG and FCa obtained funds to support the study. GG conceived the study and organised the project in collaboration with FCa, FCr, EG and MG. LY and LG-O were responsible for the diagnosis and inclusion of all patients and collected clinical data together with DLJ-F. All of the experimental, data collection and statistical analysis was closely supervised by GG, CM and MG-M. MG-M, with help from VR-A, MC-G, ET and IG-C performed all the experimental procedure to evaluate mitochondrial function. Concretely, MG-M and ET were in charge of processing all samples in the laboratory. MG-M, together with MC-G and IG-C, performed in vivo measurement of oxygen consumption of each sample. The remaining molecular measurements were performed by MG-M with the support of VR-A. The first draft of this manuscript was written by MG-M, and GG, FC, FC, LY, LG-O, DLJ-F, JCM and JMG profoundly reviewed and critiqued the manuscript, adding concepts of high relevance.

ORCID

Glòria Garrabou  <https://orcid.org/0000-0001-8973-9933>

REFERENCES

1. Visentin S, Grumolato F, Nardelli GB, Di Camillo B, Grisan E, Cosmi E. Early origins of adult disease: low birth weight and vascular remodeling. *Atherosclerosis*. 2014;237:391-399. <https://doi.org/10.1016/j.atherosclerosis.2014.09.027>
2. Lausman A, McCarthy FP, Walker M, Kingdom J. Screening, diagnosis, and management of intrauterine growth restriction. *J Obstet Gynaecol Can*. 2012;34:17-28. [https://doi.org/10.1016/S1701-2163\(16\)35129-5](https://doi.org/10.1016/S1701-2163(16)35129-5)
3. Sharma D, Shastri S, Sharma P. Intrauterine growth restriction: antenatal and postnatal aspects. *Clin Med Insights Pediatr*. 2016;10:67-83. <https://doi.org/10.4137/CMPed.S40070>
4. Temming LA, Dicke JM, Stout MJ, et al. Early second-trimester fetal growth restriction and adverse perinatal outcomes. *Obstet Gynecol*. 2017;130:865-869. <https://doi.org/10.1097/AOG.0000000000002209>
5. Crispi F, Miranda J, Gratacós E. Long-term cardiovascular consequences of fetal growth restriction: biology, clinical implications, and opportunities for prevention of adult disease. *Am J Obstet Gynecol*. 2018;218:S869-S879. <https://doi.org/10.1016/j.ajog.2017.12.012>
6. Akazawa Y, Hachiya A, Yamazaki S, et al. Cardiovascular remodeling and dysfunction across a range of growth restriction severity in small for gestational age infants—implications for fetal

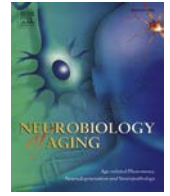
- programming. *Circ J*. 2016;80:2212-2220. <https://doi.org/10.1253/circj.CJ-16-0352>
7. Sarvari SI, Rodriguez-Lopez M, Nuñez-García M, et al. Persistence of cardiac remodeling in preadolescents with fetal growth restriction. *Circ Cardiovasc Imaging*. 2017;10. <https://doi.org/10.1161/CIRCIMAGING.116.005270>
 8. Sehgal A, Skilton MR, Crispi F. Human fetal growth restriction: a cardiovascular journey through to adolescence. *J Dev Orig Health Dis*. 2016;7:626-635. <https://doi.org/10.1017/S2040174416000337>
 9. Cruz-Lemini M, Crispi F, Valenzuela-Alcaraz B, et al. Fetal cardiovascular remodeling persists at 6 months in infants with intrauterine growth restriction. *Ultrasound Obstet Gynecol*. 2016;48:349-356. <https://doi.org/10.1002/uog.15767>
 10. Ortigosa N, Crispi F, Bailón R, et al. Heart morphology differences induced by intrauterine growth restriction and premature birth measured on the ECG in pre-adolescents. *J Electrocardiol*. 2016;49:401-409. <https://doi.org/10.1016/j.jelectrocard.2016.03.011>
 11. Figueras F, Gratacos E. An integrated approach to fetal growth restriction. *Best Pract Res Clin Obstet Gynaecol*. 2017;38:48-58. <https://doi.org/10.1016/j.bpobgyn.2016.10.006>
 12. Figueras F, Gardosi J. Intrauterine growth restriction: new concepts in antenatal surveillance, diagnosis, and management. *Am J Obstet Gynecol*. 2011;204:288-300. <https://doi.org/10.1016/j.ajog.2010.08.055>
 13. Vedmedovska N, Rezeberga D, Teibe U, Melderis I, Donders G. Placental pathology in fetal growth restriction. *Eur J Obstet Gynecol Reprod Biol*. 2011;155:36-40. <https://doi.org/10.1016/j.ejogrb.2010.11.017>
 14. Lanir N, Aharon A, Brenner B. Haemostatic mechanisms in human placenta. *Best Pract Res Clin Haematol*. 2003;16:183-195. <https://doi.org/10.1053/ybeha.2003.251>
 15. John R, Hemberger M. A placenta for life. *Reprod Biomed Online*. 2012;25:5-11
 16. Cetin I, Antonazzo P. The role of the placenta in intrauterine growth restriction (IUGR). *Semin Speech Lang*. 2009;213:84-88. <https://doi.org/10.1055/s-0029-1224143>
 17. Cetin I, Alvino G. Intrauterine growth restriction: implications for placental metabolism and transport. A review. *Placenta*. 2009;30:77-82. <https://doi.org/10.1016/j.placenta.2008.12.006>
 18. Mandò C, De Palma C, Stampalija T, et al. Placental mitochondrial content and function in intrauterine growth restriction and pre-eclampsia. *AJP Endocrinol Metab*. 2014;306:E404-E413. <https://doi.org/10.1152/ajpendo.00426.2013>
 19. Cohen J, Scott R, Schimmel T, Levron J, Willadsen S. Birth of infant after transfer of anucleate donor oocyte cytoplasm into recipient eggs. *Lancet*. 1997;350:186-187. [https://doi.org/10.1016/S0140-6736\(05\)62353-7](https://doi.org/10.1016/S0140-6736(05)62353-7)
 20. Morén C, Hernández S, Guitart-Mampel M, Garrabou G. Mitochondrial toxicity in human pregnancy: an update on clinical and experimental approaches in the last 10 years. *Int J Environ Res Public Health*. 2014;11:9897-9918. <https://doi.org/10.3390/ijerph110909897>
 21. Bertero E, Maack C. Metabolic remodelling in heart failure. *Nat Rev Cardiol*. 2018;15:457-470. <https://doi.org/10.1038/s41569-018-0044-6>
 22. Chistiakov DA, Shkurat TP, Melnichenko AA, Grechko AV, Orekhov AN. The role of mitochondrial dysfunction in cardiovascular disease: a brief review. *Ann Med*. 2018;50:121-127. <https://doi.org/10.1080/07853890.2017.1417631>
 23. Niemann B, Schwarzer M, Rohrbach S. Heart and mitochondria: pathophysiology and implications for cardiac surgeons. *Thorac Cardiovasc Surg*. 2018;66:11-19. <https://doi.org/10.1055/s-0037-1615263>
 24. Sun W, Liu C, Chen Q, Liu N, Yan Y, Liu B. SIRT3: a new regulator of cardiovascular diseases. *Oxid Med Cell Longev*. 2018;3:1-11. <https://doi.org/10.1155/2018/7293861>
 25. Koentges C, Bode C, Bugger H. SIRT3 in cardiac physiology and disease. *Front Cardiovasc Med*. 2016;3:38. <https://doi.org/10.3389/fcvm.2016.00038>
 26. Lin L, Chen K, Khalek WA, et al. Regulation of skeletal muscle oxidative capacity and muscle mass by SIRT3. *PLoS One*. 2014;9:e85636. <https://doi.org/10.1371/journal.pone.0085636>
 27. Ahn B-h, Kim H-s, Song S, et al. A role for the mitochondrial deacetylase Sirt3 in regulating energy homeostasis. *Proc Natl Acad Sci*. 2008;14447-14452. <https://doi.org/10.1073/pnas.0803790105>
 28. Wang Q, Li L, Li Cy, Pei Z, Zhou M, Li N. SIRT3 protects cells from hypoxia via PGC-1 α - and MnSOD-dependent pathways. *Neuroscience*. 2015;286:109-121. <https://doi.org/10.1016/j.neuroscience.2014.11.045>
 29. Sack MN. The role of SIRT3 in mitochondrial homeostasis and cardiac adaptation to hypertrophy and aging. *J Mol Cell Cardiol*. 2012;52:520-525. <https://doi.org/10.1016/j.yjmcc.2011.11.004>
 30. Madeleneau D, Buffat C, Mondon F, et al. Transcriptomic analysis of human placenta in intrauterine growth restriction. *Pediatr Res*. 2015;77:799-807. <https://doi.org/10.1038/pr.2015.40>
 31. Ruis-González MD, Cañete MD, Gómez-Chaparro JL, Abril N, Cañete R, López-Barea J. Alterations of protein expression in serum of infants with intrauterine growth restriction and different gestational ages. *J Proteomics*. 2015;119:169-182. <https://doi.org/10.1016/j.jprot.2015.02.003>
 32. Beyramzadeh M, Dikmen ZG, Erturk NK, Tuncer ZS, Akbiyik F. Placental respiratory chain complex activities in high risk pregnancies. *J Matern Neonatal Med*. 2017;30:2911-2917. <https://doi.org/10.1080/14767058.2016.1268594>
 33. Gonzalez-Tendero A, Torre I, Garcia-Canadilla P, et al. Intrauterine growth restriction is associated with cardiac ultrastructural and gene expression changes related to the energetic metabolism in a rabbit model. *Am J Physiol Circ Physiol*. 2013;305:H1752-H1760. <https://doi.org/10.1152/ajpheart.00514.2013>
 34. Guitart-Mampel M, Gonzalez-Tendero A, Niñerola S, et al. Cardiac and placental mitochondrial characterization in a rabbit model of intrauterine growth restriction. *Biochim Biophys Acta Gen Subj*. 2018;1862:1157-1167. <https://doi.org/10.1016/j.bbagen.2018.02.006>
 35. Figueras F, Gratacós E. Update on the diagnosis and classification of fetal growth restriction and proposal of a stage-based management protocol. *Fetal Diagn Ther*. 2014;36:86-98. <https://doi.org/10.1159/000357592>
 36. Savchev S, Figueras F, Gratacos E. Survey on the current trends in managing intrauterine growth restriction. *Fetal Diagn Ther*. 2014;36:129-135. <https://doi.org/10.1159/000360419>
 37. Casademont J, Perea M, López S, Beato A, Miró O, Cardellach F. Enzymatic diagnosis of oxidative phosphorylation defects on muscle biopsy: better on tissue homogenate or on a mitochondria-enriched suspension? *Med Sci Monit*. 2004;10:CS49-CS53.
 38. Prilutskii AS, Khodakovskii AV, Mailian EA. A method of separating mononuclears on a density gradient. *Lab Delo*. 1990:20-23.
 39. Tyrrell DJ, Bharadwaj MS, Jorgensen MJ, Register TC, Molina A. Blood cell respirometry is associated with skeletal and cardiac muscle bioenergetics: Implications for a minimally invasive biomarker of mitochondrial health. *Redox Biol*. 2016;10:65-77. <https://doi.org/10.1016/j.redox.2016.09.009>
 40. Kramer PA, Ravi S, Chacko B, Johnson MS, Darley-Usmar VM. A review of the mitochondrial and glycolytic metabolism in human platelets and leukocytes: Implications for their use as bioenergetic biomarkers. *Redox Biol*. 2014;2:206-210. <https://doi.org/10.1016/j.redox.2013.12.026>
 41. Catalan-García M, Garrabou G, Moren C, et al. Mitochondrial DNA disturbances and deregulated expression of oxidative phosphorylation and mitochondrial fusion proteins in sporadic inclusion body

- myositis. *Clin Sci*. 2016;130:1741-1751. <https://doi.org/10.1042/CS20160080>
42. Perez-Cruz M, Crispi F, Fernández M, et al. Cord blood biomarkers of cardiac dysfunction and damage in term growth-restricted fetuses classified by severity criteria. *Fetal Diagn Ther*. 2017;44:271-276. <https://doi.org/10.1159/000484315>
 43. Belenky A, Smith A, Zhang B, et al. The effect of class-specific protease inhibitors on the stabilization of B-type natriuretic peptide in human plasma. *Clin Chim Acta*. 2004;340:163-172. <https://doi.org/10.1016/j.cccn.2003.10.026>
 44. Casademont J, Garrabou G, Miró O, et al. Neuroleptic treatment effect on mitochondrial electron transport chain: peripheral blood mononuclear cells analysis in psychotic patients. *J Clin Psychopharmacol*. 2007; 27:284-288. <https://doi.org/10.1097/JCP.0b013e318054753e>
 45. Medja F, Allouche S, Frachon P, et al. Development and implementation of standardized respiratory chain spectrophotometric assays for clinical diagnosis. *Mitochondrion*. 2009;9:331-339. <https://doi.org/10.1016/j.mito.2009.05.001>
 46. Barrientos A. In vivo and in organello assessment of OXPHOS activities. *Methods*. 2002;26:307-316. [https://doi.org/10.1016/S1046-2023\(02\)00036-1](https://doi.org/10.1016/S1046-2023(02)00036-1)
 47. Morén C, González-Casacuberta I, Álvarez-Fernández C, et al. HIV-1 promonocytic and lymphoid cell lines: an in vitro model of in vivo mitochondrial and apoptotic lesion. *J Cell Mol Med*. 2017;21:402-440. <https://doi.org/10.1111/jcmm.12985>
 48. Novielli C, Mandò C, Tabano S, et al. Mitochondrial DNA content and methylation in fetal cord blood of pregnancies with placental insufficiency. *Placenta*. 2017;55:63-70. <https://doi.org/10.1016/j.placenta.2017.05.008>
 49. Holland O, Dekker Nitert M, Gallo LA, Vejzovic M, Fisher JJ, Perkins AV. Review: placental mitochondrial function and structure in gestational disorders. *Placenta*. 2017;54:2-9. <https://doi.org/10.1016/j.placenta.2016.12.012>
 50. Poidatz D, Dos Santos E, Duval F, et al. Involvement of estrogen-related receptor- γ and mitochondrial content in intrauterine growth restriction and preeclampsia. *Fertil Steril*. 2015;104:483-490. <https://doi.org/10.1016/j.fertnstert.2015.05.005>
 51. Lattuada D, Colleoni F, Martinelli A, et al. Higher mitochondrial DNA content in human IUGR placenta. *Placenta*. 2008;29:1029-1033. <https://doi.org/10.1016/j.placenta.2008.09.012>
 52. Lee H-C, Yin P-H, Lu C-Y, Chi C-W, Wei Y-H. Increase of mitochondria and mitochondrial DNA in response to oxidative stress in human cells. *Biochem J*. 2000;348:425-432. <https://doi.org/10.1042/bj3480425>
 53. Vuorinen K, Remes A, Sormunen R, Tapanainen J, Hassinen IE. Placental mitochondrial DNA and respiratory chain enzymes in the etiology of preeclampsia. *Obstet Gynecol*. 1998;91:950-955. [https://doi.org/10.1016/S0029-7844\(98\)00081-7](https://doi.org/10.1016/S0029-7844(98)00081-7)
 54. Crispi F, Hernandez-Andrade E, Pelsers MM, et al. Cardiac dysfunction and cell damage across clinical stages of severity in growth-restricted fetuses. *Am J Obstet Gynecol*. 2008;199:254.e1-254.e8. <https://doi.org/10.1016/j.ajog.2008.06.056>
 55. Girsén A, Ala-Kopsala M, Mäkilä K, Vuolteenaho O, Räsänen J. Cardiovascular hemodynamics and umbilical artery N-terminal peptide of proB-type natriuretic peptide in human fetuses with growth restriction. *Ultrasound Obstet. Gynecol*. 2007; 29:296-303. <https://doi.org/10.1002/uog.3934>
 56. Sack MN. Emerging characterization of the role of SIRT3-mediated mitochondrial protein deacetylation in the heart. *AJP Hear Circ Physiol*. 2011;301:H2191-H2197. <https://doi.org/10.1152/ajpheart.00199.2011>
 57. Sandoval-Acuña C, Ferreira J, Speisky H. Polyphenols and mitochondria: an update on their increasingly emerging ROS-scavenging independent actions. *Arch Biochem Biophys*. 2014;559:75-90. <https://doi.org/10.1016/j.abb.2014.05.017>
 58. Illsley NP, Caniggia I, Zamudio S. Placental metabolic reprogramming: do changes in the mix of energy-generating substrates modulate fetal growth? *Int J Dev Biol*. 2010;54:409-419. <https://doi.org/10.1387/ijdb.082798ni>
 59. Lefebvre T, Roche O, Seegers V, et al. Study of mitochondrial function in placental insufficiency. *Placenta*. 2018;67:1-7. <https://doi.org/10.1016/j.placenta.2018.05.007>
 60. Myatt L. Placental adaptive responses and fetal programming. *J Physiol*. 2006;572:25-30.
 61. Jauniaux E, Poston L, Burton GJ. Placental-related diseases of pregnancy: involvement of oxidative stress and implications in human evolution. *Hum Reprod Update*. 2006;12:747-755. <https://doi.org/10.1093/humupd/dml016>
 62. Zhang S, Regnault T, Barker P, et al. Placental adaptations in growth restriction. *Nutrients*. 2015;7:360-389. <https://doi.org/10.3390/nu7010360>

SUPPORTING INFORMATION

Additional supporting information may be found online in the Supporting Information section at the end of the article.

How to cite this article: Guitart-Mampel M, Juárez-Flores DL, Youssef L, et al. Mitochondrial implications in human pregnancies with intrauterine growth restriction and associated cardiac remodelling. *J Cell Mol Med*. 2019;23:3962-3973. <https://doi.org/10.1111/jcmm.14282>



Transcriptional alterations in skin fibroblasts from Parkinson's disease patients with parkin mutations



Ingrid González-Casacuberta^{a,b,1}, Constanza Morén^{a,b,1}, Diana-Luz Juárez-Flores^{a,b}, Anna Esteve-Codina^{c,d}, Cristina Sierra^e, Marc Catalán-García^{a,b}, Mariona Guitart-Mampel^{a,b}, Ester Tobías^{a,b}, José César Milisenda^{a,b}, Claustre Pont-Sunyer^{f,g}, María José Martí^{f,g}, Francesc Cardellach^{a,b}, Eduard Tolosa^{f,g}, Rafael Artuch^{b,e}, Mario Ezquerro^{f,g,*}, Rubén Fernández-Santiago^{f,g,*,2}, Glòria Garrabou^{a,b,**,2}

^aLaboratory of Muscle Research and Mitochondrial Function-CELLEX, Institut d'Investigacions Biomèdiques August Pi i Sunyer (IDIBAPS), Faculty of Medicine and Health Sciences, University of Barcelona (UB), Department of Internal Medicine-Hospital Clínic of Barcelona, Barcelona, Spain

^bCentro de Investigación Biomédica en Red de Enfermedades Raras (CIBERER), Instituto de Salud Carlos III, Madrid, Spain

^cCentro de Investigación Biomédica en Red de Enfermedades Neurodegenerativas (CIBERNED), Instituto de Salud Carlos III, Madrid, Spain

^dUniversitat Pompeu Fabra (UPF), Barcelona, Spain

^eDepartment of Clinical Biochemistry, Institut de Recerca Sant Joan de Déu, Esplugues de Llobregat, Barcelona, Spain

^fLaboratory of Parkinson Disease and Other Neurodegenerative Movement Disorders: Clinical and Experimental Research-CELLEX, IDIBAPS, Faculty of Medicine and Health Sciences, UB, Department of Neurology-Hospital Clínic of Barcelona, Barcelona, Spain

^gCentro de Investigación Biomédica en Red de Enfermedades Neurodegenerativas (CIBERNED), Instituto de Salud Carlos III, Madrid, Spain

ARTICLE INFO

Article history:

Received 8 June 2017

Received in revised form 23 January 2018

Accepted 26 January 2018

Available online 7 February 2018

Keywords:

Parkinson's disease (PD)

Parkin

RNA sequencing (RNA-seq)

Fibroblasts

Transcriptome

ABSTRACT

Mutations in the parkin gene (*PRKN*) are the most common cause of autosomal-recessive juvenile Parkinson's disease (PD). *PRKN* encodes an E3 ubiquitin ligase that is involved in multiple regulatory functions including proteasomal-mediated protein turnover, mitochondrial function, mitophagy, and cell survival. However, the precise molecular events mediated by *PRKN* mutations in *PRKN*-associated PD (*PRKN*-PD) remain unknown. To elucidate the cellular impact of parkin mutations, we performed an RNA sequencing study in skin fibroblasts from *PRKN*-PD patients carrying different *PRKN* mutations ($n = 4$) and genetically unrelated healthy subjects ($n = 4$). We identified 343 differentially expressed genes in *PRKN*-PD fibroblasts. Gene ontology and canonical pathway analysis revealed enrichment of differentially expressed genes in processes such as cell adhesion, cell growth, and amino acid and folate metabolism among others. Our findings indicate that *PRKN* mutations are associated with large global gene expression changes as observed in fibroblasts from *PRKN*-PD patients and support the view of PD as a systemic disease affecting also non-neural peripheral tissues such as the skin.

© 2018 Elsevier Inc. All rights reserved.

* Corresponding authors at: Laboratory of Parkinson Disease and Other Neurodegenerative Movement Disorders, CELLEX Building, Faculty of Medicine of University of Barcelona (UB), Institut d'Investigacions Biomèdiques August Pi i Sunyer (IDIBAPS), Hospital Clínic Universitari de Barcelona, Casanova 143, Floor 3B, 08036, Barcelona, Spain. Tel.: +34-932-275-400 ext. 4814; fax: +34-932-275-783.

** Corresponding author at: Laboratory of Muscle Research and Mitochondrial Function, CELLEX Building, Faculty of Medicine of UB, IDIBAPS, Hospital Clínic Universitari de Barcelona, Casanova 143, Floor 4B, 08036, Barcelona, Spain. Tel.: +34-932-275-400 ext. 2907; fax: +34-932-279-365.

E-mail addresses: EZQUERRA@clinic.cat (M. Ezquerro), ruben.fernandez.santiago@gmail.com (R. Fernández-Santiago), GARRABOU@clinic.cat (G. Garrabou).

¹ Contributed equally as first authors.

² Contributed equally as co-senior authors.

1. Introduction

Parkinson's disease (PD) is the most common neurodegenerative movement disorder affecting the 1%–2% of the population over the age of 65 years (Alves et al., 2008). The neuropathological hallmark of the disease is the loss of midbrain dopaminergic neurons (DANs) in the substantia nigra pars compacta (SNpc) and the presence of α -synuclein aggregates in Lewy bodies and Lewy neurites in the surviving DANs. Although the vast majority of cases are sporadic PD (sPD), patients about 10% present monogenic forms caused by pathogenic mutations in genes associated with PD (de Lau & Breteler, 2006; Simchovitz et al., 2016). Of these, loss-of-function

mutations in the parkin gene (*PRKN*) are the most frequent cause of autosomal-recessive juvenile PD, accounting for up to 50% of familial PD and about 15% of the sPD patients with an age-at-onset before 45 years (Bonifati, 2014). These pathogenic mutations in *PRKN* have been described in all 12 exons of the gene and include point missense and null mutations, as well as insertions/deletions (Klein & Westenberger, 2012). The clinicopathological picture of *PRKN*-associated PD (*PRKN*-PD) typically includes early onset, slow progression, good and lasting response to levodopa, and DA loss and gliosis in the SNpc without Lewy bodies (Bonifati et al., 2005; Klein & Westenberger, 2012).

The precise mechanisms by which *PRKN* loss-of-function mutations lead to neurodegeneration are not yet well understood. Wild-type *PRKN* encodes a multifunctional E3 ubiquitin ligase involved in key regulatory functions such as proteasomal-mediated protein turnover (Fiesel et al., 2015), mitochondrial function, and mitophagy (Clark et al., 2006b; Hasson et al., 2013; Park et al., 2006; Pickrell & Youle, 2015; Sarraf et al., 2013; Seirafi et al., 2015), thereby conferring neuroprotection and survival (Fiskin & Dikic, 2013; Zhang et al., 2015). Interestingly, recent studies have also suggested an association of *PRKN* with transcriptional deregulation of genes involved in the neurodegenerative process (da Costa et al., 2009; Duplan et al., 2013), suggesting that *PRKN* could be somehow involved in the regulation of the transcriptional activity of other genes (Tay et al., 2010; Unschuld et al., 2006). Using biological samples from PD patients, previous studies have reported transcriptomic alterations in postmortem tissues, peripheral blood mononuclear cells, and other tissues (Fernandez-Santiago et al., 2015; Grunblatt et al., 2004; Infante et al., 2015; Mutez et al., 2011). These studies have mainly focused on sPD or autosomal-dominant LRRK2-associated PD, but transcriptomic alterations potentially occurring in *PRKN*-PD are unknown.

In this context, here we have explored for the first time global gene expression changes in cultured skin fibroblasts from *PRKN*-PD patients. Skin fibroblasts from PD patients have been proposed as a cellular system to model disease (Auburger et al., 2012) able to reproduce several of the molecular alterations occurring in PD (Ambrosi et al., 2014; Hoepken et al., 2008; Romani-Aumedes et al., 2014; Yakhine-Diop et al., 2014). In addition, punch skin biopsies are minimally invasive and permit the possibility to establish primary cultures of self-propagating cells that preserve the genomic background of the patient without additional genetic manipulation. The goal of our study was to investigate whether gene expression changes occur in PD patients at peripheral non-neural tissues. More specifically, we have performed a whole-genome expression analysis by RNA sequencing (RNA-seq) in skin fibroblasts from PD patients carrying different loss-of-function mutations in *PRKN* and from genetically unrelated healthy controls. Our study identifies specific transcriptional changes, cellular processes, and molecular pathways, which are altered at the peripheral level in skin tissue from *PRKN*-PD patients.

2. Methods

2.1. Study approval

This study has been conducted conforming the principles of the Declaration of Helsinki and the Belmont Report. All participants gave written informed consent, and the study was approved by the Commission on Guarantees for Donation and Use of Human Tissues and Cells of the Instituto de Salud Carlos III and the local ethics committee at the Hospital Clínic de Barcelona. Personal data were anonymized, and subject samples were codified to preserve confidentiality.

2.2. Subjects and *PRKN* mutational screening

We selected 4 PD patients carrying mutations in the *PRKN* gene and 4 healthy unrelated subjects among patients and spouses visiting the movement disorders outpatient clinic from the Hospital Clínic de Barcelona (Barcelona, Spain). PD patients were diagnosed according to the UK Brain Bank criteria (Hughes et al., 1992). Clinical and epidemiological data of *PRKN*-PD patients are summarized in Table 1. Mutational screening of the *PRKN* was performed using the multiplex ligation-dependent probe amplification method (Schouten et al., 2002) and cycle sequencing using the BigDye Terminator v3.1 Ready Reaction (Thermo Fisher Scientific), runs on an ABI-prism automatic DNA sequencer (Thermo Fisher Scientific). Three of the patients carried homozygous or compound heterozygous deletion mutations causing loss of function of the *PRKN* protein, and 1 patient carried a rare heterozygous missense mutation previously described only in 1 family from our population whose pathogenic nature is still uncertain (Munoz et al., 2002).

2.3. Cell culture

Fibroblasts were obtained by a 6 mm of diameter punch skin biopsy from the alar surface of the nondominant arm of the subjects. Cells were cultured in Dulbecco's Modified Eagle's Medium supplemented with 10% heat-inactivated fetal bovine serum and 1% penicillin/streptomycin (Gibco; Life Technologies), following standard conditions. Cells were cultured in parallel in successive passes until optimal confluence was reached. At the same pass number, cells were collected with 2.5% Trypsin (Gibco; Life Technologies) and harvested by centrifugation 8 minutes at 500g. Cell pellets were kept dry at -80°C until RNA extraction and biochemical studies. For biochemical analyses, cell pellets were resuspended in 500 μL of saline solution. From these, an aliquot of 20 μL was used for total protein quantification using the Lowry method as an estimation of cellular content. Total amount of protein was used to normalize the biochemical parameters.

Table 1
Clinical and epidemiological data of patients and control subjects (donors of skin biopsy)

Subject	Mutation	Gender	Age of disease onset	Age at punch skin biopsy	Treatment
CTR 1	–	Female	–	66	–
CTR 2	–	Female	–	61	–
CTR 3	–	Male	–	64	–
CTR 4	–	Male	–	52	–
PRKN-PD 1	Homozygous PARK2 exon 5-6 deletion	Female	27	63	L-Dopa
PRKN-PD 2	Compound heterozygous PACRG exon 1 deletion/PARK2 exon 6 deletion/	Female	8	35	L-Dopa
PRKN-PD 3	Homozygous PARK2 exon 2-3-4 deletion	Male	35	69	L-Dopa
PRKN-PD 4	Heterozygous PARK2 Val15Met	Male	47	57	L-Dopa

No differences in mean age and gender were found between patients and control subjects.

Key: CTR, healthy control subjects (not affected by PD and any *PRKN* mutation); PACRG, parkin coregulated gene; PRKN-PD, patients with familial Parkinson's disease carrying a *PRKN* mutation; Val15Met, methionine to valine substitution at position 15.

2.4. RNA extraction and RNA-seq procedures

Total RNA was isolated from 3 million cells of each subject using AllPrep DNA/RNA/protein Kit (Qiagen) according to manufacturer's protocol and quantified using Quawell UV-Vis Spectrophotometer Q5000. Resulting concentrations were adjusted to 100 ng/μL in RNase-free water. RNA samples were assayed for quantity and quality using the Qubit RNA HS (Life Technologies) and RNA 6000 Nano assays on a Bioanalyzer 2100. RNA-seq libraries were prepared from total RNA using the TruSeq RNA Sample Prep Kit v2 (Illumina Inc), with minor modifications. Briefly, after poly-A based mRNA enrichment with oligo-dT magnetic beads using 1 μg of total RNA as the input material, the mRNA was fragmented (resulting RNA fragment size was 80–250 nucleotides (nt), with the major peak at 130 nt). After first and second strand cDNA synthesis, the double-stranded cDNA was end-repaired, 3'adenylated, and ligated to the Illumina barcoded adapters. The ligation product was enriched by 10 cycles of polymerase chain reaction (PCR). Each library was sequenced using TruSeq SBS Kit v3-HS, in paired-end mode with a read length of 2 × 76 bp. We generated over 66–76 million paired-end reads for each sample in a fraction of a sequencing lane on HiSeq 2000 (Illumina, Inc), following the manufacturer's protocol. Image analysis, base calling, and quality scoring of the run were processed using the manufacturer's software Real Time Analysis (RTA 1.13.48), followed by generation of FASTQ sequence files by CASAVA.

2.5. Bioinformatic analysis

RNA-seq reads were aligned with the GEMTools RNaseq pipeline v1.7 (<http://gemtools.github.io>), which is based on the Genome Multitool (GEM) mapper (Marco-Sola et al., 2012). The pipeline aligns all reads in a sample in 3 phases, mapping against the reference genome, against a reference transcriptome, and against a de novo transcriptome, which was generated from the input data to detect new junction sites. The transcriptome was generated from version 19 of the GENCODE annotation (<http://www.gencodegenes.org>). After mapping, all alignments were filtered to increase the number of uniquely mapped reads. The filter criteria was, to have a minimum intron length of 20 bp and a maximum exon overlap of 5 bp. Additionally, a filter step against the reference annotation was performed, checking for consistent pairs and junctions where both sites aligned to the same annotated gene. Gene quantifications were computed using the Flux Capacitor (Montgomery et al., 2010). This tool quantifies RNA-seq reads on a isoform level, and the resulting counts were summed up to gene-level counts. Normalization and differential expression analysis were done using edgeR robust approach (Zhou et al., 2014) after adjusting for sex effects in the model. Normalization was done with the trimmed mean of M-values method obtaining counts per million (cpm) values, and only genes with cpm values greater than 1 in at least 4 samples belonging to the same condition were kept (Robinson & Oshlack, 2010); edgeR robust approach includes some sort of sharing information across genes to improve inferences for small sample sizes. Moreover, to reduce the influence of extreme observations in differential expression calls, the method implements a strategy based on “observation weights”. Principal component analysis was performed with the “prcomp” R function and the “ggplot2” R package taking the top 500 most variable genes. The heatmap was done with the “pheatmap” R package with default clustering options taking the differentially expressed genes (DEGs) after restrictive multiple testing adjustment of *p*-values (<0.01) using the Benjamini-Hochberg false discovery rate (FDR) method (Benjamini and Hochberg, 1995).

2.6. Gene enrichment analyses

Upregulated and downregulated DEGs together were further analyzed using the GeneCodis bioinformatic tool (Tabas-Madrid et al., 2012; Carmona-Saez et al., 2007; Nogales-Cadenas et al., 2009). Biologically enriched gene ontology (GO) terms were considered statistically significant when passing the significance cutoff of *p* below 0.05 after adjustment for multiple testing using the FDR method. In parallel, the Core Analysis module of the Ingenuity Pathway Analysis (IPA; QIAGEN Redwood City, www.qiagen.com/ingenuity) was used to identify canonical pathway, overlapping canonical pathway, and upstream regulators analysis by using a Fisher's exact test. The significance cut-off was an adjusted *p* below 0.05.

2.7. Quantitative real-time PCR validation

To further validate the RNA-seq results, we assessed the expression of 5 DEGs by quantitative real-time PCR (qRT-PCR) in a StepOnePlus Real-Time PCR System (Thermo Fisher Scientific Inc); cDNA was synthesized from 2 μg of total RNA using a high-capacity reverse transcription kit (Thermo Fisher Scientific Inc), according to manufacturer's protocol; and cDNA was diluted 1/10 with RNase-free water before qRT-PCR. TaqMan Gene Expression Assays (Applied Biosystems) were used for the following genes: serine hydroxymethyltransferase 1 soluble (*SHMT1*), serine hydroxymethyltransferase 2 mitochondrial (*SHMT2*), methylenetetrahydrofolate dehydrogenase (NADP⁺ dependent) 2 or methenyltetrahydrofolate cyclohydrolase (*MTHFD2*), collagen type V alpha 1 (*COL5A1*), and phosphoserine aminotransferase 1 (*PSAT1*), normalized using glucuronidase beta (*GUSB*), and glyceraldehyde-3-phosphate dehydrogenase (*GAPDH*) as house-keeping genes. The qRT-PCR was performed in 96-well plates, and optimal results were obtained using 12.75 μL of TaqMan Gene Expression Master Mix, 1.25 μL of TaqMan Gene Expression Assay 20×, 8.25 μL of RNase-free water, and 2.5 μL of the diluted template cDNA in a final reaction volume of 25 μL. Thermal cycling conditions were set following manufacturer's instructions (Thermo Fisher Scientific Inc). All the samples were amplified per triplicate, and data were analyzed with the StepOne Software v.2.3 (Life Technologies). The comparative threshold cycle (*C_T*) method ($\Delta\Delta C_t$) was used for relative quantification using *GUSB* and *GAPDH* transcript levels to normalize each transcript content. Commercially available assays (Thermo Fisher Scientific Inc) are as follows: *SHMT1* (Hs00541045_m1), *SHMT2* (Hs01059263_g1), *MTHFD2* (Hs00759197_s1), *COL5A1* (Hs00609133_m1), *PSAT1* (Hs00795278_mH), *GUSB* (Hs99999908_m1), and *GAPDH* (Hs99999905_m1).

2.8. Biochemical analysis

5-Methyltetrahydrofolate (5-MTHF) and amino acid concentrations in fibroblasts were analyzed by reverse phase high-performance liquid chromatography with fluorescence detection and ion exchange chromatography of the ninyhydrin derivative, respectively, as previously reported (Ormazabal et al., 2006). Total folate concentrations were analyzed with automated chemiluminescent immunoassay according to manufacturer's protocol (ADVIA Centaur).

2.9. Statistical analysis of qRT-PCR and biochemical analyses

Statistical analysis was performed using the Statistical Package for the Social Sciences (SPSS, version 19) software (IBM SPSS Statistics; SPSS Inc, Chicago, IL, USA) to search for intergroup differences using the nonparametric Mann-Whitney *U*-test for independent samples. Results were expressed as mean ± standard

error of the mean. Significance level was set at asymptotic 2-tailed p -value below 0.05.

3. Results

3.1. Gene expression analysis

To ascertain the potential impact of *PRKN* mutations on global gene expression, we performed an RNA-seq study in skin fibroblasts from *PRKN*-PD patients and healthy controls. We found detectable gene expression of 14,230 annotated transcripts. We then performed a principal component analysis of the top 500 most variable genes to inspect overall variability among samples (Fig. 1A). The first 2 principal components showed a strong gender effect, separating females and males. Differential expression analysis between *PRKN*-PD patients and controls was accordingly conducted adjusting for sex. Under an FDR adjusted p -value below 0.01, we detected 343 DEGs (Supplemental Tables 1 and 2). Of these, 206 were upregulated and 137 downregulated in *PRKN*-PD patients (Fig. 1B). Interestingly, we found a similar expression pattern in the patient carrying the heterozygous Val15Met mutation with respect to the rest of the patients carrying homozygous loss-of-function mutations (Fig. 1B).

3.2. Functional classification of DEGs

To gain insight into the molecular mechanisms involved in PD associated with *PRKN* mutations, we performed a GO enrichment analysis using the entire list of DEGs both, upregulated and downregulated. GO analysis revealed enrichment of DEGs in processes such as cell adhesion, cell growth, amino acid metabolism, transcription, apoptosis, and interestingly, dysregulation of genes involved in guidance and extension of axons. Top significant GO terms are presented in Fig. 2.

3.3. Canonical pathways of DEGs

To further explore the biological significance of the differential gene expression affecting *PRKN*-PD, we performed a canonical pathway enrichment analysis using the IPA software. Of the 343 DEGs from our data set, 331 mapped to the IPA database. A total of 32 canonical pathways were identified to be significantly enriched (p -value below 0.05) between *PRKN*-PD patients and controls (Fig. 3). The most significant deregulated canonical pathways included serine/glycine biosynthesis, tRNA charging, fibrosis, folate metabolism, and deoxythymidine monophosphate (dTMP) de novo biosynthesis pathways, among others.

3.4. Overlapping canonical pathways

We further performed an overlapping canonical pathway analysis to identify clusters of canonical pathways related by commonly shared DEGs in our data set (Fig. 4). Interestingly, 2 independent clusters interconnecting the principal canonical pathways emerged in this analysis. The first cluster (Fig. 4A) includes pathways associated to cell development, organization of extracellular matrix, cell adhesion, proliferation, polarity, and migration of cells. The second cluster (Fig. 4A) also revealed enrichment in pathways relevant to neurons such as axon guidance, Wnt/ β -catenin, and Notch signaling. The second cluster was related with anabolic processes including the serine/glycine biosynthesis and the related 1-carbon (1C) folate-mediated metabolism (Amelio et al., 2014) and dTMP de novo biosynthesis pathway (Fig. 5A).

3.5. Analysis of upstream regulators of DEGs

To explore the cascade of potential upstream transcriptional regulators of the gene regulatory networks affected by gene expression changes, we carried out a specific upstream regulator analysis. The identified top 35 predicted upstream regulators are

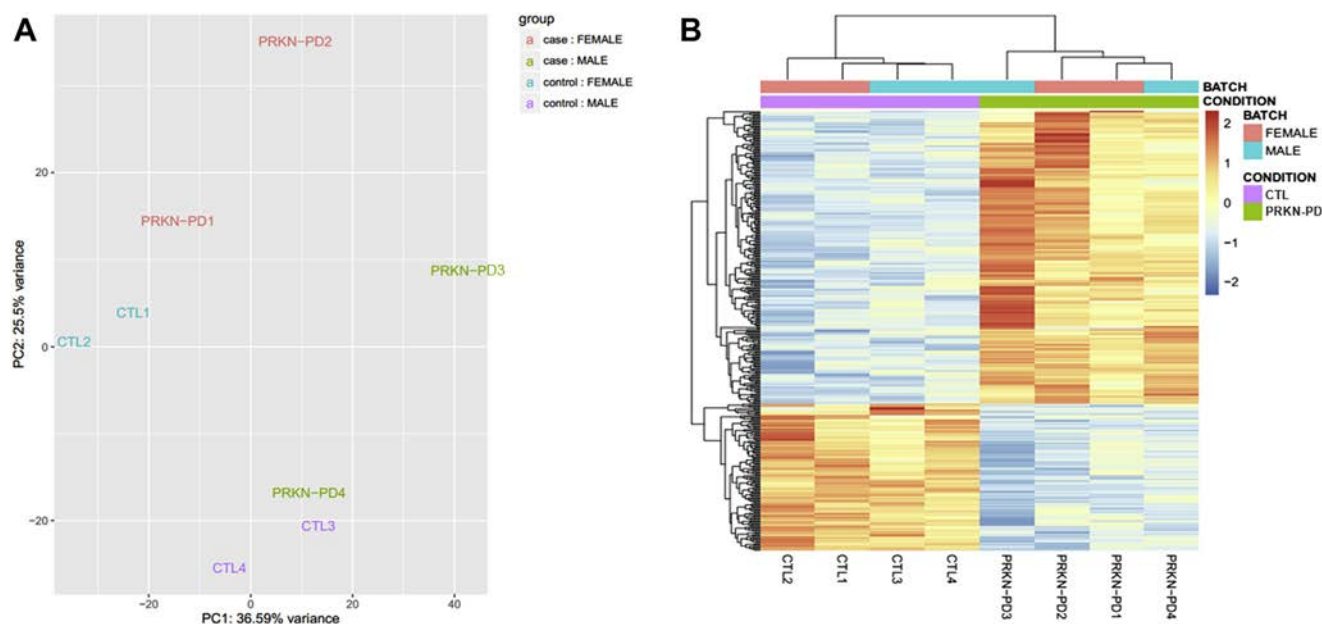


Fig. 1. (A) Principal component analysis showing the top 500 most variable genes. Principal components 1 (PC1) and 2 (PC2) explained 36.59% and 25.5% of the total variance, respectively. (B) Heatmap showing the 343 DEGs detected in fibroblasts from individuals with *PRKN*-PD as compared to healthy controls. Warm colors depict DEGs that were upregulated in the sample, and cool colors depict those downregulated. Abbreviations: CTL, control; DEGs, differentially expressed genes; *PRKN*-PD, parkin-associated Parkinson's disease. (For interpretation of the references to color in this figure legend, the reader is referred to the Web version of this article.)

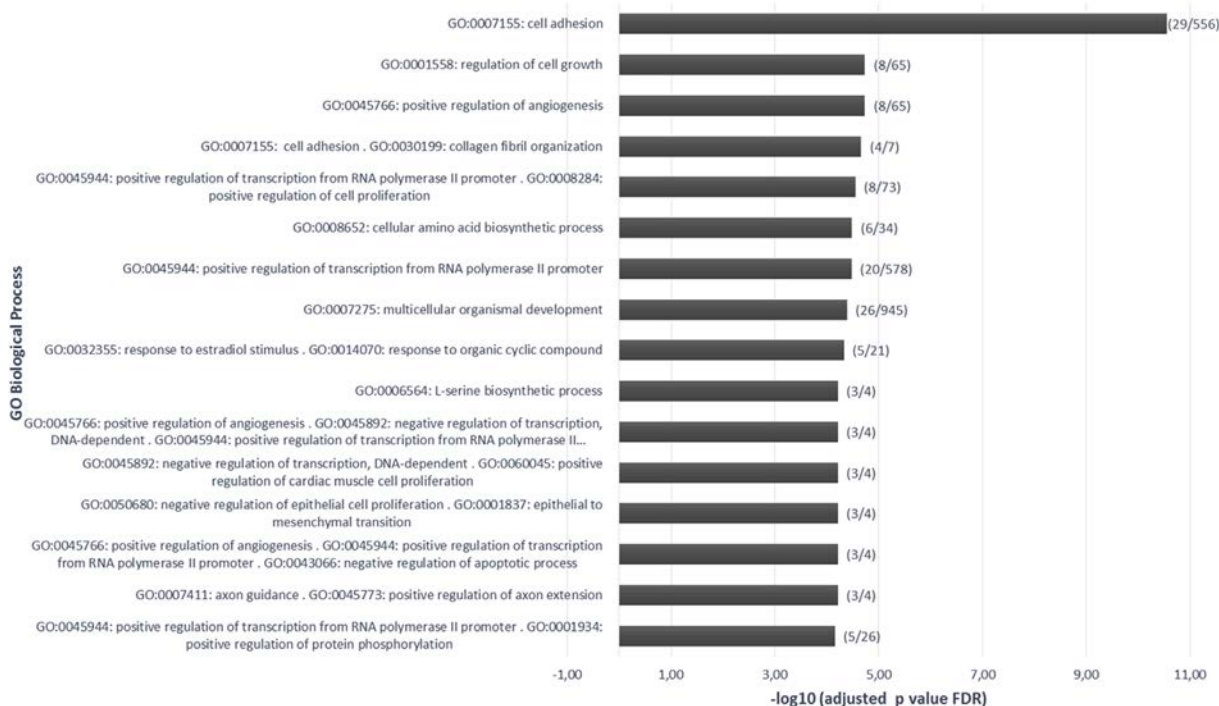


Fig. 2. Most significantly enriched annotations classified by GO terms for BPs altered in PRKN-PD fibroblasts expressed as $-\log_{10}$ (adjusted p value). In parenthesis, first the number of DEGs assigned to the GO BPs with respect to the total number of genes assigned to the process. Note $-\log_{10}(0.05) = 1.3$. Abbreviations: BP, biological process; DEGs, differentially expressed genes; GO, gene ontology; PRKN-PD, parkin-associated Parkinson's disease.

shown in Supplemental Table 3. Interestingly, the second in the list of the top predicted upstream regulator is the transcription factor ATF4 that drives the activation of the mitochondrial stress response activating targeted genes involved in the 1C folate metabolism. On

the other hand, 2 of the upstream regulators were PD upregulated DEGs within our data set, namely the fibroblast growth factor 2 (*FGF2*) and the tribbles pseudokinase 3 (*TRIB3*) genes (2.92- and 2.52-fold change; adjusted p -value = 3.55×10^{-04} and 4.84×10^{-05} ,

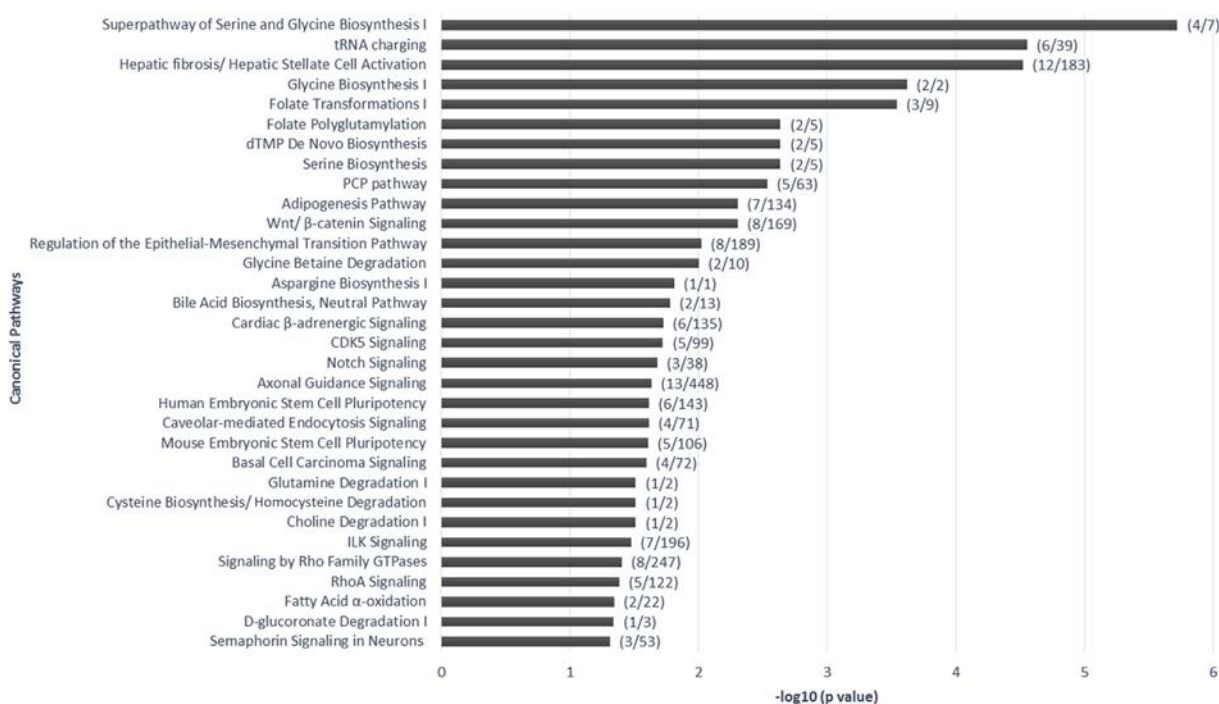


Fig. 3. Significantly enriched canonical pathways altered in PRKN-PD fibroblasts expressed as $-\log_{10}$ (p value). In parenthesis, the number of DEGs with respect to the total number of genes assigned to the canonical pathway. Note $-\log_{10}(0.05) = 1.3$. Abbreviations: CDK5, cyclin-dependent kinase 5; DEGs, differentially expressed genes; dTMP, deoxythymidine monophosphate; PCP, planar cell polarity; PRKN-PD, parkin-associated Parkinson's disease.

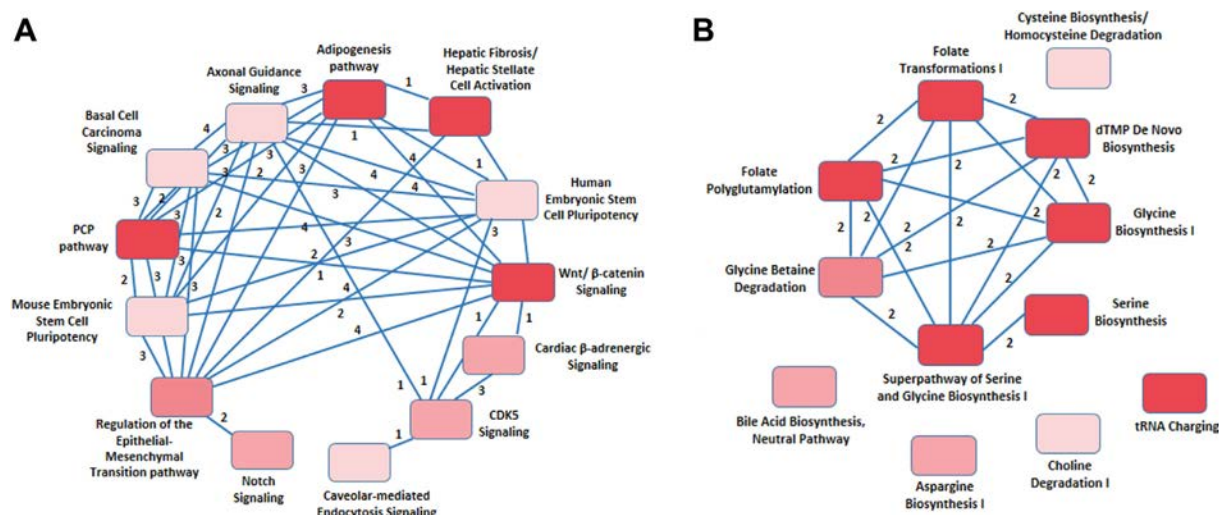


Fig. 4. (A and B) Network of overlapping canonical pathways altered in PRKN-PD fibroblasts. Each pathway is represented as a single node colored proportionally to the Fisher's exact test *p*-value, where brighter red means more significant. The line connecting the pathways contains the number of common molecules between the considered pathways. Abbreviations: dTMP, deoxythymidine monophosphate; PCP, planar cell polarity; PRKN-PD, parkin-associated Parkinson's disease. (For interpretation of the references to color in this figure legend, the reader is referred to the Web version of this article.)

respectively). These genes were predicted to affect the expression of 23 and 7 downstream genes, respectively.

3.6. Biochemical analysis

We analyzed the main methylated active form of folate (5-MTHF), total folate (methylated and nonmethylated forms), and the amino acids participating in the metabolism of this compound (serine, glycine, and methionine) in our set of fibroblasts (Fig. 5A). 5-MTHF levels were borderline significantly increased in PRKN-PD fibroblasts compared to healthy control fibroblasts (33.12 ± 1.9 vs. 23.27 ± 3.48 ; $p = 0.048$; Fig. 5B), whereas no differences were detected in total folate, glycine, and serine concentrations (Supplemental Fig. 1A–C). Methionine showed a trend of increased levels in PRKN-PD fibroblasts, without reaching statistical significance (Supplemental Fig. 1D).

3.7. Quantitative RT-PCR validation of DEGs

For technical validation of RNA-seq data, we selected the DEGs *SHMT1*, *SHMT2*, *MTHFD2*, *PSAT1*, and *COL5A1* and quantified gene expression by qRT-PCR. The selected genes were involved in the top predicted molecular processes associated to *PRKN* mutations (1C folate-mediated metabolism, de novo serine biosynthesis, and fibrosis) and had a fold change above 2. From these, 4 DEGs were significantly upregulated and 1 was downregulated in both analyses (Supplemental Fig. 2). By using this method, we validated the RNA-seq findings.

4. Discussion

We report for the first time the presence of a large number of gene expression alterations at the transcriptome level in skin fibroblasts from PD patients carrying mutations in the *PRKN*. We

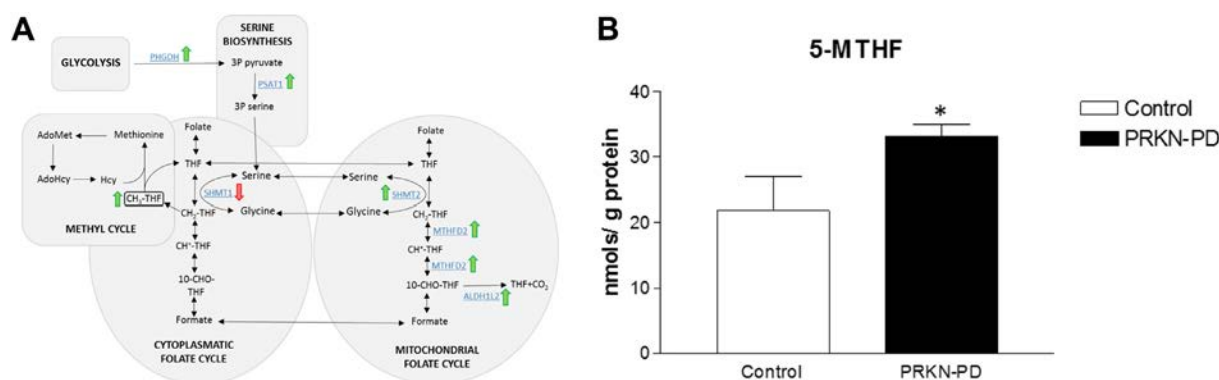


Fig. 5. (A) Summary of 1C (1-carbon) metabolism and altered pathways in PRKN-PD (parkin-associated Parkinson's disease) fibroblasts. Deregulated transcripts and metabolites are represented in blue and black, respectively. Circled metabolites and blue underlined transcripts showed significant changes in patients. Green and red arrows mean upregulation and downregulation of the molecule, respectively. (B) 5-MTHF concentration in fibroblasts from PRKN-PD patients and healthy subjects. A significant increase in 5-MTHF levels was observed in PRKN-PD fibroblasts ($*p < 0.05$). Abbreviations (transcripts): *ALDH1L2*, aldehyde dehydrogenase 1 family member L2; *MTHFD2*, methylenetetrahydrofolate dehydrogenase (NADP+ dependent) 2/methylenetetrahydrofolate cyclohydrolase; *PHGDG*, phosphoglycerate dehydrogenase; *PSAT1*, phosphoserine aminotransferase 1; *SHMT1*, serine hydroxymethyltransferase 1; *SHMT2*, serine hydroxymethyltransferase 2. Abbreviations (metabolites): 3P pyruvate, 3-phosphohydroxy pyruvate; 3P serine, 3-phosphoserine; 10-CHO-THF, 10-formyl-THF; AdoHcy, S-adenosylhomocysteine; AdoMet, S-adenosylmethionine; CH2-THF, 5,10-methylene-tetrahydrofolate; CH3-THF, 5-methyltetrahydrofolate (5-MTHF); CH+-THF, 5,10-methenyl-tetrahydrofolate; Hcy, homocysteine; THF, tetrahydrofolate. (For interpretation of the references to color in this figure legend, the reader is referred to the Web version of this article.)

identified 343 DEGs associated with PRKN-PD of which 206 were upregulated DEGs, whereas 137 were downregulated. Biological enrichment analysis revealed that these DEGs were mainly involved in cell adhesion, cell growth, amino acid biosynthesis, and folate metabolism among others.

To date, other transcriptomic studies have been performed in several biospecimens from PD patients including different post-mortem brain areas. Thus, expression studies in the SNpc from sPD patients have identified gene expression differences associated with disease mostly affecting processes relevant to PD such as dopaminergic transmission, cell adhesion, axonal guidance, inflammation, the ubiquitin-proteasome system, and mitochondrial function (Duke et al., 2006; Duke et al., 2007; Durrenberger et al., 2012; Grunblatt et al., 2004; Hauser et al., 2005). Other studies using single DANs isolated from postmortem SNpc have reported similar disturbances as those observed in SNpc sections (Elstner et al., 2011; Simunovic et al., 2010; Zheng et al., 2010). Other brain areas affected by PD, such as the putamen, cortex, and locus coeruleus, have also shown specific transcriptomic changes associated with disease (Botta-Orfila et al., 2012a,b; Naydenov et al., 2010; Stamper et al., 2008; Zhang et al., 2005). In addition, cellular studies in biopsies from olfactory mucosa of sPD patients have also revealed transcriptomic changes related with some of the aforementioned pathways (Mar et al., 2011; Matigian et al., 2010). In other peripheral tissues, reports using venous blood from sPD patients have identified deregulated genes that were related to the immune system, mitochondrial dysfunction, and axon guidance (Mutez et al., 2014; Scherzer et al., 2007). In this scenario, our study expands previous evidences of gene expression changes in PD peripheral tissues by identifying altered expression profiles in skin fibroblasts from patients carrying mutations in the *PRKN*. Our results reinforce the emerging view of PD as a systemic disease that affects not only DANs from the central nervous system (Beach et al., 2010; Chaudhuri & Schapira, 2009) but also peripheral non-neural tissues including the skin (Cardellach et al., 1993; Han et al., 2017; Hoepken et al., 2008; Lin et al., 2017).

At the clinical level, early peripheral nervous system pathology has been related to premotor symptoms of disease such as orthostatic hypotension, constipation, urinary problems, erectile dysfunction, or sweating abnormalities (Cersosimo & Benarroch, 2012; Dabby et al., 2006; Djaldetti et al., 2009; Jain, 2011). Specifically in the skin, potential PD pathology of this tissue is underexplored, but a recent study has proposed seborrheic dermatitis as a risk factor for PD (Arsic Arsenijevic et al., 2014; Ravn et al., 2017; Tanner et al., 2012). Another study has also shown that a facial skin dermatosis termed rosacea can occur as a premotor symptom of PD (Egeberg et al., 2016). Moreover, PD patients have also been suggested to have an increased risk for developing skin diseases such as cutaneous melanoma (Liu et al., 2011; Tell-Marti et al., 2015). Our findings are in line with these studies showing that PD peripheral fibroblasts exhibit large transcriptomic changes. Yet it should be mentioned that macroscopically we did not observe any apparent skin phenotype in the PRKN-PD patients. However, we cannot rule out subclinical alterations, which could remain unnoticed, or also hypothetical interconnections between dermal fibroblasts alterations and the peripheral nervous system pathology described in PD. According to our findings, future studies exploring these issues are warranted.

Primary fibroblast cultures obtained by punch skin biopsy from patients with either sPD or monogenic PD have been proposed as a cellular model of disease (Auburger et al., 2012). PD fibroblasts preserve the patient genetic background and can also reflect potential exposure to environmental cues. To date, some PD cellular phenotypes have been observed in fibroblasts from patients such as

altered protein expression (Azkona et al., 2018; Lippolis et al., 2015), including alpha-synuclein upregulation (Hoepken et al., 2008), microtubule destabilization (Cartelli et al., 2012), impaired autophagy (Dehay et al., 2012) (Rakovic et al., 2013), increased sensitivity to neurotoxins (Yakhine-Diop et al., 2014), bioenergetic deficits (Ambrosi et al., 2014; Papkovskaia et al., 2012), mitochondrial alterations (Mortiboys et al., 2008; Mortiboys et al., 2010), and enhanced apoptosis (Klinkenberg et al., 2010; Romani-Aumedes et al., 2014). Interestingly, several of these molecular phenotypes including cytoskeleton, mitochondrial, and oxidative stress defects have been observed in both PD fibroblasts (Cartelli et al., 2012; Grunewald et al., 2010; Mortiboys et al., 2008) and induced pluripotent stem cells (iPSC)-derived DANs, also in PRKN-PD (Chung et al., 2016; Imaizumi et al., 2012; Ren et al., 2015). In this scenario, our study implements previous research showing that similar to other neurodegenerative disorders (Raman et al., 2015), global gene expression changes also occur in fibroblasts from PD patients, at least in those patients carrying *PRKN* mutations.

Network analysis of the gene expression changes detected in our PRKN-PD fibroblasts showed 2 different networks. The first network (Fig. 4A) comprised pathways involved in extracellular matrix organization, cell adhesion, and cell motility. Specifically, these included Wnt/ β -catenin, cyclin-dependent kinase 5, Notch, and axon guidance pathways. These interconnected pathways regulate axon formation (Salinas, 2012), migration (Kamiguchi, 2007; Zou, 2004), regeneration (El Bejjani & Hammarlund, 2012; Onishi et al., 2014), dendritic morphogenesis, and synaptic function (Giniger, 2012; Salinas, 2012) and have been consistently associated with PD. For instance, upregulation of the Wnt pathway has been described in the ventral midbrain of parkin knockout mice (Berwick & Harvey, 2012). Another study has reported that direct parkin phosphorylation by cyclin-dependent kinase 5 modulates its ubiquitin-ligase activity and aggregation (Avraham et al., 2007). Finally, other study has demonstrated that imbalances in the Notch pathway in adult DANs impair neuronal function and survival (Imai et al., 2015). Transcriptomic alterations related to these neural cytoskeleton pathways have been found in neural tissues and blood cells of PD patients (Grunblatt et al., 2004; Miller et al., 2006; Mutez et al., 2011), and association of single-nucleotide polymorphisms involved in cell adhesion pathways has been identified by genome-wide associated studies in PD (Chapman, 2014).

The second altered network (Fig. 4B) encompassed the anabolic pathways of glycine and serine amino acid metabolism, 1C folate-mediated metabolism, and deoxythymidine monophosphate (dTMP) biosynthesis (Tibbetts & Appling, 2010). These pathways are also functionally related because glycine and serine act as carbon donors for the 1C folate metabolism, which is then connected to nucleic acid biosynthesis (Ormazabal et al., 2015; Tibbetts & Appling, 2010). Recent evidence suggests the participation of these pathways in PD and aging. For instance, 1 study in an aging mouse model of mitochondrial disease has related the aging phenotype with exacerbated serine biosynthesis and deregulation of the 1C folate metabolism leading to nucleotide imbalances (Nikkanen et al., 2016), and similar alterations were indeed also recently reported in a *Drosophila* model of PD (Tufi et al., 2014). Moreover, another study has shown deregulation of folate intermediates in PD patients (dos Santos et al., 2009). In our study, we also identified alterations in the 1C folate metabolism both at the transcriptomic and biochemical level. Specifically, we observed increased expression of transcripts participating in the de novo serine biosynthesis (*PSAT1* and *PHGDH*) and the mitochondrial folate metabolism (*SHMT2*, *MTHFD2*, and *ALDH1L2*), whereas per contrary we detected decreased expression of a transcript participating in the cytoplasmic folate metabolism (*SHMT1*) (Fig. 5A). At the biochemical level, we found that 5-MTHF levels were increased

in PRKN-PD fibroblasts (Fig. 5B). 5-MTHF is the main active form of folate, which acts as a substrate for the remethylation of homocysteine (Knowles et al., 2016), which is crucial for the physiological methylation of a wide variety of molecules (DNA, RNA, proteins) (Ormazabal et al., 2015).

According to the autosomal-recessive inheritance mode of PRKN-PD, it is commonly accepted that 1 heterozygous mutation is not sufficient to cause PD. However, heterozygous mutations in PRKN have been recently proposed to act as a strong risk factor for PD leading to haploinsufficiency or alternatively to a toxic gain of function (Clark et al., 2006a; Shulskaya et al., 2017). In this context, although our study neither explores nor proves pathogenicity of the heterozygous Val15Met mutation, it interestingly shows for the first time an expression pattern of this point mutation similar to that from pathogenic loss-of-function deletions in PRKN. Indeed, it is important to mention that we found common gene expression changes in all 4 patients despite carrying 4 different mutations in PRKN. Our findings concur with a recent study in which fibroblasts from 2 PD patients with different compound-heterozygous PRKN mutations exhibited similarly altered protein expression profiles (Lippolis et al., 2015).

Although our study does not explore the mechanism by which mutations in the PRKN associate with transcriptomic changes in PD fibroblasts, we identified 2 upregulated DEGs, *FGF2* and *TRIB3*, which were predicted as upstream transcriptional regulators of a subset of other identified DEGs. *FGF2* is a growth factor involved in neural development and maintenance, which has shown deficient expression levels in the few surviving DANs at the SNpc from PD patients (Tooyama et al., 1993; Tooyama et al., 1994). *TRIB3* is a stress-induced pro-apoptotic gene that physically interacts with PRKN at the protein level (Aime et al., 2015). In addition, *TRIB3* has shown gene and protein expression upregulation in both PD cellular models and SNpc from PD patients (Aime et al., 2015; Ryu et al., 2005). On the other hand, *TRIB3* is activated by *ATF4* (Jousse et al., 2007; Ohoka et al., 2005), the second gene in the list of the top predicted upstream regulators. *ATF4* is a transcription factor that drives the activation of the mitochondrial stress response activating targeted genes involved in the 1C folate metabolism (Suomalainen & Battersby, 2018). Previous studies have suggested the relevance of mitochondrial stress response in conditions of secondary mitochondrial DNA instability such as PD (Nikkanen et al., 2016; Suomalainen & Battersby, 2018).

Our study has some limitations. First, the sample size of our cohort is limited. Second, our study is focused in PRKN-PD, but other PD monogenic forms have not been explored. Third, all the patients were treated with L-DOPA, and thus, we cannot discard that some of the observed expression differences could be affected by treatment. Finally, we did not explore the mechanism by which PRKN mutations can be linked with gene expression changes at the skin level. In this regard, future studies performing, for instance, rescue experiments may be helpful to clarify this issue.

In summary, we found that PRKN mutations are associated with a large number of gene expression changes in fibroblasts from PRKN-PD patients supporting the view of PD as a systemic disease that affects also non-neural peripheral tissues such as the skin. Future studies performing a detailed molecular and clinical characterization of the skin or exploring potential interconnections between dermal fibroblasts and peripheral nerve pathology in PD are warranted.

Accession number

Gene expression data sets generated in this study have been deposited in the Gene Expression Omnibus (GEO) under accession GSE90514.

Disclosure statement

The authors report no actual or potential conflict of interest including any financial, personal, or other relationships with other people or organizations within 3 years of beginning the work submitted that could inappropriately influence this work.

Acknowledgements

The authors thank the patients who participated in the study and their family members. We also want to thank the programs: Supports a Grups de Recerca de la Generalitat de Catalunya 2017–2019 (grant number SGR 893/2017) and CERCA Programme/Generalitat de Catalunya. This work was developed at the building *Centre de Recerca Biomèdica Cellex*, Barcelona.

Funding: This work was supported by funds from Fondo de Investigaciones Sanitarias of the Instituto de Salud Carlos III (ISCIII; grant number PI11/00462), the Centro de Investigación Biomédica en Red de Enfermedades Raras (CIBERER), initiatives of Instituto Carlos III (ISCIII) and FEDER, and Fundació Privada Cellex. CNAG-CRG laboratory is a member of the Spanish National Bioinformatics Institute (INB), PRB2-ISCIII, and is supported by grant PT13/0001, of the PE I+D+i 2013–2016, funded by ISCIII and FEDER. R.F.-S. was supported by a Jóvenes Investigadores grant of the Spanish Ministry of Economy and Competitiveness (MINECO) (grant SAF2015-73508-JIN (AEI/FEDER/UE)).

Appendix A. Supplementary data

Supplementary data associated with this article can be found, in the online version, at <https://doi.org/10.1016/j.neurobiolaging.2018.01.021>.

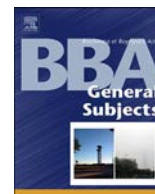
References

- Aime, P., Sun, X., Zareen, N., Rao, A., Berman, Z., Volpicelli-Daley, L., Bernd, P., Cray, J.F., Levy, O.A., Greene, L.A., 2015. Trib3 is elevated in Parkinson's disease and mediates death in Parkinson's disease models. *J. Neurosci.* 35, 10731–10749.
- Alves, G., Forsaa, E.B., Pedersen, K.F., Dreetz Gjerstad, M., Larsen, J.P., 2008. Epidemiology of Parkinson's disease. *J. Neurol.* 255 Suppl 5, 18–32.
- Ambrosi, G., Ghezzi, C., Sepe, S., Milanese, C., Payan-Gomez, C., Bombardieri, C.R., Armentero, M.T., Zangaglia, R., Pacchetti, C., Mastroberardino, P.G., Blandini, F., 2014. Bioenergetic and proteolytic defects in fibroblasts from patients with sporadic Parkinson's disease. *Biochim. Biophys. Acta* 1842, 1385–1394.
- Amelio, I., Cutruzzola, F., Antonov, A., Agostini, M., Melino, G., 2014. Serine and glycine metabolism in cancer. *Trends Biochem. Sci.* 39, 191–198.
- Arsic Arsenijevic, V.S., Milobratovic, D., Barac, A.M., Vekic, B., Marinkovic, J., Kostic, V.S., 2014. A laboratory-based study on patients with Parkinson's disease and seborrheic dermatitis: the presence and density of Malassezia yeasts, their different species and enzymes production. *BMC Dermatol.* 14, 5.
- Auburger, G., Klinckenberg, M., Drost, J., Marcus, K., Morales-Gordo, B., Kunz, W.S., Brandt, U., Broccoli, V., Reichmann, H., Gispert, S., Jendrach, M., 2012. Primary skin fibroblasts as a model of Parkinson's disease. *Mol. Neurobiol.* 46, 20–27.
- Avraham, E., Rott, R., Liani, E., Szargel, R., Engelender, S., 2007. Phosphorylation of Parkin by the cyclin-dependent kinase 5 at the linker region modulates its ubiquitin-ligase activity and aggregation. *J. Biol. Chem.* 282, 12842–12850.
- Azkona, G., Lopez de Maturana, R., Del Rio, P., Sousa, A., Vazquez, N., Zubiarrain, A., Jimenez-Blasco, D., Bolanos, J.P., Morales, B., Auburger, G., Arbelo, J.M., Sanchez-Pernaute, R., 2018. LRRK2 expression is deregulated in fibroblasts and neurons from Parkinson patients with mutations in PINK1. *Mol. Neurobiol.* 55, 506–516.
- Beach, T.G., Adler, C.H., Sue, L.L., Vedders, L., Lue, L., White III, C.L., Akiyama, H., Caviness, J.N., Shill, H.A., Sabbagh, M.N., Walker, D.G., Arizona Parkinson's Disease, C., 2010. Multi-organ distribution of phosphorylated alpha-synuclein histopathology in subjects with Lewy body disorders. *Acta Neuropathol.* 119, 689–702.
- Benjamini, Y.H., Hochberg, Y., 1995. Controlling the false discovery rate: a practical and powerful approach to multiple testing. *J. R. Stat. Soc. Ser. B (Methodological)* 57, 289–300.
- Berwick, D.C., Harvey, K., 2012. The importance of Wnt signalling for neurodegeneration in Parkinson's disease. *Biochem. Soc. Trans.* 40, 1123–1128.
- Bonifati, V., 2014. Genetics of Parkinson's disease—state of the art, 2013. *Parkinsonism Relat. Disord.* 20 Suppl 1, S23–S28.
- Bonifati, V., Rohe, C.F., Breedveld, G.J., Fabrizio, E., De Mari, M., Tassorelli, C., Tavella, A., Marconi, R., Nicholl, D.J., Chien, H.F., Fincati, E., Abbruzzese, G.,

- Marini, P., de Gaetano, A., Horstink, M.W., Maat-Kievit, J.A., Sampaio, C., Antonini, A., Stocchi, F., Montagna, P., Toni, V., Guidi, M., Dalla Libera, A., Tinazzi, M., de Pandis, F., Fabbri, G., Goldwurm, S., de Klein, A., Barbosa, E., Lopiano, L., Martignoni, E., Lamberti, P., Vanacore, N., Meco, G., Oostra, B.A., Italian Parkinson Genetics, N., 2005. Early-onset parkinsonism associated with PINK1 mutations: frequency, genotypes, and phenotypes. *Neurology* 65, 87–95.
- Botta-Orfila, T., Sanchez-Pla, A., Fernandez, M., Carmona, F., Ezquerro, M., Tolosa, E., 2012a. Brain transcriptomic profiling in idiopathic and LRRK2-associated Parkinson's disease. *Brain Res.* 1466, 152–157.
- Botta-Orfila, T., Tolosa, E., Gelpi, E., Sanchez-Pla, A., Marti, M.J., Valldeoriola, F., Fernandez, M., Carmona, F., Ezquerro, M., 2012b. Microarray expression analysis in idiopathic and LRRK2-associated Parkinson's disease. *Neurobiol. Dis.* 45, 462–468.
- Cardellach, F., Marti, M.J., Fernandez-Sola, J., Marin, C., Hoek, J.B., Tolosa, E., Urbano-Marquez, A., 1993. Mitochondrial respiratory chain activity in skeletal muscle from patients with Parkinson's disease. *Neurology* 43, 2258–2262.
- Carmona-Saez, P., Chagoyen, M., Tirado, F., Carazo, J.M., Pascual-Montano, A., 2007. GENECODIS: a web-based tool for finding significant concurrent annotations in gene lists. *Genome Biol.* 8, R3.
- Cartelli, D., Goldwurm, S., Casagrande, F., Pezzoli, G., Cappelletti, G., 2012. Microtubule destabilization is shared by genetic and idiopathic Parkinson's disease patient fibroblasts. *PLoS One* 7, e37467.
- Cersosimo, M.G., Benarroch, E.E., 2012. Autonomic involvement in Parkinson's disease: pathology, pathophysiology, clinical features and possible peripheral biomarkers. *J. Neurol. Sci.* 313, 57–63.
- Chapman, M.A., 2014. Interactions between cell adhesion and the synaptic vesicle cycle in Parkinson's disease. *Med. hypotheses* 83, 203–207.
- Chaudhuri, K.R., Schapira, A.H., 2009. Non-motor symptoms of Parkinson's disease: dopaminergic pathophysiology and treatment. *Lancet Neurol.* 8, 464–474.
- Chung, S.Y., Kishinevsky, S., Mazzulli, J.R., Graziotto, J., Mrejeru, A., Mosharof, E.V., Puspita, L., Valiulahi, P., Sulzer, D., Milner, T.A., Taldone, T., Krainc, D., Studer, L., Shim, J.W., 2016. Parkin and PINK1 patient iPSC-derived midbrain dopamine neurons exhibit mitochondrial dysfunction and alpha-synuclein accumulation. *Stem Cell Rep.* 7, 664–677.
- Clark, L.N., Afridi, S., Karlins, E., Wang, Y., Mejia-Santana, H., Harris, J., Louis, E.D., Cote, L.J., Andrews, H., Fahn, S., Waters, C., Ford, B., Frucht, S., Ottman, R., Marder, K., 2006a. Case-control study of the parkin gene in early-onset Parkinson disease. *Arch. Neurol.* 63, 548–552.
- Clark, I.E., Dodson, M.W., Jiang, C., Cao, J.H., Huh, J.R., Seol, J.H., Yoo, S.J., Hay, B.A., Guo, M., 2006b. Drosophila pink1 is required for mitochondrial function and interacts genetically with parkin. *Nature* 441, 1162–1166.
- da Costa, C.A., Sunyach, C., Giaime, E., West, A., Corti, O., Brice, A., Safe, S., Abou-Sleiman, P.M., Wood, N.W., Takahashi, H., Goldberg, M.S., Shen, J., Checler, F., 2009. Transcriptional repression of p53 by parkin and impairment by mutations associated with autosomal recessive juvenile Parkinson's disease. *Nat. Cell Biol.* 11, 1370–1375.
- Dabby, R., Djaldetti, R., Shahmurov, M., Treves, T.A., Gabai, B., Melamed, E., Sadeh, M., Avinoach, I., 2006. Skin biopsy for assessment of autonomic denervation in Parkinson's disease. *J. Neural Transm.* 113, 1169–1176.
- Dehay, B., Ramirez, A., Martinez-Vicente, M., Perier, C., Canron, M.H., Doudnikoff, E., Vital, A., Vila, M., Klein, C., Bezdard, E., 2012. Loss of P-type ATPase ATP13A2/PARK9 function induces general lysosomal deficiency and leads to Parkinson disease neurodegeneration. *Proc. Natl. Acad. Sci. U. S. A.* 109, 9611–9616.
- Djaldetti, R., Lev, N., Melamed, E., 2009. Lesions outside the CNS in Parkinson's disease. *Mov. Disord.* 24, 793–800.
- Duke, D.C., Moran, L.B., Kalaitzakis, M.E., Deprez, M., Dexter, D.T., Pearce, R.K., Graeber, M.B., 2006. Transcriptome analysis reveals link between proteasomal and mitochondrial pathways in Parkinson's disease. *Neurogenetics* 7, 139–148.
- Duke, D.C., Moran, L.B., Pearce, R.K., Graeber, M.B., 2007. The medial and lateral substantia nigra in Parkinson's disease: mRNA profiles associated with higher brain tissue vulnerability. *Neurogenetics* 8, 83–94.
- Duplan, E., Sevalle, J., Viotti, J., Goiran, T., Bauer, C., Renbaum, P., Levy-Lahad, E., Gautier, C.A., Corti, O., Leroudier, N., Checler, F., da Costa, C.A., 2013. Parkin differently regulates presenilin-1 and presenilin-2 functions by direct control of their promoter transcription. *J. Mol. Cell Biol.* 5, 132–142.
- Durrenberger, P.F., Grunblatt, E., Fernando, F.S., Monoranu, C.M., Evans, J., Riederer, P., Reynolds, R., Dexter, D.T., 2012. Inflammatory pathways in Parkinson's disease; a BNE microarray study. *Parkinsons Dis.* 2012, 214714.
- Egeberg, A., Hansen, P.R., Gislason, G.H., Thyssen, J.P., 2016. Exploring the association between rosacea and Parkinson disease: a Danish Nationwide cohort study. *JAMA Neurol.* 73, 529–534.
- El Bejjani, R., Hammarlund, M., 2012. Notch signaling inhibits axon regeneration. *Neuron* 73 (2), 268–278.
- Elstner, M., Morris, C.M., Heim, K., Bender, A., Mehta, D., Jaros, E., Klopstock, T., Meitinger, T., Turnbull, D.M., Prokisch, H., 2011. Expression analysis of dopaminergic neurons in Parkinson's disease and aging links transcriptional dysregulation of energy metabolism to cell death. *Acta Neuropathol.* 122, 75–86.
- Fernandez-Santiago, R., Carballo-Carbajal, I., Castellano, G., Torrent, R., Richaud, Y., Sanchez-Danes, A., Mosquera, J.L., Soriano, J., Lopez-Barneo, J., Canals, J.M., Alberch, J., Raya, A., Vila, M., Consiglio, A., Martin-Subero, J.L., Ezquerro, M., Tolosa, E., 2015. Aberrant epigenome in iPSC-derived dopaminergic neurons from Parkinson's disease patients. *EMBO Mol. Med.* 7, 1529–1546.
- Fiesel, F.C., Caulfield, T.R., Moussaud-Lamodiere, E.L., Ogaki, K., Dourado, D.F., Flores, S.C., Ross, O.A., Springer, W., 2015. Structural and functional impact of Parkinson disease-associated mutations in the E3 ubiquitin ligase parkin. *Hum. Mutat.* 36, 774–786.
- Fiskin, E., Dikic, I., 2013. Parkin promotes cell survival via linear ubiquitination. *EMBO J.* 32, 1072–1074.
- Ginger, E., 2012. Notch signaling and neural connectivity. *Curr. Opin. Genet. Dev.* 22, 339–346.
- Grunewald, A., Voges, L., Rakovic, A., Kasten, M., Vandebona, H., Hemmelmann, C., Lohmann, K., Orolicki, S., Ramirez, A., Schapira, A.H., Pramstaller, P.P., Sue, C.M., Klein, C., 2010. Mutant Parkin impairs mitochondrial function and morphology in human fibroblasts. *PLoS One* 5, e12962.
- Grunblatt, E., Mandel, S., Jacob-Hirsch, J., Zeligson, S., Amariglio, N., Rechavi, G., Li, J., Ravid, R., Roggendorf, W., Riederer, P., Youdim, M.B., 2004. Gene expression profiling of parkinsonian substantia nigra pars compacta; alterations in ubiquitin-proteasome, heat shock protein, iron and oxidative stress regulated proteins, cell adhesion/cellular matrix and vesicle trafficking genes. *J. Neural Transm.* 111, 1543–1573.
- Han, K., Hassanzadeh, S., Singh, K., Menazza, S., Nguyen, T.T., Stevens, M.V., Nguyen, A., San, H., Anderson, S.A., Lin, Y., Zou, J., Murphy, E., Sack, M.N., 2017. Parkin regulation of CHOP modulates susceptibility to cardiac endoplasmic reticulum stress. *Sci. Rep.* 7, 2093.
- Hasson, S.A., Kane, L.A., Yamano, K., Huang, C.H., Sliter, D.A., Buehler, E., Wang, C., Heman-Ackah, S.M., Hessa, T., Guha, R., Martin, S.E., Youle, R.J., 2013. High-content genome-wide RNAi screens identify regulators of parkin upstream of mitophagy. *Nature* 504, 291–295.
- Hauser, M.A., Li, Y.J., Xu, H., Noureddine, M.A., Shao, Y.S., Gullans, S.R., Scherzer, C.R., Jensen, R.V., McLaurin, A.C., Gibson, J.R., Scott, B.L., Jewett, R.M., Stenger, J.E., Schmechel, D.E., Hulette, C.M., Vance, J.M., 2005. Expression profiling of substantia nigra in Parkinson disease, progressive supranuclear palsy, and frontotemporal dementia with parkinsonism. *Arch. Neurol.* 62, 917–921.
- Hoepken, H.H., Gispert, S., Azizov, M., Klinkenberg, M., Ricciardi, F., Kurz, A., Morales-Gordo, B., Bonin, M., Riess, O., Gasser, T., Kogel, D., Steinmetz, H., Auburger, G., 2008. Parkinson patient fibroblasts show increased alpha-synuclein expression. *Exp. Neurol.* 212, 307–313.
- Hughes, A.J., Ben-Shlomo, Y., Daniel, S.E., Lees, A.J., 1992. What features improve the accuracy of clinical diagnosis in Parkinson's disease: a clinicopathologic study. *Neurology* 42, 1142–1146.
- Imai, Y., Kobayashi, Y., Inoshita, T., Meng, H., Arano, T., Uemura, K., Asano, T., Yoshimi, K., Zhang, C.L., Matsumoto, G., Ohtsuka, T., Kageyama, R., Kiyonari, H., Shioi, G., Nukina, N., Hattori, N., Takahashi, R., 2015. The Parkinson's disease-associated protein kinase LRRK2 modulates Notch signaling through the Endosomal pathway. *PLoS Genet.* 11, e1005503.
- Imaizumi, Y., Okada, Y., Akamatsu, W., Koike, M., Kuzumaki, N., Hayakawa, H., Nihira, T., Kobayashi, T., Ohya, M., Sato, S., Takanashi, M., Funayama, M., Hirayama, A., Soga, T., Hishiki, T., Suematsu, M., Yagi, T., Ito, D., Kosakai, A., Hayashi, K., Shouji, M., Nakanishi, A., Suzuki, N., Mizuno, Y., Mizushima, N., Amagai, M., Uchiyama, Y., Mochizuki, H., Hattori, N., Okano, H., 2012. Mitochondrial dysfunction associated with increased oxidative stress and alpha-synuclein accumulation in PARK2 iPSC-derived neurons and postmortem brain tissue. *Mol. Brain* 5, 35.
- Infante, J., Prieto, C., Sierra, M., Sanchez-Juan, P., Gonzalez-Aramburu, I., Sanchez-Quintana, C., Berciano, J., Combarros, O., Sainz, J., 2015. Identification of candidate genes for Parkinson's disease through blood transcriptome analysis in LRRK2-G2019S carriers, idiopathic cases, and controls. *Neurobiol. Aging* 36, 1105–1109.
- Jain, S., 2011. Multi-organ autonomic dysfunction in Parkinson disease. *Parkinsonism Relat. Disord.* 17, 77–83.
- Jousse, C., Deval, C., Maurin, A.C., Parry, L., Cherasse, Y., Chaveroux, C., Lefloch, R., Lenormand, P., Bruhat, A., Fafournoux, P., 2007. TRB3 inhibits the transcriptional activation of stress-regulated genes by a negative feedback on the ATF4 pathway. *J. Biol. Chem.* 282, 15851–15861.
- Kamiguchi, H., 2007. The role of cell adhesion molecules in axon growth and guidance. *Adv. Exp. Med. Biol.* 621, 95–103.
- Klein, C., Westenberger, A., 2012. Genetics of Parkinson's disease. *Cold Spring Harb. Perspect. Med.* 2, a008888.
- Klinkenberg, M., Thurov, N., Gispert, S., Ricciardi, F., Eich, F., Prehn, J.H., Auburger, G., Kogel, D., 2010. Enhanced vulnerability of PARK6 patient skin fibroblasts to apoptosis induced by proteasomal stress. *Neuroscience* 166, 422–434.
- Knowles, L., Morris, A.A., Walter, J.H., 2016. Treatment with mefolinate (5-methyltetrahydrofolate), but not folic acid or folinic acid, leads to measurable 5-methyltetrahydrofolate in cerebrospinal fluid in methyltetrahydrofolate reductase deficiency. *JIMD Rep.* 29, 103–107.
- de Lau, L.M., Breteler, M.M., 2006. Epidemiology of Parkinson's disease. *Lancet Neurol.* 5, 525–535.
- Lin, C.H., Yang, S.Y., Horng, H.E., Yang, C.C., Chieh, J.J., Chen, H.H., Liu, B.H., Chiu, M.J., 2017. Plasma alpha-synuclein predicts cognitive decline in Parkinson's disease. *J. Neurol. Neurosurg. Psychiatry* 88, 818–824.
- Liu, R., Gao, X., Lu, Y., Chen, H., 2011. Meta-analysis of the relationship between Parkinson disease and melanoma. *Neurology* 76, 2002–2009.
- Lippolis, R., Siciliano, R.A., Pacelli, C., Ferretta, A., Mazzeo, M.F., Scacco, S., Papa, F., Galbello, A., Dell'acqua, C., de Mari, M., Papa, S., Cocco, T., 2015. Altered protein expression pattern in skin fibroblasts from parkin-mutant early-onset Parkinson's disease patients. *Biochim. Biophys. Acta* 1852, 1960–1970.
- Mar, J.C., Matigian, N.A., Mackay-Sim, A., Mellick, G.D., Sue, C.M., Silburn, P.A., McGrath, J.J., Quackenbush, J., Wells, C.A., 2011. Variance of gene expression

- identifies altered network constraints in neurological disease. *PLoS Genet.* 7, e1002207.
- Marco-Sola, S., Sammeth, M., Guigo, R., Ribeca, P., 2012. The GEM mapper: fast, accurate and versatile alignment by filtration. *Nat. Methods* 9, 1185–1188.
- Matigian, N., Abrahamson, G., Sutharsan, R., Cook, A.L., Vitale, A.M., Nouwens, A., Bellette, B., An, J., Anderson, M., Beckhouse, A.G., Bennebroek, M., Cecil, R., Chalk, A.M., Cochrane, J., Fan, Y., Feron, F., McCurdy, R., McGrath, J.J., Murrell, W., Perry, C., Raju, J., Ravishankar, S., Silburn, P.A., Sutherland, G.T., Mahler, S., Mellick, G.D., Wood, S.A., Sue, C.M., Wells, C.A., Mackay-Sim, A., 2010. Disease-specific, neurosphere-derived cells as models for brain disorders. *Dis. Models Mech.* 3, 785–798.
- Miller, R.M., Kiser, G.L., Kaysser-Kranich, T.M., Lockner, R.J., Palaniappan, C., Federoff, H.J., 2006. Robust dysregulation of gene expression in substantia nigra and striatum in Parkinson's disease. *Neurobiol. Dis.* 21, 305–313.
- Montgomery, S.B., Sammeth, M., Gutierrez-Arcelus, M., Lach, R.P., Ingle, C., Nisbett, J., Guigo, R., Dermitzakis, E.T., 2010. Transcriptome genetics using second generation sequencing in a Caucasian population. *Nature* 464, 773–777.
- Mortiboys, H., Thomas, K.J., Koopman, W.J., Klaffke, S., Abou-Sleiman, P., Olpin, S., Wood, N.W., Willems, P.H., Smeitink, J.A., Cookson, M.R., Bandmann, O., 2008. Mitochondrial function and morphology are impaired in parkin-mutant fibroblasts. *Ann. Neurol.* 64, 555–565.
- Mortiboys, H., Johansen, K.K., Aasly, J.O., Bandmann, O., 2010. Mitochondrial impairment in patients with Parkinson disease with the G2019S mutation in LRRK2. *Neurology* 75, 2017–2020.
- Munoz, E., Tolosa, E., Pastor, P., Marti, M.J., Valldeoriola, F., Campdelacreu, J., Oliva, R., 2002. Relative high frequency of the c.255delA parkin gene mutation in Spanish patients with autosomal recessive parkinsonism. *J. Neurol. Neurosurg. Psychiatry* 73, 582–584.
- Mutez, E., Larvor, L., Lepretre, F., Mouroux, V., Hamalek, D., Kerckaert, J.P., Perez-Tur, J., Wauquier, N., Vanbesien-Mailliot, C., Dufloc, A., Devos, D., Dedefbre, L., Kreisler, A., Frigard, B., Destee, A., Chartier-Harlin, M.C., 2011. Transcriptional profile of Parkinson blood mononuclear cells with LRRK2 mutation. *Neurobiol. Aging* 32, 1839–1848.
- Mutez, E., Nkizila, A., Belarbi, K., de Broucker, A., Vanbesien-Mailliot, C., Bleuse, S., Bleuse, S., Dufloc, A., Comptdaer, T., Semaille, P., Blervaque, R., Hot, D., Lepretre, F., Figeac, M., Destee, A., Chartier-Harlin, M.C., 2014. Involvement of the immune system, endocytosis and EIF2 signaling in both genetically determined and sporadic forms of Parkinson's disease. *Neurobiol. Dis.* 63, 165–170.
- Naydenov, A.V., Vassoler, F., Luksik, A.S., Kaczmarek, J., Konradi, C., 2010. Mitochondrial abnormalities in the putamen in Parkinson's disease dyskinesia. *Acta Neuropathol* 120, 623–631.
- Nikkanen, J., Forsstrom, S., Euro, L., Paetau, I., Kohnz, R.A., Wang, L., Chilov, D., Viinamaki, J., Roivainen, A., Marjamaki, P., Liljenback, H., Ahola, S., Buzkova, J., Terzioglu, M., Khan, N.A., Pirnes-Karhu, S., Paetau, A., Lonnqvist, T., Sajantila, A., Isohanni, P., Tuymismaa, H., Nomura, D.K., Battersby, B.J., Velagapudi, V., Carroll, C.J., Suomalainen, A., 2016. Mitochondrial DNA replication defects disturb cellular dNTP pools and remodel one-carbon metabolism. *Cell Metab.* 23, 635–648.
- Nogales-Cadenas, R., Carmona-Saez, P., Vazquez, M., Vicente, C., Yang, X., Tirado, F., Carazo, J.M., Pascual-Montano, A., 2009. GeneCodis: interpreting gene lists through enrichment analysis and integration of diverse biological information. *Nucleic Acids Res.* 37, W317–W322.
- Ohoka, N., Yoshii, S., Hattori, T., Onozaki, K., Hayashi, H., 2005. TRB3, a novel ER stress-inducible gene, is induced via ATF4-CHOP pathway and is involved in cell death. *EMBO J.* 24, 1243–1255.
- Onishi, K., Hollis, E., Zou, Y., 2014. Axon guidance and injury-lessons from Wnts and Wnt signaling. *Curr. Opin. Neurobiol.* 27, 232–240.
- Ormazabal, A., Garcia-Cazorla, A., Perez-Duenas, B., Gonzalez, V., Fernandez-Alvarez, E., Pineda, M., Campistol, J., Artuch, R., 2006. Determination of 5-methyltetrahydrofolate in cerebrospinal fluid of paediatric patients: reference values for a paediatric population. *Clinica Chim. Acta Int. J. Clin. Chem.* 371, 159–162.
- Ormazabal, A., Casado, M., Molero-Luis, M., Montoya, J., Rahman, S., Aylett, S.B., Hargreaves, I., Heales, S., Artuch, R., 2015. Can folic acid have a role in mitochondrial disorders? *Drug Discov. Today* 20, 1349–1354.
- Papkovskaia, T.D., Chau, K.Y., Inesta-Vaquera, F., Papkovsky, D.B., Healy, D.G., Nishio, K., Staddon, J., Duchon, M.R., Hardy, J., Schapira, A.H., Cooper, J.M., 2012. G2019S leucine-rich repeat kinase 2 causes uncoupling protein-mediated mitochondrial depolarization. *Hum. Mol. Genet.* 21, 4201–4213.
- Park, J., Lee, S.B., Lee, S., Kim, Y., Song, S., Kim, S., Bae, E., Kim, J., Shong, M., Kim, J.M., Chung, J., 2006. Mitochondrial dysfunction in *Drosophila* PINK1 mutants is complemented by parkin. *Nature* 441, 1157–1161.
- Pickrell, A.M., Youle, R.J., 2015. The roles of PINK1, parkin, and mitochondrial fidelity in Parkinson's disease. *Neuron* 85, 257–273.
- Rakovic, A., Shurkewitsch, K., Seibler, P., Grunewald, A., Zanon, A., Hagenah, J., Krainc, D., Klein, C., 2013. Phosphatase and tensin homolog (PTEN)-induced putative kinase 1 (PINK1)-dependent ubiquitination of endogenous Parkin attenuates mitophagy: study in human primary fibroblasts and induced pluripotent stem cell-derived neurons. *J. Biol. Chem.* 288, 2223–2237.
- Raman, R., Allen, S.P., Goodall, E.F., Kramer, S., Ponger, L.L., Heath, P.R., Milo, M., Hollinger, H.C., Walsh, T., Highley, J.R., Olpin, S., McDermott, C.J., Shaw, P.J., Kirby, J., 2015. Gene expression signatures in motor neurone disease fibroblasts reveal dysregulation of metabolism, hypoxia-response and RNA processing functions. *Neuropathol. Appl. Neurobiol.* 41, 201–226.
- Ravn, A.H., Thyssen, J.P., Egeberg, A., 2017. Skin disorders in Parkinson's disease: potential biomarkers and risk factors. *Clin. Cosmet. Investig. Dermatol.* 10, 87–92.
- Ren, Y., Jiang, H., Hu, Z., Fan, K., Wang, J., Janoschka, S., Wang, X., Ge, S., Feng, J., 2015. Parkin mutations reduce the complexity of neuronal processes in iPSC-derived human neurons. *Stem Cells* 33, 68–78.
- Robinson, M.D., Oshlack, A., 2010. A scaling normalization method for differential expression analysis of RNA-seq data. *Genome Biol.* 11, R25.
- Romani-Aumedes, J., Canal, M., Martin-Flores, N., Sun, X., Perez-Fernandez, V., Wewering, S., Fernandez-Santiago, R., Ezquerria, M., Pont-Sunyer, C., Lafuente, A., Alberch, J., Luebbert, H., Tolosa, E., Levy, O.A., Greene, L.A., Malagelada, C., 2014. Parkin loss of function contributes to R1P801 elevation and neurodegeneration in Parkinson's disease. *Cell Death Dis.* 5, e1364.
- Ryu, E.J., Angelastro, J.M., Greene, L.A., 2005. Analysis of gene expression changes in a cellular model of Parkinson disease. *Neurobiol. Dis.* 18, 54–74.
- dos Santos, E.F., Busanello, E.N., Miglioranza, A., Zanatta, A., Barchak, A.G., Vargas, C.R., Saute, J., Rosa, C., Carrion, M.J., Camargo, D., Dalbem, A., da Costa, J.C., de Sousa Miguel, S.R., de Mello Rieder, C.R., Wajner, M., 2009. Evidence that folic acid deficiency is a major determinant of hyperhomocysteinemia in Parkinson's disease. *Metab. Brain Dis.* 24, 257–269.
- Salinas, P.C., 2012. Wnt signaling in the vertebrate central nervous system: from axon guidance to synaptic function. *Cold Spring Harb. Perspect. Biol.* 4, a008003.
- Sarraf, S.A., Raman, M., Guarani-Pereira, V., Sowa, M.E., Huttlin, E.L., Gygi, S.P., Harper, J.W., 2013. Landscape of the PARKIN-dependent ubiquitylome in response to mitochondrial depolarization. *Nature* 496, 372–376.
- Seirafi, M., Kozlov, G., Gehring, K., 2015. Parkin structure and function. *FEBS J.* 282, 2076–2088.
- Scherzer, C.R., Eklund, A.C., Morse, L.J., Liao, Z., Locascio, J.J., Fefer, D., Schwarzschild, M.A., Schlossmacher, M.G., Hauser, M.A., Vance, J.M., Sudarsky, L.R., Standaert, D.G., Growdon, J.H., Jensen, R.V., Gullans, S.R., 2007. Molecular markers of early Parkinson's disease based on gene expression in blood. *Proc. Natl. Acad. Sci. U. S. A.* 104, 955–960.
- Schouten, J.P., McElgunn, C.J., Waaijer, R., Zwijnenburg, D., Diepvens, F., Pals, G., 2002. Relative quantification of 40 nucleic acid sequences by multiplex ligation-dependent probe amplification. *Nucleic Acids Res.* 30, e57.
- Shulskaya, M.V., Shadrina, M.I., Fedotova, E.Y., Abramycheva, N.Y., Limborska, S.A., Illarionov, S.N., Slominsky, P.A., 2017. Second mutation in PARK2 is absent in patients with sporadic Parkinson's disease and heterozygous exonic deletions/duplications in parkin gene. *Int. J. Neurosci.* 127, 781–784.
- Simchovitz, A., Soreq, L., Soreq, H., 2016. Transcriptome profiling in Parkinson's leukocytes: from early diagnostics to neuroimmune therapeutic prospects. *Curr. Opin. Pharmacol.* 26, 102–109.
- Simunovic, F., Yi, M., Wang, Y., Stephens, R., Sonntag, K.C., 2010. Evidence for gender-specific transcriptional profiles of nigral dopamine neurons in Parkinson disease. *PLoS One* 5, e8856.
- Stamper, C., Siegel, A., Liang, W.S., Pearson, J.V., Stephan, D.A., Shill, H., Connor, D., Caviness, J.N., Sabbagh, M., Beach, T.G., Adler, C.H., Dunckley, T., 2008. Neuronal gene expression correlates of Parkinson's disease with dementia. *Move. Disord.* 23, 1588–1595.
- Suomalainen, A., Battersby, B.J., 2018. Mitochondrial diseases: the contribution of organelle stress responses to pathology. *Nat. Rev. Mol. Cell Biol.* 19, 77–92.
- Tabas-Madrid, D., Nogales-Cadenas, R., Pascual-Montano, A., 2012. GeneCodis3: a non-redundant and modular enrichment analysis tool for functional genomics. *Nucleic Acids Res.* 40, W478–W483.
- Tanner, C., Albers, K., Goldman, S., Fross, R., Leimpeter, A., Klingman, J., van Den Eden, S., 2012. Seborrhic dermatitis and risk of future Parkinson's disease (PD) (S42.001). *Neurology* 78 (1 Suppl), S42.001–S42.
- Tay, S.P., Yeo, C.W., Chai, C., Chua, P.J., Tan, H.M., Ang, A.X., Yip, D.L., Sung, J.X., Tan, P.H., Bay, B.H., Wong, S.H., Tang, C., Tan, J.M., Lim, K.L., 2010. Parkin enhances the expression of cyclin-dependent kinase 6 and negatively regulates the proliferation of breast cancer cells. *J. Biol. Chem.* 285, 29231–29238.
- Tell-Marti, G., Puig-Butille, J.A., Potrony, M., Badenas, C., Mila, M., Malvey, J., Marti, M.J., Ezquerria, M., Fernandez-Santiago, R., Puig, S., 2015. The MC1R melanoma risk variant p.R160W is associated with Parkinson disease. *Ann. Neurol.* 77, 889–894.
- Tibbetts, A.S., Appling, D.R., 2010. Compartmentalization of Mammalian folate-mediated one-carbon metabolism. *Annu. Rev. Nutr.* 30, 57–81.
- Tooyama, I., Kawamata, T., Walker, D., Yamada, T., Hanai, K., Kimura, H., Iwane, M., Igarashi, K., McGeer, E.G., McGeer, P.L., 1993. Loss of basic fibroblast growth factor in substantia nigra neurons in Parkinson's disease. *Neurology* 43, 372–376.
- Tooyama, I., McGeer, E.G., Kawamata, T., Kimura, H., McGeer, P.L., 1994. Retention of basic fibroblast growth factor immunoreactivity in dopaminergic neurons of the substantia nigra during normal aging in humans contrasts with loss in Parkinson's disease. *Brain Res.* 656, 165–168.
- Tufi, R., Gandhi, S., de Castro, I.P., Lehmann, S., Angelova, P.R., Dinsdale, D., Deas, E., Plun-Favreau, H., Nicotera, P., Abramov, A.Y., Willis, A.E., Mallucci, G.R., Loh, S.H., Martins, L.M., 2014. Enhancing nucleotide metabolism protects against mitochondrial dysfunction and neurodegeneration in a PINK1 model of Parkinson's disease. *Nat. Cell Biol.* 16, 157–166.
- Unschuld, P.G., Dachsel, J., Darios, F., Kohlmann, A., Casademunt, E., Lehmann-Horn, K., Dichgans, M., Ruberg, M., Brice, A., Gasser, T., Lucking, C.B., 2006.

- Parkin modulates gene expression in control and ceramide-treated PC12 cells. *Mol. Biol. Rep.* 33, 13–32.
- Yakhine-Diop, S.M., Bravo-San Pedro, J.M., Gomez-Sanchez, R., Pizarro-Estrella, E., Rodriguez-Arribas, M., Climent, V., Aiastui, A., Lopez de Munain, A., Fuentes, J.M., Gonzalez-Polo, R.A., 2014. G2019S LRRK2 mutant fibroblasts from Parkinson's disease patients show increased sensitivity to neurotoxin 1-methyl-4-phenylpyridinium dependent of autophagy. *Toxicology* 324, 1–9.
- Zhang, Y., James, M., Middleton, F.A., Davis, R.L., 2005. Transcriptional analysis of multiple brain regions in Parkinson's disease supports the involvement of specific protein processing, energy metabolism, and signaling pathways, and suggests novel disease mechanisms. *Am. J. Med. Genet. B Neuropsychiatr. Genet.* 137B1, 5–16.
- Zhang, C.W., Hang, L., Yao, T.P., Lim, K.L., 2015. Parkin regulation and neurodegenerative disorders. *Front. Aging Neurosci.* 7, 248.
- Zheng, B., Liao, Z., Locascio, J.J., Lesniak, K.A., Roderick, S.S., Watt, M.L., Eklund, A.C., Zhang-James, Y., Kim, P.D., Hauser, M.A., Grunblatt, E., Moran, L.B., Mandel, S.A., Riederer, P., Miller, R.M., Federoff, H.J., Wullner, U., Papapetropoulos, S., Youdim, M.B., Cantuti-Castelvetri, I., Young, A.B., Vance, J.M., Davis, R.L., Hedreen, J.C., Adler, C.H., Beach, T.G., Graeber, M.B., Middleton, F.A., Rochet, J.C., Scherzer, C.R., GLOBAL, P.D.G.E.C., 2010. PGC-1alpha, a potential therapeutic target for early intervention in Parkinson's disease. *Sci. Transl. Med.* 2, 52ra73.
- Zhou, X., Lindsay, H., Robinson, M.D., 2014. Robustly detecting differential expression in RNA sequencing data using observation weights. *Nucleic Acids Res.* 42, e91.
- Zou, Y., 2004. Wnt signaling in axon guidance. *Trends Neurosci.* 27, 528–532.



Cardiac and placental mitochondrial characterization in a rabbit model of intrauterine growth restriction

M. Guitart-Mampel^{a,e}, A. Gonzalez-Tendero^{b,e}, S. Niñerola^{a,e}, C. Morén^{a,e}, M. Catalán-García^{a,e}, I. González-Casacuberta^{a,e}, D.L. Juárez-Flores^{a,e}, O. Ugarteburu^{c,e}, L. Matalonga^{c,e}, M.V. Cascajo^{d,e}, F. Tort^{c,e}, A. Cortés^{d,e}, E. Tobias^{a,e}, J.C. Milisenda^{a,e}, J.M. Grau^{a,e}, F. Crispí^{b,e}, E. Gratacós^{b,e}, G. Garrabou^{a,e,*}, F. Cardellach^{a,e,*}

^a Muscle Research and Mitochondrial Function Laboratory, Cellex - IDIBAPS, Faculty of Medicine and Health Science, University of Barcelona, Internal Medicine Service, Hospital Clínic of Barcelona, Barcelona, Spain

^b BCNatal - Barcelona Center for Maternal-Fetal and Neonatal Medicine (Hospital Clínic and Hospital Sant Joan de Dew), Clinical Institute of Obstetrics, Gynecology and Neonatology, IDIBAPS, University of Barcelona, Barcelona, Spain

^c Section of Inborn Errors of Metabolism - IBC, Biochemistry and Molecular Genetics Service, Hospital Clínic of Barcelona - IDIBAPS, Barcelona, Spain

^d Centro Andaluz de Biología del Desarrollo, Universidad Pablo de Olavide - CSIC - JA, Sevilla, Spain

^e CIBERER, Madrid, Spain

ARTICLE INFO

Keywords:

Cardiovascular function
Mitochondrial dysfunction
Sirtuin3
Rabbit animal model
Fetal growth
Mitochondrial complex II

ABSTRACT

Background: Intrauterine growth restriction (IUGR) is associated with cardiovascular remodeling persisting into adulthood. Mitochondrial bioenergetics, essential for embryonic development and cardiovascular function, are regulated by nuclear effectors as sirtuins. A rabbit model of IUGR and cardiovascular remodeling was generated, in which heart mitochondrial alterations were observed by microscopic and transcriptomic analysis. We aimed to evaluate if such alterations are translated at a functional mitochondrial level to establish the etiopathology and potential therapeutic targets for this obstetric complication.

Methods: Hearts and placentas from 16 IUGR-offspring and 14 controls were included to characterize mitochondrial function.

Results: Enzymatic activities of complexes II, IV and II + III in IUGR-hearts ($-11.96 \pm 3.16\%$; $-15.58 \pm 5.32\%$; $-14.73 \pm 4.37\%$; $p < 0.05$) and II and II + III in IUGR-placentas ($-17.22 \pm 3.46\%$; $p < 0.005$ and $-29.64 \pm 4.43\%$; $p < 0.001$) significantly decreased. This was accompanied by a not significant reduction in CI-stimulated oxygen consumption and significantly decreased complex II SDHB subunit expression in placenta ($-44.12 \pm 5.88\%$; $p < 0.001$). Levels of mitochondrial content, Coenzyme Q and cellular ATP were conserved. Lipid peroxidation significantly decreased in IUGR-hearts ($-39.02 \pm 4.35\%$; $p < 0.001$), but not significantly increased in IUGR-placentas. Sirtuin3 protein expression significantly increased in IUGR-hearts ($84.21 \pm 31.58\%$; $p < 0.05$) despite conserved anti-oxidant SOD2 protein expression and activity in both tissues.

Conclusions: IUGR is associated with cardiac and placental mitochondrial CII dysfunction. Up-regulated expression of Sirtuin3 may explain attenuation of cardiac oxidative damage and preserved ATP levels under CII deficiency.

General significance: These findings may allow the design of dietary interventions to modulate Sirtuin3 expression and consequent regulation of mitochondrial imbalance associated with IUGR and derived cardiovascular remodeling.

1. Introduction

Intrauterine growth restriction (IUGR) refers to fetuses that do not reach their predefined genetic potential weight and is usually defined as

fetuses with an estimated fetal and birth weight under the 10th percentile for gestational age [1,2]. IUGR is a major cause of perinatal mortality and long-term morbidity [3]. The etiopathology of this complication remains unknown, although there is evidence suggesting

* Corresponding author at: Muscle Research and Mitochondrial Function Laboratory, Cellex - IDIBAPS, Faculty of Medicine and Health Science-University of Barcelona, Internal Medicine Service - Hospital Clinic of Barcelona, 170 Villarroel, 08036 Barcelona, Catalunya, Spain.

E-mail addresses: garrabou@clinic.ub.es (G. Garrabou), fcardell@clinic.ub.es (F. Cardellach).

<https://doi.org/10.1016/j.bbagen.2018.02.006>

Received 7 March 2017; Received in revised form 9 February 2018; Accepted 9 February 2018

Available online 13 February 2018

0304-4165/ © 2018 Elsevier B.V. All rights reserved.

that placental dysfunction followed by hypoxia could lead to IUGR by interference with molecular and bioenergetic processes [3,4]. Placenta is crucial in fetal programming in that, for example, changes in the pattern of the substrates or oxygen transported to the fetus can ultimately lead to cardiovascular or metabolic disease [5–7]. Indeed, it is well known that IUGR is associated with cardiovascular remodeling and dysfunction, persisting into adulthood [8–11]. Establishing the molecular mechanisms of cardiovascular remodeling in IUGR newborns is hampered by the difficulty of accessing the heart as a target tissue. For this reason, our group developed a rabbit model to study IUGR in which cardiovascular remodeling with altered spatial arrangement of intracellular energetic units was evidenced by microscopy in the offspring [12,13], also reflecting the hemodynamic alterations found in newborns of IUGR pregnancies. The global gene expression profile of the hearts of offspring in this IUGR-rabbit model showed alterations in different pathways, all of which converged to mitochondria, including oxygen homeostasis, mitochondrial respiratory chain (MRC) complex I, oxidative phosphorylation and NADH dehydrogenase activity [10,14].

Alternative animal models of IUGR have been developed consisting in carunclectomy, uterine artery ligation, uterine space restriction, caloric restriction or hypoxic conditions, among other procedures, in different species of animals (mainly sheep, pigs or rats models) [15–26]. Heart development is different among species (in structure, timing of maturation, morphology, function, etc.). However, cardiac remodeling have been demonstrated in most of these models [16,18–20,22,27], as well as mitochondrial alterations [24,25,28].

It is important to note that mitochondrial alterations consisting of suboptimal oxygen consumption [29], as well as altered transcriptomic profile of genes involved in mitochondrial function, oxidative phosphorylation and complexes of MRC, and thus energy production and metabolism [30], have been reported in IUGR patients. However, these findings have never been demonstrated in IUGR-hearts, in which depth characterization of mitochondrial function has not been performed to date.

Alterations in mitochondrial and metabolic pathways are critical in fetal programming within the setting of placental insufficiency [31]. Proteins regulating these crucial processes, such as sirtuins, may finally modulate the development of obstetric manifestations and associated complications. Sirtuins are a family of cellular sensors exerting a deacetylase function which regulates cell bioenergetics by synchronizing nuclear and mitochondrial activities [32–35]. Despite evidence of deregulation of sirtuins in skeletal muscle of pigs with spontaneous IUGR [36], little is known about their implication in this obstetric complication. Interestingly, growing evidence supports sirtuins involvement in cardiac disease, independent of IUGR, either by modulation of bioenergetic shift and cardiomyocyte survival [37].

The development of this study in heart and placenta of a validated IUGR animal model facilitated the evaluation of potential disturbances in tissues responsible of cardiovascular remodeling and placental insufficiency. Our hypothesis is that IUGR could be associated with mitochondrial alterations potentially leading to dysfunction of cardiomyocytes and placental metabolic adaptations to hypoxia. We have therefore analyzed whether the transcriptomic and ultrastructural alterations previously reported in cardiomyocytes from offspring of the rabbit model of IUGR with associated cardiovascular remodeling are translated to mitochondrial dysfunction in the same cell type. Second, we evaluated whether heart alterations were also present in the placental tissue, limiting oxygen and nutrient supply. Finally, we aimed to determine the molecular mechanisms responsible for downstream cell adaptations to mitochondrial imbalance, including sirtuins, in order to establish potential therapeutic targets to prevent or revert the development of this obstetric complication and associated cardiovascular remodeling.

2. Materials and methods

2.1. Animal model

Six New Zealand white pregnant rabbits were used to obtain 16 IUGR and 14 control offspring by reproducing a model of IUGR previously reported (see Table S1) [12,13]. This model was based on the selective ligation of uteroplacental vessels to reduce 40 to 50% of oxygen and nutrient supply into the fetuses in development. The ligation was performed only in one of the two uterine horns in order to obtain, in the same pregnancy, the IUGR (from the manipulated horn) and control (from the non-manipulated horn) offspring. Concretely, pregnant animals were fed with standard diet and water ad libitum, with 12 h/12 h of light cycle. At day 25 of gestation, in each pregnant rabbit, the selective ligation of uteroplacental vessels in only one of the two uterine horns was performed. Briefly, tocolysis (progesterone 0.9 mg/kg im) and antibiotic prophylaxis (Penicillin G 300.000 UI iv) were administered before uteroplacental vessel surgery. Ketamine (35 mg/kg) and xylazine (5 mg/kg) were given intramuscularly for anesthesia induction. Inhaled anesthesia was maintained with a mixture of 1–5% isoflurane and 1–1.5 l/min oxygen. After a midline laparotomy, both uterine horns were exteriorized but only one was ligated to reproduce IUGR. At day 30 (full-term pregnancy), a cesarean section was proceeded to obtain both IUGR and control offspring from the same pregnancy (all six pregnant rabbits with the same gestational age) [12,13]. After the procedure, the abdomen was closed and animals received intramuscular meloxicam 0.4 mg·kg⁻¹·24 h⁻¹·48 h, as post-operative analgesia. Offspring (from the uterine horn experimentally modified) weighting under the 10th percentile of birth weight were considered IUGR (cutoff < 60 g) and never weighting higher than any control from the not modified uterine horn and from the same nest. All newborn rabbits were sacrificed by decapitation and the hearts of newborn rabbits were removed from the chest cavity and were then weighed and preserved with Biops Medium (2.77 mM CaK₂EGTA, 7.23 mM K₂EGTA, 5.77 mM Na₂ATP, 6.56 mM MgCl₂·6H₂O, 20 mM Taurine, 15 mM Na₂Phosphocreatine, 20 mM Imidazole, 0.5 mM Dithiothreitol and 50 mM MES, pH 7.1) on ice. Likewise, the placentas of these newborn rabbits were identified, weighed and preserved with Biops Medium (prepared as mentioned previously), on ice.

All biometric parameters were measured once, following standardized protocols [12,13].

Animal handling and all the procedures were performed in accordance to the prevailing regulations and guidelines [38–40] and with the approval of the Animal Experimental Ethics Committee of the University of Barcelona (Barcelona, Spain).

2.2. Sample processing

Left ventricle was used for mitochondrial studies because is the target tissue in which previous transcriptomic and ultrastructural alterations were observed. Additionally, is the tissue were cardiomyopathies are preferentially manifested. Each left ventricle and placenta tissue were processed as follows: a piece of each tissue was maintained in fresh conditions with Biops Medium to assess mitochondrial oxygen consumption, and the remaining tissue was cryopreserved at –80 °C and further homogenized (Cafamo technologies, Ontario, Canada) at 5% (w/v) in mannitol buffer for mitochondrial analysis. The protein content was quantified in left ventricle heart and placental homogenates using the bicinchoninic acid colorimetric assay (Thermo Scientific assay kit Prod #23225, Waltham, MA, USA) to normalize experimental measures.

2.3. MRC activity and mitochondrial content in heart and placenta

In order to study MRC function, the enzymatic activities of mitochondrial complex I, II, IV, I + III and II + III (CI, CII, CIV, CI + III

and CII + III) in both heart and placental homogenates were spectrophotometrically measured at 37 °C, as reported elsewhere [41].

Citrate synthase activity was also spectrophotometrically determined in heart and placenta at 37 °C [41,42], as it is considered a reliable marker of mitochondrial content [43]. Mitochondrial content was further confirmed by alternative methods (see Section 2.8.2).

All enzymatic assays consisted of national standardized methods run in parallel with internal quality controls [41] and all the enzymatic assays, measured once per sample, simultaneously included both cases and controls.

Absorbance changes of the enzymatic activities along time were monitored in a HITACHI U2900 spectrophotometer using the UV-Solution software version 2.2 and were expressed as nanomoles of consumed substrate or generated product per minute and milligram of protein (nmol/min/mg protein).

2.4. Mitochondrial oxygen consumption in heart and placenta

To determine oxygen consumption of heart and placental tissue from IUGR and control offspring, 3–5 milligrams of each tissue were permeabilized on ice with 5% (w/v) saponine for 30 min in Biops Medium. This permeabilized tissue was washed with cold respiration medium (Mir05: 0.5 mM EGTA, 3 mM MgCl₂, 60 mM K-lactobionate, 20 mM taurine, 10 mM KH₂PO₄, 20 mM HEPES, 110 mM sucrose and 0.1% (w/v) bovine serum albumin, pH 7.1). High-resolution respirometry was performed at 37 °C by polarographic oxygen sensors in a two-chamber Oxygraph-2k system according to the manufacturer's instructions (OROBOROS Instruments, Innsbruck, Austria). Manual titration of substrates and inhibitors was performed using Hamilton syringes (Hamilton Company, Reno, NV, USA). Data was recorded using the DatLab software v5.1.1.9 (Oroboros Instruments, Innsbruck, Austria).

Glutamate and malate oxidation (GM Oxidation), corresponding to electron donation of both substrates to mitochondrial CI, was quantified once in all samples. Specific oxygen uptake rates sensitive to antimycin A (which specifically inhibits mitochondrial oxygen consumption) were obtained following the manufacturer's recommendations [44].

Oxygen consumption was normalized for the milligrams of dry tissue, thus, results were expressed as picomoles of oxygen consumed per second and milligram of tissue (pmol O₂/s/mg).

2.5. Mitochondrial coenzyme Q (CoQ) content in heart and placenta

Tissue levels of CoQ9 or CoQ10 (mobile electron transfer located within CI, CII and CIII in the MRC) were assessed in duplicates in the heart and placental homogenates from both cases and controls by high pressure liquid chromatography (HPLC in reverse form) with electrochemical detection of the reduced and oxidized molecule, as described previously [45]. Values were expressed as micromoles per liter (μmol/L).

2.6. Total cellular ATP levels in heart and placenta

Cellular ATP levels were quantified in duplicates in the heart and placental homogenates from both cases and controls using the Luminescent ATP Detection Assay Kit (Abcam, Cambridge, UK), according to the manufacturer's instructions. The results were normalized for protein content and expressed as picomolar of ATP per milligram of protein (pmol ATP/mg protein).

2.7. Lipid peroxidation in heart and placenta

Lipid peroxidation was measured in duplicates as an indicator of oxidative damage to lipid membranes of hearts and placentas using the BIOXYTECH® LPO-586™ assay by spectrophotometric measurement of malondialdehyde (MDA) and 4-hydroxyalkenal (HAE) levels (both

peroxides derived from fatty acid oxidation), according to the manufacturer's instructions (Oxis International Inc., CA, USA). The results were normalized for protein content and expressed as micromolar of MDA and HAE per milligram of protein (μM MDA + HAE/mg protein).

2.8. Western blot analysis

Twenty to forty μg of total protein homogenate of heart and placenta from both cases and controls were separated using 7/13% SDS-PAGE and transferred to nitrocellulose membranes (iBlot Gel Transfer Stacks, Life Technologies, Waltham, MA, USA). The membranes were hybridized with specific antibodies overnight at 4 °C. The expression of all studied proteins was measured once and normalized to β-actin protein (47 kDa; 1:30,000; Sigma-Aldrich, St. Louis, MO, USA) which was used as a loading control. Inter-blot control samples were used to evaluate membrane variability. The ImageQuantLD program was used to quantify chemiluminescence.

2.8.1. Expression of subunits of the MRC complexes in heart and placenta

To determine the levels of protein expression of the subunits of the MRC complexes the cleared lysates were subjected to SDS-PAGE and electroblotted. Proteins were visualized by immunostaining with anti-SDHA and anti-SDHB (both for CII; 70 kDa and 30 kDa respectively; 1:1000; Invitrogen, Paisley, UK) and also with anti-COX5A (for CIV; 16 kDa; 1:1000; MitoSciences, Oregon, USA). Results were expressed as SDHA/β-actin, SDHB/β-actin and COX5A/β-actin ratios.

2.8.2. Expression of mitochondrial import receptor subunit TOM20 (Tom20) in heart and placenta

As a mitochondrial content marker, anti-Tom20 (20 kDa; 1:1000; Santa Cruz Biotechnology, Dallas, USA) was hybridized with membranes. Results were expressed as the Tom20/β-actin ratio.

2.8.3. Expression of superoxide dismutase 2 (SOD2) in heart and placenta

SOD2 is a mitochondrial anti-oxidant enzyme pivotal in ROS release during oxidative stress. Membranes were hybridized with anti-SOD2 (24 kDa; 1:1000; ThermoFisher Scientific, Waltham, MA, USA). Results were expressed as the SOD2/β-actin ratio.

2.8.4. Expression of the acetylated form of SOD2 in heart and placenta

In order to determine the activity of SOD2 enzyme, we evaluate its acetylated form (indicating less activity) by hybridizing the membranes with anti-SOD2/MnSOD (24 kDa; 1:1000; Abcam, Cambridge, UK). Results were expressed as the acetylated SOD2/β-actin ratio or acetylated/total SOD2 ratio.

2.8.5. Expression of Sirtuin3 in heart

The protein content of Sirtuin3, which is a sensor of mitochondrial and metabolic balance, was determined by hybridizing the membrane with anti-Sirtuin3 (29 kDa; 1:500; Abcam, Cambridge, UK). Results were expressed as the Sirtuin3/β-actin ratio.

2.9. Statistical analysis

Statistical analysis was performed with the 'IBM SPSS Statistics 20' and STATA software. Biometric and experimental results were expressed as means and standard error of the mean (SEM) or as a percentage of increase/decrease of IUGR-offspring compared to control offspring after filtering for outliers. Case-control differences were sought by non-parametric statistical analysis (Mann-Whitney independent sample test) and, in case of difference, significance was adjusted by maternal influence (Random Effect regression model). Additionally, different correlations were obtained between biometric features and experimental data using the Spearman test in order to assess dependence of biometric measures in mitochondrial function or vice versa. Differences were considered significant with a p value <

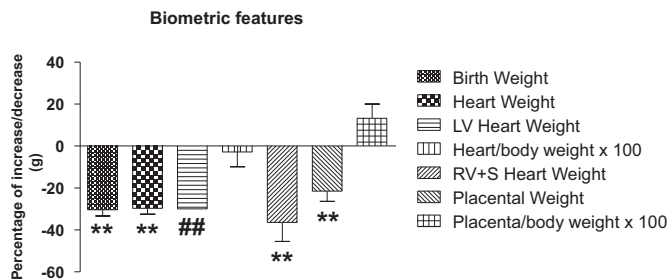


Fig. 1. Biometric results of heart and placenta from rabbit offspring with intrauterine growth restriction (IUGR). IUGR-offspring are presented as column bars demonstrating percentage of increase or decrease compared to controls (represented as the baseline 0). There was a significant decrease in birth weight in IUGR-offspring (control N = 14 and IUGR N = 16), accompanied by a reduction in heart (control N = 13 and IUGR N = 15), left (control N = 11 and IUGR N = 14) and right ventricle (control N = 10 and IUGR N = 13) and placental weight (control N = 14 and IUGR N = 16). Heart body weight relative to body weight (control N = 13 and IUGR N = 15) and also placental weight corrected by body weight (control N = 14 and IUGR N = 16) did not show significant differences between cases and controls. The results are expressed as a percentage of decrease compared to controls. Case-control differences were sought by non-parametric statistical analysis and, in case of difference, significance was adjusted by maternal influence. **: $p < 0.001$; #: $p < 0.005$; LV: left ventricle; RV + S: right ventricle and septum.

0.05.

3. Results

3.1. Biometric offspring data

The biometric results of both the IUGR and control offspring of the rabbit model are shown in Fig. 1 and Table S2. Birth weight, heart weight, left and right ventricle weight and placental weight were significantly decreased in IUGR-offspring compared to controls ($-30.35 \pm 2.99\%$, $p < 0.001$; $-29.73 \pm 2.70\%$, $p < 0.001$; $-30.00 \pm 0.00\%$, $p < 0.005$; $-36.36 \pm 9.09\%$, $p < 0.001$; $-21.49 \pm 4.85\%$, $p < 0.001$, respectively). When cardiac or placental weights were normalized to body weight, no significant differences were evidenced between IUGR and control offspring.

3.2. MRC activity, MRC expression and mitochondrial content

A significant decrease of CII, CIV and CII + III enzymatic activities ($-11.96 \pm 3.16\%$, $-15.58 \pm 5.32\%$ and $-14.73 \pm 4.37\%$, respectively; $p < 0.05$ in all cases) was found in heart of IUGR-offspring compared to controls, while other complexes (CI and CI + III) also showed a decrease, although not significant (Fig. 2A). The same pattern was observed in placenta, although the decrease in CIV did not reach statistical significance in IUGR-offspring (CII: $-17.22 \pm 3.46\%$, $p < 0.005$; CIV: $-24.03 \pm 8.26\%$, $p = \text{NS}$; CII + III: $-29.64 \pm 4.43\%$, $p < 0.001$; Fig. 2A). MRC enzymatic activities relative to citrate synthase activity confirmed absolute MRC enzymatic activities reduction. All of the raw data are presented in Table S3.

MRC CII subunits SDHA and SDHB and CIV subunit COX5A were conserved in cardiac tissue of IUGR-offspring compared to controls. Interestingly, regardless maintained expression of CII SDHA and CIV COX5A subunits in placental tissue, MRC CII SDHB subunit was significantly decreased ($-44.12 \pm 5.88\%$; $p < 0.001$) in IUGR-offspring compared to controls (Fig. 3 and Table S3).

Citrate synthase activity in both heart and placental tissues showed preserved mitochondrial content in IUGR-offspring compared to controls (Fig. 2A and Table S3). These results were confirmed by conserved Tom20 expression in these samples (Fig. S1 and Table S3).

3.3. Mitochondrial oxygen consumption

We found a not significant decrease of oxygen consumption on CI stimulation with glutamate and malate (GM oxidation) in heart and placenta from IUGR-offspring compared to controls ($-5.56 \pm 6.46\%$ and $-25.64 \pm 18.97\%$, respectively, both $p = \text{NS}$, Fig. 2B and Table S3).

3.4. Mitochondrial CoQ content

No differences were observed in CoQ9 or CoQ10 content in either cardiac or placental tissue of IUGR-offspring with respect to control individuals (Table S3).

3.5. Total cellular ATP levels

No remarkable differences were observed in total content of cellular ATP in either heart or placental tissues in IUGR and control offspring (Fig. 2D and Table S3).

3.6. Oxidative damage

Oxidative damage, estimated by the rate of lipid peroxidation, showed a significant decrease of $39.02 \pm 4.35\%$ in hearts of IUGR-offspring compared to controls ($p < 0.001$; Fig. 2C). Contrarily, lipid peroxidation was $10.65 \pm 7.33\%$ increased, albeit not significantly, in placenta from IUGR-offspring compared to the control group ($p = \text{NS}$; Fig. 2C and Table S3).

3.7. Expression and activity of SOD2

No significant differences were observed in the protein content and activity of the anti-oxidant SOD2 enzyme between cases and controls in none of the studied tissues (Figs. S2 and S3 and Table S3; either total SOD2/ β -actin content or acetylated SOD2/ β -actin). Only acetylated/total SOD2 ratio showed trends to increase in IUGR-offspring, both in heart and placental tissues (Table S3).

3.8. Expression of Sirtuin3

In heart tissue of IUGR-offspring, Sirtuin3/ β -actin protein levels showed a significant increase of $84.21 \pm 31.58\%$ ($p < 0.05$) compared to hearts from controls (Fig. 4 and Table S3).

3.9. Associations between biometric features and experimental results

Table 1 describes all the significant associations between the biometric data and experimental results in the cohorts of IUGR and control offspring from the rabbit model. The most remarkable associations are described below and showed in Fig. 5.

Firstly, birth weight was positively and significantly correlated with heart and left ventricle weight and also with placental weight ($R^2 = 0.610$, $R^2 = 0.446$ and $R^2 = 0.557$, respectively, $p < 0.001$ in all cases; Fig. 5A and B). Similarly, heart weight was correlated with left ventricle weight and placental weight ($R^2 = 0.322$, $p < 0.005$; $R^2 = 0.346$, $p < 0.001$). See Table 1 for other biometric associations.

Secondly, birth weight was positively and significantly correlated with enzymatic activities of CI, CII and CII + III in the heart of the both offspring ($R^2 = 0.157$, $p < 0.05$; $R^2 = 0.117$, $p < 0.05$; $R^2 = 0.289$, $p \leq 0.005$; respectively; Fig. 5C). The weight of the other tissues was also positively and significantly correlated with the enzymatic activity of some MRC complexes (Table 1). Similarly, body, heart, left ventricle and placental weights were significantly and positively correlated with CII SDHB protein expression in placenta ($R^2 = 0.304$, $p \leq 0.001$; $R^2 = 0.349$, $p < 0.001$; $R^2 = 0.215$, $p < 0.005$; $R^2 = 0.364$, $p < 0.05$, respectively; Fig. 5D). Interestingly, we found CII, CII + III

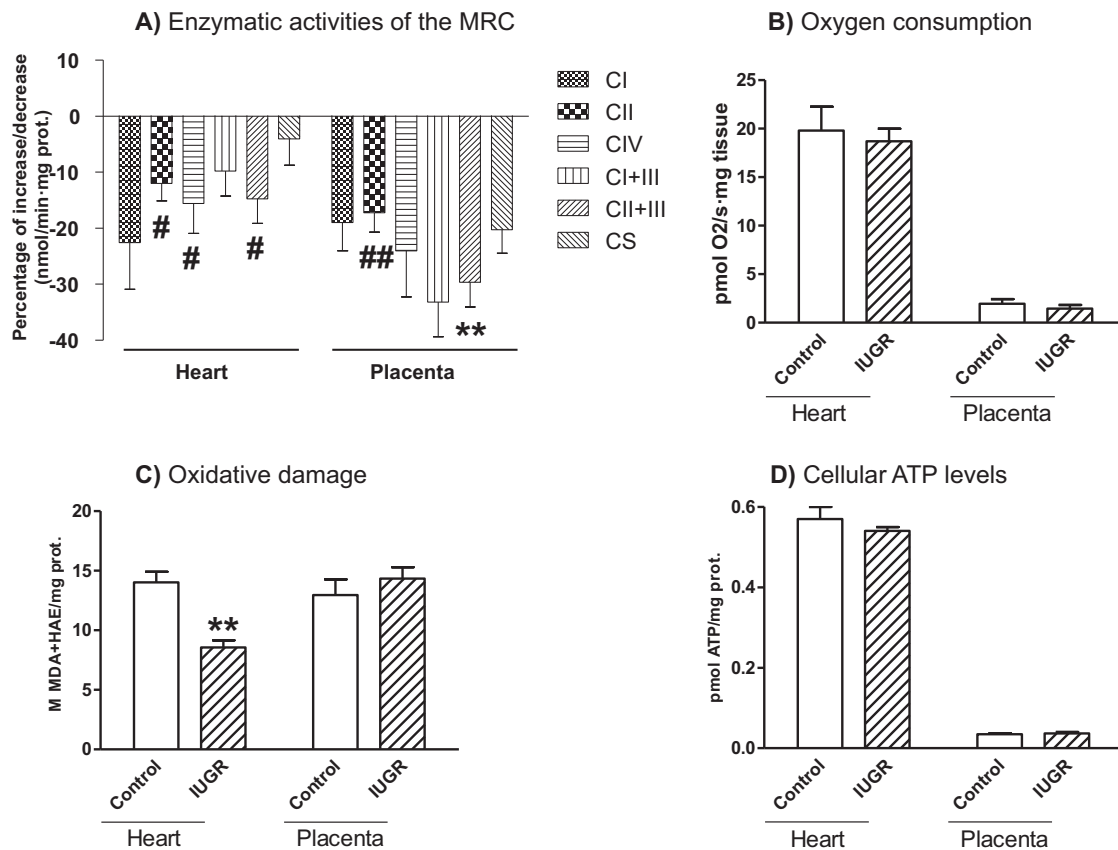


Fig. 2. Mitochondrial impairment of heart and placenta from rabbit offspring with intrauterine growth restriction (IUGR). **A)** Enzymatic activities of the mitochondrial respiratory chain (MRC) of heart (left) and placenta (right) from IUGR-offspring compared to controls (represented as the baseline). A significant decrease of CII, CIV and CII + III enzymatic activities was observed in heart of IUGR-offspring, while CI and CI + III showed a not significant decrease (control N = 10 and IUGR N = 14 for all). The same pattern was observed in placenta, although the CIV decrease did not reach statistical significance in IUGR-offspring (CI: control N = 14 and IUGR N = 14; CII and CIV: control N = 14 and IUGR N = 16; CI + III: control N = 13 and IUGR N = 15; CII + III: control N = 13 and IUGR N = 16). Citrate synthase (CS) activity (mitochondrial content) was conserved in both heart (control N = 10 and IUGR N = 14) and placental (control N = 14 and IUGR N = 16) tissues from IUGR-offspring. **B)** Mitochondrial oxygen consumption stimulated with substrates of complex I (glutamate and malate) in heart (left; control N = 11 and IUGR N = 14) and placenta (right; control N = 13 and IUGR N = 13) from IUGR-offspring (striped bars) compared to controls (empty bars). Oxygen consumption showed a not significant decrease on CI stimulation in heart and placenta from IUGR-offspring. **C)** Lipid peroxidation in heart (left; control N = 10 and IUGR N = 14) and placenta (right; control N = 13 and IUGR N = 16) from IUGR-offspring (striped bars) compared to controls (empty bars). Lipid peroxidation showed a significant decrease in hearts while showing a not significant increase in placenta from IUGR-offspring. **D)** Total cellular ATP levels in heart (left; control N = 10 and IUGR N = 14) and placenta (right; control N = 14 and IUGR N = 16) from IUGR-offspring (striped bars) compared to controls (empty bars). No remarkable differences were observed in the total cellular ATP content in either heart or placenta tissue. The results are expressed as a percentage of decrease compared to controls (A) and as means and standard error of the mean (SEM) compared to controls (B–D). Case-control differences were sought by non-parametric statistical analysis and, in case of difference, significance was adjusted by maternal influence. #: $p < 0.05$; ##: $p < 0.005$; **: $p < 0.001$; CI, CII, CIV, CI + III, CII + III: MRC complex I, II, IV, I + III, II + III; CS: Citrate synthase.

and CIV enzymatic activity positively and significantly correlated with CII SDHB subunit expression in placenta ($R^2 = 0.145$, $p < 0.005$; $R^2 = 0.192$, $p < 0.005$; $R^2 = 0.241$, $p < 0.001$, respectively). On the other hand, birth weight and heart weight showed a significant positive correlation with lipid peroxidation in heart ($R^2 = 0.325$, $p < 0.005$; $R^2 = 0.498$, $p < 0.001$; respectively; Fig. 5E). Moreover, oxidative damage in heart was positively and significantly correlated with the enzymatic activities of MRC CII and CII + III ($R^2 = 0.136$ and $R^2 = 0.173$, $p < 0.05$ in both cases).

Finally, significant negative correlations were found between both birth and heart weight and Sirtuin3/ β -actin levels ($R^2 = 0.153$, $p < 0.05$ and $R^2 = 0.266$, $p < 0.05$, respectively; Fig. 5F).

4. Discussion

A wide range of clinical manifestations has been associated with IUGR, including metabolic, neurological and cardiovascular disorders [46–51]. Among these, fetal cardiovascular remodeling has recently been demonstrated in IUGR [8,11,14,16,18–20,22,27]. However, disease modeling and investigation in cardiac or placental target tissues are lacking.

It is important to note that in the present study, offspring with induced IUGR showed altered biometric measures by significant decrease in birth weight, accompanied by a reduction in heart and placenta, as previously reported [14]. Thus, organ to body weight measures were preserved due to global and proportioned organ and body mass reduction. Cardiac hypertrophy and consequent increase in heart to body weight is not present in IUGR rabbits, resembling human conditions, in which globular and elongated hearts are usual, and hypertrophy occurs only in 17% of cases of IUGR [13,47,52–58].

Cardiac metabolic and mitochondrial impairment has been previously demonstrated in the present animal model at a transcriptional and ultrastructural level [14]. However, the bioenergetic functional imbalance has not yet been demonstrated in the target tissue of cardiovascular remodeling (heart) or in the tissue responsible for oxygen and nutrient supply (placenta), and neither have the potential causal agents or downstream cell consequences for this imbalance been described.

The present study provides evidence of mitochondrial deficiency in the cardiac tissue of IUGR-rabbits, with a significant decrease of enzymatic activities of MRC CII, CIV and CII + III. The same pattern was observed in IUGR-placentas regarding CII and CII + III. Interestingly, CII SDHB protein expression showed a significant decrease in placental

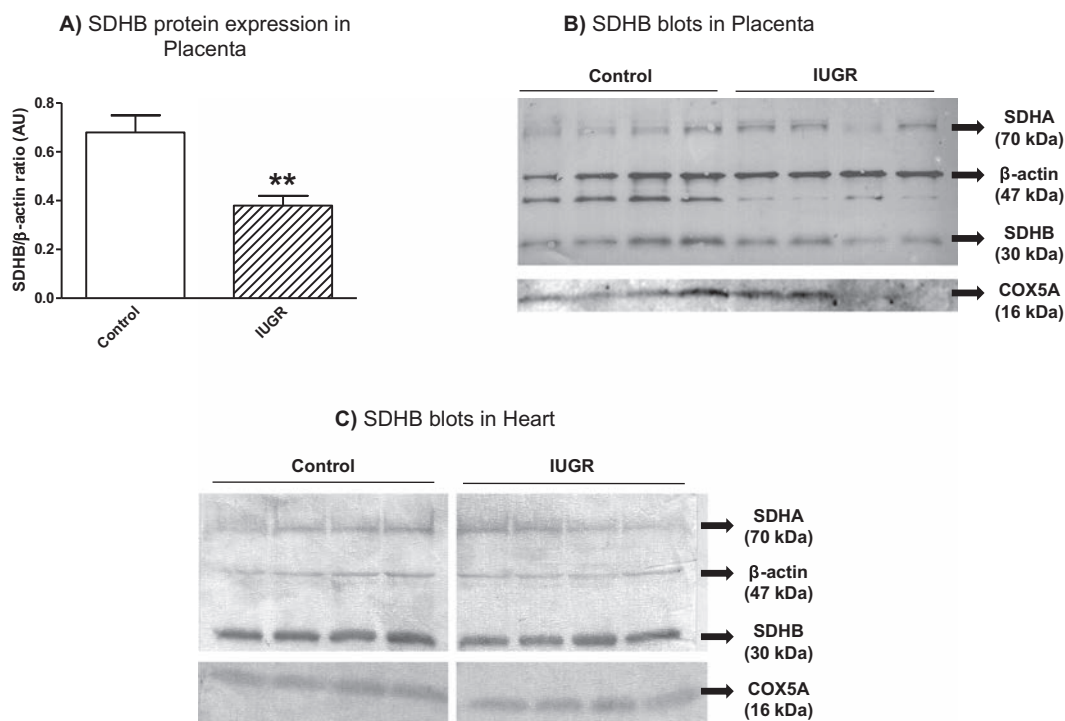


Fig. 3. Expression of the mitochondrial respiratory chain (MRC) subunits SDHA and SDHB (from complex II) and COX5A (from complex IV) in IUGR-offspring and controls. A) This column bar graph represents protein SHDB subunit levels in placenta from IUGR-offspring (striped bars; N = 16) compared to placenta from controls (empty bars; N = 14). SHDB/β-actin expression is significantly decreased in placenta from IUGR-offspring. The results are expressed as mean and standard error of the mean (SEM) compared to controls. Case-control differences were sought by non-parametric statistical analysis and, in case of difference, significance was adjusted by maternal influence. **: p < 0.001. B) A representative Western blot of SDHA, SDHB and COX5A protein expression in placenta is shown in which β-actin was used as the loading control. C) A representative Western blot of SDHA, SDHB and COX5A protein expression in heart is shown in which β-actin was used as the loading control. IUGR: Intrauterine growth restriction; SDHA: Succinate dehydrogenase complex, subunit A; SDHB: Succinate dehydrogenase complex, subunit B; COX5A: Cytochrome c oxidase subunit 5a.

tissue in front of preserved mitochondrial content, CoQ levels and ATP content. Lipid peroxidation was found to be significantly decreased in cardiomyocytes but showed a not significant increase in placental tissue. All these mitochondrial functional deficiencies validate previous transcriptomic and ultrastructural findings [14].

Interestingly, birth weight, placental and left ventricle weight were significantly and positively correlated with the enzymatic MRC activities (including CI, CII, CII + III and CIV), thereby strengthening the relevance of the need for adequate bioenergetic mitochondrial status to reach potential body, heart and placental weight.

In this sense, mitochondrial functional alterations in IUGR-offspring are not confined to the target tissue of cardiovascular remodeling (heart), but rather are also present in placenta. Mitochondrial dysfunction in placenta (and probably also in heart and other tissues) might be caused by the de novo rearrangement adaptations imposed by

the experimental hypoxia induced by the ligation of uteroplacental vessels in this animal model [6]. Similar hypoxic conditions are also present in patients with IUGR due to placental insufficiency. These are undoubtedly examples of the fetal programming, first described by Barker [5], which establishes that physiologic adaptations to the fetal environment may condition organ development and consequent disease in adulthood.

Both heart and placenta from IUGR-offspring showed a common enzymatic alteration in MRC CII dysfunction. CII, also known as succinate dehydrogenase, is the molecular link between the Krebs cycle and the MRC. The Krebs cycle is a central pathway of the mitochondrial energy metabolism, which is responsible for the oxidative degradation of the different dietetic supplies, feeding the MRC and, subsequently, activating ATP synthesis. In order to further investigate the molecular basis of CII dysfunction in heart and placenta of IUGR-offspring, the

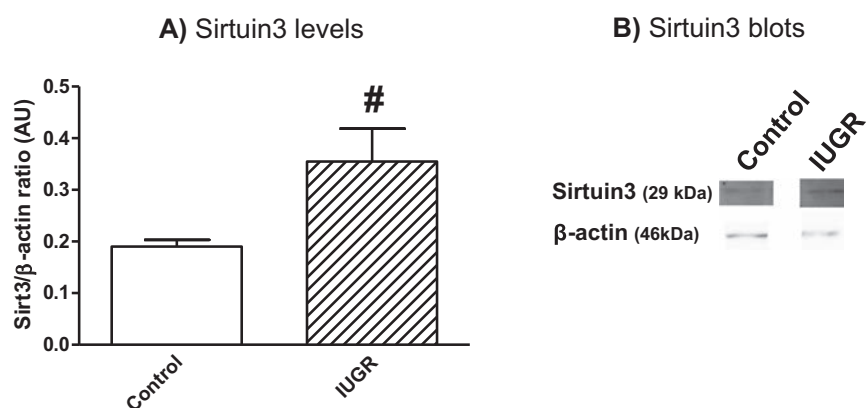


Fig. 4. Mitochondrial levels of protein Sirtuin3 (Sirt3/β-actin ratio) in heart of rabbit offspring with intrauterine growth restriction (IUGR). A) This column bar graph represents protein Sirtuin3 levels in hearts from IUGR-offspring (striped bars; N = 13) compared to hearts from controls (empty bars; N = 10). Sirtuin3/β-actin levels in heart tissue of IUGR-offspring showed a significant increase. The results are expressed as mean and standard error of the mean (SEM) compared to controls. Case-control differences were sought by non-parametric statistical analysis and, in case of difference, significance was adjusted by maternal influence. #: p < 0.05. B) A representative Western blot of Sirt3 protein expression in hearts is shown in which β-actin is used as the loading control.

Table 1
Associations between biometric data and experimental results in the IUGR and control offspring.

Parameter	With respect to	Correlation coefficient	p	R ²				
Birth weight (g)	Heart weight (g)	0.783	< 0.001	0.610				
	Left ventricle (g)	0.676	< 0.001	0.446				
	Right ventricle + septum (g)	0.735	< 0.001	0.459				
	Placental weight (g)	0.758	< 0.001	0.557				
	CI enzymatic activity ^a in heart	0.429	< 0.05	0.157				
	CII enzymatic activity ^a in heart	0.448	< 0.05	0.117				
	CII + III enzymatic activity ^a in heart	0.543	≤ 0.005	0.289				
	Citrate synthase activity ^a in heart	0.517	< 0.01	0.125				
	Lipid peroxidation ^b in heart	0.591	< 0.005	0.325				
	Sirtuin3/β-actin ratio (AU) in heart	-0.498	< 0.05	0.153				
	CI + III enzymatic activity ^a in placenta	0.380	< 0.05	0.172				
	CII + III enzymatic activity ^a in placenta	0.574	≤ 0.001	0.347				
	Citrate synthase activity ^a in placenta	0.371	< 0.05	0.217				
	SDHB/β-actin ratio (AU) in placenta	0.570	≤ 0.001	0.304				
	Heart weight (g)	Left ventricle (g)	0.511	< 0.005	0.322			
		Right ventricle + septum (g)	0.843	< 0.001	0.658			
Heart / body weight × 100 (g)		0.469	≤ 0.005	0.106				
Placental weight (g)		0.575	< 0.001	0.346				
Lipid peroxidation ^b in heart		0.710	< 0.001	0.498				
Sirtuin3/β-actin ratio (AU) in heart		-0.505	< 0.05	0.266				
CII enzymatic activity ^a in placenta		0.450	< 0.05	0.146				
CI + III enzymatic activity ^a in placenta		0.594	≤ 0.001	0.277				
CII + III enzymatic activity ^a in placenta		0.515	< 0.005	0.234				
Citrate synthase activity ^a in placenta		0.402	< 0.05	0.183				
SDHB/β-actin ratio (AU) in placenta		0.500	< 0.01	0.349				
Left ventricle (g)		Placental weight (g)	0.563	≤ 0.001	0.336			
		CII enzymatic activity ^a in heart	0.480	< 0.05	0.130			
		CII + III enzymatic activity ^a in heart	0.512	< 0.01	0.209			
		Citrate synthase activity ^a in heart	0.594	< 0.005	0.338			
		CII enzymatic activity ^a in placenta	0.461	< 0.05	0.230			
	CIV enzymatic activity ^a in placenta	0.476	< 0.05	0.412				
	CII + III enzymatic activity ^a in placenta	0.507	< 0.01	0.270				
	Citrate synthase activity ^a in placenta	0.606	≤ 0.001	0.332				
	SDHB/β-actin ratio (AU) in placenta	0.544	< 0.005	0.251				
	Right ventricle + septum (g)	Heart/body weight × 100 (g)	0.467	< 0.05	0.048			
		Sirtuin3/β-actin ratio (AU) in heart	-0.593	< 0.005	0.293			
		CI + III enzymatic activity ^a in placenta	0.459	< 0.05	0.228			
		CII + III enzymatic activity ^a in placenta	0.442	< 0.05	0.181			
		CI + III enzymatic activity ^a in placenta	0.424	< 0.05	0.018			
		Sirtuin3/α-tubulin ratio (AU) in heart	-0.551	≤ 0.01	0.053			
	Heart/body weight × 100	Placenta / body weight × 100 (g)	0.436	< 0.005	0.301			
CIV enzymatic activity ^a in placenta		0.436	< 0.05	0.245				
CII + III enzymatic activity ^a in placenta		0.548	≤ 0.001	0.267				
SDHB/β-actin ratio (AU) in placenta		0.514	< 0.005	0.364				
Sirtuin3/β-actin ratio (AU) in heart		0.732	< 0.001	0.599				
CII enzymatic activity ^a in heart		0.436	< 0.05	0.136				
Placental weight (g)	CII + III enzymatic activity ^a in heart	0.432	< 0.05	0.173				
	SDHB/β-actin ratio (AU) in heart	Total ATP levels ^c in heart	0.537	< 0.01	0.226			
	SOD2/β-actin ratio (AU) in heart	Citrate synthase activity ^a in heart	-0.418	< 0.05	0.112			
	SDHB/β-actin ratio (AU) in placenta	CII enzymatic activity ^a in placenta	0.497	< 0.005	0.145			
	Placenta/body weight × 100	CIV enzymatic activity ^a in placenta	0.617	< 0.001	0.241			
		Lipid peroxidation ^b in heart	CII + III enzymatic activity ^a in placenta	0.521	< 0.005	0.192		
		SDHB/β-actin ratio (AU) in heart	Citrate synthase activity ^a in placenta	0.613	< 0.001	0.261		
		SDHB/β-actin ratio (AU) in placenta	SOD2/β-actin ratio (AU) in placenta	0.402	< 0.05	0.314		
		Lipid peroxidation ^b in heart	CIV enzymatic activity ^a in placenta	0.409	< 0.05	0.149		
			SDHB/β-actin ratio (AU) in heart	Citrate synthase activity ^a in placenta	0.406	< 0.05	0.179	
			SDHB/β-actin ratio (AU) in placenta	CIV enzymatic activity ^a in placenta	0.429	< 0.05	0.164	
			COX5A/β-actin ratio (AU) in placenta	CIV enzymatic activity ^a in placenta	0.513	< 0.005	0.249	
				Tom20/β-actin ratio (AU) in placenta	CII + III enzymatic activity ^a in placenta	0.482	< 0.01	0.216
				SOD2/β-actin ratio (AU) in placenta				

CI: Complex I; CII: Complex II; CI + III: Complex I + III; CII + III: Complex II + III; CIV: Complex IV; SDHA: Succinate dehydrogenase complex, subunit A; SDHB: Succinate dehydrogenase complex, subunit B; COX5A: Cytochrome c oxidase subunit 5a; Tom20: Mitochondrial import receptor subunit TOM20; SOD2: Superoxide dismutase 2; AU: Arbitrary units; g: grams.

^a nmol/min-mg protein.

^b μM MDA + HAE/mg protein.

^c pmol ATP/mg protein.

expression of CII SDHA and SDHB proteins were assessed, together with CoQ levels, the electron donor for CII. Interestingly, in front of preserved CoQ levels, SDHB subunit was found significantly decreased in placenta and positively and significantly correlated with CII, CII + III and CIV enzymatic activities. These findings suggest that MRC enzymatic dysfunction may be due, at least partially, to down-regulation of

MRC subunits expression. Additionally, the significant and positive correlation between CII SDHB levels and all biometric parameters from IUGR and control offspring (body, placental and heart weights), highlighted the relevance of SDHB and CII in this obstetric complication. As CII is the only complex of the MRC exclusively encoded by the nuclear DNA [59], its deficiency may be more likely associated with alterations

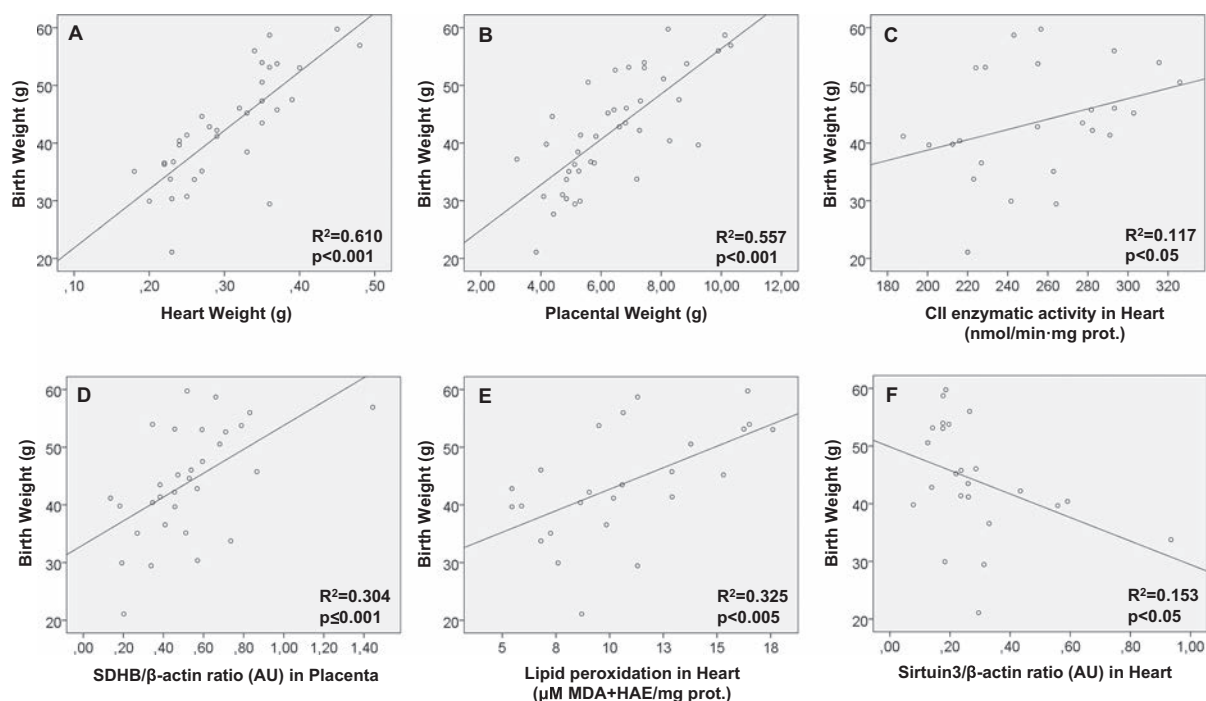


Fig. 5. Associations between birth weight of intrauterine growth restriction (IUGR) and control offspring and some biometric data or experimental results. Herein, there are correlations demonstrating the positive association between birth weight and mitochondrial parameters and also the negative association with Sirtuin3 expression, probably up-regulated as a homeostatic intent to revert mitochondrial lesion.

in the oxidative metabolism events controlled by the nucleus, rather than a regulation associated with mitochondrial genome.

Sirtuin3 is the most important mitochondrial deacetylase encoded in the nucleus and plays a role in the regulation of mitochondrial function and oxidative phosphorylation [60–62]. Interestingly, since mitochondrial CII is one of the targets of Sirtuin3 [60,63], this protein is able to simultaneously interfere with MRC and the Krebs cycle. In our study, the significant increase of cardiac Sirtuin3 observed in IUGR-offspring was associated with a significant decrease of CII enzymatic activity in both heart and placental tissues. This up-regulation in Sirtuin3 expression may be the compensatory response to imbalanced bioenergetics status. In accordance with these findings obtained in IUGR-offspring with placental hypoxia, environmental hypoxia has also been associated with alterations in the Krebs cycle [64], which may also lead to neurological or cardiac clinical consequences [65].

Additionally, Sirtuin3 has been reported to alleviate the induction of hypertrophy in heart [34] and it has been proposed that this protein has a role in antioxidation, promoting the maintenance of ATP levels, especially in hypoxic conditions [66,67]. Interestingly, in heart from IUGR-offspring, oxidative stress was found to be significantly decreased in the setting of conserved cellular ATP levels, suggesting that increased Sirtuin3 levels may protect cardiomyocytes from oxidative stress insults in placental hypoxia. Sirtuin3 would exert a compensatory role in this phenotype by modulating mitochondrial lesion in cardiomyocytes. Moreover, the presence of cardiac oxidative damage increased according to body weight, heart weight and proper MRC activity, suggesting that the antioxidant protection of Sirtuin3 may be more necessary in MRC dysfunction and abnormal fetal development. This hypothesis seems to be confirmed by the significant negative correlation of body and heart weight with cardiac Sirtuin3 levels. In parallel, cellular ATP levels were also maintained in placental tissue, albeit with a not significant increased lipid peroxidation. This juxtaposed oxidative phenotype between heart and placenta may also be explained by the poor antioxidant defenses characteristic of the placenta [68,69]. Interestingly, CoQ levels and SOD2 expression, that take part in the antioxidant defense system, did not seem to play a role in the

mitochondrial and oxidative phenotype observed in either cardiac or placental tissue. Actually, trends to higher inactivation of SOD2 (acetylated vs. total SOD2 ratio) were noticed in IUGR-offspring that, together with up-regulated expression of Sirtuin3, have been previously associated with aging [35]. Nonetheless, further research is needed to address this topic and deeper in the potential association between increased Sirtuin3 expression and observed dysfunctional mitochondrial phenotype.

The present study has some limitations and technical considerations that should be mentioned. IUGR is considered a multifactorial disease involving many pathways and etiologies which finally lead to a single phenotype. Further studies are required to elucidate the functional consequences of the loss of some enzymatic MRC complexes in order to know whether CII dysfunction is a consequence or the cause of this obstetric complication and associated cardiovascular remodeling. It is also important to keep in mind that the bioenergetic findings of the present approach may become more evident by analysis under hypoxic conditions, other than the normoxic environment of experimental mitochondrial measures. Additionally, the reduced sample size of the present study may limit statistical findings which should be interpreted as a proof of concept. Further studies including a larger sample size are needed, where additional measures may ideally be collected (brain sparing, sex distribution, timing of development and maturation of the heart, cardiac severity markers, etc) to explore underlying mechanistic pathways. Additionally, all rising evidences that support mitochondrial dysfunctional phenotype in other obstetric complications associated to placental insufficiency (for instance small for gestational age, pre-eclampsia, miscarriage or stillbirth) may strengthen the relevance of mitochondrial role in proper fetal development.

In summary, the present study shows that mitochondrial impairment is not only associated with IUGR but could also ultimately be the source of cardiac dysfunction and consequent cardiovascular remodeling. A potential mechanistic explanation for MRC CII dysfunction and decreased oxidative damage in heart of IUGR-offspring could be that Sirtuin3 regulates this unbalanced mitochondrial function by interfering MRC and Krebs cycle activity, empowering antioxidant

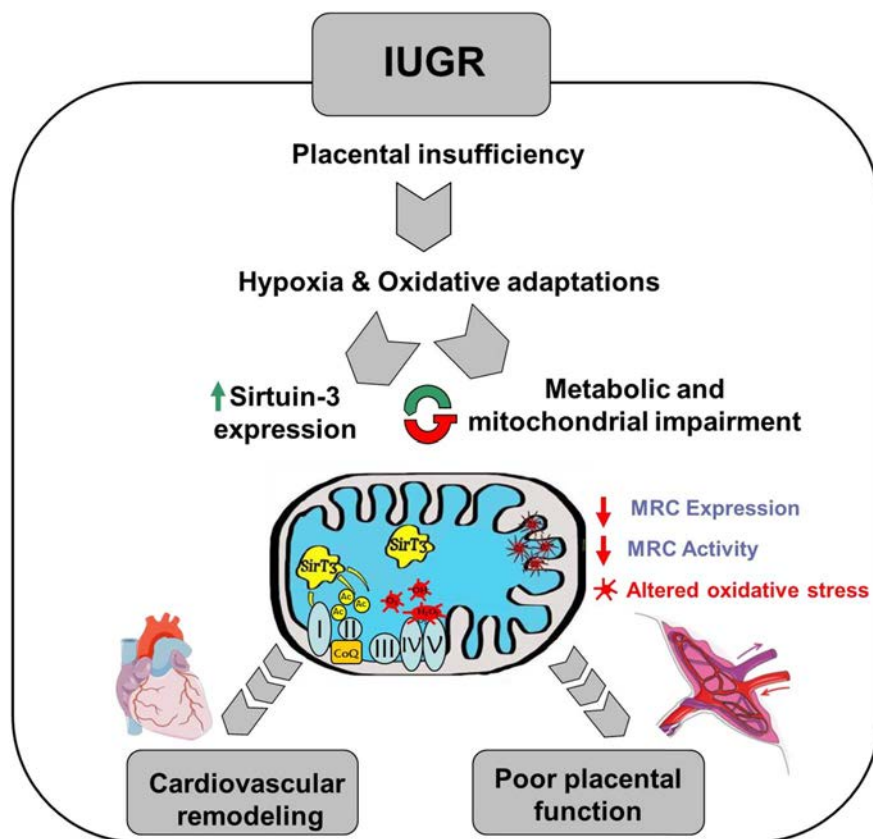


Fig. 6. Association between metabolic and mitochondrial impairment and compensation according to Sirtuin3 levels in a rabbit model of intrauterine growth restriction (IUGR) and associated cardiovascular remodeling. In the context of IUGR there is a situation of placental insufficiency that creates a hypoxic environment during fetal development leading to metabolic and mitochondrial rearrangements and cardiovascular remodeling. In these settings Sirtuin3 levels increase, probably in an attempt to regulate this adverse situation and revert the metabolic and mitochondrial imbalance that may finally lead to the development of IUGR and cardiovascular remodeling. MRC: Mitochondrial respiratory chain; CI-IV; Complex I-IV; AC: Acetylation; O_2^- : superoxide anion; H_2O_2 : Hydrogen peroxide; OH^- : Hydroxyl anion.

defenses in an attempt to recover mitochondrial function in cardiomyocytes in the setting of placental insufficiency and derived hypoxia (Fig.6).

Since sirtuins and cardiac function can be modulated through dietary interventions [37], the potential use of such non-invasive approaches in human pregnancies is a strategy that should be further investigated to reduce the risk of obstetric complications and associated diseases in adulthood.

Abbreviations

IUGR	intrauterine growth restriction
MRC	mitochondrial respiratory chain
EGTA	ethylene glycol tetraacetic acid
ATP	adenosine triphosphate
$MgCl_2$	magnesium chloride
MES	2-(N-morpholino)ethanesulfonic acid
CI	complex I
CII	complex II
CIV	complex IV
CI + III	complex I + III
CII + III	complex II + III
HEPES	4-(2-hydroxyethyl)-1-piperazineethanesulfonic acid
GM Oxidation	glutamate malate oxidation
MDA	malondialdehyde
HAE	hydroxyalkenal
SDS-PAGE	sodium dodecyl sulfate polyacrylamide gel electrophoresis
SDHA	succinate dehydrogenase complex, subunit A
SDHB	succinate dehydrogenase complex, subunit B
COX5A	cytochrome c oxidase subunit 5a
Tom20	mitochondrial import receptor subunit TOM20
SOD2	superoxide dismutase 2
SEM	standard error of the mean

Transparency document

The <http://dx.doi.org/10.1016/j.bbagen.2018.02.006> associated with this article can be found, in online version.

Acknowledgments

We would like to thank the collaboration and the valuable help of Donna Pringle for language assistance.

None of the above mentioned authors has any financial, consultant, institutional, and other relationship that might lead to bias or a conflict of interest for the information contained in the present manuscript.

Funding

This work was supported by Fondo de Investigación Sanitaria [FIS PI12/01199, PI15/00817, PI15/00903 and PI15/00130], CIBERER (an initiative of ISCIII) and InterCIBER [PIE1400061] granted by Instituto de Salud Carlos III and cofinanced by the Fondo Europeo de Desarrollo Regional de la Unión Europea “Una manera de hacer Europa”; Suports a Grups de Recerca [SGR893/2017] and CERCA Programme from the Generalitat de Catalunya; CONAcYT; Fundació La Marató de TV3 [87/C/2015]; Fundació Cellex; and “la Caixa” Foundation.

Appendix A. Supplementary data

Supplementary data to this article can be found online at <https://doi.org/10.1016/j.bbagen.2018.02.006>.

References

- [1] American College of O, Gynecologists, ACOG Practice bulletin no. 134: fetal growth restriction, *Obstet. Gynecol.* 121 (5) (2013 May) 1122–1133 (PubMed PMID: 23635765).

- [2] S. Visentin, F. Grumoloto, G.B. Nardelli, B. Di Camillo, E. Grisan, E. Cosmi, Early origins of adult disease: low birth weight and vascular remodeling, *Atherosclerosis* 237 (2) (2014 Dec) 391–399 (PubMed PMID: 25463063).
- [3] M. Alberry, P. Soothill, Management of fetal growth restriction, *Arch. Dis. Child. Fetal Neonatal Ed.* 92 (1) (2007 Jan) F62–7 (PubMed PMID: 17185432. Pubmed Central PMID: 2675309).
- [4] C.F. Rueda-Clausen, J.S. Morton, S.T. Davidge, Effects of hypoxia-induced intrauterine growth restriction on cardiopulmonary structure and function during adulthood, *Cardiovasc. Res.* 81 (4) (2009 Mar 1) 713–722 (PubMed PMID: 19088083).
- [5] D.J. Barker, Fetal origins of cardiovascular disease, *Ann. Med.* 31 (Suppl. 1) (1999 Apr) 3–6 (PubMed PMID: 10324493).
- [6] L. Myatt, Placental adaptive responses and fetal programming, *J. Physiol.* 572 (Pt 1) (2006 Apr 1) 25–30 (PubMed PMID: 16469781. Pubmed Central PMID: 1779654).
- [7] F. Crispi, B. Bijns, F. Figueras, J. Bartrons, E. Eixarch, F. Le Noble, et al., Fetal growth restriction results in remodeled and less efficient hearts in children, *Circulation* 121 (22) (2010 Jun 8) 2427–2436 (PubMed PMID: 20497977).
- [8] N. Ortigosa, M. Rodriguez-Lopez, R. Bailon, S.I. Sarvari, M. Sitges, E. Gratacos, et al., Heart morphology differences induced by intrauterine growth restriction and preterm birth measured on the ECG at preadolescent age, *J. Electrocardiol.* 49 (3) (2016 May-Jun) 401–409 (PubMed PMID: 27036371).
- [9] A. Sehgal, M.R. Skilton, F. Crispi, Human fetal growth restriction: a cardiovascular journey through to adolescence, *J. Dev. Orig. Health Dis.* 7 (2016 Jul) 1–10 (PubMed PMID: 27384077).
- [10] M. Cruz-Lemini, F. Crispi, B. Valenzuela-Alcaraz, F. Figueras, M. Sitges, B. Bijns, et al., Fetal cardiovascular remodeling persists at 6 months in infants with intrauterine growth restriction, *Ultrasound Obstet. Gynecol. Off. J. Int. Soc. Ultrasound Obstet. Gynecol.* 48 (3) (2016 Sep) 349–356 (PubMed PMID: 26415719).
- [11] Y. Akazawa, A. Hachiya, S. Yamazaki, Y. Kawasaki, C. Nakamura, Y. Takeuchi, et al., Cardiovascular remodeling and dysfunction across a range of growth restriction severity in small for gestational age infants- implications for fetal programming, *Circ. J. Off. J. Jpn. Circ. Soc.* 80 (10) (2016 Aug 18) 2212–2220, <http://dx.doi.org/10.1253/circj.CJ-16-0352> (PubMed PMID: 27535477).
- [12] E. Eixarch, F. Figueras, E. Hernandez-Andrade, F. Crispi, A. Nadal, I. Torre, et al., An experimental model of fetal growth restriction based on selective ligation of uteroplacental vessels in the pregnant rabbit, *Fetal Diagn. Ther.* 26 (4) (2009) 203–211 (PubMed PMID: 19955698).
- [13] E. Eixarch, E. Hernandez-Andrade, F. Crispi, M. Illa, I. Torre, F. Figueras, et al., Impact on fetal mortality and cardiovascular Doppler of selective ligation of uteroplacental vessels compared with undernutrition in a rabbit model of intrauterine growth restriction, *Placenta* 32 (4) (2011 Apr) 304–309 (PubMed PMID: 21334065).
- [14] A. Gonzalez-Tendero, I. Torre, P. Garcia-Canadilla, F. Crispi, F. Garcia-Garcia, J. Dopazo, et al., Intrauterine growth restriction is associated with cardiac ultrastructural and gene expression changes related to the energetic metabolism in a rabbit model, *Am. J. Physiol. Heart Circ. Physiol.* 305 (12) (2013 Dec) H1752–60 (PubMed PMID: 24097427).
- [15] J.L. Morrison, Sheep models of intrauterine growth restriction: fetal adaptations and consequences, *Clin. Exp. Pharmacol. Physiol.* 35 (7) (2008 Jul) 730–743 (PubMed PMID: 18498533).
- [16] D.A. Giussani, S.T. Davidge, Developmental programming of cardiovascular disease by prenatal hypoxia, *J. Dev. Orig. Health Dis.* 4 (5) (2013 Oct) 328–337 (PubMed PMID: 24970726).
- [17] D.A. Giussani, The fetal brain sparing response to hypoxia: physiological mechanisms, *J. Physiol.* 594 (5) (2016 Mar 01) 1215–1230 (PubMed PMID: 26496004. Pubmed Central PMID: 4721497).
- [18] Y.M. Al-Hasan, L.C. Evans, G.A. Pinkas, E.R. Dabkowski, W.C. Stanley, L.P. Thompson, Chronic hypoxia impairs cytochrome oxidase activity via oxidative stress in selected fetal Guinea pig organs, *Reprod. Sci.* 20 (3) (2013 Mar) 299–307 (PubMed PMID: 22923417. Pubmed Central PMID: 3676261).
- [19] Y.M. Al-Hasan, G.A. Pinkas, L.P. Thompson, Prenatal hypoxia reduces mitochondrial protein levels and cytochrome c oxidase activity in offspring Guinea pig hearts, *Reprod. Sci.* 21 (7) (2014 Jul) 883–891 (PubMed PMID: 24406790. Pubmed Central PMID: 4107561).
- [20] C. Oh, Y. Dong, C. Harman, H.E. Mighty, J. Kopelman, L.P. Thompson, Chronic hypoxia differentially increases glutathione content and gamma-glutamyl cysteine synthetase expression in fetal guinea pig organs, *Early Hum. Dev.* 84 (2) (2008 Feb) 121–127 (PubMed PMID: 17512683).
- [21] L.P. Thompson, Y. Al-Hasan, Impact of oxidative stress in fetal programming, *J. Pregnancy* 2012 (2012) 582748 (PubMed PMID: 22848830. Pubmed Central PMID: 3403156).
- [22] K.C. Wang, K.J. Botting, M. Padhee, S. Zhang, I.C. McMillen, C.M. Suter, et al., Early origins of heart disease: low birth weight and the role of the insulin-like growth factor system in cardiac hypertrophy, *Clin. Exp. Pharmacol. Physiol.* 39 (11) (2012 Nov) 958–964 (PubMed PMID: 22774980).
- [23] K.C. Wang, L. Zhang, I.C. McMillen, K.J. Botting, J.A. Duffield, S. Zhang, et al., Fetal growth restriction and the programming of heart growth and cardiac insulin-like growth factor 2 expression in the lamb, *J. Physiol.* 589 (Pt 19) (2011 Oct 01) 4709–4722 (PubMed PMID: 21807611. Pubmed Central PMID: 3213418).
- [24] B.S. Muhlhauser, J.A. Duffield, S.E. Ozanne, C. Pilgrim, N. Turner, J.L. Morrison, et al., The transition from fetal growth restriction to accelerated postnatal growth: a potential role for insulin signalling in skeletal muscle, *J. Physiol.* 587 (Pt 17) (2009 Sep 01) 4199–4211 (PubMed PMID: 19622603. Pubmed Central PMID: 2754360).
- [25] F. Chen, T. Wang, C. Feng, G. Lin, Y. Zhu, G. Wu, et al., Proteome differences in placenta and endometrium between normal and intrauterine growth restricted pig fetuses, *PLoS One* 10 (11) (2015) e0142396 (PubMed PMID: 26554841. Pubmed Central PMID: 4640832).
- [26] K.M. Meyer, J.M. Koch, J. Ramadoss, P.J. Kling, R.R. Magness, Ovine surgical model of uterine space restriction: interactive effects of uterine anomalies and multifetal gestations on fetal and placental growth, *Biol. Reprod.* 83 (5) (2010 Nov) 799–806 (PubMed PMID: 20574052. Pubmed Central PMID: 2959109).
- [27] J.A. Thompson, R. Gros, B.S. Richardson, K. Piorkowska, T.R. Regnault, Central stiffening in adulthood linked to aberrant aortic remodeling under suboptimal intrauterine conditions, *Am. J. Physiol. Regul. Integr. Comp. Physiol.* 301 (6) (2011 Dec) R1731–7 (PubMed PMID: 21900641).
- [28] S. Mayeur, S. Lancel, N. Theys, M.A. Lukaszewski, S. Duban-Deweer, B. Bastide, et al., Maternal calorie restriction modulates placental mitochondrial biogenesis and bioenergetic efficiency: putative involvement in fetoplacental growth defects in rats, *Am. J. Physiol. Endocrinol. Metab.* 304 (1) (2013 Jan 1) E14–22 (PubMed PMID: 23092912).
- [29] C. Mando, C. De Palma, T. Stampalija, G.M. Anelli, M. Figus, C. Novielli, et al., Placental mitochondrial content and function in intrauterine growth restriction and preeclampsia, *Am. J. Physiol. Endocrinol. Metab.* 306 (4) (2014 Feb 15) E404–13 (PubMed PMID: 24347055).
- [30] D. Madeleneau, C. Buffat, F. Mondon, H. Grimault, V. Rigourd, V. Tsatsaris, et al., Transcriptomic analysis of human placenta in intrauterine growth restriction, *Pediatr. Res.* 77 (6) (2015 Jun) 799–807 (PubMed PMID: 25734244).
- [31] T. Jansson, Placenta plays a critical role in maternal-fetal resource allocation, *Proc. Natl. Acad. Sci. U. S. A.* 113 (40) (2016 Sep 22) 11066–11068 (PubMed PMID: 27660237).
- [32] R. Nogueiras, K.M. Habegger, N. Chaudhary, B. Finan, A.S. Banks, M.G.O. Dietrich, et al., Sirtuin 1 and sirtuin 3: physiological modulators of metabolism, *Physiol. Rev.* 92 (3) (2012 Jul) 1479–1514 (PubMed PMID: 22811431. Pubmed Central PMID: 3746174).
- [33] M. Lappas, A. Mitton, R. Lim, G. Barker, C. Riley, Permezel M. SIRT1 is a novel regulator of key pathways of human labor, *Biol. Reprod.* 84 (1) (2011 Jan) 167–178 (PubMed PMID: 20844277).
- [34] D.B. Lombard, B.M. Zwaans, SIRT3: as simple as it seems? *Gerontology* 60 (1) (2014) 56–64 (PubMed PMID: 24192814. Pubmed Central PMID: 3875292).
- [35] S. Kwon, S. Seok, P. Yau, X. Li, B. Kemper, J.K. Kemper, Obesity and aging diminish sirtuin 1 (SIRT1)-mediated deacetylation of SIRT3, leading to hyperacetylation and decreased activity and stability of SIRT3, *J. Biol. Chem.* 292 (42) (2017 Oct 20) 17312–17323 (PubMed PMID: 28808064. Pubmed Central PMID: 5655509).
- [36] S. Chriett, I. Le Huerou-Luron, H. Vidal, L. Pirola, Dysregulation of sirtuins and key metabolic genes in skeletal muscle of pigs with spontaneous intrauterine growth restriction is associated with alterations of circulating IGF-1, *Gen. Comp. Endocrinol.* 232 (2016 Jun 1) 76–85 (PubMed PMID: 26769588).
- [37] M. Tanno, A. Kuno, Y. Horio, T. Miura, Emerging beneficial roles of sirtuins in heart failure, *Basic Res. Cardiol.* 107 (4) (2012 Jul) 273 (PubMed PMID: 22622703. Pubmed Central PMID: 3390697).
- [38] H. Dickinson, T.J. Moss, K.L. Gatford, K.M. Moritz, L. Akison, T. Fullston, et al., A review of fundamental principles for animal models of DoHAD research: an Australian perspective, *J. Dev. Orig. Health Dis.* 7 (5) (2016 Oct) 449–472 (PubMed PMID: 27689313).
- [39] G.B. Drummond, D.J. Paterson, J.C. McGrath, ARRIVE: new guidelines for reporting animal research, *J. Physiol.* 588 (Pt 14) (2010 Jul 15) 2517 (PubMed PMID: 20634179. Pubmed Central PMID: 2916980).
- [40] C. Kilkenny, V. Browne, I.C. Cuthill, M. Emerson, D.G. Altman, Group NCRGW, Animal research: reporting in vivo experiments: the ARRIVE guidelines, *Br. J. Pharmacol.* 160 (7) (2010 Aug) 1577–1579 (PubMed PMID: 20649561. Pubmed Central PMID: 2936830).
- [41] F. Medja, S. Allouche, P. Frachon, C. Jardel, M. Malgat, B. Mousson de Camaret, et al., Development and implementation of standardized respiratory chain spectrophotometric assays for clinical diagnosis, *Mitochondrion* 9 (5) (2009 Sep) 331–339 (PubMed PMID: 19439198).
- [42] M. Catalan-Garcia, G. Garrabou, C. Moren, M. Guitart-Mampel, A. Hernando, A. Diaz-Ramos, et al., Mitochondrial DNA disturbances and deregulated expression of oxidative phosphorylation and mitochondrial fusion proteins in sporadic inclusion body myositis, *Clin. Sci.* 130 (19) (2016 Oct 1) 1741–1751 (PubMed PMID: 27413019).
- [43] A. Barrientos, In vivo and in organello assessment of OXPHOS activities, *Methods* 26 (4) (2002 Apr) 307–316 (PubMed PMID: 12054921).
- [44] M.I. Alvarez-Mora, L. Rodriguez-Revenga, I. Madrigal, M. Guitart-Mampel, G. Garrabou, M. Mila, Impaired mitochondrial function and dynamics in the pathogenesis of FXTAS, *Mol. Neurobiol.* (2016 Oct 22) (PubMed PMID: 27771901).
- [45] D. Yubero, R. Montero, M.A. Martin, J. Montoya, A. Ribes, M. Grazina, et al., Secondary coenzyme Q10 deficiencies in oxidative phosphorylation (OXPHOS) and non-OXPHOS disorders, *Mitochondrion* 30 (2016 Sep) 51–58 (PubMed PMID: 27374853).
- [46] R. Mierzynski, D. Duski, D. Darmochwal-Kolarz, E. Poniedzialek-Czajkowska, B. Leszczynska-Gorzela, Z. Kimber-Trojnar, et al., Intra-uterine growth retardation as a risk factor for postnatal metabolic disorders, *Curr. Pharm. Biotechnol.* 17 (7) (2016) 587–596 (PubMed PMID: 26927210).
- [47] D. Batalle, E. Munoz-Moreno, A. Arbat-Plana, M. Illa, F. Figueras, E. Eixarch, et al., Long-term reorganization of structural brain networks in a rabbit model of intrauterine growth restriction, *NeuroImage* 100 (2014 Oct 15) 24–38 (PubMed PMID: 24943271).
- [48] D. Batalle, E. Munoz-Moreno, C. Tornador, N. Bargallo, G. Deco, E. Eixarch, et al., Altered resting-state whole-brain functional networks of neonates with intrauterine growth restriction, *Cortex* 77 (2016 Apr) 119–131 (PubMed PMID: 26927726).
- [49] R.V. Simoes, E. Munoz-Moreno, M. Cruz-Lemini, E. Eixarch, N. Bargallo, M. Sanz-

- Cortes, et al., Brain metabolite alterations in infants born preterm with intrauterine growth restriction: association with structural changes and neurodevelopmental outcome, *Am. J. Obstet. Gynecol.* 216 (1) (2016 Sep 22) 62.e1–62.e14, <http://dx.doi.org/10.1016/j.ajog.2016.09.089> (PubMed PMID: 27667762).
- [50] C. García-Contreras, D. Valent, M. Vazquez-Gomez, L. Arroyo, B. Isabel, S. Astiz, et al., Fetal growth-retardation and brain-sparing by malnutrition are associated to changes in neurotransmitters profile, *Int. J. Dev. Neurosci. Off. J. Int. Soc. Dev. Neurosci.* 57 (2017 Apr) 72–76 (PubMed PMID: 28104460).
- [51] J. Lopez-Tello, A. Barbero, A. Gonzalez-Bulnes, S. Astiz, M. Rodriguez, N. Formoso-Rafferty, et al., Characterization of early changes in fetoplacental hemodynamics in a diet-induced rabbit model of IUGR, *J. Dev. Orig. Health Dis.* 6 (5) (2015 Oct) 454–461 (PubMed PMID: 26268616).
- [52] M. Illa, E. Eixarch, E. Munoz-Moreno, D. Batalle, R. Leal-Campanario, A. Gruart, et al., Neurodevelopmental effects of undernutrition and placental underperfusion in fetal growth restriction rabbit models, *Fetal Diagn. Ther.* 42 (3) (2017 Jan 05) 189–197, <http://dx.doi.org/10.1159/000454859> (PubMed PMID: 28052270).
- [53] M. Illa, E. Eixarch, D. Batalle, A. Arbat-Plana, E. Munoz-Moreno, F. Figueras, et al., Long-term functional outcomes and correlation with regional brain connectivity by MRI diffusion tractography metrics in a near-term rabbit model of intrauterine growth restriction, *PLoS One* 8 (10) (2013) e76453 (PubMed PMID: 24143189. Pubmed Central PMCID: 3797044).
- [54] E. Eixarch, D. Batalle, M. Illa, E. Munoz-Moreno, A. Arbat-Plana, I. Amat-Roldan, et al., Neonatal neurobehavior and diffusion MRI changes in brain reorganization due to intrauterine growth restriction in a rabbit model, *PLoS One* 7 (2) (2012) e31497 (PubMed PMID: 22347486. Pubmed Central PMCID: 3275591).
- [55] M. Rodriguez-Lopez, M. Cruz-Lemini, B. Valenzuela-Alcaraz, L. Garcia-Otero, M. Sitges, B. Bijmens, et al., Descriptive analysis of different phenotypes of cardiac remodeling in fetal growth restriction, *Ultrasound Obstet. Gynecol. Off. J. Int. Soc. Ultrasound Obstet. Gynecol.* 50 (2) (2017 Aug) 207–214 (PubMed PMID: 27859818).
- [56] I. Torre, A. Gonzalez-Tendero, P. Garcia-Canadilla, F. Crispi, F. Garcia-Garcia, B. Bijmens, et al., Permanent cardiac sarcomere changes in a rabbit model of intrauterine growth restriction, *PLoS One* 9 (11) (2014) e113067 (PubMed PMID: 25402351. Pubmed Central PMCID: 4234642).
- [57] J. Schipke, A. Gonzalez-Tendero, L. Cornejo, A. Willfuhr, B. Bijmens, F. Crispi, et al., Experimentally induced intrauterine growth restriction in rabbits leads to differential remodelling of left versus right ventricular myocardial microstructure, *Histochem. Cell Biol.* 148 (5) (2017 Jul 10) 557–567 (PubMed PMID: 28695336).
- [58] A. Gonzalez-Tendero, C. Zhang, V. Balicevic, R. Cardenes, S. Loncaric, C. Butakoff, et al., Whole heart detailed and quantitative anatomy, myofibre structure and vasculature from X-ray phase-contrast synchrotron radiation-based micro computed tomography, *Eur. Heart J. Cardiovasc. Imaging* 18 (7) (2017 Jul 01) 732–741 (PubMed PMID: 28329054).
- [59] E.A. Schon, S. DiMauro, M. Hirano, Human mitochondrial DNA: roles of inherited and somatic mutations, *Nat. Rev. Genet.* 13 (12) (2012 Dec) 878–890 (PubMed PMID: 23154810. Pubmed Central PMCID: 3959762).
- [60] H. Cimen, M.J. Han, Y. Yang, Q. Tong, H. Koc, E.C. Koc, Regulation of succinate dehydrogenase activity by SIRT3 in mammalian mitochondria, *Biochemistry* 49 (2) (2010 Jan 19) 304–311 (PubMed PMID: 20000467. Pubmed Central PMCID: 2826167).
- [61] L. Lin, K. Chen, W. Abdel Khalek, J.L. Ward 3rd, H. Yang, B. Chabi, et al., Regulation of skeletal muscle oxidative capacity and muscle mass by SIRT3, *PLoS One* 9 (1) (2014) e85636 (PubMed PMID: 24454908. Pubmed Central PMCID: 22533670).
- [62] A. Giralt, F. Villarroja, SIRT3, a pivotal actor in mitochondrial functions: metabolism, cell death and aging, *Biochem. J.* 444 (1) (2012 May 15) 1–10 (PubMed PMID: 22533670).
- [63] L.W. Finley, W. Haas, V. Desquiret-Dumas, D.C. Wallace, V. Procaccio, S.P. Gygi, et al., Succinate dehydrogenase is a direct target of sirtuin 3 deacetylase activity, *PLoS One* 6 (8) (2011) e23295 (PubMed PMID: 21858060. Pubmed Central PMCID: 3157345).
- [64] T.M. Merz, J. Pichler Hefti, U. Hefti, A. Huber, S.M. Jakob, J. Takala, et al., Changes in mitochondrial enzymatic activities of monocytes during prolonged hypobaric hypoxia and influence of antioxidants: a randomized controlled study, *Redox Rep. Commun. Free Radic. Res.* 20 (5) (2015 Sep) 234–240 (PubMed PMID: 25867847).
- [65] M.S. Dodd, H.J. Atherton, C.A. Carr, D.J. Stuckey, J.A. West, J.L. Griffin, et al., Impaired in vivo mitochondrial Krebs cycle activity after myocardial infarction assessed using hyperpolarized magnetic resonance spectroscopy, *Circ. Cardiovasc. Imaging* 7 (6) (2014 Nov) 895–904 (PubMed PMID: 25201905. Pubmed Central PMCID: 4450075).
- [66] Q. Wang, L. Li, C.Y. Li, Z. Pei, M. Zhou, N. Li, SIRT3 protects cells from hypoxia via PGC-1alpha- and MnSOD-dependent pathways, *Neuroscience* 286 (2015 Feb 12) 109–121 (PubMed PMID: 25433241).
- [67] B.H. Ahn, H.S. Kim, S. Song, I.H. Lee, J. Liu, A. Vassilopoulos, et al., A role for the mitochondrial deacetylase Sirt3 in regulating energy homeostasis, *Proc. Natl. Acad. Sci. U. S. A.* 105 (38) (2008 Sep 23) 14447–14452 (PubMed PMID: 18794531. Pubmed Central PMCID: 2567183).
- [68] E. Jauniaux, L. Poston, G.J. Burton, Placental-related diseases of pregnancy: involvement of oxidative stress and implications in human evolution, *Hum. Reprod. Update* 12 (6) (2006 Nov-Dec) 747–755 (PubMed PMID: 16682385. Pubmed Central PMCID: 1876942).
- [69] A.L. Watson, J.N. Skepper, E. Jauniaux, G.J. Burton, Susceptibility of human placental syncytiotrophoblastic mitochondria to oxygen-mediated damage in relation to gestational age, *J. Clin. Endocrinol. Metab.* 83 (5) (1998 May) 1697–1705 (PubMed PMID: 9589679).

Imbalance in mitochondrial dynamics and apoptosis in pregnancies among HIV-infected women on HAART with obstetric complications

Mariona Guitart-Mampel^{1,2}, A. Sandra Hernandez^{3,4}, Constanza Moren^{1,2*†}, Marc Catalan-Garcia^{1,2}, Ester Tobias^{1,2}, Ingrid Gonzalez-Casacuberta^{1,2}, Diana L. Juarez-Flores^{1,2}, Josep M. Gatell⁵, Francesc Cardellach^{1,2}, Jose C. Milisenda^{1,2}, Josep M. Grau^{1,2}, Eduard Gratacos^{3,4}, Francesc Figueras^{3,4} and Gloria Garrabou^{1,2†}

¹Muscle Research and Mitochondrial Function Laboratory, Cellex-IDIBAPS, Faculty of Medicine and Health Science-University of Barcelona, Internal Medicine Service-Hospital Clínic of Barcelona, Barcelona, Spain; ²CIBERER, U722, Madrid, Spain; ³BCNatal Barcelona Center for Maternal-Fetal and Neonatal Medicine (Hospital Clínic and Hospital Sant Joan de Deu), IDIBAPS, University of Barcelona, Barcelona, Spain; ⁴CIBERER, U719, Madrid, Spain; ⁵Infectious Diseases Department, Hospital Clinic of Barcelona, Barcelona, Spain

*Corresponding author. Muscle Research and Mitochondrial Function Laboratory, Cellex-IDIBAPS, Faculty of Medicine-University of Barcelona, Hospital Clinic of Barcelona, 170 Villarroel (08036) Barcelona, Catalunya, Spain. Tel: +3493 2275400 Ext: 2907; Fax: +3493 2279365; E-mail: cmoren1@clinic.ub.es

†These authors made an equal contribution to the study.

Received 16 December 2016; returned 3 April 2017; revised 17 May 2017; accepted 23 May 2017

Background: HIV infection and HAART trigger genetic and functional mitochondrial alterations leading to cell death and adverse clinical manifestations. Mitochondrial dynamics enable mitochondrial turnover and degradation of damaged mitochondria, which may lead to apoptosis.

Objectives: To evaluate markers of mitochondrial dynamics and apoptosis in pregnancies among HIV-infected women on HAART and determine their potential association with obstetric complications.

Methods: This controlled, single-site, observational study without intervention included 26 HIV-infected pregnant women on HAART and 18 control pregnancies and their newborns. Maternal PBMCs and neonatal cord blood mononuclear cells (CBMCs) were isolated at the first trimester of gestation and at delivery. The placenta was homogenized at 5% w/v. Mitochondrial dynamics, fusion events [mitofusin 2 (Mfn2)/ β -actin] and fission events [dynamamin-related protein 1 (Drp1)/ β -actin] and apoptosis (caspase 3/ β -actin) were assessed by western blot analysis.

Results: Obstetric complications were significantly more frequent in pregnancies among HIV-infected women [OR 5.00 (95% CI 1.21–20.70)]. Mfn2/ β -actin levels in PBMCs from controls significantly decreased during pregnancy ($202.13 \pm 57.45\%$), whereas cases maintained reduced levels from the first trimester of pregnancy and no differences were observed in CBMCs. Mfn2/ β -actin and Drp1/ β -actin contents significantly decreased in the placenta of cases. Caspase 3/ β -actin levels significantly increased during pregnancy in PBMCs of cases ($50.00 \pm 7.89\%$), remaining significantly higher than in controls. No significant differences in caspase 3/ β -actin content of neonatal CBMCs were observed, but there was a slight increased trend in placenta from cases.

Conclusions: HIV- and HAART-mediated mitochondrial damage may be enhanced by decreased mitochondrial dynamics and increased apoptosis in maternal and placental compartments but not in the uninfected fetus. However, direct effects on mitochondrial dynamics and implication of apoptosis were not demonstrated in adverse obstetric outcomes.

Introduction

In developed countries, mortality and morbidity rates associated with HIV have dramatically decreased, turning this infection into a chronic disease.¹ This has been achieved thanks to HAART, a combined antiretroviral treatment that usually comprises two NRTIs combined with either a PI or an NNRTI.^{2,3} Both the virus and its treatment have been demonstrated to cause mitochondrial toxicity by either interference in mitochondrial function or apoptosis.^{4,5} It has

been proposed that these molecular disturbances are one of the aetiopathological bases of the secondary effects of HIV infection and therapy, including myopathy, hyperlactataemia, lactic acidosis, peripheral neuropathy and lipodystrophy, as well as infertility and obstetric problems.^{6–8} Furthermore, pregnancies in HIV-infected women are associated with an increased risk of adverse obstetric outcomes, including preterm delivery, pre-eclampsia,

stillbirth, low birth weight and intrauterine growth restriction (IUGR).^{9–12} Mitochondrial and apoptosis-related alterations have been described in pregnancies among HIV-infected women, including decreased mitochondrial DNA (mtDNA) levels and consequent mitochondrial dysfunction in different tissues, including oocytes, PBMCs and adipose tissue, as well as in fetal cord blood mononuclear cells (CBMCs) of exposed children.^{13–17}

Mitochondria are highly dynamic organelles, the morphology, structure and constitution of which are continually changing by fission and fusion processes.¹⁸ The frequency of these processes determines the quality as well as the morphology of mitochondria. Additionally, mitochondrial dynamics regulate mitochondrial bioenergetics, calcium signalling, mtDNA stability, mitochondrial quality, the generation of oxidative stress and cellular stress response.¹⁹ Mitochondrial fusion enables mitochondrial renewal, recycling and turnover by promoting component exchange between altered and healthy mitochondria.²⁰ Mitofusin 1 (Mfn1) and mitofusin 2 (Mfn2) are required to promote fusion of two neighbouring mitochondria. On the other hand, mitochondrial fission is mediated by dynamin-related protein 1 (Drp1), which divides a mitochondrion into two. Fission helps by splitting healthy from defective mitochondria. Damaged mitochondria should be further recycled or degraded through mitophagy;²¹ otherwise, apoptosis begins.

Considering the importance of these processes, abnormalities in mitochondrial dynamics and apoptosis have been suggested to occur early during the pathogenesis of many diseases.^{22,23} Several human pathologies, including cancer, Parkinson's disease, Alzheimer's disease and cardiovascular disorders, have been linked to abnormalities in proteins that govern mitochondrial fission or fusion phenomena or apoptosis development.^{20,24}

Previous studies support interference in cell and mitochondrial function by both HIV and HAART, leading to adverse clinical effects.^{4,5} However, few data are available about mitochondrial dynamics in the context of infectious diseases. To date, only *in vitro* models demonstrating HIV-1 viral protein R (Vpr) interaction with apoptosis and mitochondrial dynamics have been reported.²⁵ No *ex vivo* studies have been performed to assess the influence of HIV on mitochondrial dynamics or the relation between HAART and mitochondrial fusion and fission events and their potential association with an increased frequency of adverse obstetric outcomes in HIV-infected pregnant women on HAART.

The aim of this study was to evaluate Mfn2 and Drp1 levels, as markers of mitochondrial dynamics, together with caspase 3 content, indicative of apoptosis, in pregnancies among HIV-infected women on HAART and determine their potential association with obstetric and neonatal complications.

Materials and methods

Design

We performed a controlled single-site, observational study without intervention to determine the influence of mitochondrial dynamics and apoptosis on adverse obstetric outcomes of pregnancies in HIV-infected women on HAART. First, we compared longitudinal changes during pregnancy (from the first trimester of gestation to delivery) in PBMCs of HIV-infected pregnant women on HAART and uninfected pregnant controls. Second, CBMCs of uninfected but exposed newborns and the placenta of HIV-infected pregnant women on HAART were cross-sectionally compared at delivery with uninfected controls.

Patients

Twenty-six asymptomatic HIV-infected pregnant women on HAART and 18 uninfected controls were prospectively included in the first trimester of gestation during routine prenatal care in the Hospital Clinic of Barcelona (Spain) over 18 months. Inclusion criteria were age ≥ 18 years, single pregnancy, delivery at >22 weeks of gestation and, for HIV patients, previous diagnosis of HIV infection. No patients taking drugs potentially toxic to mitochondria or with a family history of mitochondrial disease were included. Epidemiological, immunovirological, therapeutic, obstetric, perinatal and experimental data were collected in a database.

Ethics

All participants provided written consent to participate in the study. The Ethics Committee of our hospital approved the study (reference code 2009/5118), which was performed following the Declaration of Helsinki guidelines.

Data collection

The epidemiological data included maternal age, ethnicity, illegal substance abuse and alcohol consumption. Immunovirological data for HIV-infected pregnant women on HAART included plasma HIV viral load, CD4 T-cell count and time from HIV infection to delivery. The therapeutic data collected included accumulated time of specific drug consumption (NRTI, NNRTI or PI) and stratification of HIV-infected pregnant women according to HAART use during pregnancy.

Therapy was administered to all HIV-infected pregnant women following international guidelines. Women naive to HAART before pregnancy started HAART (double-NRTI schedule and either PI or NNRTI) during the second trimester of gestation and continued for at least 6 months after delivery to prevent mother-to-child transmission (MTCT).

Data regarding obstetric and perinatal outcomes included pre-eclampsia (new onset of hypertension of >140 mmHg systolic or >90 mmHg diastolic blood pressure and >300 mg protein/24 h urine after 20 weeks of gestation), fetal death (>22 weeks of pregnancy), gestational age at delivery, preterm birth (<37 weeks of gestation), birth weight, small for gestational age (<10 th percentile), 5 min Apgar score <7 and global adverse perinatal outcome (including preterm birth, IUGR and preterm premature rupture of membranes).

Finally, maternal, neonatal and placental mitochondrial dynamics and apoptosis measures were collected in the first trimester of gestation and at delivery.

Samples

Twenty millilitres of maternal peripheral blood was obtained by antecubital vein puncture and collected in EDTA tubes, both in the first trimester of pregnancy (second to third months) and immediately after delivery. At delivery, 20 mL of neonatal cord blood was obtained and collected in EDTA tubes.

Maternal PBMCs and neonatal CBMCs were isolated by a Ficoll gradient procedure and cryopreserved at $-80 \pm 5^\circ\text{C}$ until analysis. Placentas were obtained at delivery and immediately frozen at $-80 \pm 5^\circ\text{C}$ until analysis. A homogenate of placental tissue (5% w/v) was prepared in mannitol buffer. Protein content was measured in PBMCs, CBMCs and placental homogenates using the bicinchoninic acid colorimetric assay (Thermo Scientific assay kit) to normalize experimental measures.

Mitochondrial studies

Mitochondrial dynamics

Mfn2 and Drp1 protein levels were examined by western blot analysis. Twenty micrograms of total protein from PBMCs, CBMCs and placenta was

Table 1. Epidemiological, immunovirological and therapeutic characteristics of HIV-infected pregnant women on HAART (HIV positive) and uninfected pregnant women (HIV negative)

Parameter ^a	HIV positive (n = 26)	HIV negative (n = 18)	P
Maternal age at delivery, years	34.7 (27–42)	34.6 (28–41)	NS
Illegal drug use, n (%)	0	0	–
Alcohol use, n (%)	0	0	–
HIV RNA at delivery, copies/mL	67.5 (49–250)	–	–
CD4 T cell count at delivery, cells/mm ³	585.5 (211–1242)	–	–
Time from diagnosis of HIV infection to delivery, months	98.1 (4–228)	–	–
NRTI before pregnancy, months	52.8 (0–106)	–	–
NNRTI before pregnancy, months	16.4 (0–86)	–	–
PI before pregnancy, months	19.6 (0–97)	–	–
Naive (HAART trimesters 2 and 3), n (%)	4 (15.4)	–	–
HAART all trimesters, n (%)	22 (84.6)	–	–
2 NRTIs + 1 PI, n (%)	14 (53.8)	–	–
2 NRTIs + 1 NNRTI, n (%)	8 (30.8)	–	–

NS, not significant.

^aData are mean (range) unless specified otherwise.

separated using 7%/13% SDS-PAGE and transferred to nitrocellulose membranes (iBlot Gel Transfer Stacks, Life Technologies), which were hybridized with anti-Mfn2 (1:2000; Abcam, Cambridge, UK) and/or anti-Drp1 (1:500; Santa Cruz, CA, USA). Quantification of Mfn2 (82 kDa) and Drp1 (80 kDa) was normalized by the content of β -actin protein (47 kDa) as a total cell protein loading control. The ImageQuantLD program was used to quantify chemiluminescence. Mfn2/ β -actin levels were interpreted as a marker of mitochondrial fusion development²⁶ and Drp1/ β -actin levels as a marker of mitochondrial fission events.²⁷

Apoptosis

Western blot analysis was performed with 20 μ g of total cell protein of PBMCs, CBMCs and placenta as described above. Nitrocellulose membranes were incubated with anti-caspase 3 (1:1000; Cell Signaling, MA, USA). Active (cleaved) caspase 3 protein expression (17–19 kDa) was normalized and quantified. The results were expressed as caspase 3/ β -actin relative content and interpreted as a marker of advanced apoptosis-related events.²⁸

Statistical analysis

Clinical and epidemiological parameters were expressed as mean and range and experimental results as mean and SEM or as a percentage increase/decrease at delivery compared with the first trimester of pregnancy or compared with controls.

Statistical analysis was performed using the IBM SPSS Statistics 20 program. Non-parametric tests were used to determine case-control differences (Mann-Whitney independent sample analysis) and the OR (χ^2 test). Additionally, different correlations were made between experimental and clinical data to assess the dependence of obstetric complications on mitochondrial dynamics or apoptosis imbalance, and the influence of therapeutic or immunovirological conditions on them (Spearman test). A *P* value <0.05 was considered significant.

Results

Clinical data

Table 1 shows the epidemiological, immunovirological and therapeutic results of patients and controls. No significant differences

were observed in epidemiological data between HIV-positive and HIV-negative pregnant women, who were all Caucasian, ranging from 27 to 42 years old. The mean time of HIV infection and of HAART prior to delivery was 98.1 and 52.8 months, respectively. All HIV-infected mothers were on HAART for at least 6 months prior to delivery to avoid MTCT, including those starting HAART during pregnancy (*n* = 4; 15.4%) and those already on HAART (*n* = 22; 84.6%). HAART consisted of administering two NRTIs and either one PI (53.8%) or one NNRTI (30.8%). At delivery, all women presented an undetectable viral load. Neither patients nor controls presented clinical manifestations of mitochondrial toxicity.

Perinatal outcomes

Table 2 shows the obstetric and neonatal outcomes of the study cohorts. All infants were HIV uninfected with no symptoms of mitochondrial toxicity, but those exposed *in utero* to HIV received 6 weeks of post-natal zidovudine chemoprophylaxis to reduce MTCT. The two cohorts showed similar gestational ages at delivery (37.9 versus 38.9 weeks), but pregnancies in HIV-infected women on HAART showed a higher trend to preterm birth (23.1% versus 11.1%), reduced birth weight (2974 versus 3080 g), higher frequency of small-for-gestational-age newborns (23.1% versus 5.6%) and significantly increased global adverse obstetric outcomes (61.5% versus 16.7%; *P* = 0.043).

Mitochondrial dynamics

Mfn2/ β -actin expression was significantly reduced, by $47.89 \pm 9.86\%$, in PBMCs of HIV-infected pregnant women on HAART compared with controls during the first trimester of pregnancy (0.74 ± 0.14 versus 1.42 ± 0.27 , *P* = 0.025; Figure 1a and Figure S1a, available as Supplementary data at JAC Online). However, at delivery, Mfn2/ β -actin expression was similar in the two cohorts ($14.89 \pm 25.53\%$ increased in HIV-infected pregnant women on HAART compared with controls; 0.54 ± 0.12 versus 0.47 ± 0.09 ; *P* = 0.705; Figure 1a and Figure S1a).

Table 2. Obstetric and neonatal outcomes of the pregnancies among HIV-infected women on HAART (HIV positive) and control pregnancies (HIV negative) included in the study

Parameter	HIV positive (n = 26)	HIV negative (n = 18)	OR (95% CI)
Preeclampsia, n (%)	0	0	-
Fetal death, n (%)	0	0	-
Gestational age at delivery (weeks) ^a	37.9 (31.3–41.2)	38.9 (34.4–41.4)	NS
Preterm birth (<37 weeks of gestation), n (%)	6 (23.1)	2 (11.1)	2.40 (0.43–13.54)
Birth weight (g) ^a	2974 (1250–4040)	3080 (2380–3905)	NS
Small newborn for gestational age (<10th percentile), n (%)	6 (23.1)	1 (5.6)	5.10 (0.56–46.68)
5 min Apgar score <7, n (%)	0	0	-
Global adverse perinatal outcome (preterm birth, IUGR and PPRM), n (%)	16 (61.5)	3 (16.7)	5.00 (1.21–20.70)

NS, not significant; IUGR, intrauterine growth restriction; PPRM, preterm premature rupture of membranes.

^aData are mean and range.

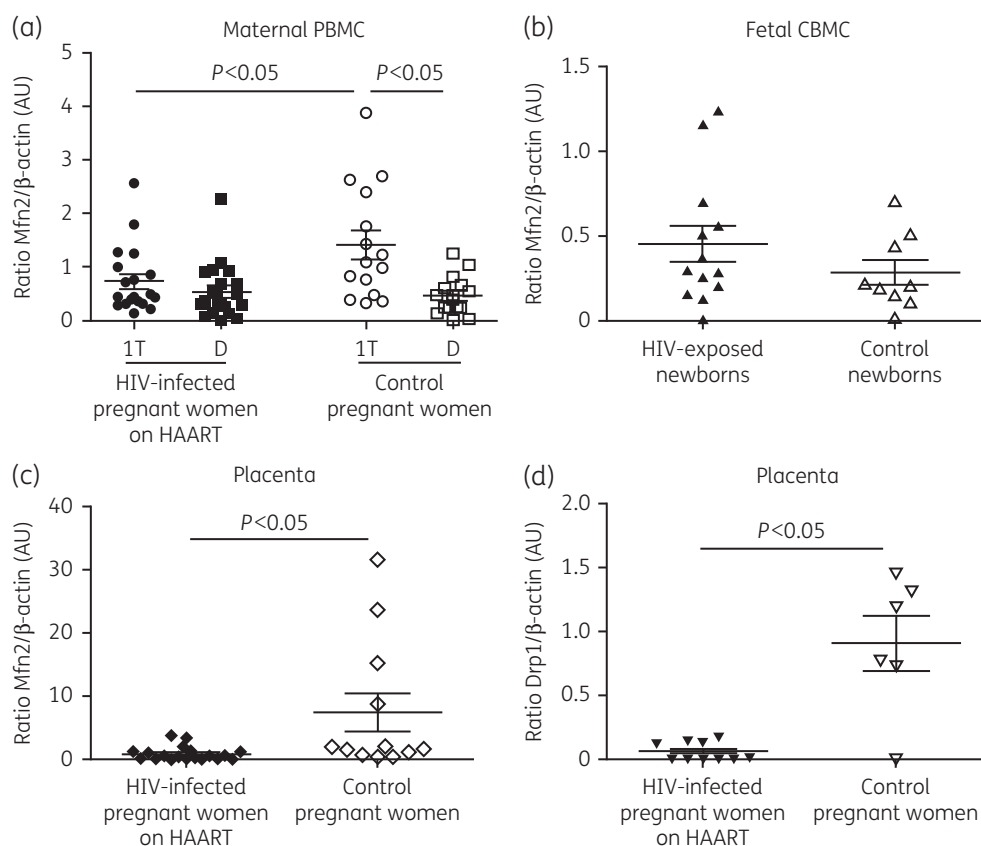


Figure 1. Markers of mitochondrial dynamics. Mfn2 and Drp1 levels relative to β-actin content in pregnancies among HIV-infected women on HAART (filled symbols) compared with control pregnancies (open symbols). (a) Mfn2 levels in maternal PBMCs at first trimester (1T) of pregnancy and at delivery (D) significantly decreased during gestation in controls, achieving values similar to those of HIV-infected pregnant women on HAART, that were significantly reduced since the first trimester of gestation. (b) Mfn2 levels in fetal CBMCs at delivery were conserved in HIV- and HAART-exposed newborns. (c) Mfn2 levels in placenta were reduced in HIV-infected pregnant women on HAART compared with controls. (d) Drp1 levels were significantly decreased in placentas of HIV-infected pregnant women on HAART compared with controls. Data are presented as mean ± SEM. AU, arbitrary units.

On longitudinal analysis, a significant decrease, of $202.13 \pm 57.45\%$, was observed in Mfn2/β-actin levels in PBMCs of control pregnancies from the first trimester of pregnancy to delivery (1.42 ± 0.27 versus 0.47 ± 0.09 ; $P = 0.003$; Figure 1a and Figure S1a).

This significant decrease was not observed in HIV-infected pregnant women on HAART ($37.04 \pm 25.93\%$ decrease; 0.74 ± 0.14 versus 0.54 ± 0.12 ; $P = 0.173$; Figure 1a and Figure S1a), since they presented significantly reduced levels compared with controls from the

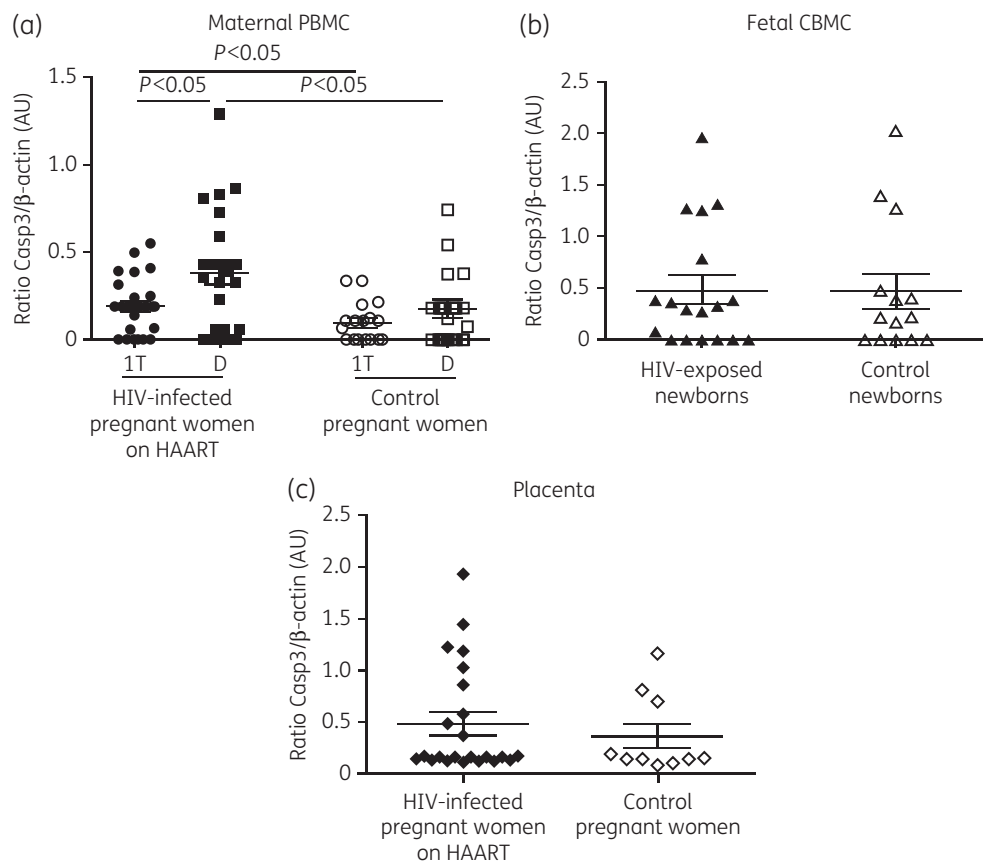


Figure 2. Markers of apoptosis. Caspase 3 (Casp3) levels normalized by β -actin content in pregnancies among HIV-infected women on HAART (filled symbols) compared with control pregnancies (open symbols). (a) Casp3 levels in maternal PBMCs at first trimester (1T) of pregnancy and at delivery (D) were significantly increased during pregnancy in HIV-infected pregnant women on HAART and remained significantly higher than in controls. (b) Casp3 levels in fetal CBMCs at delivery were similar in HIV- and HAART-exposed newborns compared with control newborns. (c) Casp3 levels in placentas showed a tendency to increase in HIV-infected pregnant women on HAART. Data are presented as mean \pm SEM. AU, arbitrary units.

first trimester of pregnancy. CBMC Mfn2/ β -actin levels were conserved in HIV- and HAART-exposed newborns (increase of $60.71 \pm 39.29\%$ versus controls; 0.45 ± 0.11 versus 0.28 ± 0.07 , $P = 0.292$; Figure 1b and Figure S1b).

Finally, Mfn2/ β -actin levels were significantly reduced, by $88.43 \pm 3.50\%$, in placentas of HIV-infected pregnant women on HAART compared with controls (0.86 ± 0.26 versus 7.43 ± 3.04 ; $P = 0.004$; Figure 1c and Figure S1c), as were Drp1/ β -actin levels (by $95.93 \pm 1.63\%$) compared with controls (0.06 ± 0.02 versus 0.91 ± 0.22 ; $P = 0.011$; Figure 1d and Figure S1c).

Apoptosis

PBMCs from pregnancies in HIV-infected women on HAART presented a significant increase in caspase 3/ β -actin levels, of $97.92 \pm 31.25\%$ (0.19 ± 0.03 versus 0.10 ± 0.03 ; $P = 0.036$; Figure 2a and Figure S1a), in the first trimester of gestation and of $123.53 \pm 35.29\%$ at delivery (0.38 ± 0.06 versus 0.17 ± 0.05 ; $P = 0.024$; Figure 2a and Figure S1a), compared with controls.

On longitudinal analysis, caspase 3/ β -actin content in PBMCs of pregnancies among HIV-infected women on HAART rose significantly, by $50.00 \pm 7.89\%$, from the first trimester of gestation to

delivery (0.19 ± 0.03 versus 0.38 ± 0.06 ; $P = 0.030$; Figure 2a and Figure S1a). This ratio also increased, albeit not significantly, in the control cohort ($43.53 \pm 17.65\%$; 0.10 ± 0.03 versus 0.17 ± 0.05 ; $P = 0.304$; Figure 2a and Figure S1a).

Caspase 3/ β -actin levels in neonatal CBMCs from pregnancies in HIV-infected women on HAART remained similar to those of controls (0.48 ± 0.14 versus 0.47 ± 0.17 ; $P = 1.000$; Figure 2b and Figure S1b) and placentas from pregnancies in HIV-infected women on HAART showed a slight trend towards an increase ($33.33 \pm 30.56\%$) compared with controls (0.48 ± 0.11 versus 0.36 ± 0.12 , respectively; $P = 0.44$; Figure 2c and Figure S1c).

Associations between experimental and clinical features

At an immunological level, CD4⁺ T cell counts in HIV-infected pregnant women on HAART at delivery significantly and positively correlated with Mfn2 levels in CBMCs from their newborns ($R^2 = 0.696$, $P = 0.002$), suggesting that proper maternal immunovirological status helps to prevent an imbalance in mitochondrial dynamics (Figure 3a).

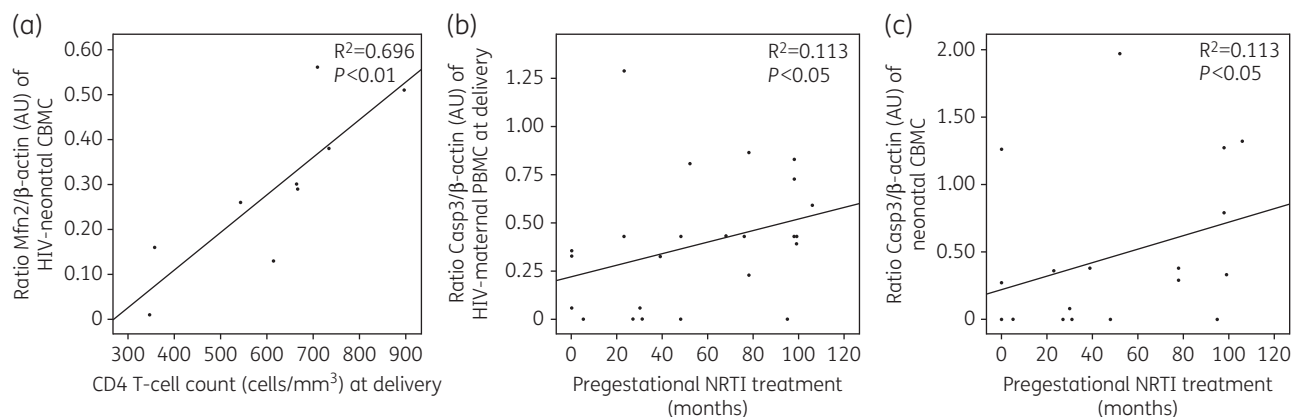


Figure 3. Associations between experimental and clinical features. (a) Significant positive correlation between Mfn2 levels in neonatal CBMCs and CD4+ T cell counts in pregnancies among HIV-infected women on HAART at delivery. (b and c) Positive correlations at limit of significance in pregnancies among HIV-infected women on HAART at delivery between apoptosis (in both maternal PBMCs and neonatal CBMCs) with respect to pregestational NRTI treatment. Casp3, caspase 3; AU, arbitrary units.

Positive correlations at the limit of significance were observed in pregnancies among HIV-infected women on HAART at delivery between apoptosis (both in maternal PBMCs and neonatal CBMCs) compared with pregestational NRTI treatment ($R^2 = 0.113$, $P = 0.044$ and $R^2 = 0.113$, $P = 0.047$, respectively), suggesting the dependence of apoptosis development on NRTI toxicity (Figure 3b and c).

Additionally, a positive correlation was found between apoptosis in CBMCs of HIV- and HAART-exposed newborns and maternal age at delivery, strengthening the involvement of ageing in cell damage and survival ($P = 0.037$, data not shown). Additionally, significant positive correlations were observed in Mfn2 levels of maternal PBMCs or caspase 3/β-actin levels between the first trimester of pregnancy and delivery, suggesting the usefulness of these biomarkers for first-trimester screening ($P = 0.005$ and $P = 0.001$, respectively; data not shown).

Finally, despite significantly increased incidence of adverse perinatal outcomes among HIV-infected women on HAART, no correlation was found between an imbalance in mitochondrial dynamics or apoptosis-related events and obstetric outcomes.

Discussion

The aetiopathology of obstetric disarrangements in pregnancies among HIV-infected women remains under debate, but mitochondrial and apoptosis-related disturbances have previously been associated with adverse clinical effects of HIV infection and its treatment.^{9–12} Mitochondrial dynamics is the mechanism by which damaged mitochondria (which may finally trigger apoptosis) are recycled. Impairment of mitochondrial dynamics and apoptosis has previously been associated with disease.^{6–8} However, mitochondrial dynamics and apoptosis deregulation in the context of human pregnancies, HIV infection and obstetric problems have never been assessed.

Previous *in vitro* studies have reported a reduction in Mfn2 and Drp1 expression mediated by Vpr,²⁴ which can be integrated on

mitochondria, leading to mitochondrial fragmentation and apoptosis.^{24,29–32} Although no study has described the involvement of HAART in mitochondrial dynamics, mitochondrial toxicity has been attributed to the NRTI component of this multidrug therapy by interfering in mtDNA replication, which may finally lead to cell death by apoptosis.²⁵

The present work demonstrates an alteration in the studied markers of mitochondrial dynamics and apoptosis in pregnancies among HIV-infected women on HAART. Additionally, the risk of adverse events in this cohort was demonstrated by trends towards increased rates of preterm birth, reduced birth weight and small-for-gestational-age newborns, and a significantly higher frequency of global adverse perinatal outcomes.

In our cohort of HIV-infected pregnant women on HAART we observed a significant decrease in Mfn2 levels in maternal PBMCs in the first trimester of pregnancy, which remained decreased during pregnancy. Similarly, we observed a significant reduction in Mfn2 and Drp1 contents in placentas of pregnancies in HIV-infected women on HAART. As previously described *in vitro*, Vpr may interfere in mitochondrial dynamics *in vivo*, but only in tissues in contact with the virus (maternal and placental cells). The fetus is uninfected and thus mitochondrial dynamics remain balanced. Experimental data suggest that decreased Mfn2 expression promotes apoptosis and hampers development by obstructing mitochondrial metabolism and disrupting mitochondrial membrane potential and cellular activity, leading to disordered embryonic development.²⁶ Consequently, imbalanced fusion and fission processes in pregnancies among HIV-infected women on HAART may underlie poor obstetric outcomes.

Additionally, these HIV-infected pregnant women on HAART present a significant increase in the expression of the apoptotic caspase 3 in PBMCs in both the first trimester of gestation and at delivery, probably mediated by the virus, as previously suggested.²⁹ Again, maternal PBMCs and placentas show a trend to an increase in apoptosis markers, but the fetus remains unaffected. Apoptosis has been associated with adverse obstetric problems in HIV-infected and uninfected pregnant women

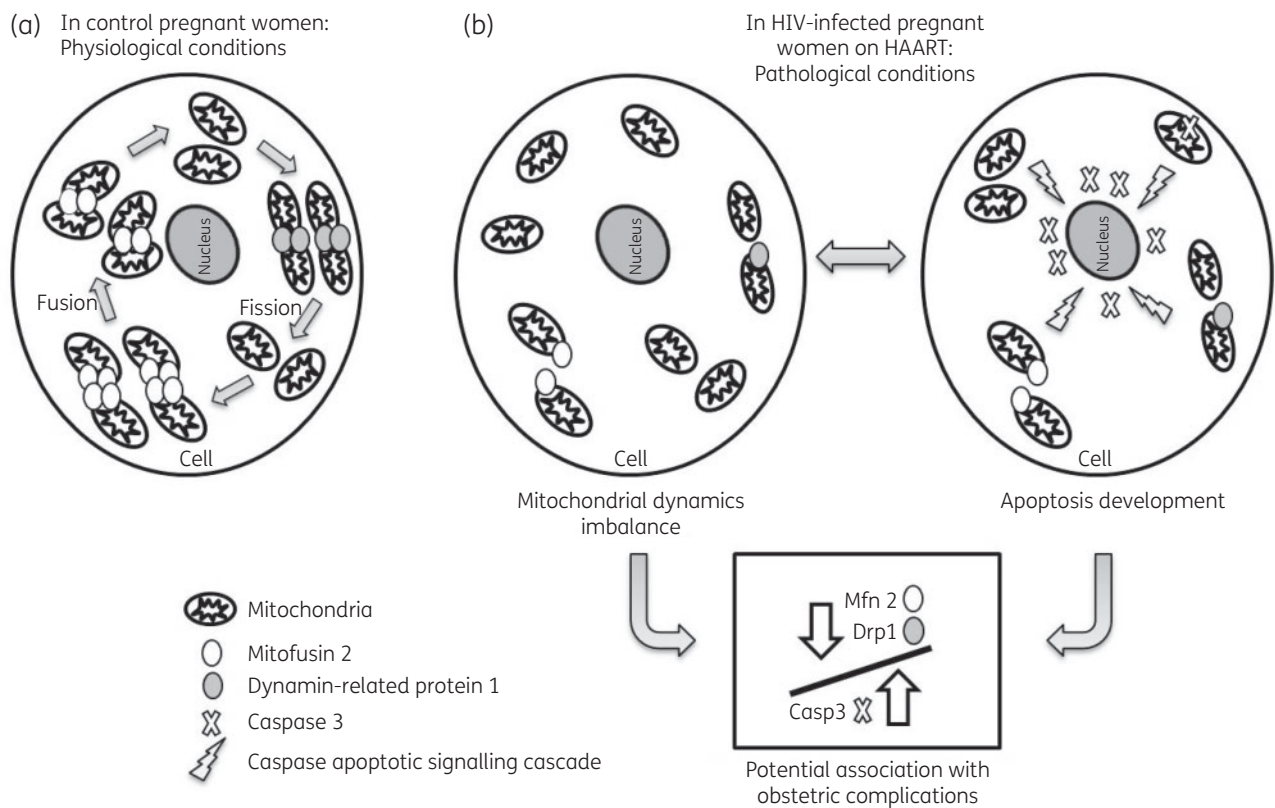


Figure 4. Association of an imbalance in mitochondrial dynamics and mitochondrial fragmentation with cell apoptosis in pregnancies among HIV-infected women on HAART. (a) Physiological conditions in normal pregnancies. Expression of Mfn2 and Drp1 maintains mitochondrial dynamics in equilibrium to promote proper mitochondrial function to avoid the development of apoptosis. (b) Potential obstetric complications in pregnancies among HIV-infected women on HAART. Altered mitochondrial dynamics could promote the increase in caspase 3 (Casp3) levels, leading to apoptosis, which could also initiate or alter mitochondrial dynamics in a bilateral manner.

presenting pre-eclampsia and IUGR.³³ Consequently, apoptosis together with an imbalance in mitochondrial dynamics may also interfere with proper neonatal development.

Interestingly, the HIV-infected cohort received HAART during gestation and consequently viral protein levels, including Vpr, should have been almost undetectable.³⁴ Thus, the imbalance in the studied markers of mitochondrial dynamics and enhanced apoptosis development observed in pregnancies among HIV-infected women on HAART may likely have been HAART- rather than virus-mediated. Alternatively, Vpr or other viral proteins may develop a toxic function when present in small amounts. In this regard, our findings suggest preserved immunovirological maternal status in association with balanced neonatal mitochondrial dynamics (Mfn2 levels). Additionally, higher exposure to NRTI would be associated with the enhancement of apoptosis development (caspase 3 expression). These associations may suggest that both the virus and its treatment, together with maternal age and other environmental agents, may simultaneously interfere with mitochondrial dynamics or apoptosis. However, further studies are needed to confirm these conclusions.

On the other hand, the association of maternal mitochondrial dynamics or apoptosis (Mfn2 and caspase 3 levels) between the first trimester of gestation and at delivery demonstrates the usefulness of these biomarkers in prenatal screening.

Additionally, Mfn2 levels in PBMCs of uninfected control women decreased from the first trimester of gestation to

delivery, achieving values similar to those in HIV-infected pregnant women on HAART, which remained underexpressed during gestation. The physiological decrease in Mfn2 in uninfected pregnant controls has not been described previously. The decrease in this marker of mitochondrial fusion during gestation could be explained by the increase in physiological apoptosis of maternal PBMCs that has been described during pregnancy.³⁵ The increase in apoptotic expression of caspase 3 in controls during gestation could thereby be associated with mitochondrial fusion and fragmentation,³⁴ regardless of any viral or drug interference. However, this increase in apoptosis markers in uninfected controls at delivery is pathologically enhanced in HIV-infected pregnant women on HAART after the first trimester of gestation, probably mediated by viral infection or treatment, and may explain the reduced Mfn2 levels observed in pregnancies among HIV-infected women since conception. An increase in apoptosis has also been reported in the placenta of HIV-infected pregnant women,³⁵ thereby explaining the reduced trends towards reduced Mfn2 content in this cohort. However, an imbalance in studied markers of mitochondrial dynamics or apoptosis was not detected in CBMCs of healthy newborns from pregnancies in HIV-infected women on HAART, probably because they were not infected, thus explaining the unaltered levels of Mfn2 or caspase 3 compared with healthy newborns from control pregnancies.

In conclusion, the increase in caspase 3 in PBMCs of HIV-infected pregnant women on HAART could be interpreted as an increase in apoptosis mediated by a reduction in Mfn2, or a reduction in Mfn2 mediated by an increase in apoptosis. Several reports have associated mitochondrial dynamics and mitochondrial fragmentation with cell apoptosis by describing the interaction among the main proteins governing both processes.^{26,36–38} Apoptosis promotes deregulation of mitochondrial dynamics, but dysfunction in mitochondrial dynamics also promotes apoptosis in a kind of bilateral feedback. Indeed, deregulation of mitochondrial dynamics and apoptosis likely go hand in hand, contributing to the associated adverse obstetric events observed in pregnancies among HIV-infected women on HAART. Apoptosis has been extensively associated with poor obstetric outcome³³ and our data suggest an additive role for the deregulation of mitochondrial dynamics markers, at least in pregnancies among HIV-infected women on HAART (Figure 4).

The present study has several limitations. The inclusion of a control group of non-pregnant HIV-infected women on HAART could have been useful to assess potential gestation interference. Another limitation may be the presence of heterogeneous HAART regimens and times of exposure to HIV or HAART, characteristic of observational studies and personalized treatment interventions, which may disclose findings closer to reality. Additionally, the implication of Vpr or alternative viral proteins in mitochondrial dynamics or apoptosis deregulation will remain speculative, as these proteins are usually quantified in plasma and we did not collect this. Finally, no significant association was found between markers of mitochondrial dynamics or apoptosis-related disturbances and obstetric problems, probably due to the reduced sample size, which hampered statistical power, or to technical limitations in the assessment of some of these markers in certain tissues.

Despite these limitations, our findings demonstrate that pregnancies in HIV-infected women on HAART with adverse obstetric outcomes show altered markers of mitochondrial dynamics and apoptosis development, probably due to viral and HAART exposure, potentially leading to increased mitochondrial fragmentation. The alteration of these mechanisms may trigger adverse obstetric outcomes in pregnancies among HIV-infected women on HAART by interfering in mitochondrial recycling and turnover and contributing to classical mitochondrial and apoptosis-related toxicity induced by the virus and its treatment. Further studies are needed to study the aetiology of obstetric problems in depth to establish new putative biomarkers and potential therapeutic targets.

Acknowledgements

We thank Donna Pringle for her valuable collaboration and for language assistance, and we are especially grateful to all the patients.

Funding

This study was funded by the Fundación para la Investigación y la Prevención del SIDA en España (FIPSE 360745/09 and 360982/10), CONACyt, Suports a Grups de Recerca (2014/SGR/376) and the CERCA Programme from the Generalitat de Catalunya, Fundació La Marató de TV3 (87/C/2015), Fundació Cellex, CIBERER (an initiative of ISCIII), Fondo de Investigación Sanitaria (FIS PI11/00462, PI12/01199, PI13/01738,

PI13/01455, PI15/00817 and PI15/00903) and InterCIBER (PIE1400061) granted by ISCIII and FEDER.

Transparency declarations

None to declare.

Supplementary data

Figure S1 is available as Supplementary data at JAC Online.

References

- Dieffenbach CW, Fauci AS. Thirty years of HIV and AIDS: future challenges and opportunities. *Ann Intern Med* 2011; **154**: 766–71.
- Rakhmanina NY, Dirajlal-Fargo S, Capparelli EV *et al*. Pharmacokinetic considerations of perinatal antiretroviral therapy. *Curr Drug Metab* 2012; **13**: 744–59.
- Volmink J, Siegfried NL, van der Merwe L *et al*. Antiretrovirals for reducing the risk of mother-to-child transmission of HIV infection. *Cochrane Database Syst Rev* 2007; issue **1**: CD003510.
- Miro O, Lopez S, Martinez E *et al*. Mitochondrial effects of HIV infection on the peripheral blood mononuclear cells of HIV-infected patients who were never treated with antiretrovirals. *Clin Infect Dis* 2004; **39**: 710–6.
- Noguera-Julian AMC, Rovira N, Garrabou G *et al*. Decreased mitochondrial function among healthy infants exposed to antiretrovirals during gestation, delivery and the neonatal period. *Pediatr Infect Dis J* 2015; **34**: 1349–54.
- Moren C, Hernandez S, Guitart-Mampel M *et al*. Mitochondrial toxicity in human pregnancy: an update on clinical and experimental approaches in the last 10 years. *Int J Environ Res Public Health* 2014; **11**: 9897–918.
- Garrabou G, Hernandez AS, Catalan Garcia M *et al*. Molecular basis of reduced birth weight in smoking pregnant women: mitochondrial dysfunction and apoptosis. *Addict Biol* 2014; **21**: 159–70.
- Mandelbrot L, Kermarrec N, Marcollet A *et al*. Case report: nucleoside analogue-induced lactic acidosis in the third trimester of pregnancy. *AIDS* 2003; **17**: 272–3.
- Tuomala RE, Shapiro DE, Mofenson LM *et al*. Antiretroviral therapy during pregnancy and the risk of an adverse outcome. *N Engl J Med* 2002; **346**: 1863–70.
- Lambert JS, Watts DH, Mofenson L *et al*. Risk factors for preterm birth, low birth weight, and intrauterine growth retardation in infants born to HIV-infected pregnant women receiving zidovudine. Pediatric AIDS Clinical Trials Group 185 Team. *AIDS* 2000; **14**: 1389–99.
- Suy A, Martinez E, Coll O *et al*. Increased risk of pre-eclampsia and fetal death in HIV-infected pregnant women receiving highly active antiretroviral therapy. *AIDS* 2006; **20**: 59–66.
- Thorne C, Patel D, Newell ML. Increased risk of adverse pregnancy outcomes in HIV-infected women treated with highly active antiretroviral therapy in Europe. *AIDS* 2004; **18**: 2337–9.
- Lopez S, Coll O, Durban M *et al*. Mitochondrial DNA depletion in oocytes of HIV-infected antiretroviral-treated infertile women. *Antivir Ther* 2008; **13**: 833–8.
- Divi RL, Walker VE, Wade NA *et al*. Mitochondrial damage and DNA depletion in cord blood and umbilical cord from infants exposed in utero to Combivir. *AIDS* 2004; **18**: 1013–21.
- Lewis W, Dalakas MC. Mitochondrial toxicity of antiviral drugs. *Nat Med* 1995; **1**: 417–22.

- 16** Garrabou G, Moren C, Gallego-Escuredo JM et al. Genetic and functional mitochondrial assessment of HIV-infected patients developing HAART-related hyperlactatemia. *J Acquir Immune Defic Syndr* 2009; **52**: 443–51.
- 17** Nasi M, Pinti M, Chiesa E et al. Decreased mitochondrial DNA content in subcutaneous fat from HIV-infected women taking antiretroviral therapy as measured at delivery. *Antivir Ther* 2011; **16**: 365–72.
- 18** Dhingra R, Kirshenbaum LA. Regulation of mitochondrial dynamics and cell fate. *Circ J* 2014; **78**: 803–10.
- 19** Babbar M, Sheikh MS. Metabolic stress and disorders related to alterations in mitochondrial fission or fusion. *Mol Cell Pharmacol* 2013; **5**: 109–33.
- 20** Archer SL. Mitochondrial dynamics—mitochondrial fission and fusion in human diseases. *N Engl J Med* 2013; **369**: 2236–51.
- 21** Yoon Y, Galloway CA, Jhun BS et al. Mitochondrial dynamics in diabetes. *Antioxid Redox Signal* 2011; **14**: 439–57.
- 22** Chen KH, Dasgupta A, Ding J et al. Role of mitofusin 2 (Mfn2) in controlling cellular proliferation. *FASEB J* 2014; **28**: 382–94.
- 23** van der Blik AM, Shen Q, Kawajiri S. Mechanisms of mitochondrial fission and fusion. *Cold Spring Harb Perspect Biol* 2013; **5**: pii=a011072.
- 24** Santel A. Get the balance right: mitofusins roles in health and disease. *Biochim Biophys Acta* 2006; **1763**: 490–9.
- 25** Huang CY, Chiang SF, Lin TY et al. HIV-1 Vpr triggers mitochondrial destruction by impairing Mfn2-mediated ER-mitochondria interaction. *PLoS One* 2012; **7**: e33657.
- 26** Zhao N, Zhang Y, Liu Q et al. Mfn2 affects embryo development via mitochondrial dysfunction and apoptosis. *PLoS One* 2015; **10**: e0125680.
- 27** Wang S, Song J, Tan M et al. Mitochondrial fission proteins in peripheral blood lymphocytes are potential biomarkers for Alzheimer's disease. *Eur J Neurol* 2012; **19**: 1015–22.
- 28** Garrabou G, Moren C, Lopez S et al. The effects of sepsis on mitochondria. *J Infect Dis* 2012; **205**: 392–400.
- 29** Muthumani K, Choo AY, Hwang DS et al. Mechanism of HIV-1 viral protein R-induced apoptosis. *Biochem Biophys Res Commun* 2003; **304**: 583–92.
- 30** Borengasser SJ, Faske J, Kang P et al. In utero exposure to prepregnancy maternal obesity and postweaning high-fat diet impair regulators of mitochondrial dynamics in rat placenta and offspring. *Physiol Genomics* 2014; **46**: 841–50.
- 31** Wappler EA, Institoris A, Dutta S et al. Mitochondrial dynamics associated with oxygen-glucose deprivation in rat primary neuronal cultures. *PLoS One* 2013; **8**: e63206.
- 32** Gall JM, Wang Z, Bonegio RG et al. Conditional knockout of proximal tubule mitofusin 2 accelerates recovery and improves survival after renal ischemia. *J Am Soc Nephrol* 2015; **26**: 1092–102.
- 33** Ishihara N, Matsuo H, Murakoshi H et al. Increased apoptosis in the syncytiotrophoblast in human term placentas complicated by either preeclampsia or intrauterine growth retardation. *Am J Obstet Gynecol* 2002; **186**: 158–66.
- 34** Lee GQ, Dong W, Mo T et al. Limited evolution of inferred HIV-1 tropism while viremia is undetectable during standard HAART therapy. *PLoS One* 2014; **9**: e99000.
- 35** Hernandez S, Moren C, Lopez M et al. Perinatal outcomes, mitochondrial toxicity and apoptosis in HIV-treated pregnant women and in-utero-exposed newborn. *AIDS* 2012; **26**: 419–28.
- 36** Wang W, Xie Q, Zhou X et al. Mitofusin-2 triggers mitochondria Ca²⁺ influx from the endoplasmic reticulum to induce apoptosis in hepatocellular carcinoma cells. *Cancer Lett* 2015; **358**: 47–58.
- 37** Brooks C, Wei Q, Feng L et al. Bak regulates mitochondrial morphology and pathology during apoptosis by interacting with mitofusins. *Proc Natl Acad Sci USA* 2007; **104**: 11649–54.
- 38** Karbowski M, Norris KL, Cleland MM et al. Role of Bax and Bak in mitochondrial morphogenesis. *Nature* 2006; **443**: 658–62.

Research Article

Colonic Oxidative and Mitochondrial Function in Parkinson's Disease and Idiopathic REM Sleep Behavior Disorder

C. Morén,¹ Í. González-Casacuberta,¹ J. Navarro-Otano,² D. Juárez-Flores,¹ D. Vilas,³
G. Garrabou,¹ J. C. Milisenda,¹ C. Pont-Sunyer,³ M. Catalán-García,¹ M. Guitart-Mampel,¹
E. Tobías,¹ F. Cardellach,¹ F. Valldeoriola,³ A. Iranzo,² and E. Tolosa³

¹Muscle Research and Mitochondrial Function Laboratory, Cellex-IDIBAPS, Faculty of Medicine and Health Sciences, University of Barcelona, Internal Medicine Department, Hospital Clínic of Barcelona, CIBERER U722, Barcelona, Spain

²Neurology Service, Hospital Clínic of Barcelona, IDIBAPS, CIBERNED, Barcelona, Spain

³Movement Disorder Unit, Neurology Service, Hospital Clínic of Barcelona, IDIBAPS, CIBERNED, Barcelona, Spain

Correspondence should be addressed to Í. González-Casacuberta; ingrid@clinic.ub.es

Received 10 January 2017; Revised 1 April 2017; Accepted 4 May 2017; Published 4 June 2017

Academic Editor: Eng King Tan

Copyright © 2017 C. Morén et al. This is an open access article distributed under the Creative Commons Attribution License, which permits unrestricted use, distribution, and reproduction in any medium, provided the original work is properly cited.

Objective. To determine potential mitochondrial and oxidative alterations in colon biopsies from idiopathic REM sleep behavior disorder (iRBD) and Parkinson's disease (PD) subjects. **Methods.** Colonic biopsies from 7 iRBD subjects, 9 subjects with clinically diagnosed PD, and 9 healthy controls were homogenized in 5% w/v mannitol. Citrate synthase (CS) and complex I (CI) were analyzed spectrophotometrically. Oxidative damage was assessed either by lipid peroxidation, through malondialdehyde and hydroxyalkenal content by spectrophotometry, or through antioxidant enzyme levels of superoxide dismutase-2 (SOD2), glutathione peroxidase-1 (Gpx1), and catalase (CAT) by western blot. The presence of mitochondrial DNA (mtDNA) deletions was assessed by long PCR and electrophoresis. **Results.** Nonsignificant trends to CI decrease in both iRBD (45.69 ± 18.15 ; 23% decrease) and PD patients (37.57 ± 12.41 ; 37% decrease) were found compared to controls (59.51 ± 12.52 , p : NS). Lipid peroxidation was maintained among groups (iRBD: 27.46 ± 3.04 , PD: 37.2 ± 3.92 , and controls: 31.71 ± 3.94 ; p : NS). Antioxidant enzymes SOD2 (iRBD: 2.30 ± 0.92 , PD: 1.48 ± 0.39 , and controls: 1.09 ± 0.318) and Gpx1 (iRBD 0.29 ± 0.12 , PD: 0.56 ± 0.33 , and controls: 0.38 ± 0.16) did not show significant differences between groups. CAT was only detected in 2 controls and 1 iRBD subject. One iRBD patient presented a single mtDNA deletion.

1. Introduction

The main pathological features of Parkinson's disease (PD) are the loss of nigral dopaminergic neurons of the central nervous system (CNS) and the presence of aggregates of abnormal α -synuclein, so-called Lewy bodies and Lewy neurites, in remaining neurons. Lewy type pathology also emerges in the peripheral autonomous nervous system (PANS) [1, 2] and is known to occur in early, prodromal stages. Abnormal aggregates of synuclein are not uncommon in the enteric neurons of PD patients and the evidence of a prion-like behavior of synuclein [3] has focused the attention on the assessment of the enteric nervous system in PD in line with the hypothesis that the gut is the initial site of synuclein aggregation [4–6]. Since abnormal aggregates of synuclein are

found in the enteric neurons in PD, a colonic biopsy could provide access to a unique tissue to study pathophysiological aspects of the disease [4–6].

Dysfunctions in mitochondrial metabolism, respiration, bioenergetics, and dynamics are suggested to play a significant role in the development of both idiopathic and genetic forms of PD [7–9]. Mitochondrial alterations related to this condition have been found in the CNS and also described in other tissues and structures such as fibroblasts [10], platelets [11], and skeletal muscle [12, 13].

Complex I (CI) dysfunction was the first depicted association between mitochondria and PD [14, 15]. Inhibition of CI can lead to the degeneration of neurons by a number of mechanisms [16]. Although the electron transport chain is a highly efficient system within mitochondria, electrons

can leak from the chain, especially from CI [17] of the mitochondrial respiratory chain (MRC), and react with oxygen to form reactive oxygen species (ROS). ROS production leads to oxidative damage and neuronal death in PD [18]. One of the principal mechanisms of ROS-derived cell damage includes the disruption of the cell membrane through lipid peroxidation. Furthermore, α -synuclein oligomers can promote lipid peroxidation and a decline of endogenous antioxidants [19]. Failure of the antioxidant enzyme machinery, such as superoxide dismutase (SOD), glutathione (GSH) peroxidase (Gpx), and catalase (CAT), could also be involved in PD, as deficiencies in such antioxidant enzymes have been directly related to this disorder [16]. Lastly, mitochondrial genetic alterations have also been described in PD [20], such as the presence of mitochondrial DNA (mtDNA) deletions, often related to ROS generation.

Although the main molecular features remaining at the core of PD etiopathogenesis are (i) mitochondrial alterations, (ii) oxidative damage, and (iii) the mishandling/degradation of proteins [21–23], only unfolded proteins have been assessed at PANS level [4–6] from subjects suffering from idiopathic REM sleep behavior disorder (iRBD), a parasomnia characterized by dream enactment behavior and atonia during REM sleep. iRBD patients are considered to suffer prodromal synucleinopathies since up to 80% of these patients develop a neurodegenerative disease, associated with Lewy body pathology [24–26].

The reported strong association of mitochondrial changes and PD led us to explore some mitochondrial and oxidative parameters in peripheral enteric tissue to potentially contribute to the study of the earliest mechanisms underlying neurodegeneration in PD. Studies on this type may provide evidence of peripheral mitochondrial dysfunction in the earliest stages of PD.

We hypothesized that mitochondrial and oxidative alterations could be present in colonic tissue from subjects with idiopathic iRBD and PD and, thus, in prodromal and clinically manifest PD patients. The aim of the study was to explore peripheral mitochondrial and oxidative function ideally as putative mitochondrial biomarkers for PD.

2. Materials and Methods

Patients were recruited from those visited at the Movement Disorders unit and the Sleep Unit of the Hospital Clínic of Barcelona. Demographic and clinical data were collected. Patients with PD and iRBD (the latter confirmed by polysomnography and lack of clinical signs of parkinsonism or cognitive dysfunction) were studied.

Control subjects with no evidence of neurologic disease or dream-enacting behaviors were prospectively and consecutively enrolled in this study. Colonic biopsies by colonoscopy were obtained. Control participants were recruited from the gastroenterology service and indications for colonoscopy included routine preventive cancer screening and follow-up of colonic adenomas, as well as workup for diarrhea. The protocol was approved by the hospital ethical committee on human experimentation before the study initiation

and written informed consent for research was obtained from all individuals participating in the study.

Nonmotor symptoms regarding gastrointestinal system were evaluated using the Non-Motor Symptoms Questionnaire (NMSQuest) items 19 to 21. Age at biopsy and disease duration (motor onset in PD patients and abnormal dream-enacting suggesting of iRBD in iRBD patients) were also documented.

Neurological evaluation of participants was carried out by means of the Movement Disorder Society-Unified Parkinson's Disease Rating Scale (MDS-UPDRS) parts I to III, the Montreal Cognitive Assessment to rule out cognitive impairment in iRBD and control subjects.

Colonic biopsies were performed in patients according to the standard procedure of the Gastroenterology Department of Hospital Clínic of Barcelona.

Standard colonoscopies and 3 to 5 biopsies were obtained from ascending, transverse, descending, and sigmoid colon using the standard biopsy forceps, as previously described [27]. Ascending and descending colonic explants were used for culture and sigmoid fragment was cryopreserved at -80°C for further analysis.

2.1. Sample Processing. Tissue explants were cut in approximately 4 pieces of 1 mm^2 and washed 3–5 times with sterilized 1x PBS supplemented with 10% penicillin, streptomycin, and fungizone (PSF). Homogenization of cryopreserved sigmoid colon biopsies was performed using 5% (w/v) mannitol buffer in potter glass at 850 rpm and further centrifuged at 650g during 20 minutes. Supernatant was kept and pellet was again resuspended in 5% (w/v) mannitol buffer, homogenized, and centrifuged at the same conditions. Supernatants from both centrifugations were mixed to obtain a mitochondrial-enriched suspension.

2.2. Experimental Assays. Total protein content was measured by bicinchoninic acid (BCA) kit assay quantification and run in microplates, by independent measurement of sample dilution duplicates. A set of internal standards were read in parallel together with a reference internal control sample.

For the quantification of the enzymatic assays [citrate synthase (CS) and CI] an internal reference pork muscle homogenate at 2 mg/ml was used. This is the gold standard material to confirm the validation of such spectrophotometric measurements, to better characterize the optimal velocity while maintaining linear kinetics relative to time and enzyme concentration.

Mitochondrial content was measured spectrophotometrically in cuvettes through CS enzymatic activity involved in the Krebs cycle, considered a reliable marker of the mitochondrial mass [28]. This assay was performed by means of the quantification of the product reaction 5,5'-dithiobis 2-nitrobenzoic acid at 412 nm and at 37°C .

The CI enzymatic activity of MRC was measured spectrophotometrically in cuvettes following the quantification of NADH substrate oxidation and using the specific inhibitor rotenone at 340 nm and at 37°C , as reported elsewhere [29].

Either protein content or CS or CI enzymatic assays were performed by standardized procedures following protocols

TABLE 1: Demographic and clinical data of the subjects included in the study.

	PD	iRBD	Control
Number of patients (M/F)	9 (7/2)	7 (6/1)	9 (4/5)
Age at biopsy (years, median, min-max)	65.18 (54.04–71.02)	72.44 (66.85–83.40)	64.79, (58.34–82.74)
Disease duration (years, median, min-max)	5.77 (0.76–13.81)	10.54 (1.64–22.25)	—
Hoehn and Yahr (median, min-max)	2 (1-2)	—	—
UPDRS I (median, min-max)	10 (1–19)	5 (1–17)	4 (0–9)
UPDRS II (median, min-max)	8 (2–14)	1 (0–8)	0 (0–3)
UPDRS III (median, min-max)	14 (5–34)	4 (1–27)	0 (0–4)
NMSQuest, gastrointestinal subdomain (median, min-max)	6 (0–16)	0 (0–9)	0.5 (0–12)

from the national Spanish Network CIBERER (unpublished protocols).

The oxidative damage was determined by the quantification of lipid peroxidation derived products: malondialdehyde and 4-hydroxyalkenals, using the assay kit OxisResearch LPO586 at 586 nm, following manufacturer instructions [30].

SOD2, Gpx1, and CAT antioxidant enzyme protein levels were assessed by western blot as follows. Sample DTT-reduced homogenates were loaded equally using SDS-PAGE (precast 12% gels, Novex; Thermo Fisher Scientific) and transferred by wet transfer onto PVDF membranes (Amersham Hybond, 0.45 μ M; GE Healthcare). Membranes were blocked using 5% powdered skim milk-PBS solution for 1 hour (RT) and then incubated with primary antibody in 1:1 blocking buffer: PBS 0.4% Tween 20 solution. SOD2 (SIGMA), CAT (AbCam), and Gpx1 (Cell Signalling) were used for immunostaining by 1-hour incubation (RT), followed by 1:2000 horseradish peroxidase- (HRP-) conjugated secondary antibodies (Biorad) for 1 hour in 1:1 blocking buffer (PBS 0.4% Tween 20 solution). Enhanced chemiluminescence (ECL) substrate (Thermo Fisher Scientific) was used to detect immunoreactive proteins on X-ray film further scanned to quantify band intensity.

MtDNA deletions were determined by long PCR using Long COX-F 5'-TTAGCAGGGAAGTACTCCCA-3' and Long H 5'-CGGATACAGTTCACCTTAGCTACCCCAAGTG-3' primers for 10.2 Kb amplicon. After amplification of mitochondrial genome, an electrophoresis was run in a 0.8% agarose gel with red safe.

Statistical analysis was performed using SPSS. Normality of the data was assessed by Kolmogorov-Smirnov test. Non-parametric *U* Mann-Whitney test for independent samples was used. Significance level was set at $p < 0.05$.

3. Results

Demographic and clinical data of the participants are summarized in Table 1. A total of 25 adult subjects were enrolled in the study including 9 PD (highest Hoehn-Yahr scale scoring of 2), 7 iRBD, and 9 healthy subjects. iRBD patients were older than PD ($p = 0.007$, Mann-Whitney *U*) whereas the difference was not significant when compared to control subjects ($p = 0.05$, Mann-Whitney *U*). As expected, UPDRS showed a more severe involvement in PD compared to iRBD

and control subjects. iRBD and control subjects with a score higher than 0 at motor evaluation (UPDRS III) were known to suffer from nonneurological movement impairment, mainly due to arthrosis. PD patients were more likely to suffer from gastrointestinal symptoms than iRBD ($p = 0.031$, Mann-Whitney *U*).

Cryopreserved homogenates were used for experimental procedures. The presence of neuronal axons was proved in the tissue explants by fluorescence confocal microscopy (Supplementary Material, Figure S1a, available online at <https://doi.org/10.1155/2017/9816095>).

Mitochondrial enzymatic activities, oxidative damage, determined by lipid peroxidation, and antioxidant levels and deletions in mitochondrial genome were measured in the cryopreserved sigmoid homogenates.

CS enzymatic activity showed equivalent mitochondrial mass in all the groups (data not shown).

No significant differential trends were observed in some of the parameters among groups. Interestingly, mitochondrial CI of MRC was slightly decreased in iRBD and PD patients compared to controls. This trend to decrease was more evident in clinically diagnosed PD patients (Figure 1(a)). Oxidative damage levels measured through lipid peroxidation by malondialdehyde and hydroxyalkenal content were slightly higher in PD but not in iRBD subjects, when compared to the controls (Figure 1(b)). The quantification of the mitochondrial parameters did not render statistically significant differences in any case.

No changes in antioxidant enzyme levels of SOD2 and Gpx1 were found between groups (Figures 2(b) and 2(c), resp.). Antioxidant enzyme CAT was only detectable in 2 controls and 1 iRBD patient. None of the PD patients showed CAT reactive staining.

MtDNA deletions were absent, although the presence of a unique mtDNA deletion in a iRBD subject was remarkable, as shown in Figure 3.

4. Discussion

Studies on the identification of surrogate in vivo peripheral prognostic markers for PD so far are relevant as they may allow minimally invasive diagnostic procedures and provide a window to early preclinical diagnosis and putative neuroprotective therapies during the prodromal phase of PD [31].

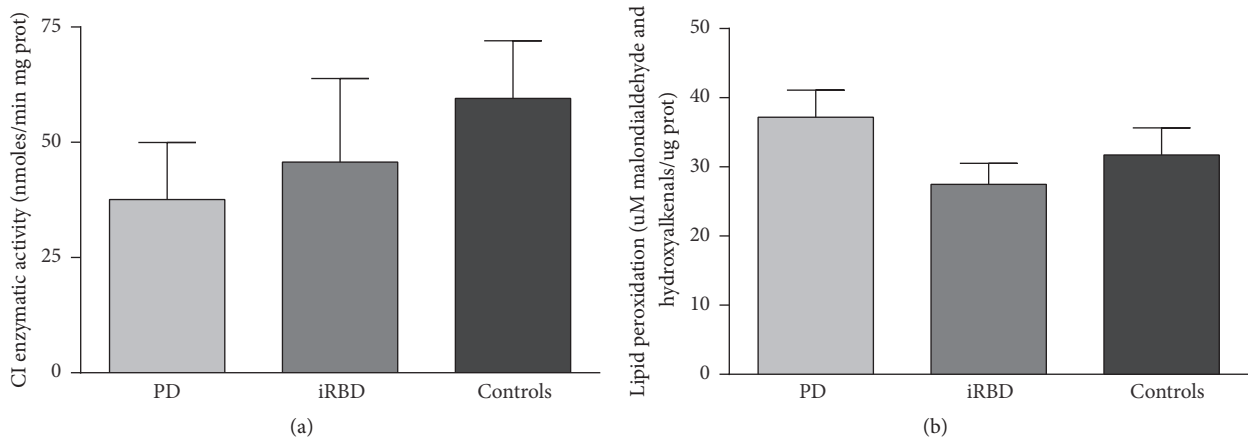


FIGURE 1: CI and lipid peroxidation assessment. (a) CI enzymatic activity of MRC. (b) Oxidative stress analysis through lipid peroxidation measured by malondialdehyde and hydroxyalkenal content. CI, complex I; MRC, mitochondrial respiratory chain; PD, Parkinson's disease; iRBD, idiopathic REM sleep behavior disorder.

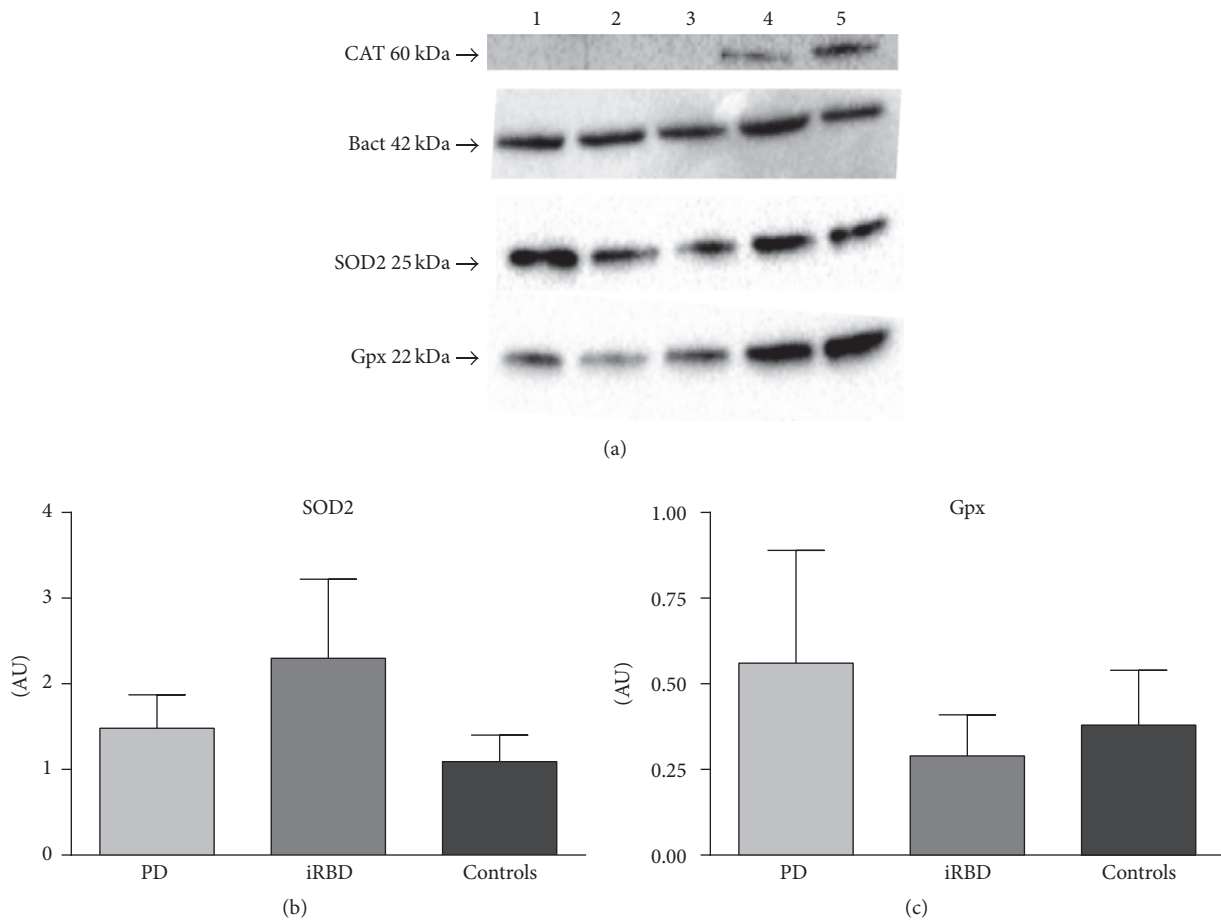


FIGURE 2: Antioxidant enzymes quantification through western analysis of controls ($n = 9$), iRBD ($n = 7$), and PD patients ($n = 9$). (a) Representative blots showing expression levels CAT, SOD2 and Gpx antioxidants, and β -actin loading control. Well ID is as follows: (1) control, (2) control, (3) iRBD, (4) iRBD, and (5) control. (b) Quantification of SOD2 levels. (c) Quantification of Gpx levels. AU, arbitrary units; SOD2, superoxide dismutase-2; Gpx, glutathione peroxidase; PD, Parkinson's disease; iRBD, idiopathic REM sleep behavior disorder.

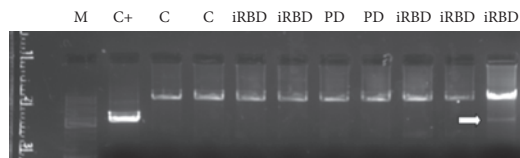


FIGURE 3: *MtDNA deletions*. 0.8%-agarose gel containing amplified mtDNA. White arrow shows a iRBD patient presenting a unique mtDNA deletion. C, controls; iRBD, idiopathic REM behavior disorder patients; PD, Parkinson's disease patients; C+, internal reference positive control; mtDNA, mitochondrial DNA.

Constipation is very common in the prodromal phase of PD and objective colonic dysfunction has been recently ascertained in PD patients [32]. At a molecular level, the presence of synuclein aggregates in colonic biopsies of PD subjects has been widely discussed as a main diagnostic factor for PD prior to the onset of clinical motor features, although providing controversial results [5, 33], and other differential factors, such as decreased intestinal acetylcholinesterase activity, have been reported in early PD [34]. Although growing attention has been focused on the search for predictive prognostic biomarkers of the disease in the enteric nervous system, no gold standard consensus has been achieved, and mitochondrial and oxidative markers in colonic samples from iRBD and PD patients have not yet been explored.

Despite the wide amount of data on mitochondrial dysfunction associated with PD, our study, reported here, in colonic biopsies of prodromal and clinically diagnosed PD patients did not detect conclusive mitochondrial alterations.

In the colonic tissue of our study subjects mitochondrial mass, estimated by CS enzymatic activity, remained similar in all the groups, suggesting that no relevant changes in mitochondrial biogenesis of the samples occur.

Although CI MRC did not present any significant changes among groups, a trend of decrease of this activity was observable in both prodromal and clinically diagnosed PD groups with respect to controls. These CI enzymatic activity levels were slightly lower in patients with manifest PD. On the other hand, oxidative damage measured by lipid peroxidation tended to not significantly increase in enteric tissue from patients but not in iRBD subjects compared to controls. These tendencies may suggest that decrease of CI enzymatic activity could occur prior to oxidative damage in PD. It is widely known that a MRC dysfunction, especially at CI level, may lead to oxidative damage due to electron leaks in the MRC and the consequent formation of ROS that promotes oxidative stress. In the present study the slight trends in CI enzymatic activity changes are observed in both iRBD and PD patients, suggesting that oxidative damage changes over time could be secondary to CI dysfunction. It is of note that previous studies in PD have pointed out to the presence of oxidative damage in the colonic submucosa either in physiological and pathological conditions [35].

Antioxidant enzyme protein levels did not show significant changes between mitochondrial SOD2 and Gpx1 enzymatic levels between groups and CAT levels were not detectable in most cases, leaving an opened question about

whether this was due to an art factual issue or due to a potential relevant molecular meaning relating on such differential data. Although our findings point out to a lack of an association between endogenous antioxidant changes in PD peripheral tissue, a recent study has described specific plasmatic changes in antioxidant levels and lipid peroxidation as potential promising PD biomarkers [36].

MtDNA deletions have been found in the *substantia nigra* of PD patients or in in vitro models of PD, but they have not been detected in other areas of the brain and it is uncommon to find mtDNA deletions in peripheral tissues. Given the use of colonic biopsies in the present study, it is not surprising that most of the patients did not show any mtDNA deletion and, indeed, the presence of a unique mtDNA deletion of a iRBD subject is remarkable.

In the present study, which included part of the cohort of a previous work [27], only one patient with positively phosphorylated synuclein aggregates in submucosal neurites was included. As discussed by Sprenger et al., the low percentage of positive cases could be related to the site of biopsy (as a rostrocaudal gradient of pathology in the gastrointestinal tract has been suggested by some authors), the possible centripetal distribution of α -synuclein pathology (from the peripheral axon to the central neuronal soma), and the depth of the biopsy, which is critical for an appropriate assessment of submucosal autonomic plexus. Unfortunately, due to these possible limitations, any adequate correlation analysis between mitochondrial function and abnormal α -synuclein aggregation could be assessed.

In summary, our findings in enteric samples do not demonstrate clear mitochondrial abnormalities in colon biopsies of iRBD or established PD patients. Such lack of mitochondrial dysfunction could be due to the type of tissue studied. Cryopreserved homogenates from colonic biopsies were used in the experimental procedures. In preliminary studies, only a few cells could be cultured and could have undergone cell death before reaching optimal confluence. Other authors were successful in obtaining neuronal cultures from the enteric system by using the entire myenteric plexus, in human fetal tissue [37] or in mouse in vitro models [38, 39]. In the present study, the amount, type, or location of the biopsies (small, with heterogeneous cell types, and superficial) could have hampered either the cell growth in the culture of enteric neurons or the detection of significant mitochondrial disturbances between groups.

Our gastrointestinal biopsies contain epithelial cells, enteric glial cells, and enteric neurons. It is important to note that, aside from neurons, the enteric glial cells and epithelial cells, which are present in a gastrointestinal biopsy, are also dysregulated in PD [40]. We have proven the presence of enteric neuronal axons in our samples. According to the longitudinal location of the biopsies, despite less prevalence of Lewy pathology in the lower compared to the upper gut, the sigmoid colon and rectum have been by far the most commonly studied sites [41]. In this study, the mitochondrial parameters were assessed from the sigmoid section of the biologic material. According to these data, global mitochondrial findings herein depicted might be considered representative of expected alterations at PANS level in the context of PD.

Despite the negative results obtained, the trends observed towards suboptimal CI enzymatic activity in both groups of patients (iRBD and PD) point to the necessity of further research in mitochondrial studies in PANS. Such studies should address the role of mitochondrial disturbances as potential PD in vivo biomarkers in different sites and depths of enteric PD biopsies in larger cohorts of patients.

Disclosure

Both C. Morén and Í. González-Casacuberta should be considered as main authors.

Conflicts of Interest

The authors declare that there are no conflicts of interest.

Acknowledgments

This work was supported by Fundació Privada Cellex, Fondo de Investigación Sanitaria [Grants nos. PI00462/11, PI13/01455, PI13/01738, PI15/00903, and PI15/00817], integrated in the Plan Estatal I+D+I and cofunded by ISCIII-Subdirección General de Evaluación and European Regional Development Fund (ERDF); Suports a Grups de Recerca de la Generalitat de Catalunya 2014–2016 [Grant no. SGR 2014/376]; InterCiber PIE1400061 and CIBER de Enfermedades Raras (CIBERER, an initiative of ISCIII). C. Morén was granted by a José Castillejo (CAS15/00140) postdoctoral grant from Spanish Ministry (Ministerio de Educación, Cultura y Deporte).

References

- [1] H. Braak, R. A. I. de Vos, J. Bohl, and K. Del Tredici, "Gastric α -synuclein immunoreactive inclusions in Meissner's and Auerbach's plexuses in cases staged for Parkinson's disease-related brain pathology," *Neuroscience Letters*, vol. 396, no. 1, pp. 67–72, 2006.
- [2] H. Braak, K. Del Tredici, U. Rüb, R. A. I. de Vos, E. N. H. Jansen Steur, and E. Braak, "Staging of brain pathology related to sporadic Parkinson's disease," *Neurobiology of Aging*, vol. 24, no. 2, pp. 197–211, 2003.
- [3] N. P. Visanji, P. L. Brooks, L. N. Hazrati, and A. E. Lang, "The prion hypothesis in Parkinson's disease: braak to the future," *Acta Neuropathologica Communications*, vol. 1, no. 1, p. 2, 2013.
- [4] S. Mrabet, N. B. Ali, A. Achouri et al., "Gastrointestinal dysfunction and neuropathologic correlations in Parkinson disease," *Journal of Clinical Gastroenterology*, vol. 50, no. 9, pp. e85–e90, 2016.
- [5] A. G. Corbillé, F. Letournel, J. H. Kordower et al., "Evaluation of alpha-synuclein immunohistochemical methods for the detection of Lewy-type synucleinopathy in gastrointestinal biopsies," *Acta Neuropathologica Communications*, vol. 4, p. 35, 2016.
- [6] M. G. Stokholm, E. H. Danielsen, S. J. Hamilton-Dutoit, and P. Borghammer, "Pathological α -synuclein in gastrointestinal tissues from prodromal Parkinson disease patients," *Annals of Neurology*, vol. 79, no. 6, pp. 940–949, 2016.
- [7] P. C. Keane, M. Kurzawa, P. G. Blain, and C. M. Morris, "Mitochondrial dysfunction in Parkinson's disease," *Parkinson's Disease*, vol. 2011, Article ID 716871, 18 pages, 2011.
- [8] A. Grünewald, K. A. Rygiel, P. D. Hepplewhite, C. M. Morris, M. Picard, and D. M. Turnbull, "Mitochondrial DNA Depletion in Respiratory Chain-Deficient Parkinson Disease Neurons," *Annals of Neurology*, vol. 79, no. 3, pp. 366–378, 2016.
- [9] D. Trudler, Y. Nash, and D. Frenkel, "New insights on Parkinson's disease genes: the link between mitochondria impairment and neuroinflammation," *Journal of Neural Transmission*, vol. 122, no. 10, pp. 1409–1419, 2015.
- [10] H. Mortiboys, R. Furnston, G. Bronstad, J. Aasly, C. Elliott, and O. Bandmann, "UDCA exerts beneficial effect on mitochondrial dysfunction in LRRK2 G2019S carriers and in vivo," *Neurology*, vol. 85, no. 10, pp. 846–852, 2015.
- [11] R. H. Haas, F. Nasirian, K. Nakano et al., "Low platelet mitochondrial complex I and complex II/III activity in early untreated Parkinson's disease," *Annals of Neurology*, vol. 37, no. 6, pp. 714–722, 1995.
- [12] L. A. Bindoff, M. A. Birch-Machin, N. E. F. Cartlidge, W. D. Parker Jr., and D. M. Turnbull, "Respiratory chain abnormalities in skeletal muscle from patients with Parkinson's disease," *Journal of the Neurological Sciences*, vol. 104, no. 2, pp. 203–208, 1991.
- [13] F. Cardellach, M. J. Marti, J. Fernandez-Sola et al., "Mitochondrial respiratory chain activity in skeletal muscle from patients with Parkinson's disease," *Neurology*, vol. 43, no. 11, pp. 2258–2262, 1993.
- [14] Y. Mizuno, S. Ohta, M. Tanaka et al., "Deficiencies in complex I subunits of the respiratory chain in Parkinson's disease," *Biochemical and Biophysical Research Communications*, vol. 163, no. 3, pp. 1450–1455, 1989.
- [15] A. H. Schapira, J. M. Cooper, D. Dexter, J. B. Clark, P. Jenner, and C. D. Marsden, "Mitochondrial complex I deficiency in Parkinson's disease," *Journal of Neurochemistry*, vol. 54, no. 3, pp. 823–827, 1990.
- [16] T. B. Sherer, R. Betarbet, and J. T. Greenamyre, "Environment, mitochondria, and Parkinson's disease," *Neuroscientist*, vol. 8, no. 3, pp. 192–197, 2002.
- [17] K. Takeshige and S. Minakami, "NADH- and NADPH-dependent formation of superoxide anions by bovine heart submitochondrial particles and NADH-ubiquinone reductase preparation," *Biochemical Journal*, vol. 180, no. 1, pp. 129–135, 1979.
- [18] A. H. V. Schapira, V. M. Mann, J. M. Cooper et al., "Anatomic and disease specificity of NADH CoQ1 reductase (complex I) deficiency in Parkinson's disease," *Journal of Neurochemistry*, vol. 55, no. 6, pp. 2142–2145, 1990.
- [19] E. Deas, N. Cremades, P. R. Angelova et al., "Alpha-synuclein oligomers interact with metal ions to induce oxidative stress and neuronal death in Parkinson's disease," *Antioxidants & Redox Signaling*, vol. 24, no. 7, pp. 376–391, 2016.
- [20] S. K. Müller, A. Bender, C. Laub et al., "Lewy body pathology is associated with mitochondrial DNA damage in Parkinson's disease," *Neurobiology of Aging*, vol. 34, no. 9, pp. 2231–2233, 2013.
- [21] A. H. V. Schapira and E. Tolosa, "Molecular and clinical prodrome of Parkinson disease: implications for treatment," *Nature Reviews Neurology*, vol. 6, no. 6, pp. 309–317, 2010.
- [22] A. M. Cuervo, E. S. P. Wong, and M. Martinez-Vicente, "Protein degradation, aggregation, and misfolding," *Movement Disorders*, vol. 25, supplement 1, pp. S49–S54, 2010.
- [23] A. P. Gatt, O. F. Duncan, J. Attems, P. T. Francis, C. G. Ballard, and J. M. Bateman, "Dementia in Parkinson's disease is associated with enhanced mitochondrial complex I deficiency," *Movement Disorders*, vol. 31, no. 3, pp. 352–359, 2016.

- [24] R. B. Postuma, J.-F. Gagnon, and J. Y. Montplaisir, "REM sleep behavior disorder: from dreams to neurodegeneration," *Neurobiology of Disease*, vol. 46, no. 3, pp. 553–558, 2012.
- [25] A. Iranzo, "Sleep-wake changes in the premotor stage of Parkinson disease," *Journal of the Neurological Sciences*, vol. 310, no. 1-2, pp. 283–285, 2011.
- [26] A. Iranzo, "Parkinson disease and sleep: sleep-wake changes in the premotor stage of Parkinson disease; impaired olfaction and other prodromal features," *Current Neurology and Neuroscience Reports*, vol. 13, no. 9, article 373, 2013.
- [27] F. S. Sprenger, N. Stefanova, E. Gelpi et al., "Enteric nervous system α -synuclein immunoreactivity in idiopathic REM sleep behavior disorder," *Neurology*, vol. 85, no. 20, pp. 1761–1768, 2015.
- [28] A. Barrientos, "In vivo and in organello assessment of OXPHOS activities," *Methods*, vol. 26, no. 4, pp. 307–316, 2002.
- [29] F. Medja, S. Allouche, P. Frachon et al., "Development and implementation of standardized respiratory chain spectrophotometric assays for clinical diagnosis," *Mitochondrion*, vol. 9, no. 5, pp. 331–339, 2009.
- [30] H. Esterbauer, R. J. Schaur, and H. Zollner, "Chemistry and biochemistry of 4-hydroxynonenal, malonaldehyde and related aldehydes," *Free Radical Biology and Medicine*, vol. 11, no. 1, pp. 81–128, 1991.
- [31] S. A. Schneider, M. Boettner, A. Alexoudi, D. Zorenkov, G. Deuschl, and T. Wedel, "Can we use peripheral tissue biopsies to diagnose Parkinson's disease? A review of the literature," *European Journal of Neurology*, vol. 23, no. 2, pp. 247–261, 2016.
- [32] K. Knudsen, T. D. Fedorova, A. C. Bekker et al., "Objective colonic dysfunction is far more prevalent than subjective constipation in Parkinson's disease: a colon transit and volume study," *Journal of Parkinson's Disease*, vol. 7, no. 2, pp. 359–367, 2017.
- [33] L. Antunes, S. Frاسquilho, M. Ostaszewski et al., "Similar α -Synuclein staining in the colon mucosa in patients with Parkinson's disease and controls," *Movement Disorders*, vol. 31, no. 10, pp. 1567–1570, 2016.
- [34] T. D. Fedorova, L. B. Seidelin, K. Knudsen et al., "Decreased intestinal acetylcholinesterase in early Parkinson disease," *Neurology*, vol. 88, no. 8, pp. 775–781, 2017.
- [35] K. M. Shannon, A. Keshavarzian, E. Mutlu et al., "Alpha-synuclein in colonic submucosa in early untreated Parkinson's disease," *Movement Disorders*, vol. 27, no. 6, pp. 709–715, 2012.
- [36] C. C. de Farias, M. Maes, K. L. Bonifácio et al., "Highly specific changes in antioxidant levels and lipid peroxidation in Parkinson's disease and its progression: disease and staging biomarkers and new drug targets," *Neuroscience Letters*, vol. 617, pp. 66–71, 2016.
- [37] N. Braidy, W.-P. Gai, Y. H. Xu et al., "Alpha-synuclein transmission and mitochondrial toxicity in primary human foetal enteric neurons in vitro," *Neurotoxicity Research*, vol. 25, no. 2, pp. 170–182, 2014.
- [38] F. Pan-Montojo, O. Nischtchik, Y. Dening et al., "Progression of Parkinson's disease pathology is reproduced by intragastric administration of rotenone in mice," *PLoS ONE*, vol. 5, no. 1, Article ID e8762, 2010.
- [39] F. Pan-Montojo, M. Schwarz, C. Winkler et al., "Environmental toxins trigger PD-like progression via increased alpha-synuclein release from enteric neurons in mice," *Scientific Reports*, vol. 2, article 898, 2012.
- [40] A. G. Corbillé, T. Clairembault, E. Coron et al., "What a gastrointestinal biopsy can tell us about Parkinson's disease?" *Neurogastroenterology & Motility*, vol. 28, no. 7, pp. 966–974, 2016.
- [41] J. B. Furness, "The enteric nervous system: normal functions and enteric neuropathies," *Neurogastroenterology and Motility*, vol. 20, supplement 1, pp. 32–38, 2008.

HIV-1 promonocytic and lymphoid cell lines: an *in vitro* model of *in vivo* mitochondrial and apoptotic lesion

Constanza Morén^{a, b, *}, Ingrid González-Casacuberta^{a, b}, Carmen Álvarez-Fernández^c,
Maria Baño^{a, b}, Marc Catalán-García^{a, b}, Mariona Guitart-Mampel^{a, b}, Diana Luz Juárez-Flores^{a, b},
Ester Tobías^{a, b}, José Milisenda^{a, b}, Francesc Cardellach^{a, b}, Josep Maria Gatell^c,
Sonsoles Sánchez-Palomino^c, Glòria Garrabou^{a, b}

^a Muscle Research and Mitochondrial Function Laboratory, Cellex-IDIBAPS, Faculty of Medicine-University of Barcelona, Internal Medicine Department-Hospital Clínic of Barcelona (HCB), Barcelona, Spain

^b Centro de Investigación Biomédica en Red (CIBER) de Enfermedades Raras (CIBERER), Madrid, Spain

^c Cellex-IDIBAPS, Faculty of Medicine-University of Barcelona, Infectious Diseases Unit-Hospital Clínic of Barcelona (HCB), Barcelona, Spain

Received: February 3, 2016; Accepted: July 21, 2016

Abstract

To characterize mitochondrial/apoptotic parameters in chronically human immunodeficiency virus (HIV-1)-infected promonocytic and lymphoid cells which could be further used as therapeutic targets to test pro-mitochondrial or anti-apoptotic strategies as *in vitro* cell platforms to deal with HIV-infection. Mitochondrial/apoptotic parameters of U1 promonocytic and ACH2 lymphoid cell lines were compared to those of their uninfected U937 and CEM counterparts. Mitochondrial DNA (mtDNA) was quantified by rt-PCR while mitochondrial complex IV (CIV) function was measured by spectrophotometry. Mitochondrial-nuclear encoded subunits II–IV of cytochrome-c-oxidase (COXII-COXIV), respectively, as well as mitochondrial apoptotic events [voltage-dependent-anion-channel-1 (VDAC-1)-content and caspase-9 levels] were quantified by western blot, with mitochondrial mass being assessed by spectrophotometry (citrate synthase) and flow cytometry (mitotracker green assay). Mitochondrial membrane potential (JC1-assay) and advanced apoptotic/necrotic events (AnexinV/propidium iodide) were measured by flow cytometry. Significant mtDNA depletion spanning 57.67% ($P < 0.01$) was found in the U1 promonocytic cells further reflected by a significant 77.43% decrease of mitochondrial CIV activity ($P < 0.01$). These changes were not significant for the ACH2 lymphoid cell line. COXII and COXIV subunits as well as VDAC-1 and caspase-9 content were sharply decreased in both chronic HIV-1-infected promonocytic and lymphoid cell lines (<0.005 in most cases). In addition, U1 and ACH2 cells showed a trend (moderate in case of ACH2), albeit not significant, to lower levels of depolarized mitochondrial membranes. The present *in vitro* lymphoid and especially promonocytic HIV model show marked mitochondrial lesion but apoptotic resistance phenotype that has been only partially demonstrated in patients. This model may provide a platform for the characterization of HIV-chronicity, to test novel therapeutic options or to study HIV reservoirs.

Keywords: apoptosis • cell models • HIV-infection • HIV progression • *in vitro* modelling • mitochondria

Introduction

Data regarding the potential role of mitochondria in the cytopathogenicity of human immunodeficiency virus (HIV) have led to great interest in the study of the relationships between these two entities [1]. Mitochondria have been closely linked to HIV infection, as a target of the deleterious effects of both HIV [2] and antiretroviral therapy (ART) [3] in relation to their involvement in the development of

apoptosis. Mitochondrial and apoptotic alterations have been widely described in both naïve and treated patients *in vivo* [4, 5].

Human immunodeficiency virus has tropism for hematopoietic cells [6]. This lentivirus is able to infect either lymphocytes or monocytes and macrophages, but the latter cells do not seem to undergo apoptosis following infection and represent a potential viral reservoir [7]. Mitochondrial and apoptotic lesions in both lymphocytes and monocytes have been associated with accelerated HIV progression in naïve patients [8, 9] and in peripheral tissues from treated patients as a result of secondary effects of medication [10]. A positive correlation

*Correspondence to: Constanza MORÉN.
E-mail: cmoren1@clinic.ub.es

has been described between apoptosis in peripheral blood lymphocytes and monocytes and the severity of HIV infection [11].

Whether mitochondrial and apoptotic malfunctions are causal factors rather than a consequence of differential HIV progression patterns remains to be elucidated. It is still unknown whether adequate mitochondrial function contributes to preventing mitochondrial-driven apoptosis of the defence cells, increasing the organism defences against a specific viral antigen. It would be conceivable that correct mitochondrial function protects defence cells to undergo apoptosis, which, in turn, would slow down the infective capacity of HIV progression.

The interaction between mitochondria, apoptosis and HIV has been well-described in HIV-infected patients [12, 13] and several groups including ours, have assessed the association between mitochondrial and apoptosis alterations and the severity of HIV infection [8, 9, 14]. Nevertheless, there is very little information on adequate mitochondrial characterization of *in vitro* models of HIV infection. Different animal models such as primate models have been used to further explore the disease and/or its treatment [15]. However, high ratios of cost/effectiveness requiring complex facilities have been associated with these models. Cell models could contribute to solve these disadvantages. In this study, we used two different types of cell models which represent the main target cells for HIV (monocytes and lymphocytes). Human immunodeficiency virus-1-infected U1 and ACH2 cell lines are, respectively, promonocytic and lymphoid cell lines derived from uninfected U937 (same U1 cell line but uninfected) and CEM (same ACH2 cell line, but uninfected) precursor cells. U1 and ACH2 lines are characterized by harbouring one and two stable integrated copies of the HIV-1 genome which replicates at a low rate, comparable to slow progression of the infection in patients. In these cell lines, HIV-1 latently auto-replicates itself, constituting a worldwide model to study chronic HIV infection [16, 17]. One previous study has shown apoptotic resistance involving modulation of the apoptotic mitochondrial pathway in persistently infected HIV-1 cells [18], however, accurate characterization of mitochondrial mechanisms and mitochondrial-derived apoptosis has yet to be performed in these models of chronically infected cells.

The hypothesis of this study was that the mitochondrial and apoptotic damage initiated by HIV infection may contribute to the persistence of infection chronicity and progression. As a proof-of-concept, we expected mitochondrial genetics, function, expression and apoptotic levels to be altered in both chronically HIV-1-infected promonocytic and lymphoid cell lines. These parameters were initially determined in the chronically HIV-1-infected promonocytic and lymphoid cell lines U1 and ACH2, being U937 and CEM non-HIV-infected cells used as *in vitro* cellular controls respectively. Mitochondrial and apoptotic involvement in the progression of HIV infection could lead to the use of putative mitochondrial or apoptotic therapeutic strategies to deal with the chronicity of HIV patients.

In depth characterization of the mitochondrial and apoptotic pathways in these cell models may lead to elucidate whether these *in vitro* models resemble *in vivo* alterations observed in patients, providing a platform to test potential targets (such as mitochondrial or apoptotic therapeutic targets) to fight HIV infection.

Materials and methods

Cell lines

Chronically infected HIV-1 promonocytic (U1) and lymphoid (ACH2) are cloned cell lines derived by limiting dilution cloning of U937 or CEM cells surviving an acute infection with HIV-1 (LAV-1 strain) first generated by Folks *et al.* [19, 20].

U1 and ACH2 cell lines, as well as their non-HIV-infected counterparts U937 and CEM, respectively, were cultured at 37°C in a fully humidified atmosphere with 5% CO₂ in RPMI-1640 medium (BioWhittaker, LONZA Portsmouth, NH, USA) supplemented with 10% foetal calf serum, and 1% penicillin-streptomycin, by trained personnel in P3 facility cores devoted to viral replication.

Mitochondrial and apoptotic parameters and experimental setups were simultaneously evaluated in these HIV-1-infected cell lines and their corresponding uninfected controls, and were run in parallel with both infected and control cell lines. Cell cultures were grown into 12 experiments (including four lines in parallel). Experimental measurements were run, at least, in triplicates.

Mitochondrial DNA depletion through multiplex real time PCR

A mitochondrial DNA (mtDNA) depletion study was performed as described. Total DNA was phenol-chloroform-extracted, spectrophotometrically quantified and diluted at 5 ng/μl. Multiplex real-time PCR (PCR Applied Biosystems (Foster City, CA, USA) 7500 Real Time PCR System) was performed with 96 round bottom well plates with the simultaneous determination of the mitochondrial 12S ribosomal RNA (mt12SrRNA) gene and the constitutive nuclear RNaseP gene (nRNaseP). The former used mtF805 (5'-CCACGGGAAACAGCAGTGAT-3') and mtR927 (5'-CTATTGACTTGGGTTAATCGTGTGA-3') with the TaqMan Probe 6FAM-5'-TGCCAGCCACCGCG-3'-MGB (Sigma-Aldrich, St. Louis, MO, USA). The latter used a commercial kit (4304437; Applied Biosystems). Each well included 25 ng of total genomic DNA diluted in 20 μl total reaction mixture containing: 1× TaqMan Universal PCR Master Mix (ABI P/N 4304437), 1 μl RNaseP commercial kit and 125 nM of each mtDNA primer and 125 nM of mtDNA probe.

The PCR was set at 2 min. at 50°C, 10 min. at 95°C, followed by 40 cycles each of 15 sec. of denaturalization at 95°C and 60 sec. of annealing/extension at 60°C. The mt12SrRNA gene was normalized by determining the nRNaseP nuclear gene and expressed as mt12SrRNA/nRNaseP ratio.

Mitochondrial function by enzymatic activities

Complex IV (CIV) enzymatic activity was measured as an experimental parameter [21] representative of mitochondrial function. The enzymatic activity of CIV was measured following national standardization rules of the Spanish network for the study of mitochondrial respiratory chain (MRC) enzyme activities. This enzymatic assay was spectrophotometrically measured at 37°C at a wavelength of 550 nm including an internal control of pig muscle sample with known reference values and expressed as nmols/min.mg protein.

Protein subunits content and mitochondrial apoptotic events by western blot

Mitochondrial and nuclear DNA encoded subunits (COXII and COXIV, respectively) of CIV, in addition to voltage-dependent anion channel-1 (VDAC-1) and caspase-9 content were analysed by western blot. In brief, 20–30 µg crude cell lysates were mixed 1:5 with a solution containing 50% glycerol, 10% SDS, 10% β-mercapto-ethanol, 0.5% bromophenol blue and 0.5 M Tris (pH 6.8), incubated at 99°C for 5 min. for protein denaturalization and electrophoresed on 0.1% SDS ranging from 7% to 13% of polyacrylamide gels. Proteins were transferred onto nitrocellulose membranes for 7 min. using an automatic system. Blots were probed with (i) a monoclonal antibody (moAb) recognizing the mtDNA-encoded human COXII subunit as a marker of the mitochondrial protein synthesis rate (A6404; Molecular Probes, Eugene, OR, USA), (ii) a moAb elicited against the nuclear DNA encoded human COXIV subunit as a marker of the nuclear protein synthesis rate (A21347; Molecular Probes) and (iii) an anti-β-actin moAb (A5441; Sigma-Aldrich) as a loading control of overall cell protein content. The protein subunits content was normalized by the content of β-actin signal to establish the relative abundance per overall cell protein. Antimouse and anti-rabbit secondary antibodies were used depending on the primary antibody [22]. Mitochondrial and nuclear protein synthesis ratios were expressed, respectively, as COXII/β-actin and COXIV/β-actin.

Apoptosis approaches were measured by western blot (as aforementioned) using the moAb raised against VDAC-1 (529536, antiporin 31HL; Calbiochem, Darmstadt, Alemania) as a marker of early apoptotic mitochondrial events and moAB against caspase-9 (ab2324; Abcam, Cambridge, UK) as marker of advanced apoptotic mitochondrial events, normalized by β-actin content and expressed as the VDAC-1/β-actin and caspase-9/β-actin ratios.

Mitochondrial content quantified by citrate synthase enzymatic activity

Citrate synthase (CS) enzymatic activity was measured as a reliable marker of mitochondrial content [21]. Enzymatic activity was spectrophotometrically measured following national standardization rules of the Spanish network for the study of MRC enzyme activities. This enzymatic assay was performed at 37°C including an internal control of pig muscle sample with known reference values and assessed at a wavelength of 412 nm and expressed as nmols/min.mg of protein.

Mitochondrial content, mitochondrial depolarization and advanced apoptosis/necrosis by flow cytometry

Mitochondrial content was determined by mitotracker green (MTG), and mitochondrial membrane potential (MMP) was estimated by JC-1 staining as reported elsewhere [23, 24] in cell lines either in the presence or absence of the mitochondrial pro-apoptotic and depolarizing stimuli valinomycin. Advanced apoptosis and necrosis phenomena were assessed using the annexin V and propidium iodide (PI) ratio by means of flow cytometric analysis. Briefly, a total of 1 ml of complete culture media containing roughly 2×10^5 cells was prepared for different reaction

procedures and subjected to incubation: (i) in the absence of any dye used for the autofluorescence calculation, (ii) with 200 nM MTG fluorophore (M-7514; Molecular Probes) for 30 min. for mitochondrial content quantification, (iii) with 0.02% JC1 dye (T-3168; Molecular Probes) for 10 min. for MMP assessment, (iv) with 0.02% JC1 fluorophore plus 0.05% valinomycin pro-apoptotic and depolarizing stimuli reagent (60403; Sigma-Aldrich) for 10 min. and (v) with 0.05% annexin V plus PI (556463; BD Biosciences, East Rutherford, NJ, USA) for 10 min. to assess advanced apoptotic and necrotic events. All cytometric analyses were performed in a FACScalibur cytometer with an argon ion laser tuned at 488 nm and a diode laser tuned at 635 nm (Becton Dickinson, San José, CA, USA). Results were expressed as median or percentage of cells with specific fluorescence.

Statistics

Results were expressed as mean ± S.E.M. Descriptive statistics were performed using the Statistical Package for the Social Sciences (SPSS) software (IBM inc. SPSS Statistics Chicago, IL, USA). A single filter was applied to discard extreme values. Statistical analysis was performed with non-parametric Kruskal–Wallis H and Mann–Whitney *U*-tests, and the level of significance was considered at $P < 0.05$ (for a confidence interval of $\alpha = 95\%$).

Results

Mitochondrial DNA content showed a significant decrease in the promonocytic latently infected HIV-1 cell line U1 compared to its respective uninfected U937 control cell line (204.64 ± 28.07 versus 483.34 ± 97.61 ; $P < 0.01$). However, the lymphoid latently infected HIV-1 cell line ACH2 showed non-significant variations of mtDNA content compared to the uninfected CEM control cells (227.32 ± 42.99 versus 162.59 ± 22.35 , $P = \text{NS}$; Fig. 1).

Mitochondrial CIV enzymatic activity was then quantified. In agreement with the above results, CIV enzymatic activity significantly decreased in infected promonocytic U1 cells with respect to uninfected U937 control cells (10.57 ± 2.46 versus 46.84 ± 7.30 , $P < 0.01$). On the other hand, this value remained non-significantly altered, although showing a trend to decrease in the infected ACH2 lymphoid cell line compared to uninfected CEM control cells (17.86 ± 6.12 versus 24.16 ± 3.45 , $P = \text{NS}$; Fig. 2).

Thereafter, the content of mitochondrial protein subunits was assessed by the expression of both the mtDNA-encoded COXII (Fig. 3A) and the nuclear encoded COXIV (Fig. 3B), components of the MRC CIV. The expression of these two subunits was reduced in both chronically HIV-1-infected cell lines studied compared to their respective uninfected control cell lines (U1 versus U937 and ACH2 versus CEM, $P < 0.001$ in all cases).

Moreover, early and advanced apoptotic mitochondrial events estimated as VDAC-1 and caspase-9 content, respectively, were significantly reduced in infected U1 and ACH2 infected cell lines versus their respective uninfected counterparts (U937 and CEM, respectively, $P < 0.05$ in all cases, except for caspase-9 in lymphoid cell lines: $P = 0.079$; Fig. 4A and B).

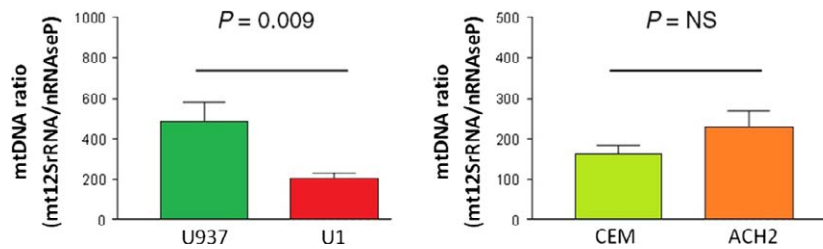


Fig. 1 mtDNA content. This figure shows the mtDNA *versus* nuclear DNA ratio (expressed in arbitrary units) in the infected promonocytic U1 cell line with respect to its uninfected U937 control (left), $P < 0.01$, as well as in the HIV-1-infected lymphoid ACH2 cell line with respect to its CEM control (right), $P = NS$. MtDNA: mitochondrial DNA, Mt12SrRNA: mitochondrial 12SrRNA ribosomal gene, nRNaseP: nuclear RNaseP gene, NS: not significant.

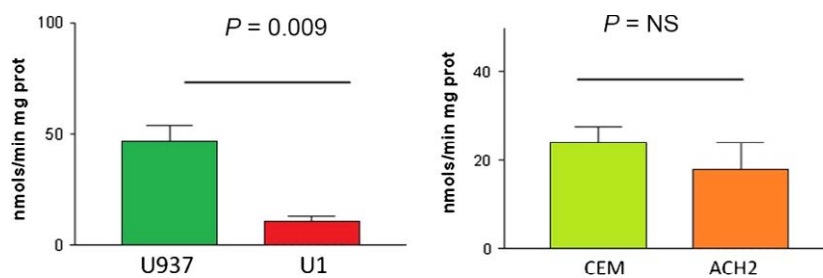


Fig. 2 CIV enzymatic activity. This figure shows the enzymatic activity of complex IV of the mitochondrial respiratory chain of promonocytic (left) and lymphoid (right) cell lines expressed in nmols/min mg protein. A significant decrease in complex IV activity was observed in the infected promonocytic cell line U1 with respect to its uninfected U937 control, $P < 0.01$. NS: not significant.

The mitochondrial content did not show any statistically significant differences, quantified by either CS activity (Fig. 5) or by the MTG assay (data not shown).

Finally, the comparisons with mitochondrial membrane depolarization in addition to advanced apoptosis and the necrosis markers assessed by flow cytometry did not reach statistical significance, although some parameters showed a bias. Thereby, the U1 promonocytic infected cell line showed a trend to lower levels of depolarized mitochondria than their uninfected U937 control cells, although these differences were not statistically significant (0.22 ± 0.16 *versus* 2.38 ± 2.38 respectively). This trend was slight in the HIV-1-infected ACH2 lymphoid cell line *versus* uninfected CEM cells (9.99 ± 9.74 *versus* 12.44 ± 10.85 , $P = NS$). The formerly described increment pattern was also exhibited in promonocytic U1 infected cells *versus* U937 uninfected control when cells were exposed to a pro-apoptotic reagent (valinomycin) (1.54 ± 1.54 *versus* 10.22 ± 10.22 , respectively), but this exacerbation pattern was not observed in ACH2 lymphoid cells *versus* uninfected control CEM cells (13.72 ± 11.51 *versus* 12.91 ± 10.88 respectively).

The rate of cells of either promonocytic or lymphoid origin undergoing apoptosis or necrosis measured by annexin V plus PI did not render significant differences. A trend towards a decrease was observed in HIV-1-infected U1 promonocytic cells with respect to their U937 controls (9.92 *versus* 27.63 respectively), whereas an increase was observed in HIV-1-infected ACH2 lymphoid cells in comparison with their CEM control cells (23.40 *versus* 4.32).

Discussion

In this study, we compared mitochondrial and apoptotic parameters in chronically HIV-1-infected promonocytic and lymphoid cell lines with their uninfected counterparts to evaluate whether they could be used as HIV infection models of the *in vivo* mitochondrial and apoptotic lesion characteristic of HIV-infected patients. Most of the mitochondrial and apoptotic parameters were altered in the HIV-infected cell lines, especially in the promonocytic lineage, resembling *in vivo* alterations in case of mitochondrial findings. However, contrarily to what is observed *in vivo*, both promonocytic and lymphoid HIV-infected models showed resistance to undergo apoptosis. In the case of the promonocytic infected cell line U1, this may lead to a useful model to study HIV reservoirs, frequently established in these cell lineages. However, *in vivo* apoptosis of lymphocytes followed by infection was not observed in the ACH2 model, except for the trends of annexin V and PI measured by flow cytometry.

Mitochondrial and apoptotic abnormalities have been postulated to be the basis of collateral effects such as the development of hyperlactatemia, lipodystrophy and neuropathy associated with both HIV infection and its treatment [25–28]. Although most mitochondrial changes are considered to be the result of HIV apoptotic capacity and the secondary effects derived from ART [12], there is a growing evidence of the crucial role of mitochondria in the dynamics of HIV infection [29]. Despite the interest in several areas of the HIV infection process such as HLA, polymorphisms in viral co-receptors,

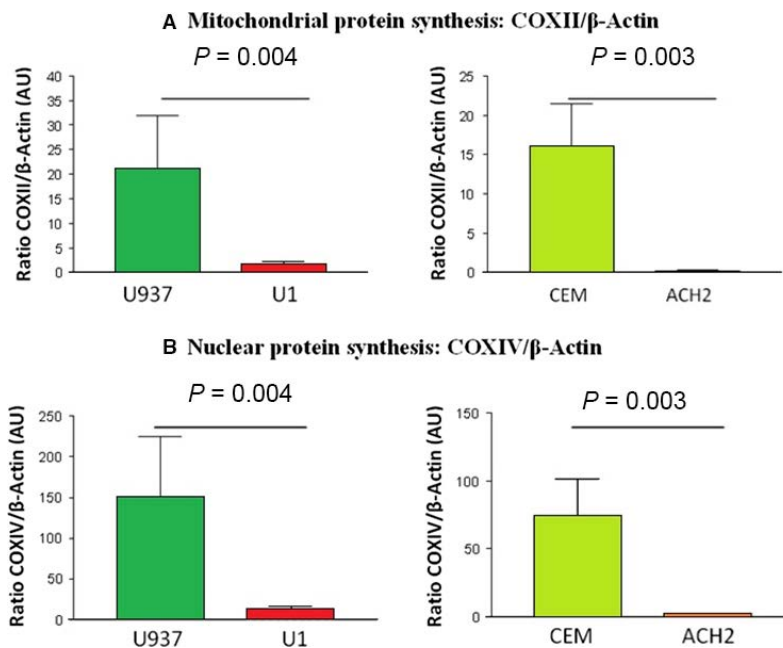


Fig. 3 (A) COXII content. This figure shows COXII protein subunit content in arbitrary units with expression of the levels of mitochondrial DNA encoded subunit II of complex IV of promonocytic (left) and lymphoid (right) cell lines normalized by β -actin content. A significant decrease in mitochondrial protein synthesis was observed in promonocytic and lymphoid U1 and ACH2 infected cell lines with respect to their uninfected U937 and CEM controls. COX: cytochrome c oxidase, AU: arbitrary units. **(B)** COXIV content. This figure shows COXIV protein subunit content in arbitrary units with expression of the levels of nuclear DNA encoded subunit IV of complex IV of promonocytic (left) and lymphoid (right) cell lines normalized by β -actin content. A significant decrease in nuclear protein synthesis was observed in promonocytic and lymphoid U1 and ACH2 infected cell lines with respect to their uninfected U937 and CEM controls. COX: cytochrome c oxidase, AU: arbitrary units.

antibodies, chemokines and defensins, among others [30, 31], the role of mitochondria has become outstanding in this process [29, 32].

The mitochondrial and apoptotic damage induced by HIV infection may exacerbate these deleterious effects in a kind of vicious cycle, terminating in the loss of cell defence capability of the host and the progression of infection. Studies performed to date have highlighted the need to establish an *in vitro* model to further investigate possible therapeutic approaches to revert mitochondrial or apoptotic damage and determine novel tools to fight HIV progression.

Mitochondrial parameters

In our cell models, most of the mitochondrial parameters were affected in both cell lines. Mitochondrial genome content and functional enzymatic activity were sharply depleted in U1 promonocytic cells, without being significantly modified in the ACH2 lymphoid cells. Both infected cell lines exhibited a marked decrease in MRC subunit expression which, in case of the promonocytic cells, goes in agreement with the outstanding dysfunction of the MRC. The expression of mitochondrial protein subunits of MRC was above 90% decreased in most cases compared to their uninfected counterparts. These mitochondrial and nuclear encoded subunits were diminished in both

HIV-1-infected cell lines, suggesting both mitochondrial and nuclear gene malfunctions in all cases.

Apoptotic parameters

A link between HIV infection and apoptosis has been widely reported [33]. Some viral proteins interact with mitochondrial targets, leading to apoptosis through different pathways [34, 35]. This is the case of the viral protein R (Vpr), the HIV-1-trans-activating protein (Tat) and the viral protease (Pr), which can directly interact with components of the mitochondrial permeability transition pore (Vpr interacts with the adenine nucleotide translocator ANT attached to VDAC, thus prompting mitochondrial depolarization) [32], translocate proapoptotic proteins into the mitochondria (Tat mediates Bim translocation) [33], activate caspases (Vpr activates caspases 3 and 9) [34] or inactivate anti-apoptotic proteins (Vpr inactivates HAX-1 and Pr inactivates Bcl-2) [34, 35], ultimately causing cell death. Consequently, the marked significant decrease in the early and advanced apoptotic markers (VDAC-1 and caspase-9 proteins) in both infected cell lines studied was unexpected. These results are in agreement with the lower levels of early apoptotic events of depolarized mitochondrial membranes observed with JC1 by flow cytometry in both infected U1 and ACH2 cell lines, although such trends did not achieve statistical significance.

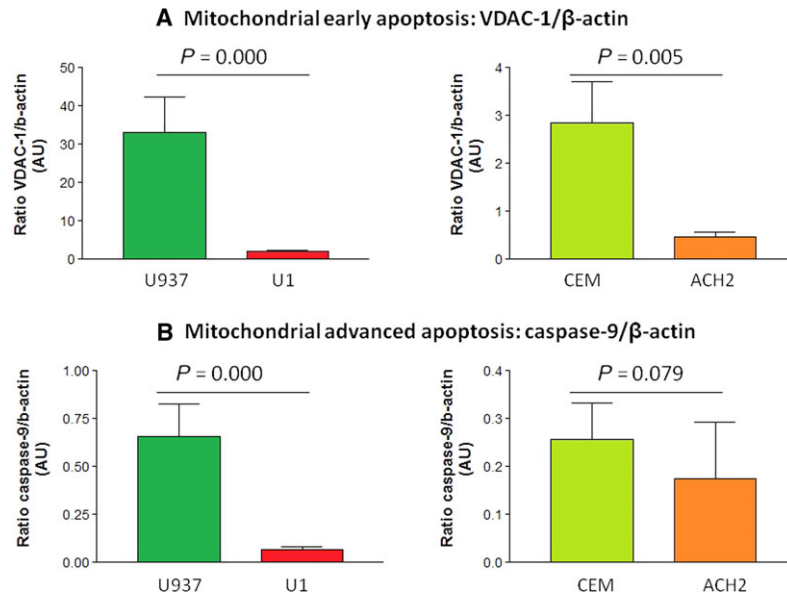


Fig. 4 (A) VDAC-1 content. This figure shows the VDAC-1 content expressed in arbitrary units. The expression of the levels of VDAC-1 content normalized by β -actin of promonocytic (left) and lymphoid (right) cells. A significant decrease in early mitochondrial apoptosis was observed in promonocytic and lymphoid U1 and ACH2 infected cell lines with respect to their uninfected U937 and CEM controls. VDAC-1: voltage-dependent anion channel-1, AU: arbitrary units. **(B)** Caspase-9 content. This figure shows the caspase-9 content expressed in arbitrary units. The expression of the levels of caspase-9 content normalized by β -actin of promonocytic (left) and lymphoid (right) cells. A decrease in advanced mitochondrial apoptosis was observed in promonocytic (significant) and lymphoid (non-significant) U1 and ACH2 infected cell lines with respect to their uninfected U937 and CEM controls. AU: arbitrary units.

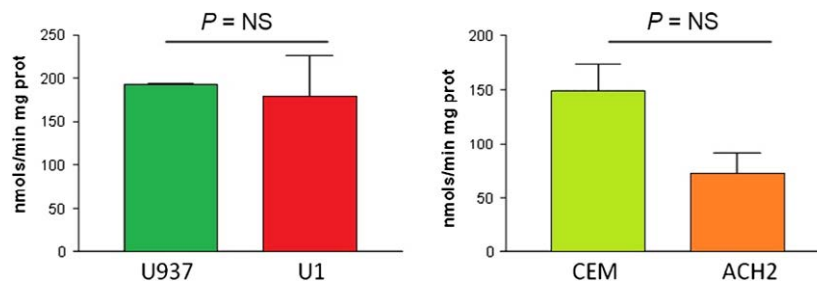


Fig. 5 Mitochondrial content. This figure shows the mitochondrial content measured by citrate synthase enzymatic activity expressed in nmols/min mg protein of promonocytic (left) and lymphoid (right) cells. No significant changes were observed in infected promonocytic and lymphoid U1 and ACH2 cell lines with respect to their uninfected U937 and CEM controls. NS: not significant.

Our data strongly indicate that latently infected cells are less susceptible to undergo apoptosis compared to uninfected cells. These results support a previous study [18] which was mainly focused on the reaction of specific cell lines against different exogenous pro-apoptotic and stress-induced stimuli. Although HIV infection most frequently leads to cell death, the latently HIV-1-infected cell lines studied only showed a reduced apoptotic behaviour which may be indicative of a viral strategy to survive [36]. In this sense, both promonocytic and lymphoid HIV-1-infected cell lines showed different patterns in advanced apoptosis and necrosis phenomena tested by flow cytometry through annexin V plus PI staining. A trend to decrease in advanced apoptotic events was observed in the infected U1

promonocytic cell lines compared to their controls, whereas a tendency to increase was observed in infected ACH2 lymphoid cell lines. These data are also in agreement with the lower sensitivity to apoptosis previously observed in promonocytic *versus* lymphoid cells [37].

Validation of both *in vitro* models

Considering all these results, our findings suggest that these cell models may at least partially reproduce *in vitro* the alterations observed *in vivo* in HIV-infected patients [4, 8, 9, 12, 13] that should be further characterized in depth.

From a mitochondrial point of view, both promonocytic and lymphoid cell lines showed pronounced abnormalities with slightly different patterns. Previous studies reported different behaviour for promonocytic and as well as lymphoid cell lines [37] or monocytes/lymphocytes [36] suggesting that different molecular mechanisms may depend on cell types considered. In our study, although both promonocytic and lymphoid cell lines showed changes in MRC expression, only the promonocytic cells (not the lymphoid lineage) showed significant alterations at the mitochondrial genetic and functional levels. In this context, it was surprising to notice the significant reduced content of subunits COXII and COXIV in the lymphoid infected lines despite the trends towards increased levels of mtDNA and only slightly reduced enzymatic activity of the complex IV. It would be conceivable that, despite the decrease in the subunit protein levels is observed, the threshold to observe a defective functionality of the enzyme had not been yet reached, probably due to the homeostatic up-regulation of mtDNA content in these cells. All these mechanisms were not observed in promonocytic infected cell lines, which showed decreased ratios in all genetic, functional and expression mitochondrial parameters fully resembling *in vivo* conditions.

From the apoptotic point of view, both infected cell lines showed a trend to a resistance to apoptotic events.

A previous study reported lower MMP in peripheral blood mononuclear cells from HIV patients, as well as higher apoptotic/necrotic events in these cells [35]. In this study non-significant trends were found in MMP. In addition, most of apoptotic/necrotic parameters measured (mitochondrial pore and caspase-9 activation or phosphatidylserine expression and nuclear DNA fragmentation) yielded to similar results suggesting the resistance to undergo apoptosis of HIV-infected cell models [18, 33] and, as opposite as *in vivo* conditions of blood cells not becoming reservoirs [4, 5].

Our findings point out the use of the present *in vitro* models as largely useful for mitochondrial monitoring. We encourage other researchers to explore in depth apoptotic events in this and other *in vitro* models. Importantly, our results clearly mimic the *in vivo* mitochondrial features of HIV infection, (especially in the promonocytic cell line), rather than the *in vivo* apoptotic conditions. Apoptotic resistance in infected lines might be derived from the genetic modification of the cancerous lineages that do not undergo apoptosis following viral genome insertion. Promonocytic apoptotic resistance may reflect the *in vivo* percentage of monocytes capable to constitute reservoirs and, subsequently, become more resistant to apoptosis. Resistance to apoptosis of ACH2 lymphoid cell line should be taken with caution when willing to reproduce *in vivo* pathophysiology of HIV infection. The observed findings, suggest that such alterations might have HIV clinical consequences as previously described *in vivo* [11] and point out to the involvement of mitochondrial status in HIV progression and

chronicity. In addition, this study provides complementary data to the apoptosis approaches previously considered [15].

In spite of strained HIV-1 replication in the infected cell lines used in this study, the assessment of the mitochondrial and apoptotic parameters investigated led to the description of significant changes compared to the respective uninfected control cell lines. It remains unknown whether these disturbances would be increased in activated HIV-1-infected cell lines (with the addition of HIV replication inducer factors).

A limitation of this study was the resistance to apoptosis of the cancerous infected cell lines, which remain viable regardless of HIV infection and would have died in natural conditions. Nonetheless, despite these limitations, due to the same cancerous origin of both control and infected lines, it is presumable that the significant changes found between cell lines are comparable and attributable to the infection itself. Thereby, we consider that the models studied may constitute adequate *in vitro* models to monitorize the patient dynamics at apoptotic and especially at mitochondrial level.

In summary, this study provides evidence that the mitochondrial and, in a lesser extent, apoptotic pathways are seriously affected in latently infected HIV-1 promonocytic and lymphoid cells. The availability of an *in vitro* HIV model is essential for translational research. Studies using these cell models of HIV infection may lead to the development of novel therapeutic tools [38], including apoptotic and mitochondrial targets [39], as strategies to reverse the lesions exerted by the virus.

Acknowledgements

Both U1 and ACH2 cell lines were first created by Dr. Thomas Folks through the NIH AIDS Reagent Program, Division of AIDS, NIAID, NIH, which we would like to thank. Foremost, we would like to express our gratitude to Florencio Varas for his critical review of the manuscript and for providing writing assistance. This work was supported by Fundación para la Investigación y la Prevención del SIDA en España (grant number FIPSE 360982/10); Fundació Cellex, Suports a Grups de Recerca de la Generalitat de Catalunya 2014-2016 (grant number SGR 2014/376) and Fondo de Investigación Sanitaria (grant numbers FIS 00462/11, FIS 01199/12, FIS 01455/13, FIS 01738/13, FIS 00903/15 and FIS 00817/15), InterCIBER (PIE1400061) and CIBER de Enfermedades Raras (CIBERER), initiatives of ISCIII and FEDER.

Conflicts of interest

None of the authors has any financial, consultant, institutional and other relationship that might lead to bias or a conflict of interest for the present manuscript.

References

1. Somasundaran M, Zapp ML, Beattie LK, *et al.* Localization of HIV RNA in mitochondria of infected cells: potential role in cytopathogenicity. *J Cell Biol.* 1994; 126: 1353–60.
2. Huang CY, Chiang SF, Lin TY, *et al.* HIV-1 Vpr triggers mitochondrial destruction by impairing Mfn2-mediated ER-mitochondria interaction. *PLoS ONE.* 2012; 7: e33657.
3. Selvaraj S, Ghebremichael M, Li M, *et al.* Antiretroviral therapy-induced mitochondrial toxicity: potential mechanisms beyond polymerase-gamma inhibition. *Clin Pharmacol Ther.* 2014; 96: 110–20.

4. **Hulgan T, Gerschenson M.** HIV and mitochondria: more than just drug toxicity. *J Infect Dis.* 2012; 205: 1769–71.
5. **Blas-Garcia A, Apostolova N, Esplugues JV.** Oxidative stress and mitochondrial impairment after treatment with anti-HIV drugs: clinical implications. *Curr Pharm Des.* 2011; 17: 4076–86.
6. **Ceresola ER, Nozza S, Sampaolo M, et al.** Performance of commonly used genotypic assays and comparison with phenotypic assays of HIV-1 coreceptor tropism in acutely HIV-1-infected patients. *J Antimicrob Chemother.* 2015; 70: 1391–5.
7. **Balestra E, Perno CF, Aquaro S, et al.** Macrophages: a crucial reservoir for human immunodeficiency virus in the body. *J Biol Regul Homeost Agents.* 2001; 15: 272–6.
8. **Pandolfi F, Pierdominici M, Oliva A, et al.** Apoptosis-related mortality *in vitro* of mononuclear cells from patients with HIV infection correlates with disease severity and progression. *J Acquir Immune Defic Syndr Hum Retrovirol.* 1995; 9: 450–8.
9. **Cossarizza A, Mussini C, Mongiardo N, et al.** Mitochondria alterations and dramatic tendency to undergo apoptosis in peripheral blood lymphocytes during acute HIV syndrome. *AIDS.* 1997; 11: 19–26.
10. **Domingo P, Gutierrez Mdel M, Gallego-Escuredo JM, et al.** Effects of switching from stavudine to raltegravir on subcutaneous adipose tissue in HIV-infected patients with HIV/HAART-associated lipodystrophy syndrome (HALS). A clinical and molecular study. *PLoS ONE.* 2014; 9: e89088.
11. **Peraire J, Miro O, Saunoy M, et al.** HIV-1-infected long-term non-progressors have milder mitochondrial impairment and lower mitochondrially-driven apoptosis in peripheral blood mononuclear cells than typical progressors. *Curr HIV Res.* 2007; 5: 467–73.
12. **Cote HC, Brumme ZL, Craib KJ, et al.** Changes in mitochondrial DNA as a marker of nucleoside toxicity in HIV-infected patients. *N Engl J Med.* 2002; 346: 811–20.
13. **Miro O, Lopez S, Martinez E, et al.** Mitochondrial effects of HIV infection on the peripheral blood mononuclear cells of HIV-infected patients who were never treated with antiretrovirals. *Clin Infect Dis.* 2004; 39: 710–6.
14. **Morén C, Bañó M, González-Casacuberta I, et al.** Mitochondrial and apoptotic *in vitro* modelling of differential HIV-1-progression and antiretroviral toxicity. *J Antimicrob Chemother.* 2015; 70: 2330–2336.
15. **Divi RL, Leonard SL, Walker BL, et al.** Erythrocytes patas monkey offspring exposed perinatally to NRTIs sustain skeletal muscle mitochondrial compromise at birth and at 1 year of age. *Toxicol Sci.* 2007; 99: 203–13.
16. **Folks TM, Justement J, Kinter A, et al.** Characterization of a promonocyte clone chronically infected with HIV and inducible by 13-phorbol-12-myristate acetate. *J Immunol.* 1988; 140: 1117–22.
17. **Poli G, Orenstein JM, Kinter A, et al.** Interferon-alpha but not AZT suppresses HIV expression in chronically infected cell lines. *Science.* 1989; 244: 575–7.
18. **Fernandez Larrosa PN, Croci DO, Riva DA, et al.** Apoptosis resistance in HIV-1 persistently-infected cells is independent of active viral replication and involves modulation of the apoptotic mitochondrial pathway. *Retrovirology.* 2008; 5: 19.
19. **Folks TM, Justement J, Kinter A, et al.** Cytokine-induced expression of HIV-1 in a chronically infected promonocyte cell line. *Science.* 1987; 238: 800–2.
20. **Clouse KA, Powell D, Washington I, et al.** Monokine regulation of human immunodeficiency virus-1 expression in a chronically infected human T cell clone. *J Immunol.* 1989; 142: 431–8.
21. **Barrientos A.** *In vivo* and in organello assessment of OXPHOS activities. *Methods.* 2002; 26: 307–16.
22. **Miro O, Lopez S, Rodriguez de la Concepcion M, et al.** Upregulatory mechanisms compensate for mitochondrial DNA depletion in asymptomatic individuals receiving stavudine plus didanosine. *J Acquir Immune Defic Syndr.* 2004; 37: 1550–5.
23. **Cossarizza A, Salvioli S.** Flow cytometric analysis of mitochondrial membrane potential using JC-1. *Curr Protoc Cytom.* 2001; Chapter 9: Unit 9.14.
24. **Lugli E, Troiano L, Cossarizza A.** Polychromatic analysis of mitochondrial membrane potential using JC-1. *Curr Protoc Cytom.* 2007; Chapter 7: Unit 7.32.
25. **Holzinger ER, Hulgan T, Ellis RJ, et al.** Mitochondrial DNA variation and HIV-associated sensory neuropathy in CHARTER. *J Neurovirol.* 2012; 18: 511–20.
26. **Walker UA, Lebrecht D, Reichard W, et al.** Zidovudine induces visceral mitochondrial toxicity and intra-abdominal fat gain in a rodent model of lipodystrophy. *Antivir Ther.* 2014; 19: 783–92.
27. **Moren C, Noguera-Julian A, Rovira N, et al.** Mitochondrial impact of human immunodeficiency virus and antiretrovirals on infected pediatric patients with or without lipodystrophy. *Pediatr Infect Dis J.* 2011; 30: 992–5.
28. **Garrabou G, Moren C, Gallego-Escuredo JM, et al.** Genetic and functional mitochondrial assessment of HIV-infected patients developing HAART-related hyperlactatemia. *J Acquir Immune Defic Syndr.* 2009; 52: 443–51.
29. **Hart AB, Samuels DC, Hulgan T.** The other genome: a systematic review of studies of mitochondrial DNA haplogroups and outcomes of HIV infection and antiretroviral therapy. *AIDS Rev.* 2013; 15: 213–20.
30. **Zapata W, Aguilar-Jimenez W, Pineda-Trujillo N, et al.** Influence of CCR5 and CCR2 genetic variants in the resistance/susceptibility to HIV in serodiscordant couples from Colombia. *AIDS Res Hum Retroviruses.* 2013; 29: 1594–603.
31. **Ding J, Tasker C, Valere K, et al.** Anti-HIV activity of human defensin 5 in primary CD4+ T cells under serum-deprived conditions is a consequence of defensin-mediated cytotoxicity. *PLoS ONE.* 2013; 8: e76038.
32. **Guzman-Fulgencio M, Jimenez JL, Garcia-Alvarez M, et al.** Mitochondrial haplogroups are associated with clinical pattern of AIDS progression in HIV-infected patients. *J Acquir Immune Defic Syndr.* 2013; 63: 178–83.
33. **Ma R, Yang L, Niu F, et al.** HIV Tat-mediated induction of human brain microvascular endothelial cell apoptosis involves endoplasmic reticulum stress and mitochondrial dysfunction. *Mol Neurobiol.* 2014; 53: 132–142.
34. **Ma R, Yang L, Niu F, et al.** HIV Tat-mediated induction of human brain microvascular endothelial cell apoptosis involves endoplasmic reticulum stress and mitochondrial dysfunction. *Mol Neurobiol.* 2016; 53: 132–42.
35. **Yedavalli VS, Shih HM, Chiang YP, et al.** Human immunodeficiency virus type 1 Vpr interacts with antiapoptotic mitochondrial protein HAX-1. *J Virol.* 2005; 79: 13735–46.
36. **Xu XN, Sreaton GR, McMichael AJ.** Virus infections: escape, resistance, and counter-attack. *Immunity.* 2001; 15: 867–70.
37. **Pinti M, Biswas P, Troiano L, et al.** Different sensitivity to apoptosis in cells of monocytic or lymphocytic origin chronically infected with human immunodeficiency virus type-1. *Exp Biol Med (Maywood).* 2003; 228: 1346–54.
38. **Li Y, Starr SE, Lisziewicz J, et al.** Inhibition of HIV-1 replication in chronically infected cell lines and peripheral blood mononuclear cells by retrovirus-mediated antitarget gene transfer. *Gene Ther.* 2000; 7: 321–8.
39. **Gupta S, Kass GE, Szegzedi E, et al.** The mitochondrial death pathway: a promising therapeutic target in diseases. *J Cell Mol Med.* 2009; 13: 1004–33.

Mitochondrial DNA disturbances and deregulated expression of oxidative phosphorylation and mitochondrial fusion proteins in sporadic inclusion body myositis

Marc Catalán-García*, Glòria Garrabou*, Constanza Morén*, Mariona Guitart-Mampel*, Adriana Hernando*, Àngels Díaz-Ramos†‡§, Ingrid González-Casacuberta*, Diana-Luz Juárez*, María Bañó*, Jennifer Enrich-Bengoa*, Sonia Emperador||, José César Milisenda*, Pedro Moreno*, Ester Tobías*, Antonio Zorzano†‡§, Julio Montoya||, Francesc Cardellach* and Josep Maria Grau*

*Muscle Research and Mitochondrial Function Laboratory, CELLEX-IDIBAPS, Faculty of Medicine, University of Barcelona; Internal Medicine Department, Hospital Clinic of Barcelona, CIBERER-U722, Barcelona, Spain

†Institute for Research in Biomedicine (IRB Barcelona), Barcelona Institute of Science and Technology, Barcelona, Spain

‡Departament de Bioquímica i Biomedicina Molecular, Facultat de Biologia, Universitat de Barcelona, 08028 Barcelona, Spain

§CIBER de Diabetes y Enfermedades Metabólicas Asociadas (CIBERDEM), Instituto de Salud Carlos III, Madrid, Spain

||Departamento de Bioquímica, Biología Molecular y Celular, Universidad de Zaragoza, CIBERER-U727, Instituto de Investigaciones Sanitarias de Aragón, Zaragoza, Spain

Abstract

Sporadic inclusion body myositis (sIBM) is one of the most common myopathies in elderly people. Mitochondrial abnormalities at the histological level are present in these patients. We hypothesize that mitochondrial dysfunction may play a role in disease aetiology. We took the following measurements of muscle and peripheral blood mononuclear cells (PBMCs) from 30 sIBM patients and 38 age- and gender-paired controls: mitochondrial DNA (mtDNA) deletions, amount of mtDNA and mtRNA, mitochondrial protein synthesis, mitochondrial respiratory chain (MRC) complex I and IV enzymatic activity, mitochondrial mass, oxidative stress and mitochondrial dynamics (mitofusin 2 and optic atrophy 1 levels). Depletion of mtDNA was present in muscle from sIBM patients and PBMCs showed deregulated expression of mitochondrial proteins in oxidative phosphorylation. MRC complex IV/citrate synthase activity was significantly decreased in both tissues and mitochondrial dynamics were affected in muscle. Depletion of mtDNA was significantly more severe in patients with mtDNA deletions, which also presented deregulation of mitochondrial fusion proteins. Imbalance in mitochondrial dynamics in muscle was associated with increased mitochondrial genetic disturbances (both depletion and deletions), demonstrating that proper mitochondrial turnover is essential for mitochondrial homeostasis and muscle function in these patients.

Key words: deletions, depletion, mitochondria, mitofusin-2, OPA1, sporadic inclusion body myositis.

INTRODUCTION

Sporadic inclusion body myositis (sIBM) is the most common inflammatory myopathy in individuals aged >50 years [1] and one of the most important myopathies associated with ageing [2]. With a male:female ratio of 3:1, it is a rare disease (ORPHA611) and its prevalence varies from 4.7 per million in the Netherlands to 14.9 per million in western Australia [3]. These rates continue

to increase, probably due to improved diagnostic protocols and increased ageing of the population. This myopathy is a devastating condition, causing slow, progressive muscle weakness and wasting, with quadriceps and finger flexors being the muscles most typically affected. Nevertheless, the clinical presentation varies considerably. This muscle weakness usually leads to falls and difficulty in standing. Around 60% of the patients also present with dysphagia. With the wide spectrum of clinical

Abbreviations: CK, creatine kinase; COX, cytochrome c oxidase; CS, citrate synthase; H&E, haematoxylin and eosin; HAE, hydroxyalkenal; IBMFRS, Inclusion Body Myositis Functional Rating Scale; MDA, malondialdehyde; MFN2, mitofusin 2; MRC, mitochondrial respiratory chain; NSE, non-specific esterase; OPA1, optic atrophy 1; ORO, Oil Red O; PAS-D, periodic acid–Schiff diastase stain; PBMC, peripheral blood mononuclear cell; RT-PCR, reverse transcriptase PCR; ROS, reactive oxygen species; SDH, succinate dehydrogenase; sIBM, sporadic inclusion body myositis; TRC, tyrosine-rich crystalloids; VDACL1, voltage-dependent anion channel 1.

Correspondence: Glòria Garrabou Tornos (email garrabou@clinic.ub.es).

manifestations in sIBM, muscle biopsy continues to be the gold standard for diagnosis [4].

The histological features observed in muscle biopsies of sIBM patients include: (i) inflammatory changes with predominant CD8+ T-cell infiltrates and the expression of MHC-I antigens by non-necrotic muscle fibres, (ii) different degrees of degenerative changes in muscle fibres and the presence of rimmed vacuoles composed mainly of β -amyloid, phosphorylated tau and caveolin proteins, among others, and (iii) mitochondrial abnormalities characterized by the presence of ragged-red fibres, cytochrome *c* oxidase (COX)-negative and succinate dehydrogenase (SDH)-positive muscle cells [5,6], all of which are widely associated with mitochondrial dysfunction and ageing [1,2,7]. However, the distribution of these histological features is not homogeneous, and they may not be simultaneously present, particularly in the early stages of the disease. For all these reasons, and due to its slow progression, diagnosis may be delayed for 5–10 years.

Mitochondria are the cell's powerhouse. They are responsible for most of the energy supply, metabolic reactions, calcium homeostasis and cell respiration. However, under pathological conditions, mitochondria are the main centres for reactive oxygen species (ROS) production and for triggering apoptosis. Mitochondria are essential for cell bioenergetics, especially in highly energetic tissues such as muscle, in which mitochondrial dysfunction may become evident much earlier. Molecular mitochondrial alterations have recently been found in sIBM by down-regulated expression of mitochondrial respiratory chain (MRC) complex I subunits and mitochondrial DNA (mtDNA) variations [7]. In addition, mtDNA deletions have also been reported in sIBM patients [6,8], but not correlated with abnormal mitochondrial function or dynamics. Despite mitochondrial abnormalities having classically been described at a histological level, mitochondrial dysfunction in sIBM patients has scarcely been assessed at a molecular level.

Mitochondrial dynamics is a recently discovered mechanism responsible for mitochondrial turnover and renewal [9]. Mitochondria constitute a complex network that is constantly undergoing fusion and fission processes to exchange genetic and structural components, which include mtDNA and MRC machinery. Deregulation of mitochondrial dynamics has been associated with disease, but has not previously been described in sIBM patients [10–16].

Although the pathological features of sIBM have been widely described, its aetiology remains unknown. It has been proposed that its development could be due to a complex interaction of environmental agents, accelerated ageing and genetic susceptibility [2,17]. As muscle tissue has a high dependence on ATP to exert its function, mitochondrial alterations in sIBM could be one of the factors involved in triggering muscle weakness and degeneration, because these alterations have been related to muscle disease by many authors [18–20]. For an in-depth evaluation of the pathological characteristics of the disease, we describe the mitochondrial phenotype at a genetic, molecular and functional level in sIBM patients.

To determine potential disease biomarkers we assessed abnormal mitochondrial fingerprints, in the target tissue of the disease (muscle) and with less invasive approaches using peri-

pheral blood mononuclear cells (PBMCs). This PBMC model is widely feasible for the evaluation of mitochondrial function [21–23]. Thus, we designed the present study to evaluate mitochondrial dysfunction in both muscle and PBMCs of sIBM patients to correlate dysfunction severity with genetic and molecular mitochondrial alterations, and determine their potential association with the deregulation of mitochondrial dynamics.

MATERIALS AND METHODS

Study design

We performed a single-site, cross-sectional, case–control, observational study.

Study population, diagnosis, clinical data and sample collection

A total of 30 patients with sIBM who had attended the Internal Medicine Department of the Hospital Clinic of Barcelona (Spain) over the last 20 years were prospectively and consecutively included. These patients were age and gender paired with 38 controls. All muscle biopsies were performed for diagnostic purposes indicated for muscle weakness or raised creatine kinase (CK) levels. Surgical muscle biopsies were obtained by trained physicians, and the samples were processed routinely in the laboratory as described elsewhere [24]. For histological studies fresh muscle samples were frozen in cooled isopentane, sectioned by cryotome at -30°C and stained with different reagents for diagnostic purposes: haematoxylin and eosin (H&E), tyrosine-rich crystalloids (TRCs), non-specific esterase (NSE), periodic acid–Schiff diastase stain (PAS-D), Oil Red O (ORO), acid and alkaline phosphatase, NADH, COX, SDH and ATPase at pH 4.3, 4.6 and 9.4, as reported elsewhere [24]. In addition some immunohistochemistry reactions such as class I antigens from the MHC as well as p62 were performed. The same expert pathologist (J.M.G.) read all the samples. Leftover biopsy material from both sIBM patients and individuals with no histological myopathy was included as patient and control samples, respectively. Histological data were collected to study inflammation and the presence of ragged-red fibres, COX-negative and SDH-positive fibres, as well as the number of vacuolated muscle cells. Diagnosis of sIBM was considered as definite or probable according to the criteria of the European Neuromuscular Centre [1,25]. Samples from 23 muscle biopsies from sIBM patients and 18 from controls were included following these criteria. In parallel, blood samples were collected from 14 sIBM patients and 20 control individuals free of muscle disease. Exclusion criteria were: age <40 years, muscle disease in the case of controls, mitochondrial disease, and family history of hereditary mitochondrial pathology, HIV infection or drug abuse. All individuals were informed, and signed written consent was obtained for inclusion in this study, which was approved by the Ethical Committee of our hospital, following the Declaration of Helsinki. All sIBM patients answered the Inclusion Body Myositis Functional Rating Scale (IBMFRS) test, which is a validated, disease-specific test to assess disease severity.

A database was created to collect epidemiological, clinical and histological data, which were further complemented with experimental results.

Leftover samples from mandatory muscle biopsy diagnosis were included in optimal cutting temperature compound (OCT) and immediately frozen and stored at -80°C until homogenization (5% w/v) with mannitol to perform experimental studies.

Around 20 ml of peripheral blood was also obtained by antecubital vein puncture and collected in EDTA tubes. PBMCs were isolated using Ficoll density gradient centrifugation, divided into aliquots and stored at -80°C until analysis.

Mitochondrial genetic studies

Total DNA from muscle biopsies and PBMCs was obtained by the standard phenol–chloroform extraction procedure. The assessment of mtDNA deletions was performed in muscle samples by long-range PCR using Phusion High-Fidelity PCR Master Mix with GC Buffer (F-532L, ThermoFisher Scientific) and the following primers: forward 5'-TTAGCAAGGGAAGTACTCCCA-3' and reverse 5'-CGGATACAGTTCCTTAGCTACCCCAAGTG-3'. The methodology of this procedure was performed as previously described [26–28]. The PCR products were electrophoresed in a 0.8% agarose gel with ethidium bromide to detect different sizes in the mitochondrial genome (see Supplementary Figure S1).

To evaluate mtDNA content, fragments of the mitochondrially encoded 12S rRNA gene and the nuclear-encoded RNase-P gene were amplified separately in triplicate by quantitative reverse transcriptase PCR (RT-PCR) using Applied Biosystems technology [29]. The relative mtDNA content was expressed as the ratio mtDNA 12S rRNA:nDNA RNase-P.

Mitochondrial transcript quantification

To evaluate mtRNA content in both muscle and PBMCs, total RNA was first extracted using the TriPure procedure and immediately retro-transcribed into cDNA using random hexamer primers, following previously described methodology [30]. The mtRNA:nRNA content was then measured by RT-PCR as previously described for mtDNA and expressed in the same units (mtRNA 12S rRNA:nRNA RNase-P).

Mitochondrial protein quantification

Mitochondrial protein quantification was assessed in muscle and PBMCs by the quantification of two mitochondrial complex IV protein subunits: COX-II (encoded by the mitochondrial genome) and COX-IV (encoded by the nuclear genome). These proteins were assessed through immunoblotting using SDS/7/13% PAGE and immunodetection using previously described reagents and antibodies [22]. Mitochondrial values normalized to nuclear-encoded COX proteins were expressed as the COX-II:COX-IV ratio, and absolute values of COX-II and COX-IV were normalized with a loading control (α -tubulin for muscle samples and β -actin for PBMC samples) and expressed as the COX-II: α -tubulin and COX-IV: α -tubulin ratios in muscle or the COX-II: β -actin and COX-IV: β -actin ratios in PBMCs. COX-II and COX-IV values were also normalized by mitochondrial mass [through constitutive voltage-dependent anion channel

1 (VDAC1) expression] and expressed as COX-II:VDAC1 and COX-IV:VDAC1 ratios in both tissues (see Supplementary Figure S2) [31].

MRC complex I and complex IV enzyme activity

MRC complex I (EC 1.6.5.3) and IV (COX – EC 1.9.3.1) enzyme activities were measured spectrophotometrically according to the methodologies of Spinazzi et al. [32] in both muscle homogenates and PBMCs. Specific enzymatic activities were expressed in absolute values as nanomoles of substrate consumed or product generated per minute per milligram of cell protein (nmol/min per mg protein) or in relative values with respect to mitochondrial content normalized by citrate synthase (CS) activity (COX:CS).

MRC complex assembly

Total oxidative phosphorylation rodent WB Antibody Cocktail (MS604, Abcam) was used to detect one subunit from each MRC complex (I–V): NDFUFB8 from complex I, SDHB from complex II, UQCRC2 from complex III, MTCO1 from complex IV and ATP5A from complex V. These subunits are labile when the respiratory complex to which they belong is not assembled and a decrease in this subunit would manifest this phenomenon. To normalize the levels of expression of these five proteins from the MRC we analysed using the SYPRO technique for the total protein content and the VDAC1 levels for the mitochondrial mass in the same membrane.

Mitochondrial mass analysis

Mitochondrial mass was analysed in both muscle and PBMCs by spectrophotometric measurement of CS (EC 4.1.3.7) enzyme activity and, in parallel, by the measurement of VDAC1 protein levels by Western blotting. CS is a mitochondrial enzyme of the citrate cycle widely considered to be a reliable marker of mitochondrial content, and VDAC1 [22] is an outer membrane anion channel also considered to be a mitochondrial mass marker [22]. CS activity was expressed as nmol/min per mg of protein and VDAC1 expression was normalized by α -tubulin in muscle and by β -actin in PBMCs, both of which are validated proteins for assessing total cell loading mass and expressed as the VDAC1: α -tubulin ratio in muscle or the VDAC-1: β -actin ratio in PBMCs.

Oxidative stress assay

Lipid peroxidation (an indicator of oxidative damage produced by ROS in cellular lipid compounds) was quantified in muscle and PBMCs using the Oxys Research kit (Deltaclon) through the spectrophotometric measurement of malondialdehyde (MDA) and 4-hydroxyalkenal (HAE), both products of fatty acid peroxide decomposition and normalized by protein content (μM MDA + HAE per mg of protein) [33].

Expression of mitochondrial fusion proteins

Mitochondrial dynamics were assessed in muscle tissue by the evaluation of both optic atrophy 1 (OPA1) and mitofusin 2 (MFN2) expression at two different levels: transcript and protein quantification. For the assessment of transcript levels of OPA1 and MFN2, mRNA, total RNA extracted by TriPure was reverse

transcribed with the SuperScript III reverse transcriptase kit (Invitrogen). Quantitative PCRs were performed with ABI Prism 7900HT real-time PCR equipment (Applied Biosystems) using materials and reagents previously described [34,35]. All measurements were normalized to glyceraldehyde-3-phosphate dehydrogenase (GAPDH) mRNA content. Protein levels of OPA1 and MFN2 were assessed in parallel using Western blotting on SDS/7/8% PAGE and posterior immunodetection using a BD antibody (612606) and an Abcam antibody (ab56889), respectively. In the case of OPA1, results were expressed as the ratio between the long and the short forms of the protein (OPA1 long:short), because this ratio decreases in abnormal mitochondrial dynamic states. In the case of MFN2, absolute values were normalized by total cell loading mass and expressed as the ratio MFN2: α -tubulin.

Statistical analysis

Statistical analysis was performed using the SPSS, version 20.00 to search for differences depending on group assignment (patients vs controls or presence vs absence of mtDNA deletions) using the non-parametric Mann–Whitney U-test for independent samples. Results were expressed as means \pm S.E.M.S or as a percentage of increase/decrease with respect to controls that were arbitrarily assigned as 0%. In all cases, $P < 0.05$ was considered statistically significant.

RESULTS

Clinical and histological data

According to the design of the study, no statistical differences were observed with regard to age and gender between sIBM patients and controls. Clinical, epidemiological, histological and mtDNA deletion data of both patients and controls are summarized in Table 1 and histological data examples are compiled in Figure 1. At the time of study inclusion the sIBM patient cohort scored 26.61 ± 1.19 out of 40 with the IBMFRS test, indicating moderate-to-advanced sIBM clinical severity.

MtDNA deletions

When assessing for the presence of mtDNA deletions in muscle from sIBM patients, 57% of the sIBM cohort presented multiple mtDNA deletions, whereas the rest showed no alterations in this parameter (see Supplementary Figure S1).

MtDNA content

MtDNA content was significantly decreased by 36% in muscle from sIBM patients compared with controls (641.6 ± 141.2 vs 979.7 ± 111.3 , respectively, $P < 0.05$) (Figure 2). Similarly, mtDNA was decreased, albeit not significantly, by 14.5% in PBMCs (Figure 2).

Mitochondrial transcript quantification

No variation was found in the levels of mtRNA in either muscle or PBMCs (Figure 2) of sIBM patients compared with controls.

Table 1 Clinical, epidemiological and histological data of patients with sIBM and controls included in the present study

Muscle biopsies	sIBM (n=23)	Controls (n=18)
Clinical and epidemiological data		
Age (years) ^a	68.64 ± 2.87	63.22 ± 2.55
Male:female ratio	0.64	0.38
IBMFRS score ^a	$26.61 \pm 1.19/40$	–
mtDNA deletions (%) ^b	57	–
Histological data (%)		
Rimmed vacuoles ^b	61.20	–
Ragged-red fibres ^b	60	–
COX-negative fibres ^b	36.36	–
SDH-positive fibres ^b	44	–
MHC-I expression ^b	57.14	–
Inflammation ^b	67.74	–
PBMC samples		
Clinical and epidemiological data		
Age (years) ^a	68.43 ± 3.28	68.55 ± 1.41
Male:female ratio	1	1.85
IBMFRS score ^a	$25.85 \pm 1.31/40$	–

^aData presented as means \pm S.E.M.S.

^bData presented as percentage.

Mitochondrial protein quantification

As shown in Figure 2, muscle from sIBM patients presented an increase of 25% in the COX-II:COX-IV ratio with respect to controls, suggesting increased expression of mitochondrial versus nuclear COX subunits (see Supplementary Figure S2). It is interesting that in PBMCs this ratio showed a statistically significant decrease of 45.46% (0.42 ± 0.05 vs 0.77 ± 0.09 , $P < 0.05$; Figure 2). In addition, in PBMCs COX-IV protein levels normalized by total cell mass showed a strong trend to be increased by 67.85% in sIBM patients compared with controls (0.47 ± 0.08 vs 0.28 ± 0.03 , $P = 0.064$; Figure 2), suggesting increased nuclear versus mitochondrial COX protein expression. This abnormality became statistically significant when COX-IV values were normalized by mitochondrial mass (COX-IV:VDAC-1), which showed a 172.72% increase in sIBM patients compared with controls (1.80 ± 0.35 vs 0.66 ± 0.01 , $P < 0.05$; Figure 2).

Mitochondrial complex I and IV activity

Measurements of respiratory chain activities showed no differences in complex I activity in muscle of patients and controls, in either absolute or relative units (data not shown). However, complex IV activity was abnormally decreased in both muscle and PBMCs of sIBM patients with respect to controls (Figure 2). Thus, taking into account absolute values, a decrease of 13.55% was found in muscle (Figure 2). These differences became statistically significant in muscle when complex IV activity was normalized to mitochondrial mass (CS), by showing a 30.31% decrease in sIBM patients compared with controls (0.26 ± 0.02 vs 0.33 ± 0.03 , $P < 0.05$; Figure 2). On analysing this parameter in PBMCs, complex IV activity was also significantly decreased by 31.4% in absolute values in patients compared with controls (24.32 ± 3.1 vs 35.45 ± 3.4 , $P < 0.05$; Figure 2) and by 28.21%

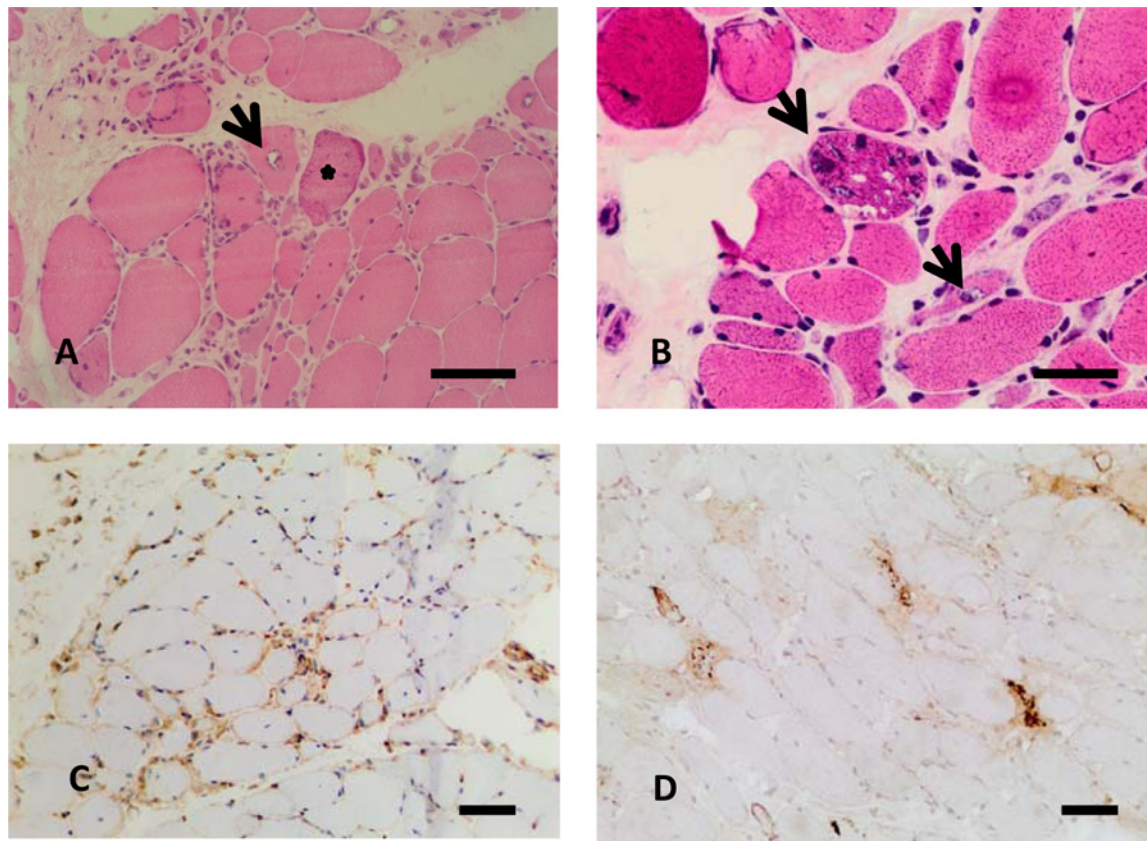


Figure 1 Images from the histological staining of sIBM muscle tissue

(A, B) H&E in frozen muscle tissue: marked variability in fibre size. Some inflammatory cells are observed in the endomysium, together with rimmed vacuoles (arrows) and a typical ragged-red fibre (star). (C) Almost universal sarcolemmal positivity of class I antigen from the MHC, a typical feature in sIBM. (D) Positivity of p62 in rimmed vacuoles, suggestive of muscle degeneration. Scale bar=50 μ m.

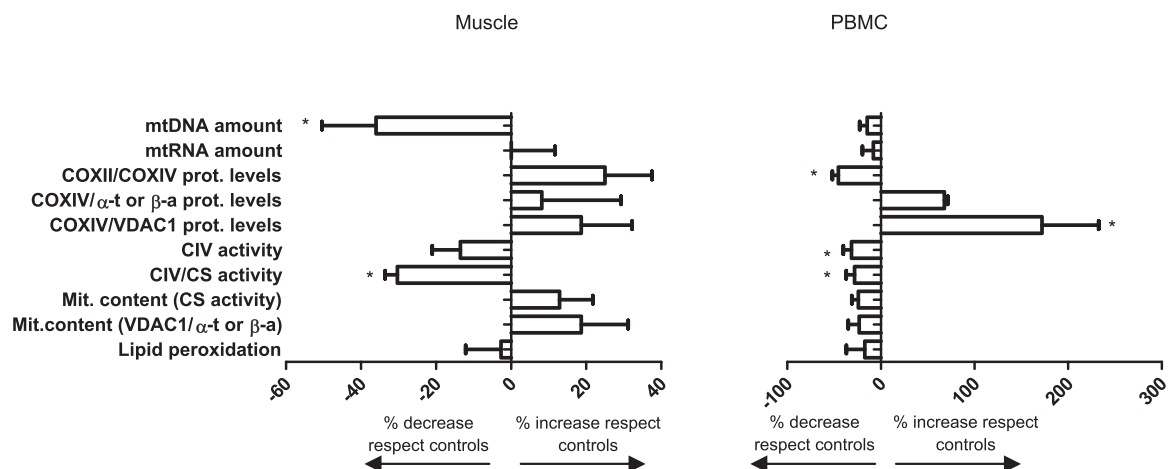


Figure 2 Mitochondrial parameters in muscle tissue and PBMCs from sIBM patients compared with controls

Mitochondrial parameters in muscle tissue and PBMCs from patients with sIBM expressed as percentage of increase/decrease compared with controls. A significant decrease in mtDNA amount and complex IV activity normalized to mitochondrial content can be observed in muscle, and also a significant decrease in COX-II:COX-IV ratio, complex IV absolute activity and complex IV activity normalized to mitochondrial content can be observed in PBMCs. In this muscle tissue, a significant increase in COX-IV subunit normalized to mitochondrial content can be observed as well as other non-significantly altered parameters. α -t, α -tubulin; β -a, β -actin; C-IV, MRC complex IV. * : $p < 0.05$.

when this parameter was normalized to the mitochondrial mass (0.28 ± 0.1 vs 0.39 ± 0.1 , $P < 0.05$; Figure 2).

MRC complexes assembly

The analysis of the subunit levels for each complex of the MRC (I–V) that correlates with the proper assembly of the respiratory chain complexes did not show differences between sIBM patients and controls, normalized to either total protein or VDAC1 content. It is interesting that the complex V subunit presented a trend towards a decrease in sIBM patients, but this difference did not reach statistical significance (Figure 3).

Mitochondrial mass content

Mitochondrial mass, assessed by both the quantification of CS enzyme activity and VDAC1 protein content, was increased in muscle of sIBM patients compared with controls (12.9% in CS activity and 18.7% in VDAC1: α -tubulin protein levels; see Figure 2) and decreased in PBMCs of sIBM patients compared with controls (by 24.18% in CS activity and 23.26% in VDAC1: β -actin protein content; see Figure 2). However, none of these results was statistically significant.

Oxidative stress levels

No differences were found in lipid peroxidation, an indicator of oxidative damage produced by ROS in lipid compounds, between sIBM patients and controls in muscle or PBMCs (see Figure 2).

Quantification of mitochondrial dynamics

Transcript levels of OPA1 showed a significant 37% reduction in muscle of sIBM patients compared with controls (0.59 ± 0.11 vs 0.94 ± 0.19 , $P < 0.05$; Figure 4). OPA1 long:short protein isoform ratios, although not significant, were decreased by 45% in muscle of sIBM patients compared with controls (0.55 ± 0.17 vs 1 ± 0.16 , $P < 0.083$; Figure 4). In the case of MFN2 transcripts, muscle of sIBM patients showed a 31% reduction. With regard to MFN2 protein expression, a strong trend towards a decrease was observed in sIBM patients, with 54% compared with controls (1.93 ± 0.3 vs 4.17 ± 0.1 , $P = 0.096$; Figure 4). The differences in MFN2 levels in either transcript or protein content were not statistically significant.

Correlation of mitochondrial parameters with regard to the presence/absence of mtDNA deletions

Last, the sIBM cohort was divided into two groups on the basis of the presence or absence of mtDNA deletions for further exploration of mitochondrial homeostasis, depending on this condition with respect to controls. The mtDNA content was slightly decreased in sIBM patients with mtDNA deletions compared with those without (Figure 5). These differences became statistically significant in sIBM patients with deletions with respect to the control group (498.50 ± 178.70 vs 979.70 ± 111.38 , $P < 0.05$). MFN2 levels showed a similar pattern to those of mtDNA content, showing the lowest content in sIBM patients with mtDNA deletions and the highest in controls (1.16 ± 0.24 vs 4.17 ± 0.96 , $P < 0.05$), with sIBM patients without mtDNA deletions presenting an intermediate value of expression (Figure 5).

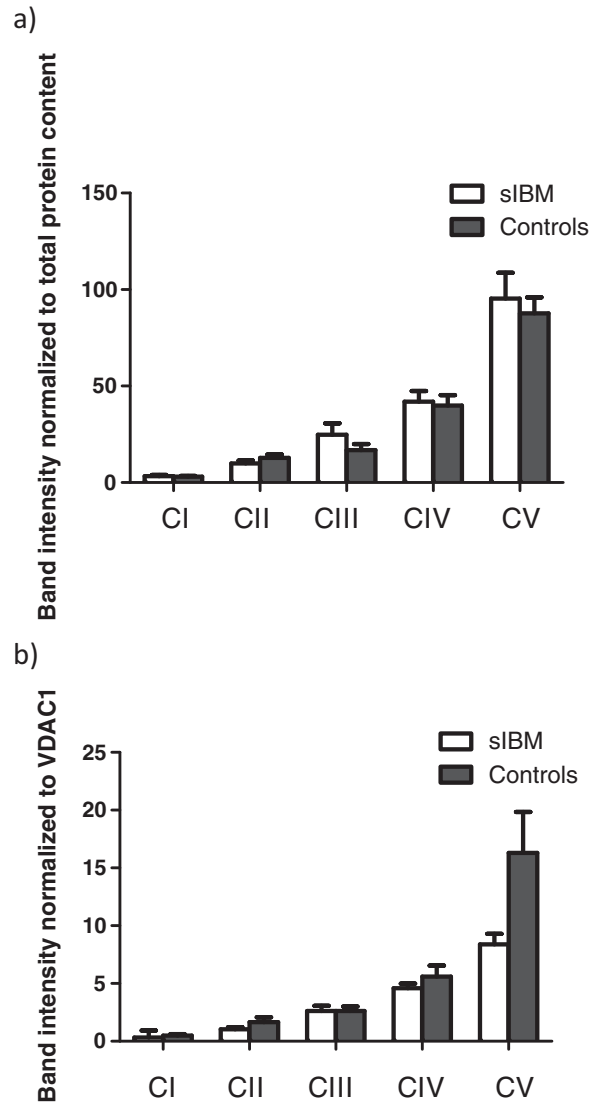


Figure 3 MRC complex assembly through the measurement of protein expression level of labile subunits of each complex in muscle tissue from sIBM patients compared with controls

No significant differences with regard to levels of specific subunits for each MRC complex were found between muscle from sIBM patients and muscle from controls, normalized to (a) total protein content and (b) the nuclear-encoded mitochondrial protein VDAC1. A trend towards increase is observed in the complex V subunit when normalized to VDAC1 which, although not significant, may give us an idea of complex V disassembly. This multiplex Western blotting measures the protein expression level of a subunit of each MRC complex (I–V), labile when the complex is not properly assembled; the following were measured: NDFUF8 from complex I (CI; 20 kDa), SDHB from complex II (CII; 30 kDa), UQCRC2 from complex III (CIII; 48 kDa), MTCO1 from complex IV (CIV; 40 kDa) and ATP5A from complex V (CV; 55 kDa).

DISCUSSION

Mitochondrial abnormalities in muscle from sIBM patients are accepted in the scientific community as a result of histological evidence [7,36]. However, little research has been performed to characterize potential functional or molecular mitochondrial

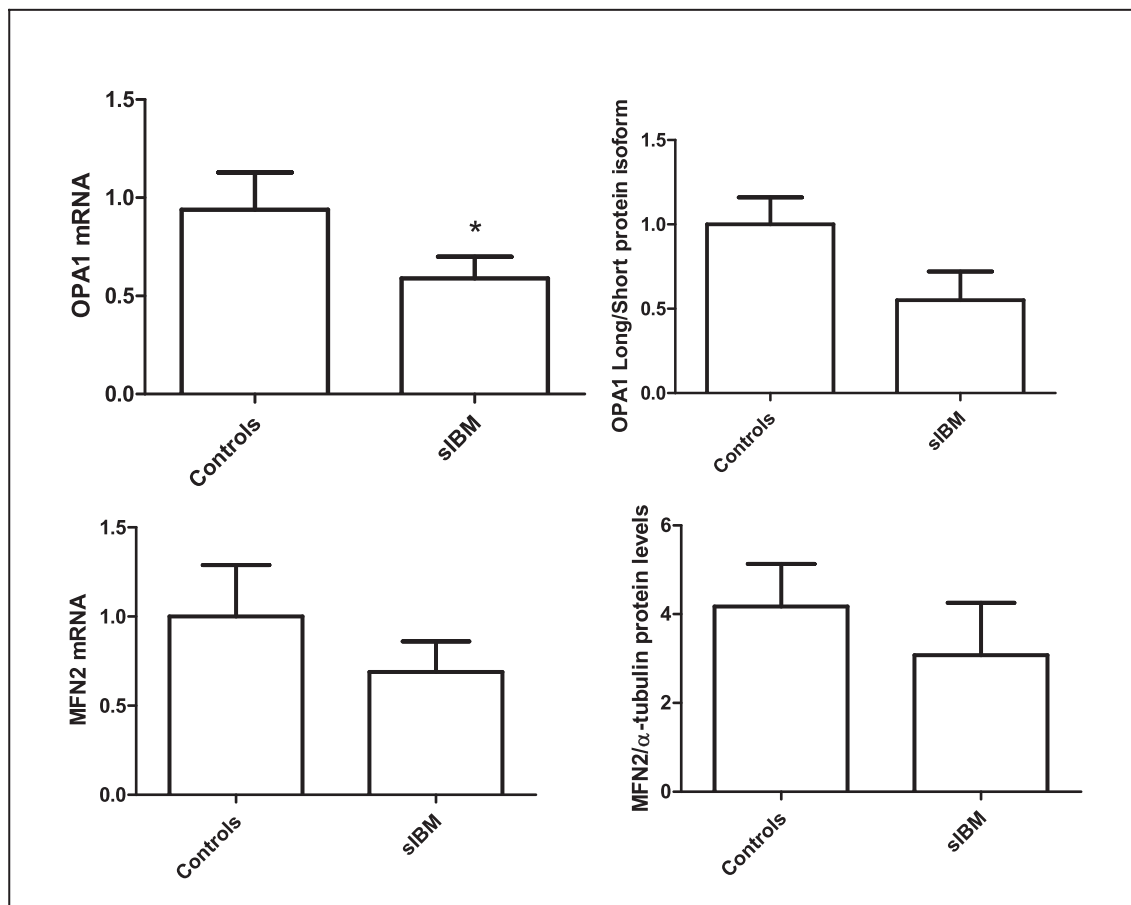


Figure 4 Mitochondrial dynamics in muscle from sIBM patients

MFN2 and OPA1 were assessed in muscle from sIBM patients at the transcript and protein levels. Significant differences were found when OPA1 mRNA levels were compared between the two groups. The other parameters showed a non-significant trend to be decreased in the sIBM respective controls. * : $p < 0.05$.

disrupted pathways [6–8]. In the present study, we evaluated mitochondrial dysfunction at a genetic and molecular level, and studied its potential association with mitochondrial dynamic deregulation. We compared mitochondrial status in muscle and PBMCs from sIBM patients with that of controls, first to evaluate its involvement in disease aetiology and, second, to determine whether mitochondrial alterations are confined to muscle tissue (the target tissue of the disease) or whether these alterations extend to other body tissues, which may allow less invasive approaches and potential follow-up as a putative biomarker.

With regard to experimental data, sIBM patients showed a decrease in mtDNA content. This mtDNA depletion was statistically significant in muscle from sIBM patients, because it is post-mitotic tissue that is prone to store mitochondrial deficiencies. On the other hand, mtDNA depletion was only mildly manifested in PBMCs, probably due to their higher renewal capacity and shorter mean lifespan. Although mtDNA depletion was found in both tissues, no significant changes were observed in mtRNA levels of either muscle or PBMCs [37].

On analysing MRC function, no differences were found in complex I activity in muscle from sIBM patients compared with

controls. Otherwise, MRC complex IV deficiency was present in both tissues (muscle and PBMCs) of sIBM patients. Absolute values of complex IV activity in muscle showed a trend towards a decrease, but, on normalizing these absolute values by mitochondrial mass, complex IV deficiency became significant. These phenomena may be due to the increase in mitochondrial biogenesis detected in muscle of sIBM patients as compensating for mitochondrial dysfunction. This increase in muscular mitochondrial content, characteristic of primary mitochondrial diseases [38], is observed in parallel in sIBM patients as an increase in CS activity and VDAC1:β-actin protein levels, as well as by the presence of ragged-red fibres. Similarly, mitochondrial protein synthesis tended to increase, albeit not significantly, in muscle from sIBM patients (COX-II:COX-IV), probably as a consequence of the trend of this homeostatic muscle to increase mitochondrial biogenesis. As mentioned previously, PBMCs present a shorter mean lifespan, thereby hindering the development of homeostatic mechanisms such as increasing mitochondrial content to deal with mitochondrial dysfunction. Thus, in PBMCs, complex IV activity was found to be significantly decreased in both absolute and relative values to mitochondrial

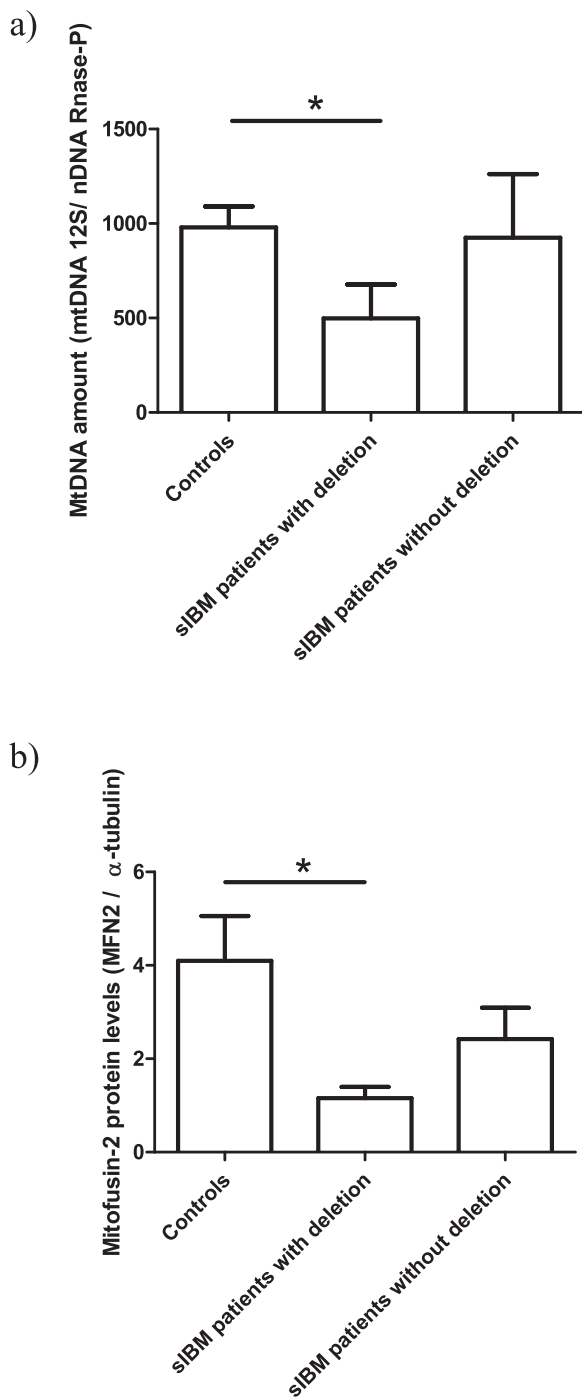


Figure 5 MtDNA amount and MFN2 protein levels in muscle of sIBM patients with and without mtDNA deletions and controls

Comparison of (a) mtDNA amount and (b) MFN2 levels among patients with sIBM with and without mtDNA deletions and controls. The patients with sIBM and mtDNA deletions showed significantly reduced muscle levels of mtDNA and MFN2 protein levels with respect to the controls. The patients with sIBM and no mtDNA deletions presented an intermediate value, suggesting the implication of mtDNA deletions in other mitochondrial alterations or the involvement of mitochondrial dynamics in mtDNA homeostasis. *: $p < 0.05$.

mass, which additionally showed trends towards a decrease, according to poor homeostatic compensation. Unlike in muscle,

in PBMC nuclear-encoded protein subunits of COX (COX-IV) were slightly increased to compensate for COX dysfunction. The trends towards up-regulation of mitochondrially encoded proteins in muscle or nuclear-encoded proteins in PBMCs, to compensate for MRC dysfunction, may depend on the levels of endoplasmic reticular stress of both cell types, which has been reported to be altered in muscle [39,40].

Mitochondrial dysfunction in sIBM patients is not caused by abnormal assembly of MRC complexes, at least as assessed through the measurement of protein levels of specific subunits that are labile in cases of complex instability. However, there was a strong trend of the complex V subunit, when normalized to mitochondrial mass, to be decreased. This decrease disappeared when the complex V subunit content was normalized to total cell protein. This could be explained by the slight increase in mitochondrial mass that underlies sIBM. Further analysis of complex V activity could be useful to elucidate whether this complex is altered in this disease.

Oxidative stress does not seem to play a role in sIBM pathogenesis, because lipid peroxidation levels are not increased in muscle or PBMCs from sIBM patients, at least in the present study cohort.

Overall, these data describe an altered mitochondrial phenotype in muscle and PBMCs of sIBM patients, with both tissues presenting a different lesion profile, probably due to different compensatory mechanisms related to the disease. It is interesting, regardless of the homeostatic attempt to preserve mitochondrial function, that COX enzymatic deficiency is present in both tissues as a common pathogenic parallelism. Thus, it seems that mitochondrial dysfunction in sIBM is not confined only to the target tissue of the disease, muscle, but may also extend to other body tissues. Whether COX/CS activity could be used as a prognostic or severity biomarker of the disease should be assessed in further studies. Alternatively, PBMC mitochondrial alterations may be interpreted as a deregulation of the immune system, non-specific for sIBM, as stated before for other diseases with inflammatory components [41–45]. Regardless of the interpretation, mitochondrial impairment is present in both PBMCs and muscle tissue of sIBM patients.

Mitochondrial dynamics are the mechanism for this organelle recycling and turnover. Imbalance of proper ratios of fusion and fission events has recently been associated with disease [13,46,47]. Mitochondrial dynamics were severely altered in muscle of sIBM patients as demonstrated by the decreased expression of OPA1 and MFN2 transcript and protein levels. Deregulation of the mitochondrial fusion:fission ratio leads to abnormal mitochondrial turnover, which is essential for the recycling of damaged and dysfunctional mitochondria [48], such as those characteristic of sIBM patients.

It is interesting that reduced expression of MFN2 in sIBM patients is associated with abnormal mitochondrial genetics (both deletions and depletion). Previous studies have reported the strong dependence of mtDNA maintenance on proper mitochondrial dynamics in physiological conditions [10]. This is the first study to report this association in the context of sIBM disease.

Whether mitochondrial genetic and molecular alterations lead to abnormal mitochondrial dynamics or, on the contrary, to an

imbalance in mitochondrial dynamics underlying the mitochondrial genetic and molecular disturbances is still a matter of debate. In any case, both adverse conditions seem to go hand in hand with the development of sIBM disease.

In summary, in the present study we demonstrate that mitochondria are impaired in sIBM, not only at histological but also at genetic, molecular and functional levels, confirming the involvement of mitochondria in the aetiology of this disease. The lesion is characterized by different patterns in both muscle and PBMCs of sIBM patients, demonstrating that mitochondrial injury is not exclusive to the target tissue of the disease but is also present in peripheral tissues. It is interesting that mitochondrial COX activity normalized by mitochondrial mass is altered in both tissues, highlighting the relevance of this parameter, and the need for further studies on this as a putative candidate diagnostic tool or therapeutic target. In addition, deregulation in mitochondrial dynamics seems to be crucial for mtDNA stability, not only in healthy conditions [10] but also in sIBM disease. Deregulation of mitochondrial dynamics in muscle leads to increased genetic alterations such as mtDNA depletion and multiple deletions, demonstrating that mitochondrial turnover is essential for proper mitochondrial health and, furthermore, for muscle function. Although further investigation is needed to demonstrate whether mitochondrial alterations are primary or secondary in sIBM, the present study provides more in-depth understanding of the role of mitochondria in this disease. It also provides knowledge related to the mechanisms implicated in order to help develop new diagnostic tools or therapeutic targets for this disease, in the absence of non-invasive diagnostic tools or effective therapy.

CLINICAL PERSPECTIVES

- The better understanding of how mitochondria is in sIBM would be useful at clinical level at different levels: to confirm that mitochondrial changes seen in the muscle biopsy of sIBM patients is a solid marker to help diagnose this disease.
- This information could be useful to develop new therapeutical strategies to treat muscle dysfunction in sIBM patients.
- The knowledge about the pathogenic mechanisms of the disease allow us to elaborate a more accurate description of the disease for the patient, as they could be able to know about the disease they're suffering.

AUTHOR CONTRIBUTION

J.M. Grau, along with F. Cardellach and G. Garrabou, conceived the study and supervised the data collection and analysis. J.M. Grau was responsible for the diagnosis and inclusion of all patients, performed the IBMFRS test and collected all the clinical data with the help of C. Morén. M. Catalán-García was responsible for the experimental analysis of the amounts of mtDNA and mtRNA (with the help of M. Bañó and J. Enrich-Bengoá), for the analysis of the MRC complex IV activity and CS activity (with the help of A. Hernando), for the analysis of the oxidative stress and mitochondrial protein synthesis (with the help of M. Guitart-Mampel and I. González-Casacuberta), and for the analysis of mitochondrial mass

by Western blotting (with the help of D.-L. Juárez). MtDNA deletions were assessed by our collaborators S. Emperador and J. Montoya, and mitochondrial dynamics-related proteins were analysed through collaboration with A. Díaz-Ramos and A. Zorzano. E. Tobías provided technical assistance for reactive preparation. M. Catalán-García created a database to collect all clinical and experimental parameters and performed the statistical analysis of the data, under the supervision of G. Garrabou and C. Morén. All authors, especially G. Garrabou, J.M. Grau, J. Montoya and A. Zorzano, participated in the revision of the manuscript, adding new concepts of high relevance.

ACKNOWLEDGEMENTS

We would like to specially thank Fundació CELLEX for funding this project and to the extraordinary generosity of sIBM patients and families.

FUNDING

This study has been funded by Instituto de Salud Carlos III (ISCIII) [PI14/00005, PI15/00903, PI15/00817 and PIE1400061] and Fondo Europeo de Desarrollo Regional (FEDER), Suports a Grups de Recerca de la Generalitat de Catalunya [SGR 2014/376], La Marató [87/C/2015], Fundació CELLEX and CIBER of Rare Diseases (CIBERER, an initiative of ISCIII).

REFERENCES

- 1 Catalan, M., Selva-O'Callaghan, A. and Grau, J.M. (2014) Diagnosis and classification of sporadic inclusion body myositis (sIBM). *Autoimmun. Rev.* **13**, 363–366 [CrossRef PubMed](#)
- 2 Needham, M., Corbett, A., Day, T, Christiansen, F., Fabian, V. and Mastaglia, F.L. (2008) Prevalence of sporadic inclusion body myositis and factors contributing to delayed diagnosis. *J. Clin. Neurosci.* **15**, 1350–1353 [CrossRef PubMed](#)
- 3 Mastaglia, F.L. (2009) Sporadic inclusion body myositis: variability in prevalence and phenotype and influence of the MHC. *Acta Myol* **28**, 66–71 [PubMed](#)
- 4 Vattemi, G., Mirabella, M., Guglielmi, V., Lucchini, M., Tomelleri, G., Ghirardello, A. and Doria, A. (2014) Muscle biopsy features of idiopathic inflammatory myopathies and differential diagnosis. *Autoimmun. Highlights* **5**, 77–85 [CrossRef](#)
- 5 Hu, J., Li, N., Yuan, J.H., Zhao, Z., Shen, H.R. and Mei, L. (2007) [A clinical and pathological analysis of inclusion body myositis.] *Zhonghua nei ke za zhi.* **46**, 658–660 [PubMed](#)
- 6 Joshi, P.R., Vetterke, M., Hauburger, A., Tacik, P, Stoltenburg, G. and Hanisch, F. (2014) Functional relevance of mitochondrial abnormalities in sporadic inclusion body myositis. *J. Clin. Neurosci.* **21**, 1959–1963 [CrossRef PubMed](#)
- 7 Rygiel, K.A., Miller, J., Grady, J.P, Rocha, M.C., Taylor, R.W. and Turnbull, D.M. (2014) Mitochondrial and inflammatory changes in sporadic inclusion body myositis. *Neuropathol. Appl. Neurobiol.* **41**, 288–303 [CrossRef](#)
- 8 Moslemi, A.R., Lindberg, C. and Oldfors, A. (1997) Analysis of multiple mitochondrial DNA deletions in inclusion body myositis. *Hum. Mut.* **10**, 381–386 [CrossRef](#)
- 9 Mishra, P and Chan, D.C. (2014) Mitochondrial dynamics and inheritance during cell division, development and disease. *Nat. Rev. Mol. Cell Biol.* **15**, 634–646 [CrossRef PubMed](#)

- 10 Chen, H., Vermulst, M., Wang, Y.E., Chomyn, A., Prolla, T.A., McCaffery, J.M. and Chan, D.C. (2010) Mitochondrial fusion is required for mtDNA stability in skeletal muscle and tolerance of mtDNA mutations. *Cell* **141**, 280–289 [CrossRef](#) [PubMed](#)
- 11 Vielhaber, S., Debska-Vielhaber, G., Peeva, V., Schoeler, S., Kudin, A.P., Minin, I., Minin, I., Schreiber, S., Dengler, R., Kollewe, K. et al. (2013) Mitofusin 2 mutations affect mitochondrial function by mitochondrial DNA depletion. *Acta Neuropathol.* **125**, 245–256 [CrossRef](#) [PubMed](#)
- 12 Chen, K.H., Dasgupta, A., Ding, J., Indig, F.E., Ghosh, P and Longo, D.L. (2014) Role of mitofusin 2 (Mfn2) in controlling cellular proliferation. *FASEB J* **28**, 382–394 [CrossRef](#) [PubMed](#)
- 13 Ni, H.M., Williams, J.A. and Ding, W.X. (2015) Mitochondrial dynamics and mitochondrial quality control. *Redox Biol.* **4**, 6–13 [CrossRef](#) [PubMed](#)
- 14 Dorn, G.W., 2nd, Vega, R.B. and Kelly, D.P. (2015) Mitochondrial biogenesis and dynamics in the developing and diseased heart. *Genes Dev* **29**, 1981–1991 [CrossRef](#) [PubMed](#)
- 15 Guedes-Dias, P., Pinho, B.R., Soares, T.R., de Proenca, J., Duchen, M.R. and Oliveira, J.M. (2016) Mitochondrial dynamics and quality control in Huntington's disease. *Neurobiol. Dis.* **90**, 51–57 [CrossRef](#) [PubMed](#)
- 16 Liesa, M., Palacin, M. and Zorzano, A. (2009) Mitochondrial dynamics in mammalian health and disease. *Physiol. Rev.* **89**, 799–845 [CrossRef](#) [PubMed](#)
- 17 Gang, Q., Bettencourt, C., Machado, P., Hanna, M.G. and Houlden, H. (2014) Sporadic inclusion body myositis: the genetic contributions to the pathogenesis. *Orphanet J. Rare Dis.* **9**, 88 [CrossRef](#) [PubMed](#)
- 18 Muller, F.L., Song, W., Jang, Y.C., Liu, Y., Sabia, M., Richardson, A. and Van Remmen, H. (2007) Denervation-induced skeletal muscle atrophy is associated with increased mitochondrial ROS production. *Am. J. Physiol. Regul. Integr. Compar. Physiol.* **293**, R1159–R1168 [CrossRef](#)
- 19 Sunitha, B., Gayathri, N., Kumar, M., Keshava Prasad, T.S., Nalini, A., Padmanabhan, B. and Srinivas Bharath, M.M. (2016) Muscle biopsies from human muscle diseases with myopathic pathology reveal common alterations in mitochondrial function. *J. Neurochem.* **138**, 174–191 [CrossRef](#) [PubMed](#)
- 20 Sivakumar, K., Vasconcelos, O., Goldfarb, L. and Dalakas, M.C. (1996) Late-onset muscle weakness in partial phosphofructokinase deficiency: a unique myopathy with vacuoles, abnormal mitochondria, and absence of the common exon 5/intron 5 junction point mutation. *Neurology* **46**, 1337–1342 [CrossRef](#) [PubMed](#)
- 21 Moren, C., Garrabou, G., Noguera-Julian, A., Rovira, N., Catalan, M., Hernandez, S., Tobías, E., Cardellach, F., Fortuny, C. and Miró, Ò. (2013) Study of oxidative, enzymatic mitochondrial respiratory chain function and apoptosis in perinatally HIV-infected pediatric patients. *Drug Chem. Toxicol.* **36**, 496–500 [CrossRef](#) [PubMed](#)
- 22 Garrabou, G., Hernandez, A.S., Catalan Garcia, M., Moren, C., Tobias, E., Cordoba, S., López, M., Figueras, F., Grau, J.M. and Cardellach, F. (2016) Molecular basis of reduced birth weight in smoking pregnant women: mitochondrial dysfunction and apoptosis. *Addict. Biol.* **21**, 159–170 [CrossRef](#) [PubMed](#)
- 23 Liu, K., Sun, Y., Liu, D., Yin, J., Qiao, L., Shi, Y., Dong, Y., Li, N., Zhang, F. and Chen, D. (2013) Mitochondrial toxicity studied with the PBMC of children from the Chinese national pediatric highly active antiretroviral therapy cohort. *PLoS One* **8**, e57223 [CrossRef](#) [PubMed](#)
- 24 Houston, M.J. (2007) Muscle Biopsy. A practical approach. Elsevier **1**, 4160 2593 6
- 25 Rose, M.R., ENMC IBM Working Group (2013) 188th ENMC International Workshop: Inclusion Body Myositis. 2–4 December 2011, Naarden, The Netherlands. *Neuromuscul. Dis.* **23**, 1044–1055 [CrossRef](#)
- 26 Ascaso, F.J., Lopez-Gallardo, E., Del Prado, E., Ruiz-Pesini, E. and Montoya, J. (2010) Macular lesion resembling adult-onset vitelliform macular dystrophy in Kearns–Sayre syndrome with multiple mtDNA deletions. *Clin. Exp. Ophthalmol.* **38**, 812–816 [CrossRef](#)
- 27 Carod-Artal, F.J., Lopez Gallardo, E., Solano, A., Dahmani, Y., Herrero, M.D. and Montoya, J. (2006) [Mitochondrial DNA deletions in Kearns–Sayre syndrome.]. *Neurología* **21**, 357–364 [PubMed](#)
- 28 Solano, A., Russo, G., Playan, A., Parisi, M., DiPietro, M., Scuderi, A., Palumbo, M., Renis, M., López-Pérez, M.J., Andreu, A.L. and Montoya, J. (2004) De Toni–Debre–Fanconi syndrome due to a palindrome-flanked deletion in mitochondrial DNA. *Pediatr. Nephrol.* **19**, 790–793 [CrossRef](#) [PubMed](#)
- 29 Montero, R., Grazina, M., Lopez-Gallardo, E., Montoya, J., Briones, P., Navarro-Sastre, A., Land, J.M., Hargreaves, I.P., Artuch, R., Coenzyme Q₁₀ Deficiency Study Group (2013) Coenzyme Q₁₀ deficiency in mitochondrial DNA depletion syndromes. *Mitochondrion* **13**, 337–341 [CrossRef](#) [PubMed](#)
- 30 Moren, C., Noguera-Julian, A., Garrabou, G., Rovira, N., Catalan, M., Bano, M., Guitart-Mampel, M., Tobías, E., Hernández, S., Cardellach, F. et al. (2015) Mitochondrial disturbances in HIV pregnancies. *AIDS* **29**, 5–12 [CrossRef](#) [PubMed](#)
- 31 Moren, C., Noguera-Julian, A., Garrabou, G., Catalan, M., Rovira, N., Tobias, E., Cardellach, F., Miró, Ò. and Fortuny, C. (2012) Mitochondrial evolution in HIV-infected children receiving first- or second-generation nucleoside analogues. *J. Acquir. Immune Defic. Syndr.* **60**, 111–116 [CrossRef](#) [PubMed](#)
- 32 Spinazzi, M., Casarin, A., Pertegato, V., Salviati, L. and Angelini, C. (2012) Assessment of mitochondrial respiratory chain enzymatic activities on tissues and cultured cells. *Nat. Protoc.* **7**, 1235–1246 [CrossRef](#) [PubMed](#)
- 33 Garrabou, G., Moren, C., Lopez, S., Tobias, E., Cardellach, F., Miro, O. and Casademont, J. (2012) The effects of sepsis on mitochondria. *J. Infect. Dis.* **205**, 392–400 [CrossRef](#) [PubMed](#)
- 34 Sebastian, D., Hernandez-Alvarez, M.I., Segales, J., Sorianello, E., Munoz, J.P., Sala, D., Waget, A., Liesa, M., Paz, J.C., Gopalacharyulu, P. et al. (2012) Mitofusin 2 (Mfn2) links mitochondrial and endoplasmic reticulum function with insulin signaling and is essential for normal glucose homeostasis. *Proc. Natl. Acad. Sci. U.S.A.* **109**, 5523–5528 [CrossRef](#) [PubMed](#)
- 35 Hernandez-Alvarez, M.I., Thabit, H., Burns, N., Shah, S., Brema, I., Hatunic, M., Finucane, F., Liesa, M., Chiellini, C., Naon, D. et al. (2010) Subjects with early-onset type 2 diabetes show defective activation of the skeletal muscle PGC-1 α /Mitofusin-2 regulatory pathway in response to physical activity. *Diabetes Care* **33**, 645–651 [CrossRef](#) [PubMed](#)
- 36 Oldfors, A., Moslemi, A.R., Jonasson, L., Ohlsson, M., Kollberg, G. and Lindberg, C. (2006) Mitochondrial abnormalities in inclusion-body myositis. *Neurology* **66** (2 Suppl 1), S49–S55 [CrossRef](#) [PubMed](#)
- 37 Herbst, A., Pak, J.W., McKenzie, D., Bua, E., Bassiouni, M. and Aiken, J.M. (2007) Accumulation of mitochondrial DNA deletion mutations in aged muscle fibers: evidence for a causal role in muscle fiber loss. *J. Gerontol. A Biol. Sci. Med. Sci.* **62**, 235–245 [CrossRef](#) [PubMed](#)
- 38 Challa, S., Kanikannan, M.A., Murthy, J.M., Bhoompally, V.R. and Surath, M. (2004) Diagnosis of mitochondrial diseases: clinical and histological study of sixty patients with ragged red fibers. *Neurol. India* **52**, 353–358 [PubMed](#)
- 39 Nogalska, A., D'Agostino, C., Terracciano, C., Engel, W.K. and Askanas, V. (2010) Impaired autophagy in sporadic inclusion-body myositis and in endoplasmic reticulum stress-provoked cultured human muscle fibers. *Am. J. Pathol.* **177**, 1377–1387 [CrossRef](#) [PubMed](#)

- 40 Nogalska, A., D'Agostino, C., Engel, W.K., Cacciottolo, M., Asada, S., Mori, K. and Askanas, V. (2015) Activation of the unfolded protein response in sporadic inclusion-body myositis but not in hereditary GNE inclusion-body myopathy. *J. Neuropathol. Exp. Neurol.* **74**, 538–546
[CrossRef](#) [PubMed](#)
- 41 Tezel, G., Fourth ARVO/Pfizer Ophthalmics Research Institute (2009) The role of glia, mitochondria, and the immune system in glaucoma. *Invest. Ophthalmol. Vis. Sci.* **50**, 1001–1012
[CrossRef](#) [PubMed](#)
- 42 Lartigue, L. and Faustin, B. (2013) Mitochondria: metabolic regulators of innate immune responses to pathogens and cell stress. *Int. J. Biochem. Cell Biol.* **45**, 2052–2056
[CrossRef](#) [PubMed](#)
- 43 West, A.P., Shadel, G.S. and Ghosh, S. (2011) Mitochondria in innate immune responses. *Nat. Rev. Immunol.* **11**, 389–402
[CrossRef](#) [PubMed](#)
- 44 Walker, M.A., Volpi, S., Sims, K.B., Walter, J.E. and Traggiai, E. (2014) Powering the immune system: mitochondria in immune function and deficiency. *J. Immunol. Res.* **2014**, 164309
[CrossRef](#) [PubMed](#)
- 45 Gomez, L., Raisky, O., Chalabreysse, L., Verschelde, C., Bonnefoy-Berard, N. and Ovize, M. (2006) Link between immune cell infiltration and mitochondria-induced cardiomyocyte death during acute cardiac graft rejection. *Am. J. Transpl.* **6**, 487–495
[CrossRef](#)
- 46 Santel, A. (2006) Get the balance right: mitofusins roles in health and disease. *Biochim. Biophys. Acta* **1763**, 490–499
[CrossRef](#) [PubMed](#)
- 47 Burte, F., Carelli, V., Chinnery, P.F. and Yu-Wai-Man, P. (2015) Disturbed mitochondrial dynamics and neurodegenerative disorders. *Nat. Rev. Neurol.* **11**, 11–24 [CrossRef](#) [PubMed](#)
- 48 Detmer, S.A. and Chan, D.C. (2007) Functions and dysfunctions of mitochondrial dynamics. *Nat. Rev. Mol. Cell Biol.* **8**, 870–879
[CrossRef](#) [PubMed](#)

Received 3 February 2016/5 July 2016; accepted 13 July 2016

Accepted Manuscript online 13 July 2016, doi: 10.1042/CS20160080

33

Drug-Induced Mitochondrial Toxicity during Pregnancy

Diana Luz Juárez-Flores^{1,3}, Ana Sandra Hernández^{2,3}, Laura García-Otero², Mariona Guitart-Mampel^{1,3}, Marc Catalán-García^{1,3}, Ingrid González-Casacuberta^{1,3}, Jose César Milisenda^{1,3}, Josep Maria Grau^{1,3}, Francesc Cardellach^{1,3}, Constanza Morén^{1,3}, and Glòria Garrabou^{1,3,*}

¹ Muscle Research and Mitochondrial Function Laboratory, Cellex-IDIBAPS, Faculty of Medicine and Health Sciences-University of Barcelona, Internal Medicine Department-Hospital Clínic of Barcelona (HCB), Barcelona, Spain

² BCNatal—Barcelona Center for Maternal-Fetal and Neonatal Medicine (Hospital Clínic and Hospital Sant Joan de Deu), IDIBAPS, University of Barcelona, Barcelona, Spain

³ CIBERER, Madrid, Spain

CHAPTER MENU

- 33.1 Mitochondria in Human Fertility, 510
- 33.2 Mitochondrial Toxicity in Human Pregnancy, 510
- 33.3 Therapeutic Approach of Drug-Induced Mitochondriopathies, 515
- 33.4 Conclusions, 516
 - Funding, 516
 - References, 517

Mitochondria are the powerhouse of the cell. Their main function is energy production coupled to cell respiration in the mitochondrial respiratory chain (MRC). They also have other important functions including lipid, carbohydrate, or protein catabolism, steroid and heme group synthesis, calcium homeostasis, and thermogenesis. However, under pathogenic conditions, mitochondria are a major source of reactive oxygen species (ROS) production and a key factor in the induction of apoptosis (Scheffler 2008; Herst et al. 2017).

Mitochondria are present in most cells of our body, so that impairment of mitochondrial bioenergetics, biogenesis, dynamics, or turnover may endanger cell survival and tissue homeostasis, leading to organ failure and ultimately threatening the life of the patient (Garrabou et al. 2011).

Importantly, they are critical in maintaining the energetic and metabolic supply essential for fertilization, implantation, and embryo development, all of which are highly energy-demanding processes, as are embryonic

cell division, migration, and differentiation. Moreover, they also regulate apoptosis development when selective pruning is crucial for successful embryo development (Nunnari et al. 2012). Consequently, any toxic agent for mitochondria is potentially able to impair oocyte or fetal viability, hampering fertility and prompting further obstetric complications.

Mitochondria contain their own genetic material encoding for 13 MRC proteins (Anderson et al., 1981), while the remaining mitochondrial proteins (thousands in mammals) are encoded by the nucleus. Therefore, intergenomic communication between these two sites is essential for normal mitochondrial function and physiologic processes as pregnancy develops. Some characteristics of primary mitochondrial diseases may arise in the case of xenobiotic mitochondrial toxicities. For instance, in the presence of mitochondrial embryonic alterations at the genetic level, wild-type and mutated mitochondrial DNA (mtDNA) molecules may coexist within a given mitochondria and cell (heteroplasmy). In this case, the type, severity, and onset of clinical manifestations derived from mitochondrial impairment will depend on

*Both authors equally contributed.

the number of mutated molecules (threshold effect) and differential distribution of these mutated mitochondrial genomes within the various tissues (mitotic segregation), all of which underlie the clinical complexity of mitochondrial toxic disorders (Garrabou et al. 2011). We should not forget that genetic lesions in nuclear DNA can also have mitochondrial consequences independent of mitochondrial genetics and that direct interference of alternative pathways independent of genetics may also arise (e.g., by interfering MRC function, altering oxidative stress or protein synthesis) (Pon and Schon 2007).

In the context of pregnancy, mitochondrial toxicity may be manifested and exclusively restricted to the carrying mother (maternal toxicity) or may be translated into the embryo (fetal toxicity). It can be manifested as infertility, as early pregnancy loss (in case of interference with implantation processes), or as obstetric complications during pregnancy (in case of further interference into fetal development). Fortunately, only few cases of lethal consequences for the newborn have been reported as due to mitochondrial toxicity (Nau et al. 1981; Poirier et al. 2015). However, milder forms of mitochondrial toxicity have been described (Barret et al. 2003; Hernández et al. 2012; Morén et al. 2015; Noguera-Julian et al. 2015; Hernandez et al. 2016), which may further contribute to the development of diseases during adulthood, such as injurious fetal cardiac remodeling (Barker 1999; Crispi et al. 2010; García-Otero et al. 2016; Timpka et al. 2016).

Many compounds can yield mitochondrial damage, and some of them are widely and frequently used in clinical settings. As discussed in this book, off-target effects of drugs can yield mitochondrial toxicity with clinical consequences, and it is a justified inference that such toxicity may entail severe consequences during fertile stages and pregnancy, taking into account that many drugs are able to cross the placental barrier and reach the fetus.

Herein we describe the mechanisms of action and potential secondary mitochondrial effects of drugs currently used in clinical practice during pregnancy in an attempt to increase awareness and caution about their management.

33.1 Mitochondria in Human Fertility

In vitro fertilization studies in humans have demonstrated that adequate mitochondrial function is essential for successful egg fertilization and uterine implantation, the first steps of fetal development (Reynier et al. 2001; Jansen and Burton 2004; Santos et al. 2006). Indeed, mitochondria are maternally inherited, and the oocyte is the sole gamete responsible for providing the mitochondrial population for the future embryo. They also affect male fertility since, although spermatozoa do not provide mitochondria to the future embryo, mitochondrial function is

essential for flagellum motility and, thus, fertilization (Guo et al. 2017). Consequently, reproductive gametes are highly susceptible to mitochondrial toxicity.

The mitochondrial bottleneck, defined as the reduction of the number of mtDNA molecules per mitochondria during meiotic oogenesis, is also crucial in the development of the future embryo (Stewart and Chinnery 2015). Briefly, mitochondrial number increases during oogenesis, accounting for approximately 23% of the ooplasm at the end of the process (Santos et al. 2006), which represents up to 100,000 mitochondria per mature oocyte. However, although the number of mitochondria increases, mtDNA levels remain constant, resulting in reduced mtDNA content per mitochondria, estimated into 100,000-600,000 molecules per mature oocyte. The aim of this evolutionary strategy is to ensure the presence of only a few molecules of mtDNA per mitochondrion to avoid heteroplasmic segregation through the maternal lineage (Santos et al. 2006). This renders the oocyte mitochondria highly susceptible to mtDNA depletion or mutagenic factors, such as infections, environmental toxins, drugs of abuse, and medications, which may exert secondary effects including infertility or obstetric complications (López et al. 2008).

33.2 Mitochondrial Toxicity in Human Pregnancy

33.2.1 Risk Categories of Mitochondrial Toxic Drugs According to their Capacity to Cause Birth Defects during Pregnancy

Once the oocyte is fertilized and implanted, mitochondria remain essential to fuel adequate fetal development. Thus, exposure to mitochondrial hazards should be minimized. Notwithstanding, some therapeutic schedules are unavoidable.

During pregnancy, acute disorders, such as migraine or infectious diseases, may require short-term treatment with potential mitochondrial toxic medication. Similarly, chronic conditions such as epilepsy, depression, or asthma may coexist and require treatment. Mothers are giving birth at increasingly older ages, which in turn increases the likelihood of chronic conditions and coexistence of pathologies associated with pregnancy such as hypertension, diabetes, and mood disorders, among others. Additionally, in early pregnancies, women who are not yet aware of their condition may use medication, increasing the risk of suffering its secondary effects.

The Food and Drug Administration (FDA) (USA) and Therapeutic Goods Administration (TGA) (AU) have established risk categories to indicate the potential of a therapeutic drug, when administered during pregnancy, to cause birth defects. Table 33.1 summarizes risk

Table 33.1 The Food and Drug Administration (FDA) (USA) and Therapeutic Goods Administration (TGA) (AU) classification for mitochondrial toxic drugs potentially used during pregnancy depending on their association to birth defects. Source: Food and Drug Administration (www.fda.gov) and Therapeutic Drugs Administration (<https://www.tga.gov.au/node/4013>)

Food and Drug Administration (USA)	Therapeutic Goods Administration (AU)	Drugs that exert mitochondrial toxicity and may be used in pregnancy
A Adequate and well-controlled studies have failed to demonstrate a risk to the fetus in the first trimester of pregnancy (and there is no evidence of risk in later trimesters)	A Drugs that have been taken by a large number of pregnant women and women of childbearing age without any proven increase in the frequency of malformations or other direct or indirect harmful effects on the fetus having been observed	Erythromycin (TGA), paracetamol (TGA), lidocaine (TGA), miconazole (TGA)
B Animal reproduction studies have failed to demonstrate a risk to the fetus, and there are no adequate and well-controlled studies in pregnant women	B1 Drugs that have been taken by only a limited number of pregnant women and women of childbearing age, without an increase in the frequency of malformation or other direct or indirect harmful effects on the human fetus having been observed. Studies in animals have not shown evidence of an increased occurrence of fetal damage	Erythromycin (FDA), azithromycin (FDA), lidocaine (FDA), didanosine (FDA), saquinavir, nelfinavir (FDA), ritonavir (FDA), nevirapine (FDA), amphotericin B (FDA)
	B2 Drugs that have been taken by only a limited number of pregnant women and women of childbearing age, without an increase in the frequency of malformation or other direct or indirect harmful effects on the human fetus having been observed. Studies in animals are inadequate or may be lacking, but available data show no evidence of an increased occurrence of fetal damage	Didanosine (TGA), nelfinavir (TGA)
	B3 Drugs that have been taken by only a limited number of pregnant women and women of childbearing age, without an increase in the frequency of malformation or other direct or indirect harmful effects on the human fetus having been observed. Studies in animals have shown evidence of an increased occurrence of fetal damage, the significance of which is considered uncertain in humans	Linezolid (TGA), clarithromycin (TGA), clozapine (FDA), stavudine (TGA), zidovudine (TGA), lamivudine (TGA), abacavir (TGA), indinavir (TGA), ritonavir (TGA), nevirapine (TGA), ketoconazole (TGA), amphotericin B (TGA)
C Animal reproduction studies have shown an adverse effect on the fetus, and there are no adequate and well-controlled studies in humans, but potential benefits may warrant use of the drug in pregnant women despite potential risks	C Drugs that, owing to their pharmacological effects, have caused or may be suspected of causing harmful effects on the human fetus or neonate without causing malformations. These effects may be reversible. Accompanying texts should be consulted for further details	Clarithromycin (FDA), rifampicin (FDA), linezolid (FDA), amitriptyline, clomipramine, fluoxetine, sertraline, haloperidol, risperidone, clozapine (TGA), paracetamol (FDA), aspirin (TGA), diazepam (TGA), bupivacaine, zalcitabine (FDA), stavudine (FDA), zidovudine (FDA), lamivudine (FDA), abacavir (FDA), indinavir (FDA), ketoconazole (FDA), miconazole (FDA), amiodarone (TGA)
D There is positive evidence of human fetal risk based on adverse reaction data from investigational or marketing experience or studies in humans, but potential benefits may warrant use of the drug in pregnant women despite potential risks	D Drugs that have caused, or are suspected to have caused or may be expected to cause, an increased incidence of human fetal malformations or irreversible damage. These drugs may also have adverse pharmacological effects. Accompanying texts should be consulted for further details	Aminoglycosides (gentamicin, amikacin), aspirin (FDA), phenytoin, phenobarbital, carbamazepine, valproic acid (TGA), diazepam (FDA), zalcitabine (TGA), amiodarone (FDA)
X Studies in animals or humans have demonstrated fetal abnormalities, and/or there is positive evidence of human fetal risk based on adverse reaction data from investigational or marketing experience, and the risks involved in the use of the drug in pregnant women clearly outweigh potential benefits	X Drugs that have such a high risk of causing permanent damage to the fetus that they should not be used in pregnancy or when there is a possibility of pregnancy	Thiamphenicol, valproic acid (FDA)

Many other therapeutic drugs are responsible for mitochondrial toxicity, but their administration is restricted during pregnancy. FDA and TGA may differ in the classification of the drugs depending on local policies, as stated in Table 33.1. Source: Food and Drug Administration (www.fda.gov) and Therapeutic Drugs Administration (<https://www.tga.gov.au/node/4013>)

categories for drugs administered during pregnancy that have been associated with mitochondrial toxicity. These agents have varying mitochondrial mechanisms of toxicity and potencies, as discussed in this chapter.

In June 2015 the FDA classification was replaced with meaningful information to patients and healthcare providers in order to allow better patient-specific counseling and informed decision making. While the new labeling improves the old format, it still does not provide definitive treatment guidance to avoid adverse events so that clinical interpretation is still required on a case-by-case basis.

33.2.2 Clinical Spectrum of Mitochondrial Toxicity during Pregnancy

Given their ubiquitous distribution and varying energetic demands of different tissues, mitochondrial toxicity can be translated into a wide spectrum of clinical symptoms that, in case of pregnancy, can affect both the maternal and the fetal compartment (Andreu and Gonzalo-Sanz 2004, Blohm 2017). Thus, it is difficult to predict the clinical picture or achieve a definite diagnosis for mitochondrial toxicity, not to mention that there are few avenues for therapeutic management.

Mitochondrial toxicity usually affects those tissues that are most energy demanding, such as the nervous system, cardiac and skeletal muscle, renal, liver, and lymphoid tissues. In the case of nonpregnant adults, the symptoms range from myopathy, neuropathy, encephalopathy, and lactic acidosis to lipodystrophy and sensory pathology such as deafness and blindness (Taylor and Turnbull 2005). However, in the context of pregnancy, mitochondrial insufficiencies have been linked to higher prevalence of obstetric complications including gestational diabetes mellitus, preterm delivery, miscarriage, stillbirth, intrauterine growth restriction, preeclampsia, premature rupture of membranes, or postnatal sudden infant death (Mando et al. 2014).

As seen in Table 33.1, a variety of drugs that are used in the clinical setting may yield mitochondrial toxicity and most of them cross the placental barrier reaching the fetus (Latini et al. 1984; Hendrick et al. 2003; Pacifici 2005, 2006; De Santis et al. 2011; Antonucci et al. 2012; Singh et al. 2016). Of all the drugs herein exposed, the less likely to reach the fetus are local anesthetics and antifungals, mainly due to the limited dosage and local effect, that hamper reaching significant blood concentrations, if any.

Although mitochondrial toxicity is widely documented in nonpregnant adults, little information is known within the context of human pregnancy, particularly in terms of *in utero* exposure and potential impact on fetal development and newborn health. Most of the data are restricted

to *in vitro* studies, cell lines, and animal models, and only few observational studies have been done in patients. Of course, studies are also needed to characterize placental permeability and hence fetal exposures.

Therapeutic drugs exert their mechanism of action through different means and, as a secondary effect of medication, mitochondrial physiology can be disturbed at different levels, such as causing genetic alterations (through depletion, deletions, and/or point mutations), MRC dysfunction (Zhang et al. 1990; Davey et al. 1998), deregulation of oxygen consumption, increase of ROS levels (Wallace and Melov 1998), depolarization of membrane potential, inhibition of mitochondrial protein synthesis (Scatena et al. 2007), imbalance of mitochondrial dynamics, or mitochondrial biogenesis, among others (see Figure 33.1). The different kinds of toxic mechanisms, together with the threshold effect and the mitotic segregation phenomenon, in case of mitochondrial genetic alterations, explain the heterogeneous clinical manifestations observed in exposed pregnant women and their newborn, regardless of similar type, time, and dose exposure to the toxic compound (Gröber 2012).

33.2.3 Classes of Mitochondrial Toxic Drugs Administered during Pregnancy

Numerous drugs have been described to potentially cause mitochondrial toxicity, such as antineoplastics (including flutamide, tamoxifen, and doxorubicin), antifungals (such as sodium azide), antidiabetics (metformin), fibrates, and antimalarials. Since their use is not indicated in pregnancy, the interested reader is referred to other sources of bibliography for a complete description of their off-target effects (Morén et al. 2014, 2016). Rather, the focus of this chapter is the description of drugs potentially administered during pregnancy having potential mitochondrial toxicity and their clinical consequences.

33.2.3.1 Antibiotics

The endosymbiotic origin of mitochondria (Margulis 1975) explains the homology shared between mitochondria and prokaryotes and why some antibiotics can exert off-target mitochondrial damage leading to severe clinical manifestations including fetal death (Lang et al. 1999). This is the case of some antibiotics, including aminoglycosides, rifampicin, linezolid, and macrolides, which act as inhibitors of bacterial and mitochondrial protein synthesis, eventually leading to well-known side effects, including deafness (Torres-Ruiz et al. 2011), peripheral neuropathy (Bressler et al. 2004), hyperlactatemia, or lactic acidosis (Del Pozo et al. 2014) in nonpregnant adults (Hong et al. 2015). Of this class of antibiotics, thiamphenicol has been used for abortive

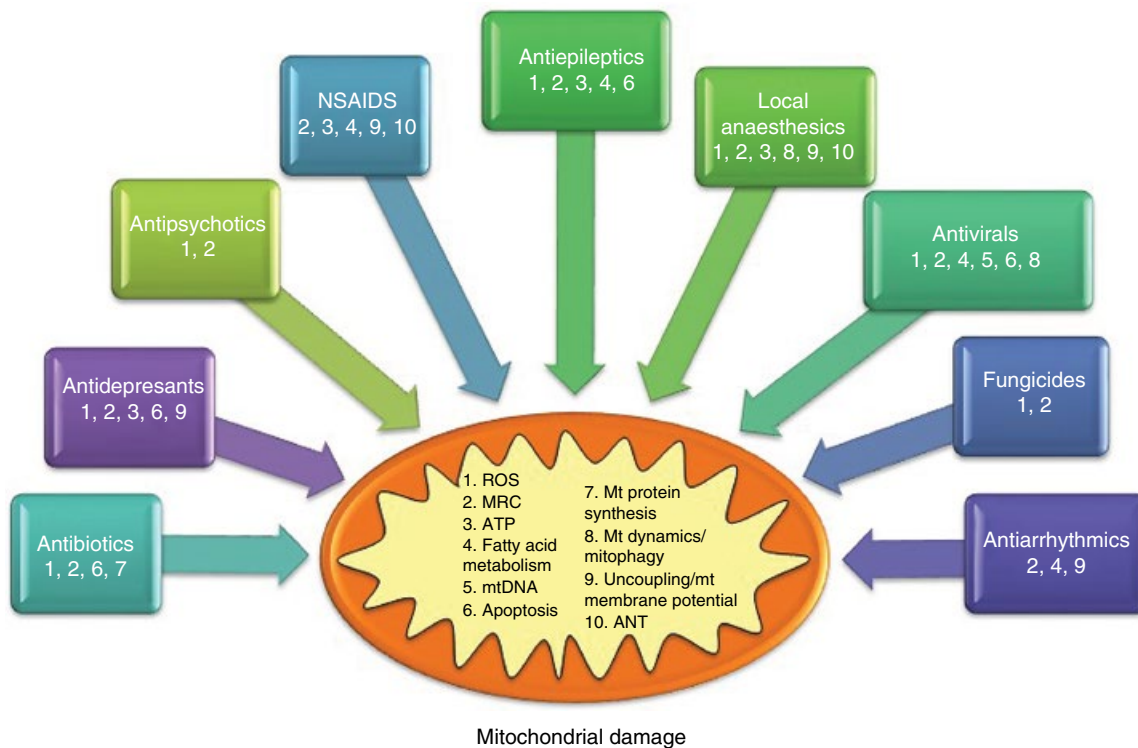


Figure 33.1 Drug-induced mitochondrial toxicity. Different degrees of evidence (in experimental models, nonpregnant humans, or human pregnancies) sustain the mitochondrial toxicity of drugs. The central mitochondria depict 10 mitochondrial alterations caused by exposition to the described drugs. The external squares represent the specific mitochondrial toxicity (in numbers) studied in experimental models (green), in nonpregnant humans (not necessarily excluding studies in experimental models; in purple), or in human pregnancies (not necessarily excluding studies in experimental models or nonpregnant humans; in blue). NOTE: The administration of the aforementioned drugs must always be prescribed by a clinician and only recommended when the therapeutic benefits exceed the potential adverse effects derived from the mitochondrial toxicity of these drugs, which should be closely monitored. ANT, adenine nucleotide translocator; ATP, adenosine triphosphate; MRC, mitochondrial respiratory chain; Mt, mitochondrial; mtDNA, mitochondrial DNA; NSAIDS, nonsteroidal anti-inflammatory drugs; ROS, reactive oxygen species.

purposes due to the severe mitochondrial toxicity for the exposed fetus (Nau et al. 1981). Macrolides, such as erythromycin, have been additionally associated with ROS-induced alteration of potassium channel kinetics, which disrupts cardiomyocyte conductance and enhances apoptosis even at concentrations lower than those to be hepatotoxic in animal models (Guo et al. 2010; Salimi et al. 2016). In population-based studies of nonpregnant adults, macrolides are associated with increased rates of cardiac defects (Bar-Oz et al. 2012; Lin et al. 2013; Bérard et al. 2015), but little is known in the context of human pregnancies.

33.2.3.2 Antidepressants

Depression is the most prevalent of the mental disorders requiring treatment during pregnancy and reproductive age. Tricyclic antidepressants (TCA) such as amitriptyline, clomipramine, and desipramine were the first drugs administered for mood disorders. Their therapeutic effect is achieved by the inhibition of serotonin, norepinephrine, and dopamine reuptake into presynaptic

vesicles in the brain in a nonselective manner, leading to significant side effects, such as memory loss. This type of drugs secondarily inhibits the enzymatic activities of MRC complexes I, II/III, and IV (Abdel-Razaq et al. 2011), thereby increasing oxidative stress and apoptosis in experimental models (Lee et al. 2015).

Selective serotonin reuptake inhibitors (SRIs) are better tolerated than TCA, making them the most widely prescribed antidepressants worldwide. Fluoxetine inhibits mitochondrial respiration at complex I (Hroudová and Fišar 2012), has effects on ATPase activity, and interferes with the physical characteristics of the inner mitochondrial membrane in animal models, which could be responsible for the gastrointestinal discomfort caused by this drug in nonpregnant adults (Curti et al. 1999). It has also been reported that fluoxetine prevents apoptosis by inhibiting mitochondrial permeability transition pore opening and cytochrome *c* release in a cell model (Nahon et al. 2005). However, no adverse effects directly related to fluoxetine have been reported in newborns of exposed women (Riggin et al. 2013). Sertraline uncouples mitochondrial oxidative

phosphorylation and inhibits the activities of CI and V, as demonstrated in an experimental model (Li et al. 2012). Although additional data are needed (Tuccori et al. 2009), sertraline has been shown to induce apoptosis in experimental models (Chen et al. 2014) and has been suggested to be responsible for an increased risk of neonatal pulmonary hypertension (Kieler et al. 2011; Andrade 2012).

Further studies are needed to confirm the safety of TCA and SRIs in the context of human pregnancy.

33.2.3.3 Antipsychotics

Although less prevalent than depression, other mental disorders such as schizophrenia, bipolar disorder, and psychotic depression may develop or become exacerbated during pregnancy. Antipsychotic drugs should be carefully managed in this setting. Mitochondrial toxicity has been reported to be the potential base of extrapyramidal disorders (Casademont et al. 2007), as well as polymorphisms in cytochrome p450 and aging, among others. Antipsychotics have been classically described to inhibit MRC complex I function (Przedborski et al. 1992; Maurer and Möller 1997), leading to an increase of oxidative stress in nonpregnant adults (Martins et al. 2008; Raudenska et al. 2013). Differential severity of molecular and clinical toxicity has been established from high to low potency as follows: haloperidol, risperidone, and clozapine (Casademont et al. 2007). Despite these toxicities, we are unaware of any studies of mitochondrial toxicity of neuroleptic drugs during human pregnancies. It is reported, though, that antipsychotics are associated with increased gestational weight and diabetes as well as with increased risk of preterm birth. The effects of antipsychotics on low birth weight or malformations are inconclusive, but these effects have been reported to be a primary cause for treatment withdrawal (Contreras-Shannon et al. 2013; Gonçalves et al. 2014).

33.2.3.4 Nonsteroidal Anti-inflammatory Drugs (NSAIDs)

Nonsteroidal anti-inflammatory drugs (NSAIDs) have been prescribed worldwide to reduce inflammation and pain and are contraindicated during pregnancy, except for paracetamol and, in case of recurrent pregnancy loss or high risk of preeclampsia, aspirin. They have been reported to induce uncoupling of oxidative phosphorylation, to increase resting state respiration, to decrease ATP synthesis and mitochondrial membrane potential, to inhibit adenine nucleotide translocase, and to alter mitochondrial lipid metabolic pathways in animal-derived experimental models, which may account for NSAID-induced gastrointestinal injury in nonpregnant adults (Matsui et al. 2011). However, little information is available on the potential effects in fetal development and obstetric complications of human pregnancies.

33.2.3.5 Antiepileptics

The administration of an adequate treatment plays a pivotal role in the well-being of the mother and the developing fetus in those pregnant women with preexistent epilepsy and those who develop seizures secondary to eclampsia. Unfortunately, this therapeutic approach is not free of adverse effects. For example, barbiturates have been shown to impair mitochondrial lipid metabolic pathways (Santos et al. 2008), and benzodiazepines may increase apoptosis in experimental models (Contreras-Shannon et al. 2013). Differential mitochondrial toxicity has been described *in vitro* with potencies from high to low with phenytoin, phenobarbital, and carbamazepine (Santos et al. 2008), inhibiting mitochondrial respiration and ATP synthesis. Valproic acid has also been strongly associated with mitochondrial toxicity through the interference of β -oxidation pathways, mitochondrial respiration, and increasing ROS metabolism (Rumbach et al. 1986; Silva et al. 2008; Komulainen et al. 2015) in experimental models. All these molecular alterations have been associated with hepatotoxicity in nonpregnant adults. Valproic acid has been additionally related to severe teratogenic effects, such as neural tube defects (Ornoy 2009). Unfortunately, scarce data are available regarding mitochondrial toxicity of these drugs in human pregnancies (Tomson et al. 2011; Battino et al. 2013).

33.2.3.6 Local Anesthetics

Local anesthetics, such as bupivacaine or lidocaine, have been reported to induce mitochondrial damage through uncoupling of oxidative phosphorylation, inhibiting mitochondrial ATPase or other MRC complexes, as well as increasing ROS and mitophagy in experimental models and patients (Szewczyk and Wojtczak 2002; Nouette-Gaulain et al. 2011). However, their use during pregnancy might be unavoidable if an intervention is needed, and, consequently, the study of derived mitochondrial toxicity in human pregnancy becomes pressing. Indeed, it has been reported that mitochondrial toxicity is associated with postoperative pain and in one case of postanesthetic myopathy (Hogan et al. 1994).

33.2.3.7 Antivirals

The use of antivirals is essential in the treatment of infection and prevention of transmission of infections caused by human immunodeficiency virus (HIV) or hepatitis C virus (HCV). Although their administration is considered safe for the mother and child, they have been associated with mitochondrial toxicity, which may trigger related adverse effects as preeclampsia, stillbirth, preterm birth, and low birth weight (Suy et al. 2006; Townsend et al. 2007; Haeri et al. 2009; Rudin et al. 2011), as well as fetal remodeling potentially leading to disease in adulthood (García-Otero et al. 2016). Importantly,

there are still lingering concerns about their short-term (Barret et al. 2003) or long-term health consequences (García-Otero et al. 2016) and the ramifications of their effects on lipid, glucose, intermediary, and mitochondrial metabolism (Kirmse et al. 2013).

The potential clinical risks associated with antiretroviral exposure in HIV pregnant women and their fetuses and infants have been described in observational studies with varying degrees of evidence and conflicting results (Brocklehurst and French 1998; Lambert et al. 2000; Thorne et al. 2004; Tuomala et al. 2005; Hernandez et al. 2017). Such risks have been mainly attributed to nucleoside reverse transcriptase inhibitors (NRTI) and, to a lesser extent, protease inhibitors (PI) and non-NRTI. First-generation NRTIs (didanosine, zidovudine, and stavudine) have long been associated with mitochondrial toxicity due to inhibition of the endogenous mitochondrial γ -DNA polymerase, the enzyme responsible for mtDNA replication and repair (Brinkman et al. 1998). γ -DNA polymerase inhibition affects the copy number and quality of mtDNA through point mutations, deletions, and depletions, ultimately triggering mitochondrial dysfunction, as has been documented in both experimental models and patients. Over time, damaged mitochondria become unable to perform metabolic functions, leading to apoptosis (Viora et al. 1997; Brinkman et al. 1999; Mallal et al. 2000; Petit et al. 2005; Opii et al. 2007; Langa-Barlow et al. 2015). Clinically, these molecular drawbacks have been linked to myopathy, hyperlactatemia, lactic acidosis, polyneuropathy, or pancreatitis in nonpregnant adults (Lewis and Dalakas 1995; Cherry and Wesselingh 2003; Garrabou et al. 2009). Fortunately, second-generation NRTIs are being commercialized with reduced mitochondrial and clinical toxicity (Morén et al. 2012; Mouton et al. 2016). Protease inhibitors are associated with mitochondrial and apoptotic effects in nonpregnant adults and clinically to metabolic syndrome and lipodystrophy, although there remains some controversy (Phenix et al. 2001; Estaquier et al. 2002). Some non-NRTIs have been weakly linked to apoptosis in nonpregnant adults, and few adverse clinical manifestations have been associated with their use.

Most of the mitochondrial studies performed in HIV pregnancies have described an increased frequency of adverse obstetric events in the HIV cohort (Poirier et al. 2003; Shiramizu et al. 2003; Aldrovandi et al. 2009; Hernández et al. 2012). Additionally, most of the studies have described different degrees of evidence of mitochondrial toxicity in pregnant women and their newborn, occasionally accompanied by the development of apoptosis in maternal, fetal, or placental tissue (Hernández et al. 2012; Ross et al. 2012; Morén et al. 2015; Noguera-Julian et al. 2015; Hernandez et al. 2016). Recent evidence points to alterations in mitochondrial dynamics and

mitophagy in cohorts of HIV pregnant women undergoing treatment (Guitart-Mampel et al. 2017). However, no direct causal effects between mitochondrial toxicity and adverse pregnancy outcomes have been demonstrated in most of these studies (Jao et al. 2017), perhaps because of their reduced statistical power. A few studies directly associate mitochondrial toxicity with rare but lethal antiretroviral exposure in children born from HIV mothers (Poirier et al. 2015). Further studies in larger cohorts are needed, see Chapter 34 for more information on HAART therapy and mitochondrial toxicity.

33.2.3.8 Antifungals

Vaginal fungal infections may also appear in the course of pregnancy. Antifungals have been reported to inhibit complex I and II enzymes of the MRC necessary for mitochondrial oxidative phosphorylation, potentially leading to increased ROS production in experimental models (Rodriguez and Acosta 1996). Examples of these drugs, mainly used topically, are ketoconazole, miconazole, and amphotericin B. As is the case for many drugs, few data are available on the potential obstetric complications in human pregnancies.

33.2.3.9 Antiarrhythmics

Exceptionally, antiarrhythmics may need to be administered to a pregnant woman. Amiodarone is used in the treatment of many ventricular and supraventricular arrhythmias and is particularly useful for converting atrial fibrillation. Its more serious adverse effects include thyroid dysfunction, hepatocellular liver damage, or pulmonary fibrosis. The hepatotoxicity mechanism could be immune or mitochondrial mediated, as an impairment of mitochondrial function, with uncoupling of oxidative phosphorylation, inhibition of MRC complexes I–III, and inhibition of fatty acid β -oxidation as has been demonstrated in experimental conditions (Spaniol et al. 2001). Again, scarce data is available in the context of pregnancy and human beings.

33.3 Therapeutic Approach of Drug-Induced Mitochondriopathies

Although acute or chronic exposure to the above mentioned mitotoxic drugs may be considered potentially harmful during conception or pregnancy, few studies have evaluated the clinical consequences and potential toxicities of such exposure in human beings. Thus, exposure to these drugs should be minimized or avoided, if possible, during pregnancy, except under specific clinical circumstances; it is always preferable to prevent, rather than to deal with, the secondary effects of therapies.

When prescription is mandatory, clinicians should be aware of early signs of mitochondrial toxicity to avoid further manifestation of adverse clinical effects. If symptoms appear, clinicians should plan strategies to revert the manifestation of symptoms. Whenever there is clinical evidence of suspect, early management should help to achieve faster mitochondrial and clinical recovery. The discontinuation of such exposure should be considered as the most efficient therapeutic approach. Unfortunately, this may not always be possible. If the withdrawal of the given mitotoxic drug is not feasible, then secondary effects should be treated. To date, mitochondrial treatments are exclusively supportive and symptomatic with limited proven efficacy and, again, not yet evaluated in pregnant women. Such mitochondrial treatments may consist of the administration of certain mitochondrial-targeted drugs (vitamins, enzymatic cofactors, or antioxidants), performing blood transfusions, hemodialysis, dietary measures (Finsterer 2010; Monteiro et al. 2014), and physiotherapy (Andreu and Gonzalo-Sanz 2004; Pedrol et al. 2005; Artuch et al. 2006; Finsterer 2009).

Despite of the restricted possibilities, these strategies have been demonstrated to modify the onset, evolution, and outcomes of patients suffering from mitochondrial toxicities. This has been widely shown in HIV-infected nonpregnant adults. Current guidelines of HIV infection and antiviral treatment in case of mitochondrial toxicity promote strategies based on (i) substituting antivirals to less toxic regimens for mitochondria, (ii) reducing antiretroviral doses, (iii) changing antiviral schedules to nucleoside-sparing therapies, or (iv) implementing structured treatment interruptions (Mussini et al. 2005; Negrodo et al. 2009; Negrodo et al. 2010). Similarly, in case of symptomatic hyperlactatemia and lactic acidosis as consequences of mitochondrial toxicity during HIV management in nonpregnant adults, concomitant administration of mitochondrial treatments (L-carnitine, B6 and C vitamins, thiamine, and hydroxocobalamin) has been associated with faster and most efficient recovery of patients (Pedrol et al. 2005). The utility of these supportive measures remains controversial as long as they are not tested in pregnant women.

In case of human pregnancies, novel approaches based on *in silico* modeling and system pharmacology, aimed to design and predict on-target and off-target effects of a drug before administration, should be considered in order to maximize its therapeutic action and minimize its toxic consequences (Bai et al. 2014). This way, the assessment of the therapeutic/safety index would be taken into account during drug development to prompt an adequate benefit/risk ratio.

Additionally, the implementation of biomarkers to monitor mitochondrial toxicity derived from the intake

of these drugs should also be considered in the clinical settings and in the cohort of pregnant women and those wishing to conceive.

33.4 Conclusions

Few therapies, if any, are free of adverse effects. The aforementioned therapeutic drugs currently used in medical practice may trigger mitochondrial toxicity, which may ultimately underlie adverse clinical events. Although their manifestations are usually subclinical, they may occasionally lead to serious off-target effects in both mother and fetus. Most of these adverse mitochondrial effects are manifested through infertility or obstetric complications. However, mitochondrial toxicity may also contribute to fetal diseases and, by triggering irreversible physiologic alterations and fetal remodeling, to pathology emerging during adulthood.

As the current mitochondrial therapies are symptomatic rather than therapeutic, the prevention of mitochondrial toxicities is the best prophylactic choice.

As a matter of course, medication should be avoided in case of pregnant women or those wishing to conceive, unless strongly needed. In case of compulsory treatment, medical advice has to take precedence over secondary mitochondrial events. Clinicians should be aware of these toxicities and circumventing strategies (especially treatment interruption or substitution of toxic drugs by alternative compounds).

Further studies are needed to better understand these mitochondrial toxicities in human pregnant women based on observational clinical case studies or large epidemiologic cohorts follow-up, especially in the case of chronic or unavoidable treatments.

In case of mandatory or accidental therapeutic exposures to these mitotoxic drugs, there is the crucial need to (i) find less toxic substances, (ii) establish novel or already described biomarkers into clinical settings for monitoring toxicity during pregnancy, and (iii) elaborate guidelines to assess risk–benefit ratios in cases of therapy administration.

Funding

Fondo de Investigación Sanitaria (FIS 00462/11, FIS 01199/12, FIS 01455/13, FIS 01738/13, FIS 00903/15 and FIS 00817/15), CIBERER (an initiative of ISCIII) and InterCIBER (PIE1400061) granted by ISCIII and FEDER (a way to build Europe); Suports a Grups de Recerca (2014/SGR/376, PERIS PI044859) and CERCA Programme from the Generalitat de Catalunya; Fundació La Marató de TV3 (87/C/2015); and Fundació Cellex.

References

- Abdel-Razaq, W., Kendall, D.A. and Bates, T.E., 2011. The effects of antidepressants on mitochondrial function in a model cell system and isolated mitochondria. *Neurochemical Research*, **36**(2), pp. 327–38.
- Aldrovandi, G.M. et al., 2009. Antiretroviral exposure and lymphocyte mtDNA content among uninfected infants of HIV-1-infected women. *Pediatrics*, **124**(6), pp. e1189–97.
- Anderson, S., 1981. Sequence and organization of the human mitochondrial genome. *Nature*, **5806**(290), pp. 457–65.
- Andrade, C., 2012. Selective serotonin reuptake inhibitors and persistent pulmonary hypertension of the newborn. *The Journal of Clinical Psychiatry*, **73**(5), pp. e601–5.
- Andreu, A.L. and Gonzalo-Sanz, R., 2004. Mitochondrial disorders: a classification for the 21st century. *Neurología (Barcelona, Spain)*, **19**(1), pp. 15–22.
- Antonucci, R. et al., 2012. Use of non-steroidal anti-inflammatory drugs in pregnancy: impact on the fetus and newborn. *Current Drug Metabolism*, **13**(4), pp. 474–90.
- Artuch, R. et al., 2006. Cerebellar ataxia with coenzyme Q10 deficiency: diagnosis and follow-up after coenzyme Q10 supplementation. *Journal of the Neurological Sciences*, **246**(1–2), pp. 153–8.
- Bai, J.P.F. et al., 2014. Systems pharmacology modeling: an approach to improving drug safety. *Biopharmaceutics & Drug Disposition*, **35**(1), pp. 1–14.
- Bar-Oz, B. et al., 2012. The outcomes of pregnancy in women exposed to the new macrolides in the first trimester. *Drug Safety*, **35**(7), pp. 589–98.
- Barker, D.J., 1999. Fetal origins of cardiovascular disease. *Annals of Medicine*, **31** Suppl 1, pp. 3–6.
- Barret, B. et al., 2003. Persistent mitochondrial dysfunction in HIV-1-exposed but uninfected infants: clinical screening in a large prospective cohort. *AIDS (London, England)*, **17**(12), pp. 1769–85.
- Battino, D. et al., 2013. Seizure control and treatment changes in pregnancy: observations from the EURAP epilepsy pregnancy registry. *Epilepsia*, **54**(9), pp. 1621–7.
- Bérard, A. et al., 2015. Use of macrolides during pregnancy and the risk of birth defects: a population-based study. *Pharmacoepidemiology and Drug Safety*, **24**(12), pp. 1241–8.
- Blohm, E., Lai, J. and Neavyn, M., 2017. Drug-induced hyperlactatemia. *Clinical Toxicology*, **55**(8), pp. 869–78.
- Bressler, A.M. et al., 2004. Peripheral neuropathy associated with prolonged use of linezolid. *The Lancet Infectious Diseases*, **4**(8), pp. 528–31.
- Brinkman, K. et al., 1998. Adverse effects of reverse transcriptase inhibitors: mitochondrial toxicity as common pathway. *AIDS (London, England)*, **12**(14), pp. 1735–44.
- Brinkman, K. et al., 1999. Mitochondrial toxicity induced by nucleoside-analogue reverse-transcriptase inhibitors is a key factor in the pathogenesis of antiretroviral-therapy-related lipodystrophy. *Lancet (London, England)*, **354**(9184), pp. 1112–5.
- Brocklehurst, P. and French, R., 1998. The association between maternal HIV infection and perinatal outcome: a systematic review of the literature and meta-analysis. *British Journal of Obstetrics and Gynaecology*, **105**(8), pp. 836–48.
- Casademont, J. et al., 2007. Neuroleptic treatment effect on mitochondrial electron transport chain: peripheral blood mononuclear cells analysis in psychotic patients. *Journal of Clinical Psychopharmacology*, **27**(3), pp. 284–8.
- Chen, S. et al., 2014. Sertraline, an antidepressant, induces apoptosis in hepatic cells through the mitogen-activated protein kinase pathway. *Toxicological Sciences: An Official Journal of the Society of Toxicology*, **137**(2), pp. 404–15.
- Cherry, C.L. and Wesselingh, S.L., 2003. Nucleoside analogues and HIV: the combined cost to mitochondria. *The Journal of Antimicrobial Chemotherapy*, **51**(5), pp. 1091–3.
- Contreras-Shannon, V. et al., 2013. Clozapine-induced mitochondria alterations and inflammation in brain and insulin-responsive cells. *PLoS One*, **8**(3), p. e59012.
- Crispi, F. et al., 2010. Fetal growth restriction results in remodeled and less efficient hearts in children. *Circulation*, **121**(22), pp. 2427–36.
- Curti, C. et al., 1999. Fluoxetine interacts with the lipid bilayer of the inner membrane in isolated rat brain mitochondria, inhibiting electron transport and F1F0-ATPase activity. *Molecular and Cellular Biochemistry*, **199**(1–2), pp. 103–9.
- Davey, G.P., Peuchen, S. and Clark, J.B., 1998. Energy thresholds in brain mitochondria: potential involvement in neurodegeneration. *Journal of Biological Chemistry*, **273**(21), pp. 12753–7.
- De Santis, M. et al., 2011. Antiepileptic drugs during pregnancy: pharmacokinetics and transplacental transfer. *Current Pharmaceutical Biotechnology*, **12**(5), pp. 781–8.
- Del Pozo, J.L. et al., 2014. Linezolid-induced lactic acidosis in two liver transplant patients with the mitochondrial DNA A2706G polymorphism. *Antimicrobial Agents and Chemotherapy*, **58**(7), pp. 4227–9.
- Estaquier, J. et al., 2002. Effects of antiretroviral drugs on human immunodeficiency virus type 1-induced CD4(+) T-cell death. *Journal of Virology*, **76**(12), pp. 5966–73.
- Finsterer, J., 2009. Management of mitochondrial stroke-like-episodes. *European Journal of Neurology: The Official Journal of the European Federation of Neurological Societies*, **16**(11), pp. 1178–84.
- Finsterer, J., 2010. Treatment of mitochondrial disorders. *European Journal of Paediatric Neurology: EJPN: Official Journal of the European Paediatric Neurology Society*, **14**(1), pp. 29–44.
- García-Otero, L. et al., 2016. Zidovudine treatment in HIV-infected pregnant women is associated with fetal cardiac remodelling. *AIDS*, **30**(9), pp. 1393–401.

- Garrabou, G. et al., 2009. Genetic and functional mitochondrial assessment of HIV-infected patients developing HAART-related hyperlactatemia. *JAIDS Journal of Acquired Immune Deficiency Syndromes*, **52**(4), pp. 443–51.
- Garrabou, G. et al., 2011. *Mitochondrial Pathophysiology*, Transworld Research Network, pp. 249–79.
- Gonçalves, V.F. et al., 2014. A hypothesis-driven association study of 28 nuclear-encoded mitochondrial genes with antipsychotic-induced weight gain in schizophrenia. *Neuropsychopharmacology: Official Publication of the American College of Neuropsychopharmacology*, **39**(6), pp. 1347–54.
- Gröber, U., 2012. Mitochondrial toxicity of drugs. *Medizinische Monatsschrift für Pharmazeuten*, **35**(12), pp. 445–56.
- Guitart-Mampel, M. et al., 2017. Altered mitochondrial dynamics and apoptosis in HIV-pregnancies with obstetric complications. *The Journal of Antimicrobial Chemotherapy*, **72**(9), pp. 2578–86.
- Guo, D. et al., 2010. The cardiotoxicity of macrolides: a systematic review. *Die Pharmazie*, **65**(9), pp. 631–40.
- Guo, H. et al., 2017. Relationships between mitochondrial DNA content, mitochondrial activity, and boar sperm motility. *Theriogenology*, **87**, pp. 276–83.
- Haeri, S. et al., 2009. Obstetric and newborn infant outcomes in human immunodeficiency virus-infected women who receive highly active antiretroviral therapy. *American Journal of Obstetrics and Gynecology*, **201**(3), pp. 315.e1–e5.
- Hendrick, V. et al., 2003. Placental passage of antidepressant medications. *American Journal of Psychiatry*, **160**(5), pp. 993–6.
- Hernandez, S. et al., 2016. Mitochondrial toxicity and caspase activation in HIV pregnant women. *Journal of Cellular and Molecular Medicine*, **21**(1): 26–34.
- Hernández, S. et al., 2012. Perinatal outcomes, mitochondrial toxicity and apoptosis in HIV-treated pregnant women and in-utero-exposed newborn. *AIDS*, **26**(4), pp. 419–28.
- Hernández, S. et al., 2017. Placental mitochondrial toxicity, oxidative stress, apoptosis, and adverse perinatal outcomes in HIV pregnancies under antiretroviral treatment containing zidovudine. *JAIDS Journal of Acquired Immune Deficiency Syndromes*, **75**(4), pp. e113–9.
- Herst, P.M. et al., 2017. Functional mitochondria in health and disease. *Frontiers in Endocrinology*, **8**, p. 296.
- Hogan, Q. et al., 1994. Local anesthetic myotoxicity: a case and review. *Anesthesiology*, **80**(4), pp. 942–7.
- Hong, S. et al., 2015. Evidence that antibiotics bind to human mitochondrial ribosomal RNA has implications for aminoglycoside toxicity. *The Journal of Biological Chemistry*, **290**(31): 19273–86.
- Hroudová, J. and Fišar, Z., 2012. *In vitro* inhibition of mitochondrial respiratory rate by antidepressants. *Toxicology Letters*, **213**(3), pp. 345–52.
- Jansen, R.P.S. and Burton, G.J., 2004. Mitochondrial dysfunction in reproduction. *Mitochondrion*, **4**(5–6), pp. 577–600.
- Jao, J. and Abrams, E.J., 2014. Metabolic complications of in utero maternal HIV and antiretroviral exposure in HIV-exposed infants. *The Pediatric Infectious Disease Journal*, **33**(7), pp. 734–40.
- Kieler, H. et al., 2011. Selective serotonin reuptake inhibitors during pregnancy and risk of persistent pulmonary hypertension in the newborn: population based cohort study from the five Nordic countries. *BMJ*, **344**(jan12 3), pp. d8012–d8012.
- Kirmse, B., Baumgart, S. and Rakhmanina, N., 2013. Metabolic and mitochondrial effects of antiretroviral drug exposure in pregnancy and postpartum: implications for fetal and future health. *Seminars in Fetal and Neonatal Medicine*, **18**(1), pp. 48–55.
- Komulainen, T. et al., 2015. Sodium valproate induces mitochondrial respiration dysfunction in HepG2 *in vitro* cell model. *Toxicology*, **331**, pp. 47–56.
- Lambert, J.S. et al., 2000. Risk factors for preterm birth, low birth weight, and intrauterine growth retardation in infants born to HIV-infected pregnant women receiving zidovudine. Pediatric AIDS Clinical Trials Group 185 Team. *AIDS (London, England)*, **14**(10), pp. 1389–99.
- Lang, B.F., Gray, M.W. and Burger, G., 1999. Mitochondrial genome evolution and the origin of eukaryotes. *Annual Review of Genetics*, **33**(1), pp. 351–97.
- Langs-Barlow, A. et al., 2015. Association of circulating cytochrome c with clinical manifestations of antiretroviral-induced toxicity. *Mitochondrion*, **20**, pp. 71–4.
- Latini, R., Tognoni, G. and Kates, R.E., 1984. Clinical pharmacokinetics of amiodarone. *Clinical Pharmacokinetics*, **9**(2), pp. 136–56.
- Lee, M. et al., 2015. Tricyclic antidepressants amitriptyline and desipramine induced neurotoxicity associated with Parkinson's disease. *Molecules and Cells*, **38**(8), pp. 734–40.
- Lewis, W. and Dalakas, M.C., 1995. Mitochondrial toxicity of antiviral drugs. *Nature Medicine*, **1**(5), pp. 417–22.
- Li, Y. et al., 2012. Mitochondrial dysfunction induced by sertraline, an antidepressant agent. *Toxicological Sciences: An Official Journal of the Society of Toxicology*, **127**(2), pp. 582–91.
- Lin, K.J. et al., 2013. Safety of macrolides during pregnancy. *American Journal of Obstetrics and Gynecology*, **208**(3), pp. 221.e1–8.
- López, S. et al., 2008. Mitochondrial DNA depletion in oocytes of HIV-infected antiretroviral-treated infertile women. *Antiviral Therapy*, **13**(6), pp. 833–8.
- Mallal, S.A. et al., 2000. Contribution of nucleoside analogue reverse transcriptase inhibitors to subcutaneous fat wasting in patients with HIV infection. *AIDS (London, England)*, **14**(10), pp. 1309–16.

- Mando, C. et al., 2014. Placental mitochondrial content and function in intrauterine growth restriction and preeclampsia. *AJP: Endocrinology and Metabolism*, **306**(4), pp. E404–13.
- Margulis, L., 1975. Symbiotic theory of the origin of eukaryotic organelles; criteria for proof. *Symposia of the Society for Experimental Biology*, (29), pp. 21–38.
- Martins, M.R. et al., 2008. Antipsychotic-induced oxidative stress in rat brain. *Neurotoxicity Research*, **13**(1), pp. 63–9.
- Matsui, H. et al., 2011. The pathophysiology of non-steroidal anti-inflammatory drug (NSAID)-induced mucosal injuries in stomach and small intestine. *Journal of Clinical Biochemistry and Nutrition*, **48**(2), pp. 107–11.
- Maurer, I. and Möller, H.J., 1997. Inhibition of complex I by neuroleptics in normal human brain cortex parallels the extrapyramidal toxicity of neuroleptics. *Molecular and Cellular Biochemistry*, **174**(1–2), pp. 255–9.
- Monteiro, J.P. et al., 2014. Mitochondrial membrane lipids in life and death and their molecular modulation by diet: tuning the furnace. *Current Drug Targets*, **15**(8), pp. 797–810.
- Morén, C. et al., 2014. Mitochondrial toxicity in human pregnancy: an update on clinical and experimental approaches in the last 10 years. *International Journal of Environmental Research and Public Health*, **11**(9), pp. 9897–918.
- Morén, C. et al., 2015. Mitochondrial disturbances in HIV pregnancies. *AIDS*, **29**(1), pp. 5–12.
- Morén, C. et al., 2016. The role of therapeutic drugs on acquired mitochondrial toxicity. *Current Drug Metabolism*, **17**(999), pp. 1–1.
- Mouton, J.P., Cohen, K. and Maartens, G., 2016. Key toxicity issues with the WHO-recommended first-line antiretroviral therapy regimen. *Expert review of clinical pharmacology*, **9**(11), pp. 1493–503.
- Mussini, C. et al., 2005. Effect of treatment interruption monitored by CD4 cell count on mitochondrial DNA content in HIV-infected patients: a prospective study. *AIDS (London, England)*, **19**(15), pp. 1627–33.
- Nahon, E. et al., 2005. Fluoxetine (Prozac) interaction with the mitochondrial voltage-dependent anion channel and protection against apoptotic cell death. *FEBS Letters*, **579**(22), pp. 5105–10.
- Nau, H. et al., 1981. Thiamphenicol during the first trimester of human pregnancy: placental transfer *in vivo*, placental uptake *in vitro*, and inhibition of mitochondrial function. *Toxicology and Applied Pharmacology*, **60**(1), pp. 131–41.
- Negredo, E. et al., 2009. Improvement of mitochondrial toxicity in patients receiving a nucleoside reverse-transcriptase inhibitor-sparing strategy: results from the Multicenter Study with Nevirapine and Kaletra (MULTINEKA). *Clinical Infectious Diseases: An Official Publication of the Infectious Diseases Society of America*, **49**(6), pp. 892–900.
- Negredo, E. et al., 2010. Mild improvement in mitochondrial function after a 3-year antiretroviral treatment interruption despite persistent impairment of mitochondrial DNA content. *Current HIV Research*, **8**(5), pp. 379–85.
- Noguera-Julian, A. et al., 2015. Decreased mitochondrial function among healthy infants exposed to antiretrovirals during gestation, delivery and the neonatal period. *The Pediatric Infectious Disease Journal*, **34**(12), pp. 1349–54.
- Nouette-Gaulain, K. et al., 2011. From analgesia to myopathy: when local anesthetics impair the mitochondrion. *The International Journal of Biochemistry & Cell Biology*, **43**(1), pp. 14–9.
- Nunnari, J. et al., 2012. Mitochondria: in sickness and in health. *Cell*, **148**(6), pp. 1145–59.
- Opii, W.O. et al., 2007. Oxidative stress and toxicity induced by the nucleoside reverse transcriptase inhibitor (NRTI)—2',3'-dideoxycytidine (ddC): relevance to HIV-dementia. *Experimental Neurology*, **204**(1), pp. 29–38.
- Ornoy, A., 2009. Valproic acid in pregnancy: how much are we endangering the embryo and fetus? *Reproductive Toxicology*, **28**(1), pp. 1–10.
- Pacifici, G.M., 2005. Transfer of antivirals across the human placenta. *Early Human Development*, **81**(8), pp. 647–54.
- Pacifici, G.M., 2006. Placental transfer of antibiotics administered to the mother: a review. *International Journal of Clinical Pharmacology and Therapeutics*, **44**(2), pp. 57–63.
- Pedrol, E. et al., 2005. Treatment of symptomatic hyperlactatemia and lactic acidosis in HIV+ patients under nucleoside reverse transcriptase inhibitors. *Medicina Clínica*, **125**(6), pp. 201–4.
- Petit, F. et al., 2005. Mitochondria are sensors for HIV drugs. *Trends in Pharmacological Sciences*, **26**(5), pp. 258–64.
- Phenix, B.N. et al., 2001. Antiapoptotic mechanism of HIV protease inhibitors: preventing mitochondrial transmembrane potential loss. *Blood*, **98**(4), pp. 1078–85.
- Poirier, M.C. et al., 2003. Long-term mitochondrial toxicity in HIV-uninfected infants born to HIV-infected mothers. *Journal of Acquired Immune Deficiency Syndromes (1999)*, **33**(2), pp. 175–83.
- Poirier, M.C. et al., 2015. Fetal consequences of maternal antiretroviral nucleoside reverse transcriptase inhibitor use in human and nonhuman primate pregnancy. *Current Opinion in Pediatrics*, **27**(2), pp. 233–9.
- Pon, L.A. and Schon, E.A., 2007. *Mitochondria*, 2nd ed., San Diego, CA: Elsevier.
- Przedborski, S. et al., 1992. Transgenic mice with increased Cu/Zn-superoxide dismutase activity are resistant to N-methyl-4-phenyl-1,2,3,6-tetrahydropyridine-induced neurotoxicity. *The Journal of Neuroscience: The Official Journal of the Society for Neuroscience*, **12**(5), pp. 1658–67.
- Raudenska, M. et al., 2013. Haloperidol cytotoxicity and its relation to oxidative stress. *Mini Reviews in Medicinal Chemistry*, **13**(14), pp. 1993–8.

- Reynier, P. et al., 2001. Mitochondrial DNA content affects the fertilizability of human oocytes. *Molecular Human Reproduction*, **7**(5), pp. 425–9.
- Riggin, L. et al., 2013. The fetal safety of fluoxetine: a systematic review and meta-analysis. *Journal of Obstetrics and Gynaecology Canada*, **35**(4), pp. 362–9.
- Rodriguez, R.J. and Acosta, D., 1996. Inhibition of mitochondrial function in isolated rat liver mitochondria by azole antifungals. *Journal of Biochemical Toxicology*, **11**(3), pp. 127–31.
- Ross, A.C. et al., 2012. Effects of in utero antiretroviral exposure on mitochondrial DNA levels, mitochondrial function and oxidative stress. *HIV Medicine*, **13**(2), pp. 98–106.
- Rudin, C. et al., 2011. Antiretroviral therapy during pregnancy and premature birth: analysis of Swiss data. *HIV Medicine*, **12**(4), pp. 228–35.
- Rumbach, L. et al., 1986. Effects of sodium valproate on mitochondrial membranes: electron paramagnetic resonance and transmembrane protein movement studies. *Molecular Pharmacology*, **30**(3), pp. 270–3.
- Salimi, A. et al., 2016. Toxicity of macrolide antibiotics on isolated heart mitochondria: a justification for their cardiotoxic adverse effect. *Xenobiotica; The Fate of Foreign Compounds in Biological Systems*, **46**(1), pp. 82–93.
- Santos, N.A.G. et al., 2008. Aromatic antiepileptic drugs and mitochondrial toxicity: effects on mitochondria isolated from rat liver. *Toxicology in Vitro: An International Journal Published in Association with BIBRA*, **22**(5), pp. 1143–52.
- Santos, T.A., El Shourbagy, S. and St. John, J.C., 2006. Mitochondrial content reflects oocyte variability and fertilization outcome. *Fertility and Sterility*, **85**(3), pp. 584–91.
- Scatena, R. et al., 2007. The role of mitochondria in pharmacotoxicology: a reevaluation of an old, newly emerging topic. *American Journal of Physiology. Cell Physiology*, **293**(1), pp. C12–21.
- Scheffler, I.E., 2008. *Mitochondria*, 2nd ed., Hoboken, NJ: Wiley-Liss.
- Shiramizu, B. et al., 2003. Placenta and cord blood mitochondrial DNA toxicity in HIV-infected women receiving nucleoside reverse transcriptase inhibitors during pregnancy. *Journal of Acquired Immune Deficiency Syndromes (1999)*, **32**(4), pp. 370–4.
- Silva, M.F.B. et al., 2008. Valproic acid metabolism and its effects on mitochondrial fatty acid oxidation: a review. *Journal of Inherited Metabolic Disease*, **31**(2), pp. 205–16.
- Singh, K.P., Singh, M.K. and Gautam, S., 2016. Effect of *in utero* exposure to the atypical anti-psychotic risperidone on histopathological features of the rat placenta. *International Journal of Experimental Pathology*, **97**(2), pp. 125–32.
- Spaniol, M. et al., 2001. Toxicity of amiodarone and amiodarone analogues on isolated rat liver mitochondria. *Journal of Hepatology*, **35**(5), pp. 628–36.
- Stewart, J.B. and Chinnery, P.F., 2015. The dynamics of mitochondrial DNA heteroplasmy: implications for human health and disease. *Nature Reviews Genetics*, **16**(9), pp. 530–42.
- Suy, A. et al., 2006. Increased risk of pre-eclampsia and fetal death in HIV-infected pregnant women receiving highly active antiretroviral therapy. *AIDS (London, England)*, **20**(1), pp. 59–66.
- Szewczyk, A. and Wojtczak, L., 2002. Mitochondria as a pharmacological target. *Pharmacological Reviews*, **54**(1), pp. 101–27.
- Taylor, R.W. and Turnbull, D.M., 2005. Mitochondrial DNA mutations in human disease. *Nature Reviews Genetics*, **6**(5), pp. 389–402.
- Thorne, C., Patel, D. and Newell, M.-L., 2004. Increased risk of adverse pregnancy outcomes in HIV-infected women treated with highly active antiretroviral therapy in Europe. *AIDS (London, England)*, **18**(17), pp. 2337–9.
- Timpka, S. et al., 2016. Hypertensive disorders of pregnancy and offspring cardiac structure and function in adolescence. *Journal of the American Heart Association*, **5**(11), p. e003906.
- Tomson, T. et al., 2011. Dose-dependent risk of malformations with antiepileptic drugs: an analysis of data from the EURAP epilepsy and pregnancy registry. *The Lancet Neurology*, **10**(7), pp. 609–17.
- Torres-Ruiz, N.M., Granados, O. and Meza, G., 2011. Aminoglycosides: therapeutics, ototoxicity and hypersensitivity of mitochondrial genetic origin. *Proceedings of the Western Pharmacology Society*, **54**, pp. 49–51.
- Townsend, C.L. et al., 2007. Antiretroviral therapy and premature delivery in diagnosed HIV-infected women in the United Kingdom and Ireland. *AIDS*, **21**(8), pp. 1019–26.
- Tuccori, M. et al., 2009. Safety concerns associated with the use of serotonin reuptake inhibitors and other serotonergic/noradrenergic antidepressants during pregnancy: a review. *Clinical Therapeutics*, **31**, pp. 1426–53.
- Tuomala, R.E. et al., 2005. Improved obstetric outcomes and few maternal toxicities are associated with antiretroviral therapy, including highly active antiretroviral therapy during pregnancy. *Journal of Acquired Immune Deficiency Syndromes (1999)*, **38**(4), pp. 449–73.
- Viora, M. et al., 1997. Interference with cell cycle progression and induction of apoptosis by dideoxynucleoside analogs. *International Journal of Immunopharmacology*, **19**(6), pp. 311–21.
- Wallace, D.C. and Melov, S., 1998. Radicals r'aging. *Nature Genetics*, **19**(2), pp. 105–6.
- Zhang, Y. et al., 1990. The oxidative inactivation of mitochondrial electron transport chain components and ATPase. *The Journal of Biological Chemistry*, **265**(27), pp. 16330–6.

The Role of Therapeutic Drugs on Acquired Mitochondrial Toxicity

Constanza Morén, Diana Luz Juárez-Flores*, Francesc Cardellach and Glòria Garrabou

Muscle Research and Mitochondrial Function Laboratory, Muscle Research Unit, Cellex-IDIBAPS-Faculty of Medicine, University of Barcelona, Internal Medicine Department-Hospital Clínic of Barcelona (Barcelona, Spain) and U722-CIBERER (ISCIII, Madrid, Spain)

Abstract: Certain therapeutic drugs used in medical practice may trigger mitochondrial toxicity leading to a wide range of clinical symptoms including deafness, neuropathy, myopathy, hyperlactatemia, lactic acidosis, pancreatitis and lipodystrophy, among others, which could even compromise the life of the patient.

The aim of this work is to review the potential mitochondrial toxicity derived from drugs used in health care, including anesthetics, antiepileptics, neuroleptics, antidepressants, antivirals, antibiotics, antifungals, antimalarics, antineoplastics, antidiabetics, hypolipemians, antiarrhythmics, anti-inflammatories and nitric oxide.

We herein have reviewed data from experimental and clinical studies to document the molecular mitochondrial basis, potential biomarkers and putative clinical symptoms associated to secondary effects of drugs.

Since treatment of acquired mitochondrial pathologies remains supportive and therapeutic interventions cannot be avoided, information of molecular and clinical consequences of toxic exposure becomes fundamental to assess risk-benefit imbalance of treatment prescription. Additionally, there is a crucial need to develop less mitochondrial toxic compounds, novel biomarkers to follow up mitochondrial toxicity (or implement those already proposed) and new approaches to prevent or revert unintended mitochondrial damage.

Keywords: Mitochondria, toxicity, medication, secondary mitochondrial pathologies, adverse effects, mitotoxicity.

1. INTRODUCTION

Cell survival and viability is highly dependent on proper mitochondrial function. It is widely known that mitochondria are the powerhouse of the cell, since their main function is energy production through adenosine triphosphate (ATP) synthesis. However, mitochondria have other important functions including cellular respiration, calcium homeostasis, thermogenesis, steroid synthesis and lipid, carbohydrate or protein catabolism. Most importantly, mitochondrion is the primary site of reactive oxygen species (ROS) production or reactive nitric oxide species signaling, and it is the organelle that regulates cell death through apoptosis development. As mitochondria are present in almost all the cells of our body, any disruption in the aforementioned pathways could potentially endanger cell survival leading to tissue damage, organ failure and, in the most severe cases, compromise the life of the patient [1].

Mitochondrion's endosymbiotic origin [2] has given rise to a multifunctional, semiautonomous and dynamic organelle whose double membrane makes possible to have a highly alkaline, negatively-charged milieu that contains a double stranded circular DNA (mtDNA) which encodes 13 of the proteins of the mitochondrial respiratory chain (MRC) and 22 transfer RNA and 2 ribosomal RNA essential for mtDNA translation. The inner mitochondrial membrane, enriched in cardiolipin content, contains all the proteins of the MRC, the disruption of which may lead to a massive generation of ROS that may easily exert oxidative damage to lipidic, glucidic, proteinic or genetic structures entailing a vicious circle of cell death and pathological consequences.

There are natural and synthetic compounds able to promote mitochondrial lesion. Any person exposed to such agents may be affected, but the two populations that are more prone to develop

mitochondrial toxicity are: patients primarily affected by a mitochondrial disease and pregnant women or those aiming to procreate. Patients with inherited mitochondrial diseases should avoid contact with toxic agents for mitochondria, unless supervised by a medical authority, in order to prevent disease onset or worsening. Pregnant women or those willing to conceive should minimize contact with mitochondrial hazards, unless medically supervised, as they may exert mitochondrial fetal damage either by direct or vertical toxicity. As for the latter, it should be kept in mind that oocytes are the only mitochondria-carrying gametes; consequently, if the maternally inherited mitochondria have a previous genetic lesion, it may be transmittable to the fetus. Nonetheless, since most of the mitochondrial proteins are nuclear-encoded, disturbances in the intergenomic cross talk and nuclear genome could also originate mitochondrial disarrangements. In case of mitochondrial alterations at genetic level, wild and mutated mtDNA molecules may coexist within mitochondria (heteroplasmy) and mitochondrial disease onset may arise depending on the number of mutated molecules (threshold effect) and differential distribution of these mutated mitochondrial genomes within body tissues (mitotic segregation), characteristics which may partially explain the complexity of mitochondrial toxic disorders [1].

Acquired mitochondrial diseases involve those alterations triggered by contact with toxic compounds. Therapeutic drugs exert their mechanism of action by very different means and mitochondrial physiology can result disturbed at different levels, causing genetic alterations (through depletion, deletions and/or point mutations), MRC enzymatic dysfunction [3,4], impairment of oxygen consumption, ROS generation [5], membrane potential depolarization, mitochondrial protein synthesis inhibition [6], mitochondrial dynamics deregulation and mitochondrial biogenesis impairment, among others. Exogenous toxic compounds may initially exert mitochondrial damage in one specific level, however, after a continuous exposition, the isolated effect may ultimately lead to a general mitochondrial dysfunction with severe consequences for the cell viability. Depending on the specific pathway of mitochondrial func-



Diana Luz Juárez-Flores

*Address correspondence to this author at the Muscle Research and Mitochondrial Function Laboratory, Muscle Research Unit, Cellex-IDIBAPS-Faculty of Medicine, University of Barcelona, Internal Medicine Department-Hospital Clínic of Barcelona (Barcelona, Spain) and U722-CIBERER (ISCIII, Madrid, Spain); E-mail: DJUAREZ@clinic.ub.es

tion that is disrupted, pharmacokinetics and pharmacodynamics of the drug, dosage, time of treatment and individual susceptibility to drug exposition, clinical consequences will ultimately translate in a wide spectrum of symptoms [7], ranging from almost asymptomatic patients to severe cases with fatal consequences. All these considerations together with the threshold effect and the mitotic segregation phenomenon, in case of mitochondrial genetic alterations, explain the differential clinical manifestations after the same kind and time of toxic exposure [8].

Usually, the clinical suspicion of mitochondrial lesion after a toxic exposure is feasible because most clinical symptoms are similar to those of inherited mitochondrial disorders. An example of this parallelism among acquired and inherited mitochondrial disorders is the drug-induced MELAS (mitochondrial encephalopathy with lactic acidosis and stroke syndrome), which is classically a maternally inherited syndrome with spontaneous early onset, that can also be induced by antiepileptic drugs, statins and propofol [9]. Similarly, Madelung lipomatosis resembles clinical manifestations of antiretroviral-mediated lipodystrophy.

A variety of drugs are known to prompt mitochondrial toxicity; many of them are frequently used in medical practice. This is the case of certain anesthetics, antiepileptics, neuroleptics, antidepressants, antivirals, antibiotics, antifungals, antimalarics, antineoplastics, antidiabetics, hypolipemiant, antiarrhythmic, anti-inflammatories and nitric oxide. The mitochondrial toxicity derived from the intake of some of these drugs may underlie non-negligible secondary adverse events (Table 1). These agents present different toxicity mechanisms and damage capacity, some of which are currently being established (Fig. 1, Table 1).

The present manuscript reviews experimental and human data of the etiopathological pathways, potential biomarkers and clinical manifestations of exposition to those mitochondrial toxic therapeutic drugs in order to raise awareness and minimize the incidence of their secondary effects.

The following data is of relevance to diverse areas of biomedicine, as it brings attention to different and previously unnoticed mechanisms of disease after taking a drug, making it imperative to assess the potential toxicity of these and other compounds, in the whole pharmaceutical development procedure. Physicians should be familiarized not only with these adverse effects but also on their mechanism of action, since some patients may develop symptoms in a more dramatic way than others, whereas for having a previous mitochondrial disease or as a first sign of underlying mitochondrial dysfunction. Finally, general population may benefit from this knowledge in order to be aware of the presence of clinical symptoms of toxicity and seek medical advice immediately.

2. MITOCHONDRIAL TOXIC COMPOUNDS

The information provided in this roster might not include all mitochondrial toxic medications or all off target mechanisms disrupted. The large amount of knowledge in this topic requires a limited summary implying to highlight only some of the most relevant points and to unavoidably leave behind other aspects out of the scope of these review. Noticeably, different degrees of toxicity and/or evidence support the depicted findings.

Few therapies are free of adverse effects. We will focus our attention in the mitochondrial alterations derived from the administration of therapeutic drugs to consider risk-benefit ratio of drug administration with respect the therapeutic goals that are pursued in every particular case.

Anesthetics and Sedatives

These drugs are commonly used in clinical practice that involves surgery, to reduce sensitivity and awareness of pain or consciousness.

General anesthetics are involved in the inhibition of the opening of the ion channel in a postsynaptic ligand-gated membrane protein but their actions are based on the particularities of the plas-

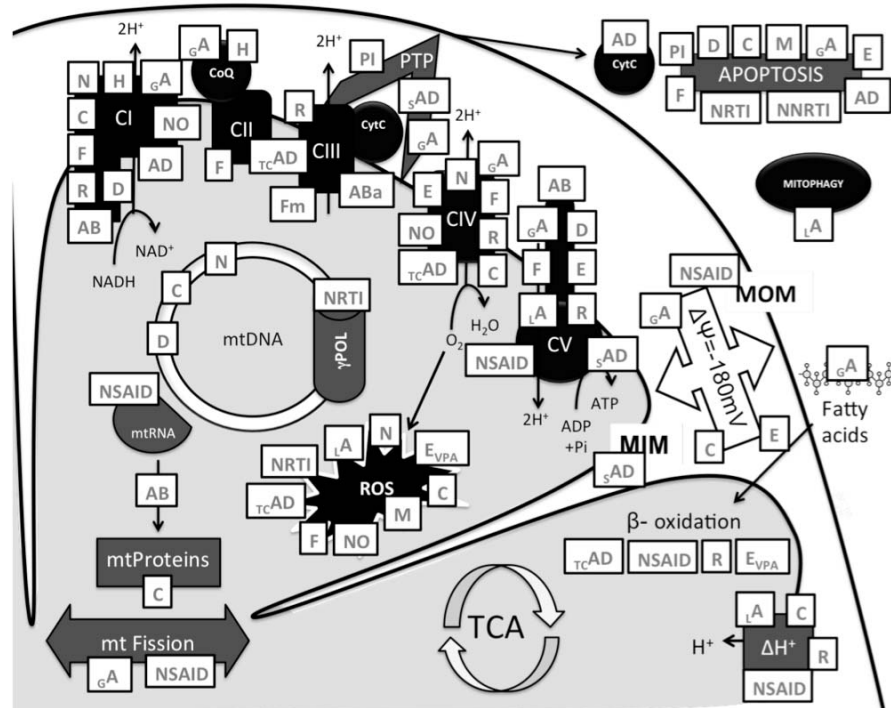


Fig. (1). Illustration of a mitochondrion, showing part of the mitochondrion's outer membrane (MOM), mitochondrion's inner membrane (MIM), intermembrane space, cristae and matrix. A, anesthetics; gA, general anesthetics; LA, local anesthetics; AB, antibiotics; AD, antidepressants; tcAD, tricyclic antidepressants; sAD selective serotonin reuptake inhibitors; C, chemotherapy; D, antidiabetic drugs; E, antiepileptics; F, fungal drugs; H, hypolipemiant; M, antimalarial drugs; N, neuroleptic drugs; NRTI, nucleoside reverse transcriptase inhibitors; NNRTI, non-NRTI; NSAID, non steroidal anti-inflammatories; NO, nitric oxide; PI, protease inhibitors; R, antiarrhythmic drugs.

matic membranes and their environmental interaction, as it will depend on complex mechanistic and thermodynamic complexes including the lateral pressure at which they are subjected [10]. It has been demonstrated that they affect mitochondrial function and oxygen consumption capacity in both human and experimental models [11]. General anesthetic inhalants such as halothane, isoflurane and sevoflurane inhibit MRC Complex I (CI) activity of cardiac pig mitochondria (Fig. 1, Table 1) [12]. Such molecular mechanism may underlie associated hepatotoxicity, neurological impairment and cardiac adverse effects. Mitochondrial-like myopathies may occur after intravenous anesthetics as in propofol infusion syndrome [13]. This syndrome is associated to free fatty acid metabolism failure, through an inhibition of free fatty acid entrance into the mitochondria and interference at specific sites in the MRC [14].

Ketamine is another widely used general anesthetic recently reported to induce mitochondrial toxicity in human iPSC-derived neurons. It has been related to an increase of ROS production and activation of caspase 3/7 activity, dissipating the mitochondrial membrane potential at high doses. And, even at a lower concentration, it can cause a reduction in ATP levels, an increase in mitochondrial fission and an increase in the nicotinamide-adenine dinucleotide/nicotinamide-adenine (NADH/NAD⁺) ratio, suggesting insufficient consumption of NADH during oxidative phosphorylation (Fig. 1, Table 1) [15], which could be responsible of associated hepatotoxicity.

Barbiturates, such as phenobarbital, (used as sedatives, anesthetics, anxiolytics, hypnotics and anticonvulsants), have also been described to block initial MRC electron transport between CI (Fe-S center) and ubiquinone [16] in children receiving this antiepileptic drug as the first option for treatment (Fig. 1, Table 1).

Benzodiazepines, of which diazepam is the most widely known, have been associated with multiple mitochondrial effects as they bind to a mitochondrial receptor involved in steroid-synthesis and permeability transition pore opening to promote apoptosis development. This was demonstrated when a cancer-derived cell model was exposed to midazolam [17].

It has been described that the concomitant administration of the neuromuscular relaxant drug pancuronium and anti-inflammatory steroids in patients receiving mechanical ventilation may be related to the development of toxic myopathy [18,19]. This effect was later confirmed *in vitro* by alterations in mitochondrial membrane potential and increased apoptosis in cultured lymphocytes exposed to pancuronium [20]. Despite the safety of depolarizing and non depolarizing neuromuscular relaxants has been previously documented in patients with mitochondrial disease [21,22], a unique fatal case of postoperative myopathy was recently described in a child with mtDNA depletion syndrome after vecuronium administration [23].

Local anesthetics have been described to cause mitochondrial damage through uncoupling oxidative phosphorylation and inhibiting mitochondrial Complex V (CV) or ATPase as well as alternative MRC complexes [24] in experimental models and patients (Fig. 1, Table 1). For example, bupivacaine inhibits mitochondrial function, increases ROS production, reduces oxidative phosphorylation and induces mitophagy in patients, resulting in myopathy, characterized by postoperative muscle pain and dysfunction [25].

Antiepileptics

Epilepsy is one of the most common causes of neurological attention in the clinical practice, and many efforts have been made to find an adequate, effective and secure pharmacological agent that helps patients to prevent and control seizures.

Many antiepileptic drugs are known to produce alterations in mitochondrial function [26]. Paradoxically, it is not rare to find them as the backbone for the treatment of mitochondrial disorders, which in many cases are accompanied by epilepsy. Such is the case

of Leigh Syndrome, Alpers Huttenlocher disease, MELAS and MERRF (myoclonic epilepsy with ragged red fibers). As it has recently been reviewed [27], antiepileptic treatment should take into consideration that these drugs can have a mitochondrial toxic effect that could trigger or worsen a previous condition [28], and may even be fatal in some cases.

The aromatic antiepileptic drugs have been recently studied for *in vitro* mitochondrial toxicity, and it was demonstrated that all drugs, when bioactivated, intensely affected mitochondrial respiration and ATP synthesis (Fig. 1, Table 1) that may underlie associated hepatotoxicity. The differential toxic capacity to cause mitochondrial dysfunction *in vitro* was described (from high to low) as follows: Phenytoin > Phenobarbital > Carbamazepine [29].

Among the therapeutic options for antiepileptic treatment, Valproic acid (VPA) is the most commonly related to mitochondrial toxicity and associated hepatotoxicity [30] through β -oxidation pathway interference [31], supported by several experimental findings. Various mechanisms have been proposed to explain VPA hepatotoxicity such as mitochondrial respiration dysfunction [32], compromised free-radical scavenging activity or enhanced production of ROS (Fig. 1, Table 1) [33]. This mitochondrial pathologic phenotype results specially altered in carriers of POLG gene mutation, responsible for encoding γ DNA polymerase (γ DNApol), in which mtDNA depletion, increased PTP opening and an higher apoptotic sensitivity have been also described [34]. Such mitochondrial toxicity of VPA prompted medical guidelines to circumvent its administration in case of known or suspected mitochondrial disease such as CPEO (chronic progressive external ophthalmoplegia), since it may lead to fulminant hepatic failure [35]. In this sense, new antiepileptic drugs have been developed as a safer option [36].

Neuroleptics or Antipsychotics

Neuroleptics are widely used as a therapeutic option for schizophrenia, paranoia and organic/functional psychosis related mood disorders. These drugs are related to secondary effects in both the peripheral and central nervous system [37].

Extrapyramidal effects, such as dystonia, akathisia and parkinsonism, probably represent the most relevant clinical consequences and have been associated with different risk factors such as the time of treatment, patient's age [38,39] and polymorphisms in cytochrome p450 [40], among others [41,42]. MRC CI activity inhibition may help to explain unsolved questions regarding the onset of extrapyramidal movement disorders [43,44], as well as the ROS production derived from CI dysfunction (Fig. 1, Table 1) [45,46], which has been demonstrated in experimental models and also documented in patients.

Balijepalli *et al.* [47] demonstrated that, when administered as a single dose, haloperidol causes CI dysfunction only in striatum and midbrain of mice (extrapyramidal region), as opposed to chronic administration (commonly used in clinical settings), in which CI dysfunction occurs also in the frontal cortex and hippocampus.

Because extrapyramidal manifestations are sometimes non-reversible despite antipsychotic discontinuation, some authors have proposed a permanent alteration in mtDNA (Fig. 1, Table 1) as the etiology of the secondary effect [48], which has not been further confirmed by other authors [49].

Our group assessed mitochondrial toxicity in schizophrenic patients undergoing differential neuroleptic treatment and confirmed MRC CI dysfunction at enzymatic and oxidative level [50]. The differential mitochondrial toxicity reflected through the MRC CI dysfunction depending on the type of neuroleptic administered (haloperidol > risperidone > clozapine) was similar to the frequency of prevalence of extrapyramidal movement disorders caused by these drugs, suggesting an association between mitochondrial damage and the severity of clinical secondary effects (Fig. 2).

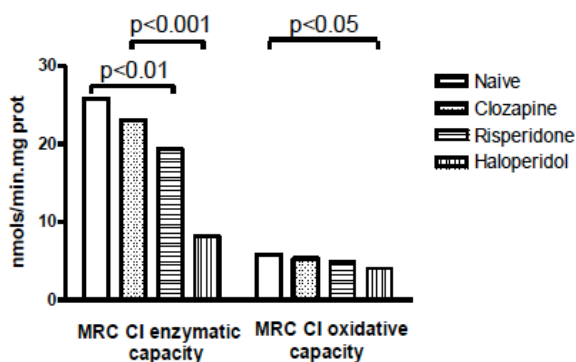


Fig. (2). Mitochondrial respiratory chain complex I (MRC CI) enzymatic and oxidative activities in different naive or treated (with clozapine, risperidone or haloperidol) schizophrenic patients. Differential CI enzymatic dysfunction is observed in concordance to severity of extrapyramidal movement disorders as follows: haloperidol>risperidone>clozapine. Figure reproduced with permission of the authors of the article: Casademont *et al*, published in the *J Clin Psychopharmacol* 2007; 27: 284 [50].

It has also been recently described that mitochondrial damage and ROS production are responsible for weight gain and metabolic syndrome in patients treated with antipsychotics, which is reported to be an important cause of treatment withdrawal [51,52].

Antidepressants

This kind of drugs is widely used in the clinical practice. As stated by their name, they are used for major depression and dysthymias but also for many other conditions such as chronic and neuropathic pain, eating disorders, sleep disorders, migraine and attention-deficit hyperactivity disorder (ADHD), among others.

Tricyclic antidepressants (TCA) were one of the first drugs discovered for mood disorders, they inhibit the reuptake of serotonin, norepinephrine and dopamine into presynaptic vesicles in the brain in a non selective manner, leading to significant and often intolerable side effects, such as memory impairment, that limits in an important way their clinical utility. It has been recently suggested that chronic use of antidepressants may lead to Parkinson's Disease and that the underlying mechanism may involve mitochondrial dysfunction [53]. Amitriptyline is one of the most prescribed TCA and it has been thoroughly studied in order to elucidate the different mechanisms that may be involved in the appearance of adverse effects. González-Pardo reported a general pattern of decrease in the oxidative metabolism in limbic regions of animal models [54]. More recently, it was demonstrated *in vitro* an inhibition of mitochondrial activity with a secondary increase in oxidative stress, production of ROS and cell death when using an amitriptyline concentration similar to the one used for patients with severe depression [53] (Fig. 1, Table 1). Another interesting work [55] demonstrated an apoptotic activity of clomipramine and desipramine, with significant inhibition of the activities of CI, complex II/III (CII/III) and complex IV (CIV) in a cell model and in isolated mitochondria (Fig. 1, Table 1).

Selective serotonin reuptake inhibitors (SSRIs) are the most widely prescribed antidepressants worldwide, primarily because they are better tolerated than previously described antidepressants. The most common adverse effects associated with SSRIs are not life threatening and dose dependent, except for the case of fluoxetine-induced skin reactions that appear to be idiosyncratic [56]. As for mitochondrial disturbances, fluoxetine and sertraline have both been reported to cause mitochondrial toxicity *in vitro*. It has been demonstrated in animal models that fluoxetine inhibits mitochondrial respiration through CI [57], affects ATPase activity, and inter-

feres with the physical characteristics of the inner mitochondrial membrane, which could be responsible of associated gastrointestinal discomfort [58] (Fig. 1, Table 1). Although sertraline is considered to be relatively safe, liver injury has been documented and it has been demonstrated *in vitro* that sertraline uncouples mitochondrial oxidative phosphorylation and inhibits the activities of CI and CV [59] and induces apoptosis [60] (Fig. 1, Table 1). It has been recently reported that sertraline can reduce total ATP levels in human platelets, although this effect was only seen in higher much higher concentrations than the ones used in the clinical practice [61], effect previously described in other organisms [62].

Fluoxetine has also been reported to prevent apoptosis by inhibiting mitochondrial permeability transition pore (PTP) opening and cytochrome c release [63], which supports previous experiments carried out in animal models where malignant cell growth was demonstrated at clinically relevant doses [64]. However, there is also contradictory data at this respect, as was reported later by Cloonan and Williams [65]. Similarly, sertraline has been reported to inhibit and proliferate apoptosis on Jurkat lymphoma cells, although the specific apoptotic pathway has not yet been elucidated [66]. Whether antidepressants have a beneficial effect on cancer therapy or, on the other hand, promote malignant growth, has been a matter of great interest for years [67,68], giving rise to many considerations that exceed the scope of this article but should be kept in mind when evaluating mitochondrial toxicity of this kind of components.

Antivirals

Antivirals used to treat Human Immunodeficiency Virus (HIV) or Hepatitis C Virus (HCV) infection have been associated to mitochondrial impairment, which may rely on the basis for adverse effects. Mitochondrial toxicity of antiretrovirals has been mainly attributed to nucleoside reverse transcriptase inhibitors (NRTI), and to a lesser extent, protease inhibitors (PI) and non-NRTI (NNRTI).

Nucleoside analogue reverse transcriptase inhibitors exert their therapeutic activity of blocking viral cycle by inhibiting the retrotranscriptase enzyme of the virus. Thymidine analogues including didanosine (ddI), zidovudine (AZT) and stavudine (d4T) are the most related to mitochondrial toxicity [69]. Clinically, they are associated to myopathy, hyperlactatemia, lactic acidosis, polyneuropathy or pancreatitis [70–72]. Some of these symptoms may turn into severe clinical consequences in chronically infected and treated patients.

Mitochondrial toxicity and secondary effects derived from NRTIs are caused by the inhibition of the endogenous mitochondrial γ DNAPol, the only enzyme responsible for mtDNA replication and repair [73]. γ DNAPol inhibition affects both the mtDNA copy number and quality through point mutations, deletions and depletions, ultimately leading to mitochondrial dysfunction, which has been documented in experimental models and in treated patients. Over time, dysfunctional mitochondria become unable to perform metabolic functions, such as oxidation of fatty acid and oxidative phosphorylation. Oxidative stress and energetic deprivation trigger intrinsic apoptosis [74–78], especially deleterious when it is the responsible for the depletion of CD4+ T-lymphocytes of HIV-infected patients. The hierarchical capacity of NRTI to inhibit γ DNAPol was established *in vitro*: ddC (zalcitabine) > ddI > d4T (stavudine) >>> AZT > 3TC (lamivudine) > ABC (abacavir) = TDF (tenofovir) [79].

Some compensatory homeostatic mechanisms for NRTI-induced mitochondrial damage and associated mtDNA depletion have been reported by transcriptional and/or translational up regulation [80,81]. Also, epigenetic factors driven by oxidative stress have been associated to long term side effects that should be taken into account when prescribing this kind of drugs [82].

Fortunately, second generation of antiretroviral drugs are being commercialized with reduced mitochondrial toxicity and associated adverse effects (Fig. 3).

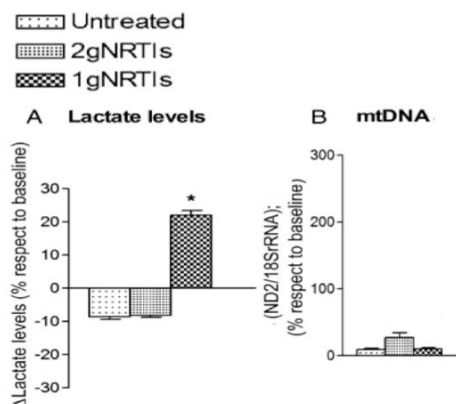


Fig. (3). **A.** Lactate levels, which constitute a plasmatic biomarker of mitochondrial dysfunction were similar in all groups at baseline, but significantly increased after 2 years of treatment with first generation nucleoside analogue reverse transcriptase inhibitors (1gNRTIs) with respect to HIV-infected untreated controls or second generation nucleoside analogue transcriptase inhibitor treated patients (2gNRTIs). **B.** Mitochondrial DNA content (mtDNA), as a biomarker of mitochondrial toxicity, was also higher in second generation-treated patients. Figure reproduced with permission of the authors of the article: Morén *et al.*, published in the *Journal of acquired immune deficiency syndromes* 2012; 60(2), pp.111–6 [83].

Protease inhibitors block viral protein processing. The similarities between cellular and viral proteins are the cause for the PI-derived lipid and carbohydrate metabolic disturbances, which could, in turn, remain at the basis of the onset of the metabolic syndrome and lipodystrophy, typically associated with these antiviral drugs.

To date, there is still controversial data about the mitochondrial and apoptotic effects of PI. Some anti-apoptotic and mitochondrial PI-protective benefits have been reported, based on the PI-mediated capacity to prevent mitochondria depolarization and mitochondrial apoptosis development [84]. Meanwhile, other authors have reported that higher doses of PI depolarize mitochondria leading to apoptotic development (Fig. 1, Table 1) [85]. Most authors accept a dual model of PI-mediated anti/pro-apoptotic behavior and beneficial/deleterious effects of PI with respect to mitochondria in a dose-dependent manner. Data supporting the pro-mitochondrial and anti-apoptotic effects of PI have been obtained *in vitro* using drug concentrations under physiologic values [86–88]. Curiously, most studies using PI concentrations in plasma have described mitochondrial toxicity and pro-apoptotic properties for these drugs [77].

Non-nucleoside reverse transcriptase inhibitors (NNRTI) are a third group of antiviral drugs that also aim to block viral reverse transcriptase. Compared to NRTIs, these antiretrovirals lack secondary inhibition of mitochondrial γ DNAPol. However, efavirenz, the most commonly used NNRTI, has been associated to enhanced apoptosis development (Fig. 1, Table 1) [89] and interfere on adipocyte differentiation [90]. Recent *in vitro* data suggests that efavirenz produces mitochondrial dysfunction in hepatocytes and neurons [91,92] and nevirapine, associated to hepatotoxicity [93] may contrarily reduce the rate of apoptosis [94]. These adverse effects moved pharmaceutical companies to develop new NNRTI such as rilpivirine, etravirine and delavirdine, that do not affect mitochondrial function [95]. Additionally, new antiviral drug families as fusion, entry and integrase inhibitors, with few or null mitochondrial toxicity are currently available as therapeutic options for HIV management [96].

Antibiotics

Antibiotics are used for the treatment of bacterial infections. They are commonly classified depending on their antibacterial activity.

Due to the endosymbiotic origin of mitochondria [2], mitochondria share homology with prokaryotes and, consequently, some antibiotics can exert secondary mitochondrial lesion which may lead to severe clinical manifestations [97].

Some antibiotics such as valinomycin and gramicidin exert an uncoupler effect by disturbing the mitochondrial electrochemical gradient and preventing ATP synthesis (Fig. 1, Table 1), as demonstrated in experimental models and patients. Other antibiotics, including piericidin A, antimycin A and oligomycin, produce the specific inhibition of some of the MRC complexes leading, in most of cases, to a suboptimal cellular respiration. Piericidin specifically inhibits MRC CI (the electron transfer between NADH and ubiquinone), antimycin A specifically blocks MRC CIII (electron transfer between cytochromes b and c) and oligomycin specifically prevents MRC CV function, both in *in vitro* and *in vivo* studies (Fig. 1, Table 1).

Mitochondrial toxicity derived from chloramphenicol, tetracycline, erythromycin, linezolid, aminoglycosides and rifampicin [98], has been well documented both in experimental models and patients (Fig. 4). The deleterious consequence for all the above-mentioned antibiotics is the decrease of mitochondrial protein synthesis, which may lead to mitochondrial dysfunction at the basis of many clinical manifestations such as ear loss and myopathy [99]. For instance, it is widely known that aminoglycosides (such as gentamicin) produce side effects such as auditory, renal and muscle disorders that are related to mitochondrial dysfunction. Since the main target of aminoglycosides is the prokaryotic inhibition of the binding site for bacterial tRNA binding to rRNA, it has been recently demonstrated that the high homology shared between both prokaryote and mitochondrial ribosomes, results in an off-target inhibition of mitochondrial protein synthesis (Fig. 1, Table 1) contributing to the earlier mentioned side effects [100]. A novel agent, tedizolid, has been recently introduced as a therapeutic alternative to linezolid (associated to lactic acidosis, hematologic disturbances, gastrointestinal discomfort or neuropathy) given the evidence in preclinical studies, both *in vitro* and in animals, that mitochondrial function is less disturbed, even though it decreases mitochondrial protein synthesis at a larger scale than linezolid when used at similar doses [101].

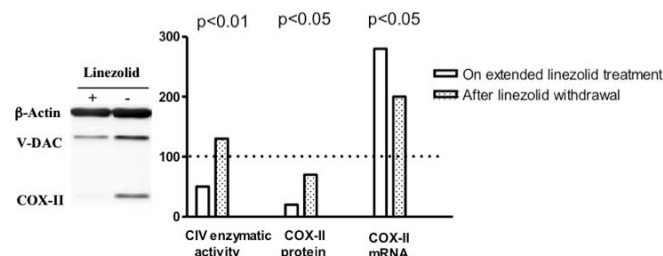


Fig. (4). **(Left)** Quantification of mitochondrial protein before (-) or after (+) extended linezolid administration. β -actin as cell loading control; V-DAC (voltage dependent anion channel) as mitochondrial loading control; COX-II (subunit II of the cytochrome c oxidase) as mitochondrial encoded and synthesized protein. It is remarkable the decrease of CIV protein content and enzymatic activity despite increased mitochondrial transcription when patients are under linezolid therapy. Mitochondrial RNA levels increase, probably, due to a homeostatic intent to preserve the mitochondrial protein rate. Figure reproduced with permission of the authors of the article: Garrabou *et al.*, published in the *Antimicrobial agents and chemotherapy* 2007, 51(3), pp.962–7 [99].

A word has to be said about the recently described, albeit rare, cardiotoxic effects of macrolides which have been recently associated to a ROS-induced alteration of the kinetics of potassium channels, which disrupt cardiomyocytes conductance and enhances apoptosis signalling as a secondary effect of cytochrome c release from heart mitochondria into cardiomyocytes cytosol, at even lesser concentrations than the ones found to be hepatotoxic in the same animal model [102].

Fungicides

Drugs focused on the treatment of fungal infections, such as ketoconazole (associated to hepatotoxicity) and miconazole (but not fluconazole) directly inhibit the NADH and succinate oxidase enzymes necessary for mitochondrial oxidative phosphorylation in an experimental model (Fig. 1, Table 1) [103].

Other antifungals, including mixotiazol (responsible for MRC CIII blockade), sodium azide (which inhibits mitochondrial CIV function) or rutamicine (also used as an antibiotic; responsible for ATP-synthase inhibition) (Fig. 1, Table 1, Table 1), can also seriously impair mitochondrial function, ultimately leading to cell death either in animal models or human treated patients.

An increase in the production of ROS levels has additionally been reported for several antifungal drugs (Fig. 1) such as ciclopirox, amphotericin B and miconazole in *Candida albicans* and *Saccharomyces cerevisiae* [104].

Antimalarial Drugs

These type of drugs used to treat *Plasmodium sp* infection have also been described as toxic agents for the mitochondria. Quinine is the classic example of antimalarial drug and, in an animal model using bovine heart, it has been reported to influence potassium pathways in mitochondria, mainly by mitoKATP channel inhibition [105].

Artemisinin compounds are used to treat drug-resistant malaria. An exhaustive review by Rodrigues *et al.* describes an increase in the generation of ROS levels via MRC dysfunction and the induction of cell death via apoptosis, among other mitochondrial effects (Fig. 1, Table 1) [106].

Interestingly, the MRC chain of *Plasmodium falciparum* is an attractive new target for treatment because its functional significance varies from that of the equivalent mammalian system which is a great advantage in the clinical setting [107]. However, close attention will have to be focused on potential cross-over toxicity.

Antineoplastics and Chemotherapies

The therapeutic activity of some anticancer drugs consists of an induction of damage cell death through apoptosis by interfering with mitochondrial pathways. This is the case of flutamide [108], tamoxifen [109,110] and doxorubicin [111], which are chemotherapy drugs used for prostate, breast and soft-tissue cancer treatment, respectively, that have been reported to interfere with mitochondrial respiration, uncoupling of the oxidative phosphorylation system and, specifically, the electron transference from MRC CI by a redox cycling mechanism in experimental models and in patients (Fig. 1, Table 1). Doxorubicin also forms a stable complex with Fe³⁺ which then reacts with hydrogen peroxide to form hydroxyl radicals, which could explain why dexrazoxane, a ferric chelator, prevents cardiomyocyte induced mitochondrial dysfunction [112]. Finally, it has also been stated that the interaction of doxorubicin with cardiac mitochondrial proteins as a result of the drug's interaction with cardiolipin, which is a lipid that gives structure to the mitochondrial inner membrane, by which it is excluded and indirectly causes damage to MRC [113].

Cisplatin is also associated with various kinds of mitochondrial toxicities. Recent research has shown an impairment of mitochondrial oxidative function *in vitro*, with mtDNA alterations and rise in lipid peroxidation as a result of ROS production (Fig. 1, Table 1) and a decrease of antioxidant status [114].

Antidiabetics

Antidiabetics are used in clinical practice to treat *Diabetes Mellitus* by lowering glucose levels in blood. Besides, these drugs have also been related to mitochondrial damage through specific MRC impairment in experimental models. For instance, metformin and other biguanides specifically inhibit MRC CI activity (Fig. 1, Table 1) [115,116]. It has been shown that CI inhibition triggers a complete inhibition of gluconeogenesis. In addition, the respiration of submitochondrial particles was much more resistant to metformin than mitochondria on intact cells, suggesting that slow membrane potential-driven accumulation of metformin across the inner membrane into the mitochondrial matrix was required for inhibiting CI, all of the above by a mechanism still unknown but that could involve the interaction of hydrocarbon parts of the molecule and membrane phospholipids and ulterior interaction with the phospholipid phosphate group [117].

Thiazolidinediones improve insulin resistance by acting as ligands for the nuclear peroxisome proliferator-activated receptor- γ (PPAR γ). Troglitazone (TRO) was the first thiazolidinedione used. Unfortunately, it caused serious hepatic damage and was withdrawn from the market. Evidence suggests that TRO caused mitochondrial dysfunction and induction of apoptosis in an *in vitro* model of human hepatocytes, and damage to mtDNA has been demonstrated to be the initiating event involved in TRO-mitochondrial induced dysfunction and hepatotoxicity [118]. However, due to a different chemical composition, Rosiglitazone has been proved to be a safer option to improve insulin resistance as it does not cause mtDNA damage *in vitro* and no serious adverse effects have been reported in the clinical setting [119].

Hypolipemiant

Hypolipemiant are used to treat dyslipidemias. Their therapeutic activity consists of decreasing the amount of lipids in blood. There are different types of hypolipemiant agents.

Statins are the most frequently administered anticholesterolemics and they decrease cholesterol levels by blocking its synthesis through competitive inhibition with the enzyme acetyl coenzyme a (HMG CoA) reductase. Cholesterol, and the remaining fatty acids, are initially synthesized through CoA in the mitochondria. The degradation process (through β -oxidation) undertakes just the opposite pathway to generate CoA, in the mitochondria as well. Statin blockade of cholesterol synthesis has been associated with a reduction in mitochondrial Coenzyme Q content (the mobile electron transfer located between MRC CI, II and III) (Fig. 1, Table 1) that can be clinically accompanied by a wide range of symptoms (Fig. 5), from the asymptomatic rise of creatine kinase to severe rhabdomyolysis or the development of a myopathic syndrome (increase of creatine kinase, severe muscle weakness, rhabdomyolysis and myoglobinuria) which, in some cases, may lead to death [1]. Fortunately, the frequency of statin-induced myopathy is quite reduced (about 1% of patients on treatment per year), tends to be dose-dependent and may be solved when lowering or discontinuing the drug. However, certain drug combinations may increase its incidence. This is the case of concomitant administration of statins with the immunosuppressor cyclosporine, in renal or cardiac transplanted patients, in which myopathy frequency increases up to 30% [18]; or the combination of statins with the antihypertensive treatment propranolol. Furthermore, the association of statins with other

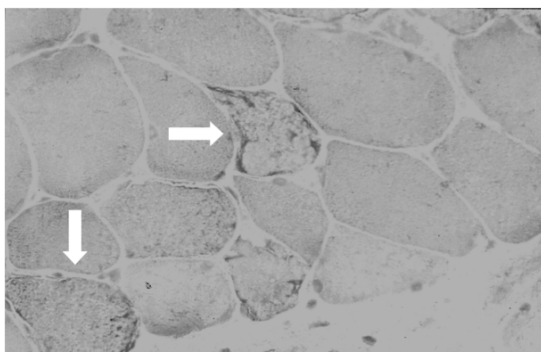


Fig. (5). Gomori trichrome staining in a frozen section of skeletal muscle from a patient with symptomatic statin toxicity. Observe classical ragged-red fibers, characteristic of mitochondrial disease (white arrows). Figure reproduced with permission of the authors of the chapter “Secondary mitochondrialopathies” from the book *Mitochondrial Pathophysiology*, 2011:249-279 [1].

hypolipemiant agents such as fibrates notoriously increases the risk of the myopathy onset, especially when the patient is over 70 and kidney function is compromised [120]. There are some other drug combinations that may lead to higher serum drug levels because of competition for cytochrome P450 metabolism in the liver, such as erythromycin, diltiazem, nefazodone and azolic antifungals.

Fibrates are used to treat hyperlipidemia and have also been associated with mitochondrial damage, especially if concomitantly administered with statins, as aforementioned. Individual fibrates induce mitochondrial dysfunction, as demonstrated in experimental models through different molecular mechanisms to finally impair cell respiration. For instance, fenofibrate, predominantly acts by inhibition of the MRC CI enzymatic activity (Fig. 1, Table 1) [115].

Antiarrhythmics

Antiarrhythmic agents are a group of pharmaceutical drugs used to suppress abnormal cardiac rhythms, which are a common cause of death and disease.

Antiarrhythmic drugs are classified based on their mechanism of action as follows: (i) Class I interfere with sodium channels, (ii) Class II are anti-sympathetic nervous system agents, most agents of this class are beta blockers, (iii) Class III affect potassium efflux from the cell, (iv) Class IV affect calcium channels and the atrioventricular node and (v) class V agent work by other or unknown mechanisms.

Class I antiarrhythmic drugs, as quinidine and lidocaine, have been associated with ATP-synthase inhibition in animal models, probably due to their lipophilicity and membrane stabilizing activity, typical of these drugs [121].

Amiodarone is one of the most effective antiarrhythmic agents, with class III activity, which is used in the treatment of many ventricular and supraventricular dysrhythmias and is particularly useful for converting atrial fibrillation. Its more serious adverse effects include hepatocellular liver damage, pulmonary fibrosis or thyroid dysfunction. The hepatotoxicity mechanism could be immune or mitochondrial-mediated, as it has been demonstrated in rat liver cells, where amiodarone accumulates in the mitochondria leading to an impairment of mitochondrial function that include uncoupling of oxidative phosphorylation, inhibition of CI-III and inhibition of fatty acid β -oxidation (Fig. 1, Table 1) [122].

Non-Steroidal Anti-Inflammatory Drugs

Non-steroidal anti-inflammatory drugs (NSAIDs), such as aspirin, ibuprofen or acetaminophen, represent the most widely pre-

scribed drugs around the world. They reduce inflammation and pain through cyclooxygenase inhibition with the consequent decrease in prostaglandin production.

Anti-inflammatory derived mitochondrial damaging mechanisms have been well described. NSAIDs have been reported to cause an uncoupling of the oxidative phosphorylation pathway, an increase in resting state respiration, a decrease in ATP synthesis and mitochondrial membrane potential, inhibition of adenine nucleotide translocase and to cause an alteration of mitochondrial lipid metabolic pathways, all these through the inhibition of β -oxidation in multiple *in vitro* models (Fig. 1, Table 1), thoroughly reviewed by Szewczyk [123].

The derived mitochondrial damage, together with cyclooxygenase inhibition and inflammatory tissue-reaction, has been proposed as responsible for some clinical secondary events such as hepatotoxicity and gastrointestinal damage (ulcers, gastrointestinal perforation and bleeding) associated with NSAID administration. Reye's syndrome, a disorder characterized by liver disease and encephalopathy, was also initially associated with aspirin administration and potential mitochondrial damage, anyhow this association is weakening, and currently it is thought that an underlying metabolic alteration seems to trigger this condition [124].

Acetaminophen –also known as paracetamol– is another widely used NSAID whose most important adverse reaction is hepatotoxicity when administered at high doses. For a long time, the mechanism of this damage remained unknown, but it has been recently demonstrated in human hepatic cells that mitochondrial CI dysfunction, and reduction of the expression of those genes involved in the MRC complex assembly, electron and proton transport, and those that participate in mitochondrial membrane permeability, may be involved in the etiopathology of the disease [125] (Fig. 1, Table 1).

Nimesulide is another anti-inflammatory frequently used in the clinical practice that may cause idiosyncratic hepatotoxicity. It has been described that nimesulide may influence mitochondrial physiology by interfering with its membrane structure and dynamics [126]. The latter and some other studies [127] demonstrate the importance of the integrity of mitochondrial membranes and their evaluation as potential targets for toxicity that should be addressed to when developing or prescribing anti-inflammatories [128].

Nitric Oxide

Nitric oxide (NO) is a short half-life, inorganic molecule that diffuses freely through the membranes and inhibits mitochondrial respiration and cytochrome oxidase activity (CIV). It is naturally produced by NO synthases through arginin, oxygen and NADPH consumption and is metabolized to peroxynitrite (NOO⁻) in combination with oxygen. NO directly binds and inhibits CIV function (Fig. 1, Table 1) and the resultant peroxynitrite has been reported to inhibit MRC CI activity through impairment of poly ADP-ribose polymerase-1 (PARP-1) function and a decrease in NAD⁺/NADH content in *in vitro* models aimed to resemble various biological systems [129].

It has primarily a vasodilator function but is also known to play a role in a variety of physiological processes such as neurotransmission and immune response [130]. However, sustained levels of NO production or chronic gas exposure result in direct tissue toxicity, leading to the development of carcinomas and inflammatory conditions.

Nowadays its usage is approved for the treatment of pulmonary hypertension in neonatology [131] and studies are being held for its use in other forms of pulmonary hypertension such as asthma and acute respiratory distress syndrome [132]. Although there are not proven *in vivo* clinical effects of secondary mitochondrial toxicity,

it exerts mitochondrial damage *in vitro*, and, additionally, it is known to induce cell death by a variety of mechanisms unrelated to respiratory inhibition [133].

Also worthy of mention is nitroglycerin, a precursor of NO with a potent vasodilator capacity commonly used in medical practice as an antianginal medication. It exerts this effect by the release of NO, raising controversies about its mitochondrial potential toxicity, specially since it was demonstrated that it inhibits mitochondrial respiration and increases mitochondrial ROS production in animal models [134]. However, it has been recently demonstrated that this damage is not exerted via NO [135], suggesting again an alternative mechanism of mitochondrial and cell damage independent of NO production.

3. TREATMENT OF DRUG-INDUCED MITOCHONDRIOPATHIES

When secondary mitochondrial toxicity is suspected, the most efficient therapeutic measure to be applied is the discontinuation of the exposure to the toxic compound. However, this may not always be possible, for example, in cases of therapeutic regimens necessary for the quality of life of the patient. If toxic withdrawal is not feasible, then treatment of secondary mitochondrial diseases becomes necessary. Treatment of mitochondrial diseases should be individualized because of the peculiarities and high-variability of mitochondriopathies. To date, mitochondrial treatments are exclusively supportive and symptomatic. Such treatment consists on administering mitochondrial drugs, blood transfusions, hemodialysis, invasive measures, surgery, dietary measures and physiotherapy [136].

Knowledge of mitochondrial disorders has dramatically increased in the last years and some 'mitochondrial treatments' including vitamins, enzymatic cofactors or antioxidants, have been proposed in order to minimize their consequences [7,137,138]. Resveratrol is currently being prescribed and studied because its antioxidant capacity has proven to reverse mitochondrial toxicity secondary to various compounds [124,139]. However, most of the treatments are palliative or supportive with limited proven efficacy.

For the treatment of some manifestations secondary to mitochondrial disease, including diabetes, hyperlipidemia or epilepsy, dietary measures can be offered (such as ketogenic diet or anaplerotic diet) [140,141].

Despite limited possibilities, symptomatic treatment should be provided to treat patients with mitochondriopathies, since it may have a significant impact on the onset, course and outcome of the disease. For instance, in case of symptomatic hyperlactatemia and lactic acidosis as secondary mitochondriopathies derived by both HIV-infection and antiretroviral treatment, concomitant administration of mitochondrial non-specific drugs (L-carnitine, B6 and C vitamins, thiamine and hydroxycobalamin) has been associated with faster and better amelioration of affected patients [137]. The current data available on mitochondrial toxicity induced by HIV infection and antiviral treatment has led to antiretroviral guidelines for restrictive strategies based on: (i) substituting antivirals described to present high mitochondrial toxic properties, by less potent toxic regimens for mitochondria, (ii) reducing antiretroviral doses, or (iii) changing antiviral schedules to nucleoside-sparing therapies or (iv) the implementation of structured-treatment interruptions [142–144]. Probably these measures could be applied to other mitochondrial toxic treatments.

In secondary mitochondrial disturbances caused by toxic drug administration, clinicians should be aware of which drug to choose, the doses and combinations of both. Also they must be aware of any suspect of mitochondrial toxicity, early signs or symptoms of toxic-

ity undergoing a subsequent change in therapy not only after the manifestation of toxicity but also prior to its development. Although mitochondrial recovery is not always possible in some cases after discontinuation of the toxic agents, it is preferable to prevent, rather than to deal with, the secondary effects of therapies and, once the secondary effect has developed, early management will help to achieve mitochondrial and clinical recovery.

A novel and different approach that should be considered is system's pharmacology, which is aimed to delineate and predict the effects of a drug from its on-target beneficial effect and off-target adverse effects through the systems pathways and networks [145]. This way, the understanding and assessment of its safety and overall therapeutic index could be taken into account. This approach, from a mitocentric point of view, would improve the yield of the future drug products by prompting an adequate benefit/risk ratio.

4. CONCLUSIONS

Certain therapeutic drugs used in medical practice may trigger mitochondrial toxicity, which may lie at the basis of adverse clinical manifestations. Although their administration usually entails subclinical conditions, they may occasionally lead to serious adverse events.

Different degrees of evidence support mitochondrial toxicity in each case (based on experimental models or *ex vivo* data directly extracted from patients). Among those drugs frequently administered in whose adverse effects are clearly secondary to mitochondrial damage we must highlight neuroleptics, antivirals and antibiotics. Apart from these, two other categories of drugs that should be kept in mind are anesthetics and antiepileptics, for they may exceptionally cause life-threatening complications, such as toxic myopathy and fulminant liver failure, respectively.

Few therapies are free of adverse effects. Thus, it is important to remark that medical prescriptions have to take precedence even over secondary mitochondrial events, as long as the clinicians are aware of potential mitochondrial derived toxicities. These drugs are seriously discouraged in case of high risk populations as patients with inherited mitochondrial diseases, pregnant women or women in reproductive stage. Compromised patient wellness and socio-sanitary and economic burden of clinical management of these complications are raising concern into the clinical and scientific community. Most of secondary effects are reversible after disruption of toxic exposition. However, since therapeutic interventions cannot always be avoided, secondary effects may remain permanently or be hardly reversible, and treatment of acquired mitochondriopathies remains supportive.

First, it is fundamental to raise awareness of mitochondrial toxicity of these therapeutic drugs into the medical personnel to follow-up potential secondary effects and avoid synergic toxic interactions. Information of molecular and clinical consequences of toxic exposure becomes fundamental to assess risk-benefit imbalance of treatment prescription. Second, currently described biomarkers of mitochondrial toxicity should be implemented in routinely clinical practice to monitor high-risk population in which these drugs should be avoided or disrupted in case of clinical complications. Third, it is mandatory to search and promote the use of novel drugs with less mitochondrial toxicity while conserving its therapeutic efficacy.

Continuing the refinement of this information regarding mechanisms underlying mitochondrial toxicity of therapeutic drugs will surely come in the foreseeable future leading to the development of novel strategies of treatment and prevention of deleterious effects associated to mitochondrial toxicity.

Table 1. Summary of the therapeutic drugs reviewed, potential mitochondrial-related clinical effects that may arise from exposition and potential off target mechanism of action. It is important to note that each drug may exert some other secondary effects but, as they may not be secondary to mitochondrial toxicity, they are not mentioned in this review. ⊙: mitochondrial toxic effects demonstrated in humans, •: mitochondrial toxic effects demonstrated in animal models, *ex vivo* or *in vitro*, but not on the clinical setting. The hierarchical capacity to exert mitochondrial toxicity is stated when possible (see text). ND: Adverse effects not demonstrated on clinical settings, EP: Extrapyramidal effects, GID: Gastrointestinal damage, LA: Lactic acidosis.

THERAPEUTIC DRUGS ASSOCIATED TO MITOCHONDRIAL TOXICITY		MECHANISM OF ACTION AT MITOCHONDRIAL LEVEL																							
CLINICAL USE	DRUGS		CLINICAL ADVERSE EFFECTS THAT MAY BE RELATED TO MITOCHONDRIAL TOXICITY																						
	CLASS	NAME	CI	CII	CIII	CIV	CV	ROS	mtDNA	ATP	OXPPOS	β oxidation	mtPTP	Cyt C	Other	MIM	MOM	ΔΨ	Mt Membrane	Mt dynamics	Mt proteins	Mytophagy			
Anaesthetics	Barbiturates	Halothane	•																						
		Isoflurane	•																						
		Sevoflurane	•																						
	Benzodiazepines	Propofol										⊙													
		Ketamine																							
		Phenobarbital																							
		Diazepam																							
	Muscular relaxants	Pancuronium																							
		Vecuronium																							
	Local	Bupivacaine																							
Phenytoin																									
Phenobarbital																									
Antiepileptics	Aromatic	Carbamazepine																							
		Valproic acid																							
	Non aromatic	Haloperidol																							
Neuroleptics	Atypical	Risperidone																							
		Clozapine																							
Antidepressants	Tricyclic antidepressants	Amytriptilin																							
		Clomipramine																							
		Desipramine																							
	Selective serotonin reuptake inhibitors (SSRIs)	Fluoxetine																							
		Sertraline																							

Table (1) contd....

THERAPEUTIC DRUGS ASSOCIATED TO MITOCHONDRIAL TOXICITY			MECHANISM OF ACTION AT MITOCHONDRIAL LEVEL																				
CLINICAL USE	DRUGS		CLINICAL ADVERSE EFFECTS THAT MAY BE RELATED TO MITOCHONDRIAL TOXICITY	MECHANISM OF ACTION AT MITOCHONDRIAL LEVEL																			
	CLASS	NAME		MRC	Aptosis	Mt Membrane	Mt dynamics	Mt proteins	Mytophagy	β oxidation	OXPHOS	ATP	mtDNA	ROS	CV	CTV	CIII	CII	CI				
Fungicides		Ketoconazole	Hepatotoxicity																				
		Miconazole																					
		Mixotiazol																					
		Sodium azyde																					
		Rutamicine																					
		Ciclopirox																					
Antimalarics		Amphotericine B	ND																				
		Quinine																					
Antineoplastics		Artemisinin derivatives	ND																				
		Flutamide																					
		Tamoxifen																					
		Doxorubicin																					
		Cisplatin																					
Antidiabetics		Metformin	ND																				
		Biguanides																					
Hypolipemiant		Troglitazone	Hepatotoxicity																				
		Statins																					
		Fibrates																					
Antiarrithmics		Atrovastatin	Rhabdomyolisis, myopathic syndrome																				
		Fenoibrate																					
		Lidocaine																					
Non steroidal Antinflammatories		Quinidine	Hepatotoxicity																				
		Amiodarone																					
		Aspirine																					
		Ibuprofen																					
Nitric oxide		Acetaminophen	Hepatotoxicity, GID																				
		Nimesulide																					

ABBREVIATIONS

ABC	=	Abacavir
ADHD	=	Attention-deficit hyperactivity disorder
ATP	=	Adenosine triphosphate
AZT	=	Zidovudine
CI	=	Complex I
CII	=	Complex II
CIII	=	Complex III
CIV	=	Complex IV
CV	=	Complex V
CPEO	=	Chronic progressive external ophthalmoplegia
ddC	=	zalcitabine
ddI	=	Didanosine
d4T	=	stavudine
DNA	=	Deoxyribonucleic acid
γDNApol	=	γDNA polymerase
Fe-S	=	Iron-sulfur
HCV	=	Hepatitis C virus
HIV	=	Human immunodeficiency virus
HMG CoA	=	acetyl coenzyme a
iPSC	=	Induced pluripotent stem cells
MELAS	=	Mitochondrial encephalopathy with lactic acidosis and stroke syndrome
MERRF	=	Myoclonic epilepsy with ragged red fibers
MRC	=	Mitochondrial Respiratory Chain
mtDNA	=	Mitochondrial DNA
NAD	=	nicotinamide-adenine
NADH	=	nicotinamide-adenine-dinucleotide
NNRTI	=	non-nucleoside reverse transcriptase inhibitors
NRTI	=	nucleoside reverse transcriptase inhibitors
NSAID	=	Non steroidal anti-inflammatory drugs
PPARγ	=	peroxisome proliferator-activated receptor-γ
PTP	=	Permeability transition pore
RNA	=	Rybonucleic acid
ROS	=	Reactive oxygen species
SSRIs	=	Selective serotonin reuptake inhibitors
TDF	=	Tenofovir
TCA	=	Tricyclic antidepressants
TRO	=	Troglitazone
VPA	=	Valproic acid

CONFLICT OF INTEREST

The authors confirm that this article content has no conflict of interest.

ACKNOWLEDGEMENTS

This work was supported by Fundación para la Investigación y la Prevención del SIDA en España (FIPSE 360982/10); Fundación Cellex; Fondo de Investigación Sanitaria (FIS 00462/11, FIS 01199/12, FIS 01455/13, FIS 01738/13, FIS 00817/15 and FIS 00903/15); InterCIBER PIE1400061; CONACyT, México; Marató de TV3 87C/2015; Suports a Grups de Recerca de la Generalitat de Catalunya 2014-2016 (SGR 2014/376) and Centro de Investigación en Red de Enfermedades Raras (CIBERER, an initiative of ISCIII).

We would like to thank Melisa Gabriela Altaparro for her counseling in English-language writing.

REFERENCES

- Garrabou, G.; Morén, C.; Nicolás, M.; Grau, J. M.; Casademont, J.; Miró, Ó.; Cardellach, F. *Mitochondrial Pathophysiology*; Transworld Research Network, 2011.
- Margulis, L. Symbiotic Theory of the Origin of Eukaryotic Organelles; Criteria for Proof. *Symp. Soc. Exp. Biol.* **1975**, No. 29, 21–38.
- Zhang, Y.; Marcillat, O.; Giulivi, C.; Ernster, L.; Davies, K. J. The Oxidative Inactivation of Mitochondrial Electron Transport Chain Components and ATPase. *J. Biol. Chem.* **1990**, *265* (27), 16330–16336.
- Davey, G. P.; Peuchen, S.; Clark, J. B. Energy Thresholds in Brain Mitochondria: POTENTIAL INVOLVEMENT IN NEURODEGENERATION. *J. Biol. Chem.* **1998**, *273* (21), 12753–12757.
- Wallace, D. C.; Melov, S. Radicals R'aging. *Nat. Genet.* **1998**, *19* (2), 105–106.
- Scatena, R.; Bottoni, P.; Botta, G.; Martorana, G. E.; Giardina, B. The Role of Mitochondria in Pharmacotoxicology: A Reevaluation of an Old, Newly Emerging Topic. *Am. J. Physiol. Cell Physiol.* **2007**, *293* (1), C12–C21.
- Andreu, A. L.; Gonzalo-Sanz, R. [Mitochondrial Disorders: A Classification for the 21st Century]. *Neurologia* **2004**, *19* (1), 15–22.
- Gröber, U. [Mitochondrial Toxicity of Drugs]. *Med. Monatsschr. Pharm.* **2012**, *35* (12), 445–456.
- Pasnoor, M.; Barohn, R. J.; Dimachkie, M. M. Toxic Myopathies. *Neurol. Clin.* **2014**, *32* (3), 647–670, viii.
- Cantor, R. S. The Lateral Pressure Profile in Membranes: A Physical Mechanism of General Anesthesia. *Biochemistry* **1997**, *36* (9), 2339–2344.
- Miró, O.; Barrientos, A.; Alonso, J. R.; Casademont, J.; Jarreta, D.; Urbano-Márquez, A.; Cardellach, F. Effects of General Anaesthetic Procedures on Mitochondrial Function of Human Skeletal Muscle. *Eur. J. Clin. Pharmacol.* **1999**, *55* (1), 35–41.
- Hanley, P. J.; Ray, J.; Brandt, U.; Daut, J. Halothane, Isoflurane and Sevoflurane Inhibit NADH:ubiquinone Oxidoreductase (Complex I) of Cardiac Mitochondria. *J. Physiol.* **2002**, *544* (Pt 3), 687–693.
- Mirakhimov, A. E.; Voore, P.; Halytsky, O.; Khan, M.; Ali, A. M. Propofol Infusion Syndrome in Adults: A Clinical Update. *Crit. Care Res. Pract.* **2015**, *2015*, 260385.
- Short, T. G.; Young, Y. Toxicity of Intravenous Anaesthetics. *Best Pract. Res. Clin. Anaesthesiol.* **2003**, *17* (1), 77–89.
- Ito, H.; Uchida, T.; Makita, K. Ketamine Causes Mitochondrial Dysfunction in Human Induced Pluripotent Stem Cell-Derived Neurons. *PLoS One* **2015**, *10* (5), e0128445.
- Berger, I.; Segal, I.; Shmueli, D.; Saada, A. The Effect of Antiepileptic Drugs on Mitochondrial Activity: A Pilot Study. *J. Child Neurol.* **2010**, *25* (5), 541–545.
- Ohno, S.; Kobayashi, K.; Uchida, S.; Amano, O.; Sakagami, H.; Nagasaka, H. Cytotoxicity and Type of Cell Death Induced by Midazolam in Human Oral Normal and Tumor Cells. *Anticancer Res.* **2012**, *32* (11), 4737–4747.
- Illa Sendra, I. [Recent Advances in Toxic Myopathies]. *Med. Clin. (Barc).* **1993**, *100* (19), 741–742.
- Matsubara, S.; Okada, T.; Yoshida, M. Mitochondrial Changes in Acute Myopathy after Treatment of Respiratory Failure with Mechanical Ventilation (Acute Relaxant-Steroid Myopathy). *Acta Neuropathol.* **1994**, *88* (5), 475–478.
- Delogu, G.; Moretti, S.; Marcellini, S.; Antonucci, A.; Tellan, G.; Marandola, M.; Signore, M.; Famularo, G. Pancuronium Bromide, a Non-Depolarizing Muscle Relaxant Which Promotes Apoptosis of Blood Lymphocytes *in vitro*. *Acta Anaesthesiol. Scand.* **2003**, *47* (9), 1138–1144.
- Wiesel, S.; Bevan, J. C.; Samuel, J.; Donati, F. Vecuronium Neuromuscular Blockade in a Child with Mitochondrial Myopathy. *Anesth. Analg.* **1991**, *72* (5), 696–699.
- Footitt, E. J.; Sinha, M. D.; Raiman, J. A. J.; Dhawan, A.; Moganasundram, S.; Champion, M. P. Mitochondrial Disorders and General Anaesthesia: A Case Series and Review. *Br. J. Anaesth.* **2008**, *100* (4), 436–441.
- Thomas, M.; Salpietro, V.; Canham, N.; Ruggieri, M.; Phadke, R.; Kinali, M. Mitochondria DNA Depletion Syndrome in a Infant with Multiple Congenital Malformations, Severe Myopathy, and Prolonged Postoperative Paralysis. *J. Child Neurol.* **2015**, *30* (5), 654–658.
- Szewczyk, A.; Wojtczak, L. Mitochondria as a Pharmacological Target. *Pharmacol. Rev.* **2002**, *54* (1), 101–127.

- [25] Nouette-Gaulain, K.; Jose, C.; Capdevila, X.; Rossignol, R. From Analgesia to Myopathy: When Local Anesthetics Impair the Mitochondrion. *Int. J. Biochem. Cell Biol.* **2011**, *43* (1), 14–19.
- [26] Gilbert, J. C.; Wyllie, M. G. Effects of Anticonvulsant and Convulsant Drugs on the ATPase Activities of Synaptosomes and Their Components. *Br. J. Pharmacol.* **1976**, *56* (1), 49–57.
- [27] Finsterer, J.; Zarrouk Mahjoub, S. Mitochondrial Toxicity of Antiepileptic Drugs and Their Tolerability in Mitochondrial Disorders. *Expert Opin. Drug Metab. Toxicol.* **2012**, *8* (1), 71–79.
- [28] Chaudhry, N.; Patidar, Y.; Puri, V. Mitochondrial Myopathy, Encephalopathy, Lactic Acidosis, and Stroke-like Episodes Unveiled by Valproate. *J. Pediatr. Neurosci.* **2013**, *8* (2), 135–137.
- [29] Santos, N. A. G.; Medina, W. S. G.; Martins, N. M.; Mingatto, F. E.; Curti, C.; Santos, A. C. Aromatic Antiepileptic Drugs and Mitochondrial Toxicity: Effects on Mitochondria Isolated from Rat Liver. *Toxicol. In vitro* **2008**, *22* (5), 1143–1152.
- [30] Rumbach, L.; Mutet, C.; Creml, G.; Marescaux, C. A.; Micheletti, G.; Warter, J. M.; Waksman, A. Effects of Sodium Valproate on Mitochondrial Membranes: Electron Paramagnetic Resonance and Transmembrane Protein Movement Studies. *Mol. Pharmacol.* **1986**, *30* (3), 270–273.
- [31] Sztajnkrzyca, M. D. Valproic Acid Toxicity: Overview and Management. *J. Toxicol. Clin. Toxicol.* **2002**, *40* (6), 789–801.
- [32] Komulainen, T.; Lodge, T.; Hinttala, R.; Bolszak, M.; Pietilä, M.; Koivunen, P.; Hakola, J.; Poulton, J.; Morten, K. J.; Uusimaa, J. Sodium Valproate Induces Mitochondrial Respiration Dysfunction in HepG2 *in vitro* Cell Model. *Toxicology* **2015**, *331*, 47–56.
- [33] Silva, M. F. B.; Aires, C. C. P.; Luis, P. B. M.; Rutter, J. P. N.; Iljst, L.; Duran, M.; Wanders, R. J. A.; Tavares de Almeida, I. Valproic Acid Metabolism and Its Effects on Mitochondrial Fatty Acid Oxidation: A Review. *J. Inher. Metab. Dis.* **2008**, *31* (2), 205–216.
- [34] Jafarian, I.; Eskandari, M. R.; Mashayekhi, V.; Ahadpour, M.; Hosseini, M.-J. Toxicity of Valproic Acid in Isolated Rat Liver Mitochondria. *Toxicol. Mech. Methods* **2013**, *23* (8), 617–623.
- [35] Krähenbühl, S.; Brandner, S.; Kleinle, S.; Liechti, S.; Straumann, D. Mitochondrial Diseases Represent a Risk Factor for Valproate-Induced Fulminant Liver Failure. *Liver* **2000**, *20* (4), 346–348.
- [36] Beghi, E. Efficacy and Tolerability of the New Antiepileptic Drugs: Comparison of Two Recent Guidelines. *Lancet. Neurol.* **2004**, *3* (10), 618–621.
- [37] Elmorsy, E.; Smith, P. A. Bioenergetic Disruption of Human Micro-Vascular Endothelial Cells by Antipsychotics. *Biochem. Biophys. Res. Commun.* **2015**, *460* (3), 857–862.
- [38] Goff, D. C.; Tsai, G.; Beal, M. F.; Coyle, J. T. Tardive Dyskinesia and Substrates of Energy Metabolism in CSF. *Am. J. Psychiatry* **1995**, *152* (12), 1730–1736.
- [39] Wolfarth, S.; Ossowska, K. Can the Supersensitivity of Rodents to Dopamine Be Regarded as a Model of Tardive Dyskinesia? *Prog. Neuropsychopharmacol. Biol. Psychiatry* **1989**, *13* (6), 799–840.
- [40] Schillevoort, I.; de Boer, A.; van der Weide, J.; Steijns, L. S. W.; Roos, R. A. C.; Jansen, P. A. F.; Leufkens, H. G. M. Antipsychotic-Induced Extrapyramidal Syndromes and Cytochrome P450 2D6 Genotype: A Case-Control Study. *Pharmacogenetics* **2002**, *12* (3), 235–240.
- [41] Pickar, D. Prospects for Pharmacotherapy of Schizophrenia. *Lancet (London, England)* **1995**, *345* (8949), 557–562.
- [42] Dean, C. E. Antipsychotic-Associated Neuronal Changes in the Brain: Toxic, Therapeutic, or Irrelevant to the Long-Term Outcome of Schizophrenia? *Prog. Neuropsychopharmacol. Biol. Psychiatry* **2006**, *30* (2), 174–189.
- [43] Przedborski, S.; Kostic, V.; Jackson-Lewis, V.; Naini, A. B.; Simonetti, S.; Fahn, S.; Carlson, E.; Epstein, C. J.; Cadet, J. L. Transgenic Mice with Increased Cu/Zn-Superoxide Dismutase Activity Are Resistant to N-Methyl-4-Phenyl-1,2,3,6-Tetrahydropyridine-Induced Neurotoxicity. *J. Neurosci.* **1992**, *12* (5), 1658–1667.
- [44] Maurer, I.; Möller, H. J. Inhibition of Complex I by Neuroleptics in Normal Human Brain Cortex Parallels the Extrapyramidal Toxicity of Neuroleptics. *Mol. Cell. Biochem.* **1997**, *174* (1–2), 255–259.
- [45] Raudenska, M.; Gumulec, J.; Babula, P.; Stracina, T.; Sztalmachova, M.; Polanska, H.; Adam, V.; Kizek, R.; Novakova, M.; Masarik, M. Haloperidol Cytotoxicity and Its Relation to Oxidative Stress. *Mini Rev. Med. Chem.* **2013**, *13* (14), 1993–1998.
- [46] Martins, M. R.; Petronilho, F. C.; Gomes, K. M.; Dal-Pizzol, F.; Streck, E. L.; Quevedo, J. Antipsychotic-Induced Oxidative Stress in Rat Brain. *Neurotox. Res.* **2008**, *13* (1), 63–69.
- [47] Balijepalli, S.; Kenchappa, R. S.; Boyd, M. R.; Ravindranath, V. Protein Thiol Oxidation by Haloperidol Results in Inhibition of Mitochondrial Complex I in Brain Regions: Comparison with Atypical Antipsychotics. *Neurochem. Int.* **2001**, *38* (5), 425–435.
- [48] Burkhardt, C.; Kelly, J. P.; Lim, Y. H.; Filley, C. M.; Parker, W. D. Neuroleptic Medications Inhibit Complex I of the Electron Transport Chain. *Ann. Neurol.* **1993**, *33* (5), 512–517.
- [49] Barrientos, A.; Marín, C.; Miró, O.; Casademont, J.; Gómez, M.; Nunes, V.; Tolosa, E.; Urbano-Márquez, A.; Cardellach, F. Biochemical and Molecular Effects of Chronic Haloperidol Administration on Brain and Muscle Mitochondria of Rats. *J. Neurosci. Res.* **1998**, *53* (4), 475–481.
- [50] Casademont, J.; Garrabou, G.; Miró, O.; López, S.; Pons, A.; Bernard, M.; Cardellach, F. Neuroleptic Treatment Effect on Mitochondrial Electron Transport Chain: Peripheral Blood Mononuclear Cells Analysis in Psychotic Patients. *J. Clin. Psychopharmacol.* **2007**, *27* (3), 284–288.
- [51] Gonçalves, V. F.; Zai, C. C.; Tiwari, A. K.; Brandl, E. J.; Derkach, A.; Meltzer, H. Y.; Lieberman, J. A.; Müller, D. J.; Sun, L.; Kennedy, J. L. A Hypothesis-Driven Association Study of 28 Nuclear-Encoded Mitochondrial Genes with Antipsychotic-Induced Weight Gain in Schizophrenia. *Neuropsychopharmacology* **2014**, *39* (6), 1347–1354.
- [52] Contreras-Shannon, V.; Heart, D. L.; Paredes, R. M.; Navaira, E.; Catano, G.; Maffi, S. K.; Walss-Bass, C. Clozapine-Induced Mitochondria Alterations and Inflammation in Brain and Insulin-Responsive Cells. *PLoS One* **2013**, *8* (3), e59012.
- [53] Lee, M.; Hong, S.; Kim, N.; Shin, K. S.; Kang, S. J. Tricyclic Antidepressants Amitriptyline and Desipramine Induced Neurotoxicity Associated with Parkinson's Disease. *Mol. Cells* **2015**, *38* (8), 734–740.
- [54] González-Pardo, H.; Conejo, N. M.; Arias, J. L.; Monleón, S.; Vinader-Caerols, C.; Parra, A. Changes in Brain Oxidative Metabolism Induced by Inhibitory Avoidance Learning and Acute Administration of Amitriptyline. *Pharmacol. Biochem. Behav.* **2008**, *89* (3), 456–462.
- [55] Abdel-Razaq, W.; Kendall, D. A.; Bates, T. E. The Effects of Antidepressants on Mitochondrial Function in a Model Cell System and Isolated Mitochondria. *Neurochem. Res.* **2011**, *36* (2), 327–338.
- [56] Ferguson, J. M. SSRI Antidepressant Medications: Adverse Effects and Tolerability. *Prim. Care Companion J. Clin. Psychiatry* **2001**, *3* (1), 22–27.
- [57] Hroudová, J.; Fišar, Z. *In vitro* Inhibition of Mitochondrial Respiratory Rate by Antidepressants. *Toxicol. Lett.* **2012**, *213* (3), 345–352.
- [58] Curti, C.; Mingatto, F. E.; Polizello, A. C.; Galastri, L. O.; Uye-mura, S. A.; Santos, A. C. Fluoxetine Interacts with the Lipid Bilayer of the Inner Membrane in Isolated Rat Brain Mitochondria, Inhibiting Electron Transport and F1F0-ATPase Activity. *Mol. Cell. Biochem.* **1999**, *199* (1–2), 103–109.
- [59] Li, Y.; Couch, L.; Higuchi, M.; Fang, J.-L.; Guo, L. Mitochondrial Dysfunction Induced by Sertraline, an Antidepressant Agent. *Toxicol. Sci.* **2012**, *127* (2), 582–591.
- [60] Chen, S.; Xuan, J.; Wan, L.; Lin, H.; Couch, L.; Mei, N.; Dobrovol'sky, V. N.; Guo, L. Sertraline, an Antidepressant, Induces Apoptosis in Hepatic Cells through the Mitogen-Activated Protein Kinase Pathway. *Toxicol. Sci.* **2014**, *137* (2), 404–415.
- [61] Rodrigues, D. O.; Bristot, I. J.; Klamt, F.; Frizzo, M. E. Sertraline Reduces Glutamate Uptake in Human Platelets. *Neurotoxicology* **2015**, *51*, 192–197.
- [62] Palit, P.; Ali, N. Oral Therapy with Sertraline, a Selective Serotonin Reuptake Inhibitor, Shows Activity against Leishmania Donovanii. *J. Antimicrob. Chemother.* **2008**, *61* (5), 1120–1124.
- [63] Nahon, E.; Israelson, A.; Abu-Hamad, S.; Varda, S.-B. Fluoxetine (Prozac) Interaction with the Mitochondrial Voltage-Dependent Anion Channel and Protection against Apoptotic Cell Death. *FEBS Lett.* **2005**, *579* (22), 5105–5110.
- [64] Brandes, L.; Arron, R.; Bogdanovic, R. Stimulation of Malignant Growth in Rodents by Antidepressant Drugs at Clinically Relevant Doses. *Cancer Res.* **1992**.
- [65] Cloonan, S. M.; Williams, D. C. The Antidepressants Maprotiline and Fluoxetine Induce Type II Autophagic Cell Death in Drug-Resistant Burkitt's Lymphoma. *Int. J. Cancer* **2011**, *128* (7), 1712–1723.
- [66] Amit, B. H.; Gil-Ad, I.; Taler, M.; Bar, M.; Zolokov, A.; Weizman, A. Proapoptotic and Chemosensitizing Effects of Selective Sero-

- tonin Reuptake Inhibitors on T Cell Lymphoma/leukemia (Jurkat) *in vitro*. *Eur. Neuropsychopharmacol.* **2009**, *19* (10), 726–734.
- [67] Frick, L. R.; Rapanelli, M. Antidepressants: Influence on Cancer and Immunity? *Life Sci.* **2013**, *92* (10), 525–532.
- [68] Steingart, A. B.; Cotterchio, M. Do Antidepressants Cause, Promote, or Inhibit Cancers? *J. Clin. Epidemiol.* **1995**, *48* (11), 1407–1412.
- [69] Margolis, A. M.; Heverling, H.; Pham, P. A.; Stolbach, A. A Review of the Toxicity of HIV Medications. *J. Med. Toxicol.* **2014**, *10* (1), 26–39.
- [70] Lewis, W.; Dalakas, M. C. Mitochondrial Toxicity of Antiviral Drugs. *Nat. Med.* **1995**, *1* (5), 417–422.
- [71] Garrabou, G.; Morén, C.; Gallego-Escuredo, J. M.; Milinkovic, A.; Villarroya, F.; Negro, E.; Giralt, M.; Vidal, F.; Pedrol, E.; Martínez, E.; Cardellach, F.; Gatell, J. M.; Miró, O. Genetic and Functional Mitochondrial Assessment of HIV-Infected Patients Developing HAART-Related Hyperlactatemia. *JAIDS J. Acquir. Immune Defic. Syndr.* **2009**, *52* (4), 443–451.
- [72] Cherry, C. L.; Wesselingh, S. L. Nucleoside Analogues and HIV: The Combined Cost to Mitochondria. *J. Antimicrob. Chemother.* **2003**, *51* (5), 1091–1093.
- [73] Brinkman, K.; ter Hofstede, H. J.; Burger, D. M.; Smeitink, J. A.; Koopmans, P. P. Adverse Effects of Reverse Transcriptase Inhibitors: Mitochondrial Toxicity as Common Pathway. *AIDS* **1998**, *12* (14), 1735–1744.
- [74] Opii, W. O.; Sultana, R.; Abdul, H. M.; Ansari, M. A.; Nath, A.; Butterfield, D. A. Oxidative Stress and Toxicity Induced by the Nucleoside Reverse Transcriptase Inhibitor (NRTI)—2',3'-Dideoxycytidine (ddC): Relevance to HIV-Dementia. *Exp. Neurol.* **2007**, *204* (1), 29–38.
- [75] Mallal, S. A.; John, M.; Moore, C. B.; James, I. R.; McKinnon, E. J. Contribution of Nucleoside Analogue Reverse Transcriptase Inhibitors to Subcutaneous Fat Wasting in Patients with HIV Infection. *AIDS* **2000**, *14* (10), 1309–1316.
- [76] Brinkman, K.; Smeitink, J. A.; Romijn, J. A.; Reiss, P. Mitochondrial Toxicity Induced by Nucleoside-Analogue Reverse Transcriptase Inhibitors Is a Key Factor in the Pathogenesis of Antiretroviral-Therapy-Related Lipodystrophy. *Lancet (London, England)* **1999**, *354* (9184), 1112–1115.
- [77] Petit, F.; Fromenty, B.; Owen, A.; Estaquier, J. Mitochondria Are Sensors for HIV Drugs. *Trends Pharmacol. Sci.* **2005**, *26* (5), 258–264.
- [78] Viora, M.; Di Genova, G.; Rivabene, R.; Malorni, W.; Fattorossi, A. Interference with Cell Cycle Progression and Induction of Apoptosis by Dideoxynucleoside Analogs. *Int. J. Immunopharmacol.* **1997**, *19* (6), 311–321.
- [79] Kakuda, T. N. Pharmacology of Nucleoside and Nucleotide Reverse Transcriptase Inhibitor-Induced Mitochondrial Toxicity. *Clin. Ther.* **2000**, *22* (6), 685–708.
- [80] Miró, O.; López, S.; Rodríguez de la Concepción, M.; Martínez, E.; Pedrol, E.; Garrabou, G.; Giralt, M.; Cardellach, F.; Gatell, J. M.; Villarroya, F.; Casademont, J. Upregulatory Mechanisms Compensate for Mitochondrial DNA Depletion in Asymptomatic Individuals Receiving Stavudine plus Didanosine. *J. Acquir. Immune Defic. Syndr.* **2004**, *37* (5), 1550–1555.
- [81] Morén, C.; Noguera-Julian, A.; Rovira, N.; Garrabou, G.; Nicolàs, M.; Cardellach, F.; Martínez, E.; Sánchez, E.; Miró, O.; Fortuny, C. Mitochondrial Assessment in Asymptomatic HIV-Infected Paediatric Patients on HAART. *Antivir. Ther.* **2011**, *16* (5), 719–724.
- [82] Koczor, C. A.; Jiao, Z.; Fields, E. J.; Russ, R.; Ludaway, T.; Lewis, W. AZT-Induced Mitochondrial Toxicity: An Epigenetic Paradigm for Dysregulation of Gene Expression through Mitochondrial Oxidative Stress. *Physiol. Genomics* **2015**, physiogenomics.00045.2015.
- [83] Morén, C.; Noguera-Julian, A.; Garrabou, G.; Catalán, M.; Rovira, N.; Tobías, E.; Cardellach, F.; Miró, O.; Fortuny, C. Mitochondrial Evolution in HIV-Infected Children Receiving First- or Second-Generation Nucleoside Analogues. *J. Acquir. Immune Defic. Syndr.* **2012**, *60* (2), 111–116.
- [84] Phenix, B. N.; Lum, J. J.; Nie, Z.; Sanchez-Dardon, J.; Badley, A. D. Antiapoptotic Mechanism of HIV Protease Inhibitors: Preventing Mitochondrial Transmembrane Potential Loss. *Blood* **2001**, *98* (4), 1078–1085.
- [85] Estaquier, J.; Lelièvre, J.-D.; Petit, F.; Brunner, T.; Moutouh-De Parseval, L.; Richman, D. D.; Ameisen, J. C.; Corbeil, J. Effects of Antiretroviral Drugs on Human Immunodeficiency Virus Type 1-Induced CD4(+) T-Cell Death. *J. Virol.* **2002**, *76* (12), 5966–5973.
- [86] Sloand, E. M.; Maciejewski, J.; Kumar, P.; Kim, S.; Chaudhuri, A.; Young, N. Protease Inhibitors Stimulate Hematopoiesis and Decrease Apoptosis and ICE Expression in CD34(+) Cells. *Blood* **2000**, *96* (8), 2735–2739.
- [87] Sloand, E. M.; Kumar, P. N.; Kim, S.; Chaudhuri, A.; Weichold, F. F.; Young, N. S. Human Immunodeficiency Virus Type 1 Protease Inhibitor Modulates Activation of Peripheral Blood CD4(+) T Cells and Decreases Their Susceptibility to Apoptosis *in vitro* and *in vivo*. *Blood* **1999**, *94* (3), 1021–1027.
- [88] Phenix, B. N.; Angel, J. B.; Mandy, F.; Kravcik, S.; Parato, K.; Chambers, K. A.; Gallicano, K.; Hawley-Foss, N.; Cassol, S.; Cameron, D. W.; Badley, A. D. Decreased HIV-Associated T Cell Apoptosis by HIV Protease Inhibitors. *AIDS Res. Hum. Retroviruses* **2000**, *16* (6), 559–567.
- [89] Pilon, A. A.; Lum, J. J.; Sanchez-Dardon, J.; Phenix, B. N.; Douglas, R.; Badley, A. D. Induction of Apoptosis by a Nonnucleoside Human Immunodeficiency Virus Type 1 Reverse Transcriptase Inhibitor. *Antimicrob. Agents Chemother.* **2002**, *46* (8), 2687–2691.
- [90] Fève, B.; Glorian, M.; Hadri, K. El. Pathophysiology of the HIV-Associated Lipodystrophy Syndrome. *Metab. Syndr. Relat. Disord.* **2004**, *2* (4), 274–286.
- [91] Apostolova, N.; Gomez-Sucerquia, L. J.; Moran, A.; Alvarez, A.; Blas-García, A.; Esplugues, J. V. Enhanced Oxidative Stress and Increased Mitochondrial Mass during Efavirenz-Induced Apoptosis in Human Hepatic Cells. *Br. J. Pharmacol.* **2010**, *160* (8), 2069–2084.
- [92] Robertson, K.; Liner, J.; Meeker, R. B. Antiretroviral Neurotoxicity. *J. Neurovirol.* **2012**, *18* (5), 388–399.
- [93] Mallolas, J. Nevirapine-Associated Hepatotoxicity in Virologically Suppressed Patients—Role of Gender and CD4+ Cell Counts. *AIDS Rev.* **2005**, *8* (4), 238–239.
- [94] Rodríguez de la Concepción, M. L.; Yubero, P.; Domingo, J. C.; Iglesias, R.; Domingo, P.; Villarroya, F.; Giralt, M. Reverse Transcriptase Inhibitors Alter Uncoupling Protein-1 and Mitochondrial Biogenesis in Brown Adipocytes. *Antivir. Ther.* **2005**, *10* (4), 515–526.
- [95] Blas-García, A.; Polo, M.; Alegre, F.; Funes, H. A.; Martínez, E.; Apostolova, N.; Esplugues, J. V. Lack of Mitochondrial Toxicity of Darunavir, Raltegravir and Rilpivirine in Neurons and Hepatocytes: A Comparison with Efavirenz. *J. Antimicrob. Chemother.* **2014**, *69* (11), 2995–3000.
- [96] Gulick, R. M. New Antiretroviral Drugs. *Clin. Microbiol. Infect.* **2003**, *9* (3), 186–193.
- [97] Lang, B. F.; Gray, M. W.; Burger, G. MITOCHONDRIAL GENOME EVOLUTION AND THE ORIGIN OF EUKARYOTES. *Annu. Rev. Genet.* **1999**, *33* (1), 351–397.
- [98] Erokhina, M. V.; Kurylnina, A. V.; Onishchenko, G. E. Mitochondria Are Targets for the Antituberculosis Drug Rifampicin in Cultured Epithelial Cells. *Biochem. Biokhimiia* **2013**, *78* (10), 1155–1163.
- [99] Garrabou, G.; Soriano, A.; López, S.; Guallar, J. P.; Giralt, M.; Villarroya, F.; Martínez, J. A.; Casademont, J.; Cardellach, F.; Mensa, J.; Miró, O. Reversible Inhibition of Mitochondrial Protein Synthesis during Linezolid-Related Hyperlactatemia. *Antimicrob. Agents Chemother.* **2007**, *51* (3), 962–967.
- [100] Hong, S.; Harris, K. A.; Fanning, K. D.; Sarachan, K. L.; Frohlich, K. M.; Agris, P. F. Evidence That Antibiotics Bind to Human Mitochondrial Ribosomal RNA Has Implications for Aminoglycoside Toxicity. *J. Biol. Chem.* **2015**.
- [101] Flanagan, S.; McKee, E. E.; Das, D.; Tulkens, P. M.; Hosako, H.; Fiedler-Kelly, J.; Passarelli, J.; Radovsky, A.; Prokocimer, P. Non-clinical and Pharmacokinetic Assessments To Evaluate the Potential of Tedizolid and Linezolid To Affect Mitochondrial Function. *Antimicrob. Agents Chemother.* **2015**, *59* (1), 178–185.
- [102] Salimi, A.; Eybagi, S.; Seydi, E.; Naserzadeh, P.; Kazerouni, N. P.; Pourahmad, J. Toxicity of Macrolide Antibiotics on Isolated Heart Mitochondria: A Justification for Their Cardiotoxic Adverse Effect. *Xenobiotica* **2015**, 1–12.
- [103] Rodriguez, R. J.; Acosta, D. Inhibition of Mitochondrial Function in Isolated Rate Liver Mitochondria by Azole Antifungals. *J. Biochem. Toxicol.* **1996**, *11* (3), 127–131.
- [104] Belenky, P.; Camacho, D.; Collins, J. J. Fungicidal Drugs Induce a Common Oxidative-Damage Cellular Death Pathway. *Cell Rep.* **2013**, *3* (2), 350–358.
- [105] Bednarczyk, P.; Kicińska, A.; Kominkova, V.; Ondrias, K.; Dolowy, K.; Szewczyk, A. Quinine Inhibits Mitochondrial ATP-Regulated Potassium Channel from Bovine Heart. *J. Membr. Biol.* **2004**, *199* (2), 63–72.

- [106] Rodrigues, T.; Lopes, F.; Moreira, R. Inhibitors of the Mitochondrial Electron Transport Chain and de Novo Pyrimidine Biosynthesis as Antimalarials: The Present Status. *Curr. Med. Chem.* **2010**, *17* (10), 929–956.
- [107] Stocks, P. A.; Barton, V.; Antoine, T.; Biagini, G. A.; Ward, S. A.; O'Neill, P. M. Novel Inhibitors of the Plasmodium Falciparum Electron Transport Chain. *Parasitology* **2014**, *141* (01), 50–65.
- [108] Fau, D.; Eugene, D.; Berson, A.; Letteron, P.; Fromenty, B.; Fisch, C.; Pessayre, D. Toxicity of the Antiandrogen Flutamide in Isolated Rat Hepatocytes. *J. Pharmacol. Exp. Ther.* **1994**, *269* (3), 954–962.
- [109] Cardoso, C. M.; Custódio, J. B.; Almeida, L. M.; Moreno, A. J. Mechanisms of the Deleterious Effects of Tamoxifen on Mitochondrial Respiration Rate and Phosphorylation Efficiency. *Toxicol. Appl. Pharmacol.* **2001**, *176* (3), 145–152.
- [110] Ribeiro, M. P. C.; Santos, A. E.; Custódio, J. B. A. Mitochondria: The Gateway for Tamoxifen-Induced Liver Injury. *Toxicology* **2014**, *323*, 10–18.
- [111] Wallace, K. B. Doxorubicin-Induced Cardiac Mitochondriopathy. *Pharmacol. Toxicol.* **2003**, *93* (3), 105–115.
- [112] Hasinoff, B. B.; Schnabl, K. L.; Marusak, R. A.; Patel, D.; Huebner, E. Dexrazoxane (ICRF-187) Protects Cardiac Myocytes against Doxorubicin by Preventing Damage to Mitochondria. *Cardiovasc. Toxicol.* **2003**, *3* (2), 89–99.
- [113] Monteiro, J. P.; Oliveira, P. J.; Jurado, A. S. Mitochondrial Membrane Lipid Remodeling in Pathophysiology: A New Target for Diet and Therapeutic Interventions. *Prog. Lipid Res.* **2013**, *52* (4), 513–528.
- [114] Waseem, M.; Bhardwaj, M.; Tabassum, H.; Raisuddin, S.; Parvez, S. Cisplatin Hepatotoxicity Mediated by Mitochondrial Stress. *Drug Chem. Toxicol.* **2015**, 1–8.
- [115] Brunmair, B.; Lest, A.; Staniek, K.; Gras, F.; Scharf, N.; Roden, M.; Nohl, H.; Waldhäusl, W.; Fürsinn, C. Fenofibrate Impairs Rat Mitochondrial Function by Inhibition of Respiratory Complex I. *J. Pharmacol. Exp. Ther.* **2004**, *311* (1), 109–114.
- [116] Matsuzaki, S.; Humphries, K. M. Selective Inhibition of Deactivated Mitochondrial Complex I by Biguanides. *Biochemistry* **2015**, *54* (11), 2011–2021.
- [117] Chan, K.; Truong, D.; Shangari, N.; O'Brien, P. J. Drug-Induced Mitochondrial Toxicity. *Expert Opin. Drug Metab. Toxicol.* **2005**, *1* (4), 655–669.
- [118] Hu, D.; Wu, C.; Li, Z.; Liu, Y.; Fan, X.; Wang, Q.; Ding, R. Characterizing the Mechanism of Thiazolidinedione-Induced Hepatotoxicity: An *in vitro* Model in Mitochondria. *Toxicol. Appl. Pharmacol.* **2015**, *284* (2), 134–141.
- [119] Racheck, L. I.; Yuzefovych, L. V.; Ledoux, S. P.; Julie, N. L.; Wilson, G. L. Troglitazone, but Not Rosiglitazone, Damages Mitochondrial DNA and Induces Mitochondrial Dysfunction and Cell Death in Human Hepatocytes. *Toxicol. Appl. Pharmacol.* **2009**, *240* (3), 348–354.
- [120] Bosch, X.; Poch, E.; Grau, J. M. Rhabdomyolysis and Acute Kidney Injury. *N. Engl. J. Med.* **2009**, *361* (1), 62–72.
- [121] Almotrefi, A. A. Effects of Class I Antiarrhythmic Drugs on Mitochondrial ATPase Activity in Guinea Pig Heart Preparations. *Gen. Pharmacol.* **1993**, *24* (1), 233–237.
- [122] Spaniol, M.; Bracher, R.; Ha, H. R.; Follath, F.; Krähenbühl, S. Toxicity of Amiodarone and Amiodarone Analogues on Isolated Rat Liver Mitochondria. *J. Hepatol.* **2001**, *35* (5), 628–636.
- [123] Olszewska, A.; Szewczyk, A. Mitochondria as a Pharmacological Target: Magnum Overview. *IUBMB Life* **2013**, *65* (3), 273–281.
- [124] Abdin, A.; Sarhan, N. Resveratrol Protects against Experimental Induced Reye's Syndrome by Prohibition of Oxidative Stress and Restoration of Complex I Activity. *Can. J. Physiol. Pharmacol.* **2014**, *92* (9), 780–788.
- [125] Jiang, J.; Briedé, J. J.; Jennen, D. G. J.; Van Summeren, A.; Saritas-Brauers, K.; Schaart, G.; Kleinjans, J. C. S.; de Kok, T. M. C. M. Increased Mitochondrial ROS Formation by Acetaminophen in Human Hepatic Cells Is Associated with Gene Expression Changes Suggesting Disruption of the Mitochondrial Electron Transport Chain. *Toxicol. Lett.* **2015**, *234* (2), 139–150.
- [126] Monteiro, J. P.; Martins, A. F.; Lúcio, M.; Reis, S.; Pinheiro, T. J. T.; Geraldes, C. F. G. C.; Oliveira, P. J.; Jurado, A. S. Nimesulide Interaction with Membrane Model Systems: Are Membrane Physical Effects Involved in Nimesulide Mitochondrial Toxicity? *Toxicol. In vitro* **2011**, *25* (6), 1215–1223.
- [127] Nunes, C.; Brezesinski, G.; Pereira-Leite, C.; Lima, J. L. F. C.; Reis, S.; Lúcio, M. NSAIDs Interactions with Membranes: A Biophysical Approach. *Langmuir* **2011**, *27* (17), 10847–10858.
- [128] Monteiro, J. P.; Martins, A. F.; Lúcio, M.; Reis, S.; Geraldes, C. F. G. C.; Oliveira, P. J.; Jurado, A. S. Interaction of Carbonyl cyanide P-Trifluoromethoxyphenylhydrazone (FCCP) with Lipid Membrane Systems: A Biophysical Approach with Relevance to Mitochondrial Uncoupling. *J. Bioenerg. Biomembr.* **2011**, *43* (3), 287–298.
- [129] Galkin, A.; Higgs, A.; Moncada, S. Nitric Oxide and Hypoxia. *Essays Biochem.* **2007**, *43*, 29–42.
- [130] Poderoso, J. J.; Carreras, M. C.; Lisdero, C.; Riobó, N.; Schöpfer, F.; Boveris, A. Nitric Oxide Inhibits Electron Transfer and Increases Superoxide Radical Production in Rat Heart Mitochondria and Submitochondrial Particles. *Arch. Biochem. Biophys.* **1996**, *328* (1), 85–92.
- [131] Soll, R. F. Inhaled Nitric Oxide in the Neonate. *J. Perinatol.* **2009**, *29* Suppl 2, S63–S67.
- [132] Creagh-Brown, B. C.; Griffiths, M. J. D.; Evans, T. W. Bench-to-Bedside Review: Inhaled Nitric Oxide Therapy in Adults. *Crit. Care* **2009**, *13* (3), 221.
- [133] Brown, G. C.; Borutaite, V. Nitric Oxide Inhibition of Mitochondrial Respiration and Its Role in Cell Death. *Free Radic. Biol. Med.* **2002**, *33* (11), 1440–1450.
- [134] Mayer, B. Bioactivation of Nitroglycerin—a New Piece in the Puzzle. *Angew. Chem. Int. Ed. Engl.* **2003**, *42* (4), 388–391.
- [135] Dungal, P.; Haindl, S.; Behling, T.; Mayer, B.; Redl, H.; Kozlov, A. V. Neither Nitrite nor Nitric Oxide Mediate Toxic Effects of Nitroglycerin on Mitochondria. *J. Biochem. Mol. Toxicol.* **2011**, *25* (5), 297–302.
- [136] Finsterer, J. Management of Mitochondrial Stroke-like Episodes. *Eur. J. Neurol.* **2009**, *16* (11), 1178–1184.
- [137] Pedrol, E.; Ribell, M.; Deig, E.; Villà, M. del C.; Miró, O.; Garabou, G.; Soler, A. Treatment of Symptomatic Hyperlactatemia and Lactic Acidosis in HIV+ Patients under Nucleoside Reverse Transcriptase Inhibitors. *Med. Clin. (Barc.)* **2005**, *125* (6), 201–204.
- [138] Artuch, R.; Brea-Calvo, G.; Briones, P.; Aracil, A.; Galván, M.; Espinós, C.; Corral, J.; Volpini, V.; Ribes, A.; Andreu, A. L.; Pallau, F.; Sánchez-Alcázar, J. A.; Navas, P.; Pineda, M. Cerebellar Ataxia with Coenzyme Q10 Deficiency: Diagnosis and Follow-up after Coenzyme Q10 Supplementation. *J. Neurol. Sci.* **2006**, *246* (1–2), 153–158.
- [139] Park, E.-J.; Pezzuto, J. M. The Pharmacology of Resveratrol in Animals and Humans. *Biochim. Biophys. Acta* **2015**, *1852* (6), 1071–1113.
- [140] Monteiro, J. P.; Morais, C. M.; Oliveira, P. J.; Jurado, A. S. Mitochondrial Membrane Lipids in Life and Death and Their Molecular Modulation by Diet: Tuning the Furnace. *Curr. Drug Targets* **2014**, *15* (8), 797–810.
- [141] Finsterer, J. Treatment of Mitochondrial Disorders. *Eur. J. Paediatr. Neurol.* **2010**, *14* (1), 29–44.
- [142] Mussini, C.; Pinti, M.; Bugarini, R.; Borghi, V.; Nasi, M.; Nemes, E.; Troiano, L.; Guaraldi, G.; Bedini, A.; Sabin, C.; Esposito, R.; Cossarizza, A. Effect of Treatment Interruption Monitored by CD4 Cell Count on Mitochondrial DNA Content in HIV-Infected Patients: A Prospective Study. *AIDS* **2005**, *19* (15), 1627–1633.
- [143] Negro, E.; Miró, O.; Rodríguez-Santiago, B.; Garrabou, G.; Estany, C.; Masabeu, A.; Force, L.; Barrufet, P.; Cucurull, J.; Domingo, P.; Alonso-Villaverde, C.; Bonjoch, A.; Morén, C.; Pérez-Alvarez, N.; Clotet, B. Improvement of Mitochondrial Toxicity in Patients Receiving a Nucleoside Reverse-Transcriptase Inhibitor-Sparing Strategy: Results from the Multicenter Study with Nevirapine and Kaletra (MULTINEKA). *Clin. Infect. Dis.* **2009**, *49* (6), 892–900.
- [144] Negro, E.; Romeu, J.; Rodríguez-Santiago, B.; Miró, O.; Garrabou, G.; Puig, J.; Pérez-Alvarez, N.; Moren, C.; Ruiz, L.; Bellido, R.; Miranda, C.; Clotet, B. Mild Improvement in Mitochondrial Function after a 3-Year Antiretroviral Treatment Interruption despite Persistent Impairment of Mitochondrial DNA Content. *Curr. HIV Res.* **2010**, *8* (5), 379–385.
- [145] Bai, J. P. F.; Fontana, R. J.; Price, N. D.; Sangar, V. Systems Pharmacology Modeling: An Approach to Improving Drug Safety. *Biopharm. Drug Dispos.* **2014**, *35* (1), 1–14.

Mitohormesis and autophagic balance in Parkinson disease

Diana Luz Juarez-Flores, Ingrid Gonzalez-Casacuberta, Gloria Garrabou

Parkinson's disease (PD) is the second most prevalent neurodegenerative disorder worldwide, affecting 2% of the population over 65 years. This number will continue to rise as the life expectancy increases. Aging is the most important risk factor for developing PD; nevertheless the precise mechanisms leading to the clinical presence of the disease remain largely unknown. The fact that the age at onset of PD importantly modifies the natural history of the disease raises significant questions on the biological link between them. However, it must be acknowledged that 98% of the elderly population will not develop PD, thus suggesting the existence of some kind of 'healthy aging'. Strikingly, for different reasons, aging is a variable rarely incorporated in most of experimental approaches in the study of PD [1].

Considering the definition of aging as "*a persistent decline in the age-specific fitness components of an organism due to internal physiological degeneration*" [2] the fact that the degeneration process is not the same for all tissues within the same organism, and consequently not for all individuals, is critical when developing experimental models directed to the study of neurodegenerative diseases. Additionally, the recent recognition that PD is not a disease constrained to the loss of dopaminergic neurons in the *substantia nigra*, but a complex series of events that lead to a common clinical outcome, has greatly increased the potential areas of investigation directed towards the establishment of novel experimental models, biomarkers and disease-modifying therapies [3]. In this sense, the use of patient's derived cell models for research preserving aging-related variables of patients and individual genetic and some epigenetics' characteristics is gaining relevance.

While most of PD cases are idiopathic, monogenic forms of the disease are demonstrated in 5-10% of the cases. The study of the genes responsible for these monogenic forms of the disease has proven to be of great utility to further dissect the pathogenic mechanisms and metabolic pathways that lead to PD. Interestingly, the role of mitochondrial function (responsible of energy supply and oxidative stress generation) and autophagy (aimed to remove and recycle damaged cell components) are being tested in these patients and these models as a trigger or a protective factor for the development of both aging and PD.

On this matter, our research has focused on the study of mitochondrial and autophagic function in fibroblasts derived from subjects carrying mutations associated to PD, either with or without clinical manifestations of the disease. Our results suggest that an optimal mitochondrial bioenergetics, dynamics and autophagic function, and the capacity to adapt to challenging environments, play a role in the onset of clinically manifest PD due to LRRK2 mutations [4]. Current ongoing studies point out the importance of an optimal mitochondrial function necessary to achieve high ATP demands in response to an upregulation of anabolic cellular pathways that has been recently evidenced through transcriptomic and biochemical approaches in patients carrying *PRKN* mutation [5]. Strikingly, and in accordance to our findings, Y. Teves et al. have described the differential morphological, mitochondrial and autophagic phenotype in fibroblasts obtained from idiopathic PD patients. An increased anabolism, distinct morphology and special cellular organization was described, together with significantly compromised mitochondrial structure and function and altered macroautophagy [6]. Further research is needed in order to uncover the mechanisms by which these alterations lead to dopaminergic neural death.

Altogether, the above-described studies highlight the importance of mitohormesis and proper autophagic function as putative protective factors from neurodegeneration in PD and validate the use of fibroblasts as a proper model to study the disease, confirming the existence of molecular alterations in non-neural tissues. We hypothesize that a deficient mitochondrial function and impaired autophagic flux would limit the cellular energy supply and increase the accumulation of waste products, principally oligomeric α -synuclein, leading to accelerated neural aging in PD.

Perhaps in the future, strategies directed toward preserving mitochondrial function and autophagic balance may be of use to promote healthy aging and prevent PD but also to achieve a greater life expectancy with the best possible quality of life throughout this journey called "life".

REFERENCES

1. Collier TJ, et al. *Mov Disord.* 2017; 32:983–90. <https://doi.org/10.1002/mds.27037>

2. Rose MR. Evolutionary Biology of Aging. New York: Oxford University Press; 1991.
3. Kalia LV, Lang AE. Parkinson's disease. Lancet (London, England). Elsevier; 2015; 386: 896–912.
4. Juárez-Flores DL, et al. J Transl Med. 2018; 16:160. <https://doi.org/10.1186/s12967-018-1526-3>
5. González-Casacuberta I, et al. Neurobiol Aging. 2018; 65:206–16. <https://doi.org/10.1016/j.neurobiolaging.2018.01.021>
6. Teves JM, et al. Front Neurosci. 2018; 11:737. <https://doi.org/10.3389/fnins.2017.00737>

Gloria Garrabou: Muscle Research and Mitochondrial Function Laboratory, Cellex-IDIBAPS, Faculty of Medicine and Health Science, University of Barcelona, Internal Medicine Service, Hospital Clínic of Barcelona, Barcelona and CIBERER, Spain

Correspondence: Gloria Garrabou

Email: GARRABOU@clinic.cat

Keywords: Parkinson disease, mitochondria, autophagy, fibroblasts, systemic disease

Copyright: Juárez-Flores et al. This is an open-access article distributed under the terms of the Creative Commons Attribution License (CC BY 3.0), which permits unrestricted use, distribution, and reproduction in any medium, provided the original author and source are credited

Received: October 14, 2018

Published: January 16, 2019

This thesis was made possible thanks to a scholarship granted by the
Consejo Nacional de Ciencia y Tecnología (CONACyT),
México to Diana Luz Juárez Flores (CVU 617816) during the period 2014-2018.